NASA CR 71198

C6-332/3061 Copy 4

APPLICATION OF GYROCOMPASSING TO SPACE MISSIONS

FINAL TECHNICAL REPORT
(Study Contract NAS8-20192)

11 February 1966

Approved:

H L Dibble
H. L. Dibble
Manager, Systems Engineering
Astrionics Division

J. J. Fischer
J. J. Fischer
Chief Engineer
Astrionics Division

AUTONETICS
A DIVISION OF NORTH AMERICAN AVIATION, INC.

Unless otherwise expressly restricted on the face of this document, all use, disclosure and reproduction thereof by or on behalf of the Government is expressly authorized. The recipient of this document, if other than the Government of the United States of America, shall not duplicate, use or disclose, in whole or in part, the information disclosed herein, except for or on behalf of the Government to fulfill the purposes for which the document was delivered to him by the Government

CONTENTS

Page

I. Introduction 1

1. Gyrocompassing 1
2. Classes of Techniques 1
   2.1 Definitions 1
   2.2 Measurement Gyrocompassing 2
   2.3 Indirect Gyrocompassing 2
   2.4 Exotic Gyrocompassing 3
   2.5 Applications 4

II. Notation 5

1. Matrices of Base Vectors and Transformations 5
2. Angular Velocity 6
3. Reference Frames 8
   3.1 Celestial (Inertial) Frame (I) 8
   3.2 Orbital Frame (O) 8
   3.3 Local Reference Frame 10
   3.4 Orientation Angles (Roll, Pitch, and Yaw) 11
   3.5 Vehicle Frame (v) for Gyrocompassing in Orbit 12
   3.6 Reference Frame Summary 13
4. Other Conventions 13
   4.1 Subscripts and Superscripts 13
   4.2 Differentiation 15

III. Sensors 16

1. Sensors for Gyrocompassing 16
2. The Gyroscope 16
   2.1 The Single Axis Platform 16
   2.2 Vibration; Kinematic Drift 21
   2.3 The Gyroscope Error Model 23
3. Accelerometers 26
4. Gravity Gradient Attitude Detection 27
   4.1 Principles of Operation 27
   4.2 Practical Prospects 37
5. Horizon Sensor 38
   5.1 Second Harmonic Edge Tracking Horizon Scanner, Fixed Heads 40
   5.2 Tracker Mechanization Equations, Edge Tracker 44
   5.3 Second Harmonic Edge Tracker Horizon Sensor With Azimuth Rotation 47
   5.4 Development Considerations For Future Designs 47

CONTENTS (Continued)

Page

5.5 Conical Scan Horizon Sensors 48
5.6 Large-Angle Mechanization 51
5.7 Small-Angle Mechanization For The Conical Scan Horizon Scanner 56
5.8 Right Angle Conical Scan Mechanization 58
5.9 Small-Angle Mechanization 61
5.10 Radiation Balance of Edge Tracking 64

IV. Fixed-Sight Indirect-Gyrocompassing 66

1. Introduction 66
2. Basic Logic 68
2.1 Level 68
2.2 Azimuth 70
2.3 Inherent Coupling 72
2.4 Error Sources 74
2.5 Gyrocompassing At A Fixed Point Not On The Equator 74
2.6 Extension To A Moving Vehicle 76
3. Comments 79
3.1 Arbitrarily Oriented Instruments 79
3.2 Variations On The Loop Transfer Function 80
4. Examination Of The System Common To Cruise Vehicles 81
4.1 Characteristics Equation And Final Error Values 82
5. Performance And Sensitivity Coefficients 85
5.1 Computer Simulation 85

V. Direct Terrestrial Gyrocompassing 88

1. The Strapdown System 88
1.1 Gyroscopes 88
2. Coordinate Transformations in Strapped Down Systems 89
3. Errors 92
3.1 Simplification of the Error Analysis 98
4. General Considerations 101
5. Vibrational Effects 102
6. Multiple Readings 102

VI. Operation on Bodies Other Than The Earth 105

1. Introduction 105
2. Performance on Other Planets 105
2.1 An Example of Indirect Gyrocompassing With Small W_y and g 106
2.2 Theoretical Optimum 108
2.3 Knowledge of Local Vertical 109

CONTENTS (Continued)

Page

3. Knowledge of Latitude 110
4. Required Accuracy 111

VII. Indirect Gyrocompassing With an Inertial Platform in Orbit 112

1. Introduction 112
2. Coordinate Systems 113
3. Preliminary Considerations to Orbital Gyrocompass Alinement Mechanization 114
    - 3.1 General 114
    - 3.2 In-Orbit Leveling Considerations 115
    - 3.3 In-Orbit Azimuth Alinement Considerations 116
    - 3.4 General Discussion on Gyrocompass Alinement Mechanization 117
4. Summary Discussion 123
5. Detailed Mechanization Equations 130
    - 5.1 Attitude Determination 130
    - 5.2 Angular Velocity - Platform Torquing Rate 132
    - 5.3 Platform Torquing Rate Error-The Platform Attitude Error Propagation Equations 135
    - 5.4 Characteristics of Free-Inertial Response (Open Loop Attitude Mechanization) 140
        - 5.4.1 Constant Coefficient Solution 140
        - 5.4.2 Time-Varying Coefficient Solution 144
        - 5.4.3 Analysis of the Effect of Orbital Eccentricity 148
            - 5.4.3.1 Initial Condition Errors 148
            - 5.4.3.2 Gyro Drift 148
6. Gyrocompass Mechanization 152
    - 6.1 General 152
    - 6.2 Platform Pitch Axis Stabilization 154
        - 6.2.1 Closed Loop Mechanization 156
        - 6.2.2 Effect of Noise 157
            - 6.2.2.1 Integral Plus Proportional 158
            - 6.2.2.2 Mean Squared Error 159
        - 6.2.3 Effect of Incorrect Platform Level Torquing Errors 159
        - 6.2.4 Summary of Errors 161
    - 6.3 Case 1-Open Loop Roll-Yaw 161
        - 6.3.1 Roll Caging Torque as Measure of Yaw 164
        - 6.3.2 Roll and Yaw in Free-Inertial Mode 168
    - 6.4 Case 2-Damping the Roll-Yaw Channels 174
    - 6.5 Case 3-Torquing Yaw Gyro with Proportional Roll Error 174
    - 6.6 Case 4-Torque the Roll and Yaw Gyros with Proportional Roll Error 176

CONTENTS (Continued)

	Page
6.7 Cases 5 to 7 - Derivative Plus Proportional Control	185
6.8 Cases 8 and 9 - Torquing with Integral Plus Proportional Roll Error	185
6.9 Case 10 - Integral Plus Proportional Control on Roll and Yaw Gyro	186
6.9.1 Transient Characteristics	188
6.9.2 Mean Squared Error Characteristics	191
6.10 Cases 11 to 13 - Torquing with a Bilinear Transfer Function	191
6.11 Case 14	193
6.11.1 Torquing Transfer Functions	193
6.11.2 Mechanization Error Equations	196
6.11.3 A Basic Lower Bound to Alinement Accuracy	199
6.11.4 Roll-Yaw Stabilization	201
6.11.5 Stability Characteristics	201
6.11.6 Roots of the Characteristic Equation	202
6.11.7 A Literal Factorization (By Lin's Method)	207
6.11.8 Steady State Characteristics	212
6.11.9 Mean Squared Error Characteristics	213
6.11.10 Asympotic Cases	219
7. System Mechanization Errors	221
7.1 General	221
7.2 Platform Torquing Mechanization	222
7.2.1 Generalized Platform Tilt Equations	222
7.2.2 Coupled Platform Tilt Equations	223
7.2.3 The Effect of Navigational Errors in the Mechanization	228
7.2.4 The Effect of Perturbations	229
8. High Precision Gyro Mechanization	230
References	231
VIII. Measurement Gyrocompassing in Orbit	232
1. Introduction	232
2. Preliminary Mechanization Considerations for Strapdown In-Orbit Gyrocompass Alinement	233
2.1 Definition of Gyrocompass Alinement Modes	233
2.2 Systems Considerations	239
2.3 Strapdown Platforms	241
3. Open Loop Attitude Determination and Error Characteristics	243
3.1 General	243
3.2 Case 1 - Open Loop Yaw From Roll Gyro Rate Output	243

CONTENTS (Continued)

Page

3.2.1 Error Characteristics 247
3.2.2 Smoothing Errors 249
3.2.3 Compensation Errors 252
3.3 Case 2-Integration of Attitude Deviation 252
3.3.1 Updating The Attitude Error Matrix 254
3.3.2 Error Analysis 255
4. General Theory of Computational Strapdown Gyrocompass Alinement 255
4.1 General 255
4.2 Attitude Determination Equations 255
4.2.1 Direction Cosine Equations 255
4.2.2 Attitude Error Propagation Equation (The Gyrocompass Equation) 256
4.2.3 Horizon Error Equation 259
4.3 Mechanization Schemes 260
4.3.1 Basic Equations 260
4.3.2 Continuous Computational Self-Alinement Gyrocompass Techniques 261
4.3.3 One-Point Mechanization Schemes for Initial Attitude Determination 262
4.3.4 An Alternate Scheme 269
4.3.5 Alinement Relative to Arbitrary Frames of Reference 270
4.3.6 Two-Point Gyrocompass Mode 271
4.3.7 Updating the Attitude Matrix 272
4.4 Fine Alinement Schemes (Closed Loop) 273
4.4.1 Orthonormality Constraint 277
4.4.2 A Psuedo Inverse Scheme 279
5. High Precision Gyrocompass Alinement 284
5.1 Preliminary Considerations 284
5.2 A Multipoint Gyrocompass Alinement Scheme 286
5.3 Analytical Transition Matrix 291
5.4 Discussion 292
6. Strapdown ESG Orbital Gyrocompass Alinement 292
6.1 Attitude Determination 293
6.2 Gyrocompass Alinement 294
6.2.1 One-Point Scheme 295
6.2.2 Two-Point or Multipoint Schemes 296
7. Gyrocompass Error Equations 298
References 303

IX. Special Situations and Techniques 304

1. Introduction 304
2. Gyrocompassing During Powered Lift Into Orbit 304

CONTENTS (Continued)

Page

2.1 High Pitch Rate 304
2.2 Vertical Reference 305
3. Spin Stabilized Vehicles 306
4. Operation on Interplanetary Orbits 306
4.1 Utilization of Arbitrary Vertical References 307
4.2 Out of Plane Objects 307

Appendix A - Time History of Alinement Errors for One Example of Indirect Terrestrial Gyrocompassing

Appendix B - Time History of Alinement Errors For Three Examples of Indirect Orbital Gyrocompassing

Appendix C - Mechanization of Strapdown ESG Attitude and Angular Rate Determination

ILLUSTRATIONS

Page

Chapter III

2.1 Schematic Representation of a Single-Axis Platform 17
3.1 Schematic Diagram of a Pendulous Mass Integrating Gyro Accelerometer Showing the x, y, and z-axis Notation 28
4.1 Differential Accelerometer Orientation for $\partial g_{z'}/\partial g_{x'}$ 35
4.2 Differential Accelerometer Orientation for $\partial g_{x'}/\partial g_{z'}$ 36
5.1 Edge Tracking 41
5.2 Output vs Sweep 42
5.3 Mirror Scanning Mechanism 43
5.4 Attitude Mechanization for Small Angles 44
5.5 Angular Relations for Large Angle Inclination, Edge Tracker 46
5.6 Conical Scan Paths 48
5.7 Conical Scan and Output Waveforms 49
5.8 Horizon Profile Curves for 14-16 CO_2 and Two Slicing Levels 50
5.9 Tangent Relationships 52
5.10 Cone Angles 54
5.11 Rolled Disposition of the Tangent Lines of Sight Zero Pitch 56
5.12 Pitched Disposition of the Tangent Lines of Sight, Zero Roll 57
5.13 Right Angle Conical Scan Mechanization 58
5.14 Tangent Lines for Right Angle Cones 59
5.15 Angular Relationships for $\underline{T}_3$ or $\underline{T}_4$, Right Angle Cones 60
5.16 Angular Relationships for T_1 and T_2 61
5.17 System C, Head Layout 62
5.18 System E, Head Layout 62
5.19 System A, Head Layout 63
5.20 System B, Head Layout 63
5.21 Triangular Aperture Edge Tracker, Image Plane View of Horizon 64

Chapter IV

2.1 Block Diagram for Simple Level Mechanism Associated With The Y-Axis 71
2.2 Stabilized Level Mechanism for the Y-Axis 71
2.3 Block Diagram Showing Level Loops and Coupled Azimuth Correction 73
2.4 Complete Block Diagram Showing Leveling Loops and Coupled Azimuth 75
2.5 Error Block Diagram for Gyrocompassing With a Nonstationary Vehicle 78
5.1 Instrument Configuration 87

ILLUSTRATIONS (Continued)

Chapter V

1.1 Three Single-Axis Platform Configurations for a Strapped Down System 90
3.1 Pictorial Representation of ϕ_x^L 96

Chapter VII

3.1 A Three-Axis Level Platform 114
3.2 Angle Relations Between True (Orbital) Vehicle and Platform Defined Frames 115
3.3 Vehicle Oriented Platform 118
3.4 Orbit Oriented Platform 118
3.5 Open Loop Yaw Indication from Measuring Roll Gimbal Angle Rate with Caged Platform 119
3.6 Open-Loop Yaw Indicator Mechanization 119
3.7 Generalized Gyrocompass Self-Alinement Diagram 120
6.1 Closed-Loop Pitch Axis Stabilization 156
6.2 An Error Diagram of an Open-Loop Mechanization of Roll and Yaw 164
6.3 Damping the Roll-Yaw Response 168
6.4 Error Diagram of Gyrocompass Loop for Case 4 177
6.5 Steady-State Sensitivities Due to Sensor Bias 183
6.6 Roll-Yaw Characteristics of Case 4 at Damping Ratio of .5 184
6.7 Frequency Response of $G(s) = 1/s+K$ 194
6.8 Frequency Response of $G(s) = K/s+K$ 195
6.9 Error Block Diagram of Alinement Scheme 197
6.10 Pitch Axis Response Characteristics 200
6.11 Roll and Yaw Torquing Gain Constant Domains in Terms of Filter in Terms of Filter Band Pass 203
6.12 Routh's Criterion 204
6.13 Stability Domains 206
6.14 Stability Domains 208
6.15 Natural Frequency Domains 209
6.16 Natural Frequency Domains 210
6.17 Permissible Domains for Damping Ratio 211
6.18 Routh's Criterion and Steady-State Sensitivity Ratio Resulting from Sensor Bias 214
6.19 Plots of Steady-State Roll Error Sensitivities and Ratio of Steady-State Yaw to Roll Errors Due to Horizon Sensor Bias 215
6.20 Mean Squared Roll and Yaw Error Characteristics Random Sensor (White) Noise 220

ILLUSTRATIONS (Continued)

Page

Chapter VIII

1. One-Point Gyrocompass Mode 238
2. Two-Point Gyrocompass Mode 238
3. Overall System Diagram of In-Orbit Strapdown Computational Gyrocompass Mode 240
4. Three Single-Axis Platforms 242
5. Rate Gyro Package 242
6. Roll Rate Compensation 246
7. Roll Rate Network 247
8. RMS Gyrocompass Error Due to Random Roll Rate Coupling 251

Chapter IX

4.1 Representation of Lines-of-Sight From the Sun to Vehicle and to Out-of-Plane Object at Point "a" 308

Appendix C

A-1 ESG Gyro Readout Latitude Circle Geometry
A-2 Time Series of Pulses Read From Pickoff Ports
A-3 Top View of Readout Latitude Circle

TABLES

Page

Chapter II

1. Summary of Definition of Reference Frames 14

Chapter VII

4.1 Summary Roll-Yaw Platform Response Characteristics for Locally Level Orbiting Gyro-Platform 125
4.2 Summary of Steady State Errors 128
4.3 Summary of Settling Times 129
5.1 Open Loop Platform Attitude Error Propagation 143
6.1 Summary of Pitch Axis Error Response Characteristics for Undamped Modes 162
6.2 Steady State Errors Closed Loop on Pitch Open Loop Roll-Yaw 167
6.3 Summary of Steady State Platforms Errors in the Damped Leveling Mode 173

Chapter VIII

1. Summary of Gross Errors of Gyrocompassing Techniques 236
2. Summary of Open Loop Gyrocompass Errors 248

FOREWORD

This report was prepared by the Autonetics Division of North American Aviation, Inc., as a requirement of NASA Contract No. NAS 8-20192. The study contract originated at George C. Marshall Space Flight Center, Huntsville, Alabama, and the execution of the contract was under the direction of John W. Cole, NASA contracting officers' representative.

The principal investigator at Autonetics was Dr. John F. Sanford. Significant contributions were made by Mr. K. C. Kochi and Mr. F. M. Pelteson. Dr. R. E. Roberson, Professor of Engineering at UCLA, served as Technical Consultant.

CHAPTER I

INTRODUCTION

1. Gyrocompassing

A classical gyrocompass designed for use on the surface of the Earth - - more precisely, at sea - - consists of a gyroscope with a nominally horizontal spin axis and a center of mass below the point of support of the gyro gimbal. The lowered center of mass tends to keep the input axis of the gyro horizontal (in the absence of lateral translational accelerations), and the gyro responds to the component of the Earth's angular velocity on this inpoint axis. Damping in the device settles the gyro into such an orientation that the sensed Earth rate is zero, whence the spin axis points North along the local meridian.

The two essential ingredients of the classical gyrocompass, therefore, are a means of sensing a known angular rate and a means of establishing a known "line of sight" (in this case, the geographic vertical). From this information, the orientation of the device may be deduced.

In more general terms, one can define gyrocompassing as any means of establishing orientation by one line of sight or its equivalent, together with one component of angular rate, however obtained.

The purpose of this work is to pursue the subject of gyrocompassing in general, considering both the situations under which it is used and the instrumentation utilized. Uses considered include operation at a fixed site on the Earth or any other celestial body, or in a moving vehicle (e.g. ship, aircraft, etc.) more or less confined to the surface of such a body, or in a vehicle in free orbital flight about such a body.

2. Classes of Techniques

2.1 Definitions

It is convenient to distinguish two broad classes of techniques. These do not have standard names, so they are called here simply:

1. Measurement (or direct) gyrocompassing
2. Indirect gyrocompassing

The names are not completely descriptive, so the categories are perhaps best visualized by analogies to elementary measuring devices which are divided into two types, ordinarily described as "direct-reading instruments" and "nulled instruments". The measurement gyrocompass techniques are analogous to direct-reading instruments, the indirect gyrocompassing to nulled instruments.

2.2 Measurement Gyrocompassing

Measurement gyrocompassing is the process of determining the direction of rotation and the direction of the local vertical by direct measurement employing such instruments as horizon sensors, optical telescopes, accelerometers, gyroscopes, and possibly others. This is the basic approach utilized by a strapdown system, so there might be some justification for calling it strapdown gyrocompassing. However, other simpler forms of azimuth determination are also included in this general category. For instance, one might design a single degree of freedom gyroscope with its spin axis parallel to its mounting base. The axis of freedom would be perpendicular to the base. If such an instrument was operated with the base leveled, the earth's rotation would cause the gyro to precess. With proper damping were provided, the gyro would come to rest with the spin axis alined with the component of earth's rotation lying in the base plane, i.e., perpendicular to the gyro axis of freedom. Thus, if the gyro base were carefully leveled, the spin axis would indicate the northerly direction. Other examples can be thought of.

Results obtained from measurement gyrocompassing are degraded by instrument errors, such as electronic noise, and instrument misalinement, and by spurious rotations of the instrument package. Improvement may be obtained with statistical filtering techniques. In some applications, improvement has been sought by placing the instruments on a stable platform. A stable platform is basically a gimballed platform whose attitude is controlled by gyroscopes and associated servo systems. It is designed to remain fixed in inertial space unless commanded to change attitude. It is kept locally level by the accelerometers mounted on it, and can provide isolation from angular motion for the gyroscope being used for earth rate measurement.

2.3 Indirect Gyrocompassing

The concept of a stable platform introduces the second approach to gyrocompassing. In this method, no direct measurement of the direction of the reference rotation vector is made, rather the direction of the vector is inferred through use of the measurements which are made; hence the name, "indirect gyrocompassing".

The logic proceeds as follows. Let us assume that an inertial platform is located at a point on the earth's equator. Its attitude will remain fixed in inertial space. As the earth rotates, the platform will appear to rotate with respect to the earth. If the platform is to remain locally level, it must be rotated about its north pointing axis at earth rate. But, we do not know where north is. Let us rotate the platform about an axis we think is north. The platform can remain locally level only if the axis about which it is rotating is indeed pointed north and if the angular velocity is indeed earth rate. We can use the accelerometers to measure platform tilt. Any indicated acceleration in the horizontal axes is actually equivalent to the acceleration of gravity times the small tilt angle. Through proper utilization of tilt information, we can rotate the platform in azimuth until its rotation axis points north, and also make any small adjustment to platform rotation rate which may be necessary to make it equal to earth rate.

The problem in logic may essentially be stated as follows. "There exists a platform which is rotating about a specified platform axis at an angular velocity equivalent to that of the earth. Find the one and only orientation of the platform for which it will remain locally level". The complete solution proceeds from a knowledge of tilt angles only. Some reasonably good estimate of proper rotation rate is helpful though not necessary. One can also see that this process works equally well whether the gyrocompassing platform is on the equator or elsewhere. If the platform is not on the equator, the fixed rotation rate is divided between platform vertical axis and platform north seeking axis. A slight extension to the logic will make this approach applicable to a vehicle moving over the earth's furface.

The indirect gyrocompassing method utilizing a platform offers a process by which vibration and undesired vehicle motion which degrades the measurement gyrocompassing process may be filtered out. Knowledge of attitude is improved, up to a point, by continued observation. Very little computation is required.

There is no reason why the same logic may not be applied to the strapdown case. The sensing instruments may be body mounted, but an imaginary platform can be created, and the indirect gyrocompassing mechanization employed. In this situation, more computational capacity is required.

2.4 Exotic Gyrocompassing

As has been mentioned, measurements of local vertical and angular rotation are degraded by deterministic and stochastic errors. Modern filtering techniques might be expected to improve the results. For instance, Kalman's technique which essentially employs time varying coefficients is used effectively for rapid alinement of the platform in some inertial navigation systems for cruise vehicles. Present technology in adaptive control systems suggests the possibility of further improvements.

These more sophisticated approaches require more computational capabilities than the more direct methods. They were not extensively considered as a part of this study.

2.5 Applications

It appears reasonable to divide gyrocompassing into regions of application such as prelaunch alinement; final stages of boost; in orbit around the earth; etc. That procedure has been followed in this document. In addition, each application has been further divided into the two categories, i.e., measurement gyrocompassing and indirect gyrocompassing.

CHAPTER II

NOTATION

1. Matrices of Base Vectors and Transformations

To simplify the respresentation of the triad of unit vectors associated with a particular reference frame, a single symbol may be used to define the complete triad. A triad of orthonormal vectors, $\underline{1}_x$, $\underline{1}_y$, $\underline{1}_z$, associated with an orthogonal frame is defined symbolically as a column matrix of the unit vectors.

$$\underline{1} = [\underline{1}_x \; \underline{1}_y \; \underline{1}_z]^T$$

The superscript T denotes matrix transpose.

Subscripts may be used to identify certain coordinate frames, as for instance, $\underline{1}_v$ may be used to designate the vehicle coordinate triad. This leads to double subscripts for the x, y, and z unit vectors, as $\underline{1}_{vx}$, $\underline{1}_{vy}$, and $\underline{1}_{vz}$.

All direction cosine matrices are specified by the following "self-defining" notation. Let $\underline{1}_a$ and $\underline{1}_b$ define two triads of orthogonal coordinate systems. The forward direction cosine transformation matrix, S of frame $\underline{1}_a$ to frame $\underline{1}_b$ is defined as

$$\underline{1}_b = S^{ba} \, \underline{1}_a \tag{1}$$

and the inverse as

$$\underline{1}_a = S^{ab} \, \underline{1}_b = (S^{ba})^{-1} \, \underline{1}_b = (S^{ba})^T \, \underline{1}_b \quad . \tag{2}$$

In this work linear orthogonal transformations are of primary concern, for which the inverse of the transformation matrix is equal to its transpose.

The ba superscript on the direction cosine matrix of Eq. (1) indicates that the matrix will rotate a column matrix from the a frame into the b frame. The direction cosine angles are measured from a to b. This convention for direction of measurement of the angles is important. If the angles were measured from b to a, the signs of the elements of the S^{ba} matrix would be transposed about the principle diagonal from that defined by Eq. (1).

Using this notation, a chain of transformation can be represented as

$$\underline{1}_b = S^{ba}\,\underline{1}_a$$

$$\underline{1}_c = S^{cb}\,\underline{1}_b = S^{cb}\,S^{ba}\,\underline{1}_a = S^{ca}\,\underline{1}_a \tag{3}$$

and the inverse

$$\underline{1}_a = (S^{cb}\,S^{ba})^{-1}\,\underline{1}_c = S^{ab}\,S^{bc}\,\underline{1}_c = (S^{cb}\,S^{ba})^{T}\,\underline{1}_c \tag{4}$$

2. Angular Velocity

To specify the angular velocity of one triad relative to another, a convenient notation is to use a double superscript. The angular velocity matrix in turn can be related to the direction cosine matrix. The angular velocity of triad b relative to triad a resolved into triad b can be expressed as the vector

$$\underline{\omega}^{ba} = \omega_x^{ba}\,\underline{1}_{bx} + \omega_y^{ba}\,\underline{1}_{by} + \omega_z^{ba}\,\underline{1}_{bz} = {\omega^{ba}}^{T}\,\underline{1}_b \tag{5}$$

With any column matrix such as ω^{ba} can be associated a skew-symmetric matrix $\tilde{\omega}^{ba}$ defined by[1]

$$\tilde{\omega}^{ba} = [\tilde{\omega}^{ba}_{\alpha\beta}] = [\epsilon_{\alpha\lambda\beta}\;\omega^{ba}_{\lambda}]$$

---

[1] The summation convention is used for repeated subscripts. Greek lower case indices have the range 1, 2, 3; when x, y, z subscripts are used, they are to be considered equivalent to 1, 2, 3 respectively.

$$\tilde{\omega}^{ba} = \begin{bmatrix} 0 & -\omega_z^{ba} & \omega_y^{ba} \\ \omega_z^{ba} & 0 & -\omega_x^{ba} \\ -\omega_y^{ba} & \omega_x^{ba} & 0 \end{bmatrix} \tag{6}$$

where $\varepsilon_{\alpha\lambda\beta}$ are the epsilon symbols of tensor analysis.

It can be shown that

$$\tilde{\omega}^{ba} = -\dot{S}^{ba} S^{ab} \quad . \tag{7}$$

Thus the angular velocity of two frames can be found in terms of the derivative of the direction cosine matrix which connects them.

The skew-symmetric matrix of Eq. (6) plays an especially important role in the matrix representation of vector cross products. Let R^b be the vector, $\underline{R}$, represented in the b- frame. The cross product $\underline{\omega}^{ba}$ x $\underline{R}$ resolved into the b- frame can be written in matrix notation as $\omega^{ba} R^b$.

In case the direction cosine matrix consists of a chain of transformations, typically as a product of two direction cosine matrices

$$S^{ca} = S^{cb} S^{ba} \quad ,$$

then

$$\tilde{\omega}^{ca} = \dot{\overline{(S^{cb} S^{ba})}} \, (S^{cb} S^{ba})^T = \tilde{\omega}^{cb} + S^{cb} \tilde{\omega}^{ba} S^{bc} \quad , \tag{8}$$

This corresponds to the vector representation in the $\underline{1}_c$ frame

$$\underline{\omega}^{ca} = \underline{\omega}^{cb} + S^{cb} \underline{\omega}^{ba} \quad , \tag{9}$$

and expresses the total angular rate of triad $\underline{1}_c$ with respect to triad $\underline{1}_a$.

3. Reference Frames

3.1 Celestial (Inertial) Frame (I)

This frame is typically defined by the triad

$$\underline{I} = \begin{bmatrix} \underline{I} \\ \underline{J} \\ \underline{K} \end{bmatrix} = \begin{bmatrix} \underline{J} \times \underline{K} \\ \text{North Celestial Pole} \\ \text{Direction of First Point of Aries} \end{bmatrix} \tag{10}$$

3.2 Orbital Frame (0)

This frame is locally level and defined by the orbital trajectory of the vehicle center-of-mass

$$\underline{1}_0 = \begin{bmatrix} \underline{1}_x \\ \underline{1}_y \\ \underline{1}_z \end{bmatrix} = \begin{bmatrix} \underline{1}_y \times \underline{1}_z \text{ (Downrange)} \\ \text{Normal (out-of-plane) to Instantaneous Orbital Plane} \\ \text{Direction (Radial) to Geocenter} \end{bmatrix} \tag{11}$$

For the gyrocompass problem in particular, this frame is used to reference vehicle roll, pitch, and yaw rotations. Nominally body roll, pitch, and yaw axes, respectively, are represented:

$$\underline{1}_0 = \begin{bmatrix} \underline{1}_x \\ \underline{1}_y \\ \underline{1}_z \end{bmatrix} = \begin{matrix} \text{Nominal Roll} \\ \text{Nominal Pitch} \\ \text{Nominal Yaw} \end{matrix} \tag{12}$$

The actual roll, pitch, and yaw are, of course, measured relative to the vehicle axes.

The orbital frame is described in terms of the inertial by the equation

$$\underline{1}_0 = S^{0I}\,\underline{I} \qquad (13)$$

where S^{0I} is determined from the knowledge of the position and velocity (navigation information) of the vehicle center-of-mass in the inertial frame of reference. The navigation data typically is determined from orbit determination. As an example, S^{0I} can be determined from the position and velocity vectors, $\underline{r}$ and $\underline{v}$.

$$\left.\begin{aligned}
\underline{r} &= x\,\underline{I} + y\,\underline{J} + z\,\underline{K} = \text{represented in celestial frame} \\
\underline{v} &= \dot{x}\,\underline{I} + \dot{y}\,\underline{J} + \dot{z}\,\underline{K} = \text{represented in celestial frame} \\
\underline{1}_z &= \frac{\underline{r}}{r}, \quad r = \sqrt{\underline{r}\cdot\underline{r}} \\
\underline{1}_y &= \frac{\underline{r}\times\underline{v}}{\sqrt{\mu p}}, \quad \sqrt{\mu p} = \sqrt{(\underline{r}\times\underline{v})\cdot(\underline{r}\times\underline{v})} \\
\underline{1}_x &= \underline{1}_y \times \underline{1}_z = \frac{(\underline{r}\times\underline{v})}{\sqrt{\mu p}} \times \frac{\underline{r}}{r}
\end{aligned}\right\} \qquad (14)$$

Equations (14) can be expanded in terms of the unit vectors $\underline{I}$, $\underline{J}$, and $\underline{K}$ from which the elements of S^{0I} can be represented.

One convenient representation for S^{0I} is given in terms of the orbital constants and the true anomaly

$$\begin{bmatrix}
-s\Omega\, su + c\Omega\, c\gamma\, cu & s\gamma\, cu & -c\Omega\, su - s\Omega\, c\gamma\, cu \\
-c\Omega\, s\gamma & c\gamma & s\Omega\, s\gamma \\
s\Omega\, cu + c\Omega\, s\gamma\, su & s\gamma\, su & c\, cu - s\Omega\, c\gamma\, su
\end{bmatrix} \qquad (15)$$

where

Ω = right ascension of Aries

u = $+ v$ = argument of latitude

ω = argument of perigee

v = true anomaly

γ = inclination of orbital plane to equator plane

and s, c, abbreviate sin and cos.

3.3 Local Reference Frame

When utilizing gyrocompassing on the earth for prelaunch alinement, it is convenient to define a locally level reference frame as follows

$$\underline{1}_L = \begin{bmatrix} \underline{1}_x \\ \underline{1}_y \\ \underline{1}_z \end{bmatrix} \begin{bmatrix} \underline{1}_y \times \underline{1}_z \text{ (East)} \\ \text{Due North} \\ \text{Vertically upward from the location} \\ \text{of the vehicle} \end{bmatrix} \qquad (16)$$

This frame is used as a reference for roll, pitch, and yaw of the vehicle's inertial platform in a manner identical to Eq. (12).

Typically, the direction of a plumb line is taken as the local vertical defined as $\underline{1}_z$. Because of the earth's rotation, this is not the geocentric vertical except at the equator. The effective acceleration of gravity measured at the earth's surface includes the centripetal acceleration resulting from planet rotation. This latter acceleration is a function of local latitude, as well as planet diameter and rotation rate.

Presumably the direction of the local "apparent" gravity vector will be known with respect to the geocentric vertical at any terrestrial launch site. Alinement of the inertial platform with the local "apparent" gravity defined vertical may be used, or the acceleration which would be sensed by each accelerometer with the platform alined to the geocentric vertical may be computed and applied as a negative bias to accelerometer output.

3.4 Orientation Angles (Roll, Pitch, and Yaw)

In most cases we are concerned with the attitude of the platform with respect to the reference set, be it orbital or locally level on earth. Occasionally we may be concerned with the alinement of an imaginary coordinate frame defined in the vehicle navigation computation, but this is treated similarly to the situation where a physical platform is used.

The platform will have its own x, y, and z axes, which will be nominally alined with the reference set, but which actually, of course, are not. Thus, Eq. (2.16) obtain

$$\underline{1}_p = S^{PO}\,\underline{1}_O \text{ in orbit}$$

or

$$\underline{1}_p = S^{PL}\,\underline{1}_L \text{ on earth} \qquad (17)$$

In order to characterize the elements of the S direction cosine matrix, the canonical Euler angle representation may be used. A convenient description is

$$S^{vO} = E_R(\phi)\,E_p(\theta)\,E_y(\Psi) \qquad (18)$$

where ϕ, θ, and Ψ represent Euler angles of rotation about the roll, pitch, and yaw axes, or the x, y, and z axes, respectively. It further follows that

$$E_R(\phi) = \begin{bmatrix} 1 & 0 & 0 \\ 0 & c\phi & s\phi \\ 0 & -s\phi & c\phi \end{bmatrix} \qquad (19)$$

$$E_p(\theta) = \begin{bmatrix} c\theta & 0 & -s\theta \\ 0 & 1 & 0 \\ s\theta & 0 & c\theta \end{bmatrix} \qquad (20)$$

and

$$E_y(\Psi) = \begin{bmatrix} c\Psi & s\Psi & 0 \\ -s\Psi & c\Psi & 0 \\ 0 & 0 & 1 \end{bmatrix} . \qquad (21)$$

If indeed the platform axes are nominally alined to the orbital (local level) frame, then small deviations of the platform axes from the orbital frame are characterized as

$$S^{PO} = I - \tilde{\phi} \qquad (22)$$

where

$$I = \begin{bmatrix} 1 & 0 & 0 \\ 0 & 1 & 0 \\ 0 & 0 & 1 \end{bmatrix} = \text{unit matrix} \qquad (23)$$

and

$$\tilde{\phi} = \begin{bmatrix} 0 & -\Psi & \theta \\ \Psi & 0 & -\phi \\ -\theta & \phi & 0 \end{bmatrix} = -(\Delta S^{PO})\, S^{OP} \qquad (24)$$

Equation (22) can be obtained from Eq. (18) by setting $c\theta = 1$, $s\theta = \theta$, and performing the operation of Eq. (24).

Alternate representations of S^{PO} are possible by interchanging E_R, E_p, and E_y; however, the small angle formulation (24) will be the same.

3.5 Vehicle Frame (v) For Gyrocompassing in Orbit

This frame is fixed in the vehicle. One can imagine this frame to be designated by three marker lines, mutually orthogonal, scribed in the structure of the vehicle. Again, for the gyrocompass problem, a convenient orientation of this frame is in alinement with the orbital frame. In this configuration the vehicle attitude deviation can be described by roll, pitch, and yaw angle deviations relative to the orbital frame. The various transformations to describe this triad are given on the next page.

$$\underline{1}_v = S^{vo}\,\underline{1}_0 = S^{v0}\,S^{0I}\,1_I$$

$$\underline{1}_v = \begin{bmatrix} 1_{vx} = \text{roll axis} \\ 1_{vy} = \text{pitch axis} \\ 1_{vz} = \text{yaw axis} \end{bmatrix} \qquad (25)$$

3.6 Reference Frame Summary

Some of the more important reference frames required for this study are summarized in Table 1.

4. Other Conventions

4.1 Subscripts and Superscripts

The use of superscripts and subscripts has, in general, already been covered above.

Superscripts are used to designate relative quantities, as in the case of ω^{ca}, which is the angular rotation of frame c with respect to frame a. When expressed in matrix form, it would be in the c system. Thus the superscript may also be used to designate the reference frame to which the elements of a matrix are related.

Subscripts are utilized to indicate elements of a matrix or components of a vector such as ω_x^{ca}, ω_y^{ca}, and also as a part of the definition quantity such as $\underline{1}_p$, $\underline{1}_{py}$, and $\underline{1}_{pz}$.

In certain cases where the intent is obvious, superscripts and subscripts may be left off. For example, Ω is commonly used for earth's rotation vector. Properly this should be designated as Ω^{LI} where L stands for earth fixed locally level coordinate frame and I for the inertially fixed frame. Superscripts in this situation are really unnecessary and will not be employed.

In some instances there will be duplication of symbols. In the foregoing paragraph Ω was used to represent earth rate. This symbol is also commonly found as the right ascension of Aries. Since the two are not likely to be found in the same discussion, this duplication should pose no real problem. It is felt by the authors that use of commonly accepted symbols will offset, for most readers, any inconvenience resulting from duplication.

$$\underline{I} = \begin{bmatrix}\underline{I}\\ \underline{J}\\ \underline{K}\end{bmatrix} = \begin{bmatrix}\underline{J}\times\underline{K}\\ \text{North celestial pole}\\ \text{Direction of first point of aries}\end{bmatrix} \qquad \text{celestial frame}$$

$$\underline{1}_O = \begin{bmatrix}\underline{1}_x\\ \underline{1}_y\\ \underline{1}_z\end{bmatrix} = \begin{bmatrix}\text{Down range}\\ \text{Out-of-plane}\\ \text{Radial}\end{bmatrix} = S^{OI}\,\underline{I} \qquad \text{orbital frame}$$

$$\underline{1}_v = \begin{bmatrix}\underline{1}_{vx}\\ \underline{1}_{vy}\\ \underline{1}_{vz}\end{bmatrix} = \begin{bmatrix}\text{Roll}\\ \text{Pitch}\\ \text{Yaw}\end{bmatrix} = S^{vO}\,\underline{1}_O = S^{vO}\,S^{OI}\,\underline{I} \qquad \text{vehicle axes}$$

$$\underline{1}_p = \begin{bmatrix}\underline{1}_{px}\\ \underline{1}_{py}\\ \underline{1}_{pz}\end{bmatrix} = \begin{bmatrix}\text{Platform Roll}\\ \text{Platform Pitch}\\ \text{Platform Yaw}\end{bmatrix} \begin{array}{l} \left.\begin{aligned} &= S^{pv}\,\underline{1}_v = S^{pv}\,S^{vO}\,\underline{1}_O \\ &= S^{pv}\,S^{vO}\,S^{OI}\,\underline{I} \end{aligned}\right\}\text{in orbit} \\ \text{or} \quad = S^{PL}\,\underline{1}_L \qquad \text{on earth} \end{array} \quad \begin{array}{c}\text{platform}\\ \text{frame}\end{array}$$

$$\underline{1}_L = \begin{bmatrix}\underline{1}_{Lx}\\ \underline{1}_{Ly}\\ \underline{1}_{Lz}\end{bmatrix} = \begin{bmatrix}\text{East}\\ \text{North}\\ \text{Up}\end{bmatrix} \qquad \begin{array}{l}\text{Locally level frame}\\ \text{on the earth.}\end{array}$$

Table 1

Summary of Definition of Reference Frames

4.2 Differentiation

The total derivative of a vector or column matrix will be indicated by a dot over the symbol representing the vector. In many situations, differentiation with respect to the vector reference frame is desired rather than the total derivative. This will be indicated by a small circle in place of the dot. The reference frame will be indicated by the superscript (or the first symbol of the superscript if there are two), unless it has been specified clearly by other means.

CHAPTER III

SENSORS

1. Sensors For Gyrocompassing

The gyrocompassing problem is concerned with the measurement, directly of indirectly, of a rotation vector and a line-of-sight vector or its equivalent. Several types of devices can be used, at least in principle, to implement such measurements. They include gyroscopes, accelerometers, horizon sensors, and optical telescopes. The behavior of these instruments is well understood and well documented. Their essential characteristics are summarized briefly in this chapter to the extent needed for the gyrocompassing study.

2. The Gyroscope

2.1 The Single Axis Platform

There is a vast literature on the nature and behavior of gyroscopes. Therefore, it is assumed that the reader is relatively familiar with general characteristics of gyros. Thus the briefest possible description should suffice here.

The discussion focuses on the single axis, two-gimbal gyroscope with a servo follow-up controlling the outer gimbal generally called a single axis platform. Figure 2.1 is a schematic representation of such a device.

It will be convenient to define the following quantities:

h_s = angular momentum of the spinning wheel

h^i = angular momentum of the inner gimbal system and wheel, expressed in terms of the inner gimbal reference coordinate frame as indicated by the superscript "i".

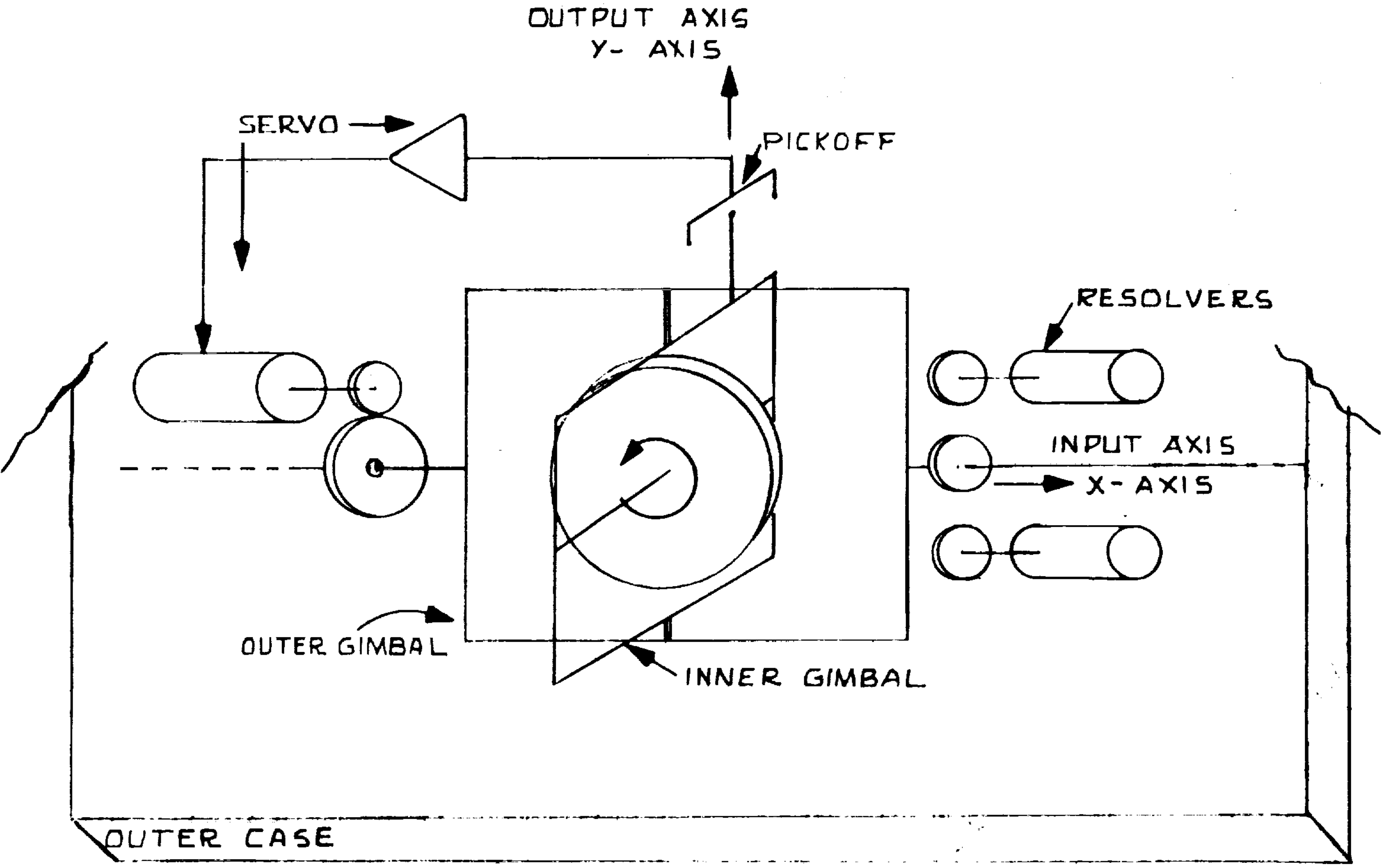
OUTPUT AXIS
Y- AXIS
SERVO
PICKOFF
RESOLVERS
INPUT AXIS
X- AXIS
OUTER GIMBAL
INNER GIMBAL
OUTER CASE

Fig. 2.1

A schematic representation of a single axis platform. The z-axis is the spin axis of the gyro wheel. The resolvers are not important to this discussion, but they demonstrate the means by which angular position of the shaft with respect to the outer case may be measured.

$h^i = h^i \text{ gimbal} + h^i \text{ wheel} = j^i \omega^i + h^i_s$

j^i = moment of inertia of the inner gimbal and wheel (except that, of course, the moment of inertia of the wheel does not effect the moment of inertia of the gimbal system about the axis parallel to the wheel spin axis)

$$j^i = \begin{bmatrix} J_{11} & 0 & 0 \\ 0 & J_{22} & 0 \\ 0 & 0 & J_{33} \end{bmatrix}^i$$

Ω^i = total angular velocity of the outer case expressed in the inner gimbal coordinate frame

ω^i = total angular velocity of the inner gimbal expressed in the inner gimbal frame

ρ^i = angular velocity of the inner gimbal with respect to the outer case

$\omega^i = \rho^i + \Omega^i$

From an understanding of the basic behavior of gyroscopes, one knows that the spin axis of the wheel will try to aline itself with the direction of any externally applied rotation of the case. If such external rotation is about the z-axis, however, the spinning wheel cannot sense this. If the rotation is about the y-axis, no precession is possible because the servo holds the outer gimbal firmly so that the wheel is not free to precess about the x-axis. It is true that sufficient rotation of the outer gimbal about the y-axis would move the pickoff away from null as a result of the inertia of the inner gimbal. Only a small torquing signal from the servo is required to overcome this. Such an effect is insignificant.

If, on the other hand, the case is rotated about the x-axis, the wheel will precess about the y-axis so as to aline its spin vector with the case spin vector. In order to hold the pickoff at null, the servo must rotate the outer gimbal in the opposite direction from the case rotation so as to hold the x-axis shaft at a constant angular position with respect to inertial space. Let T^i represent the total torque on the inner gimbal. It is now possible to construct the basic Euler's equation of motion for the inner gimbal.

$$\overset{\circ}{h}^{i} + \tilde{\omega}^{i} h^{i} = T^{i} = \overset{\circ}{h}^{i} + \tilde{\rho}^{i} h_{s} + \tilde{\Omega}^{i} h_{s} + \tilde{\omega}^{i} J^{i} \omega^{i} \qquad (2.1)$$

But,

$$\overset{\circ}{h}^{i} = J^{i} \overset{\circ}{\omega}^{i} \qquad (2.2)$$

The small circle indicates derivative with respect to the specific coordinate frame.

Equation (2.1) may be rewritten using Eq. (2.2) and the basic definitions.

$$\begin{bmatrix} J_{11} & 0 & 0 \\ 0 & J_{22} & 0 \\ 0 & 0 & J_{33} \end{bmatrix}^{i} \begin{bmatrix} \overset{\circ}{\omega}_{x} \\ \overset{\circ}{\omega}_{y} \\ \overset{\circ}{\omega}_{z} \end{bmatrix}^{i} + \begin{bmatrix} 0 & -\rho_{z} & \rho_{z} \\ \rho_{z} & 0 & -\rho_{x} \\ -\rho_{z} & \rho_{x} & 0 \end{bmatrix} \begin{bmatrix} 0 \\ 0 \\ h_{s} \end{bmatrix}^{i}$$

$$+ \begin{bmatrix} 0 & -\Omega_{z} & \Omega_{z} \\ \Omega_{z} & 0 & -\Omega_{x} \\ -\Omega_{z} & \Omega_{x} & 0 \end{bmatrix}^{i} \begin{bmatrix} 0 \\ 0 \\ h_{s} \end{bmatrix}^{i} + \begin{bmatrix} 0 & -\omega_{z} & \omega_{z} \\ \omega_{z} & 0 & -\omega_{x} \\ -\omega_{z} & \omega_{x} & 0 \end{bmatrix}^{i} \begin{bmatrix} J_{11} & 0 & 0 \\ 0 & J_{22} & 0 \\ 0 & 0 & J_{33} \end{bmatrix} \begin{bmatrix} \omega_{x} \\ \omega_{y} \\ \omega_{z} \end{bmatrix}^{i}$$

$$= \begin{bmatrix} T_{x} \\ 0 \\ T_{z} \end{bmatrix}^{i} \qquad (2.3)$$

which reduces to

$$\begin{bmatrix} J_{11}\ \dot{\omega}_x \\ J_{22}\ \dot{\omega}_y \\ J_{33}\ \dot{\omega}_z \end{bmatrix}^i + \begin{bmatrix} \rho_z h_s \\ -\rho_x h_s \\ 0 \end{bmatrix}^i + \begin{bmatrix} \Omega_z h_s \\ -\Omega_x h_s \\ 0 \end{bmatrix}^i + \begin{bmatrix} \omega_z\ \omega_z (J_{33}-J_{22}) \\ \omega_z\ \omega_x (J_{11}-J_{33}) \\ \omega_z\ \omega_x (J_{22}-J_{11}) \end{bmatrix}^i$$

$$= \begin{bmatrix} T_x \\ 0 \\ T_z \end{bmatrix}^i \qquad (2.4)$$

The first and third rows of matrix Eq. (2.4) are not of primary concern. The components T_x and T_z of total torque are transmitted to the outer gimbal. Since the outer gimbal is servo controlled, it can and will sustain any torques required to satisfy the desired control conditions. The second row represents the summation of torques about the y-axis. No torques may be transmitted to the outer gimbal about the y-axis because there is a free bearing on this axis. Hence the servo control must sense the pickoff angle and rotate the x-axis in proper fashion to precess the gyroscope back to pickoff null. For convenience, the second row of Eq. (2.4) is displayed again.

$$\frac{J_{22}\ \dot{\omega}_y}{h_s} + \frac{\omega_x\ \omega_z}{h_s}\ (J_{11} - J_{33}) = \rho_x + \Omega_x \qquad (2.5)$$

Under ideal conditions, J_{11} and J_{33} are made equal so that the second term is identically zero. The Ω_x term represents the component of case rotation along the x-axis of the inner gimbal. When the pickoff angle is zero, the x-axis of the inner gimbal is coincident with the x-axis of the outer gimbal and the outer case. In order to maintain the pickoff angle at zero, $\dot{\omega}_y$ must be maintained at zero. This is accomplished through the mechanism of the servo controller driving the outer gimbal x-axis at an angular velocity equal to $-\Omega_x$, (i.e., $\rho_x = -\Omega_x$). This only reiterates what has been said before. The servo must rotate the outer gimbal in the opposite direction from the case rotation about the case x-axis.

It is apparent then that the x-axis of the outer gimbal (under ideal circumstances) does not rotate in inertial space, even though the case to which it is mounted may rotate. As an extension of this process, one can envision three such gyroscopes mounted on a common platform in such a way that their input axes are mutually orthogonal. In this way the platform could be held fixed in attitude with respect to inertial space.

2.2 Vibration; Kinematic Drift

It is instructive to examine the behavior of the single axis gyroscope when there is a small pickoff angle. For this purpose, let the pickoff angle be defined as θ. Further, let W be the total angular velocity of the outer gimbal in Fig. 2.1, expressed in terms of the outer gimbal coordinate system. The angular velocity of the inner gimbal may be expressed in terms of W, θ, and $\dot{\theta}$,

$$\left.\begin{array}{l}\omega_x \approx W_x - W_z\theta \\ \omega_y \approx W_y + \dot{\theta} \\ \omega_z \approx W_z + W_x\theta \\ \dot{\omega}_y = \dot{W}_y + \ddot{\theta}\end{array}\right] \qquad (2.6)$$

where derivatives of θ and W are taken with respect to their respective coordinate frames. By substitution of Eq. (2.6) into Eq. (2.5), the following expression may be obtained.

$$\frac{J_{22}}{h_s}(\dot{W}_z + \ddot{\theta}) + \frac{W_xW_z - W_z^{\,2}\,\theta + W_x^{\,2}\,\theta - W_xW_z\,\theta^2}{h_s}(J_{11} - J_{33}) = W_x - W_z\,\theta \qquad (2.7)$$

Usually $(J_{11} - J_{33})$ can be safely assumed to be equal to zero. However, this term should be kept in mind; because if it is non-zero, it can result in rectification of rotary vibration. This is apparent because products of components of W as well as the squares of W components appear as coefficients. Assuming the term to be zero results in a simplification.

$$W_x = \frac{J_{22}}{h_s}\dot{W}_y + \frac{J_{22}}{h_s}\ddot{\theta} + W_z\,\theta \qquad (2.8)$$

It is well to mention once again that the desired condition is that W_x, the true inertial rotation of the outer gimbal about the x-axis, be equal to zero. The right hand terms of Eq. (2.8) constitute error terms. The average value of $\ddot{\theta}$ is zero so this term cannot contribute to any average error. The $\dot{W}_y$ term will, in general, have zero mean though this is not necessarily true in all situations. Of more direct concern is the $W_z\,\theta$ term.

The servo controller functions to hold θ equal to zero, but if the outer case is subject to vibrations at a frequency above the pass band of the servo, θ will not be held to zero. Let it be assumed that friction and spring force on the inner gimbal are negligible (indeed they have been assumed so thus far). As an approach toward the worst possible behavior, a function for θ may be obtained from Eq. (2.8) by assuming that $W_z\,\theta$ can be dropped.

$$\left.\begin{aligned} \frac{h_s}{J_{22}} W_x - \mathring{W}_y &= \ddot{\theta} \\ \theta &= \iint \left(\frac{h_s}{J_{22}} W_x - \mathring{W}_y \right) dt^2 \end{aligned}\right] \qquad (2.9)$$

This worst case function can be used to evaluate the $W_z\,\theta$ error term in Eq. (2.8).

$$W_z\,\theta = W_z \iint \frac{h_s}{J_{22}} W_x\, dt^2 - W_z \int W_z\, dt \qquad (2.10)$$

Consider the case where the disturbing vibration is located midway between the x, y, and z reference directions. The component of this vibration on each axis may be described as

$$\int W_x\, dt = \int W_z\, dt = \int W_z\, dt = A \sin \Omega\, t \qquad (2.11)$$

Equation (2.10) now becomes

$$W_z \, \theta \; = \; - \frac{A^2 \, h_s}{J_{22}} (\cos\Omega t)^2 - A^2 \Omega \cos\Omega t \sin\Omega t \qquad (2.12)$$

The last term on the right is not important except under conditions where there is a phase difference between the driving rotary vibration and the oscillatory response of θ. Unfortunately such a situation would not be uncommon. The first term on the right obviously rectifies rotary vibration and has an average value of

$$\frac{h_s \, A^2}{2J_{22}}$$

This corresponds to a drift rate resulting from unfortunately phased rotary vibration.

On the other hand, it should be noted that the term which is definitely undesirable involves W_x. But the vibrational frequency under consideration is above the pass band of the servo. If the inertia of the servo drive does not restrain the x-axis shaft, then the freedom of the bearing and inertia of the gimbal assembly will provide partial isolation from rotation about the x-axis.

The discussion thus far has concerned itself with rotary vibration. Translational vibration can be damaging to accuracy also. The gimbals and wheel of the gyroscope are designed with great care so that the mass of each is symmetrically distributed about each axis around which that element or collection of elements is free to rotate. Any pendulous mass will produce a torque in the presence of translational vibration. Through this mechanism, translational vibration may be converted into rotational vibration with the possibility of creating some non-zero-mean gyro-drift error.

The study of instrument response to vibration is a very detailed problem. It is closely associated with the actual design and construction of the particular instrument and the environment in which it is used.

2.3 The Gyroscope Error Model

From a practical viewpoint, gyroscope errors may be characterized by the following error equation.

$$\dot{\phi}_x' = \beta_y \dot{\phi}_z + \beta_z \dot{\phi}_y + P_1 A_x + P_2 A_y + P_3 A_z + P_{11} A_x^2$$

$$+ P_{12} A_x A_y + P_{13} A_x A_z + P_{22} A_y^2 + P_{23} A_y A_z = P_{33} A_z^2$$

$$+ \eta + T \dot{\theta}_x + \dots \qquad (2.13)$$

where

$\dot{\phi}_x'$ = gyro drift (i.e., error)

β_y and β_z = misalinement of the input axis as described by small rotations about the y and z axes

A_x, A_y, and A_z are the orthogonalized components of total sensed acceleration

$\dot{\phi}_y$ and $\dot{\phi}_z$ = rotation rates of the case about the y and z axes

η = random drift of the instrument

P = instrument error parameters

$\dot{\theta}$ = input axis rate commanded by any external torquing signal

T = torquing scale factor error

The β misalinement angles are really alinement errors. They represent errors in positioning of the input axis at the time the gyroscope is mounted in the vehicle or platform.

The torquing scale factor error applies only to rotation of the input axis in response to external commands. It is not applicable to closed loop servo control represented in Eq. (2.5). In that instance sufficient torque will be generated to drive the pickoff to null because of the feedback.

Equation (2.13) might be extended to include higher order P terms, but this is usually not done. In fact, Eq. (2.13) includes terms in excess of the number usually found to be significant. The number of which are significant depends upon the type and design of the instrument and its intended use. The β, P, η, and T parameters are obtained empirically. In most cases theoretical justification for their existence may be found. Parameter values may be obtained from experimentation on each individual instrument, or they may be inferred statistically for the ensemble through experiments performed on a random sample. In the first instance, the actual value is obtained for the instrument, with a rms measurement error. In the second instance, there is still an rms measurement error as well as the individual instruments deviation from the mean for the ensemble.

There are two possible ways of dealing with the error parameters which apply regardless of the measurement technique. If the parameter has a non-zero mean, corrections may be made in the on-board navigation computations, but need not be. If they are not, then a deterministic error in the output of the instrument will result. If the parameter has zero mean, then, of course, corrections are uncalled for. In either case, the rms variation from the mean, which may be caused by measurement error or parameter shift since measurement, cannot be compensated by on-board means. In most cases, significant error parameters will be compensated in one way or another so that the error analysis for the instrument deals solely with rms values for the β, P, and T parameters. A suitable error model for a typical single axis gyroscope might include only the misalinement terms, η, P_1, P_2, P_3, and P_{13}.

When dealing with the two-axis gyro, Eq. (2.13) must be repeated for the other input axis. In this case there will likely be correlation between similar parameters for the two axes.

A gyroscope may not be mounted on a platform (either single axis or three axis), for some applications but may be affixed firmly to the vehicle. The outer case and associated servo control system depicted in Fig. 2.1 would then be absent. The outer gimbal would be mounted directly to the body of the vehicle. Now, unless some means is found to apply torque to the inner gimbal, the gyro wheel will precess away from pickoff null. The required torque is usually supplied by electric induction. The servo system of Fig. 2.1 is replaced by another one which applies torque directly to the inner gimbal (now the only gimbal). Measurement of the torquing current required to maintain the gyro at pickoff null gives an exact indication of the angular rotation of the vehicle about the gyro input axis. The error equation for the strapdown gyro would be identical to Eq. (2.13). Conceptually, the problem is not much different from the single axis platform case.

3. Accelerometers

Accelerometers are devices which measure vehicular acceleration with respect to inertial space as well as gravitational acceleration. Indeed, the instrument cannot differentiate between the two types of acceleration. The sum of the two may be referred to as sensed acceleration.

The error model for an accelerometer may be expressed in general form as follows

$$\begin{aligned} A_x' = {} & A_x + \beta_y A_z + \beta_z A_y + F_1 A_x + F_2 A_y + F_3 A_z \\ & + F_{11} A_x^2 + F_{12} A_x A_y + F_{13} A_x A_z + F_{22} A_y^2 + F_{23} A_y A_z \\ & + F_{33} A_z^2 + N + B + \dots \end{aligned} \tag{3.1}$$

where

A_x' is the accelerometer output

A_x = the desired measurable (sensed acceleration along the input axis)

β_y and β_z represent misalinement of the input axis described as small rotations about the y and z axes

A_x, A_y, and A_z are the orthogonalized components of total sensed acceleration, of which A_x is the quantity being measured.

F_1, F_2, etc., are constants peculiar to the particular instrument

N = random noise

B = bias

The equation could be continued to higher order F terms, but this is seldom required.

The previous discussion of gyroscope parameters is directly applicable to accelerometers. The β misalinement terms refer to inaccuracy in orientation of the input axis and not anything inherent to the accelerometer. They are similar in nature to F_2 and F_3, which are peculiar to the nature of the instrument. It is possible to calibrate the accelerometers after assembly if used on an inertial platform. By this means the misalinement errors may be reduced to an rms residual measurement (or calibration) error. Such calibration after mounting will be employed only where high accuracy is essential. Measurement of instrument errors and calibration of instruments before and after mounting are normal practices in the inertial guidance industry and are in no way peculiar to gyrocompassing. Consequently they will not be covered in greater detail.

The generality of Eq. (3.1) makes it applicable to any sort of accelerometer. Perhaps the most common instrument available today is the PIGA (Pendulous Integrating Gyro Accelerometer). In this case Fig. (3.1) may be used to describe more clearly the significance of each of the F parameters in terms of input, output, and spin axes.

A typical error model for a PIGA would include the F_1 and F_3 coefficients, bias, noise, and the misalinement terms. This is the model which will be employed in this document. Because the PIGA is basically a single axis platform with a pendulous mass added to the spin axis, it is sensitive to rotations about the input axis. Whether platform-mounted or body-mounted, the output of the PIGA's must be corrected for rotation of their input axes. This poses no real problem since rotational information is available. The gyroscopes measure the rotation of a strapdown system. In the case of the inertial platform system, the platform remains inertially fixed in attitude unless commanded to rotate by an external torquing signal which is known or can be measured.

Because the PIGA is basically a single axis platform, it may be subject to the rotational vibration errors discussed in Section 2.2. The error model given by Eq. (3.1) also indicates that rectification of translational vibration is possible. Any terms involving products of acceleration components or squares of single components will produce rectification errors. Again, unfortunately, evaluation of the extent to which vibration will perturb the system is an involved process closely associated with the peculiarities of the particular instruments being used.

4. Gravity Gradient Attitude Detection

4.1 Principles of Operation

Orbiting vehicles or vehicles that are in free fall, i.e., whose center of mass O is in free fall, sustain an acceleration at point O that is equal to the gravity field value at O

$$\ddot{\underline{R}}_o - \underline{G}_o = \underline{0}$$

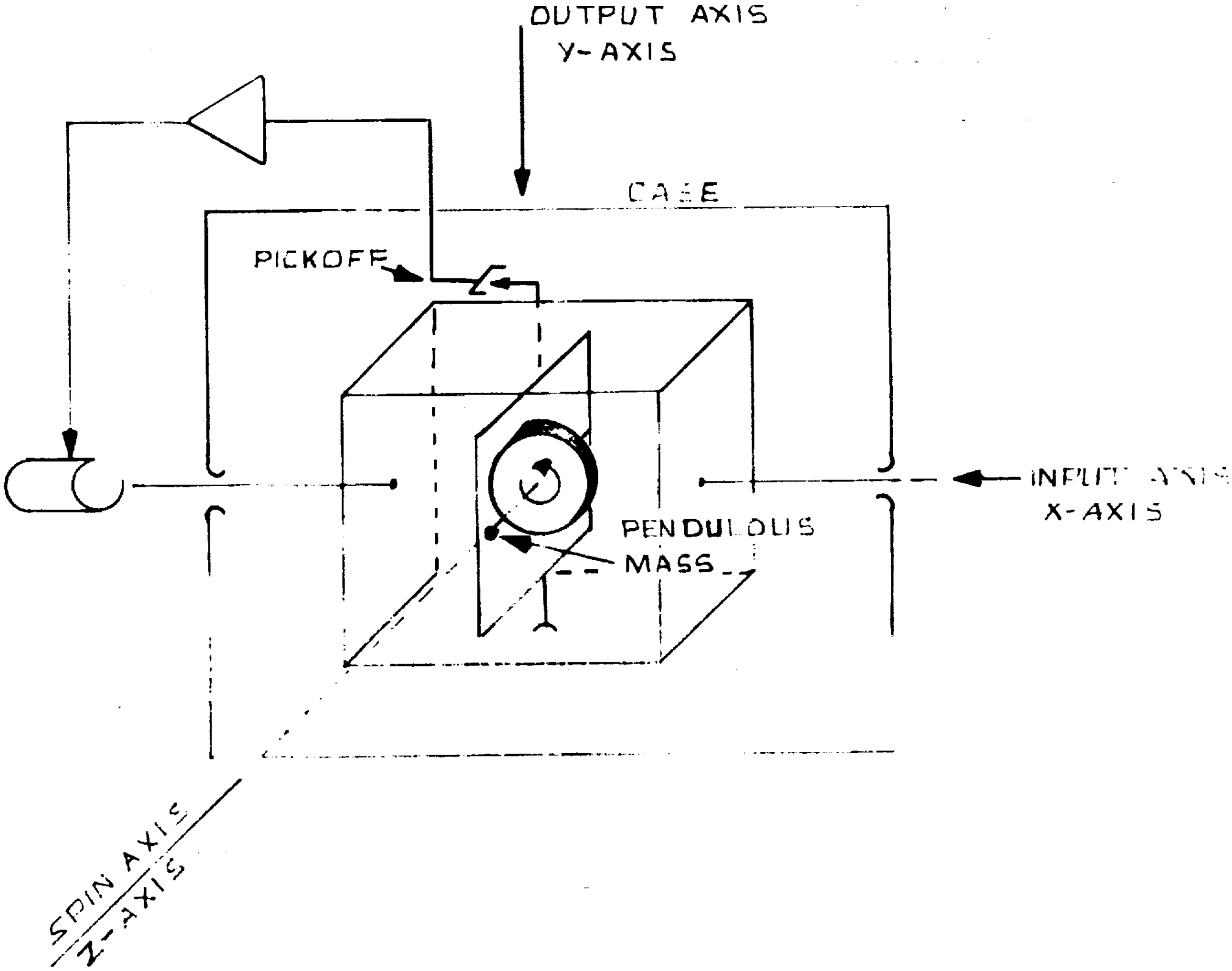
OUTPUT AXIS
Y-AXIS
CASE
PICKOFF
INPUT AXIS
X-AXIS
PENDULOUS
MASS
SPIN AXIS
Z-AXIS

Fig. 3.1

Schematic diagram of a Pendulous Mass Integrating Gyro Accelerometer showing the x, y, and z axis notation.

An accelerometer at a nearby point, whose acceleration with respect to O is structurally constrained to be $\ddot{\underline{r}}$ and which has an increment of gravity $\Delta\underline{g}$ due to being removed from point O, will measure

$$\ddot{\underline{A}} = (\ddot{\underline{R}}_0 + \ddot{\underline{r}}) - (\underline{G}_0 + \Delta\underline{g}) = \ddot{\underline{r}} - \Delta\underline{g}$$

If the vehicle is rigid and not rotating, $\ddot{\underline{r}} = \underline{0}$, and such an accelerometer measures only the desired gravitational difference $- \Delta\underline{g} = \underline{\underline{\phi}} \cdot \underline{r}$, where $\underline{\phi}$ is the gravity gradient tensor.

It remains to be shown how accelerometers should be arranged so that the gravity gradient principle may be profitably employed to indicate vehicle attitude. In order to do this, it becomes necessary to recognize that the gravity gradient has nine components; i.e., it is a tensor of rank 2 being made up of all possible partial derivatives of the gravity vector with respect to the position vector. With this in mind, it is possible to state that the vehicle attitude can be represented by that transformation matrix which diagonalizes the gravity gradient tensor, namely that transformation matrix which relates the eigenvectors of the gravity gradient tensor to the principal axes of the vehicle. The mechanization associated with this definition can be simplified considerably if one realizes that for gyrocompassing-in-orbit, it is desirable to indicate the attitude tilt deviation from null rather than the total attitude. There are two possible such mechanizations which indicate first order sensitivity to tilt. For simplicity only the inverse square central force field is assumed. Two coordinate systems are assumed: The base coordinate system and the vehicle coordinate system.

Considering the inverse square law, let the gravity vector $\underline{g}$ in the base coordinate system, denoted by unit vectors $\underline{i}$, $\underline{j}$, and $\underline{k}$ be expressed as follows

$$\underline{g} = \frac{-\mu}{(x^2 + y^2 + 3^2)^{3/2}} (\underline{i}\, x + \underline{j}\, y + \underline{k}\, z) = \underline{i}\, \underline{g} \cdot \underline{i} + \underline{j}\, \underline{g} \cdot \underline{j} + \underline{k}\, \underline{g} \cdot \underline{k},$$

$$= \underline{i}\, g_x + \underline{j}\, g_y + \underline{k}\, g_z \tag{4.1}$$

where $\underline{i}\, x + \underline{j}\, y + \underline{k}\, z$ is the vehicle location relative to the force center, and the force center is located at the origin of the coordinate axes.

The vehicle axes, denoted by $\underline{i}'$, $\underline{j}'$, and $\underline{k}'$ are related by an orthogonal transformation T to $\underline{i}$, $\underline{j}$, and $\underline{k}$, as follows

$$\begin{bmatrix} \underline{i}' \\ \underline{j}' \\ \underline{i}' \end{bmatrix} = \begin{bmatrix} \underline{i}'\cdot\underline{i} & \underline{i}'\cdot\underline{j} & \underline{i}'\cdot\underline{k} \\ \underline{j}'\cdot\underline{i} & \underline{j}'\cdot\underline{j} & \underline{j}'\cdot\underline{k} \\ \underline{i}'\cdot\underline{i} & \underline{k}'\cdot\underline{j} & \underline{k}'\cdot\underline{k} \end{bmatrix} \begin{bmatrix} \underline{i} \\ \underline{j} \\ \underline{k} \end{bmatrix} = T \begin{bmatrix} \underline{i} \\ \underline{j} \\ \underline{k} \end{bmatrix} \tag{4.2}$$

First, it becomes necessary to obtain $\underline{g}$ in vehicle coordinates; that is to find $\underline{i}'\underline{g}\cdot\underline{i}' + \underline{j}'\underline{g}\cdot\underline{j}' + \underline{k}'\underline{g}\cdot\underline{k}'$ from Eq. (4.2) and (4.1)

$$\left.\begin{aligned} g\cdot\underline{i}' &= (g\cdot\underline{i}\,\underline{i} + g\cdot\underline{j}\,\underline{j} + g\cdot\underline{k}\,\underline{k})\cdot(\underline{i}'\cdot\underline{i}\,\underline{i} + \underline{i}'\cdot\underline{j}\,\underline{j} + \underline{i}'\cdot\underline{k}\,\underline{k}) \\ &= (g\cdot\underline{i})\underline{i}'\cdot\underline{i} + (g\cdot\underline{j})\underline{i}'\cdot\underline{j} + (g\cdot\underline{k})\underline{i}'\cdot\underline{k} \\ \text{Similarly,}\quad g\cdot\underline{j}' &= (g\cdot\underline{i})\underline{j}'\cdot\underline{i} + (g\cdot\underline{j})\underline{j}'\cdot\underline{j} + (g\cdot\underline{k})\underline{j}'\cdot\underline{k} \\ \text{and}\quad g\cdot\underline{k}' &= (g\cdot\underline{i})\underline{k}'\cdot\underline{i} + (g\cdot\underline{j})\underline{k}'\cdot\underline{j} + (g\cdot\underline{k})\underline{k}'\cdot\underline{k} \end{aligned}\right\} \tag{4.3}$$

or, in matrix form

$$\left.\begin{aligned} \begin{bmatrix} g_{x'} \\ g_{y'} \\ g_{z'} \end{bmatrix} = \begin{bmatrix} g\cdot\underline{i}' \\ g\cdot\underline{j}' \\ g\cdot\underline{k}' \end{bmatrix} &= \begin{bmatrix} \underline{i}'\cdot\underline{i} & \underline{i}'\cdot\underline{j} & \underline{i}'\cdot\underline{k} \\ \underline{j}'\cdot\underline{i} & \underline{j}'\cdot\underline{i} & \underline{j}'\cdot\underline{j} \\ \underline{k}'\cdot\underline{i} & \underline{k}'\cdot\underline{j} & \underline{k}'\cdot\underline{k} \end{bmatrix} \begin{bmatrix} g\cdot\underline{i} \\ g\cdot\underline{j} \\ g\cdot\underline{k} \end{bmatrix} \\ &= T \begin{bmatrix} g\cdot\underline{i}' \\ g\cdot\underline{j}' \\ g\cdot\underline{k}' \end{bmatrix} = T \begin{bmatrix} g_x \\ g_x \\ g_x \end{bmatrix} \end{aligned}\right\} \tag{4.4}$$

The position vector $\underline{i}x + \underline{j}y + \underline{k}z = \underline{r}$ can be projected along vehicle coordinates axes as follows

$$\begin{bmatrix} x' \\ y' \\ z' \end{bmatrix} = \begin{bmatrix} \underline{r}\cdot\underline{i}' \\ \underline{r}\cdot\underline{j}' \\ \underline{r}\cdot\underline{k}' \end{bmatrix} = \begin{bmatrix} x\underline{i}'\cdot\underline{i} & + & y\underline{i}'\cdot\underline{j} & + & z\underline{i}'\cdot\underline{k} \\ x\underline{j}'\cdot\underline{i} & + & y\underline{j}'\cdot\underline{j} & + & z\underline{j}'\cdot\underline{k} \\ x\underline{k}'\cdot\underline{i} & + & y\underline{k}'\cdot\underline{j} & + & z\underline{k}'\cdot\underline{k} \end{bmatrix}$$

$$= T \begin{bmatrix} \underline{r}\cdot\underline{i} \\ \underline{r}\cdot\underline{j} \\ \underline{r}\cdot\underline{k} \end{bmatrix} = T \begin{bmatrix} x \\ y \\ z \end{bmatrix} \tag{4.5}$$

The inverse of T is the transposed matrix T^T, since T is orthogonal. Hence Eq. (4.5) inverts to the following with an added convenient redefinition of T stated as well

$$\begin{bmatrix} x \\ y \\ z \end{bmatrix} = T^T \begin{bmatrix} x' \\ y' \\ z' \end{bmatrix} = \begin{bmatrix} \frac{\partial x}{\partial x'} & \frac{\partial x}{\partial y'} & \frac{\partial x}{\partial z'} \\ \frac{\partial y}{\partial x'} & \frac{\partial y}{\partial y'} & \frac{\partial y}{\partial z'} \\ \frac{\partial z}{\partial x'} & \frac{\partial z}{\partial y'} & \frac{\partial z}{\partial z'} \end{bmatrix} \begin{bmatrix} x' \\ y' \\ z' \end{bmatrix} \tag{4.6}$$

From the rules of partial differentiation for cascaded variables

$$\frac{\partial g_{x'}}{\partial x'} = \frac{\partial g_{x'}}{\partial x}\frac{\partial x}{\partial x'} + \frac{\partial g_{x'}}{\partial y}\frac{\partial y}{\partial x'} + \frac{\partial g_{x'}}{\partial z}\frac{\partial z}{\partial x'} \tag{4.7}$$

Applying this same pattern of differentiation to all nine partial derivatives of the three components of $\underline{g}$ with respect to the three components of $\underline{r}$ (the gravity gradient tensor), one obtains

$$\begin{bmatrix} \frac{\partial g_{x'}}{\partial x'} & \frac{\partial g_{y'}}{\partial x'} & \frac{\partial g_{z'}}{\partial x'} \\ \frac{\partial g_{x'}}{\partial y'} & \frac{\partial g_{y'}}{\partial y'} & \frac{\partial g_{z'}}{\partial y'} \\ \frac{\partial g_{x'}}{\partial z'} & \frac{\partial g_{y'}}{\partial z'} & \frac{\partial g_{z'}}{\partial z'} \end{bmatrix} = \begin{bmatrix} \frac{\partial x}{\partial x'} & \frac{\partial y}{\partial x'} & \frac{\partial z}{\partial x'} \\ \frac{\partial x}{\partial y'} & \frac{\partial y}{\partial y'} & \frac{\partial z}{\partial y'} \\ \frac{\partial x}{\partial z'} & \frac{\partial y}{\partial z'} & \frac{\partial z}{\partial z'} \end{bmatrix} \begin{bmatrix} \frac{\partial g_{x'}}{\partial x} & \frac{\partial g_{y'}}{\partial x} & \frac{\partial g_{z'}}{\partial x} \\ \frac{\partial g_{x'}}{\partial y} & \frac{\partial g_{y'}}{\partial y} & \frac{\partial g_{z'}}{\partial y} \\ \frac{\partial g_{x'}}{\partial z} & \frac{\partial g_{y'}}{\partial z} & \frac{\partial g_{z'}}{\partial z} \end{bmatrix} \tag{4.8}$$

and from Eq. (4.6), this is restated as

$$= T \begin{bmatrix} \frac{\partial g_{x'}}{\partial x} & \cdot & \cdot \\ \cdot & \cdot & \cdot \\ \cdot & \cdot & \frac{\partial g_{z'}}{\partial z} \end{bmatrix} \tag{4.9}$$

By transposing Eq. (4.4)

$$(g_{x'}\ g_{y'}\ g_{z'}) = (g_x\ g_y\ g_z)T^T \tag{4.10}$$

Taking $\frac{\partial}{\partial x}$ $\frac{\partial}{\partial y}$, and $\frac{\partial}{\partial z}$ of Eq. (4.3), arranging it in matrix form, and substituting in Eq. (4.9) one obtains

$$\begin{bmatrix} \frac{\partial g_{x'}}{\partial x'} & \frac{\partial g_{y'}}{\partial x'} & \frac{\partial g_{z'}}{\partial x'} \\ \frac{\partial g_{x'}}{\partial y'} & \frac{\partial g_{y'}}{\partial y'} & \frac{\partial g_{z'}}{\partial y'} \\ \frac{\partial g_{x'}}{\partial z'} & \frac{\partial g_{y'}}{\partial z'} & \frac{\partial g_{z'}}{\partial z'} \end{bmatrix} = T \begin{bmatrix} \frac{\partial g_{x}}{\partial x} & \frac{\partial g_{y}}{\partial x} & \frac{\partial g_{z}}{\partial x} \\ \frac{\partial g_{x}}{\partial y} & \frac{\partial g_{y}}{\partial y} & \frac{\partial g_{z}}{\partial y} \\ \frac{\partial g_{x}}{\partial z} & \frac{\partial g_{y}}{\partial z} & \frac{\partial g_{z}}{\partial z} \end{bmatrix} T^T \qquad (4.11)$$

The significance of Eq. (4.11) is that the gravity gradient tensor in vehicle coordinates is merely the similarity-transformed gravity gradient tensor in base coordinates. Transformation T is the vehicle attitude transformation.

The transformation T represents only a small angle approximation for gyrocompassing in orbit. Consequently, it is permissible to let

$$T = \begin{bmatrix} 1 & \phi_z & -\phi_y \\ -\phi_z & 1 & \phi_x \\ \phi_y & -\phi_x & 1 \end{bmatrix} \qquad (4.12)$$

where ϕ_x, ϕ_y, and ϕ_z are small-angle tilts.

Taking partial derivatives on Eq. (4.1), and arranging in matrix form, one obtains

$$\begin{bmatrix} \frac{\partial g_{x}}{\partial x} & \frac{\partial g_{y}}{\partial x} & \frac{\partial g_{z}}{\partial x} \\ \frac{\partial g_{x}}{\partial y} & \frac{\partial g_{y}}{\partial y} & \frac{\partial g_{z}}{\partial y} \\ \frac{\partial g_{x}}{\partial z} & \frac{\partial g_{y}}{\partial z} & \frac{\partial g_{z}}{\partial z} \end{bmatrix} = \frac{\mu}{r^5} \begin{bmatrix} -(-2x^2+y^2+z^2) & 3xy & 3xz \\ 3xy & -(x^2-2y^2+z^2) & 3yz \\ 3xz & 3yz & -(x^2+y^2-2z^2) \end{bmatrix} \qquad (4.13)$$

where $r^2 = x^2 + y^2 + z^2$. Note that this matrix is symmetric, implying mutually perpendicular eigenvectors. Selecting the base coordinates to be the local level coordinates to which it is desired to null

$$\underline{i}x + \underline{j}y + \underline{k}z = \underline{i}0 + \underline{j}0 + \underline{k}r$$

The gravity gradient tensor becomes

$$\begin{bmatrix} \frac{\partial g_x}{\partial x} & \frac{\partial g_y}{\partial x} & \frac{\partial g_z}{\partial x} \\ \frac{\partial g_x}{\partial y} & \frac{\partial g_y}{\partial y} & \frac{\partial g_z}{\partial y} \\ \frac{\partial g_x}{\partial z} & \frac{\partial g_y}{\partial z} & \frac{\partial g_z}{\partial z} \end{bmatrix} = \frac{+\mu}{r^3} \begin{bmatrix} -1 & 0 & 0 \\ 0 & -1 & 0 \\ 0 & 0 & +2 \end{bmatrix} \qquad (4.15)$$

Transforming this into vehicle coordinates, according to Eq. (4.12) and (4.11),

$$\begin{bmatrix} \frac{\partial g_{x'}}{\partial x} & \frac{\partial g_{y'}}{\partial x} & \frac{\partial g_{z'}}{\partial x} \\ \frac{\partial g_{x'}}{\partial y} & \frac{\partial g_{y'}}{\partial y} & \frac{\partial g_{z'}}{\partial y} \\ \frac{\partial g_{x'}}{\partial z} & \frac{\partial g_{y'}}{\partial z} & \frac{\partial g_{z'}}{\partial z} \end{bmatrix} = \frac{-\mu}{r^3} \begin{bmatrix} 1+\phi_z^2+2\phi_y^2 & -2\phi_y\phi_x & 3\phi_y-\phi_z\phi_x \\ 2\phi_y\phi_x & 1+\phi_z^2-2\phi_x^2 & -3\phi_x-\phi_y\phi_z \\ 3\phi_y-\phi_x\phi_z & -3\phi_x-\phi_y\phi_z & -2+\phi_x^2+\phi_y^2 \end{bmatrix}$$

(4.16)

Neglecting all ϕ terms of power 2 (a valid assumption for small angles) results in the following very simple gravity gradient tensor as a function of tilt

$$\begin{bmatrix} \frac{\partial g_{x'}}{\partial x} & \frac{\partial g_{y'}}{\partial x} & \frac{\partial g_{z'}}{\partial x} \\ \frac{\partial g_{x'}}{\partial y} & \frac{\partial g_{y'}}{\partial y} & \frac{\partial g_{z'}}{\partial y} \\ \frac{\partial g_{x'}}{\partial z} & \frac{\partial g_{y'}}{\partial z} & \frac{\partial g_{z'}}{\partial z} \end{bmatrix} = \frac{-\mu}{r^3} \begin{bmatrix} 1 & 0 & 3\phi_y \\ 0 & 1 & -3\phi_x \\ 3\phi_y & -3\phi_x & -2 \end{bmatrix} \qquad (4.17)$$

One sees that only the following four gravity gradient expressions are functions of tilt in the tensor Eq. (4.17)

$$\frac{\partial g_{z'}}{\partial x'} = \frac{\partial g_{x'}}{\partial z'} = \frac{-3\phi_y \mu}{r^3} \qquad (4.18)$$

and

$$\frac{\partial g_{z'}}{\partial y'} = \frac{\partial g_{y'}}{\partial z'} = \frac{+3\phi_x \mu}{r^3} \qquad (4.19)$$

Based on the above expressions, one can mechanize approximately for tilt angle ϕ_y by placing accelerometers in either of two ways as shown in Figs. 4.1 and 4.2.

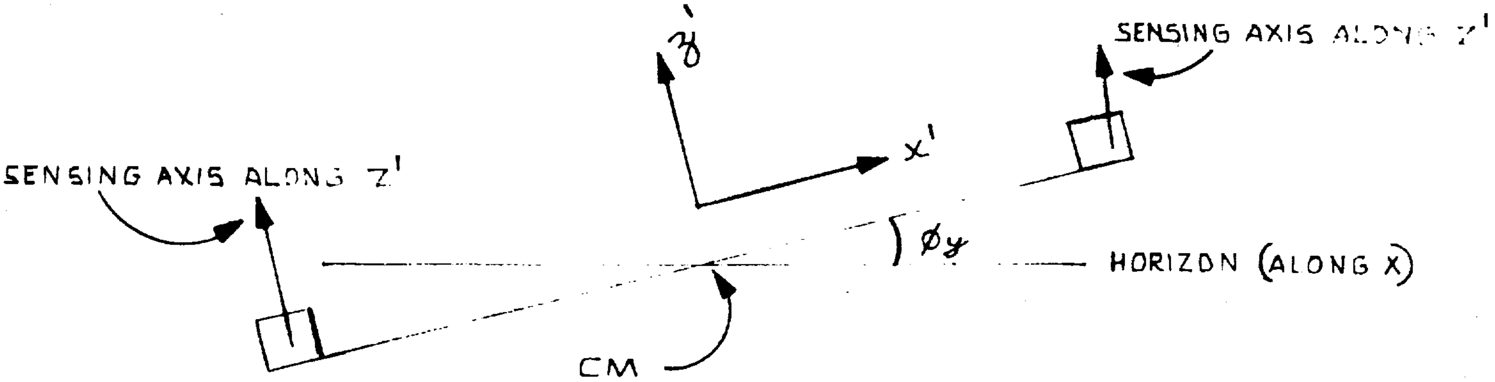

Fig. 4.1

for $\frac{\partial g_{z'}}{\partial x'}$

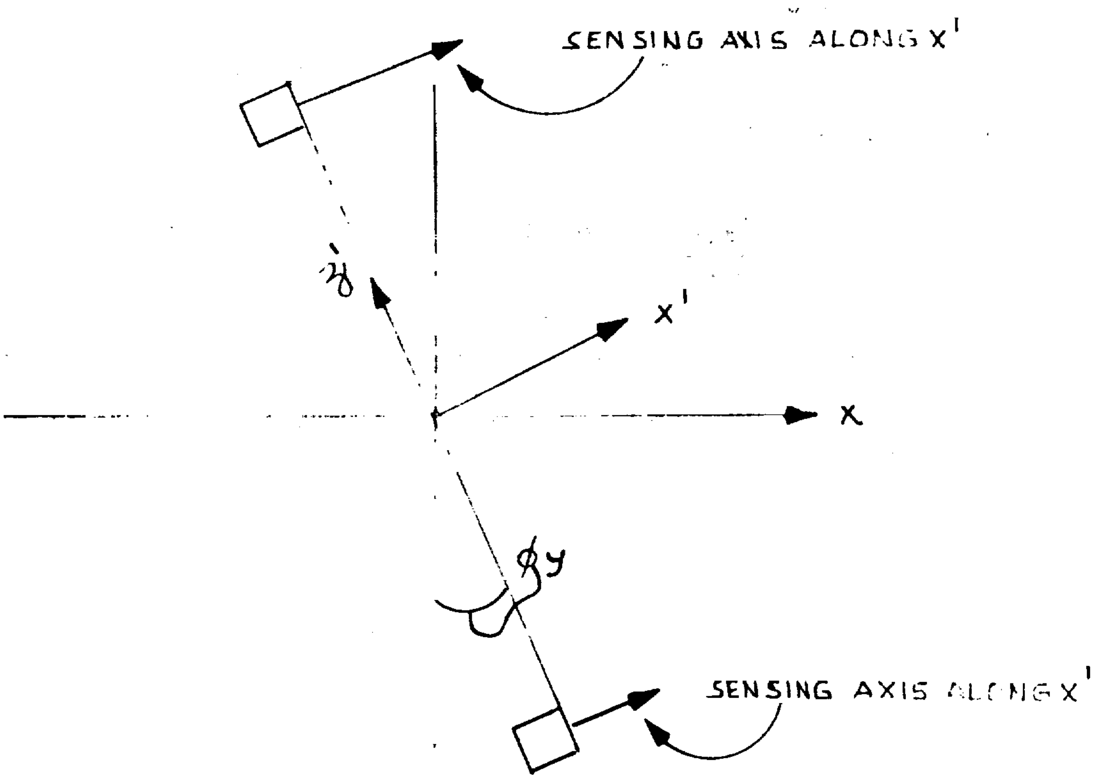

Fig. 4.2

for $\frac{\partial g_{x'}}{\partial z'}$

According to some investigators, it is possible to continually rotate an accelerometer with the sensing axis tangential to the circle of rotation. This produces a sinusoidal output[1], which can be resolved back to determine ϕ_x and ϕ_y. In this case, T is a sinusoidal time-varying transformation and the resulting

$$\frac{\partial g_{x'}}{\partial z'} \quad \text{or} \quad \frac{\partial g_{y'}}{\partial z'}$$

terms vary sinusoidally. This approach provides the capability of separating inertial and gravitational accelerations as well as avoiding the requirement for accelerometer matching.

---

[1] Diesel, John W., "A New Approach to Gravitational Gradient Determination of the Vertical", AIAA Journal Vol. 2, No. 7, July 1964.

4.2 Practical Prospects

Accelerometer performance or moment arm length may be specified on the basis of acceptable tilt performance through the use of the following equations

$$\frac{\partial g_{z'}}{\partial x'} = \frac{3\phi_y \mu}{r^3} \qquad (4.20)$$

in accordance with Eq. (4.15) or (4.16). Gyrocompassing in orbit requires consideration of the two possible extremes: low altitude orbits and synchronous orbits. For low altitude orbits it is appropriate to consider a tilt error due to threshold accelerometer error of not more than 1 min, which is about 0.3 mr. At sea level

$$\frac{\mu}{r_o^2} = g_o \quad \text{or} \quad \mu = g_o r_o^2 \qquad (4.21)$$

Hence,

$$\frac{\partial g_{z'}}{\partial x} = 3\phi_y \frac{g_o r_o^2}{r^3} \qquad (4.22)$$

Assuming r_o = 6370 km and r = 6700 km, one obtains a threshold gravity gradient measurement of

$$\frac{g_{z'}}{x'} = g_o \cdot \frac{3 \times 0.3 \times 10^{-3}}{6700 \text{ km}} \times {\frac{6.37}{6.7}}^{2} \text{ g's/km} \qquad (4.23)$$

$$= 1.35 \times 10^{-7} \text{ g's/km for a 1 min tilt}$$

Threshold sensitivities lower than 10^{-6} g's are rare in accelerometer state-of-the-art development. Consequently, one would have to mount such an accelerometer at a moment arm of at least

$$dx = \frac{dg_{z'}}{1.35 \times 10^{-7}} \text{ km} = \frac{10^{-6}}{1.35 \times 10^{-7}} = 7.4 \text{ km} \qquad (4.24)$$

Considering practical accelerometers, with 10^{-5}g sensitivity, the moment arm would have to be ten times this length or 74 km. Clearly orbiting structures of this magnitude are not practical. Until accelerometers of two to three orders of magnitude finer sensitivity are built (and can be suitably ground-tested), the accelerometer-measured attitude method will not be applicable to gyrocompassing in orbit. When such devices do become available, noise problems due to structural accelerations will still have to be dealt with as indicated in Ref. A. At the synchronous altitude, assuming a requirement for 0.1 min in tilt, one would require a boom of 20,000 km for a threshold sensitivity of 10^{-6}g's, which is even more far fetched.

Because the accelerometers are tangentially oriented, any vehicle attitude control torques will seriously disturb the instruments, further compounding the difficulty. The need for rotational isolation arises, and the method of Ref. A serves to eliminate this.

5. Horizon Sensor

The Close-Body Optical Sensor, more commonly known as the Horizon Sensor, has great promise of playing a key role in orbital gyrocompassing. It is used, by definition, with those orbits which closely graze the surface of the planet, and consequently provide the largest angular rate of the vertical. The characteristic is most desirable for effective gyrocompassing. At the present, the horizon sensor is the only device which has the capability of sharply defining the vertical direction to the orbiting craft. It is not burdened by the inherent angular momentum coupling of stabilization techniques utilizing gravity gradient, and it does not require the extreme sensitivity of the gravity gradient sensing devices. On the other hand, depending on the planet sensed, the horizon sensor has phenomenological limitations, which have been dealt with to varying degrees of success and continue to interest various investigators.

The key feature to keep in mind when dealing with horizon sensors is their role in orbital gyrocompassing. In the literature, horizon scanners are generally treated from the standpoint of their ability to detect the position of the vertical, i.e., the static ability. However, when gyrocompassing is contemplated, both the static and the dynamic performance need to be taken into account. According to R. Gordon[1], the azimuth error is related to the sensed roll error by the following equation in Laplace transform notation

$$\psi(s) = \frac{(sK_B - K_A\Omega)\phi(s)}{-[s^2 + sK_A + \Omega(\Omega + K_B)]} \tag{5.1}$$

---

[1] AIAA Paper No. 64-238, "An Orbital Gyrocompass Heading Reference for Satellite Vehicles", by Robert Gordon

where

ψ = Azimuth error

K_A = Horizon sensor to roll axis gain

K_B = Horizon sensor to azimuth axis gain

Ω = Orbital angular rate

$\phi(s)$ = Roll error

It is assumed that gyrocompassing is performed by coupling the horizon sensor to a nominally level gimballed platform; feeding the horizon sensor outputs to the leveling gyros; and feeding the horizon sensor roll output to the azimuth gyro as well.

According to Gordon[1], gains K_A and K_B are set at 5 rad/hr and 2.25 rad/hr to give well behaved responses to a wide variety of input error sources. The value of Ω is typically 4 rad/hr, for close earth orbit. Assuming a steady state response Eq. (5.1) reduces to

$$\psi = \frac{K_A}{\Omega + K_B} \quad \phi \cong 0.8\,\phi \tag{5.2}$$

Assuming this type of mechanization, one can state, as a rule of thumb, that the azimuth error is roughly equal to the roll error for orbital gyrocompassing at low altitudes. The gain relations can probably be adjusted to provide similar results for gyrocompassing in orbit about the moon and other planets. Gordon believes it should be possible to obtain an azimuth error of 1.08 min with compensation for oblateness, instrument error, latitude, season, and diurnal variation. The largest uncompensatable error source seems to be diurnal variation, and the resulting instrument compensation error. These amount to .55 and .75 min respectively. Present hardware has not achieved this type of performance, but the theoretical analysis indicates potential for the future.

F. Singer[2] reports that according to D. Q. Wark and J. Alishouse of the U.S. Weather Bureau, the sharpest, cleanest horizon is seen as filtered radiance in the carbon dioxide band at 15 micron wavelength. This is an infra-red wavelength which also minimizes sensitivity to solar radiation interference. Furthermore, the horizon provided by the 15 micron band is invariant with day or night, eliminating the need for terminator compensation and the resulting special scanning techniques. Mars will pose problems since it has only a weak atmosphere resulting in slight diffusion of the horizon, according to Barnes Engineering Co.[3] The absence of atmosphere on the moon creates even more severe problems in this regard. Most investigations have shown that Albedo and air glow are poor alternate phenomena for horizon scanning at present (Singer). More experimental work is proceeding in this area.

---

[1] IBID

[2] Torques and Attitude Sensing in Earth Satellites, S. F. Singer, Academic Press, 1964

[3] Infrared Horizon Sensor Techniques for Lunar and Planetary Approaches, Gerald Falbel, Tech Planning Staff, Barnes Engineering Co. Paper 63-358.

Scanning schemes for near body sensors tend to fall into two categories:

1. Conical scanning
2. Edge tracking

Edge tracking is subdivided into three types:

1. Several vibrating heads fixed in the craft
2. One or more vibrating heads rotating in azimuth
3. Radiation balancing, using specially shaped apertures

Conical scan employed on such space crafts as Mercury and Tiros has shown only moderate accuracy performance. However, work to improve this approach and compensate for the errors is continuous. The edge trackers employing vibrating heads show promise as candidates for high accuracy gyrocompassing in orbit. The rotating azimuth action, by neutralizing scanner instrument bias, should provide the highest form of compensation possible. According to E. W. Morales[1], the potential instrument accuracy for this scheme may be 0.6 minutes. Hence, the vibrating head scheme is most important to describe in detail for the purpose of gyrocompassing in orbit.

Early developmental work is also proceeding on an edge tracker employing the principle of radiation balance. However, this will require further proof as to its applicability to gyrocompassing.

5.1 Second Harmonic Edge Tracking Horizon Scanner-Fixed Heads

The second harmonic edge tracking scanner consists of four fixed telescopes which use vibrating deflection mirror for scanning. Each field of view is sinusoidally dithered across the horizon, as illustrated in Fig. 5.1, in sweeps of a few degrees approximately normal to the horizon. Fig. 5.2 shows how the second harmonic output is derived. The radiance variance as a function height above mean sea level as reported by Singer[2] is shown in upper left. The dither motion of the mirror is drawn as an input to the curve. The resulting sensor output, shown upper right, has a second harmonic content. For this system, the horizon is defined as the condition under which the second harmonic content of the output waveform is zero. It turns out that the shape of the radiance curve for various geographic locations and seasons has been experimentally verified to be quite similar. Hence, even with variations in peak radiance, the second harmonic null horizon is fairly insensitive to peak radiance variations, mainly due to the steepness of the radiance slope and the amplitude of the dither sweep (about 4 degrees). The second harmonic error signal so derived would be used to drive the horizon scanner to null, i.e., to second harmonic zero content. It is always preferable to employ such a horizon scanner as part of a closed loop, rather than as an open loop measuring device, because it has poor scale-factor stability due to radiance level variations, but has good null stability for the reasons mentioned. The tracker output to the gyrocompassing system would be the properly transformed nulled central mirror angles relative to the base, i.e., the pitch and roll errors of the base.

---

[1] "Second Harmonic Edge Tracking Horizon Scanner, Edge Tracking Type", Eleazar W. Morales, Proceedings of the First Symposium on Infrared Horizon Scanners for Spacecraft Guidance and Control, May 1965.

[2] "Torques and Attitude Sensing in Earth Satellites", S. F. Singer, Academic Press, 1964.

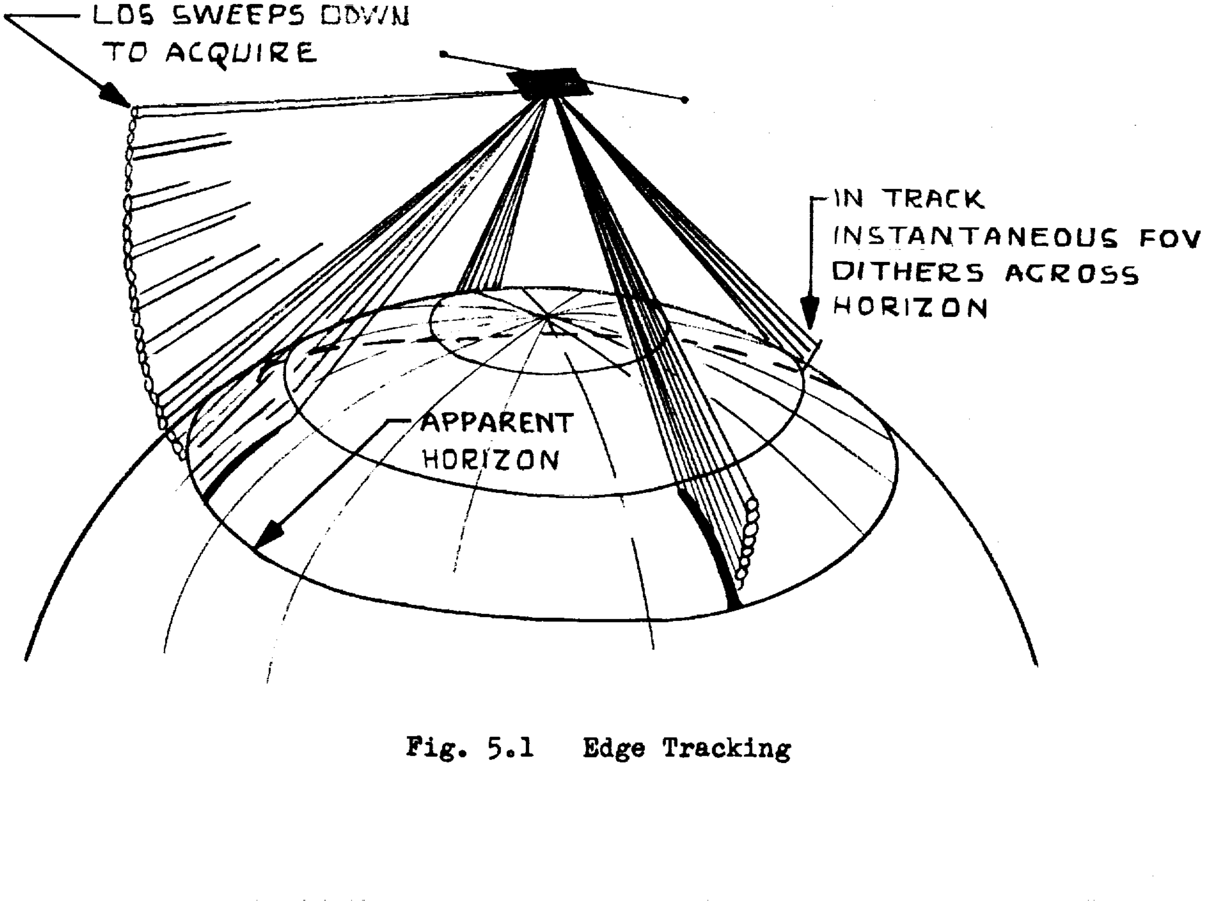
LOS SWEEPS DOWN TO ACQUIRE
IN TRACK INSTANTANEOUS FOV DITHERS ACROSS HORIZON
APPARENT HORIZON

Fig. 5.1 Edge Tracking

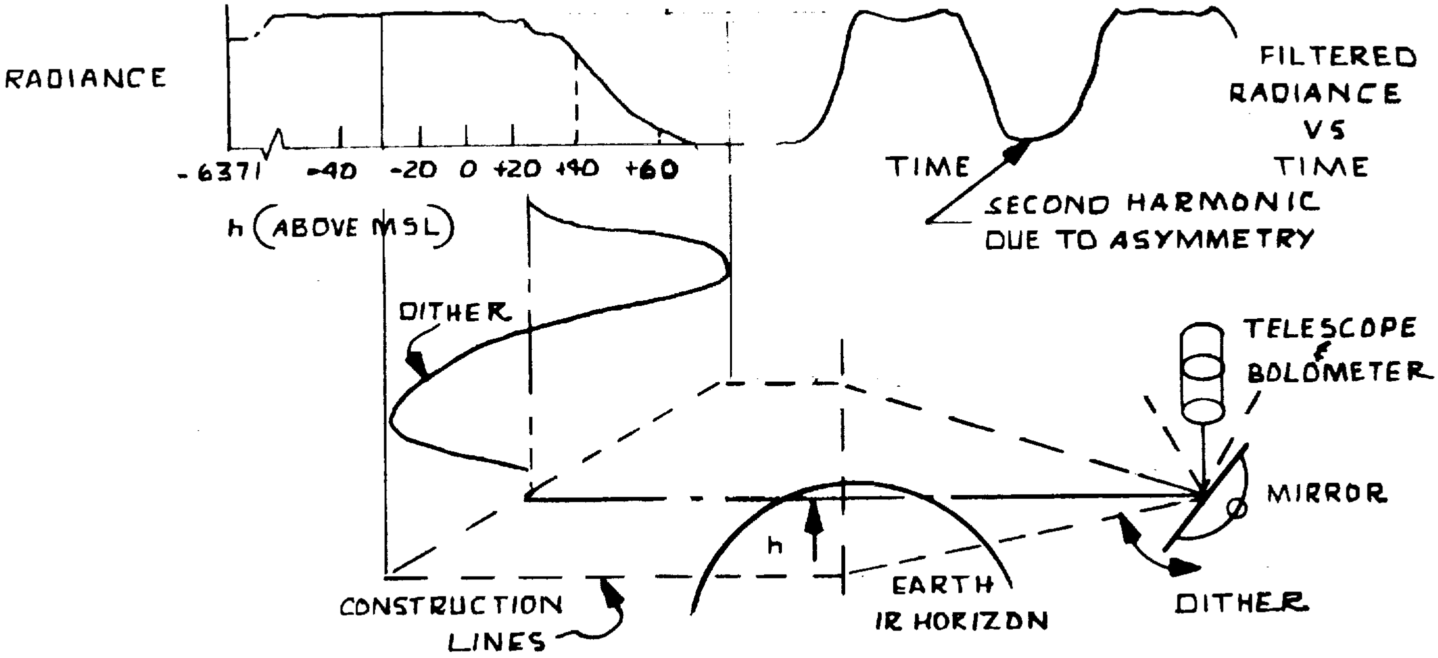
RADIANCE
-6371
-40
-20
0
+20
+40
+60
h (ABOVE MSL)
FILTERED RADIANCE VS TIME
TIME
TIME
SECOND HARMONIC DUE TO ASYMMETRY
DITHER
TELESCOPE & BOLOMETER
MIRROR
h
EARTH IR HORIZON
DITHER
CONSTRUCTION LINES

Fig. 5.2 Output vs Sweep

Second harmonic detection is very simply mechanized. As is well known from Fourier analysis, one can obtain frequency components of a waveform by multiplying it by a sine wave of the frequency to be analyzed, and averaging the product. Hence, one can employ the same frequency that is used to vibrate the mirror, double it to get the second harmonic, multiply the sensor output, and average-filter the product. Even simpler than multiplying by the second harmonic is switching the sensor output at the second harmonic frequency, using a synchronous rectifier.

A construction of the vibrating mirror is shown in Fig. 5.3.

This "meter movement" type of drive structure has the ability to position the mirror precisely both in the wide search angle as well as the narrow dither angle. A D-C flux through the drive coil deflects the mirror, until the flexure pivot torsion counterbalances the electromagnetic torque. Since the flexure pivot torsion is not precisely calibrated, the position of the mirror is picked off electromagnetically. A 5 kc voltage is applied to the field coils. The drive coils 5 kc output voltage is a function of mirror angle.

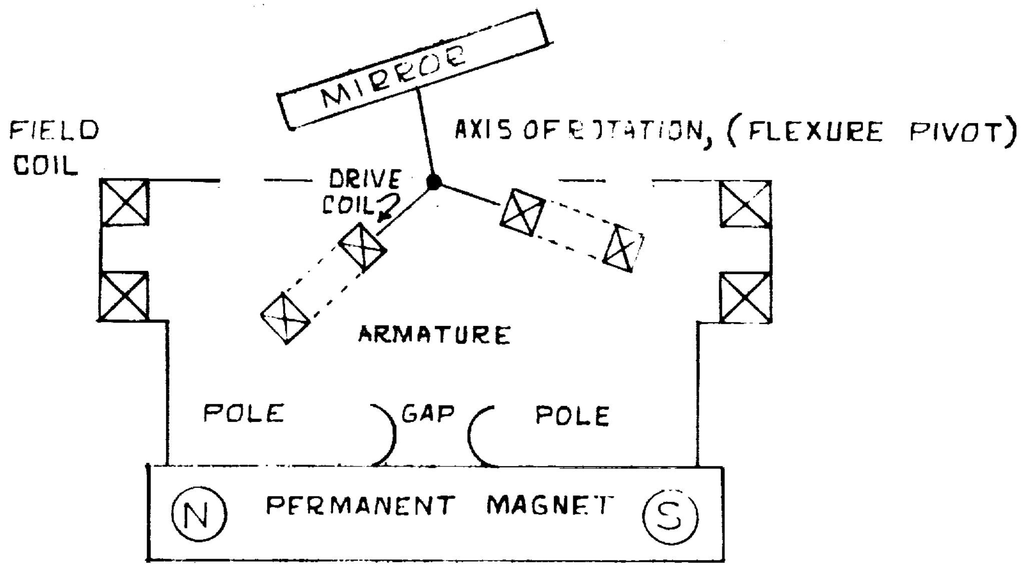

FIGURE 5.3 MIRROR SCANNING MECHANISM

Because of the higher sensitivity of this horizon scanner, it is affected by the near presence of other celestial bodies. Hence, when the sun appears in the field of view of one of the trackers, the affected telescope output is momentarily ignored while the remaining three trackers are used in a different logic mode.

5.2 Tracker Mechanization Equations, Edge Tracker

The tracker's primary purpose is to indicate to the gyrocompassing system only the infinitesimal rotation errors of the tracker base about the roll and pitch axes. Consequently the uncompensated mechanization equations are extremely simple. From a mechanizational viewpoint, the mirrors can be visualized as being slaved to the horizon at their particular location as indicated in Fig. 5.4.

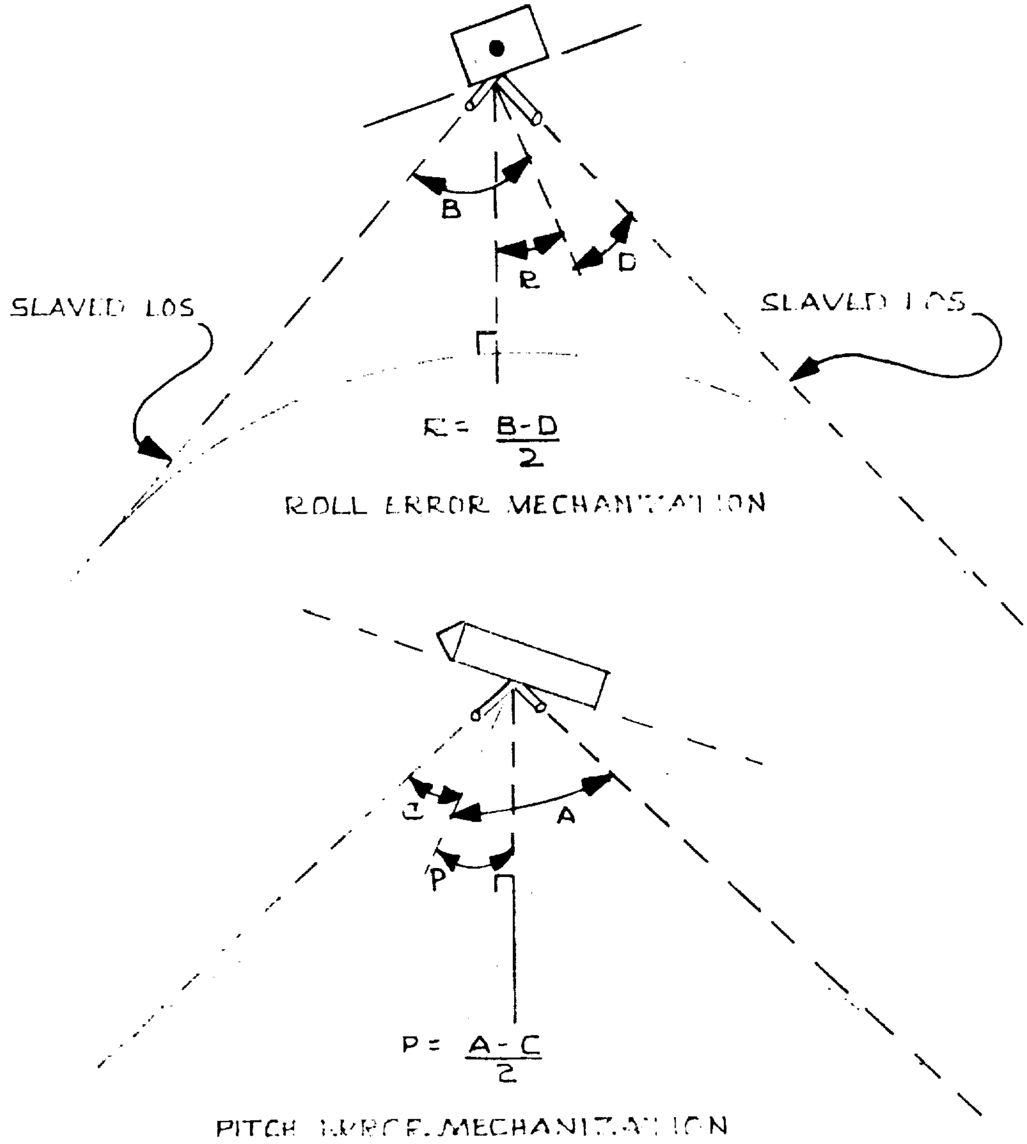
B
R
D
SLAVED LOS
SLAVED LOS
R = $\frac{B-D}{2}$
ROLL ERROR MECHANIZATION
C
A
P
P = $\frac{A-C}{2}$
PITCH ERROR MECHANIZATION

Fig. 5.4

Attitude Mechanization for Small Angles

Note that the sensors have a wide angle capability so that they can slave themselves to the horizon at a large variety of altitudes and attitudes. The assumption in the above mechanization is that the attitudes are not cross-coupled; that is, the vehicle attitude is close enough to level that Euler angles need not be employed. In the event that large base attitude inclinations are encountered, the attitude mechanization becomes more complicated. In this case, (see Fig. 5.5) the direction cosines of the vertical relative to the scanner-defined base becomes:

$$\left(\tan\frac{(A-C)}{2},\ -\tan\frac{(B-D)}{2},\ 1\right) \div \sqrt{1 + \tan^2\frac{(A-C)}{2} + \tan^2\frac{(B-D)}{2}} \qquad (5.3)$$

and the corresponding Euler angle equalities may be set up; in these the direction cosines are defined as

$$(\sin\theta,\ -\cos\theta\sin\phi,\ \cos\theta\cos\phi)$$

where ϕ is the rotation about the roll axis, and θ the rotation about the rolled pitch axis. Consequently pitch θ is

$$\theta = \tan^{-1}\left(\tan\frac{(A-C)}{2}\ \cos\frac{(B-D)}{2}\right) \qquad (5.4)$$

and roll ϕ is

$$\phi = \frac{B-D}{2} \qquad (5.5)$$

According to R. Caveney[1], a computer study was made of the second harmonic null variation due to the variation of radiance with altitude function given by Singer. The results of this study showed a peak variation of 0.09 deg at a 100 mile altitude, which swamps out the potential instrument errors. The instrument errors did not exceed 0.02 deg.

---

[1] "Second Harmonic Edge Tracker Horizon Sensor, Fixed Point Type", Robert Caveney, Advance Technology Laboratories, Proceedings of the First Symposium on Infrared Sensors for Spacecraft Guidance and Control, May 1965.

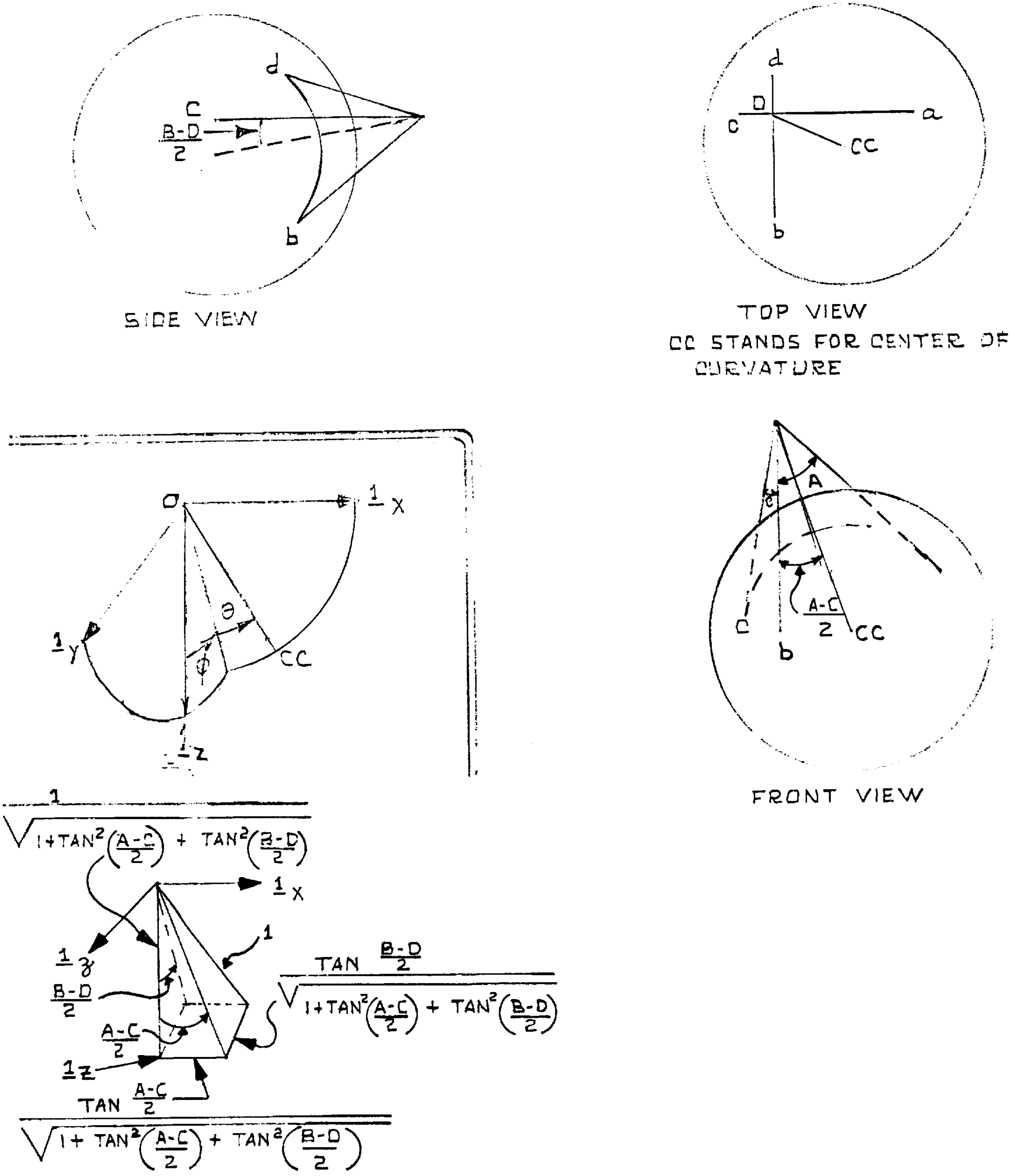
SIDE VIEW

TOP VIEW
CC STANDS FOR CENTER OF CURVATURE

FRONT VIEW

d
C
$\frac{B-D}{2}$
b
d
D
c
a
CC
b
O
1x
1y
θ
φ
CC
1z
A
c
$\frac{A-C}{2}$
c
b
CC
$\frac{1}{\sqrt{1+\tan^2\left(\frac{A-C}{2}\right)+\tan^2\left(\frac{B-D}{2}\right)}}$
1x
1y
1
$\frac{B-D}{2}$
$\frac{A-C}{2}$
1z
$\frac{\tan\frac{B-D}{2}}{\sqrt{1+\tan^2\left(\frac{A-C}{2}\right)+\tan^2\left(\frac{B-D}{2}\right)}}$
$\frac{\tan\frac{A-C}{2}}{\sqrt{1+\tan^2\left(\frac{A-C}{2}\right)+\tan^2\left(\frac{B-D}{2}\right)}}$

Fig. 5.5

Angular Relations for Large Angle Inclinations,
Edge Tracker

5.3 Second Harmonic Edge Tracker Horizon Sensor with Azimuth Rotation

Since the possibility of local horizon anomalies exists (cold clouds for instance), it appears possible to eliminate these by averaging out their effect through continual rotation of the previously discussed tracker configuration in azimuth. Even with this feature the 0.09 deg error mentioned above cannot be circumvented. Hence the extra complexity of this scheme is difficult to justify.

5.4 Development Considerations for Future Designs

According to Morales[1] it is possible to propose a design accuracy (except for the above mentioned horizon variations) near 0.01 degree. For instance one could have four telescopes mounted on a common azimuth base and separated in azimuth by 90°. The dither frequency would be set quite high to permit high tracking loop gain relative to the azimuth frequency employed. Fast optics would be employed to obtain an adequate signal to noise ratio. Instantaneous readout of the telescope angles would be required, and all pitch and roll data processing would be digital. Altitude and ellipticity compensation would be digitally computed, and suitable relation to the absolute yaw angle would be incorporated. A rigid structure and mounting would be required to prevent permanent mechanical distortion during launch. This approach begins to become expensive in terms of weight, size and power.

The horizon sensor should be operated continuously at null, (i.e., keeping the azimuth axis near vertical) in order to eliminate scalefactor, nonlinearity, and cross coupling problems, leaving only the null error. Fastening the sensor cluster to a stable gyrostabilized platform directly would improve the accuracy. However, since this type of scanner is by no means small, the gimbal structure surrounding such a device would become prohibitively large. Remote gimballed slaving to a stable platform is the other alternative, but here the complexity costs due to the large number of servos and digital encoders are high. Reduction in the number of telescopes would help, but may degrade operation when the sun is near the horizon, (sun-illuminated telescope rejection) otherwise possible with four telescopes. At present the azimuth scanning is used only for ± 180 deg, since slip rings cannot operate in space according to Morales[1].

Because of the complexity of any azimuth scanning system, especially when gimballed, consideration has to be given to the non-scanning systems. However, such systems generate optical alinement requirements comparable to the accuracy of the sensor. These requirements are not easily satisfied at the wavelengths involved and with the physical size of the optics available.

---

[1] Morales, E. W., "Second Harmonic Edge Tracking Horizon Scanner, Edge Tracking Type", Proceedings of the First Symposium on Infrared Horizon Scanners for Spacecraft Guidance and Control, May 1965.

The horizontal telescope field of view of a gimballed non-scanning system would not be critical. The telescope aberrations in that direction are of no concern. A wide horizontal field of view is actually desirable; since to some extent it accomplishes the horizon averaging done by an azimuth scanning system. However this requires sophisticated optical design.

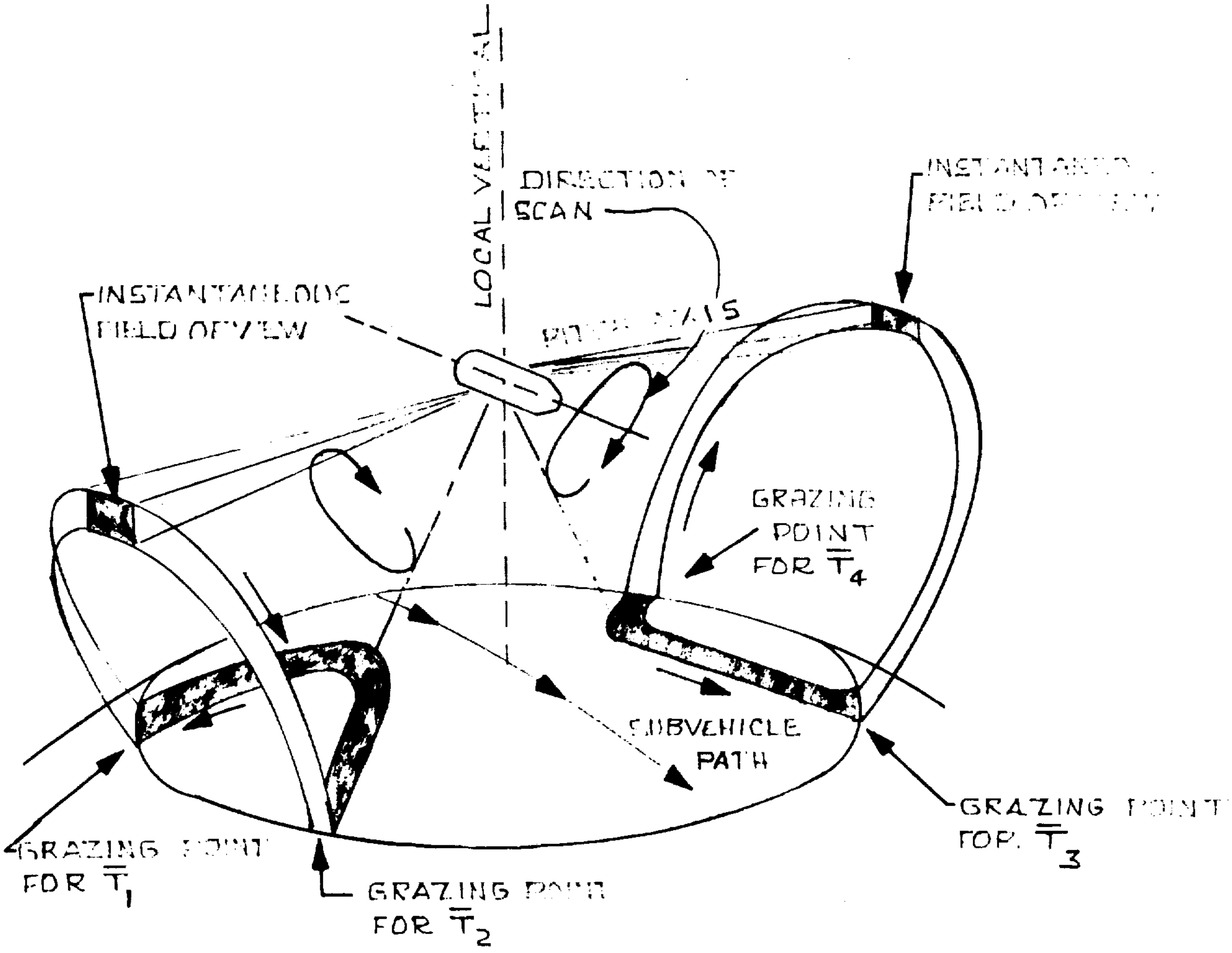
LOCAL VERTICAL
DIRECTION OF SCAN
INSTANTANEOUS FIELD OF VIEW
INSTANTANEOUS FIELD OF VIEW
PITCH AXIS
GRAZING POINT FOR $\overline{T}_4$
SUBVEHICLE PATH
GRAZING POINT FOR $\overline{T}_1$
GRAZING POINT FOR $\overline{T}_2$
GRAZING POINT FOR $\overline{T}_3$

Fig. 5.6

Conical Scan Paths

5.5 Conical Scan Horizon Sensors

The conical scanning horizon scanner, illustrated in Fig. 5.6 sweeps out large angle cones at a rapid rate (approximately 20 to 30 cps) using 1 to 3° fields of view. It must determine the vehicle attitude relative to the vertical from the dark-bright duty cycle and phase.

Operation is in the infrared spectrum for reasons already mentioned. A sun rejection process is also included, since according to S. Spielberger[1], the 6000°K sun can produce large disturbances. Typical output of the conical scanner illustrates the difficulties with this mechanization. As shown in Fig. 5.7 the effects of cold clouds and sun set up spurious zero crossings that require special clarification in the system electronics. What starts out to be a very simple mechanization, based on taking the average of an unsymmetrical duty cycle square wave, turns out to be greatly complicated in order to compensate for the phenomena. In fact, it results in scanning large areas of sky and ground that have no bearing on the problem of finding the vehicle attitude, and of then rejecting these unwanted areas.

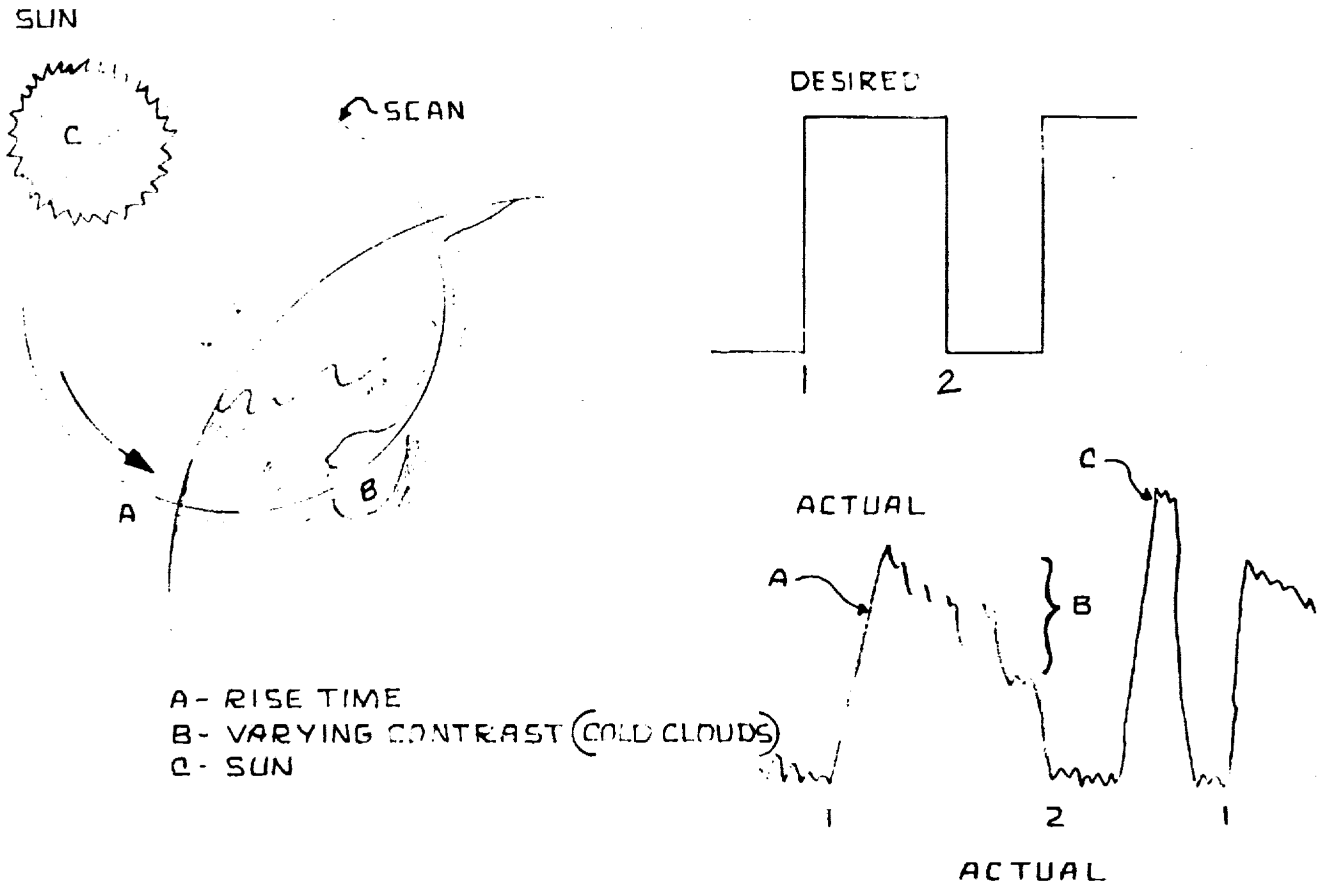

Fig. 5.7 Conical Scan and Output Waveforms

---

[1] "Conical Scan Horizon Sensor", S. Spielberger, Proc. for the First Symposium on I. R. Sensors for Spacecraft G&C, May 1965

Instrument accuracies vary from ± 0.2° to ± 1° depending on the method of slicing, optics, and the sensors employed[1]. According to F. Schwartz, K. Ward, and T. Falk[2], evolutionary development is continuing, in which the above inaccuracy promises to be reduced by a factor of 10. They describe a scanner output made responsive to two slicing levels as shown in Fig. 5.8.

By using two slicing levels a constant amplitude pulse, whose duration is inversely proportional to the slope of the horizon profile, can be obtained. Thus the slope of the horizon gradient so obtained could be used to correct for the variation in the horizon gradient at any location and at any season, using the slope-intercept method of analytic geometry. In Fig. 5.7 the extrapolated zero radiance intercepts vary only

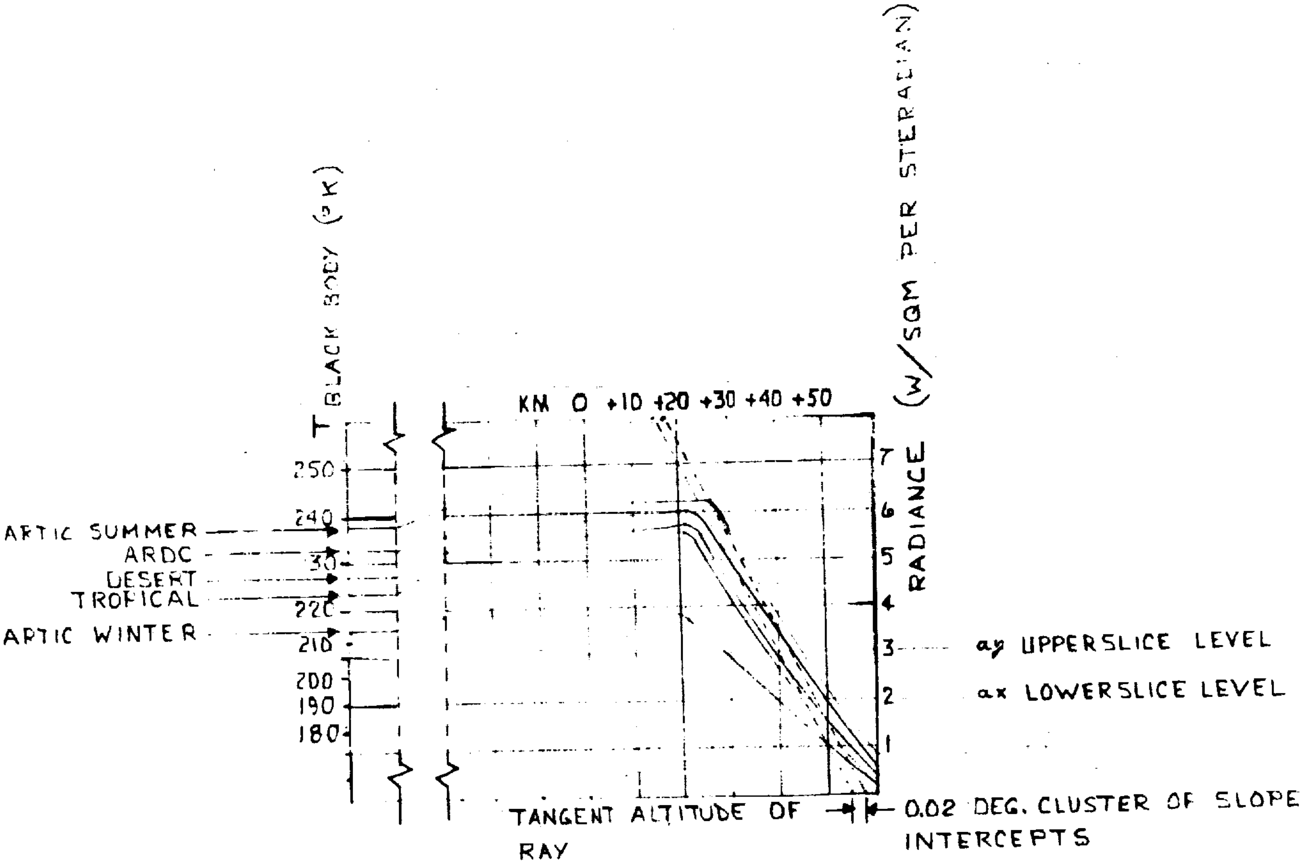

Fig. 5.8

Horizon Profile Curves for 14-16 CO_2 and Two Slicing Levels by 0.02 deg, giving inspiration to this technique. Sensor response time is critical and is taken into account. Laboratory work with an artificial horizon, having a built-in gradient, indicated that a 0.5 deg error was corrected to 0.03 deg with the slope correction method. Flight proof testing remains to be done.

---

[1] IBID

[2] "A High Accuracy Conical Scan Horizon Sensor Operating in the 15 CO_2 Band", F. Schwartz, K. Ward & T. Falk, Pro. for the First Symposium on I. R. Sensors for Spacecraft Guidance and Control, May 1965

The basic problem can be simply stated. Four lines of sight having the following characteristics

1. Their coordinates are known in vehicle coordinates
2. They lie on the conical surfaces swept out by the scanners
3. Each is tangent to the planet surface (considered as a sphere here for simplicity) where the radiance gradient is sensed.

Problem: Find the direction of the vertical in vehicle coordinates. This problem simplifies considerably if pitch and roll attitude angles are assumed to be small, since then it is permissible to solve for pitch and roll separately; that is, i.e., to treat pitch as a phase angle and roll as a problem unaffected by pitch. If the attitude angles are large the above simplifications are no longer valid.

5.6 Large-Angle Mechanization

Let the unit vectors that lie in the cone and tangent to the sphere be called $\underline{T}_1$, $\underline{T}_3$, and $\underline{T}_4$, as shown in Fig. 5.9. Let $\underline{V}$ be the unknown unit vertical vector. The triangles that are formed by the tangent lines, the vertical, and the rays from earth center to point of tangency are all congruent. Therefore the angle between the vertical and a tangent line is equal to the angle between vertical and any other tangent line. Consequently in vector notation,

$$\underline{V} \cdot \underline{T}_1 = \underline{V} \cdot \underline{T}_2 = \underline{V} \cdot \underline{T}_3 = \underline{V} \cdot \underline{T}_4 \qquad (5.6)$$

Since $\underline{T}_1$, $\underline{T}_2$, $\underline{T}_3$, and $\underline{T}_4$ are assumed known in vehicle coordinates, one can solve for unit vertical vector $\underline{V}$. Since it is only necessary to obtain the direction of $\underline{V}$, i.e., the ratio $V_x:V_y:V_z$, only two equations in three unknowns are required.

$$\begin{aligned} \underline{V} \cdot \underline{T}_1 &= \underline{V} \cdot \underline{T}_2 \\ \underline{V} \cdot \underline{T}_2 &= \underline{V} \cdot \underline{T}_3 \end{aligned} \qquad (5.7)$$

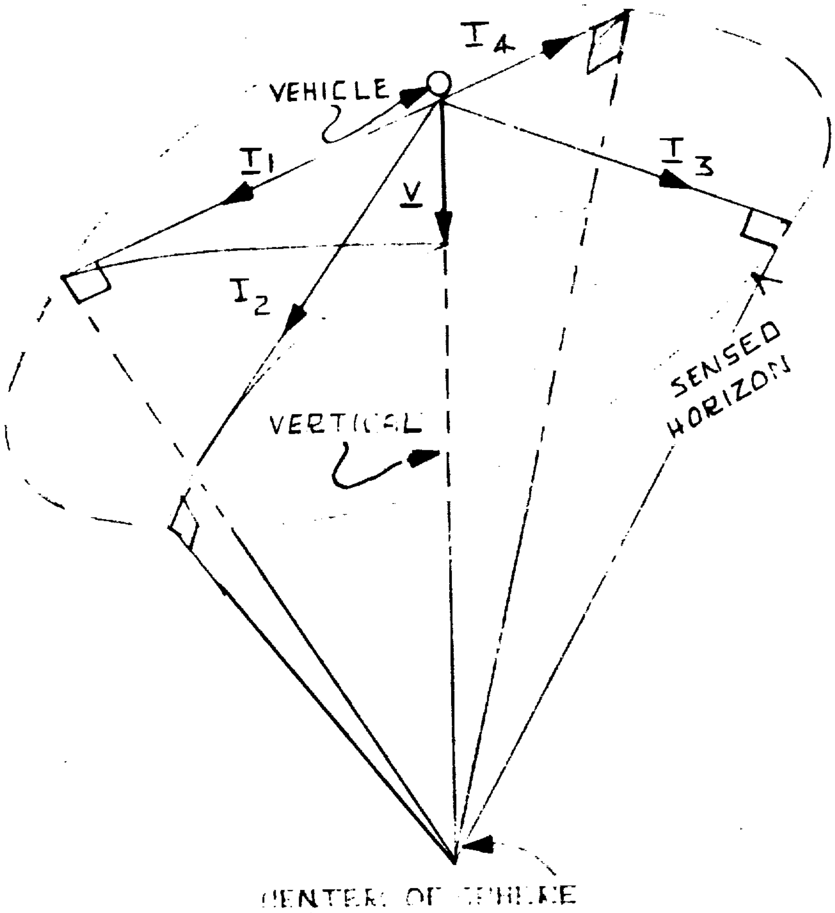
T4
VEHICLE
T1
V
T3
T2
SENSED HORIZON
VERTICAL
CENTER OF SPHERE

Fig. 5.9

Tangent Relationships

The tangent line $\underline{T}_4$ is a redundant value. The two equations can be rewritten in component form as

$$\begin{bmatrix} T_{1_1} - T_{2_1}, & T_{1_2} - T_{2_2} \\ T_{2_1} - T_{3_1}, & T_{2_2} - T_{3_2} \end{bmatrix} \begin{bmatrix} V_x \\ V_y \end{bmatrix} = - \begin{bmatrix} T_{1_3} & - & T_{2_3} \\ T_{2_3} & - & T_{3_3} \end{bmatrix} V_z \qquad (5.8)$$

Inverting this,

$$\begin{bmatrix} V_x \\ V_y \end{bmatrix} = - \frac{\begin{bmatrix} T_{2_2} - T_{3_3}, & -(T_{1_1} - T_{2_2}) \\ -(T_{2_2} - T_{3_3}), & T_{1_1} - T_{2_2} \end{bmatrix} \begin{bmatrix} T_{1_3} - T_{2_3} \\ T_{2_3} - T_{3_3} \end{bmatrix} V_z}{\begin{vmatrix} T_{1_1} - T_{2_1} & T_{1_2} - T_{2_2} \\ T_{2_1} - T_{3_1} & T_{2_2} - T_{3_2} \end{vmatrix}} \tag{5.9}$$

or

$$\frac{V_x}{(T_{1_2}-T_{2_2})(T_{2_3}-T_{3_3})-(T_{1_3}-T_{2_3})(T_{2_3}-T_{3_3})} = \frac{V_y}{(T_{1_3}-T_{2_3})(T_{2_1}-T_{3_1})-(T_{1_1}-T_{2_1})(T_{2_3}-T_{3_3})}$$

$$= \frac{V_z}{(T_{1_1}-T_{2_1})(T_{2_2}-T_{3_2})-(T_{1_2}-T_{2_2})(T_{2_1}-T_{3_1})} \tag{5.10}$$

Note that the denominators are the components of the cross-product $(\underline{T}_1 - \underline{T}_2) \times (\underline{T}_2 - \underline{T}_3)$. Hence, the direction of $\underline{V}$ is equal to the direction of this cross-product. The direction cosines of $\underline{V}$, which are used to determine cosines of the above cross-product or the components of the unit vector, are given by

$$\frac{(\underline{T}_1 - \underline{T}_2) \times (\underline{T}_2 - \underline{T}_3)}{|(\underline{T}_1 - \underline{T}_2) \times (\underline{T}_2 - \underline{T}_3)|} \tag{5.11}$$

The measured information is the cone angle of the four tangent lines. From this the direction of $\underline{T}_1$, $\underline{T}_2$, $\underline{T}_3$, and $\underline{T}_4$ are calculated. Consequently, the transformation of a line of sight into the $\underline{1}_x$, $\underline{1}_y$, $\underline{1}_z$ coordinates is performed on the basis of the following set of general transformations.

For T_3 and T_4:

$$\begin{bmatrix} T_{ix} \\ T_{iy} \\ T_{iz} \end{bmatrix} = \begin{bmatrix} \mathrm{Cos}D & 0 & -\mathrm{Sin}D \\ 0 & 1 & 0 \\ \mathrm{Sin}D & 0 & \mathrm{Cos}D \end{bmatrix} \begin{bmatrix} 1 & 0 & 0 \\ 0 & \mathrm{Cos}S_i & -\mathrm{Sin}S_i \\ 0 & \mathrm{Sin}S_i & \mathrm{Cos}S_i \end{bmatrix} \begin{bmatrix} \mathrm{Cos}H & -\mathrm{Sin}H & 0 \\ \mathrm{Sin}H & \mathrm{Cos}H & 0 \\ 0 & 0 & 1 \end{bmatrix} \begin{bmatrix} 1 \\ 0 \\ 0 \end{bmatrix}$$

where i = 3 or 4. (5.12)

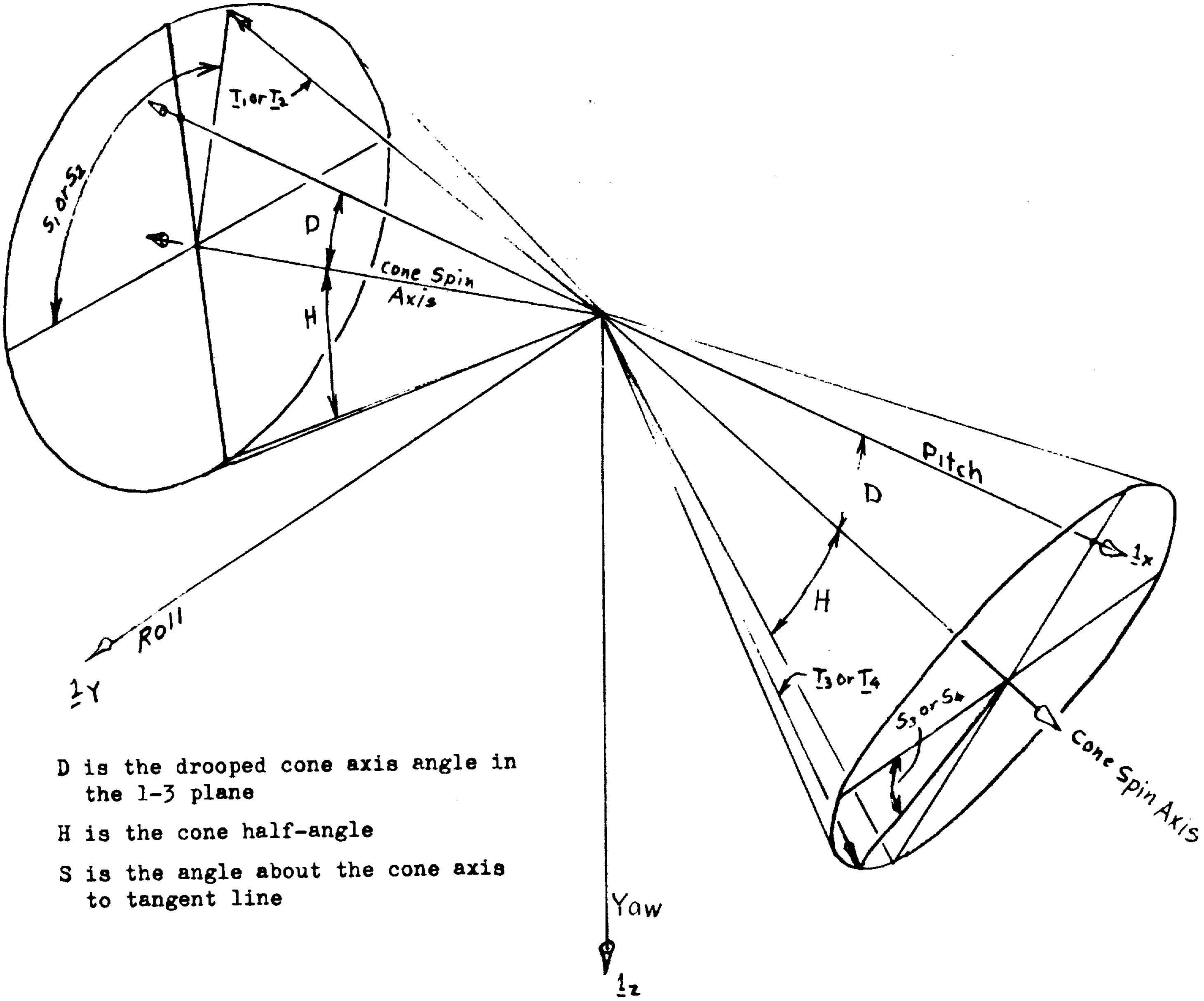
T1 or T2
S1 or S2
D
H
Cone Spin Axis
Roll
1Y
Pitch
D
H
1x
T3 or T4
S3 or S4
Cone Spin Axis
Yaw
1z

D is the drooped cone axis angle in the 1-3 plane

H is the cone half-angle

S is the angle about the cone axis to tangent line

Fig. 5.10
Cone Angles

And, for T_1 and T_2:

$$\begin{bmatrix} T_{jx} \\ T_{jy} \\ T_{jz} \end{bmatrix} = \begin{bmatrix} -\mathrm{CosD} & 0 & -\mathrm{SinD} \\ 0 & 1 & 0 \\ \mathrm{SinD} & 0 & -\mathrm{CosD} \end{bmatrix} \begin{bmatrix} 1 & 0 & 0 \\ 0 & \mathrm{CosS}_j & -\mathrm{SinS}_j \\ 0 & \mathrm{SinS}_j & \mathrm{CosS}_j \end{bmatrix} \begin{bmatrix} \mathrm{CosH} & -\mathrm{SinH} & 0 \\ \mathrm{SinH} & \mathrm{CosH} & 0 \\ 0 & 0 & 1 \end{bmatrix} \begin{bmatrix} 1 \\ 0 \\ 0 \end{bmatrix} \qquad (5.13)$$

Where S is the angle, measured counter clockwise about the drooped cone axis, and j may be either 1 or 2.

The components of $\underline{V}$ are obtained from Eq. (5.11).

$$V_x = \frac{1}{\Delta}\left\{-\mathrm{Sin}^2\mathrm{H}\ \mathrm{CosD}\ [\mathrm{Sin}(S_1+S_3) + \mathrm{Sin}(S_2-S_1)-\mathrm{Sin}(S_2+S_3)]\right\}$$

$$V_y = \frac{1}{\Delta}\left\{(\mathrm{SinS}_2-\mathrm{SinS}_1)[-2\mathrm{SinH}\ \mathrm{CosH}\ \mathrm{Cos}^2\mathrm{D} + 2\mathrm{Sin}^2\mathrm{H}\ \mathrm{CosD}\ \mathrm{SinD}\ \mathrm{SinS}_3]\right\} \qquad (5.14)$$

$$V_z = \frac{1}{\Delta}\left\{\mathrm{sin}^2\mathrm{H}\ \mathrm{SinD}[\mathrm{Sin}(S_3-S_2)+\mathrm{Sin}(S_2-S_1)+\mathrm{Sin}(S_3-S_1)+2\mathrm{SinH}\ \mathrm{CosH}\ \mathrm{CosD}\ (\mathrm{CosS}_1-\mathrm{CosS}_2)\right\}$$

where Δ is such that

$$V_x{}^2 + V_y{}^2 + V_z{}^2 = 1$$

or $= [(\text{numerator } V_1)^2 + (\text{numerator } V_2)^2 + (\text{numerator } V_3)^2]^{\frac{1}{2}}$ (5.15)

Then,

$$\phi = \mathrm{Sin}^{-1} V_x$$

and

$$\theta = \mathrm{Sin}^{-1} \frac{V_y}{-\mathrm{Cos}\phi}$$

analogous to the Euler angle equalities of Fig. 5.10.

Clearly the large-angle mechanization equations are complex, and difficult to implement, especially in view of the fact that S_1, S_2 and S_3 vary rapidly. However, the small angle approximations may safely be used because the angular errors are minimized by the gyrocompassing mechanization.

5.7 Small-Angle Mechanization for the Conical Scan Horizon Scanner

Here, roll and pitch can be treated independently. The assumption is made that the roll error is zero. Consequently the unit vectors are symmetrically disposed about the 1_z plane, as indicated in Fig. 5.11.

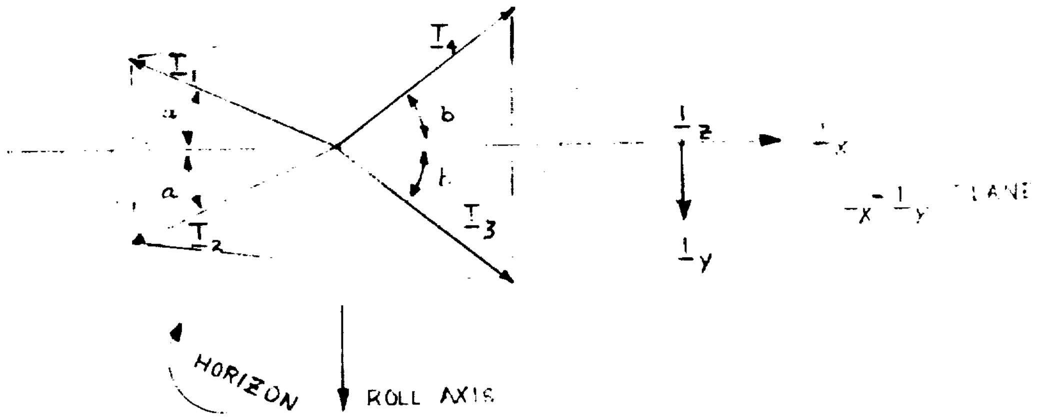
$\underline{T}_1$
$\underline{T}_2$
$\underline{T}_3$
$\underline{T}_4$
a
a
b
b
$\underline{1}_z$
$\underline{1}_x$
$\underline{1}_y$
$\underline{1}_x - \underline{1}_y$ PLANE
HORIZON
ROLL AXIS

Fig. 5.11 Rolled Disposition of the Tangent Lines of Sight, Zero Pitch

Using the convention of Fig. 5.10 the following approximations may be made.

$$\begin{aligned} \operatorname{Sin}S_1 &= \operatorname{Sin}S_2 \\ \operatorname{Sin}S_3 &= -\operatorname{Sin}(S_1 + \Delta S) \end{aligned} \tag{5.16}$$

leading to

$$\phi = \frac{\operatorname{Sin}H \operatorname{Cos}S_1 \operatorname{Cos}D \,\Delta S}{2(\operatorname{Cos}H \operatorname{Cos}D + \operatorname{Sin}H \operatorname{Sin}D \operatorname{Sin}S_1)} \tag{5.17}$$

The difference in cone angle Δ S or the difference in duty cycles is proportional to the roll error. In practice, this proportionality factor is experimentally determined, so that roll angle

$$\phi = K \Delta S$$

where ΔS is the difference in cone angles across the cones.

Here the simplifying assumptions that

$$\sin S_2 = \sin(S_1 + \Delta S)$$

$$\cos S_2 = -\cos(S_1 + \Delta S)$$

$$\sin S_3 = -\sin S_2$$

$$\cos S_3 = \cos S_2$$

are made, consequently

$$\frac{\Delta S \cos D}{2} = \theta \qquad (5.18)$$

where ΔS is the difference in cone angle along a cone.

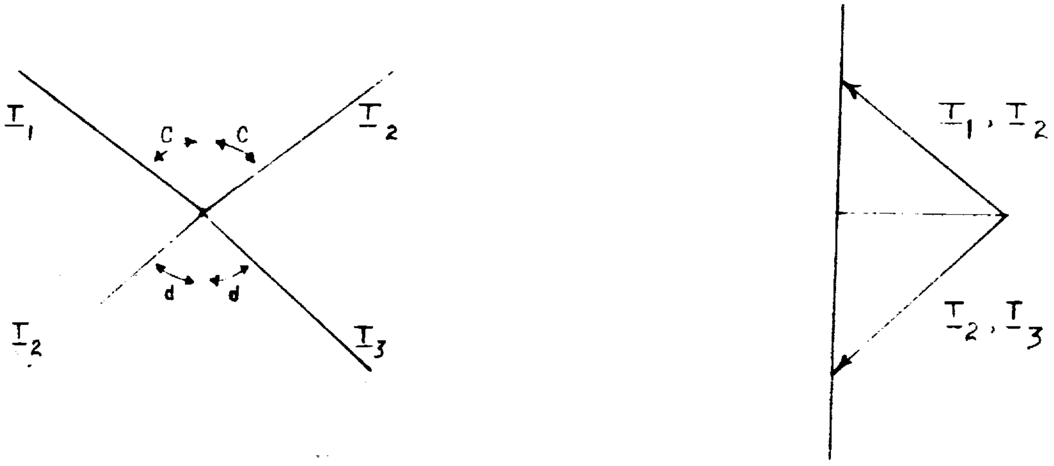

Fig. 5.12 Pitched Disposition of the Tangent Lines of Sight - Zero Roll

5.8 Right Angle Conical Scan Mechanization

The conical horizon scanner mechanization described on the previous page is convenient to use when it is only permissible to view the horizon from opposite sides of the spacecraft. When it is possible to view the horizon at right angles, the mechanization shown in Fig. 5.13 may be used. In this mechanization roll and pitch are very simply mechanized as proportional to the phase angles about the cone axes when small angles are assumed, but as before, fairly complex mechanizations for large angles would be required.

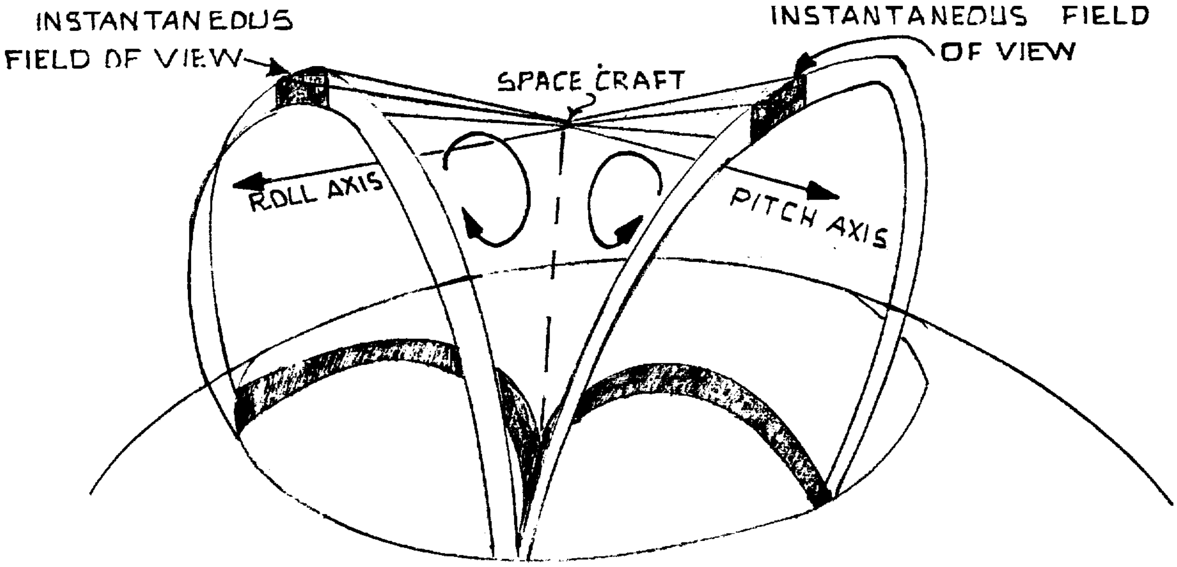
INSTANTANEOUS FIELD OF VIEW
INSTANTANEOUS FIELD OF VIEW
SPACE CRAFT
ROLL AXIS
PITCH AXIS

Fig. 5.13

Right Angle Conical Scan Machanization

The theory is based on the same thoughts as before. As illustrated in Fig. 5.14, the tangent vectors are disposed differently:

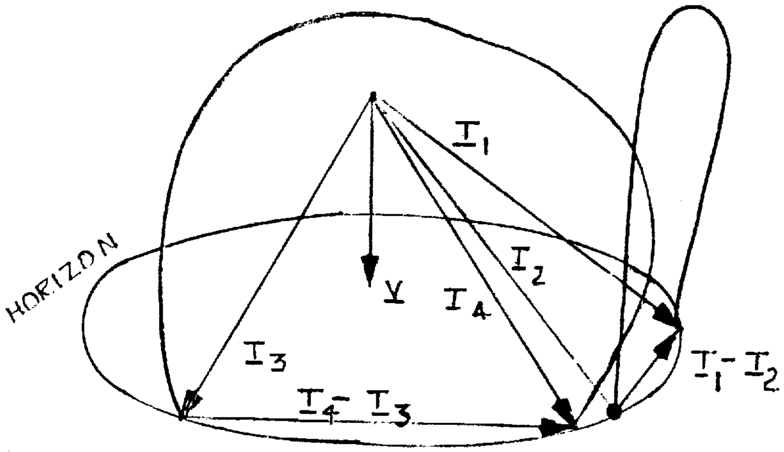
HORIZON
$\underline{T}_1$
$\underline{T}_2$
$\underline{V}$
$\underline{T}_4$
$\underline{T}_3$
$\underline{T}_1 - \underline{T}_2$
$\underline{T}_4 - \underline{T}_3$

Fig. 5.14

Tangent Lines for Right Angle Cones

The unit vertical vector can be constructed by forming

$$\underline{V} = \frac{(\underline{T}_1 - \underline{T}_2) \times (\underline{T}_4 - \underline{T}_3)}{|(\underline{T}_1 - \underline{T}_2) \times (\underline{T}_4 - \underline{T}_3)|} \tag{5.19}$$

where $\underline{T}_1$, $\underline{T}_2$, $\underline{T}_3$ and $\underline{T}_4$ are given in terms of measured cone angles S_1, S_2, S_3 and S_4. In general this mechanization makes use of cones that are not dipped in the 1-3 and 2-3 planes.

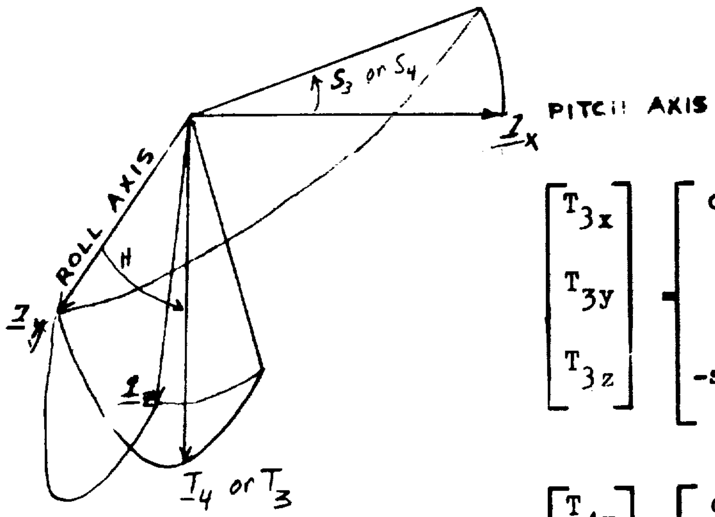

$$\begin{bmatrix} T_{3x} \\ T_{3y} \\ T_{3z} \end{bmatrix} = \begin{bmatrix} \cos S_3 & 0 & \sin S_3 \\ 0 & 1 & 0 \\ -\sin S_3 & 0 & \cos S_3 \end{bmatrix} \begin{bmatrix} 1 & 0 & 0 \\ 0 & \cos H & -\sin H \\ 0 & \sin H & \cos H \end{bmatrix} \begin{bmatrix} 0 \\ 1 \\ 0 \end{bmatrix} \quad (20)$$

$$\begin{bmatrix} T_{4x} \\ T_{4y} \\ T_{4z} \end{bmatrix} = \begin{bmatrix} \cos S_4 & 0 & \sin S_4 \\ 0 & 1 & 0 \\ -\sin S_4 & 0 & \cos S_4 \end{bmatrix} \begin{bmatrix} 1 & 0 & 0 \\ 0 & \cos H & -\sin H \\ 0 & \sin H & \cos H \end{bmatrix} \begin{bmatrix} 0 \\ 1 \\ 0 \end{bmatrix} \quad (21)$$

Fig. 5.15 Angular Relationships for $\underline{T}_3$ or $\underline{T}_4$, Right Angle Cones

Hence, for large attitude angles, using the above relation for $\overline{V}$

$$V_x = (\cos S_1 - \sin S_2)(\sin S_4 - \sin S_3)/\Delta \quad = \quad \sin \phi \text{ for roll}$$

$$V_y = (\sin S_1 - \sin S_2)(\sin S_4 - \sin S_3)/\Delta \quad = \quad -\sin \theta \cos \phi \text{ for pitch}$$

$$V_z = (\cos S_1 - \cos S_2)(\sin S_4 - \sin S_3)/\Delta \quad = \quad \text{not used}$$

$$\text{where } \Delta = \sqrt{(\text{numerator } V_1)^2 + (\text{numerator } V_2)^2 + (\text{numerator } V_3)^2}$$

Again it is seen that this is complex, and possibly unnecessary for servoed applications.

5.9 Small-Angle Mechanization

For the roll mechanization the effect of pitch is neglected, i.e., one may assume that no pitch angle exists. Consequently letting

$$\theta = 0, \quad \mathrm{Sin}S_1 = \mathrm{Sin}S_2, \quad S_4 = S_o - \Delta S,$$

$$\mathrm{Cos}S_1 = -\mathrm{Cos}S_2, \quad S_3 = 360 - (S_o + \Delta S),$$

then $\phi = 4\ \mathrm{Cos}S_1\ \mathrm{Sin}S_o\ \Delta S$, or ϕ is proportional to the phase angle of the roll cone. Note that $V_2 = 0$ and $V_3 = 1$. For the pitch mechanization the effect of roll is neglected. Consequently letting

$$\phi = 0, \quad \mathrm{Sin}S_3 = -\mathrm{Sin}S_4, \quad S_1 = 180 - (S_o + \Delta S)$$

$$\mathrm{Cos}S_3 = \mathrm{Cos}S_4, \quad S_2 = S_o - \Delta S$$

$V_2 = 4\mathrm{Sin}S_4\ \mathrm{Cos}S_o\ \Delta S = -\theta$, or the pitch angle is proportional to the phase error of the pitch cone. Note also that $V_1 = 0$, $V_3 = 1$.

It appears that the constants of proportionality in this type of conical arrangement are independent of H, the cone half angle. Furthermore the sensitivity varies with $\mathrm{Cos}S_o$ for θ and $\mathrm{Sin}S_o$ for ϕ. The lower the altitude, the better the sensitivity. The angles S_1, S_2, S_3 and S_4 are really dependent on H however. A wider cone is desirable to the increase sensitivity. However, practical considerations such as optics design and signal-noise considerations limit the cone half angle.

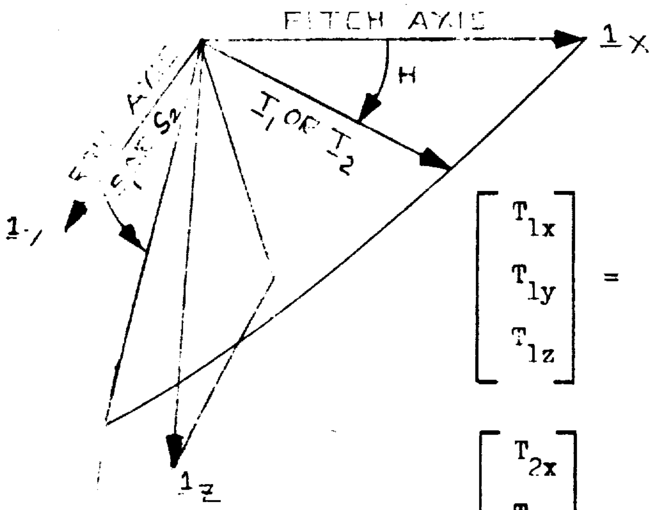

$$\begin{bmatrix} T_{1x} \\ T_{1y} \\ T_{1z} \end{bmatrix} = \begin{bmatrix} 1 & 0 & 0 \\ 0 & \cos S_1 & -\sin S_1 \\ 0 & \sin S_1 & \cos S_1 \end{bmatrix} \begin{bmatrix} \cos H & -\sin H & 0 \\ \sin H & \cos H & 0 \\ 0 & 0 & 1 \end{bmatrix} \begin{bmatrix} 1 \\ 0 \\ 0 \end{bmatrix} \qquad (5.22)$$

$$\begin{bmatrix} T_{2x} \\ T_{2y} \\ T_{2z} \end{bmatrix} = \begin{bmatrix} 1 & 0 & 0 \\ 0 & \cos S_2 & -\sin S_2 \\ 0 & \sin S_2 & \cos S_2 \end{bmatrix} \begin{bmatrix} \cos H & -\sin H & 0 \\ \sin H & \cos H & 0 \\ 0 & 0 & 1 \end{bmatrix} \begin{bmatrix} 1 \\ 0 \\ 0 \end{bmatrix} \qquad (5.23)$$

Fig. 5.16

Angular Relationships for T_1 and T_2

Figs. 5.17-5.20 reproduced through the courtesy of Barnes Engineering

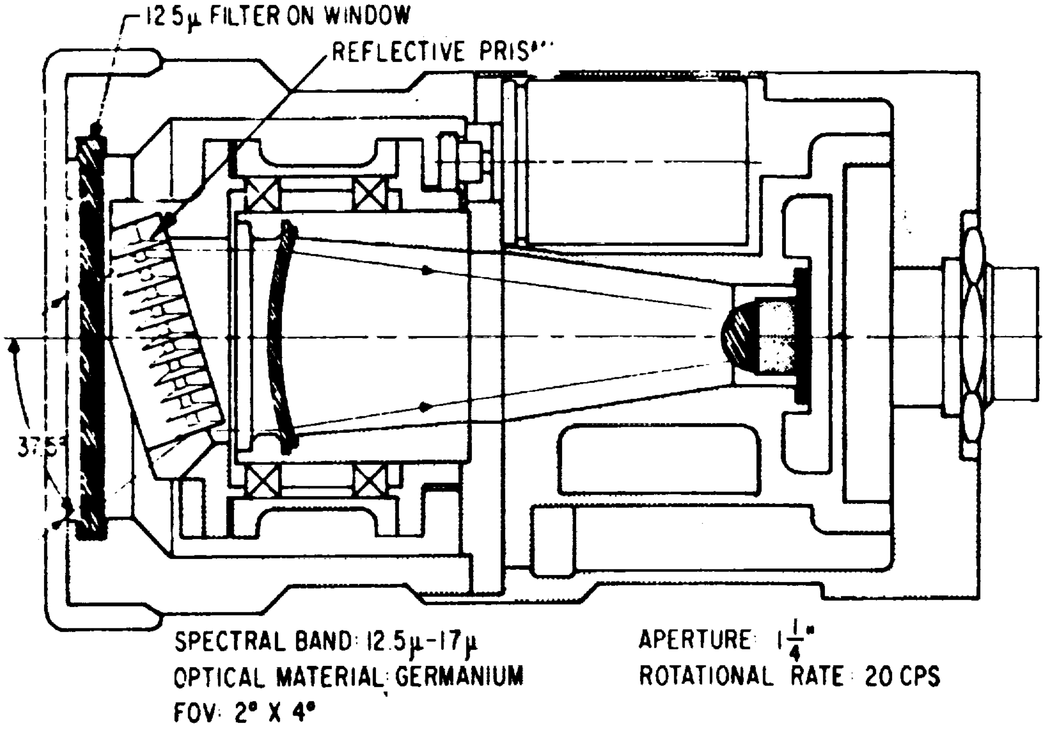
12.5μ FILTER ON WINDOW
REFLECTIVE PRIS''
37.5°
SPECTRAL BAND: 12.5μ-17μ
OPTICAL MATERIAL: GERMANIUM
FOV: 2° X 4°
APERTURE: 1 1/4"
ROTATIONAL RATE: 20 CPS

Fig. 5.17 SYSTEM C, HEAD LAYOUT

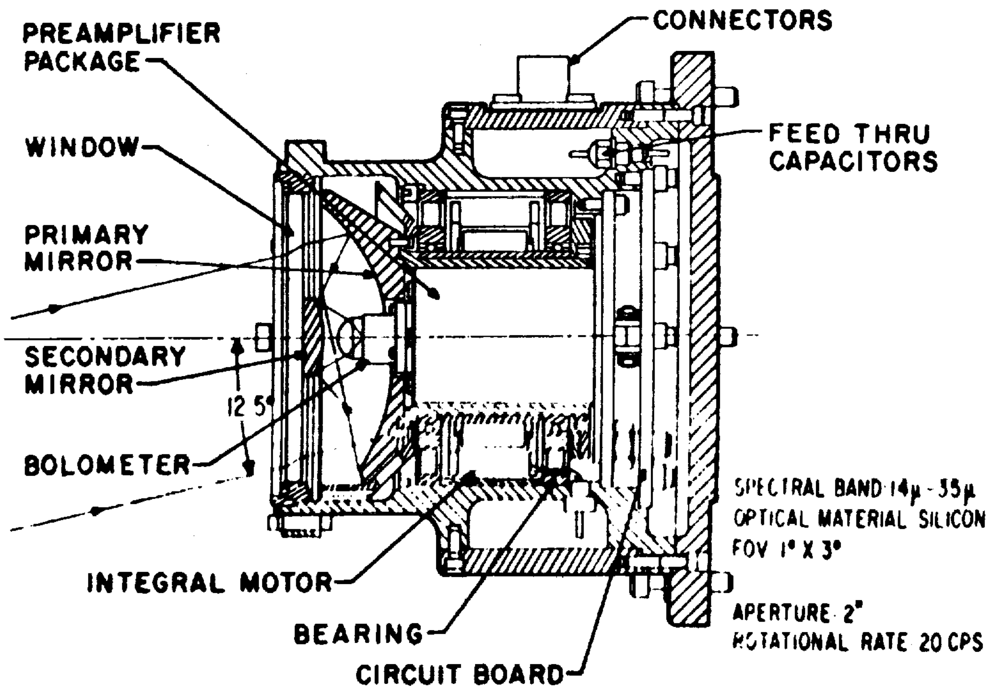
CONNECTORS
PREAMPLIFIER PACKAGE
WINDOW
FEED THRU CAPACITORS
PRIMARY MIRROR
SECONDARY MIRROR
12.5°
BOLOMETER
SPECTRAL BAND 14μ-35μ
OPTICAL MATERIAL SILICON
FOV 1° X 3°
INTEGRAL MOTOR
APERTURE 2"
ROTATIONAL RATE 20 CPS
BEARING
CIRCUIT BOARD

Fig. 5.18 SYSTEM E, HEAD LAYOUT

Figs. 5.17-5.20 reproduced through the courtesy of Barnes Engineering

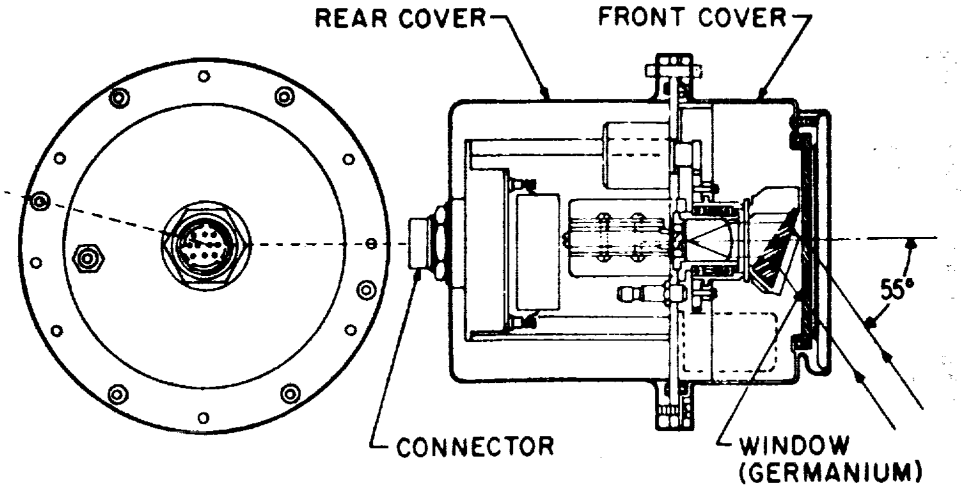
REAR COVER
FRONT COVER
55°
CONNECTOR
WINDOW (GERMANIUM)

SPECTRAL BAND: 1.7μ - 17μ
FOV: 2° X 8°
APERTURE: 5/8"
ROTATIONAL RATE: 30 CPS

Fig. 19 SYSTEM A, HEAD LAYOUT

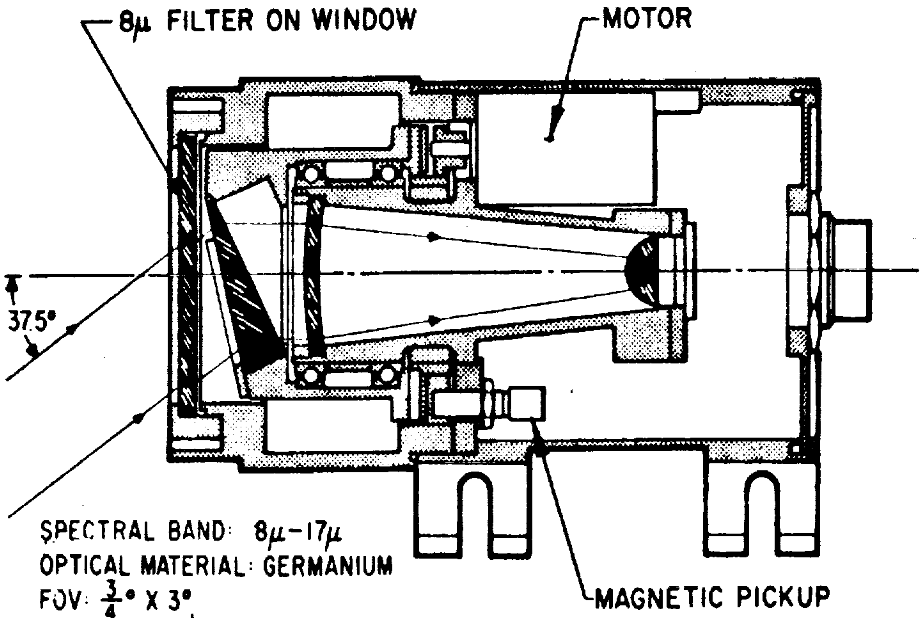
8μ FILTER ON WINDOW
MOTOR
37.5°
MAGNETIC PICKUP

SPECTRAL BAND: 8μ-17μ
OPTICAL MATERIAL: GERMANIUM
FOV: $\frac{3}{4}$° X 3°
APERTURE: $1\frac{1}{4}$"
ROTATIONAL RATE: 30 CPS

Fig. 5.20 SYSTEM B, HEAD LAYOUT

Typical cone half angles vary from 12.5° to 55° according to Spielberger. Representative Conical Scan Configurations are illustrated in Figures 17, 18, 19 and 20, and are some of the advanced configurations mentioned by Spielberger.

5.10 Radiation Balance of Edge Tracking

There is always a strong interest in eliminating the rapidly vibrating and rotating parts of the scanning type of horizon sensor for reliability reasons. The argument for the vibrating sensor is that the same sensing element does the comparing between the light and dark side of the horizon edge. If two sensors are used, one to measure the dark side of the horizon, while the other measures the light side, a sensor comparison error based on the inherent mismatch of sensor biases and gain is introduced. Consequently, there is always a trade-off between the moving part vibrating sensor and the non-moving part sensor pair. So far the moving part sensor continues to win out where high accuracy applications as gyrocompassing prevail.

In the case of edge tracking with a pair of sensors provision must be made to output a monotonic function of horizon error. One solution to this problem is to employ a pair of triangular apertured sensors side by side, with one of the triangles inverted, as shown in Fig. 5.21. By properly ratioing the illumination level outputs produced by areas A and B as shown, a continuous function of the horizon location can be generated in analog signal processing fashion. This function is independent of the value of illumination, i.e., of the amount of earth radiance.

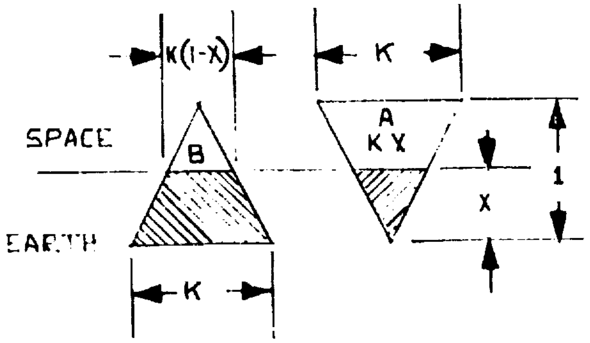

SHADED AREAS (BRIGHT EARTH)

AREA $A = \frac{1}{2}KX^2$

$$\frac{A}{B} = \frac{\frac{1}{2}X}{1-\frac{1}{2}X}$$

AREA $B = K\left(X - \frac{1}{2}X^2\right)$

OR, SOLVING FOR X, $X = \frac{2A}{A+B}$

Fig. 5.21 Triangular Aperture Edge Tracker, Image Plane View of Horizon

According to J. Kruse[1] the principal application problems stem from sensor bias and sensor responsivity mismatch. An attempt at compensating these is mentioned. An offset heat source in the optical path is provided to keep the active junction at ambient temperature when that junction is looking at cold space. The radiation balance detector can be mechanized similarly to the vibrating mirror edge scanner from the standpoint of the total attitude sensor; that is four such detectors can be pointed at 90 degree azimuth spacing, and can be made to slave to the horizon based on some predetermined sensor balance point. This type of attitude sensor is capable of reducing the present 3 to 5 deg errors of conventional radiation balance sensors to errors of less than one degree even with severe earth radiance unbalances on opposite sides of the horizon.

---

[1] "Radiance Compensating Horizon Sensor", John Kruse, Proc. of the First Symposium on I. R. Sensors for G&C, May 1965

CHAPTER IV

FIXED-SITE INDIRECT-GYROCOMPASSING

1. Introduction

It is possible that the first knowledgeable observation of gyroscopic phenomena occured during the lifespan of Sir Isac Newton. At this time considerable interest arose concerning the motion of our planet. As early as 1836 E. Sang[1] suggested that a gyroscope might be used to demonstrate rotation of the earth. In 1852 Jean Bernard Foucault, a French physicist, successfully performed such an experiment. The potential value of the gyroscope as a navigational instrument was certainly realized at this time. But it remained for a German, Hermann Anschutz Kaempfe, to develop and patent the first practical gyrocompass in 1908. He was followed three years later by Elmer A. Sperry of the United States, who developed a slightly different version of the same instrument. Both instruments were designed for nautical navigation. Both utilized a spinning rotor, gimbals, and an off-center weight. The weight essentially served as a plumb, tending to keep the spin axis in the horizontal plane. Thus constrained the spin axis rotated toward true north. It would be correct to say that the north seeking capability of the instrument was dependent upon the dynamic behavior of the gyroscope. The gyroscope would experience precession unless its spin axis were coincident with the horizontal component of the earth's spin vector. Because the distinction between direct and indirect gyrocompassing is a rather subtle one, it is difficult to classify these instruments. Since they are not useful for space systems the issue may be sidestepped; though it appears that they could be analyzed from the point of view of indirect gyrocompassing.

---

[1] E. Sang, Trans. of the Royal Scottish Society, Arts. 4, 1856, 416.

The Anschutz and Sperry types of gyrocompasses still find extensive service as marine navigational compasses. They are less suited for faster moving vehicles and are not as accurate as some of the more modern gyrocompassing schemes. They are, of course, not applicable to extraterrestrial use since they depend upon the force of gravity.

During World War II there appeared a clear need for automatic navigation and guidance systems. For example some German rocketry developed during the war utilized what is commonly called inertial guidance. Following the war the inertial navigation technique proved so promising that its application was extended not only to aircraft but even to marine use, notably the submarine, where it has proved exceedingly valuable.

The basic principle of inertial navigation involves keeping track of the acceleration of the vehicle with respect to inertial space and performing successive integrations to obtain the change in position. Since position, thus obtained, is relative to an inertially fixed coordinate frame; proper transformations are required to relate the inertial position to a meaningful terrestrial position. During the process the acceleration of gravity at the present location is computed and extracted from the measured acceleration in order to obtain acceleration with respect to inertial space. The original approach to the problem led to construction of a small platform which would be attached to the vehicle through a series of gimbals so that its attitude could remain fixed in inertial space regardless of vehicle motion. Gyroscopes were used to stabilize the platform, and accelerometers were mounted on the platform. Present systems are constructed the same way, but the concept of a strapped down system is receiving increased attention today.

Inasmuch as the accelerometers which are used to supply information about vehicle motion are mounted on the platform, it is important that precise knowledge of the initial orientation of the platform is available. One possible method of initial alinement embodies gyrocompassing (indirect gyrocompassing to be precise). Because the primary concern is indeed navigation, tutorial expositions[1] of inertial navigation are commonly developed along lines of the navigation equations and gyrocompassing is included as a supplementary item. The following discussion proceeds along a rather interesting reverse path which assumes that the primary purpose is to provide a continuous and accurate attitude reference for vehicles on the earth's surface, and that information as to position and velocity are available as a slight extension to the logic.

This chapter is intended to develop a concise picture of gyrocompassing with an inertial platform at a fixed site on the earth's surface. Further it deals only with that particular utilization of the platform which does not involve gyroscopes except for stabilization of the platform. Interestingly enough the gyroscopes do not measure the earth's rotation vector.

---

[1] For example, see: Leondes, C. T., Guidance and Control of Aerospace Vehicles, McGraw-Hill, New York, 1963; or Pitman, G. R. Jr., Inertial Guidance, John Wiley & Sons, New York, 1962.

Although such information might be extracted by looking at the torquing currents in the gyroscope servos, this is not commonly done. If other means of holding the platform fixed in inertial space were available, this form of gyrocompassing could function without gyroscopes at all. For this reason the process has been named "indirect gyrocompassing". The process is of special interest for ground alinement of space systems because it requires only the inertial guidance equipment presently on board for space probes, with the possible exception of a requirement for additional computer capability.

It should be stated at this point that although the following logic may appear heuristic, it is none the less rigorous. The process requires exact specification of the desired output conditions. A simple feedback control system is then designed which will have zero error signal only when the desired output does indeed exist. If the feedback system can be shown to be stable over the required range of input and output signals, then it is a practical solution to the problem. This reasoning process is quite commonly employed in the design of control systems. Optimizing over the ensemble of possible control systems is indeed another question. Attempts at reasonable answers to this question will be made in this and other chapters.

The chapter on Indirect Gyrocompassing in Orbit proceeds with a similar development but with slight variations, and the reader may wish to refer to this chapter during or after the reading of the present one. The work done on the in-orbit case is more extensive since the possibilities for mechanization are more varied.

2. Basic Logic

In order to simplify the approach, the first situation to be considered will be that of gyrocompassing with an inertial platform at a fixed location on the earth's equator. The logic to be followed may be outlined as follows.

2.1 Level

The basic requirement of an inertial platform is that it maintains its attitude invariant with respect to inertial space unless intentionally directed to do otherwise. The only practical method of achieving this involves the use of gyroscopes, associated servos, and gimbals. For the present discussion, three single-axis gyroscopes will be assumed located with their input axes orthogonally oriented; one nominally pointed east, one nominally pointed north, and one nominally pointed up. These directions will be designated as x, y, and z, respectively. They constitute the platform reference coordinate frame. Thus the x-gyro and associated servo control rotation about the platform x-axis, and so on. Initially the platform is locally level. If it is to remain level, it must be rotated about its y-axis at a rate equivalent to the earth's rotation rate. This is achieved by an external torquing signal applied to the y-gyro. The platform now rotates with respect to inertial space in a manner equivalent and opposite to the rotation of the earth, and, if everything functions perfectly, it will remain locally level. The process may be termed open loop control.

It is unreasonable to expect perfect functioning of this or any set of hardware. If, in reality, the platform is to remain alined with the true, locally-level, coordinate frame (i.e. the true east, north, and up unit vectors), some mechanism must be provided whereby deviations from the correct alinement may be sensed if they occur. Because the platform is stationary on the earth's surface, accelerometers mounted on the platform offer excellent information about tilt. Indeed only two accelerometers are needed for this; one pointed along the x-axis and one along the y-axis. Should the platform be tilted about the y-axis, for example, the x-pointed accelerometer will measure the local acceleration of gravity times the sine of the tilt angle. For small angles, this is equivalent to gravity times the angle itself. The accelerometer output may be used as an error signal to torque the platform about the y-axis until it is level. A similar argument may be constructed for rotations about the x-platform-axis.

It is possible to operate on the accelerometer error signal with any sort of filter. However, the physical characteristics of the instrument must be considered. Accelerometers of the PIGA type typically indicate velocity at discrete time points, as a result of the readout mechanism. In other words, they might better be called velocity meters, because they supply accurately only the integral of acceleration over a given time period. If this output were multiplied by a gain constant and used to torque the appropriate gyro, the block diagram for the y-axis control would be as depicted in Fig. 2.1.

The total angular misalinement of the platform from the true or local level set is designated ϕ, and is measured from the true set to the platform. Because ϕ is a small angle, it can be dealt with as three independent rotations about the true x, y, and z axes. It is important to keep in mind that all of this analysis is predicated on the assumption that only small angles will be present. A glance at any table of natural functions for angles in radians will satisfy the reader that use of unity for the cosine, and the angle itself for the sine, is accurate to within 10 percent up to 25 degrees. The small angle assumption is not a very limiting one.

The negative sign associated with the gravity acceleration, g, deserves an explanation. If the platform is rotated in the positive sense about the y-axis, this will dip the x-axis of the platform so that the unit vector pointing along that axis now points downward toward the earth. The x-accelerometer will read a fraction of the acceleration of gravity. Since the apparent acceleration of gravity as measured by an accelerometer is upward, the x-accelerometer indicates a velocity in the negative-x direction. If this is used directly to generate a torquing signal it will be a negative signal, which is desired in order to rotate backward along the y-axis and level the platform.

Integrations are represented by a 1/s symbol in keeping with Laplace Transform notation. Signals input to the box labeled "y-gyro" are equivalent torquing signals having dimensions of radians per second. The transfer function for the gyro itself is assumed to be 1/s so that the output of the "gyro" box has the dimensions of radians. Actually, the gyro and associated servo system cannot have a perfect integration, but its behavior for signals within the frequency band of interest is close enough to perfect integration that little error is incurred through this assumption.

Unfortunately the block diagram reveals two integrations in the servo loop, and the system is undamped. In the practical case instrument errors will make the system unstable. Instability may be eliminated through the addition of a minor loop feedback around the accelerometer. An actual measure of acceleration is not physically available except by direct differentiation of the accelerometer (velocity meter) output. But it is possible to apply feedback to the instrument through the mechanism of torquing currents within the PIGA, or to mechanize an equivalent feedback loop within the navigation computer. For this reason, the most practical solution to the stability problem is to alter the block diagram as shown in Fig. 2.2.

2.2 Azimuth

The feedback control allows the platform to maintain itself locally level. It even allows it to level from an initial misalinement. But feedback fromthe azimuth control has not been discussed. To arrive at a suitable mechanization for azimuth control, it is necessary to recall that the platform has been preprogrammed to rotate about the y-axis at earth rate. Let it be assumed that the y-axis rotation is precisely accurate, but that the platform has drifted in azimuth. In order to remain locally level the platform must be rotated about the true north-pointing axis. But with the existance of an azimuth error, the actual rotation of the platform will be about some axis pointing slightly east or west of north. If the azimuth error is a negative rotation from the true set then the y-platfrom-axis points east of north, and as the earth rotates the unit vector directed along this axis will appear to swing upward from the earth's surface. To an observer on the earth, it appears that the platform is developing a positive tilt rotation about the x-axis. The reason for this is as follows. If the only rotation of the platform is about its own y-axis, then this axis itself must remain fixed in inertial space. If the axis points north from a location on the earth's equator, then it will remain locally level because it remains fixed in attitude in inertial space. If, however, the axis is pointed east of north then it fails to experience the required rotation equivalent to the earth's rotation and, because it does remain fixed in inertial space, it appears to rotate in attitude with respect to the earth.

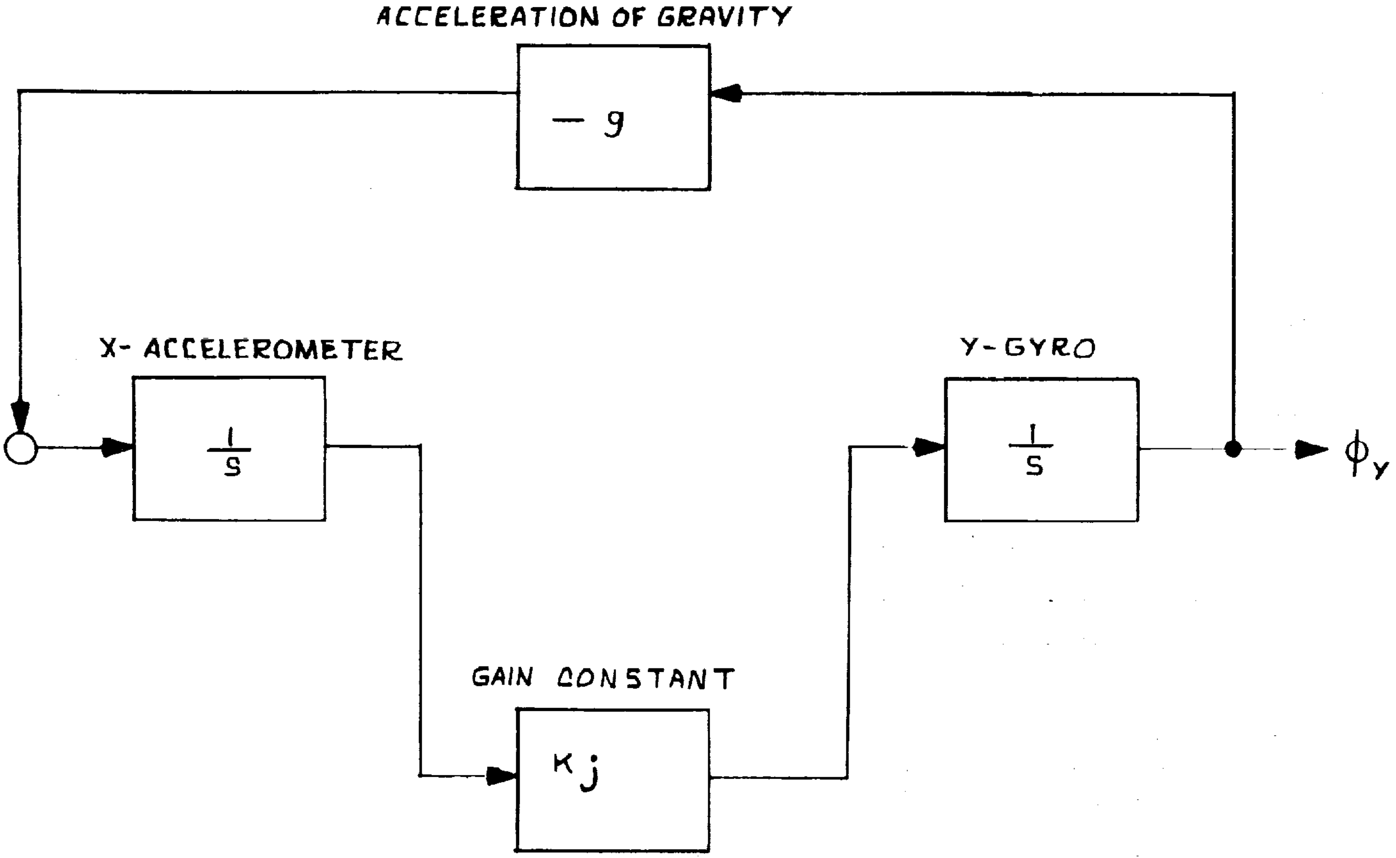
ACCELERATION OF GRAVITY
$-g$
X- ACCELEROMETER
$\frac{1}{s}$
Y-GYRO
$\frac{1}{s}$
ϕ_Y
GAIN CONSTANT
K_j

Fig. 2.1
Block Diagram for Simple Level Mechanism
Associated with the Y-Axis

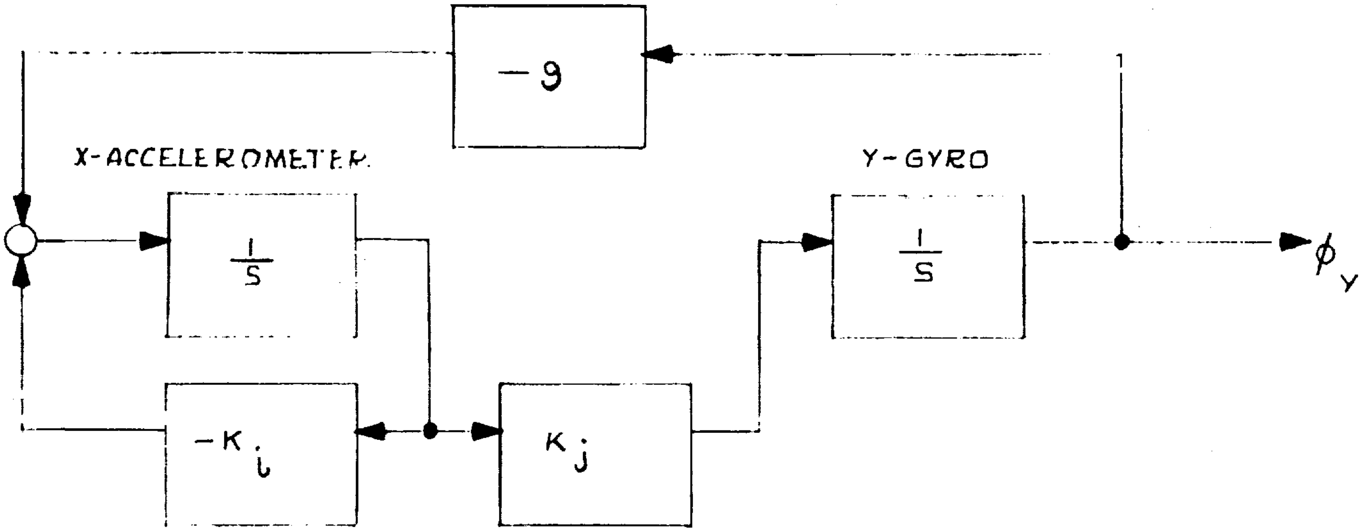
$-g$
X-ACCELEROMETER
$\frac{1}{s}$
Y-GYRO
$\frac{1}{s}$
ϕ_Y
$-K_i$
K_j

Fig. 2.2
Stabilized Level Mechanism for the Y-Axis

It would appear then that the natural solution would be to apply x-axis tilt information as a feedback error signal to control azimuth. The error signal will be zero only if there is no azimuth error, and also no x-axis tilt from other sources. Figure 2.3 shows a block diagram for the x-axis mechanization along these lines.

The gravity constant in the x-channel feedback path is not negative because a positive tilt rotation about the x-axis tends to point the y-axis upward and thus the y-accelerometer will have a positive reading. The negative sign must be supplied externally in order to assure stability. It appears with the constant K_d.

It has already been decided that a negative error rotation about the z-axis will point the y-axis east of north. This will result in an upward tilt of the y-axis, positive tilt rotation about the x-axis, and a positive accelerometer indication in the y-channel. Application of the positive torquing signal to the z-gyro will tend to correct the negative rotational error. The signal path from ϕ_x through to ϕ_z has the proper sign without the addition of any phase inversion.

2.3 Inherent Coupling

The block diagram developed thus far is not entirely accurate. Consideration must be given to the effect of torquing the platform about one of its axes in the presence of a rotational misalinement from the true (i.e. locally level) coordinate set. Let the total platform rotation be described by the vector $\underline{W}$. The misalinement angle will be called ϕ. In terms of small angle notation, the vector $\underline{W}$ may be expressed in matrix form as follows:

$$W^L = B^{LP}\, W^P = \left\{ I + \begin{bmatrix} 0 & -\phi_z & \phi_z \\ \phi_z & 0 & -\phi_x \\ -\phi_z & \phi_x & 0 \end{bmatrix} \right\} W^P \qquad (2.1)$$

where

$$B^{LP} = -\, S^{LP} \qquad (2.2)$$

The superscript L represents the locally level set and P the platform set. The direction cosine matrix is designated as B rather than S because the angle ϕ has been defined as a rotation from the L set into the P set. This is the reverse of the definition for rotation reference given in the chapter on notation. The unit matrix is designated by I.

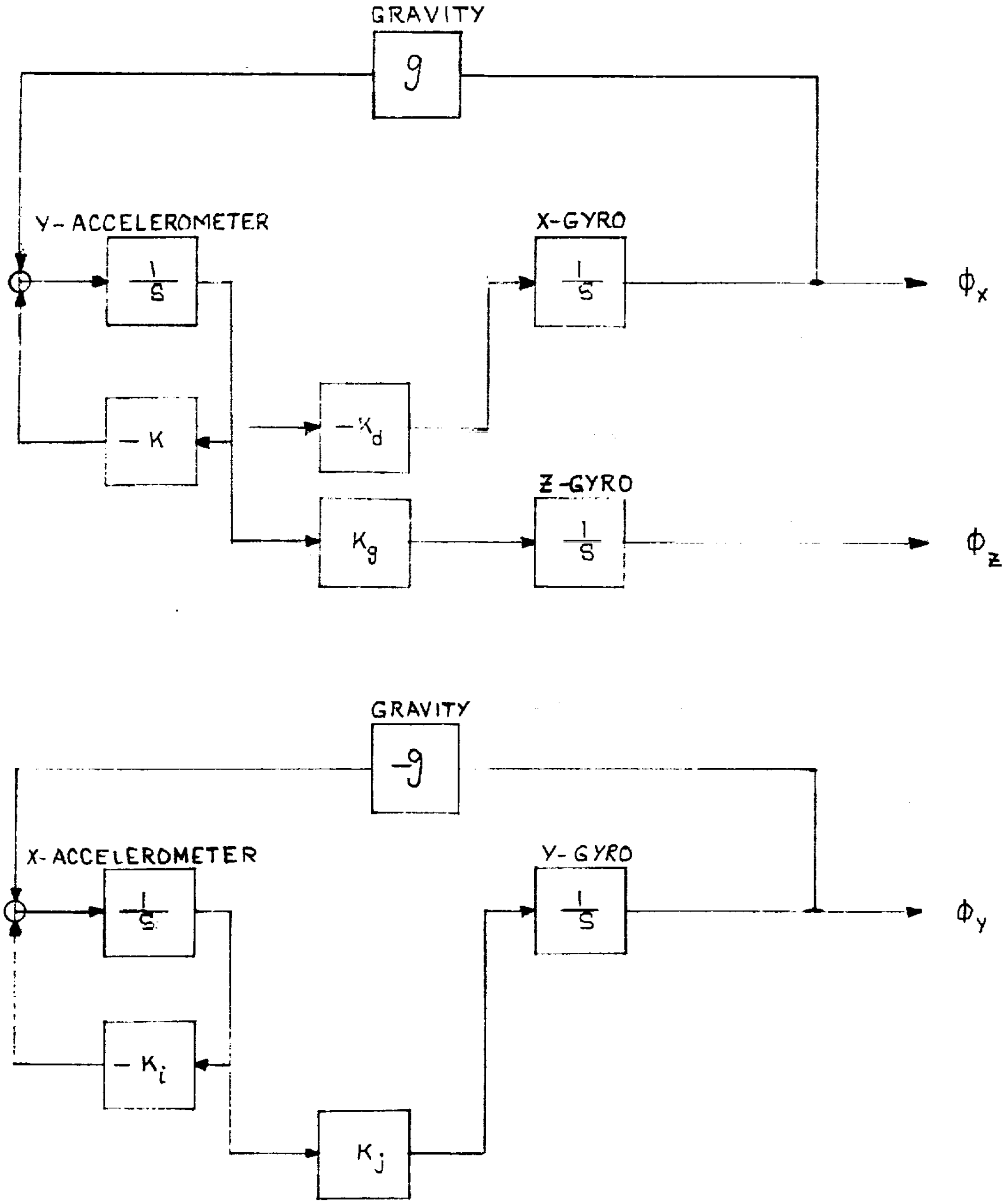
GRAVITY
g
Y- ACCELEROMETER
1/S
X-GYRO
1/S
ϕ_x
− K
$-K_d$
Z-GYRO
K_g
1/S
ϕ_z
GRAVITY
−g
X- ACCELEROMETER
1/S
Y- GYRO
1/S
ϕ_y
$-K_i$
K_j

Fig. 2.3

Block diagram showing leveling loops and coupled azimuth correction. This diagram is not correct yet. Further additions are to be developed in the test.

Equation 2.1 says that the total platform rotation rate expressed in the locally level coordinate frame is essentially equivalent to the total rotational velocity with the misalinement assumed to be zero, plus the vector product of the misalinement angle crossed into the total angular rate. It is important to understand that the cross product involves the total angular rate and not relative rate.

Let it be assumed that the locally level set rotates with a velocity ω with respect to inertial space. Then the velocity difference between the platform and the locally level set is given by:

$$\text{Velocity Difference} = \underline{W} + \underline{\phi} \times \underline{W} - \underline{\omega} \tag{2.3}$$

The angle ϕ is not really a vector but, under the small angle assumption, it may be treated as such.

Figure 2.4 has been drawn to include the cross product coupling due to misalinement and the $\underline{W} - \underline{\omega}$ term. The block diagram has been developed as a model of the actual system mechanization. The inclusion of the $\underline{W} - \underline{\omega}$ error makes it an error block diagram. Other error sources are easily added as inputs to appropriate points of the loop.

2.4 Error Sources

Gyro errors such as random drift rate, gravity dependent drift rate, misalinement induced error, and torquer scale factor are entered as inputs to the gyro box on the block diagram. Accelerometer errors are entered as inputs to the summation point to the left of the accelerometer box. Initial angular misalinement errors are initial conditions on the integrators representing the gyroscope transfer functions. Thus, if a Laplace transform solution is undertaken, initial misalinements may be entered as constants at the left of the gyro transfer functions. Other errors must be entered as Laplace transforms of their time functions.

2.5 Gyrocompassing At A Fixed Point Not on the Equator

The selection of an equatorial point for gyrocompassing has not resulted in loss of generality, but only served to simplify the picture for initial presentation. If the location of the fixed point is not equatorial, the earth's rotation rate must be divided between the y and z platform axes. All of the previous arguments are still valid. However, uncertainty in knowledge of latitude now presents a new error source since it results in improper division of the earth rate vector. Errors in the preprogrammed torquing rate (nominally earth rate) are coupled into all channels whereas they were confined to the ϕ_y channel before.

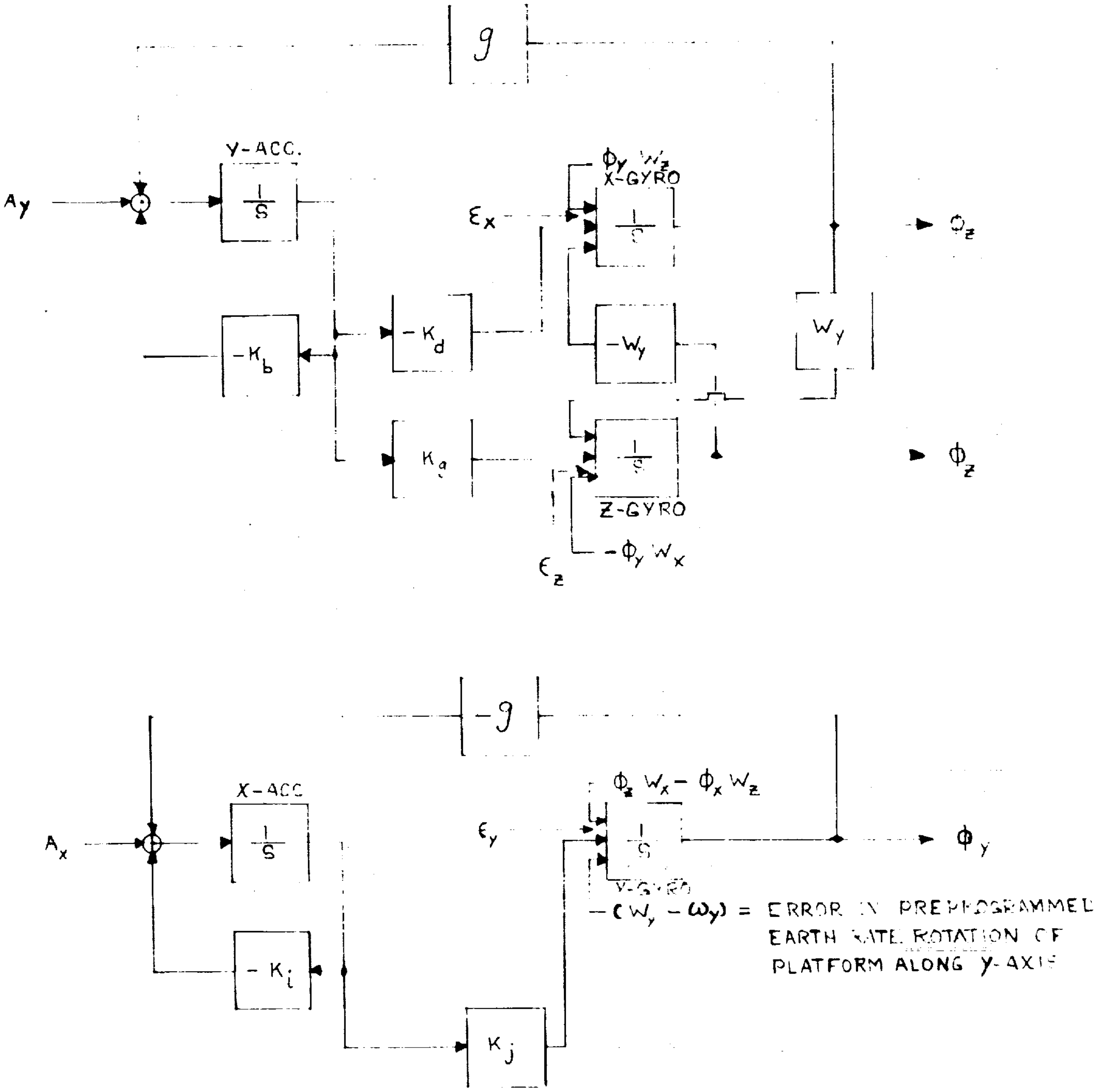
g
Y-ACC.
$\frac{1}{S}$
A_y
ϵ_x
$\phi_y W_z$
X-GYRO
$\frac{1}{S}$
ϕ_z
$-K_b$
$-K_d$
$-W_y$
W_y
K_a
$\frac{1}{S}$
Z-GYRO
$-\phi_y W_x$
ϵ_z
ϕ_z
$-g$
X-ACC
A_x
$\frac{1}{S}$
ϵ_y
$\phi_z W_x - \phi_x W_z$
$\frac{1}{S}$
Y-GYRO
ϕ_y
$-(W_y - \omega_y)$ = ERROR IN PREPROGRAMMED EARTH RATE ROTATION OF PLATFORM ALONG Y-AXIS
$-K_i$
K_j

Fig. 2.4

Complete block diagram showing leveling loops azimuth. The quantities ϵ_x, ϵ_y, ϵ_z and A_x, A_y are discussed later in the text.

It may be noted that the total rotation of the platform is predominately earth rate. The only other platform rotational velocity results from the action of the feedback systems and gyro drift, both of which generate small angular velocities compared to earth rate. At the equator earth rate is entirely represented by W_y. In this case $Ø_y$ is completely uncoupled from $Ø_x$ and $Ø_z$, as can be seen by referral to Fig. 2.4. Thus even if the programmed rotation rate, W_y, is not quite equal to earth rate, the $Ø_y$ feedback system will correct for this and no error in azimuth will result. In fact making the characteristic equation third order through the addition of more filtering eliminates the $Ø_y$ error from this source. When not on the equator this uncoupled situation does not exist, and an error in $\underline{W}$ cannot be corrected. Specifically an error in W_z must appear as an error in $Ø_x$ or $Ø_z$ or both. An undesirable negative rotation rate about the z-axis and an undesirable positive rotation rate about the x-axis produces the same measurable output from the y-accelerometer, namely a positive acceleration reading. The system has no way to distinguish between the two sources. Clearly it cannot precisely eliminate what it cannot identify.

System performance deteriorates as the gyrocompassing location approaches either terrestrial pole. This is not difficult to understand, because at either pole the earth rate vector is vertical. It is easy to level the platform, but because there is no horizontal component of earth rate, azimuth determination is impossible.

2.6 Extension to a Moving Vehicle

This work is not concerned with the problem of a vehicle moving over the surface of the earth. As an interesting digression, however, the previous arguments will be extended to this situation.

The only programmed rotation of a stationary platform was equivalent to earth rate. If the platform is moving additional rotation, equivalent to the velocity over the earth's surface divided by the distance from the center of the earth, (V/R), must be provided. The direction of rotation is the direction indicated by the cross product of $\underline{R}$ into $\underline{V}$. The platform-mounted accelerometers indicate velocity which includes velocity over the earth and the apparent velocity resulting from platform tilt. On normal cruise vehicles the indicated velocity resulting from tilt will be small compared to that resulting from vehicle motion. Thus the output of the accelerometers (better called velocity meters) may be used to compute V/R directly. The radius of the earth, of course, is known.

But the indication of platform tilt is now hopelessly degraded by vehicle velocity. The only effective way to correct this is to have a separate indication of vehicle velocity or platform tilt. The common practice is to employ doppler radar for an indication of true velocity over the surface of the earth. The difference between the accelerometer indicated velocity and the radar indicated velocity is attributed to platform tilt. This signal may be used in the gyrocompassing loop just as in the previous discussion.

Figure 2.5 has been drawn to include the additions for a moving vehicle. It must be remembered that the block diagram has now become an error diagram. The feedback from the ϕ angle is an error. The 1/R box indicates the way in which tilt and accelerometer errors propagate into gyro torque as a result of using the total accelerometer output to compute the V/R rotation rate. The quantity δV_r is used to indicate error in velocity measured by radar. It is entered into the loop at the same point that the total radar-measured velocity is subtracted from the total accelerometer output. The error in accelerometer indicated velocity is designated ΔV. If this is integrated, as shown in the figure, the result is the error in the indicated motion over the earth's surface indicated as Δr for the lack of a better symbol.

The question immediately comes to mind, "Why not use the doppler radar information directly for the computation of V/R?" The answer is that some variations on the basic theme would certainly be possible, but the representation of Fig. 2.5 seems most widely used in practice. It must be borne in mind, that in the inertial navigation problem, gyrocompassing is really an alinement scheme. A vehicle may gyrocompass continuously, or it may run in the free inertial mode without the gyrocompassing loop. In the free inertial mode the platform is controlled open loop. The proper attitude of the platform is determined from the computer estimate of vehicle location. To put it another way the platform is torqued for earth rate and for vehicle motion. The former is apportioned between y and z axes according to the estimated latitude, and the latter is computed as V/R from the accelerometer outputs.

The mechanization depicted in the figure deals only with attitude and heading reference. When moving about on the earth's surface, one wishes to know the latitude and longitude also. The integration of vehicle velocity does not yield such information because one mile eastward motion at 80 degrees latitude does not represent the same longitude change that one mile eastward motion at the equator does. It is necessary for a computer to operate on velocity information to update the computed position of the vehicle. In this manner the computer keeps track of latitude and longitude. With such a mechanization the platform attitude must be strongly correlated with the computer estimate of position. The usual procedure for analysis of this situation involves definition of a third coordinate frame called the computer coordinate set. The three coordinate frames of interest now are the locally level set (often called the true set), the platform set, and the computer set. Accelerometer readings and other information are resolved in the computer coordinate frame. Torque commands for the gyros are computed in the computer coordinate frame. The equivalent of the $\underline{\phi}$ cross $\underline{W}$ coupling still exists; but $\underline{\phi}$ becomes $\underline{\Psi}$, the

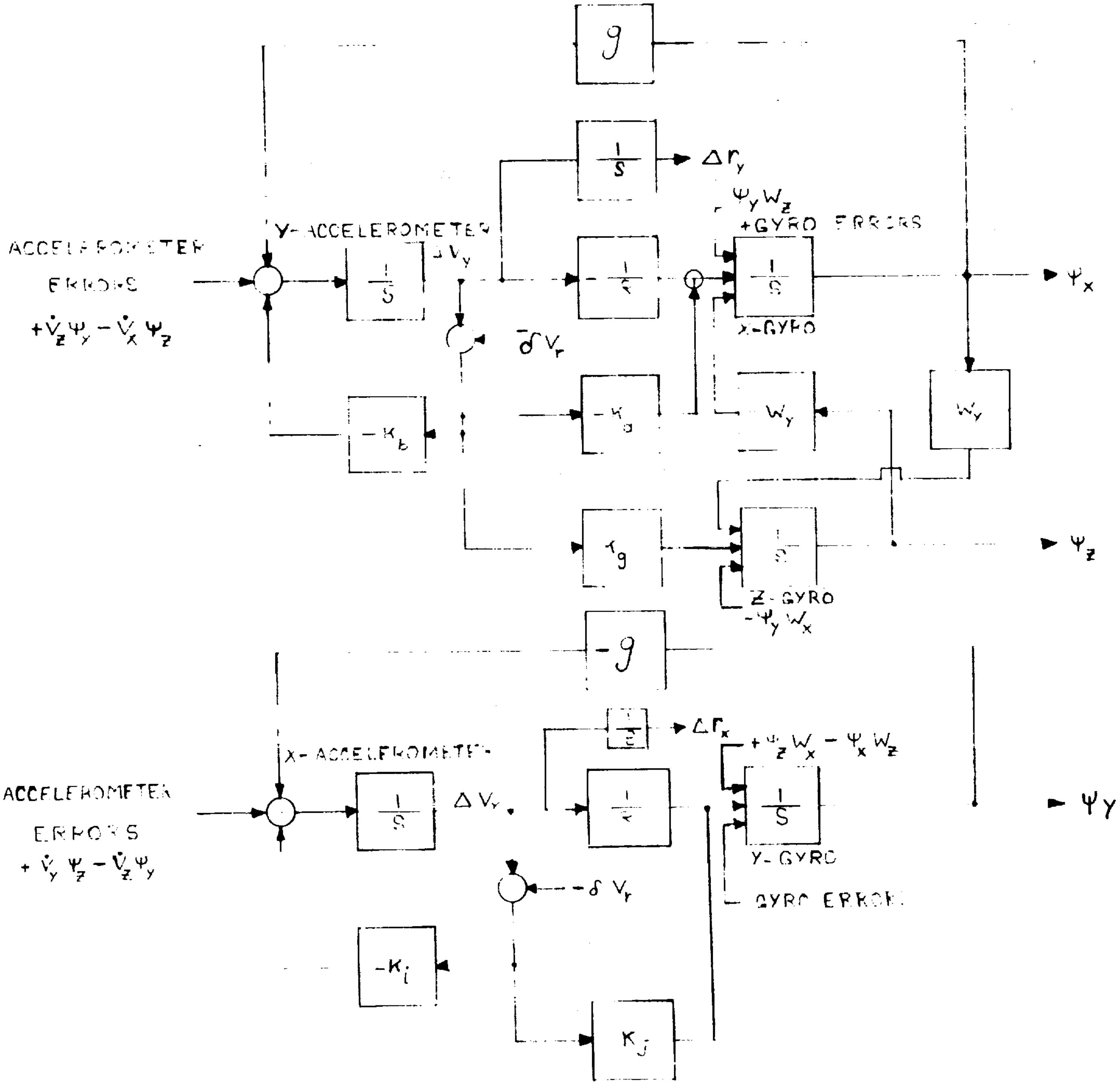
g
$\frac{1}{S}$
Δr_y
$\Psi_y W_z$
+GYRO ERRORS
ACCELEROMETER ERRORS
$+\dot{V}_z \Psi_y - \dot{V}_x \Psi_z$
Y-ACCELEROMETER
ΔV_y
$\frac{1}{S}$
$\frac{1}{R}$
$\frac{1}{S}$
X-GYRO
Ψ_x
$-\delta V_r$
$-K_b$
$-K_a$
W_y
W_y
K_g
$\frac{1}{S}$
Z-GYRO
$-\Psi_y W_x$
Ψ_z
$-g$
$\frac{1}{R}$
Δr_x
$+\Psi_z W_x - \Psi_x W_z$
X-ACCELEROMETER
ACCELEROMETER ERRORS
$+\dot{V}_y \Psi_z - \dot{V}_z \Psi_y$
$\frac{1}{S}$
ΔV_x
$\frac{1}{R}$
$\frac{1}{S}$
Y-GYRO
Ψ_Y
$-\delta V_r$
GYRO ERRORS
$-K_i$
K_j

Fig. 2.5

Error block diagram for gyrocompassing with a nonstationary vehicle. Accelerometer and gyro errors are discussed in the chapter on auxiliary sensors. The angle $\underline{\psi}$ representing misalinement of the platform with respect to the computer is used in place of $\underline{\phi}$. The $-\delta V_r$ is entered at the point where Doppler radar velocity is subtracted from accelerometer indicated velocity.

angle between the computer and the platform measured from the computer coordinate frame; and $\underline{W}$ is the rotation rate computed by the computer. The outputs from the gyro transfer function boxes on the diagram become ψ_x, ψ_y, and ψ_z. The error between computer coordinate frame and the locally level coordinate frame may be described by the angle $\underline{\delta\theta}$, measured from the true locally level set. About the x-axis this is equal to the error in computed latitude. About the y-axis it is equivalent to longitude error times the cosine of latitude. And about the z-axis it is equal to the longitude error times the sine of latitude. In other words,

$$\begin{aligned} \phi_x &= \delta\theta_x + \psi_x \\ \phi_y &= \delta\theta_y + \psi_y \qquad\qquad (2.4) \\ \phi_z &= \delta\theta_y \frac{\text{sin latitude}}{\text{cos latitude}} + \psi_z \end{aligned}$$

The usual accelerometer and gyroscope error sources exist. These have been discussed in the chapter on auxiliary sensors. In addition there is a new error source resulting from the platform misalinement from the computer coordinate frame. The accelerometer measurements are taken in the platform reference coordinates, but they are interpreted in the computer set. The resultant error arises by a mechanism similar to the ϕ cross $\underline{W}$ (now $\underline{\psi}$ cross $\underline{W}$) error, but it is taken in reverse, i.e. $\underline{\dot{V}}$ cross $\underline{\psi}$. The symbol $\dot{V}$ is used to indicate that portion of measured acceleration which results from vehicle motion and not gravity. The error in the portion sensed acceleration which is attributable to gravity is already accounted for by the feedback path from the output of the gyro blocks.

This digression is by no means intended to be definitive on the topic of inertial guidance for moving vehicles. It is intended merely to show the tie between stationary gyrocompassing and nonstationery gyrocompassing on the earth's surface. For more complete information the reader is referred to any standard test on the subject.[1]

3. Comments

3.1 Arbitrarily Oriented Instruments

During the presentation of basic logic some simplifying assumptions were made. It was assumed that the gyros and accelerometers were mounted along the x, y, and z axes of the platform. In fact this requirement is not necessary. The readings of any number of arbitrarily oriented accelerometers may be transformed into equivalent indicated acceleration along the three platform axes. Similarly the gyro torquing commands can be resolved into any coordinate frame, orthogonal or not, which is suited to the actual gyro orientations. Analysis of the system performance then proceeds along precisely the same lines as those of the previous section.

---

[1] Again, the following texts are recommended: Leondes, C. T., Guidance and Control of Aerospace Vehicles, McGraw-Hill, New York, 1963; and Pitman, G.R.,Jr. Inertial Guidance, John Wiley & Sons, New York, 1962.

For general navigation during power flight the only requirement on the accelerometers is that there be at least three pointed in different directions, not all in the same plane. In order to solve the gyrocompassing problem a minimum of two accelerometers, pointing in different directions, is required. The sensitivity of an accelerometer to platform tilts is increased as the input axis approaches the horizontal. However, this may be offset as by instrument deadband which the instrument may exhibit near zero-input acceleration. An optimum location for accelerometers used for gyrocompassing is in the horizontal plane or near it.

If more than a sufficient number of instruments is utilized, an algorithm must be supplied which will indicate how the redundant information is to be used.

Only a slightly greater stretch of the imagination is required to envision a platform stabilized with non-orthogonally oriented gyroscopes. But the resultant complication of the mechanization would be difficult to justify. A minimum of three gyros is required; all three must not be in a plane nor can any two be identically oriented.

What has been said for the elements is also true for the platform. An imaginary platform can be defined in the computational program. The actual platform can be arbitrarily oriented. Sensed acceleration information may be transformed into the imaginary platform coordinate frame. The proper gyro commands may be originated in the imaginary platform coordinate set and transformed back to the platform (or gyro) coordinate frame. There is no problem here, but excessive computation is required. Whereas a minimum of computer capability is required when the platform is oriented locally level, and the gyros and accelerometers are alined along the platform axes as assumed during earlier discussions.

3.2 Variations on the Loop Transfer Function

The block diagram of Fig. 2.4 is really the simplest mechanization available for the usual inertial platform utilizing pendulous integrating gyro accelerometers (PIGA) and single (or double) axis gyros. The integration associated with the accelerometers is inherent in the readout mechanism. The feedback around the accelerometers may be accomplished by a torquing current in the PIGA. The other integrations are inherent in the gyroscopes. Accelerometer outputs are digitalized. These must be multiplied by the appropriate gains and applied to the appropriate gains and applied to the appropriate gyro torquing mechanisms. The performance of this operation does not really entail use of a computer in the real sense of the word. If arbitrary orientations are chosen for the instruments and/or the platform orientation, then a small computer would be required, but essentially this system functions without the requirements for a navigation computer.

Now that the basic philosophy of the indirect gyrocompassing or closed loop at a fixed point on the earth has been outlined, the servo engineer can recognize that it is possible to alter the loop transfer function through the introduction of other filtering functions. For instance if an accelerometer were available which gave a direct reading of acceleration, the initial 1/s with minor loop feedback would not be necessary. The sensed acceleration could be applied directly to the gyro torquing motors. The accelerometers are only supplying a measure of platform tilt, and unlike the navigation gyrocompassing does not require knowledge of velocity or position. The accelerometers on the ground perform the equivalent function of the horizon sensor in orbit. Reference to the chapter on indirect orbital gyrocompassing will illustrate other possible mechanizations.

One important problem associated with accelerometers capable of large g measurement is that of deadband or non-linear performance near zero g. It is possible that bubble levels or pendulums may prove more satisfactory for platform alinement. Such instruments do not have an inherent integration, but provide a direct indication of angle. This means that any of the other filters discussed later in Chapter VII are applicable. Case 4 of that chapter deserves particular attention as being the simplest mechanization for the direct angle reading instrument.

Obtaining an optimum over the ensemble of all possible mechanizations would be quite tedious. However, the mechanization of Fig. 2.4 seems to be a reasonable solution. An improvement to this would be the used of advanced filtering techniques such as Kalman filtering and others. These approaches do require digital computer. Their primary value lies in rapidity of alinement, for example six to ten minutes. The Fig. 2.4 system will provide comparable alinement in 35 to 40 minutes which is no problem for prelaunch alinement of space vehicle platforms.

It should be emphasized here that the final accuracy is to a considerable degree bounded by the quality of the equipment used. Neither the approach of Fig. 2.4 nor advanced time varying coefficient filtering techniques will achieve the same results with poor accelerometers and gyroscopes as they will with good ones.

4. Examination of the System Common to Cruise Vehicles

The system developed in Section II and depicted in Fig. 2.4 is in widespread use with inertial navigation systems for terrestrial cruise vehicles, where it appears to be a simple and reasonable approach campatibel with existing equipment. Further attention will be focused on this system.

4.1 Characteristic Equation and Final Error Values

When gyrocompassing is performed at a stationary point not on the equator, the $\underline{\phi}$ cross $\underline{W}$ term provides coupling between the ϕ_y and ϕ_x, ϕ_z channels. This means that, in the general case, determination of the characteristic equation is somewhat involved. System behavior is easily analyzed with an electronic computer. Either an analog or digital computer is suitable, but the digital computer offers greater accuracy and ease of treatment of correlated noise.

The behavior of the system may be understood by considering the equatorial case. On the equator ϕ_x and ϕ_z are uncoupled from ϕ_y. The only important platform rotational velocity is W_y which is equal to earth rate. Under these conditions the following equations describe the ϕ_x, ϕ_y channel. Laplace Transform notation is used. The caret over certain quantities indicates that the quantities are to be interpreted as Laplace Transforms of their time functions.

$$\hat{\phi}_x = \frac{s + K_b}{A(s)} \quad s(\hat{\varepsilon}_x + \phi_{xo}) - W_y(\hat{\varepsilon}_z + \phi_{zo}) - \frac{sK_d + W_y K_g}{s + K_b} A_y \qquad (4.1)$$

$$\hat{\phi}_z = \frac{s + K_b}{A(s)} \quad \left(W_y + \frac{K_g g}{s + K_b}\right) (\hat{\varepsilon}_x + \phi_{xo}) + \left(s + \frac{K_d g}{s + K_b}\right) (\hat{\varepsilon}_z + \phi_{zo})$$

$$+ \left(\frac{sK_g - W_y K_d}{s + K_b}\right) A_y \qquad (4.2)$$

$$A(s) = s^3 + K_b s^2 + (gK_d + W_y^2) s + W_y^2 K_b + W_y gK_g \qquad (4.3)$$

Behavior of the ϕ_y channel is described by,

$$\hat{\phi}_y = \frac{1}{B(s)} \quad (s + K_i) (\hat{\varepsilon}_y + \phi_{yo}) + K_i A_x \qquad (4.4)$$

$$B(s) = s^2 + K_i s + gK_j \qquad (4.5)$$

The Epsilon ($\hat{\varepsilon}$) quantities are inputs to the loop just before the gyro indicated by the subscript. Primarily the epsilons may be thought of as the Laplace Transforms of constant gyro drift. This may include gravity dependent drift rates, which because the motion of the platform relative to the gravity vector will be small and may be neglected. By the same token drift rate resulting from individual axis misalinement may be included; under the assumption that the principle motion of the platform is equal to earth rate and is essentially constant even in platform coordinates.

The ϕ_{xo}, ϕ_{yo}, and ϕ_{zo} quantities represent initial values of platform misalinement. These are assumed to enter the loop at the input to the gyro transfer functions. In this case the 1/s of the gyro provides the 1/s required for the Laplace transform, and the ϕ_o quantities in Eq 4.1 through 4.5 are simple numbers. The $\hat{a}$ quantities represent accelerometer errors such as bias. Again only independent error sources may be used with these equations.

Examination of the final values of platform misalinement resulting from the error sources may be informative. To obtain final values let $\hat{\varepsilon}$ and $\hat{a}$ be ε/s and a/s which would be the case for a constant gyro drift rate, and a constant accelerometer bias. The Final Value Theorem requires that the function be multiplied by s and the limit taken as s approaches zero. This yields the following results:

$$\phi_x \text{ Final Value} = \frac{K_b}{W_y K_b + K_g g} \quad - \varepsilon_z \; \frac{-K_g}{K_b} \; A_y \tag{4.6}$$

$$\phi_z \text{ Final Value} = \frac{\varepsilon_x}{W_y} + \frac{K_b}{W_y K_b + K_g g} \; \frac{K_d g \varepsilon_z}{W_y K_b} - A_y \tag{4.7}$$

$$\phi_y \text{ Final Value} = \frac{K_i}{g K_j} \left(\varepsilon_y + A_x\right) \tag{4.8}$$

It can be seen that initial misalinement errors vanish, but instrument errors propagate into alinement errors. Also of note is the fact that the rotation rate W_y does not appear in the final value of ϕ_y.

On the other hand the final value of ϕ_z includes the term ε_x/W_y, and no adjustment of gain constants can alter this. One way to satisfy oneself that this is reasonable is to consider the situation where the platform has a small offset angle ϕ'_z. Now if the platform is locally level, and if it is to remain locally level, it should be torqued about its own x-axis at a rate equivalent to $W_y \phi_z$. Normally this would not be done, and therefore the platform would not remain level and the accelerometers would sense an error. However if the x-gyro has a constant drift rate of $W_y \phi_z$ then the platform can remain level even in the face of the azimuth error. Indeed, the azimuth error is required in order to maintain level.

Consider the case with a constant drift rate about the z-axis. In general this case will propagate into a constant error in both azimuth and tilt about the x-axis. This accrues in the following fashion. If the azimuth error is to remain constant, sufficient feedback signal must be present to cancel the drift of the z-gyro. As may be seen from Fig. 2.4, there are two feedback paths from ϕ_x to ϕ_z, so that the following equation may be written for the steady state.

$$-W_y \phi_x - \frac{gK_g}{K_b} \phi_x = \varepsilon_z$$

$$\phi_x = \frac{-K_b}{W_y K_b + gK_g \varepsilon_z} \qquad (4.9)$$

The sum of the steady state feedback signals into the x-gyro is,

$$W_y \phi_z + \frac{gK_d}{K_b} = 0 \qquad (4.10)$$

Substitution of Eq 4.9 into Eq 4.10 produces

$$\phi_z = \frac{gK_d}{W_y (W_y K_b + gK_g)} \varepsilon_z \qquad (4.11)$$

Suppose that the feed around the accelerometer were a feed forward instead of backward. The transfer function for this part of the system would then be $(1/s) + K_b$. The circuit would still be stable, and the perfect integration would provide a self-biasing mechanism. Such a forward feed might not be easy with the PIGA. In any event since the output of the integrator can be other than zero when ϕ_x is zero, it can provide a corrective bias to compensate for a finite z-gyro drift. The sum of drift rates into the z-gyro would be

$$K_g \text{ (integral)} + \varepsilon_z = 0 \qquad (4.12)$$

The value of the integral must be $-\varepsilon_z/K_g$, under the assumption that ϕ_x was equal to zero. Summing the drift rate signals at the x-gyro yields

$$\phi_z = \frac{K_d}{K_g W_y} \epsilon_z \tag{4.13}$$

So it is clear that, with the integral plus proportional filter, it would be possible to cancel out a constant z-gyro drift rate through the self-biasing mechanism without the requirement for any final ϕ_x error.

As a parenthetical note, it must be admitted that these comments are only rigorous for system representation of Fig. 2.4 without added cross coupling. However the effect of cross coupling arising from gyro axes misalinements and operation slightly north or south of the equator will be small enough as to create no major discrepancies with the foregoing observations.

The discussions of the preceding few paragraphs have been presented only to emphasize a precept well known to servo engineers. That is that a feedback system can be tailored for optimum performance in the face of any disturbance, given that the form of the disturbance is known. Often such tailoring degrades some other aspect of performance.

5.0 Performance and Sensitivity Coefficients

When the system of Fig. 2.4 is used in cruise vehicles, the choice of constants is usually made on the basis of desired system time constants. From this point of view the system equation for a third order system would be written as

$$\left(s + \frac{1}{T_2}\right)\left(s^2 + \frac{2}{T} s + \frac{1}{T^2 \zeta^2}\right)$$

$$= s^3 + \left(\frac{2}{T} + \frac{1}{T_2}\right) s^2 + \left(\frac{2}{TT_2} + \frac{1}{T^2 \zeta^2}\right) s + \frac{1}{T_2 T^2 \zeta^2} \tag{5.1}$$

The problem of system parameter adjustments is considered in more detail in Chapter VII. The large number of error sources, including noise sources, makes it difficult if not impossible to say anything generally definitive on the subject. One must treat each case individually. Selection of system parameters will inevitably lead to a trade-off between sensitivity to instrument errors and sensitivity to noise inputs.

5.1 Computer Simulation

The time response resulting from error analysis on the 7094 IBM digital computer is presented in Appendix A. For this simulation all the cross coupling terms discussed in the previous work were included.

The outputs are in graphic form with titles indicating the error source responsible for the indicated output. Error sources are assumed to be r.m.s. values for quantities having zero mean. The displayed outputs are likewise r.m.s. quantities naturally.

Error models for the instruments are those presented in the chapter on auxiliary sensors. However most of the gravity dependent terms vanish because of the instrument configuration.

Figure 5.1 describes the instrument configuration.

Launch point is assumed to be the Atlantic Missile Range at latitude 28.6 degrees north.

The system equation is as follows. It is sixth order because of the inclusion of all cross coupling terms associated with the $\Psi \times \underline{W}$ terms.

$$\begin{aligned} & s^6 + 0.01978\, s^5 + 1.756 \times 10^{-4}\, s^4 + 8.811 \times 10^{-7}\, s^3 \\ & + 2.619 \times 10^{-9}\, s^2 + 4.355 \times 10^{-12}\, s + 3.137 \times 10^{15} \\ & = (s + 3.359 \times 10^{-3} + j\, 2.42. \times 10^{-3})\,(s + 3.359 \times 10^{-3} - j\, 2.42. \times 10^{-3}) \\ & \quad (s + 3.308 \times 10^{-3} + j\, 2.576 \times 10^{-3})\,(s + 3.308 \times 10^{-3} - j\, 2.576 \times 10^{-3}) \\ & \quad (s + 3.225 \times 10^{-3} + j\, 1.999 \times 10^{-4})\,(s + 3.225 \times 10^{-3} - j\, 1.199 \times 10^{-4}) \end{aligned} \tag{5.2}$$

It will be noted that all time constants are of the order of five minutes. The damping factor is equal to 0.8. This means that alinement time will be in the order of half an hour, which is a reasonable figure.

All of the r.m.s. output quantities scale directly with the magnitude of the r.m.s. error source except the correlation time associated with correlated noise. In the case of noise amplitude scales, but autocorrelation time does not.

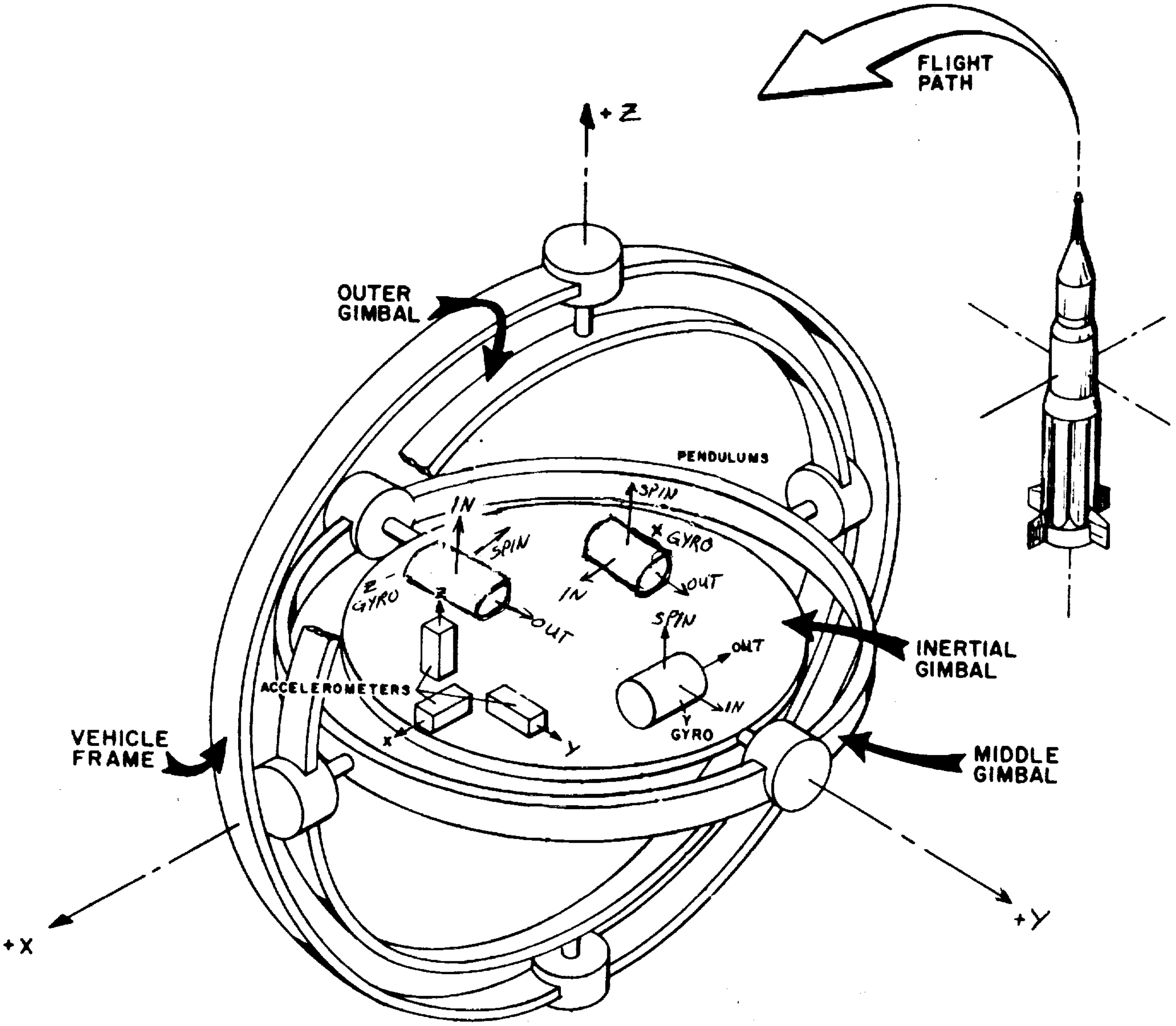
FLIGHT PATH
+Z
OUTER GIMBAL
PENDULUMS
IN
SPIN
SPIN
X GYRO
Z GYRO
Z
IN
OUT
OUT
SPIN
OUT
ACCELEROMETERS
IN
Y GYRO
X
Y
INERTIAL GIMBAL
VEHICLE FRAME
MIDDLE GIMBAL
+X
+Y

Fig. 5.1 Instrument Configuration

CHAPTER V

DIRECT TERRESTRIAL GYROCOMPASSING

1. The Strapdown System

In the foreseeable future space probes may be equiped with strapped down or modified strapped inertial guidance systems. In such a system the accelerometers and gyroscopes are firmly affixed to the vehicle body. Such systems will require initial alinement before launching, and for this purpose gyrocompassing may prove useful. The process would fit under the definition of Direct Gyrocompassing since direct measurement of earth rate and gravity would be used to provide a direction cosine matrix relating vehicle coordinates to north, east, and local vertical. An investigation of the general procedure follows.

1.1 Gyroscopes

The gyroscopes may be of two kinds - the single axis platform and the full strapped down rate gyro.

The single axis platform was discussed in chapter three. Fig. 2.1 of chapter three presents a schematic representation of such an instrument. Equation (2.5) of chapter three is the input axis equation. The gyroscope ideally does not rotate about its input axis, (with respect to inertial space). Therefore the vehicle rotation about the input axis may be measured by observing the rotation of the input axis gimbal with respect to the vehicle.

The full strapped down gyro is similar to the single axis platform of Fig. 2.1, chapter three but without the outer gimbal. The spin axis is maintained in proper relation to the pickoff by externally applied torque about the output axis. The magnitude and direction of this torque is a measure of the vehicle rotation about the input axis.

Both instruments are generically similar. The full strapped down instrument has fewer moving parts, but the single axis platforms will have no more gimbals than the accelerometers if pendulous integrating gyro accelerometers are used. Figure 1.1 indicates schematically a configuration for three single axis platforms in a strapped down system. Accelerometers would be located along the same axes.

2. Coordinate Transformations in Strapped Down Systems

While Fig. 1.1 depicts an orthogonal orientation there is no real constraint of this nature. Instruments may be arbitrarily located provided that there is sufficient number to provide all the information about the rotation of the acceleration vector. For instance all the gyroscopes may not be in one plane; because they will not provide information on rotation directed orthogonal to that plane. If there are more than a sufficient number of instruments, arbitrary decisions must be made as to how to treat the information from each.

In general three gyros and three accelerometers will be used. Consider the case of three gyros arbitrarily oriented. The problem is to make use of the information from each. Let the vehicle coordinate frame be designated by the superscript v. The gyro coordinate frames will be g_1, g_2, and g_3. It is not difficult to obtain a direction cosine matrix S^{g_1v} which rotates quantities from vehicle coordinates into the g_1 coordinate frame. Similarly, there exist S^{g_2v} and S^{g_3v}. Each gyro coordinate frame will be defined such that the input axis of the instrument lies along the x-axis of its coordinate frame. Since the instrument will measure only that component of rotation which is directed along its input axis, the only important rows of the S^{gv} matrices are the first rows. Other rows pertain to the instrument y and z axes and not the input axes.

The three input axes of the three instruments form a coordinate frame which in the general case will be non-orthogonal. None the less any vector may be uniquely defined by its components along the input axes provided the axes do not all lie in a plane and no two are parallel. Let the matrix which transforms a column matrix from the vehicle frame into the coordinate frame of input axes be designated $(Q^g)^{-1}$. It is composed of the rows of the S^{gv} matrices. The first row of $(Q^g)^{-1}$ is the first row of S^{g_1v}; the second row is the first row of S^{g_2v}; and the third row is the first row of S^{g_3v}. Now the inverse of $(Q^g)^{-1}$ is the matrix which transforms the outputs, or angular rate measurements, of the three gyros uniquely into the total vehicle angular-rotation-vector in terms of vehicle coordinates. Let this be designated Q^g. In the special case where the instrument input axes are orthogonal, the $(Q^g)^{-1}$ matrix is orthogonal, and $(Q^g)^{-1}$ equal $(Q^g)^T$. By similar logic, S^{av} and Q^a may be found for the accelerometers.

The S^{av} and S^{gv} matrices must be used to transform gravity and earth rotation rate into the instrument coordinate frames for formation of the instrument error models. The instrument error models are constructed in the instrument's own coordinate frame using the error model equations given in the chapter on auxiliary sensors. The instrument error is expressed as a spurious reading. This output is transformed into vehicle coordinates via the proper Q matrix.

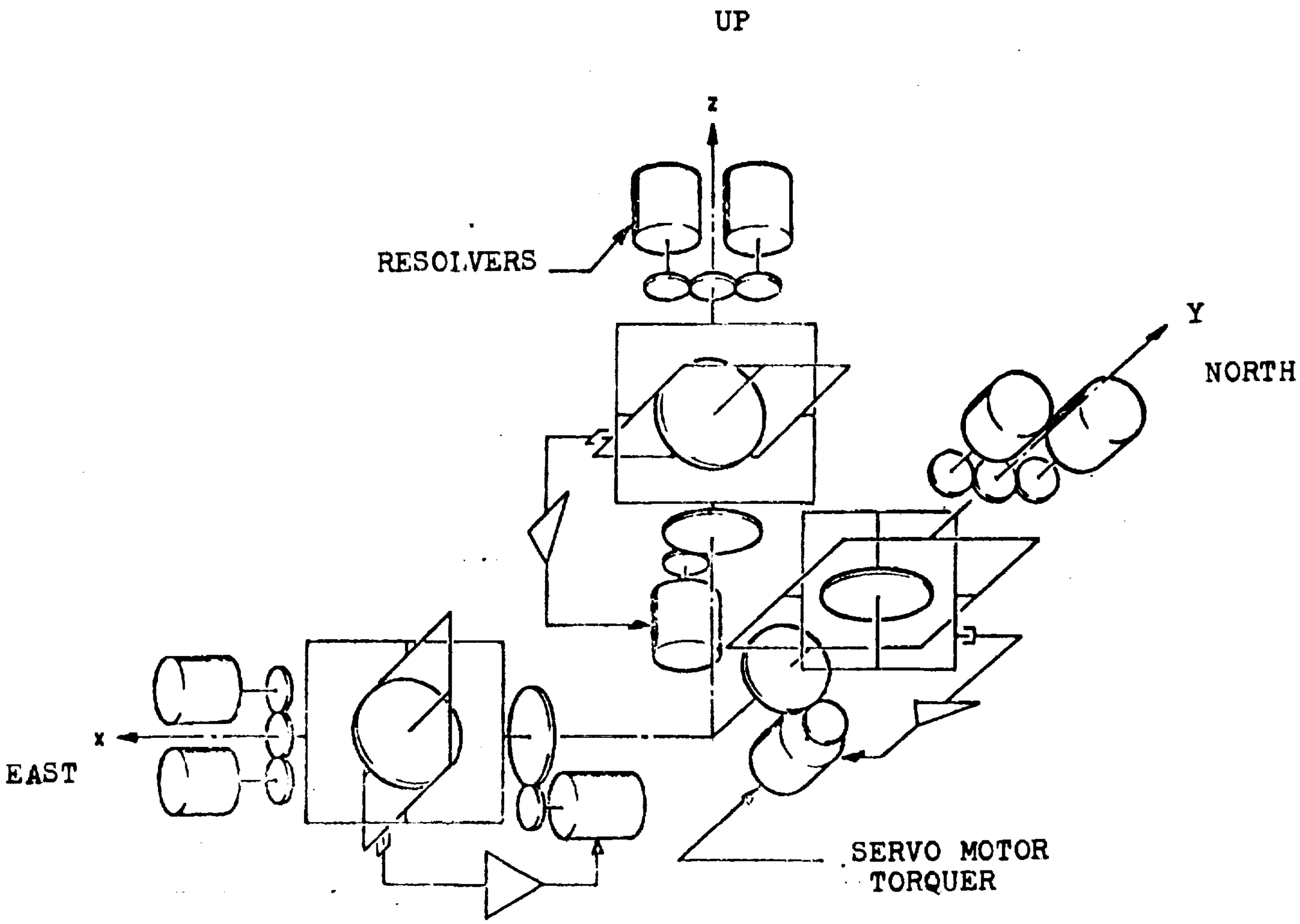
UP
z
RESOLVERS
Y
NORTH
x
EAST
SERVO MOTOR
TORQUER

Fig. 1.1 Three Single Axis Platform Configuration for a Strapped Down System

The accelerometers actually measure the acceleration of gravity plus the centripetal acceleration resulting from the earth's rotation. The latter is small and may safely be ignored. Gravity anomalies resulting from oblateness of the earth may be larger, but these will be also neglected. The gravity measured by the accelerometers, but displayed in vehicle coordinates will be assumed to present a sufficiently accurate indication of the local vertical. This will be true for any space vehicle launches presently envisioned. The gyroscopes are used to measure the total earth rate vector, Ω , in vehicle coordinates.

Since the accelerometers will indicate gravity as an upward acceleration, the vector $\underline{G}$ will be assumed to be directed upward and coincident with the z-axis of the earth-fixed locally-level coordinate set. Easterly direction is indicated by the vector product of earth rate and $\underline{G}$. The direction of north completes the triad which may be described by the following equations.

$$G^v = G^v \tag{2.1}$$

$$E^v = \tilde{\Omega}^v G^v \tag{2.2}$$

$$N^v = \widetilde{(\tilde{\Omega}^v G^v)} G^v = (\underline{\Omega} \times \underline{G}) \times G \tag{2.3}$$

The superscript v indicates that the superscripted quantity is expressed in the vehicle coordinate system.

There exists some direction cosine matrix which rotates the locally level set into the vehicle set. This shall be designated S^{vL}. It is easily obtained by recognizing that if the components of $\underline{G}$ in vehicle coordinates are normalized, they themselves constitute the direction cosines which rotate the true local vertical into the vehicle triad. The matrix S^{vL} is then composed as follows.

$$\left.\begin{aligned}
\frac{G^v}{\|G\|} &= \text{the third column of } S^{vL} \\
\frac{E^v}{\|E\|} &= \frac{\tilde{\Omega}^v G^v}{\|\underline{\Omega} \times \underline{G}\|} = \text{the first column of } S^{vL} \\
\frac{N^v}{\|N\|} &= \frac{\widetilde{(\tilde{\Omega}^v G^v)}\, G^v}{\|(\underline{\Omega} \times \underline{G}) \times \underline{G}\|} = \text{the second column of } S^{vL}
\end{aligned}\right\} \tag{2.4}$$

The double vertical lines indicate absolute value.

3. Errors

The mechanization is now in hand. How does the error analysis procede? The error models for accelerometers and gyros have already been discussed. In order to simplify the following discussion, the accelerometer errors will be limited to constant bias, B; scale factor error, F_1; and misalinement errors, β_y and β_z. Gyro error sources will be limited to long time correlation (i.e., nearly constant) drift rate, η ; misalinement angles, β_y and β_z; and a scale factor error which shall be called k.

The error matrix for one accelerometer may be written as follows, where ΔG_x, ΔG_y, and ΔG_z are errors in the components of the gravity vector $\underline{G}$ in vehicle coordinates.

$$\begin{bmatrix} \Delta G_x \\ \Delta G_y \\ \Delta G_z \end{bmatrix}^{v}_{\text{from } a_1 \text{ only}} = Q^{a} \begin{bmatrix} 1 & G_x & G_z & -G_y \\ 0 & 0 & 0 & 0 \\ 0 & 0 & 0 & 0 \end{bmatrix}^{a_1} \begin{bmatrix} B \\ F_1 \\ \beta_2 \\ \beta_3 \end{bmatrix} \qquad (3.1)$$

This may be rewritten as:

$$\begin{bmatrix} \Delta G_x \\ \Delta G_y \\ \Delta G_z \end{bmatrix}_{\text{from } a_1 \text{ only}} = \begin{bmatrix} Q^{a}_{11} & Q^{a}_{11}G^{a_1}_{x} & Q^{a}_{11}G^{a_1}_{z} & -Q^{a}_{11}G^{a_1}_{y} \\ Q^{a}_{21} & Q^{a}_{21}G^{a_1}_{x} & Q^{a}_{21}G^{a_1}_{z} & -Q^{a}_{21}G^{a_1}_{y} \\ Q^{a}_{31} & Q^{a}_{31}G^{a_1}_{x} & Q^{a}_{31}G^{a_1}_{z} & -Q^{a}_{31}G^{a_1}_{y} \end{bmatrix} \begin{bmatrix} B \\ F_1 \\ \beta_2 \\ \beta_3 \end{bmatrix}^{a_1} \qquad (3.2)$$

The superscripts v and a_1 refer to vehicle coordinates and accelerometer number one respectively. The components of gravity $G^{a_1}_{x}$, $G^{a_1}_{y}$, and $G^{a_1}_{z}$ are the components in the number one accelerometer coordinate frame. It is necessary to transform them into this frame from the locally level set via the S^{alv} matrix and the S^{vL} matrix. This, of course, means that the nominal value of S^{vL} must be known in order to proceed with the error analysis. A similar approach leads to an error matrix for each gyroscope, and the aggregate may be written as given by Eq. (3.3) on the following page.

The large rectangular matrix may be partitioned into sections pertaining to each instrument. Let this matrix be designated as M. In the same manner, the long column matrix at the right may be partitioned into sections pertaining to each instrument. This naturally corresponds to the partitioning of the M matrix. Let the column matrix be designated γ . The treatment of the instruments must be kept separate because the instrument error sources are uncorrelated from one instrument to the next.

$$\begin{bmatrix} \Delta\Omega_x \\ \Delta\Omega_y \\ \Delta\Omega_z \\ \Delta G_x \\ \Delta G_y \\ \Delta G_z \end{bmatrix} = \begin{bmatrix} Q^g{}_{11} & Q^g{}_{11}\Omega^{g1}_x & Q^g{}_{11}\Omega^{g1}_z & -Q^g{}_{11}\Omega^{g1}_y \\ Q^g{}_{21} & Q^g{}_{21}\Omega^{g1}_x & Q^g{}_{21}\Omega^{g1}_z & -Q^g{}_{21}\Omega^{g1}_y \\ Q^g{}_{31} & Q^g{}_{31}\Omega^{g1}_x & Q^g{}_{31}\Omega^{g1}_z & -Q^g{}_{31}\Omega^{g1}_y \\ 0 & 0 & 0 & 0 \\ 0 & 0 & 0 & 0 \\ 0 & 0 & 0 & 0 \end{bmatrix}$$

$$\left|\begin{array}{cccc|c}
Q^g_{12} & Q^g_{12}\Omega^{g2}_x & Q^g_{12}\Omega^{g2}_z & -Q^g_{12}\Omega^{g2}_y & Q^g_{13} \\
Q^g_{22} & Q^g_{22}\Omega^{g2}_x & Q^g_{22}\Omega^{g2}_z & -Q^g_{22}\Omega^{g2}_y & Q^g_{23} \\
Q^g_{32} & Q^g_{32}\Omega^{g2}_x & Q^g_{32}\Omega^{g2}_z & -Q^g_{32}\Omega^{g2}_y & Q^g_{23} \\
0 & 0 & 0 & 0 & 0 \\
0 & 0 & 0 & 0 & 0 \\
0 & 0 & 0 & 0 & 0
\end{array}\right.$$

53 ②

$$\begin{array}{ccc|ccc}
Q^{g}_{13}\Omega^{g3}_{x} & Q^{g}_{13}\Omega^{g3}_{z} & -Q^{g}_{13}\Omega^{g3}_{y} & 0 & 0 & 0 \\
Q^{g}_{23}\Omega^{g3}_{x} & Q^{g}_{23}\Omega^{g3}_{z} & -Q^{g}_{23}\Omega^{g2}_{y} & 0 & 0 & 0 \\
Q^{g}_{33}\Omega^{g3}_{x} & Q^{g}_{33}\Omega^{g3}_{z} & -Q^{g}_{33}\Omega^{g3}_{y} & 0 & 0 & 0 \\
0 & 0 & 0 & Q^{a}_{11} & Q^{a}_{11}G^{a1}_{x} & Q^{a}_{11}G^{a}_{z} \\
0 & 0 & 0 & Q^{a}_{21} & Q^{a}_{21}G^{a1}_{x} & Q^{a}_{21}G^{a}_{z} \\
0 & 0 & 0 & Q^{a}_{31} & Q^{a}_{31}G^{a1}_{x} & Q^{a}_{31}G^{a}_{z}
\end{array}$$

93 ③

$$
\begin{array}{cc|cccc|}
 & 0 & 0 & 0 & 0 & 0 \\
 & 0 & 0 & 0 & 0 & 0 \\
 & 0 & 0 & 0 & 0 & 0 \\
1 & -Q^{a}_{11}G^{a_1}_{y} & Q^{a}_{12} & Q^{a}_{12}G^{a_2}_{x} & Q^{a}_{12}G^{a_2}_{z} & -Q^{a}_{12}G^{a_2}_{y} \\
1 & -Q^{a}_{21}G^{a_1}_{y} & Q^{a}_{22} & Q^{a}_{22}G^{a_2}_{x} & Q^{a}_{22}G^{a_2}_{z} & -Q^{a}_{22}G^{a_2}_{y} \\
1 & -Q^{a}_{31}G^{a_1}_{y} & Q^{a}_{32} & Q^{a}_{32}G^{a_2}_{x} & Q^{a}_{32}G^{a_2}_{z} & -Q^{a}_{32}G^{a_2}_{y}
\end{array}
$$

93④

$$\begin{bmatrix}
0 & 0 & 0 & 0 \\
0 & 0 & 0 & 0 \\
0 & 0 & 0 & 0 \\
Q^{a}_{13} & Q^{a}_{13}G_{x}^{a_3} & Q^{a}_{13}G_{z}^{a_3} & -Q^{a}_{13}G_{y}^{a_3} \\
Q^{a}_{23} & Q^{a}_{23}G_{x}^{a_3} & Q^{a}_{23}G_{z}^{a_3} & -Q^{a}_{23}G_{y}^{a_3} \\
Q^{a}_{33} & Q^{a}_{33}G_{x}^{a_3} & Q^{a}_{33}G_{z}^{a_3} & -Q^{a}_{33}G_{y}^{a_3}
\end{bmatrix}
\qquad
\begin{bmatrix}
\eta^{g_1} \\
K^{g_1} \\
\beta_{y}^{g_1} \\
\beta_{z}^{g_1} \\
\eta^{g_2} \\
K^{g_2} \\
\beta_{y}^{g_2} \\
\beta_{t}^{g_2} \\
\eta^{g_3} \\
K^{g_3} \\
\beta_{y}^{g_3} \\
\beta_{z}^{g_3} \\
B^{a_1} \\
F_{1}^{a_1} \\
\beta_{y}^{a_1} \\
\beta_{2}^{a_1} \\
B^{a_2} \\
F_{1}^{a_2} \\
\beta_{y}^{a_2} \\
\beta_{z}^{a_2} \\
B^{a_3} \\
F_{1}^{a_3} \\
\beta_{y}^{a_3} \\
\beta_{z}^{a_3}
\end{bmatrix}$$

(3.3)

⑤

Actually the instrument error sources could be handled even if there were inter-instrument correlation. The desired result is a covariance matrix for total attitude error. The process of obtaining this total covariance matrix involves acquisition of the covariance matrix of instrument errors. This is the expectation of $\gamma\gamma^T$. If the error sources are uncorrelated, this is a diagonal matrix consisting of the square of the rms numbers for instrument errors. If there is correlation and if the correlation factors are known, then off-diagonal terms may be filled in. Only if the correlation were unity, i.e., if the numbers for each instrument were identical, could all the instruments be lumped together. Equation (3.3) may be rewritten as follows

$$\begin{bmatrix} \Delta\Omega \\ \Delta G \end{bmatrix} = M\gamma \tag{3.4}$$

The problem now is to discover how $\Delta\Omega$ and ΔG are transferred into attitude errors. The solution is obtained by perturbing Eqs. (2.1) and (2.2). There is no need to perturb Eq. (2.3) because it is clear that North must be orthogonal to Up and East. Equation (2.3) really adds no new information.

It appears intuitively clear that errors in level will depend entirely upon error in measuring G. Level error may be described as small rotations about the two level axes of the earth fixed latitude-longitude system. Let these rotations be ϕ_x and ϕ_y. Errors in azimuth should depend upon level and errors in measurement of earth rate. Azimuth error is described as a small rotation, ϕ_z, about the third axis of the locally level set. This is the vertical axis.

The rotation matrix, S^{vL}, was defined by Eq. (2.4). For a first order approximation of error this matrix will be assumed correct. It will be used to transform errors in G^v and Ω^v from the vehicle coordinate frame to the locally level frame designated by the superscript L in the following equations. The transpose of V^{vL} is, of course, S^{Lv}.

$$(G+\Delta G)^L = S^{Lv}(G+\Delta G)^v = \begin{bmatrix} S_{11}^{Lv}(G_x+\Delta G_x)^v & S_{12}^{Lv}(G_y+\Delta G_y)^v & S_{13}^{Lv}(G_z+\Delta G_z)^v \\ S_{21}^{Lv}(G_x+\Delta G_x)^v & S_{22}^{Lv}(G_y+\Delta G_y)^v & S_{23}^{Lv}(G_z+\Delta G_z)^v \\ S_{31}^{Lv}(G_x+\Delta G_x)^v & S_{32}^{Lv}(G_y+\Delta G_y)^v & S_{33}^{Lv}(G_z+\Delta G_z)^v \end{bmatrix} \tag{3.5}$$

$$(\Omega+\Delta\Omega)^{L} = \begin{bmatrix} S_{11}^{Lv}(\Omega_x+\Delta\Omega_x)^{v} & S_{12}^{Lv}(\Omega_y+\Delta\Omega_y)^{v} & S_{13}^{Lv}(\Omega_z+\Delta\Omega_z) \\ S_{21}^{Lv}(\Omega_x+\Delta\Omega_x)^{v} & S_{22}^{Lv}(\Omega_y+\Delta\Omega_y)^{v} & S_{23}^{Lv}(\Omega_z+\Delta\Omega_z) \\ S_{31}^{Lv}(\Omega_x+\Delta\Omega_x)^{v} & S_{32}^{Lv}(\Omega_y+\Delta\Omega_y)^{v} & S_{33}^{Lv}(\Omega_z+\Delta\Omega_z) \end{bmatrix} \qquad (3.6)$$

Now to a first order approximation, the error angle ϕ_x^L can be seen to be:

$$\phi_x^L = \frac{-\Delta G_y^L}{G_z^L} = \frac{S_{21}^{Lv}\,\Delta G_x^v + S_{22}^{Lv}\,\Delta G_y^v + S_{23}^{Lv}\,\Delta G_z^v}{S_{31}^{Lv}\,G_x^v + S_{32}^{Lv}\,G_y^v + S_{33}^{Lv}\,G_z^v} \qquad (3.7)$$

Also, ϕ_2^E can be seen to be:

$$\phi_y^L = \frac{\Delta G_x^L}{G_z^L} = \frac{S_{11}^{Lv}\,\Delta G_x^v + S_{12}^{Lv}\,\Delta G_y^v + S_{13}^{Lv}\,\Delta G_z^v}{S_{31}^{Lv}\,G_x^v + S_{32}^{Lv}\,G_y^v + S_{33}^{Lv}\,G_z^v} \qquad (3.8)$$

The philosophy behind Eqs. (3.7) and (3.8) is simply that the error resulting from an angular misalinement is the cross product of the angle and the original vector quantity. This is true for small angular displacements. Fig. 3.1 may clarify this logic.

The Easterly reference direction is obtained from the cross product of earth rate and $\underline{G}$. The error E^E may be expressed as follows

$$\Delta E^L = S^{Lv}\,\Delta E^v = S^{Lv} \begin{bmatrix} G_z\Delta\Omega_y + \Omega_y\,\Delta G_z - \Omega_z\Delta G_y - G_y\Delta\Omega_z \\ \Omega_z\Delta G_x + G_x\Delta\Omega_z - \Omega_x\Delta G_z - G_z\Delta\Omega_x \\ \Omega_x\Delta G_x + G_y\Delta\Omega_x - \Omega_y\Delta G_x - G_x\Delta\Omega_y \end{bmatrix}^{v} \qquad (3.9)$$

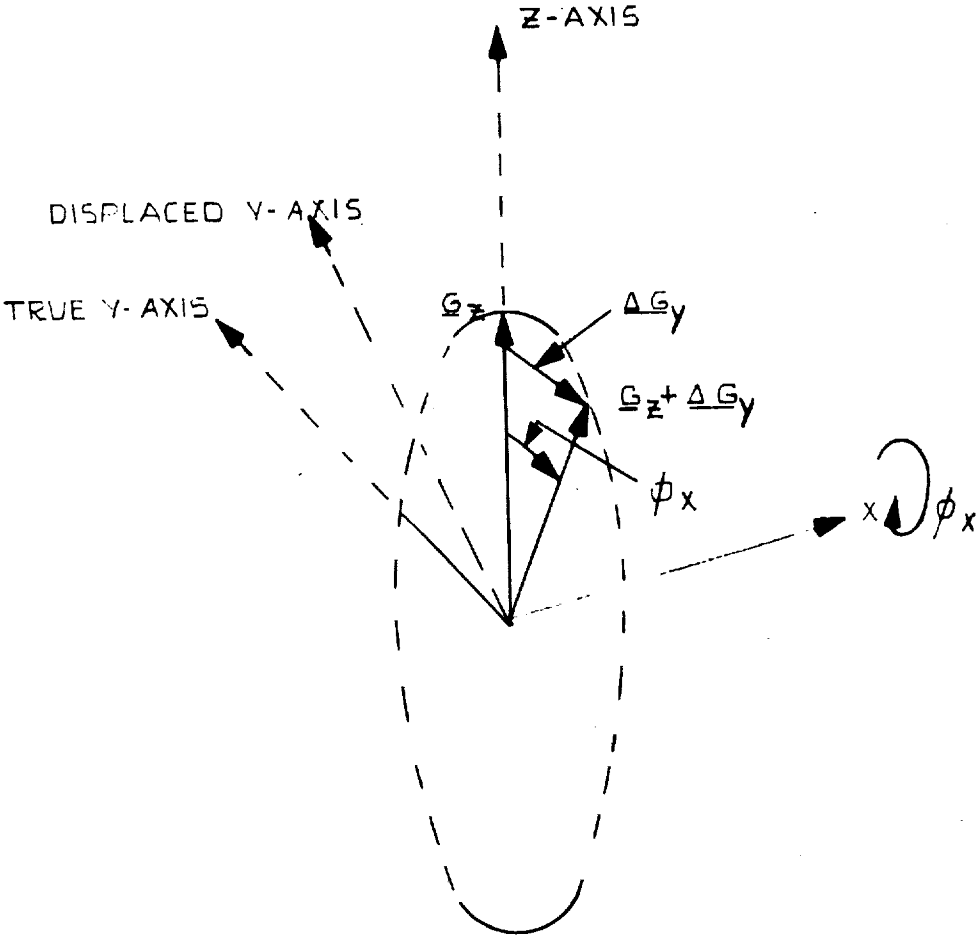
Z-AXIS
DISPLACED Y-AXIS
TRUE Y-AXIS
$\underline{G}_z$
$\Delta \underline{G}_y$
$\underline{G}_z + \Delta \underline{G}_y$
ϕ_x
x
ϕ_x

Fig. 3.1

Pictorial Representation of ϕ_x^L .
Actual, G_z is the total gravity vector $\underline{G}$.

This arises from perturbation of the basic equation:

$$E^{v} = \tilde{\Omega}^{v} G^{v} = \begin{bmatrix} \Omega_y G_z - \Omega_z G_y \\ \Omega_z G_x - \Omega_x G_z \\ \Omega_x G_y - \Omega_y G_x \end{bmatrix}^{v} \tag{3.10}$$

Azimuth error, ϕ_z^L, is then given by the following relation.

$$\phi_z^L = \frac{\Delta E_y^L}{E_x^L} = \frac{S_{21}^{Lv}(G_z \Delta\Omega_y + \Omega_y \Delta G_z - \Omega_z \Delta G_y - G_y \Delta\Omega_z)^v}{S_{11}^{Lv}(\Omega_y G_z - \Omega_z G_y)^v + S_{12}^{Lv}(\Omega_z G_x - \Omega_x G_z)^v + S_{13}^{Lv}(\Omega_x G_y - \Omega_y G_x)^v}$$

$$+ \frac{S_{22}^{Lv}(\Omega_z \Delta G_x + G_x \Delta\Omega_z - \Omega_x \Delta G_z - G_z \Delta\Omega_x)^v}{S_{11}^{Lv}(\Omega_y G_z - \Omega_z G_y)^v + S_{12}^{Lv}(\Omega_z G_x - \Omega_x G_z)^v + S_{13}^{Lv}(\Omega_x G_y - \Omega_y G_x)^v}$$

$$+ \frac{S_{23}^{Lv}(\Omega_x \Delta G_y + G_y \Delta\Omega_x - \Omega_y \Delta G_x - G_x \Delta\Omega_y)^v}{S_{11}^{Lv}(\Omega_y G_z - \Omega_z G_y)^v + S_{12}^{Lv}(\Omega_z G_x - \Omega_x G_z)^v + S_{13}^{Lv}(\Omega_x G_y - \Omega_y G_x)^v} \tag{3.11}$$

It is now possible to combine Eqs. (3.7), (3.8), and (3.11) into one matrix equation as follows

$$\begin{bmatrix} \phi_x \\ \phi_y \\ \phi_z \end{bmatrix}^L = \begin{bmatrix} 0 & 0 & 0 & -\frac{S_{21}^{Lv}}{\|G\|} & -\frac{S_{22}^{Lv}}{\|G\|} & -\frac{S_{23}^{Lv}}{\|G\|} \\ 0 & 0 & 0 & \frac{S_{11}^{Lv}}{\|G\|} & \frac{S_{12}^{Lv}}{\|G\|} & \frac{S_{13}^{Lv}}{\|G\|} \\ \frac{S_{23}^{Lv}G_y^v - S_{22}^{Lv}G_z^v}{E_x^L} & \frac{S_{21}^{Lv}G_z^v - S_{23}^{Lv}G_x^v}{E_x^L} & \frac{S_{22}^{Lv}G_x^v - S_{21}^{Lv}G_y^v}{E_x^L} & \frac{S_{22}^{Lv}\Omega_z^v - S_{23}^{Lv}\Omega_y^v}{E_x^L} & \frac{S_{23}^{Lv}\Omega_x^v - S_{21}^{Lv}\Omega_z^v}{E_x^L} & \frac{S_{21}^{Lv}\Omega_y^v - S_{22}^{Lv}\Omega_x^v}{E_x^L} \end{bmatrix} \begin{bmatrix} \Delta\Omega_x^v \\ \Delta\Omega_y^v \\ \Delta\Omega_z^v \\ \Delta G_x^v \\ \Delta G_y^v \\ \Delta G_z^v \end{bmatrix} \tag{3.12}$$

Let the large rectangular matrix of Eq. (3.12) be designated by the symbol N. Equations (3.12) and (3.4) may now be combined as follows

$$\phi^L = N \; M \gamma \tag{3.13}$$

Equation (3.13) is the error equation for the alinement process in the absence of broad spectrum noise. The covariance matrix for misalinement is formed as follows, where Ex means Expectation in the statistical sense.

$$E_x(\phi^L \phi^{L^T}) = E_x(N \, M \gamma \gamma^T M^T N^T) = N \, M \, E_x(\gamma \gamma^T) M^T N^T \tag{3.14}$$

3.1 Simplification of the Error Analysis

Equation (3.12) is quite involved. The complication may be attributed to the freedom allowed in the choice of coordinate frames and instrument orientation. If the input axes of the instruments were chosen coinsident with axes of the vehicle coordinate system, and if the vehicle coordinates were chosen coinsident with the earth-fixed locally-level set, considerable simplification would result. Naturally in practice, the vehicle triad will not be so conveniently oriented. If such orientation were possible, there would be no need for gyrocompassing. However looking at this case will prove informative. There is probably no advantage to be gained by having the vehicle triad close to coinsidence with the locally level triad. But if an advantage did exist such alinement could usually be made to within 20 degrees, and that would be close enough for the following discussion to prove applicable.

If the vehicle coordinate frame and locally level frame are close to identity, then S^{VL} may be assumed an identity matrix. Further the gravity component G_z^V is essentially the total $\underline{G}$ vector, E_x^V becomes the total $\underline{E}$ vector, and the value of Ω_x^v becomes zero. Equation (3.12) now becomes the following.

$$\begin{bmatrix} \phi_x \\ \phi_y \\ \phi_z \end{bmatrix} = \begin{bmatrix} 0 & 0 & 0 & 0 & -\dfrac{1}{\|G\|} & 0 \\ 0 & 0 & 0 & -\dfrac{1}{\|G\|} & 0 & 0 \\ -\dfrac{G}{\|E\|} & 0 & 0 & \dfrac{G_z^v}{\|E\|} & 0 & 0 \end{bmatrix} \begin{bmatrix} \Delta\Omega_x^v \\ \Delta\Omega_y^v \\ \Delta\Omega_z^v \\ \Delta G_x^v \\ \Delta G_y^v \\ \Delta G_z^v \end{bmatrix} \tag{3.15}$$

The 15 and 24 elements of the large matrix are seen to arise directly from Eqs. (3.7) and (3.8).

The magnitude of $\underline{E}$ is seen to be the magnitude of $\Omega_y G_z$ or simply the product of the y-component of earth rate and the total gravity acceleration.

After multiplication by the column matrix of $\Delta\Omega$ and ΔG, the 31 element of the rectangular matrix becomes $\Delta\Omega_x/\Omega_y$. This angular error is similar to the error depicted in Fig. 3.1. But now the 34 element becomes

$$\frac{\Delta G_x \ \Omega_z}{G \ \Omega_y} = \phi_y \frac{\Omega_z}{\Omega_y} \tag{3.16}$$

The exact physical significance of this term may be a little difficult to perceive. It actually arises from the fact that if the x-y plane of the vehicle coordinates is tilted about the y-axis, and if the total earth rate vector is not coinsident with the y-axis, then the earth rate vector will exhibit an apparent error in azimuth when observed from the tilted coordinates.

Because the instruments are now assumed alined with the coordinate axes, the Q matrices are also unit matrices. Equation (3.3) is considerably simplified, and the expectation of $(M \gamma\gamma^T M^T)$ is a sixth order diagonal matrix in which each diagonal element represents the total mean square error associated with one of the six instruments. The mean square errors of the instruments appear separately because only one instrument contributes to measurement error, in either gravity or earth rate, along any one of the axes.

Equation (3.14) now becomes the following.

$$E_x(\phi\,\phi^T) = E_x(\,M\;M\,\gamma\gamma^T\,M^T\,N^T) =$$

$$\begin{bmatrix} 0 & 0 & 0 & 0 & \frac{-1}{G} & 0 \\ 0 & 0 & 0 & \frac{1}{G} & 0 & 0 \\ \frac{-G}{\Omega_y G} & 0 & 0 & \frac{\Omega_z}{\Omega_y G} & 0 & 0 \end{bmatrix} \begin{bmatrix} \Delta\Omega_x^2 & 0 & 0 & 0 & 0 & 0 \\ 0 & \Delta\Omega_y^2 & 0 & 0 & 0 & 0 \\ 0 & 0 & \Delta\Omega_z^2 & 0 & 0 & 0 \\ 0 & 0 & 0 & \Delta G_x^2 & 0 & 0 \\ 0 & 0 & 0 & 0 & \Delta G_y^2 & 0 \\ 0 & 0 & 0 & 0 & 0 & \Delta G_z^2 \end{bmatrix} \begin{bmatrix} 0 & 0 & \frac{-G}{\Omega_y G} \\ 0 & 0 & 0 \\ 0 & 0 & 0 \\ 0 & \frac{1}{G} & \frac{\Omega_z}{\Omega_y G} \\ \frac{-1}{G} & 0 & 0 \\ 0 & 0 & 0 \end{bmatrix} =$$

$$\begin{bmatrix} \frac{\Delta G_y^2}{G^2} & 0 & 0 \\ 0 & \frac{\Delta G_x^2}{G^2} & \frac{\Omega_z}{\Omega_y}\frac{\Delta G_x^2}{G^2} \\ 0 & \frac{\Omega_z}{\Omega_y}\frac{\Delta G_y^2}{G^2} & \frac{\Omega_z^2}{\Omega_y^2}\frac{\Delta G_x^2}{G^2} + \frac{\Delta\Omega_x^2}{\Omega_y^2} \end{bmatrix} \qquad (3.17)$$

It can be seen that in this special situation, there is cross correlation between the x and y accelerometers only. Furthermore the only gyro contributing to first order errors is the x-gyro.

At first these results may appear strange. The reader might think that the x-gyro could simply be ignored since it is not contributing much anyway. The truth is that while the x-gyro is measuring a small quantity, it is the most important rotational measurement being made. If indeed the x-gyro is horizontal, then its reading is equal to the product of the azimuth misalinement of the vehicle coordinates and the horizontal component of earth rate. Since earth rate is known, this is a direct measurement of azimuth misalinement. The fact is that if the vehicle coordinate frame is nearly coinsident with the true, locally-level coordinate-triad, then the other gyros might be ignored, but not the x-gyro.

It must also be pointed out that the error analysis has proceeded under the assumption that all errors were small. The preceding obviously does not apply to the case where one gyro or one accelerometer generates extremely large errors, an order of magnitude or greater because the description of misalinement errors as small Euler angles is no longer valid.

The delta terms pertain to the total mean square individual instrument errors. For example G_x^2 obtained from Eq. (3.2) under the assumption of unit Q^a matrix is the following

$$\Delta G_x^2 = B^2 + G_x^2 F_1^2 + \beta_2^2 G_z^2 + \beta_3^2 G_y^2 \tag{3.18}$$

And since G_x and G_y are zero for accelerometer number one, this becomes

$$\Delta G_x^2 = B^2 + \beta_2^2 G_z^2 \tag{3.19}$$

The instrument error models must be formed in their own coordinate frame, so that for the y-axis accelerometer the components of the gravity vector must be rotated from vehicle coordinates into y-accelerometer coordinates.

4. General Considerations

One might inquire as to the overall effect of changes in instrument orientation. The answer is that since instrument errors are a function of their position with respect to gravity and rotation vectors, an optimum orientation might exist. Its existence would depend upon the characteristics of the instruments being used.

If the instruments have identical rms errors such as identical scale factor uncertainties and if they are orthogonally mounted, then the orientation of the instrument package does not alter the principle diagonal of the attitude error covariance matrix. This is because the surface of equal error probability forms a sphere about the coordinate origin. The correlation between errors in ϕ_x, ϕ_y, and ϕ_z changes with orientation of the instrument package, but not the standard deviation of the angles themselves.

It is interesting to note that the horizontal component of earth rate appears in the denominator of the error terms relating to azimuth. This quantity diminishes as either of the geographic poles is approached and vanishes at the poles. This, of course, demonstrates that gyrocompassing is poorly conditioned to the far northern or southern latitudes, but it does not present a practical problem to gyrocompassing for ground alinement of space vehicle guidance systems.

5. Vibrational Effects

Rectification of vibration was discussed briefly in Chapter III. Complete analysis of associated errors must proceed from an intimate knowledge of the particular instruments involved. Furthermore it is necessary to characterize the vibration, both rotational and translational, to which the instruments are subjected. This is often far from a simple task. To some degree the rectification problem may be diminished by shock mounting the instruments.

In the absence of noise alinement time may not exceed several minutes. Vibrational noise and electronic noise, if applicable, constitute additive errors. Standard filtering techniques are applicable to this problem. The simplest approach might be to perform periodic alinements and use a least squares estimation procedure. The sampling times should be chosen far enough apart that the noise samples may be considered uncorrelated.

Optimum filtering depends upon the nature of the noise, and the locations at which it enters the system. Filtering may be applied directly to the output of the instruments, or to the final alinement information, or both. It seems apparent that if sufficient time is available for alinement, and if sufficient computational capability is present, that the effect of zero mean noise may be mitigated to any desirable degree.

6. Multiple Readings

The dominant azimuth error is x-gyro error divided by the y component of earth rate. Much of the x-gyro error is deterministic in nature, but completely accurate measurements of magnitudes cannot be obtained for the error coefficients. Such would be the case for gravity dependent errors and misalinement errors. There are also gyro drift rate errors which are essentially random in nature but with long correlation times. If the autocorrelation times for random drifts are long with respect to the time duration for several measurements, then these drift rates are essentially constant and may be considered deterministic during the alinement period.

The interesting feature about deterministic errors is that their effect may be canceled out by taking repeated readings with the instrument (or instruments) judiciously repositioned for each reading. For example suppose that the x-gyro had a constant bias, i.e., constant drift rate. If two readings are taken, one with the gyro pointed east and one with it pointed west, the first reading minus the second will be equal to twice the true rotation rate about the x-axis. The constant bias will have been canceled out by the subtraction.

The true strapdown system offers no possibility for repositioning of the instruments. If the guidance system employs an inertial platform, several options are available. The platform may be mechanized according to the discussions in Chapter V. However, better performance may be achieved if the platform can be operated as a strapdown system. The platform may be precision torqued into preselected positions and locked in those positions. Measurement of earth rate may be made at each position by monitoring the torquing currents required to keep the gyroscopes at null while the platform is locked.

Error analysis for such a process procedes in a manner similar to that described earlier in this chapter. The total transition matrix must be found that transforms each set of readings into a final determination of x, y, and z components of earth rate and gravity. This matrix will be similar to Eq. (3.3), but the large rectangular matrix will have added columns for each of the multiple positions. The column vector or error sources at the right of Eq. (3.3) will have added rows associated with each of the multiple positions. From this point on the analysis proceeds as before. It is important to note however, that $_y$ and $_z$ were used to represent the total misalinements of the input axes from the direction in which they were assumed to be pointing. This misalinement must be broken into two components where multiple positions are used. One component will be the misalinement of the entire platform from the desired position, and the other will be the misalinement of the sensitive axes with respect to the platform coordinate frame. For example if the platform were rotated 180° about the z axis between two readings, the misalinement of the x-gyro, measured around the platform x-axis, would result in an error of the same magnitude and sign in each position. Misalinement of the platform about the y-axis would result in an error of equivalent magnitude but opposite signs in the two positions. Therefore these two error sources must be kept separate.

Selection of positions for measurement must be made so as to minimize the effect of the important error sources without introducing new ones of equivalent magnitude. The new error sources would arise from inaccuracies in precision torquing of the platform to each new position.

The ability to precision torque the platform, to lock it in position, and to measure individual gyro torquing currents represents added capabilities over and above those normally found on a platform designed for space applications. Perhaps a simpler solution to the problem of achieving an accurate azimuth alinement would be to mechanize the platform self leveling loops only. A fourth gyro of high quality might be mounted on the platform for the purpose of measuring the component of earth rate in the plane of the platform, nominally the level plane. Typically this might be a rate gyro which would be positioned pointing eastward first and then westward. This would afford effective cancellation of the gyro drift rate, random in nature but with long autocorrelation time. This is usually the largest gyro error source, principally because it will have changed considerably since laboratory calibration, and thus cannot be easily compensated.

Gyro error analysis for this case is the same as that just discussed, but easier in that only one gyro is repositioned. Platform tilt will represent a first order error source and must be considered. Platform angular rotation rate would present an uncorrectable error, but this is essentially nonexistent in the steady state, except for the effect of vehicle vibration.

Platform level errors would be the same as those for the y-axis leveling loop discussed in Chapter IV.

CHAPTER VI

OPERATION ON BODIES OTHER THAN THE EARTH

1. Introduction

Gyrocompassing at a fixed location on the surface of other planets would be desirable in certain situations. Such situations would include alignment prior to launch from a planet for a return trip; erection of an antenna; or preliminary to star-sighting. Consideration of this problem breaks naturally into three parts. One part is concerned with the practicality of gyrocompassing on other planets. The second part involves consideration of how well vehicle location on the planet will be known. The third asks the question, "What accuracy is required for launch from another planet in connection with a typical space mission?"

2. Performance on Other Planets

It is interesting to observe the similarities in errors obtained from both direct and indirect gyrocompassing. All of these mechanisms have an azimuth error term given by gyro drift rate divided by earth rate, or the horizontal component of earth rate.

Chapter VII developes extensively several mechanizations for indirect gyrocompassing in orbit. Essentially, the same results apply to terrestrial application. In most cases results are similar to those presented by Eqs. (4.6) through (4.8) of Chapter IV. That is, x-gyro drift rate divided by total nominal rotation rate is an azimuth error term. The strapped-down system is also subject to the same error but has an additional error of z-gyro rate with a multiplicative constant in both azimuth and x-axis tilt. The constant is different for the two axes, and generally different from one candidate system to another. This constant contains the total nominal rotation rate, W_y, (or ω_0 in Chapter VII, in the denominator, but it appears in conjunction with other gain constants so that some adjustment is possible. In other words, the effect of a diminished W_y may be in some measure offset by adjustment of system gains for the error term involving the z-gyro drift rate. This is not true for the x-gyro.

2.1 An Example of Indirect Gyrocompassing with small W_y and g

By way of example of the capability for compensating adjustment of system gains, let the system depicted in Fig. 2.4 of Chapter IV be considered. The characteristic equation for that system is:

$$S^3 + k_b S^2 + (gk_d + W_y^2)S + W_y^2 k_b + gW_y\, k_g = 0 \tag{2.1}$$

This may be represented in time constant form as:

$$\left(S + \frac{1}{T_2}\right) \left(S^2 + \frac{2}{T}S + \frac{1}{T^2 \zeta^2}\right) =$$

$$S^3 + \left(\frac{2}{T} + \frac{1}{T_2}\right)S^2 + \left(\frac{2}{TT_2} + \frac{1}{T^2 \zeta^2}\right) S + \frac{1}{T_2 T^2 \zeta^2} = 0 \tag{2.2}$$

System gains may be expressed in terms of time constants by equating terms of Eqs. (2.1) and (2.2). The results follow.

$$\frac{2}{T} + \frac{1}{T_2} = k_b \tag{2.3}$$

$$\frac{2}{TT_2} + \frac{1}{T^2\;{}^2} = gk_d + W_y^2 \tag{2.4}$$

$$\frac{1}{T_2 T^2 \zeta^2} = W_y^2 k_b + gW_y k_g = W_y(W_y k_b + gkg) \tag{2.5}$$

The final error values are repeated from Eqs. (4.6) through (4.8) of Chapter IV.

$$\phi_x \text{ final value} = \frac{k_b}{W_y k_b + k_g\, g} \left[-\epsilon_z + \frac{k_g}{k_b} A_y \right] \tag{2.6}$$

$$\phi_z \text{ final value} = \frac{k_b}{W_y k_b + k_g g} \left[\frac{gk_d}{W_y k_b}\, \epsilon_z - A_y \right] + \frac{\epsilon_x}{W_y} \tag{2.7}$$

$$\phi_y \text{ final value} = \frac{k_i}{gk_j} (\epsilon_y + A_x) \tag{2.8}$$

The y-axis control is a second order loop. The characteristic equation appears in Chapter IV, as Eq. (4.5). Reference to this Chapter makes it immediately evident that if the y-channel time constant is held constant, then k_i/gk_j is constant and the y-axis tilt errors are not primarily affected by reduction in planet rotation rate or variations in gravity, so long as gravity does not approach zero or the limit of sensitivity of the accelerometer. For operation on or near the equator, the y-axis rotation does not strongly couple into aximuth, and for this reason one would not expect planet rotation rate to be important. Indeed the local level may be established even in the absence of planet rotation.

Equations (2.6) and (2.7) may be rewritten as follows in terms of the time constants.

$$\phi_x \text{ final value} = T_2 T^2 \zeta^2 \left[-W_y k_b \epsilon_z + k_g W_y A_y \right] \qquad (2.9)$$

$$\phi_z \text{ final value} = T_2 T^2 \zeta^2 \left[g k_d \epsilon_z - k_b W_y A_y + \frac{\epsilon_x}{W_y} \right] \qquad (2.10)$$

The effect of z-gyro drift rate on aximuth may be determined by an examination of $T_2 T^2 \zeta^2 g\, k_d$. Equation (2.4) indicates that the time constants and damping ratio may be chosen such that gk_d is equal to zero. On the earth, this could be accomplished with damping of 0.8 and time constants slightly greater than 15 minutes. If W_y were decreased by an order of magnitude, the time constants would have to be increased by approximately an order of magnitude in order to maintain cancellation of the ϵ_z term in Eq. (2.10).

But this increase in time constants results in an order of magnitude decrease in k_b as may be seen from Eq. (2.3). The coefficient of ϵ_z in Eq. (2.9) is $T_2 T^2 \zeta^2 W_y k_b$. The total effect on this coefficient is an order of magnitude increase. Some improvement may be obtained by adjusting the time constants independently, but the basic indication is that this system is poorly conditioned to operation with low values of W_y. On the contrary large W_y is no problem. The effect of x-gyro drift is increased in direct proportion to W_y decrease.

Consider the effect of accelerometer bias, A_y, in the presence of an order of magnitude decrease in W_y and a compensating order of magnitude increase in T and T_2. The effect on ϕ_z is increased by order of magnitude as can be seen from its correspondence to ϵ_z in Eq. (2.9). In order to determine the effect of A_y on ϕ_x it is necessary to consider k_g. From consideration of Eq. (2.5), it appears that gk_g must decrease by about two orders of magnitude. The value of k_g naturally depends upon g. But if g were decreased by no more than an order of magnitude, then k_g would be decreased by at least an order of magnitude, and the effect of A_y on ϕ_x would be increased by no more than an order of magnitude.

It would appear that a decrease in planet rotation rate below earth rate effects an approximately proportional degradation in overall system performance for the system just considered, provided the system gains are adjusted. If no adjustment is made, degradation may be considerably worse.

There are many alternative mechanizations for indirect gyrocompassing with a platform. Several examples are enumerated in Table 4.1 of Chapter VII. Some of these may be better suited to operation with low rotation rates.

The effect of decreased g is considerably less. This is understandable, because gravity is essentially part of the gain of the tilt sensing device. The practical limitation on low g level is one of signal to noise level and sensitivity of the sensing device. These are the same factors which limit the usefulness of accelerometers for orbital use. In orbit, the accelerometer located at the center of mass of the satellite will have zero signal to measure. However, just above or below this point the effective acceleration of gravity is not zero, but is quite small. Thus accelerometers may be used for gyrocompassing in orbit if they are sufficiently sensitive.

At low g levels, such as might be experienced on the moon, the signal to noise levels of the accelerometers may become sufficiently poor as to require attention. In this event, adjustment of the system for optimum performance will not be confined to minimization of the final values indicated by Laplace Transform Final Value Theorem, (Eqs. (2.6) through (2.8), but must include consideration of noise rejection. Some discussions along the lines of optimum noise rejection are also included in Chapter VII.

Thus it is clear that optimization is a function of the individual instruments employed and the system transfer function. Trade-off studies among the possible candidate systems should include optimization of the systems for the instrumentation available and the W_y and g levels expected and comparison of the cost and performance of the optimized systems.

2.2 Theoretical Optimum

Some inference of the theoretically best attainable performance is available from an investigation of the basic measurable quantities. It is clear that the basic limitation on performance must be the ability of the instruments to measure the two basic quantities, gravity and planet rotation. From this point of view, the analysis is similar to the investigation of the strapped-down system, which measures these quantities directly.

The indication of azimuth comes either directly or indirectly from the measurement of planet rotation. It can never be better than the normalized drift rate of the gyroscopes. That is to say, the indication of azimuth can never be better than the x-gyro drift rate divided by planet rotation rate. It will be noted that this term appears in all the residual errors of all the indirect gyrocompassing systems as well as the strapped down system.

Improvement over this limitation is achievable only from sophisticated data reduction techniques employed with multiple measurements often involving multiple positions of the instruments.

The indication of local level comes from the measurement of gravity. It can never be better than the normalized errors in the x and y accelerometers (or equivalent measuring instruments such as bubble levels). Again, stochastic errors may be diminished in a statistical sense by statistical inference, and deterministic errors may often be eliminated or diminished by averaging over multiple observations involving various instrument positions.

It should be kept in mind that gyrocompassing with an inertial platform (indirect gyrocompassing) does not admit multiple positioning of the instruments so as to cancel gravity induced errors or constant errors and, as such, does not offer as accurate a final answer as is theoretically possible from direct measurement. Furthermore, as was mentioned in Section 2, the indirect method has added error terms not present for direct measurement systems. On the other side of the question, the indirect method requires essentially no computer and results in a physically alined platform. If an inertial platform is to be used for space navigation and if the inertial measurement instruments on the platform are the only ones available, then the indirect method may prove to be the only reasonable approach. It is true that direct measurement techniques may offer more accurate resolution of azimuth and level in the computer, but positioning of the platform with respect to the computer coordinates is only as good as the gimbal readout mechanism. The introduction of the computer complicates the picture; and in the end, increased accuracy may involve considerable increase in cost. Answers to questions such as these are obtainable only from a knowledge of specific mission requirements and the capabilities of the instruments available for use.

2.3 Knowledge of Local Vertical

Knowledge of the local vertical is obtained from the planet gravitational field. Two factors perturb the symmetry of the apparent gravity field at the location of the vehicle. One is the centrifugal force on the vehicle resulting from the planet rotation. The other is gravitational anomalies resulting from nonhomogeneity of the planet's composition and planet oblateness. On the earth, these error sources are not sufficiently large to cause concern for prelaunch alinement. Other planets must be considered on their own characteristics.

The direct measurement technique of gyrocompassing makes available information concerning the magnitude of planet rotation components in the locally level plane and along the local vertical. From this information and a preknowledge of planet diameter, the perturbation attributable to centrifugal force may be calculated and corrected.

Information concerning the vertical and horizontal components of planet rotation vector gives an exact indication of vehicle latitude on the planet. This will also allow correction to gravity for oblateness and other anomalies dependent upon latitude to the extent to which such anomalies are known. No indication of longitude is available from gyrocompassing measurements.

These considerations may be largely academic. No situation presently envisioned would require such accuracy as to make corrections for centrifugal force and gravity anomalies necessary. In any event if such accuracy were required, navigation would undoubtedly proceed from a celestial basis; i.e., with respect to the stars rather than relative to the planet as is done with gyrocompassing.

3. Knowledge of Latitude

Gyrocompassing supplies only relative information. This information allows positioning of a platform, or definition of a coordinate frame relative to the local vertical defined by the planet gravity vector at the vehicle location, and local north as defined by the planet rotation vector.

There is no way in which longitude information can be obtained from such measurements. However, this is not important because longitude information is not essential to the general space launch problem.

Latitude, on the other hand, is essential information for an effect space launch from the planet surface; and this information may be obtained as a by-product of gyrocompassing alinement. If the coordinates of the planet rotation rate vector are established in the locally level reference frame, the latitude is given by the arc tangent of the ratio of vertical component to the horizontal component.

This algorithm ignores the fact that the local vertical is established by means of the local apparent gravity vector, which includes centripetal acceleration. The error involved is small and may be treated as a linear perturbation. As such it may be ignored until the "almost correct" latitude has been found, at which time correction may be made.

The direct measurement (strapdown) system obtains the components of the planet rotation vector directly and can provide adequate latitude determination even in the absence of prior knowledge of the planet rotation rotational velocity.

The indirect (inertial platform) gyrocompassing system provides latitude information equally well provided that the magnitude of the total rotation velocity vector is known a priori. As will be recalled, the platform must be programmed to rotate with the same velocity as the planet. This rotational velocity must be apportioned between the y and z platform axes according to latitude. The y-gyro must be torqued at a rate equivalent to the planet rate times the cosine of latitude. If latitude is not known, then the y-axis torquing rate will not be correct and an error signal will build up indicating tilt about that axis. This information may be used to adjust the estimate of latitude until the y-tilt error signal falls to zero indicating that the y-gyro is being torqued with the proper horizontal component of planet rotation rate.

If knowledge of planet rotational velocity is not available, then performance of the gyrocompassing platform system will be considerably degraded. In the absence of any programmed rotation, the platform will assume some misalinement in tilt and azimuth such that the error signals are sufficient to supply proper rotation rates for the y and z axes. After the system has reached steady state, the y and z rotation rates may be measured; but the price will be considerable misalinement of the platform.

4. Required Accuracy

The final point of interest is simply the accuracy required for gyrocompassing on other planets. This involves mission requirements as well as the function intended to be served by gyrocompassing. Uses of a gyrocompass on an alien planet may be categorized as either alinement for non-navigational purposes such as for the erection of an antenna or for prelaunch alinement. Evaluation of exact accuracy requirements lie beyond the scope of this report.

CHAPTER VII

INDIRECT GYROCOMPASSING WITH AN INERTIAL PLATFORM IN ORBIT

1.0 Introduction

This chapter considers mechanization techniques for the orbital gyrocompass alinement of a gimballed locally level platform. The emphasis is on real time mechanizations with minimal onboard computation. Optimal parameter estimation techniques, while having promise for high precision gyrocompass alinement, are not considered at any length because of the implied high computational requirements. The techniques which are particularly emphasized are continuous self-alinement techniques with continuous leveling and azimuthing control signals being provided by horizon sensor derived error signals.

The study centers primarily around a locally level "true north" platform configuration; here true north is defined by the orbital pole. Classical gyrocompass alinement has its origin with the local level true north system (see Ref. 1); and it is for this reason the local level system is being initially considered for the orbital problem. The purpose is to draw as many similarities as possible with the fixed site and cruise system gyrocompass problem so that the alinement problem can be better understood for the other platform configuration, such as the inertial and strapdown.

The chief difficulty of actually applying a local level configuration for orbital operation is, of course, the required high platform torquing rate. This disadvantage, however, is offset by its advantages which are several: gyrocompass alinement mechanization is perhaps the simplest in this frame; minimal attitude determination computation relative to the orbital frame; and it is geometrically ideal for reading pitch, roll, and yaw relative to the orbital plane.

It should be emphasized that the mechanization study considered herein is very preliminary. Until better quantitative measures of the characteristics of the instrument induced and phenomenon induced errors of the horizon sensor are available, it is difficult to conclude what final form the mechanization will assume.

For this reason, various kinds of mechanizations have been considered, each with a characteristic of its own. For example, derivative type control may be used to minimize the effect of bias if noise levels are kept low. On the other hand, integral control can be used to minimize noise effects if bias type errors can be kept within tolerable bounds. In addition, transient characteristics such as settling time constants must be considered in order to bound the effects of system drift and attenuate the effects of initial errors. The overall design considerations will involve weighting the relative effects from the several sources of errors that potentially limit system performance.

2. Coordinate Systems

Some of the more important coordinate reference frames required for the study of orbital gyrocompassing are defined in Chapter 2.

As a reminder it may be mentioned that pitch, roll and yaw are designated by the small angles θ, ϕ and ψ measured from the orbital frame. The orbital frame is the true locally level triad at the vehicle location.

3.0 Preliminary Considerations to Orbital Gyrocompass Alinement Mechanization

3.1 General

The present section is a preliminary discussion on the orbital gyrocompass problem. General discussion is given to the in-orbit leveling and azimuthing a gimballed locally level platform. Further detailed discussion on cruise and fixed site mechanizations are contained in Ref. 1. Figure 3.1 shows a locally level platform configuration. The roll and yaw gyro spin axes are along the pitch axis to minimize the platform servo control problem to maintain local level. While this configuration is not germane to the alinement problem, it eases the analysis.

The pitch gyro, however, must be driven with orbital rate. The high angular rate (about 16 times earth rate) implied for orbital local level systems may severely limit its application. However, classical gyrocompass alinement for cruise systems originated with the locally level configuration, and for this reason the initial study based on this configuration has value aside from questions regarding its utility.

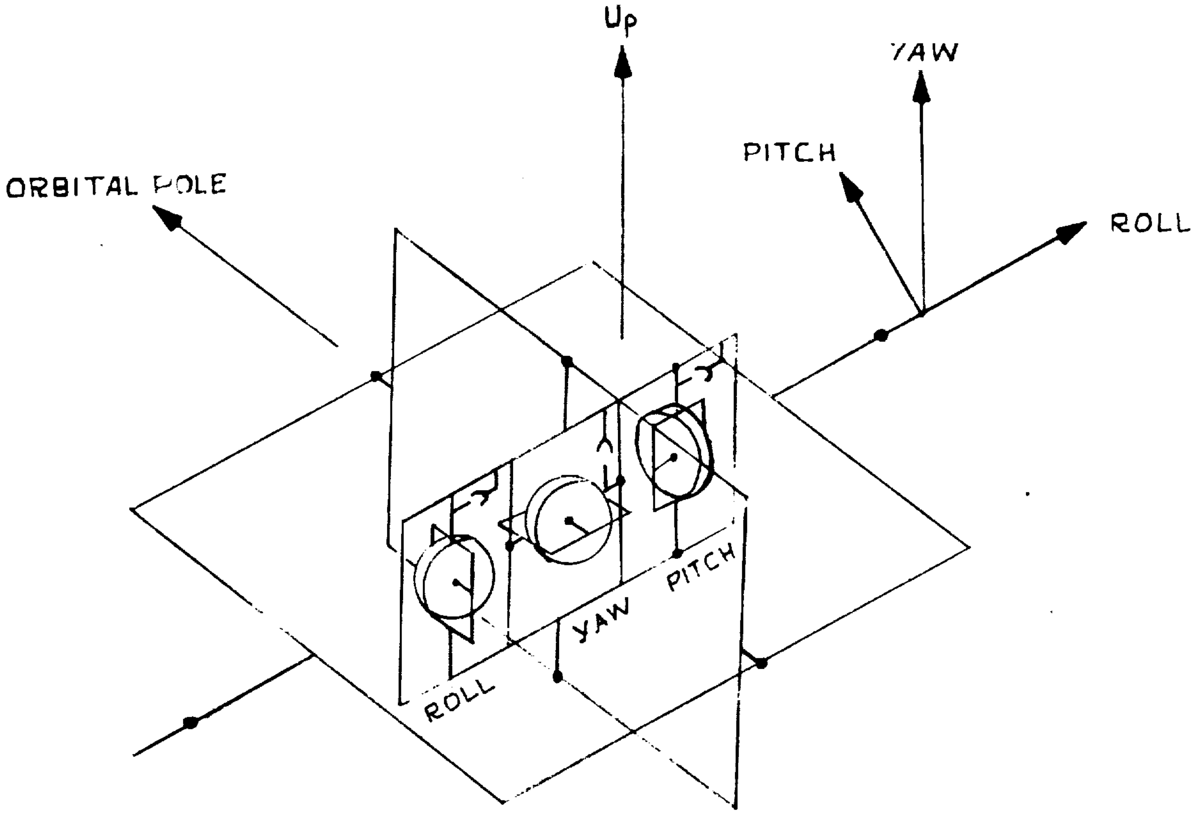

Fig. 3.1

A Three-Axis Level Platform

3.2 In-Orbit Leveling Considerations

To give insight into the level error parameters which are required to be stabilized, Fig. 3.2 shows the relative configuration of the platform, vehicle, and orbital level references. The true vertical (O) is here defined as the vertical determined on the basis of the orbital parameters, the vehicle vertical (v) is defined as the horizon sensor vertical (assuming sensor axis fixed in vehicle); and the platform vertical (p) is defined on the basis of the computed direction to the local vertical. Shown in this figure is the pitch error; a similar configuration holds for the roll axis.

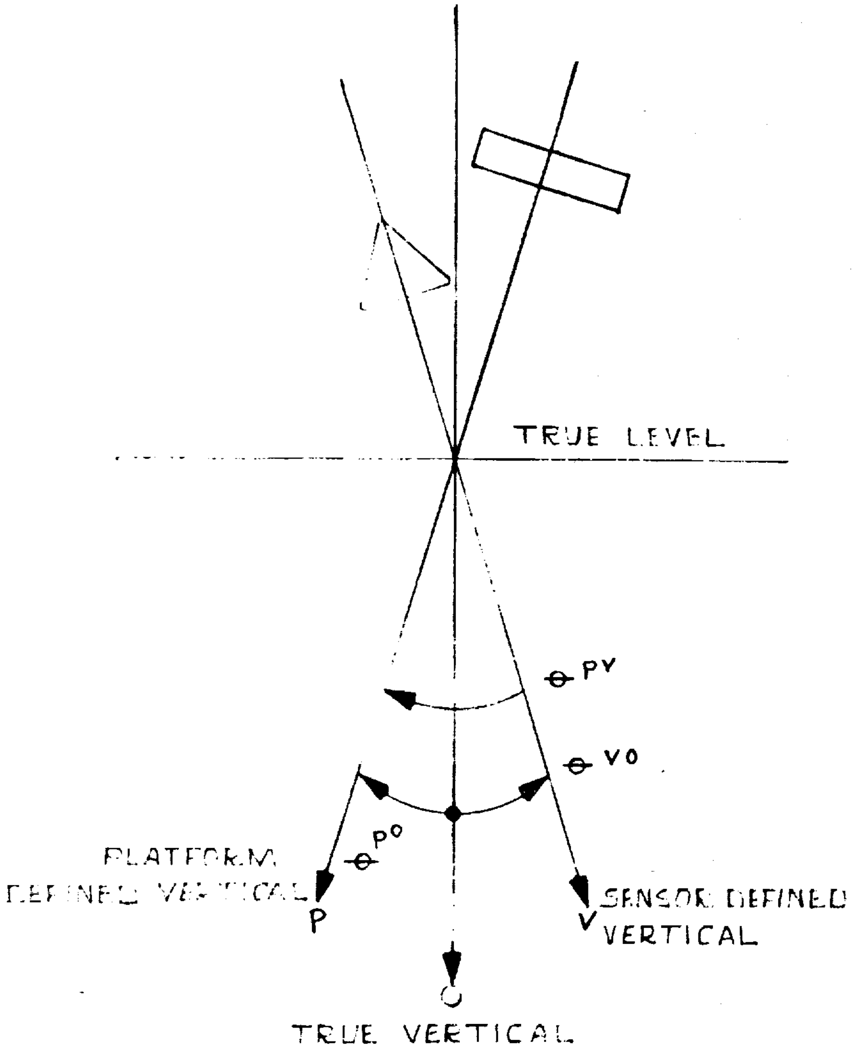
TRUE LEVEL
θ^{PV}
θ^{VO}
θ^{PO}
PLATFORM DEFINED VERTICAL
P
SENSOR DEFINED VERTICAL
V
O
TRUE VERTICAL

Fig. 3.2

Angle Relations Between True (Orbital) Vehicle and Platform Defined Frames

The pitch error θ^{vO}, between the vehicle and the orbital frame, is unknown. The angle θ^{pv} is directly available in the gimbal angle readout. The angle θ^{pO} is the platform drift error relative to the orbital frame.

In a general leveling configuration it is desired to null θ^{pO}; that is to level the platform frame to the orbital frame, in the presence of arbitrary vehicle motion θ^{vO}. As seen in Fig. 3.2 $\theta^{pO} = \theta^{pv} + \theta^{vO}$. If θ^{pO} were equal to zero then $\theta^{vO} = - \theta^{pv}$ (gimbal readouts). The leveling alinement problem is to stabilize and bound the inertial platform level tilt errors θ^{pv} and ϕ^{pO} to null.

To be even more general, it should be recognized that there is still another error parameter. This is the error in the navigation data. Depending upon how the platform is torqued to maintain level, potentially, gyrocompass alinement is limited by the coupling of the navigation error. Unfortunately there is no way of separating the angular navigation error from platform tilt error unless a separate mode is introduced to specifically damp out the navigation errors (such as via orbit re-determination). This problem is considered in detail in the later sections.

Drawing a similarity with cruise system gyrocompassing, the navigation errors are damped out via a separate mode, wherein a comparison is made of the system velocity output with an external reference doppler radar velocity. This essentially effects damping out platform torquing errors arising from navigation errors.

3.3 In-Orbit Azimuth Alinement Considerations

The orbital gyrocompass alinement problem for stable platforms can be described by a pair of simple diagrams. Assuming the platform has been leveled, the top view of a three-gyro locally level platform is shown in Figs. 3.3 and 3.4 in the azimuth misalined and alined configurations. Figure 3.3 shows the platform alined to the vehicle frame, but the vehicle frame is misalined relative to the orbital frame. This is the misalined configuration of platform azimuth. It is always possible to aline the platform axes to the vehicle frame by nulling the observed platform gimbal angles provided, of course, the vehicle motion is reasonably stable. The problem is to determine the azimuth misalinement of the vehicle. In the configuration of Fig. 3.3 this azimuth deviation indicated by the angle ψ, is undeterminable unless angular rates are measured.

To describe the effect of angular rates about wrong axes, it is necessary to consider the mechanization involved in torquing the platform to maintain local level. Assuming for the moment that the azimuth error is zero in Fig. 3.3, the platform must be torqued about the platform frame pitch axis with the orbital rate, ω_O, to maintain platform level. In the presence of a platform azimuth error ψ, the platform will still be torqued about the same pitch axis of the platform which is now misalined relative to the true ("north") orbital rate axis by the angle ψ. This is because there is no way of knowing that the platform is tilted in azimuth. If indeed the azimuth error were measurable and the platform were to be torqued along the direction of the true orbital polar axis, then the platform will maintain level. To maintain level then, a torque is required about the roll axis (roll gyro) to yield a roll rate which is equal to $\omega_O \psi$. The required torque to the pitch gyro will be given by $\omega_O \cos \psi$ which, for small ψ, is essentially given to the first order by ω_O (the nominal torque). Thus to maintain platform level in the presence of azimuth error, it is required to add a torque of $\omega_O \psi$ to the roll gyro.

Since the platform is actually being torqued about the misalined platform pitch axis, in effect then, the platform will appear to drift relative to the vehicle frame by the amount $-\omega_o \psi$ along roll. This effect is the observed platform drift rate resulting from torquing the platform with the nominal orbital rate in the presence of platform misalinements. The rate is observable about the platform outer roll gimbal provided, of course, that the vehicle frame rate is stabilized.

In Fig. 3.4 the platform frame is seen in a position of alinement with the orbital frame with the vehicle frame misalined in azimuth relative to the orbital frame. The platform is still being torqued about the pitch axis of the platform frame. In this configuration there is no component of the orbital rate about the roll gyro. Hence, assuming that the orbital rate is the only rate appearing on the platform, the platform will maintain level, the outer gimbal frame will maintain level, and assuming the vehicle frame is stabilized in the vertical, the roll gimbal angular rate output essentially reads zero to the first order. In this condition the platform frame is alined to the orbital frame and vehicle yaw is indicated by the platform yaw gimbal angle transducer output.

3.4 General Discussion on Gyrocompass Alinement Mechanization

The two different configurations represented by Figs. 3.3 and 3.4 suggest various mechanization possibilities for determining the vehicle yaw or for the self-alinement of the platform in yaw. Figure 3.3 suggests a very simple open loop mechanization. In the misalined condition (recognize the system is always alineable to the vehicle frame) the roll gimbal angle output allows a rate to be measured which is proportional to the yaw error. This mechanization, shown in the diagram Fig. 3.5, is considered further in a later section. It is an open loop scheme because no error signals are used to aline the platform except as to null ("cage") the gimbal angles relative to the vehicle frame, which in turn are assumed to be alined to the local vertical via the horizon sensor.

In the mechanization of Fig. 3.5 the gyros essentially serve the function of holding the platform stable. The gyro torquing transfer functions $G_p(s)$, $G_R(s)$, $G_y(s)$ are filters which smooths out fluctuations of vehicle motion due to the vehicle attitude control system and the random errors of the horizon sensor which is the basis for holding the vehicle to the local vertical. The output of the roll gimbal angle must also be smoothed with a filter to eliminate the vehicle roll motion.

Note that this mechanization is essentially the same mechanization as that arising from reading the rate output of a roll rate gyro which is strapped to the vehicle. Fig. 3.6 shows a typical mechanization. The only difference with this configuration and that which gives the present mechanization a promise of improvement is that the vehicle motion can be isolated (or filtered) from the platform frame so that roll rate coupling is

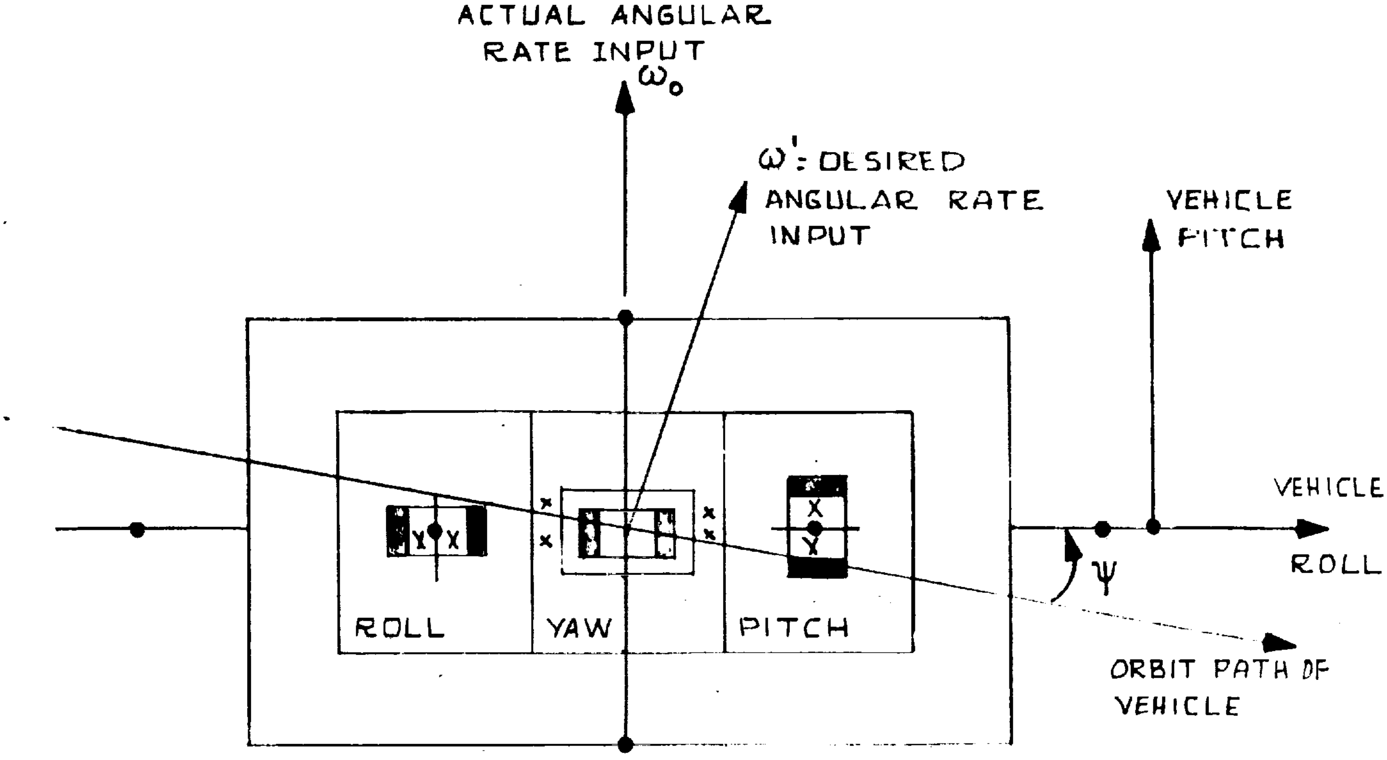
ACTUAL ANGULAR RATE INPUT
ω_0
ω': DESIRED ANGULAR RATE INPUT
VEHICLE PITCH
VEHICLE ROLL
ψ
ORBIT PATH OF VEHICLE
ROLL
YAW
PITCH
X
Y

Fig. 3.3

Vehicle Oriented Platform

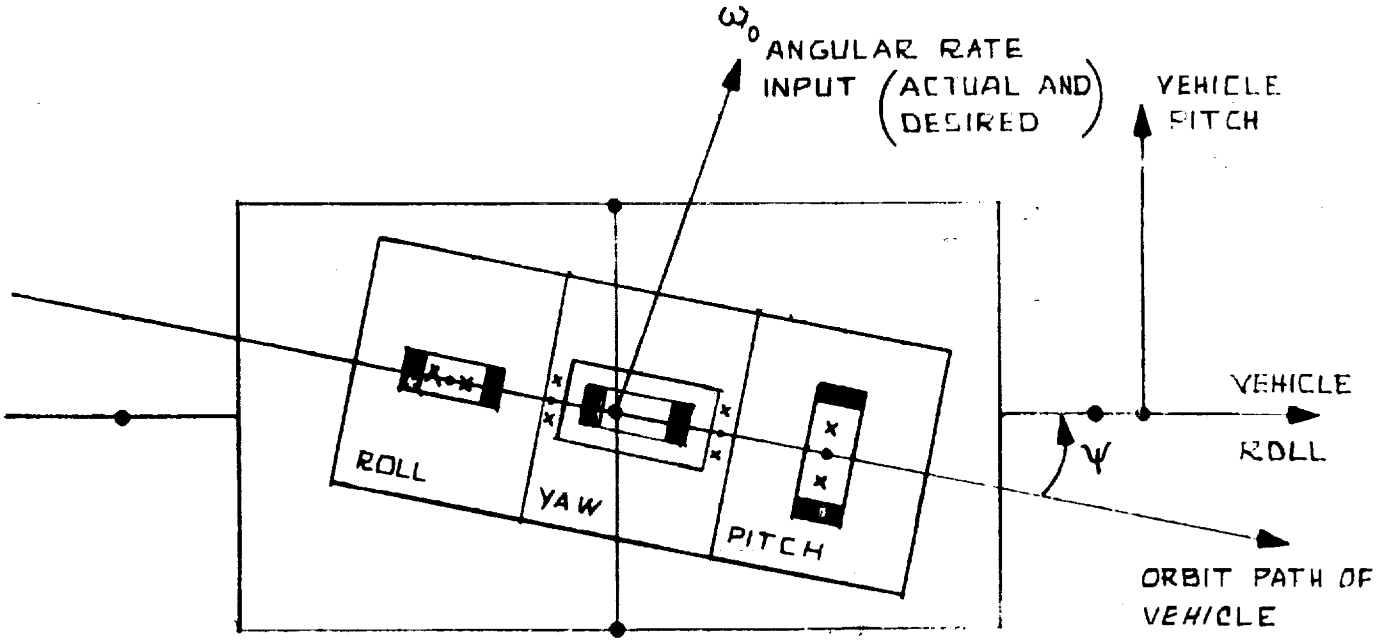
ω_0 ANGULAR RATE INPUT (ACTUAL AND DESIRED)
VEHICLE PITCH
VEHICLE ROLL
ψ
ORBIT PATH OF VEHICLE
ROLL
YAW
PITCH

Fig. 3.4

Orbit Oriented Platform

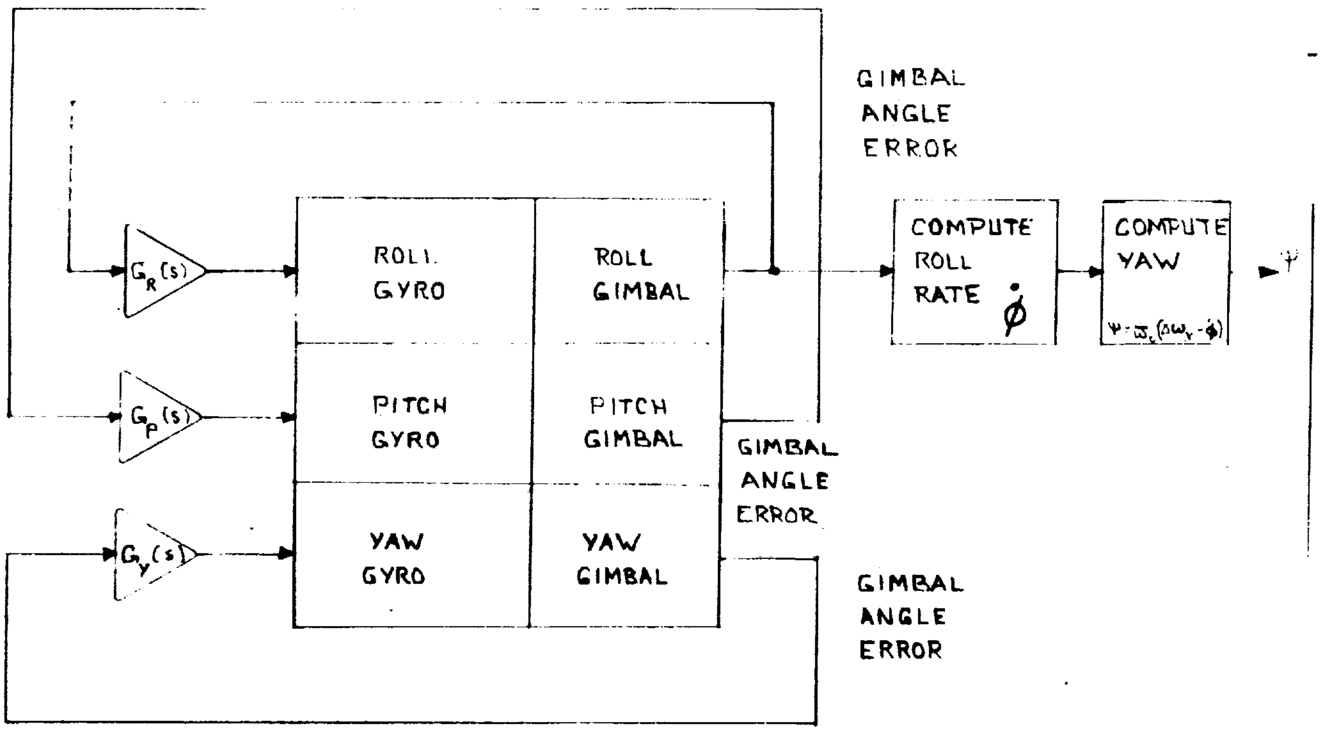
GIMBAL ANGLE ERROR
$G_R(s)$
$G_P(s)$
$G_Y(s)$
ROLL GYRO
ROLL GIMBAL
PITCH GYRO
PITCH GIMBAL
YAW GYRO
YAW GIMBAL
GIMBAL ANGLE ERROR
GIMBAL ANGLE ERROR
COMPUTE ROLL RATE $\dot{\phi}$
COMPUTE YAW
$\Psi = \bar{\omega}_o(\Delta\omega_y - \dot{\phi})$
Ψ

Fig. 3.5
Open Loop Yaw Indication from Measuring Roll Gimbal Angle Rate with Caged Platform

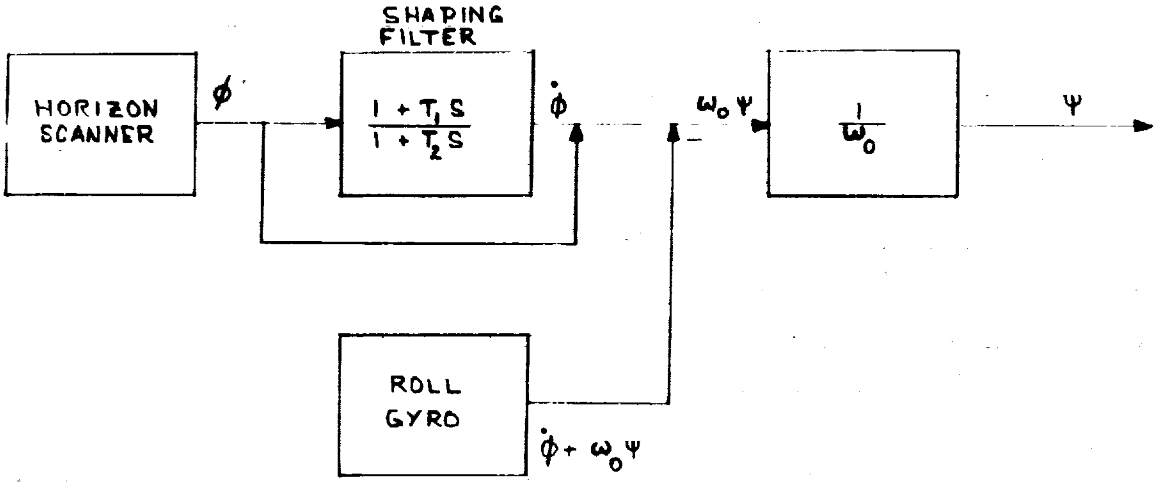
HORIZON SCANNER
ϕ
SHAPING FILTER
$\frac{1 + T_1 S}{1 + T_2 S}$
$\dot{\phi}$
$\omega_o \Psi$
$-$
$\frac{1}{\omega_o}$
Ψ
ROLL GYRO
$\dot{\phi} + \omega_o \Psi$

Fig. 3.6
Open Loop Yaw Indicator Mechanization

minimized. In the case of a vehicle strapped gyro, the output directly reflects all of the vehicle motion, and compensation for roll rate is a difficult problem. For the gimballed system the proper caging of the gyros can be taken advantage of to attenuate the effect of vehicle motion. The roll rate signal, however, must be smoothed or compensated in both mechanization so that the real isolation of vehicle roll motion is not eliminated entirely.

In general, the measuring of roll rate to infer azimuth error is an undesirable approach to mechanization for yaw indication because roll rate must somehow be compensated to extract the desired effect of yaw coupling. To measure roll rate which is free of the azimuth coupling, the horizon sensor derived roll error signal may be differentiated to yield the roll rate $\dot{\phi}$. This is subtracted from the roll gyro indicated roll rate to yield $\omega_0 \psi$. However, all available literature on horizon sensors point to large noise content in the resolution of level indication imply discrimination of rate indication to be extremely difficult; therefore, the determination of the horizon sensor derived rate signal is presently considered an impractical approach to mechanization. Further discussion on roll rate determination errors are found in Ref. 2 and 3.

Figure 3.4 in the alined condition allows the yaw indication to be read off at the azimuth gimbal axis. This mechanization depends upon the alinement of the platform frame to the orbital frame. Since the steady state roll error is proportional to the steady state yaw error, a mechanization which suggests itself is to drive the yaw gyro with a signal proportional as the roll error; the error signals being a measure of platform error relative to the orbital frame.

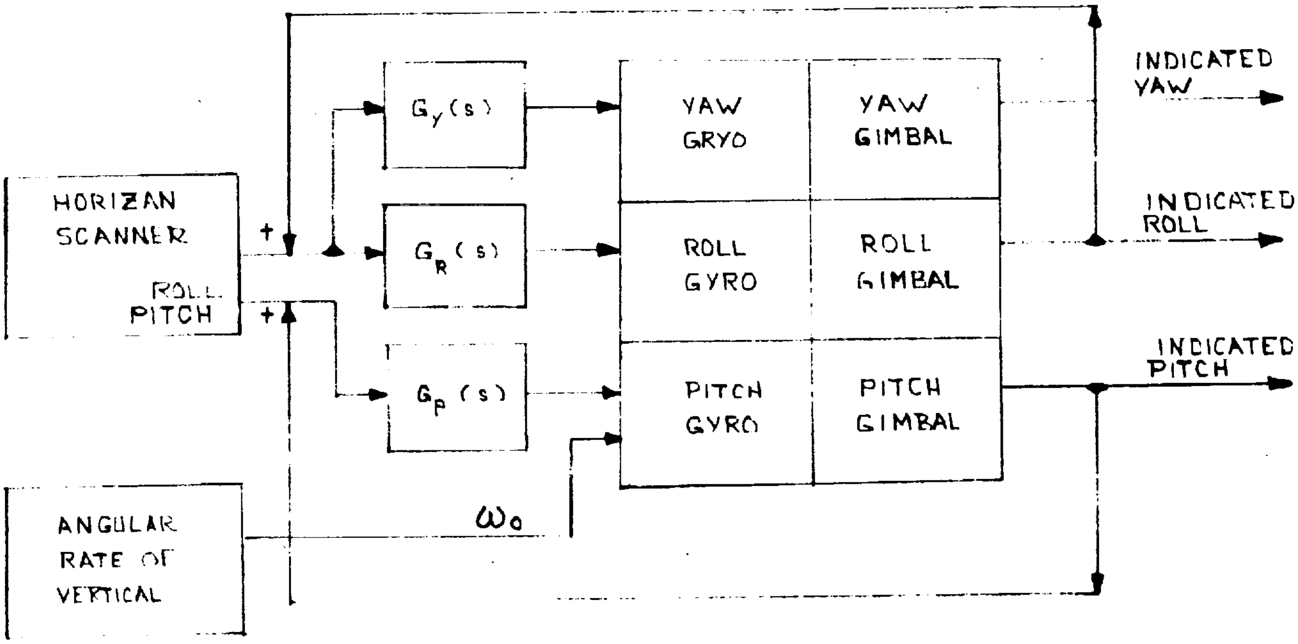

Fig. 3.7

Generalized Gyrocompass Self-Alinement Diagram

More specifically, the simultaneous torquing of the roll and yaw gyro with a signal proportional to the roll platform error might secure self-alinement of the platform to the orbital frame. The basic insight provided by this mechanization is that it is a direct analog of the cruise and fixed site gyrocompass mechanization considered in the earlier sections of the present study.

Figure 3.7 is a generalized diagram of a self-alinement gyrocompass scheme. The basic objective of self-alinement here is to effect platform alinement to the orbital frame as shown in Fig. 3.4. The block diagram of Fig. 3.7 is seen to be analogous to the fixed site gyrocompass problem except for small differences in the technique of derived signals for torquing the gyros. Here the roll and yaw gyros are torqued with the angle error signals obtained from the platform gimbals and the horizon sensor. The torques applied to the gyros can be given in terms of a generalized transfer functions

$$T_R = G_R(s)\,(\phi^{po} + \Delta\phi)$$

$$T_y = G_y(s)\,(\phi^{po} + \Delta\phi)$$

$$T_p = G_p(s)\,(\theta^{po} + \Delta\theta)$$

where $G_R(s)$ and $G_y(s)$ are arbitrary transfer functions converting the measured roll into gyro torquing signals. The parameter $\Delta\phi$ is primarily the resolution error of the horizon sensor consisting of a bias and random noise components.

A generalized representation can be given to the response of the attitude deviation in the presence of the feedback torques. For a nominally locally level alined platform the deivation propagation equation with feedback are shown in a later section to be given as

$$S\theta + G_p(s)\theta = -G_p(s)\Delta\theta + \varepsilon_y \qquad \text{Pitch}$$

$$S\phi + \omega_o\psi + G_R(s)\phi = -G_R(s)\Delta\phi + \varepsilon_x \qquad \text{Roll}$$

$$s\psi - \omega_o\phi - G_y(s)\phi = +G_y(s)\Delta\phi + \varepsilon_z \qquad \text{Yaw}$$

and the generalized response is given as

$$\theta = \frac{G_p(s)}{s+G_p(s)}\Delta\theta + \frac{\varepsilon_y}{s+G_p(s)}$$

$$\phi = \frac{s\ \varepsilon_x - \omega_o\ \varepsilon_z}{\nabla(s)}\quad\theta - \frac{(sG_R(s)+\omega_o G_y(s))}{\nabla(s)}\quad\phi$$

$$\psi = \frac{(\omega_o+G_y(s))\,\varepsilon_x+(s+G_R(s))\,\varepsilon_z}{\nabla(s)} + \frac{sG_y(s)\,\omega_o G_R(s)}{\nabla(s)}\quad\phi$$

where $\nabla(s) = S^2 + sG_R(s) + \omega_o(\omega_o + G_y(s))$ is the characteristic equation.

The following sections will consider the response characteristics associated with various forms of the transfer functions $G_R(s)$, $G_p(s)$, and $G_y(s)$.

4.0 Summary Discussion

A summary discussion of the various gyrocompass alinement mechanizations considered for the local level platform is given here. The following sections contain the detailed developments.

Table 4.1 is a summary of various response characteristics of the roll and yaw platform axes to various transfer functions $G_R(s)$ and $G_Y(s)$. The transient, steadystate, and noise response characteristics are shown for each case.

The pitch axis analysis is given separately because it is decoupled from the other two axes and because it is comparatively an easier problem. In general, a proportional feedback using the pitch error is probably an adequate mechanization. This control will damp the initial pitch errors and bound the effect of gyro drift. However, performance is limited by sensor errors.

The various cases listed in the table include most of the possible kinds of feedback control on the roll and/or yaw gyros; assuming the horizon sensor error signal is the only externally available observable.

For all mechanizations, it is shown that a basic error limitation to stabilizing the yaw channel in orbit arises from the coupling of roll gyro drift rate. No mechanization which utilizes level error signals to stabilize the yaw channel (the classical gyrocompass alinement problem) can attenuate the effect of this error source. The basic steady state platform yaw error resulting from gyrocompass alinement and which is independent of mechanization is

$$\Delta\psi = \frac{1}{\omega_0} \varepsilon_x$$

Other error sources are, of course, present but their effects can be attenuated to a certain degree by the adjustment of the system gain.

This ultimate yaw resolution error has its counterpart in the fixed site and cruise mechanization. Here, however, ω_0 is orbital rate which is about sixteen times larger than earth rate; consequently in orbital operation, yaw indication error from gyro drift is automatically attenuated in the ratio of sixteen to one. As a result for orbital operations, it can be expected that gyro drift is not really the error source which would limit system performance.

Another basic error source which cannot be attenuated by mechanization is the effect of horizon sensor bias as it affects the pitch axis. The steady state pitch error is limited by the sensor bias. This effect has its counterpart in the fixed site case where accelerometer bias sets the basic limitation to alinement accuracy.

form Response Characteristics for ting Gyro-Platform

: Gyro ıg ;	Asymptotic Mean Square Response Due to Random Gyro Drift Rate and Horizon Sensor Pointing Error (Assume No Cross Correlation)	Comments (It is Assumed that Pitch Axis is Stabilized)
:	$\overline{\phi}^2$ and $\overline{\psi}^2 \approx \frac{\overline{\epsilon}^2\beta t}{\beta^2+\omega_y^2}$	1. Open Loop Response 2. Conditional Stability to System Axis Inputs 3. Initial Errors Undamped 4. Unbounded Platform Drift Rate Due to Random Gyro Drift
	$\overline{\phi}^2 = \frac{\overline{\epsilon}_x^2\beta+\overline{\epsilon}_z^2(K_R+\beta)}{K_R(K_R\beta+\omega_y^2+\beta^2)} + \frac{K_R\gamma\overline{\Delta\phi}^2}{K_R\gamma+\omega_y^2+\gamma^2}$ $\overline{\psi}^2 = \frac{\overline{\epsilon}_x^2(K_R+\beta)+\overline{\epsilon}_z^2(\omega_y^2\beta+K_R^3+\beta K_R^2}{K_R(K_R\beta+\omega_y^2+\beta^2)}$ $+ \frac{K_R(K_R+\gamma)\overline{\Delta\phi}^2}{K_R\gamma+\omega_y^2+\gamma^2}$	1. Promising 2. Damped Response in Roll and Yaw 3. Initial Errors Damping 4. Undesirable-Natural Frequency of System is Fixed to Orbital Frequency 5. For Steady-State Desirable or Choose K_R as Small as Possible
	$\overline{\phi}^2 \approx \frac{\overline{\epsilon}^2\beta t}{\beta^2+\omega_y(\omega_y+K_y)} + \frac{\omega_y^2K_y^2\overline{\Delta\phi}^2\gamma t}{\gamma^2+\omega_y(\omega_y+K_y)}$ $\overline{\psi}^2 \approx \frac{(\omega_y+K_y)^2\overline{\epsilon}^2\beta t}{\beta^2+\omega_y(\omega_y+K_y)} + \frac{K_y^2\Delta\psi^2\gamma t}{\gamma^2+\omega_y(\omega_y+K_y)}$	1. Conditional Stability to Systematic Inputs (Increased Natural Frequency) 2. Initial Errors Undamped 3. Unbounded Platform Drift Due to Random Gyro Drift and Horizon Sensor Error
	$\overline{\phi}^2 = \left[\frac{\beta\epsilon_x^2}{K_R} + \frac{\omega_y(K_R+\beta)\epsilon_z^2}{K_R(\omega_y+K_y)}\right] + [K_R\beta+\omega_y(\omega_y+K_y)+\beta^2]$ $+ \overline{\Delta\phi}^2 \frac{K_R^2\gamma(\omega_y+K_y)+K_y^2\omega_y(K_R+\gamma)}{K_R(\omega_y+K_y)[K_R\beta+\omega_y(\omega_y+K_y)+\gamma^2]}$ $\overline{\psi}^2 = \frac{(\omega_y+K_y)(K_R+\beta)\overline{\epsilon}_x^2}{\omega_yK_R[K_R\beta+\omega_y(\omega_y+K_y)+\beta^2]}$ $+ \frac{[\beta\omega_y(\omega_y+K_y)+K_R(K_R+\beta)\epsilon_z^2]}{K_R\omega_y(\omega_y+K_y)[K_R\beta+\omega_y(\omega_y+K_y)+\beta^2]}$ $+ \overline{\Delta\phi}^2 \frac{K_y^2(\omega_y+K_y)\gamma+K_R^2\omega_y(K_R+\gamma)}{K_R(\omega_y+K_y)[K_R\beta+\omega_y(\omega_y+K_y)+\gamma^2]}$	1. Promising 2. Stable With Natural Frequency Increased 3. Initial Errors Damped 4. Steady-State Sensor Errors Linear in Roll and Yaw 5. Loop Stiffness Limited by Amplification of Sensor Bias 6. Steady-State Choose K_R Small and K_y Large
		1. Stable With Natural Frequency Changeable 2. Initial Errors Damped 3. Undesirable: Differential Sensor Data 4. Steady-State Yaw Limited by Sensor Errors
		1. Stable Plus Natural Frequency Can Be Increased Above Orbital 2. Initial Condition Damped 3. Undesirable: Differential Horizon Sensor Data 4. Steady-State Roll Limited by Sensor Error
;] $)\Delta\phi$]		1. Stable. Natural Frequency Can Be Increased 2. Essentially Same Considerations as 5 and 6 Except Both Roll and Yaw Steady-State Limited by Sensor Errors
		1. Natural Frequency of Roll-Yaw Mode Can Be Increased Above Orbital 2. Azimuth Error Integrates Horizon Sensor Bias and Gyro Drift 3. Initial Errors Damped 4. Steady-State Roll Limited by Sensor Bias

②

TABLE 4.1 CONTINUED

GYRO CONTROL TRANSFER		ROLL - YAW RESPONSE
9) —	$k_{y2} + \frac{k_{y3}}{s}$	CHARACTERISTIC EQUATION: $\Delta(s) = s^3 + \omega_y(\omega_y + k_{y2})s + k_{y3}$
10) $k_{R1} + \frac{k_{R2}}{s}$	$k_{y1} + \frac{k_{y2}}{s}$	$\begin{matrix} \phi \\ \psi \end{matrix} = \frac{s}{\Delta(s)} \begin{matrix} s & -\omega_0 \\ \omega_0 + k_{y1} + \frac{k_{y2}}{s} & s + k_{R1} + \frac{k_{R2}}{s} \end{matrix} \begin{matrix} \epsilon_x - (k_{R1} + \\ \epsilon_z + (k_{y1} + \end{matrix}$ $\Delta(s) = s^3 + s^2 k_{R1} + s(\omega_0^2 + \omega_0 k_{y1} + k_{R2}) + \omega_0 k$
11) $\frac{k_{R1}s + k_{R2}}{k_{R3}s + k_{R4}}$ FILTER FUNCTION	—	$\begin{bmatrix} \phi \\ \psi \end{bmatrix} = \frac{k_{R3}s + k_{R4}}{\Delta(s)} \begin{bmatrix} s & -\omega_y \\ \omega_y & \frac{k_{R3}s^2 + (k_{R4} + k_{R1})s + k_{R2}}{k_{R3}s + k_{R4}} \end{bmatrix} \begin{bmatrix} \epsilon_x - \\ \epsilon_z + \end{bmatrix}$ $\Delta(s) = k_{R3}s^3 + s^2(k_{R4} + k_{R1}) + s(k_{R2} + k_{R3}\omega_y^2) +$
12) —	$\frac{k_{y1}s + k_{y2}}{k_{y3}s + k_{y4}}$	CHARACTERISTIC EQUATION: $\Delta(s) = k_{y3}s^3 + s^2 k_{y4} + s(\omega_y^2 k_{y3} + \omega_y k_{y1}) + \omega_y^2 k$
13) $\frac{k_{R1}s + k_{R2}}{k_{R3}s + k_{R4}}$	$\frac{k_{y1}s + k_{y2}}{k_{y3}s + k_{y4}}$	CHARACTERISTIC EQUATION: $\Delta(s) = s^2(k_{R3}s + k_{R4})(k_{y3}s + k_{y4}) + s(k_{R1}s + k_{R2})($ $+ \omega_y(k_{y1}s + k_{y2})(k_{R3}s + k_{R4}) + \omega_y^2(k_{R3}s +$
14) $\frac{-k_{R1}}{s + k_{R2}}$	$\frac{k_{y1}}{s + k_{R2}}$	$\phi = \frac{s + k_{R2}}{\Delta(s)} \left[s\epsilon_x - \omega_0 \epsilon_z + \frac{s k_{R1} + \omega_0 k_{y1}}{s + k_{R2}} \Delta\phi \right.$ $\psi = \frac{s + k_{R2}}{\Delta(s)} \left[(\omega_0 + \frac{k_{y1}}{s + k_{R2}})\epsilon_x + (s + \frac{k_{R1}}{s + k_{R2}})\epsilon_z + (\right.$ $\Delta(s) = s^3 + s^2 k_{R2} + s(k_{R1} + \omega_0^2) + \omega_0^2 k_{R2}$

$) \Delta\phi$ $) \Delta\phi$ $Y2$	$\dot{\phi}_{ss} = -\Delta\dot{\phi}$ $\psi_{ss} = \frac{\epsilon_x}{\omega_0} + \frac{k_{R2}}{\omega_0 k_{Y2}} \epsilon_z - \frac{k_{R2}}{k_{Y2}} \Delta\phi$
$\frac{S + k_{R2}}{R3 S + k_{R4}} \Delta\phi + \phi_0 \big]$ ψ_0 $\omega_y^2 k_{R4}$	$\begin{bmatrix} \phi_{ss} \\ \psi_{ss} \end{bmatrix} = \begin{bmatrix} 0 & \frac{-1}{\omega_Y} \\ \frac{1}{\omega_Y} & \frac{k_{R2}}{k_{R4}} \end{bmatrix} \begin{bmatrix} \epsilon_x - \frac{k_{R2}}{k_{R4}} \Delta\phi \\ \epsilon_z \end{bmatrix}$
$+ \omega_y k_{Y2}$	
$_3 s + k_{Y4})$ $_{R4})(k_{Y3} S + k_{Y4})$	
$\frac{K_{Y1} - \omega_0 K_{R1}}{S + K_{R2}}) \Delta\phi \big]$ $+ \omega_0 k_{Y1}$	$\phi_{ss} = \frac{k_{R2}}{\omega_0(\omega_0 k_{R2} + k_{Y1})} \left[-\omega_0 \epsilon_z - \frac{\omega_0 k_{Y1}}{k_{R2}} \Delta\phi \right]$ $\psi_{ss} = \frac{\epsilon_x}{\omega_0} + \frac{k_{R1}}{\omega_0(\omega_0 k_{R2} + k_{Y1})} \left[\epsilon_z - \omega_0 \Delta\phi \right]$

SE	COMMENTS
	1. UNINTERESTING CASE 2. UNSTABLE CHARACTERSTIC EQUATION – INTEGRATES NOISE (GYRO AND SENSOR)
	1. VERY PROMISING 2. DISADVANTAGE: ROLL LIMITED BY SENSOR BIAS 3. INCREASING YAW GYRO INTEGRAL GAIN RESULTS IN NEAR OPTIMUM STEADY STATE RESPONSE 4. INTEGRAL ERRORS CASE 8 COMPLETELY ELIMINATED
	1. STEADY STATE RESPONSE SAME AS 2 2. HAS PROMIS BECAUSE TRANSIENT AND STEADY STATE RESPONSE CAN BE SHAPED BECAUSE OF LARGE NUMBER OF DEGREES OF FREEDOM IN PARAMETER VARIATIONS 3. UNDESIRABLE FEATURES ARE DIFFERENTIAL GYRO DRIFT AND SENSOR DATA
	SAME CONSIDERATIONS AS ABOVE
	1. GENERALIZED MECHANIZATION 2. SAME CONSIDERATIONS AS ABOVE BUT 4th ORDER SYSTEM 3. DESIRABLE LARGE NUMBER OF GAIN PARAMETERS TO BE ADJUSTED FOR SHAPING STEADY STATE, TRANSIENT, AND SPECTRAL RESPONSE CHARACTERISTICS 4. UNDESIRABLE BECAUSE OF MORE COMPLEX ERRORS; COMPONENTS 5. See Text (Section 6.12)
	1. SIMILAR TO FIXED SITE CASE, AND CRUISE SYSTEM MECHANIZATION 2. PROMISING 3. STEADY STATE RESPONSE SAME AS CASE 4 4. FREQUENCY RESPONSE MAY BE IMPROVED BY SHAPING

3

Case 1 gives the open loop characteristics. Without feedback the roll and yaw channel errors oscillate with orbital frequency. If gyro drift and mechanization errors are bounded to small values, and if the system can be initialized at some arbitrary epoch, the free-inertial platfrom drift would be bounded and propagate sinusoidally. The vehicle attitude in roll, pitch, and yaw is obtained from the platform gimbals. In the presence of noise, as might result from random gyro drift rate, a conditionally stable system will tend to give rise to unbounded errors in roll and yaw over long term operation. For an earth pointing vehicle the roll error can be bounded while the yaw error will always remain unbounded.

Case 2 considers a proportional control on the roll gyro utilizing the roll error signal which is derived from the horizon sensor and the roll gimbal angle output. This simple control effects damping in both the roll and yaw channels. However, it lacks stiffness to the extent that the transient settling time is bounded below by the orbital frequency. This implies a minimum time constant of about 15 minutes for a low altitude vehicle. The interesting result, however, is that both roll and yaw are damped simply by torquing the roll gyro.

Case 3 considers the same kind of proportional control on the yaw gyro only. This control effects no damping, the system remains conditionally stable. However, the frequency response has been raised. A higher natural system frequency is desirable from the point of view of decreasing the settling time. This, however, is achieved at the expense of amplifying the effects of high frequency noise (such as arising from the sensor).

Case 4 considers torquing both the roll and yaw gyro with a proportional roll signal. As expected, the characteristic equation exhibits the two desirable characteristics associated with Cases 2 and 3. Roll torquing introduces damping in both channels, yaw torquing provides for increasing the natural frequency. Consequently settling time can be decreased below the 15 min of Case 2 by increasing the gain to the yaw gyro. Increasing gain however, is achieved at the expense of increasing the effect from sensor bias as can be seen in Table 4.1.

Case 5 to 7 considers combinations of derivative plus proportional control using the roll error signal. This case presently lacks interest because a rate signal must be generated from the horizon sensor derived pointing data (Ref. 2). Current literature shows that rate information derived from sensor data is extremely poor (Ref. 3).

Cases 8 to 10 considers integral plus proportional control. Integral control will tend to minimize the effect of noise but will enhance the effect of bias. Reference 2 considers compensation techniques for sensor bias. The effect of gyro bias will, however, remain. Both in Cases 8 and 9, in particular, the integrated effect is evident. However, in Case 1, where both roll and yaw gyros are torqued with an integral plus proportional roll error signal, the integrated errors arising from both gyro and sensor errors cancel out in the mechanization. Further studies regarding this mechanization from the point of view of the effects of noise is required.

Cases 11 to 14 include a generalized filter (bilinear) functions. All previous cases can be considered as special cases to this case. This generalized approach might be considered for shaping the system response for transient settling times, and minimizing the effect of bias and noise.

The design considerations depend upon the relative error characteristics of noise and bias from the gyros and the sensor. Since the basic measurable obtainable from the horizon sensor is of limited resolution anyway, (unlike the fixed site and cruise alinement where high precision measurable are available as outputs of the accelerometers) it would appear sufficient to consider only the simplest mechanizations for orbital operations. Three particular cases satisfying the requirement for simplicity are based on proportional control. These are:

1. Case 1 - closed loop proportional control on pitch axis, with roll - yaw in open loop

2. Case 2 - closed loop proportional control on pitch and roll

3. Case 4 - closed loop proportional control on pitch, roll and yaw. The roll and yaw gyros being fed with roll, the pitch with pitch error.

In Case 1 the system response is independent of sensor errors, however, initial roll-yaw tilt errors are undamped and oscillate. In Case 2 system response is independent (i.e., in steady state) to initial errors but is limited by the sensor errors; and minimum time constant is limited to the orbital period. In Case 4 system response is independent of initial errors; response time can be decreased, but is also limited by sensor errors.

Error Source		Case 1	
		Pitch	Roll
Initial Errors			
Pitch θ_0	1.0 mil		
Roll ϕ_0	1.0 mil		$1.0c\,\omega_0 t$
Yaw ψ_0	1.0 mil		$3.0s\,\omega_0 t$
Constant Gyro Drift			
Pitch ε_y	0.1°/hr	$0.4\,\frac{\omega_0}{K_p}$	
Roll ε_x	0.1°/hr		$0.4s\,\omega_0 t$
Yaw ε_z	0.1°/hr		$0.4(1-c\omega_0 t)$
Random Gyro Drift			
Pitch ε_y rms	0.1°/hr	$0.4\sqrt{\frac{\omega_0^2}{K_p(K_p+\beta)}}$	
Roll ε_x rms	0.1°/hr		$0.4\sqrt{\beta t}$
Yaw ε_z rms	0.1°/hr		$0.4\sqrt{\beta t}$
Horizon Sensor Bias			
Pitch $\Delta\theta$	1 mil	1.0	
Roll $\Delta\phi$	1 mil		
Noise			
Pitch $\Delta\theta$rms	1 mil	$1.0\sqrt{\frac{K_p}{K_p+\gamma}}$	
Roll $\Delta\phi$rms	1 mil		

128 ①

Table 4.2 Summary of Steady State Errors

	Case 2		
Yaw	Pitch	Roll	
$-1.0s\,\omega_0 t$ $3.0c\,\omega_0 t$			
$-0.4(1-e\omega_0 t)$ $0.4s\,\omega_0 t$	$0.4\frac{\omega_0}{K_p}$	0.4	
	$0.4\sqrt{\frac{\omega_0^2}{K_R(K_p+\beta)}}$		
$0.4\sqrt{\beta t}$		$0.4\sqrt{\frac{\beta\omega_0^2}{K_R(\omega_0^2+K_R^2)}}$	$0.4\sqrt{\ }$
$0.4\sqrt{\beta t}$		$0.4\sqrt{\frac{\beta\omega_0^2}{K_R(\omega_0^2+K_R^2)}}$	$0.4\sqrt{\ }$
	1.0		1.
	$1.0\sqrt{\frac{K_p}{K_p+\gamma}}$		
		$1.0\sqrt{\frac{K_R}{K_R^2+\omega_0^2}}$	1.

	Case 4		
Yaw	Pitch	Roll	Yaw
0.4 0.8ζ	$0.4\,\frac{\omega_0}{K_p}$	$0.4\,\frac{\omega_0^2}{\omega_N^2}$	0.4 $0.8\,\zeta\,\frac{\omega_0}{\omega_N}$
$\frac{\omega_0^2(K_R+\beta)}{K_R(\omega_0^2+K_R^2)}$ $\frac{K_R^2}{K_R^2+\omega_0^2}$	$0.4\sqrt{\frac{\omega_0^2}{K_p(K_p+\beta)}}$	$0.4\sqrt{\frac{\frac{\beta}{\omega_N}\,\frac{\omega_0^2}{\omega_p^2}}{2\zeta(1+4\zeta^2+\frac{\beta^2}{\omega_N^2})}}$ $0.4\sqrt{\frac{2\zeta+\frac{\beta}{\omega_N}}{2\zeta(1+4\zeta^2+\frac{\beta^2}{\omega_N^2})}}$	$0.4\sqrt{\frac{2\zeta+\frac{\beta}{\omega_N}}{2\zeta(1+4\zeta^2+\frac{\beta^2}{\omega_N^2}}}$ $0.4\,\frac{\omega_0}{\omega_N}\sqrt{\frac{\frac{\beta}{\omega_N}+4\zeta^2(2\zeta+\frac{\beta}{\omega_N})}{2\zeta(1+4\zeta^2+\frac{\beta^2}{\omega_N^2})}}$
$0\,\frac{K_R}{\omega_0}$	1.0	$(1-\frac{\omega_0^2}{\omega_N^2})$	$2.0\,\frac{\zeta\omega_0}{\omega_N}$
$0\sqrt{\frac{K_R+\gamma}{K_R^2+\omega_0^2}}$	$1.0\sqrt{\frac{K_p}{K_p+\gamma}}$	1.0(I)	1.0(II)

Comments
Cases 2 and 4 initial conditions dampout
$I = \sqrt{\dfrac{4\zeta^2 \frac{\gamma}{\omega_N} + \left(1 - \frac{\omega_0^2}{\omega_N^2}\right)^2 \left(2\zeta + \frac{\gamma}{\omega_N}\right)}{2\zeta\left(1 + 4\zeta^2 + \frac{\gamma^2}{\omega_N^2}\right)}}$ $II = \sqrt{\dfrac{\left(1 - \frac{\omega_0^2}{\omega_N^2}\right)^2 \frac{\omega_N^2}{\omega_0^2} \frac{\gamma}{\omega_N} + \frac{\omega_0}{\omega_N} 4\zeta^2\left(2\zeta + \frac{\gamma}{\omega_N}\right)}{2\zeta\left(1 + 4\zeta^2 + \frac{\gamma^2}{\omega_N^2}\right)}}$ 25

4

The other cases, of course, merit further study; however, as noted previously, the fact that present-day sensors do not yield high performance; imply that the consideration of sophisticated networks at this stage is not necessary except as perhaps for shaping the response but this depends upon knowing the input characteristics very accurately.

To provide insight into the basic accuracy capability of horizon sensor slaved gyrocompass alinement mechanizations, simplified steady error response characteristics are summarized in Table 4.2 for Cases 1, 2 and 4. These three cases appear to typify the characteristic error responses of all the other cases. They have been selected here, not as recommended mechanizations, but primarily because their complete error responses are fairly easy to describe analytically. Table 4.3 is a summary of the associated time constants of the alinement loops.

Case 1 See Section 6.3	Sinusoidal in Roll - Yaw Pitch $\frac{1}{K_p}$
Case 2 See Section 6.4	Roll - Yaw $\frac{1}{\zeta\omega_0} = \frac{2}{K_R} = \frac{15\ \text{min}}{\zeta}$ Pitch $\frac{1}{K_p}$
Case 4 See Section 6.6	Roll - Yaw $\frac{1}{\zeta\omega_N} = \frac{2}{K_R} = 15\left(\frac{\omega_0}{\zeta\omega_N}\right)$ (min) Pitch $\frac{1}{K_p}$

Table 4.3

Summary of Settling Times

In particular, mechanizations having promise for further studies are Cases 10 and 14. In Case 14 a lag filter is used, leading to a third order system with the desirable characteristic that the effect of sensor errors can be bounded by the adjustment of system gain. In Case 10 the steady response shows the roll error to be limited by the sensor bias which cannot be reduced by adjustment of system gain.

5.0 Detailed Mechanization Equations

5.1 Attitude Determination

If the direction cosine matrix, S^{pO}, of the platform frame relative to the orbital frame is known as a function of time, the complete attitude history of the vehicle frame relative to the orbital frame S^{vO} can be determined via the equation

$$S^{vO} = S^{vp} S^{pO} \tag{5.1}$$

where S^{vp} is determined from the platform gimbal angle transducer outputs (via Euler angles). Nominally $S^{pO} = I$ so that the vehicle pitch, roll and yaw is obtained from

$$S^{vO} = S^{vp} \tag{5.2}$$

That is, for a locally level platform alined to the orbital frame, vehicle attitude relative to local level is obtained directly from the platform gimbal angles via Eq.(5.2). If the vehicle is earth pointing then one can assume that its principal axis is also nominally alined to the orbital frame, and from Eq. (5.2) the pitch, roll, and yaw of the vehicle can be expressed in terms of the corresponding small gimbal angles (i.e., $S^{pO} \approx I$ and $S^{vO} \approx I$ also implies that $S^{vp} \approx I$)

$$\begin{aligned} S^{vO} &= I + \Delta S^{vO} = (I + \Delta S^{vO} S^{Ov}) = I - \tilde{\phi}^{vO} \\ &= S^{vp} = I + \Delta S^{vp} = (I + \Delta S^{vp} S^{pv}) = I - \tilde{\phi}^{vp} \end{aligned} \tag{5.3}$$

or

$$\tilde{\phi}^{v0} = \tilde{\phi}^{vp}$$

where

$$\tilde{\phi}^{v0} = \begin{bmatrix} 0 & -\psi & \theta \\ \psi & 0 & -\phi \\ -\theta & \phi & 0 \end{bmatrix} \qquad \begin{array}{l} \psi = \text{vehicle yaw} \\ \theta = \text{vehicle pitch} \\ \phi = \text{vehicle roll} \end{array} \tag{5.4}$$

$$\tilde{\phi}^{vp} = \begin{bmatrix} 0 & -\phi_z & \phi_y \\ \phi_z & 0 & -\phi_x \\ -\phi_y & \phi_x & 0 \end{bmatrix} \qquad \begin{array}{l} \phi_x = \text{gimbal angle along roll axis} \\ \phi_y = \text{gimbal angle along pitch axis} \\ \phi_z = \text{gimbal angle along yaw axis} \end{array} \tag{5.5}$$

In general the platform frame will drift (due to gyro drift rates, etc) causing S^{p0} to deviate from its unitary value. The objective of the alinement mechanization is to continuously determine the correction on the actual value of S^{p0} so as to cause it to maintain its unitary value. This is accomplished by slaving the platform frame either computationally or physically to the local vertical (as defined by the horizon sensor), measuring deviations of the platform torquing rates (via platform gimbal readouts) to maintain local level and "north"; and determining correction torquing signals to the gyros to cause the platform error $\tilde{\phi}^{p0}$ to seek null. From Eq. (5.1) the variations of vehicle attitude is more correctly represented

$$I - \tilde{\phi}^{v0} = (I - \tilde{\phi}^{vp})(I - \tilde{\phi}^{p0})$$

which implies that

$$\tilde{\phi}^{v0} = \tilde{\phi}^{vp} + \tilde{\phi}^{p0} = -\tilde{\phi}^{pv} + \tilde{\phi}^{p0} \tag{5.6}$$

where $\tilde{\phi}^{pO}$ is the platform attitude error relative to the orbital frame. If indeed the platform is perfectly alined, $\tilde{\phi}^{pO} = 0$, then the vehicle attitude relative to the orbital frame is given directly as the gimbal angle readouts $\tilde{\phi}^{vp}$. In the general case the absolute requirement $S^{pO} = I$ is not necessary; only that S^{pO} can be corrected and/or updated.

Stated in this way, the alinement mechanization is identical to the conventional gyrocompassing problem for stationary or in-flight alinement of a three axis local level platform (see Ref. 1). There, gyrocompass alinement is achieved by slaving the level channels to the gravity vertical, measuring deviations in platform torquing rates via accelerometer outputs (these deviations are principally ascribed to platform azimuth tilt), and torquing the gyros so as to cause the platform error relative to local level and true north, as sensed by the accelerometers to seek null. In the orbital case the "reference" sensing of platform deviations is accomplished with the horizon sensor and the platform gimbal angle transducer outputs. In the convential stationary alinement, both vertical and angular rate sensing is accomplished via accelerometer outputs.

5.2 Angular Velocity - Platform Torquing Rate

To maintain local level the platform must be rotated at orbital rate. The direction cosine matrix of the platform relative to inertial space is expressed as

$$S^{pI} = S^{pv} S^{vO} S^{OI} = S^{pO} S^{OI} \tag{5.7}$$

where S^{OI} is the transformation matrix between the orbital frame and inertial space (defined by the navigation equations). The total actual platform torquing rate to maintain local level true "north" is given by

$$\tilde{\omega}^{pI} = -\dot{S}^{pI} S^{Ip} = -\dot{S}^{pv} S^{vp} =$$

$$S^{pv} \dot{S}^{vO} S^{Ov} S^{vp} - S^{pv} S^{vO} \dot{S}^{OI} S^{OI} S^{Ov} S^{vp}$$

$$\tilde{\omega}^{pI} = \tilde{\omega}^{pv} + S^{pv} \tilde{\omega}^{vO} S^{vp} + S^{pO} \tilde{\omega}_0 S^{Op} \tag{5.8}$$

$$\tilde{\omega}^{pI} = \tilde{\omega}^{pO} + S^{pO} \tilde{\omega}_0 S^{Op} \tag{5.9}$$

where

$\tilde{\omega}_O = -\dot{S}^{OI} S^{IO}$ = inertial angular velocity of orbital frame whose components are expressed in the orbital frame

$\tilde{\omega}^{vO} = -\dot{S}^{vO} S^{Ov}$ = angular velocity of vehicle frame relative to the orbital frame whose components are expressed in the vehicle frame

$\tilde{\omega}^{pv} = -\dot{S}^{pv} S^{vp}$ = angular velocity of platform frame relative to the vehicle frame whose components are expressed in the platform frame

$\tilde{\omega}^{pO} = -\dot{S}^{pO} S^{Op}$ = angular velocity of the platform frame relative to the orbital frame whose components are expressed in the platform frame

If the platform is maintained truly locally level then $\tilde{\omega}^{pO} = 0$ and the nominal torquing rate to maintain alinement to the orbital frame is

$$\tilde{\omega}^{pI}_{T} = S^{pO}\,\tilde{\omega}_O\,S^{Op} = \tilde{\omega}_O \tag{5.10}$$

where subscript T is used to denote the "true" torquing rate. In addition, if the trajectory is planar as is the case for two-body orbits, $\tilde{\omega}_O$ is

$$\tilde{\omega}_O = -\dot{S}^{OI} S^{IO} = \begin{bmatrix} 0 & 0 & \omega_y \\ 0 & 0 & 0 \\ -\omega_y & 0 & 0 \end{bmatrix} = \tilde{\omega}^{pI} = \begin{bmatrix} 0 & -\omega^{pI}_z & \omega^{pI}_y \\ \omega^{pI}_z & 0 & -\omega^{pI}_x \\ -\omega^{pI}_y & \omega^{pI}_x & 0 \end{bmatrix} \tag{5.11}$$

where

$$\begin{bmatrix} -S\Omega Su + C\Omega C\gamma Cu & -C\Omega S\gamma & S\Omega Cu + C\Omega C\gamma Su \\ S\gamma Cu & C\gamma & S\gamma Su \\ -C\Omega Su - S\Omega C\gamma Cu & S\Omega S\gamma & C\Omega Cu - S\Omega C\gamma Su \end{bmatrix} \qquad (5.12)$$

and Ω, γ are constants for two-body orbits. For planar motion, therefore, the components of the nominal torquing rates are

$$\omega_x^{pI} = 0 = \text{roll platform torque}$$

$$\omega_y^{pI} = \omega_y = \text{pitch platform torque}$$

$$\omega_z^{pI} = 0 = \text{yaw platform torque}$$

One further point is made here. In a general orbital motion perturbations, on the vehicle center-of-mass, are present (Ω and γ are not constants) and to define the local level true "north" frame, it can be shown that the components of $\bar{\omega}_0$ are given by

$$\begin{aligned} \omega_{0x} &= 0 \\ \omega_{0y} &= \omega_y = \dot{u} + \Omega C\gamma \\ \omega_{0z} &= \omega_z = \dot{\Omega} Su\, S\gamma + \dot{\gamma} Cu \end{aligned} \qquad (5.13)$$

where ω_y and ω_z are well defined in terms of the perturbation force models affecting the motion of the vehicle center-of-mass. The gross orbital motion, however, is approximately described by Eq. (5.12) and, therefore, the discussion of the general case as expressed by Eq. (5.13) will be deferred to a later section.

It should be noted that the nominal platform torquing rate, as expressed by Eq. (5.11) and (5.13), is based upon the orbital parameters which are assumed to be known without error. Actually, however, in an "open-loop" torquing mechanization, the level torquing can be maintained either via computation or by the direct slaving of the level channels to the horizon sensor defined vertical. In both cases feedback corrections to the gyro torquing signals, based on sensor and gimbal angle deviations, are introduced to null the indicated errors. These considerations are discussed further in a later section. For present purposes, however, it will be assumed that the nominal torquing of the platform is without error.

5.3 Platform Torquing Rate Error - The Platform Attitude Error Propagation Equations

Subtracting Eq. (5.10) from Eq. (5.8) and (5.9) the deviation in the torquing rate is obtained.

$$\Delta\tilde{\omega}^{pI} \equiv \tilde{\omega}^{pI} - \tilde{\omega}_T^{pI} = \tilde{\omega}^{pI} - \tilde{\omega}_0 = \tilde{\omega}^{pv} + S^{pv}\ \tilde{\omega}^{v0} + S^{p0}\ \tilde{\omega}_0\ S^{0p} - \tilde{\omega}_0 \quad (5.14)$$

$$= \tilde{\omega}^{p0} + S^{p0}\ \tilde{\omega}_0\ S^{0p} - \tilde{\omega}_0 \quad (5.15)$$

This equation is used to relate the error in torquing the platform to platform attitude error.

Note that the total error in torquing is due to the angular motion of the platform frame relative to the orbital frame $\tilde{\omega}^{p0}$ (nominally equal to zero) and the alinement error of this frame (as expressed by S^{p0} being different from its nominal unitary value) relative to the orbital frame.

The two forms given by Eq. (5.14) and (5.15) suggest two different mechanizations. Either the platform frame can be corrected relative to the vehicle frame (Eq. (5.14)) or corrected relative to the orbital frame (Eq. (5.15)). The former would appear to be less desirable since oscillatory modes of the vehicle attitude arising from limit cycle motion resulting from the vehicle attitude control system must be accounted for in the alinement mechanization. In the latter form the platform motion relative to the orbital frame would be considerably more "smooth" (of orbital frequency) governed largely by gyro drift; therefore, alinement of the system should be a simpler problem.

It is next desired to express Eq. (5.14) as a linear equation in terms of platform attitude deviation. Assuming the platform frame deviates from the orbital frame by small angles, the linearized platform attitude error equation can be developed as follows. From Eq. (5.14)

$$\Delta\tilde{\omega}^{pI} = \tilde{\omega}^{pO} + S^{pO}\,\tilde{\omega}_O\,S^{Op} - \tilde{\omega}_O \tag{5.16}$$

$$\tilde{\omega}^{pO} = -\dot{S}^{pO}\,S^{Op}$$

Let the estimated or computed value of S^{pO} be designated with a hat (^) symbol. Then

$$\hat{S}^{pO} = S^{pO} + \Delta S^{pO} \tag{5.17}$$

where ΔS^{pO} is a first variation on the elements of S^{pO}. From Eq. (5.16)

$$\begin{aligned}\hat{S}^{pO} &= (I + \Delta S^{pO}\,S^{Op})S^{pO}\\ &= (I - \tilde{\phi}^{pO})S^{pO} = I - \tilde{\phi}^{pO}\end{aligned} \tag{5.18}$$

where $\tilde{\phi}^{pO} = -\Delta S^{pO}\,S^{Op}$ is antisymmetric matrix

$$\tilde{\phi}^{pO} = \begin{bmatrix} 0 & -\psi^{pO} & \theta^{pO} \\ \psi^{pO} & 0 & -\phi^{pO} \\ -\theta^{pO} & \phi^{pO} & 0 \end{bmatrix} \tag{5.19}$$

obtained from a general Euler rotation matrix by assuming small angles.

Returning to Eq. (5.16), substituting Eq. (5.19) into Eq. (5.16) by assuming the S^{pO} is really the computed value, the linearized platform attitude error equation is obtained. The development is as follows.

$$\Delta\tilde{\omega}^{pI} = \Delta\tilde{\omega}^{pO} + \Delta S^{pO} \ \tilde{\omega}_O \ S^{Op} + S^{pO} \ \tilde{\omega}_O \ \Delta S^{Op} \tag{5.20}$$

$$\Delta\tilde{\omega}_O = 0 = \text{no navigation error} \tag{5.21}$$

where from Eq. (5.16)

$$\Delta\tilde{\omega}^{pO} = -\Delta\dot{S}^{pO} \ S^{Op} - \dot{S}^{Op} \ \Delta S^{Op} \tag{5.22}$$

Equation (5.22) is reduced in terms of $\tilde{\phi}^{pO}$ (by Eq. 5.18) as follows

$$\tilde{\phi}^{pO} \equiv -\Delta S^{pO} \ S^{Op} \tag{5.23}$$

$$\dot{\tilde{\phi}}^{pO} \equiv -\Delta\dot{S}^{pO} \ S^{Op} - \Delta S^{pO} \ \dot{S}^{Op} = -\Delta\dot{S}^{pO} \ S^{Op} - \Delta S^{pO} \ S^{Op} \ S^{pO} \ \dot{S}^{Op} \tag{5.24}$$

$$= -\Delta\dot{S}^{pO} \ S^{Op} + \tilde{\phi}^{pO}(\dot{S}^{pO} \ S^{Op})^T = -\Delta\dot{S}^{pO} \ S^{Op} - \tilde{\phi}^{pO} \ \tilde{\omega}^{pO} \tag{5.25}$$

Substituting Eq. (5.24) into Eq. (5.22) and further reducing

$$\Delta\tilde{\omega}^{pO} = \dot{\tilde{\phi}}^{pO} + \tilde{\phi}^{pO} \ \tilde{\omega}^{pO} - \tilde{\omega}^{pO} \ \tilde{\phi}^{pO} \tag{5.26}$$

Substituting Eq. (5.25) into Eq. (5.20) and further reducing

$$\Delta\tilde{\omega}^{pI} = \dot{\tilde{\phi}}^{pO} + \tilde{\phi}^{pO}(\tilde{\omega}^{pO} + S^{pO} \ \tilde{\omega}_O \ S^{Op}) - (\tilde{\omega}^{pO} + S^{pO} \ \tilde{\omega}_O \ S^{Op})\tilde{\phi}^{pO} \tag{5.27}$$

$$= \dot{\tilde{\phi}}^{pO} + \tilde{\phi}^{pO} \ \tilde{\omega}^{pI} - \tilde{\omega}^{pI} \ \tilde{\phi}^{pO} \tag{5.28}$$

This equation has the familiar vector equivalent

$$\Delta\underline{\omega}^{pI} = \dot{\underline{\phi}}^{pO} + \underline{\omega}^{pI} \times \underline{\phi}^{pO} \tag{5.29}$$

The input to this equation $\Delta\underline{\omega}^{pI}$ is composed of the gyro drift rates, $\underline{\epsilon}$, gyro torquing scale factor errors, $k\underline{\omega}^{pI}$, the feedback gyro torquing rates, $\underline{T}$, and the actual deviation between the actual required torquing rate resulting from platform drift and the desired nominal orbital frame torquing rate, $\Delta\underline{M}$.

$$\Delta\underline{\omega}^{pI} = \underline{\epsilon} + \underline{T} + \Delta\underline{M} + k\underline{\omega}^{pI} \qquad (5.30)$$

Equation (5.29) is more specifically written as

$$\dot{\underline{\phi}}^{pO} + \underline{\omega}^{pI} \times \underline{\phi}^{pO} = \underline{\epsilon} + \underline{T} + \Delta\underline{M} + k\underline{\omega}^{pI} \qquad (5.31)$$

This equation is the basic platform attitude error propagation equation and is the basis for the present gyrocompass mechanization studies. If the input side of this equation and the initial conditions are known as a function of time, the integration of this equation will yield the platform attitude deviation as a function of time.

Assuming the dominate error frames arise from gyro drift and incorrect mechanization, Eq. (5.31) expanded in terms of components is given as (superscripts are removed for convenience)

$$\underline{\omega}^{pI} = \begin{bmatrix} 0 \\ \omega_y \\ \omega_z \end{bmatrix} = \begin{bmatrix} 0 \\ \dot{u} + \dot{\Omega}\, C\gamma \\ \dot{\Omega}\, Su\, S\gamma + \dot{\gamma}\, Cu \end{bmatrix} \qquad (5.32)$$

where $\underline{\omega}^{pI}$ is given to the first order (i.e., exclusive of body rates)

$$\begin{aligned} \dot{\phi} + \omega_y \Psi - \omega_z \theta &= \epsilon_x + T_x \\ \dot{\theta} + \omega_z \phi &= \epsilon_y + T_y \\ \dot{\Psi} - \omega_y \phi &= \epsilon_z + T_z \end{aligned} \qquad (5.33)$$

These three equations describe the general platform tilt error relative to the orbital frame as a function of time. As shown the three axes are coupled with one another for a general perturbed orbit. That is, in a general motion, the vehicle center-of-mass is perturbed by other than the central force field (i.e., oblateness). The trajectory will not be planar, and as a result, the platform attitude errors of all three axes will be coupled with one another complicating the problem of stabilizing the platform frame. To be even more rigorous the effect of gravity gradient loading on the platform due to unsymmetrical mass distribution must be included in these equations.

For most orbits of interest ω_z and the effect of gravity gradient is several orders of magnitude smaller than ω_y so that Eq. (5.33) may be further simplified to

$$\begin{aligned} \dot{\phi} + \omega_y \Psi &= \varepsilon_x + T_x \\ \dot{\theta} &= \varepsilon_y + T_y \\ \dot{\Psi} - \omega_y \phi &= \varepsilon_z + T_z \end{aligned} \tag{5.34}$$

where ω_y is the orbital angular rate of the vehicle center-of-mass. These equations are sufficient for analysis purposes of the gyrocompass alinement mechanization. For an eccentric two-body orbit ω_y is

$$\omega_y = \sqrt{\frac{\mu}{p^3}} \; \frac{p}{r} = \sqrt{\frac{\mu}{p^3}} \; (1 + e \cos v) \tag{5.35}$$

μ = gravitational and constant

p = semi-latus rectum of orbit

R = radial distance to vehicle center-of-mass

e = orbital eccentricity

v = true anomaly

It is, therefore, seen that a locally level "true" north alined platform in a two-body field, to a first order, the pitch axis error propagation is de-coupled from the roll and yaw. The roll and yaw axes are coupled via the orbital rate ω_y which for nearly circular orbit is approximately by the mean motion, ω_0.

5.4 Characteristics of Free-Inertial Response (Open Loop Attitude Mechanization)

In an open loop mechanization the platform is operated in a free-inertial mode. That is, no feedback error correcting torque is applied to the gyros; and the platform is allowed to drift, it being assumed that the error sources such as arising from gyro drift and initial condition uncertainties are negligible. This corresponds to setting $\underline{T} = 0$ in Eq. (5.31). The vehicle attitude is determined directly from the gimbal angle readouts.

Except for short term operation, an open loop mechanization will not be used in practive because gyro drift and initial condition errors will limit the accuracy of the readout. It is instructive, nevertheless, to characterize the platform attitude error response in the free-inertial mode to provide basic insight into the mature of its propagation with respect to time.

Closed form integrals can be obtained to Eq. (5.33) for the case where the components of $\underline{\omega}^{pI}$ are constant, and for the general elliptic unperturbed orbit case. Both of these integrals are given here for the purpose of defining the regimes of validity for the general constant $\underline{\omega}^{pI}$ case, which is much simpler to use for the mechanization analysis.

5.4.1 Constant Coefficient Solution

This condition obtains for circular orbits to the same order of exactness of the equations themselves. Since most orbits are nearly circular, the circular orbit characteristics will typify a large class of non-circular orbits.

Assuming the components of $\underline{\omega}^{pI}$ are constant with time in general closed form integral solution to Eq. (5.31) can be given as

$$\underline{\phi}^{pO}(t) = \int_0^t [\cos \omega_0 \tau \; I - \frac{\tilde{\underline{\omega}}^{pI}}{\tilde{\omega}_0} \sin \omega_0 \tau + \frac{\underline{\omega}^{pI} (\underline{\omega}^{pI})^T}{\omega_0^2} (1 - \cos \omega_0 \tau)] \Delta \underline{\omega}(t - \tau) dt$$

(equation continued on next page)

$$+ \left[\cos \omega_0\tau \; I - \frac{\tilde{\omega}^{pI}}{\omega_0} \sin \omega_0\tau + \frac{\omega^{pI}(\omega^{pI})^T}{\omega_0^2}(1-\cos \omega_0\tau)\right] \phi_0^{pO} \qquad (5.36)$$

where I is a 3x3 unit matrix, and $\Delta\omega = \epsilon + \Delta M + k\omega^{pI}$. This general solution shows that a constant error such as might result from constant gyro drift rate will cause an unbounded platform error with time. The particular term which contributes to this unbounded error (denoted by asterisk) is

$$\phi^*(t) = \int_0^t \frac{\omega^{pI}(\omega^{pI})^T}{\omega_0^2}(1-\cos \omega_0\tau)\Delta\omega(t-\tau)d\tau \qquad (5.37)$$

In the particular case where the platform is nominally alined to the orbital frame to a first order

$$\omega^{pI} = \begin{bmatrix} 0 \\ \omega_0 \\ 0 \end{bmatrix} \qquad (5.38)$$

and, therefore, the components of Eq. (5.36) are

$$\phi_x^* = 0 = \text{platform roll error}$$

$$\phi_y^* = \int_0^t (1-\cos \omega_0\tau)\Delta\omega_y(t-\tau)d\tau = \text{pitch error}$$

$$\phi_z^* = 0 \qquad = \text{yaw error}$$

The components of Eq. (5.36) expressed in terms of local level "north" system for a circular orbit is $\underline{\phi}^{pO} = (\phi \text{ roll}, \theta \text{ pitch}, \psi \text{ yaw})$

$$\phi = \phi_0 \cos \omega(t - t_0) - \psi_0 \sin \omega(t - t_0)$$

$$+ \int_{t_0}^{t} [\cos \omega_0(t - \tau)\epsilon_x(\tau) - \sin \omega_0(t - \tau)\epsilon_z(\tau)]d\tau$$

$$\theta = \theta_0 + \int_{t_0}^{t} \epsilon_y(\tau)d\tau \tag{5.39}$$

$$\psi = \psi_0 \cos \omega_0(t - t_0) + \phi_0 \sin \omega_0(t - t_0)$$

$$+ \int_{t_0}^{t} [\cos \omega_0(t - \tau)\, \epsilon_z(\tau) - \sin\, \omega_0(t - \tau)\epsilon_x(\tau)]$$

Table 5.1 shows a summary of the platform attitude error response characteristics for an open loop mechanization. The pitch and roll initial errors are assumed to be defined by the horizon level resolution error of the vehicle control system. It is assumed in this mechanization that horizon sensor defined error signals are not used to control the platform. Thus for a locally level true "north" oriented platform the unbounded platform tilt occurs only in the pitch channel. For the general perturbed trajectory, unbounded errors are also possible in the roll and yaw channels; however, the error effect is measured by the small perturbation forces which can be ignored for the present discussion.

From a measure of $\underline{\phi}$ the direction cosine matrix S^{p0} is updated or corrected in the following way. From Eq. (5.17)

$$\hat{S}^{p0} = S^{p0} + \Delta S^{p0} = I - \tilde{\phi}^{p0} \tag{5.40}$$

The estimate $\tilde{\phi}^{p0}$ is used to reset $\hat{S}^{p0}$.

Error Source	Error Magnitude	Roll ϕ (mil)	Pitch θ (mil)	Yaw ψ (mil)
1) Initial Tilt Error				
Roll ϕ_0	1 mil	$1.0 \cos \omega_0 t$		$-1.0 \sin \omega_0 t$
Pitch θ_0	1 mil		1.0	
Yaw ψ_0	3 mil	$3.0 \sin \omega_0 t$		$3.0 \cos \omega_0 t$
2) Drift Rate				
Constant Roll Gyro Drift ε_x	0.1°/hr	$0.4 \sin \omega_0 t$	1.7 t(hrs)	$-.4(1-\cos \omega_0 t)$
Constant Pitch Gyro ε_y	0.1°/hr			
Constant Yaw Gyro ε_z	0.1°/hr	$0.4(1-C\ \omega_0 t)$		$0.4 \sin \omega_0 t$

Table 5.1

Open Loop Platform Attitude
Error Propagation

5.4.2 Time-Varying Coefficient Solution

In the case where the effect of orbital eccentricity is not negligible, the roll-yaw equation (5.34) leads to a Mathieu type equation. Solving these equations simultaneously leads to the time varying coefficient differential equations governing roll and yaw

$$\ddot{\phi} - \frac{\dot{\omega}_y}{\omega_y} \dot{\psi} + \omega_y^{2} \phi = - \frac{\dot{\omega}_y}{\omega_y} \varepsilon_x + \dot{\varepsilon}_x - \omega_y \varepsilon_z \qquad (5.41)$$

$$\ddot{\psi} - \frac{\dot{\omega}_y}{\omega_y} \dot{\psi} + \omega_y^{2} \psi = - \frac{\dot{\omega}_y}{\omega_y} \varepsilon_x + \dot{\varepsilon}_z + \omega_y \varepsilon_x \qquad (5.42)$$

Since

$$\omega_y = \sqrt{\frac{\mu_p}{p^2}}$$

$$\frac{\dot{\omega}_y}{\omega_y} = - 2 \sqrt{\frac{\mu}{p^3}} \frac{p}{r} e \, sv$$

These equations are written as

$$\ddot{\phi} + 2 \sqrt{\frac{\mu}{p^3}} \frac{p}{r} e \, sv \, \dot{\phi} + \left(\sqrt{\frac{\mu}{p^3}}\right) (1 + e \, cv)^{2} \phi = A_x \qquad (5.44)$$

The yaw equation has an identical form.

If the $\dot{\phi}$ and $e^2 \cos v^2 \phi$ term were absent in the equations, a Mathieu equation results. The presence of these terms, though small, yields essentially different kinds of solutions than the characteristic solutions associated with Mathieu equations which can have unstable modes. As shown on the next page this particular equation has a closed form integral which yields a bounded solution for constant inputs.

If the equations are transformed from time differentiation to true anomaly differentiation, the resulting equation will be found to have an exact integral. Consider the roll equation. Let

$$\omega_y = \frac{dv}{dt}$$

then

$$\frac{d}{dt} = \frac{d}{dv}\,\frac{dv}{dt} = \omega_y \frac{d}{dv} \tag{5.45}$$

$$\frac{d^2}{dt^2} = \dot{\omega}_y \frac{d}{dv} + \omega_y^{\,2} \frac{d^2}{dv^2}$$

Substituting these operations into the roll equation, there results

$$\omega_y^{\,2} \left(\frac{d^2\phi}{dv^2} + \phi \right) = - \frac{d\,\omega_y}{dv} \varepsilon_x + \dot{\varepsilon}_x - \omega_y \varepsilon_z \tag{5.46}$$

or

$$\frac{d^2\phi}{dv^2} + \phi = - \frac{1}{\omega_y^{\,2}} \frac{d\,\omega_y}{dv} \varepsilon_x + \frac{1}{\omega_y} \frac{d\,\omega_x}{dv} - \frac{1}{\omega_y} \varepsilon_z$$

$$= \frac{d}{dv} \left(\frac{\varepsilon_x}{\omega_y} \right) - \frac{1}{\omega_y} \varepsilon_z \tag{5.47}$$

the integral can be expressed as

$$\phi(v) = \phi_0(cv - v_0) + \frac{\dot{\phi}_0}{\omega_{y0}} s(v - v_0)$$

$$+ \int_0^v s(v - u) \frac{d}{du} \left(\frac{\varepsilon_x}{\omega_y} \right) du$$

$$- \int_0^v s(v - u) \frac{1}{\omega_y(u)} \varepsilon_z(u) du$$

Assuming that at $t = t_0$, $\varepsilon_x(t_0) = 0$, and at $t = 0^+$, $\varepsilon_x(t_0^+) = 0$, the solution can be expressed further as

$$\phi(v) = \phi_0 \, c(v - v_0) + \frac{\dot{\phi}_0}{\omega_{y0}} s(v - v_0)$$

$$+ \int_0^v \frac{\varepsilon_x(u)}{\omega_y(u)} c(v - u) du - \int_0^v \frac{\varepsilon_z(u)}{\omega_y(u)} s(v - u) du$$

A similar solution can be written for the yaw error

$$\psi(v) = \psi_0 \, c(v - v_0) + \frac{\dot{\psi}_0}{\omega_{y0}} \, s(v - v_0)$$

$$+ \int_0^t \frac{\varepsilon_x(u)}{\omega_y(u)} \, s(v - u) du$$

$$+ \int_0^t \frac{\varepsilon_z(u)}{\omega_y(u)} \, c(v - u) du$$

Equations (5.49) and (5.50) represent the exact solution to the free inertial platform tilt equation (5.34) for an arbitrary eccentric orbit.

For comparison the constant coefficient solution (circular orbit) is given as

$$\phi = \phi_0 \, c \, \omega_0(t - t_0) + \frac{\dot{\phi}_0}{\omega_0} \, s \, \omega_0(t - t_0)$$

$$+ \int_0^t \varepsilon_x \, c \omega_0(t - \tau) d\tau - \int_0^t \varepsilon_z \, s \omega_0(t - \tau) d\tau \tag{5.51}$$

$$\psi = \psi_0 \, c \omega_0(t - t_0) + \frac{\dot{\psi}_0}{\omega_0} \, s \omega_0(t - t_0)$$

$$+ \int_0^t \varepsilon_x \, s \omega_0(t - \tau) d\tau + \int_0^t \varepsilon_z \, s \omega_0(t - \tau) d\tau \tag{5.52}$$

5.4.3 Analysis of the Effect of Orbital Eccentricity

In this section the effect of orbital eccentricity on the free-inertial propagation of the platform tilt errors is examined for constant gyro drift rates and initial errors. The analysis affects only the roll and yaw axes (to the first order) since, as noted earlier, the pitch is decoupled from roll-yaw, and its propagation is independent of the orbital motion.

The purpose in examining the effect of the eccentricity is to attempt to define regimes of operation where the more simple constant coefficient equations can be the basis for gyrocompass mechanization. Specifically, it is desired to uncover tilt propagation which have unbounded response. Any unbounded roll error can be detected if the vehicle is stabilized in the local vertical. However, azimuth errors are undetectable in the free-inertial mode.

5.4.3.1 Initial Condition Errors

The effect of eccentricity can be determined by comparing $\cos(v-v_0)$ and $\frac{s(v-v_0)}{\omega_y(0)}$ (Eq. 5.48 and 5.49) with $\cos \omega_0(t - t_0)$ and $\frac{s\,\omega_0(t-t_0)}{\omega_0}$. This comparison can be made by expressing the true anomaly in terms of the mean motion, M. To a first order in the eccentricity

$$sv = sM + e\ s\ 2M$$

$$cv \approx cM + e\ c\ 2M - e$$

The effect on the initial errors, therefore, is seen to be of the order of $e\ s\ 2M$ and $e(1 - c\ 2M)$. For orbital eccentricities of the order of $e = 0.1$ the error is at most 10% of the circular orbit effect.

5.4.3.2 Gyro Drift

To examine the effect of constant gyro drift, consider the roll error due to yaw gyro drift of Eq. (5.49)

$$\phi = \int_0^v \frac{\varepsilon_z}{\omega_y(u)}\ s(v - u)du$$

where

$$\omega_y(u) = \sqrt{\frac{\mu}{p^3}}\,(1 + e\ c\ u)^2 = \frac{dv}{dt}$$

substituting into the integral

$$\phi = \sqrt{\frac{p^3}{\mu}}\,\varepsilon_z \int_0^v \frac{s(v-u)}{(1+e\ c\ u)^2}\,du$$

$$= \sqrt{\frac{p^3}{\mu}}\,\varepsilon_z \int_0^v s(v-u)\,\sqrt{\frac{\mu}{p^3}}\,dt$$

$$= \varepsilon_z \int_0^v (s\ v\ c\ u - c\ v\ s\ u)dt$$

since

$$cu = \frac{cE-e}{1-e\ c\ E} \qquad su = \frac{\sqrt{1-e2\ s\ E}}{1-e\ c\ E}$$

$$\sqrt{\frac{\mu}{u^3}}\,dt = d\ E(1-e\ c\ E)$$

Expressing in terms of the eccentric anomaly

$$\phi = \varepsilon_x \sqrt{\frac{u^3}{\mu}} \int_0^E (sv(c\ E-e) - cv\,\sqrt{1-e2}\ \ sE)dE$$

where v is held constant

$$= \frac{\varepsilon_z}{\omega_0} \left[sv[sE - eE] - cv \sqrt{1-e^2} \, [1 - cE] \right]$$

$$= \frac{\varepsilon_z}{\omega_0} \frac{\sqrt{1 - e^2}}{1 - e\, cE} \left[1 - cE - eE\, sE + e(1 - cE) \right]$$

Finally it is necessary to expand the eccentric anomaly in terms of the mean motion. To first order in e

$$sE = sM + e\, s\, 2M$$

$$E = M + e\, s\, M$$

$$cE = \frac{1}{2} e + cM + \frac{e}{2} cM$$

Substituting and reducing, the final result is obtained

$$\phi = \frac{\varepsilon_z}{\omega_0} \left[1 - cM + \frac{1}{2} e\, (1 - c\, 2M) + e(1 - M) sM \right]$$

This expression is to be compared with the circular orbit (or constant coefficient) solution

$$\phi = \frac{\varepsilon_z}{\omega_0} (1 - cM)$$

The error due to eccentricity is

$$\Delta\phi = \frac{\varepsilon_x}{\omega_0} (e) \left(\frac{1}{2} (1 - c\, 2M) + (1 - M) sM \right)$$

For long term operation the secular increase of the error is due to the second term

$$\Delta\phi = \left(\frac{\varepsilon_z}{\omega_0}\right) e(1 - M)sM$$

where M is directly proportional to time. Similar expressions can be obtained for the x-gyro drift. The effect being proportional to $e(1 - M)cM$. The yaw axis will experience a similar effect from the roll and yaw gyros.

The conclusion is that while the effect of the error is bounded, for circular orbits, an unbounded error proportional to $e(1 - M)sM$ or $e(1 - M)cM$ can result for eccentric orbits. The effect, however, is attenuated by the eccentricity parameter so that for nearly circular orbits, the error will be small.

In the subsequent gyrocompass mechanization studies, the constant coefficient platform tilt equations will be assumed. If the vehicle is stabilized relative to the local vertical, large tilt errors in the roll channel will be detected and corrected. Hence, ignoring this error effect may be valid. However, the error in the azimuth channel will go uncorrected unless an error correcting mechanization is incorporated into the system.

6.0 Gyrocompass Mechanization

6.1 General

This section considers several particular cases of the feedback transfer functions shown in the generalized diagram of Fig. 3.7 and summarized in Table 4.1. The mechanization consideration will center around the circular orbit. As noted in section 5.4.3, the first order effect due to eccentric orbits was of the order of the eccentricity parameter. For nearly circular orbits, where gyrocompassing has its real utility, the mechanization analysis on the basis of circular orbits would probably be valid. Further analysis of the effect of eccentricity on the particular mechanizations would have to depend upon simulation studies.

The initial portion of this section considers the pitch axis stabilization problem; this is considered separately because, to a first order, pitch motion is decoupled from roll and yaw. For the pitch mode, two specific cases of the feedback transfer function are considered; a simple proportional control, and an integral plus proportional control.

Following this the roll-yaw stabilization problem is examined. Various combinations of the transfer functions $G_R(S)$ and $G_Y(S)$ are considered. These range from a simple proportional to a generalized bilinear transfer function.

It is well to note here a basic error characteristic in gyrocompass alinements which no mechanization can really eliminate. The stabilization of roll and yaw axes using feedback of the roll sensor error will effect certain desired characteristics in the response. However, the yaw channel will always be limited by the roll gyro drift rate. The error in yaw determination which is independent of all mechanization of the above kind is

$$\psi(\text{error in yaw}) = \frac{\epsilon_x}{\omega_0}$$

This result is easy to show. Assume a generalized transfer function for roll and yaw which will yield the control torques

$$T_R = G_R(S)\ (\phi + \Delta\phi)$$

$$T_y = G_y(S)\ (\phi + \Delta\phi)$$

The condition on $G_R(S)$ and $G_y(S)$ is that the resulting characteristic equation is at least stable. The roll-yaw response can be given the generalized representation

$$\dot{\phi} + \omega_0\ \psi = \epsilon_x - G_R(\phi + \Delta\phi)$$

$$\dot{\psi} - \omega_0\ \phi = \epsilon_z + G_y(\phi + \Delta\phi)$$

Solving the system there results

$$\begin{pmatrix} \phi \\ \psi \end{pmatrix} = \frac{1}{\Delta(S)} \begin{bmatrix} S & -\omega_0 \\ +(\omega_0 + G_y(S)) & S + G_R(S) \end{bmatrix} \begin{bmatrix} \epsilon_x - G_R\,\Delta\phi \\ \epsilon_z + G_y\,\Delta\phi \end{bmatrix}$$

where the characteristic equation $\Delta(S)$ is

$$\Delta(S) = S^2 + S\,G_R(S) + \omega_0(\omega_0 + G_y(S))$$

In the steady state

$$\begin{pmatrix} \phi_{SS} \\ \psi_{SS} \end{pmatrix} = \frac{1}{w_0(\omega_0 + G_y(S))} \begin{bmatrix} 0 & -\omega_0 \\ +(\omega_0 + G_y(S)) & G_R(S) \end{bmatrix} \begin{bmatrix} \epsilon_x - G_R\,\Delta\phi \\ \epsilon_z + G_y\,\Delta\phi \end{bmatrix}$$

or

$$\phi_{SS} = -\frac{1}{\omega_0 + G_y(S)}\,(\epsilon_x - G_R\,\Delta\phi)$$

$$\psi_{SS} = -\frac{1}{\omega_0}\,\epsilon_x + \frac{G_R(S)}{\omega_0(\omega_0 + G_y(S))}\,\epsilon_z - \frac{G_R(S)}{\omega_0 + G_y(S)}\,\Delta\phi$$

For all error sources except the roll gyro error in the yaw channel, the possibility of shaping the response by the selection of the proper function $G_R(S)$ and $G_y(S)$ is possible. This shows that an error no mechanization will take care of is the yaw error due to roll gyro drift rate.

The foregoing error effect has also been seen to be characteristic of the fixed site and cruise system mechanization. For the present orbit of case, however, the effect is about sixteen times smaller for close earth vehicles; and for this reason, this unmechanizable effect poses no difficulty in orbital operations. The effect is roughly attenuated by the ratio of earth rate to orbital rate.

A consequence implied by the foregoing is that for earth orbital operations where the angular rates are larger, the effect of gyro drift would be relatively unimportant. The basic error sources limiting system performance would be associated with external measurables such as derived from the horizon sensor.

One additional characteristic in connection to the foregoing discussion is noted here. If the feedback to the roll gyro is absent, then the system tends to be conditionally stable. For example, the characteristic equation may be generalized as:

$$\Delta(S) = S^2 + SG_R(S) + \omega_0(\omega_0 + G_y(S))$$

If $G_R(S) = 0$ then

$$\Delta(S) = S^2 + \omega_0(\omega_0 + G_y(S))$$

Assuming a second order system $\Delta(S)$ is unstable unless

$$\Delta(S) = S^2 + \omega_0^2 + \omega_0 \; G_y(S) = S^2 + aS + b$$

which implies that

$$\omega_0 \; G_y(S) = aS + b - \omega_0^2$$

Thus a damped system can only result provided that yaw control includes at least a derivative feedback.

6.2 Platform Pitch Axis Stabilization

As noted in Eq. (5.33) the pitch axis is weakly coupled to the roll axis. For planar trajectories it is completely decoupled. Since orbital trajectories are closely approximated by planar trajectories (except for perturbations), it is possible to consider the stabilization of the pitch axis independently of roll and yaw. For this reason, pitch stabilization is considered separately in the present section.

From Eq. (34) the platform pitch error propagation is given by

$$\dot{\theta} = \epsilon_y + T_y \tag{6.1}$$

In the absence of a feedback correction the open loop pitch tilt is given by

$$\theta = \theta_0 + \int_{t_0}^{t} \epsilon_y \, dt \tag{6.2}$$

where the initial tilt error t_0 is defined by the horizon sensor resolution error resulting from stabilizing the vehicle to local vertical. If a horizon sensor is not used for external control of the vehicle, the initial platform tilt may be larger than the sensor resolution error and will be determined largely by gyro drift.

The specific error sources causing tilt are due to initial sources, constant and random gyro drift rates. The steady long term error for constant gyro drift and initial condition error is given by

$$\theta = \theta_0 + \epsilon_y t$$

The mean square error resulting from random gyro drift is approximated given by (assume βt)

$$\overline{\theta^2} \cong \frac{2\overline{\epsilon_y^2}\, t}{\beta} \tag{6.3}$$

where β is one reciprocal gyro drift not correlation time. This result is obtained assuming a MARKOV process for gyro drift with an autocorrelation function

$$\phi_\epsilon(\tau) = \overline{\epsilon_y^2}\, e^{-\beta|\tau|} \tag{6.4}$$

6.2.1 Closed Loop Mechanization

The pitch error in an open loop mechanization is seen to be unbounded with time due to gyro drift. To bound the steady state error, damping may be introduced by beginning the pitch gyro with a signal proportional to the sum of the Horizon Sensor error and the pitch gimbal (Fig 3.2)

$$
\begin{aligned}
T_p &= -K_p(\theta^{pv} + \theta^{v0} + \Delta\theta) \\
&= -K_p(\theta^{p0} + \Delta\theta) = -K_p(\theta + \Delta\theta) \qquad (6.5)
\end{aligned}
$$

where θ is the error introduced by the horizon sensor. Since $\theta^{p0} \equiv \theta$, substituting Eq. (6.5) into Eq. (6.1) yields

$$\dot{\theta} + K_p\,\theta = \epsilon_y - K_p\,\Delta\theta \qquad (6.6)$$

which has the solution

$$\theta = \theta_o\, e^{-K_p(t-t_0)} + \int_{t_0}^{t} e^{-K_p(t-\tau)}(\epsilon_y(\tau) - K_p\,\Delta\theta)dt \qquad (6.7)$$

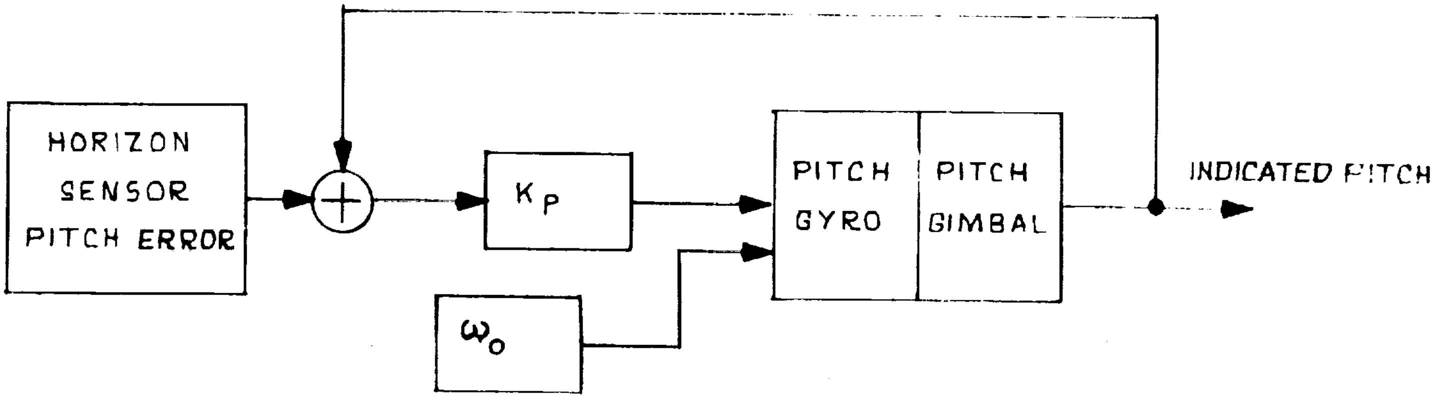

Fig. 6.1

Closed Loop Pitch Axis Stabilization

This solution shows that initial errors are damped out, but at the expense of introducing a new error source $K_p \Theta$. The steady state response assuring gyro drift rate and sensor bias errors is

$$\Theta_{SS} = \frac{\epsilon_y}{K_p} - \Delta\Theta \tag{6.8}$$

Thus damping eliminates initial error, provides the possibility of attenuating (bounding) the effect of gyro drift, but introduces the sensor error as an additional error source.

Comparing the long term response between the open loop and present closed loop mechanization, it is noted that the initial pitch tilt error has been traded for the horizon sensor bias error, and the effect of gyro drift has been bounded.

6.2.2 Effect of Noise

To compare the effect of random errors, the tilt error is given in terms of Laplace transforms

$$\Theta = \frac{\epsilon_y}{S+K_p} - \frac{K_p \Delta\Theta}{S+K_p} \tag{6.9}$$

Assuming drift rate is uncorrelated with horizon sensor bias uncertainty, a steady state mean squared error in pitch can be obtained in terms of the spectral characteristic of the noise processes. For simplicity in the derivation assume that the autocorrelation function for both gyro drift and the sensor noise can be given as

$$\phi_{-}(\tau) = \overline{\epsilon_y^2}\, e^{-\beta|\tau|} \tag{6.10}$$

$$\phi_{\Delta\Theta}(\tau) = \overline{\Delta\Theta^2}\, e^{-\gamma|\tau|} \tag{6.11}$$

where γ is the reciprocal correlation time of the sensor noise.

The power spectral density corresponding to these autocorrelation functions are

$$\Phi_{\epsilon}(\omega) = \frac{2\,\overline{\epsilon_y^2}\,\beta}{\omega^2 + \beta 2} \qquad (6.12)$$

$$\Phi_{\Delta t}(\omega) = \frac{2\,\overline{\Delta\theta^2}\,\gamma}{\gamma^2 + \beta 2} \qquad (6.13)$$

The steady state mean squared pitch tilt error is

$$\overline{\theta^2} = \frac{1}{2\pi j}\int_{-\infty}^{j\infty} Y_1(j\omega)\,Y_1(-j\omega)\,\frac{2\,\overline{\epsilon_y^2}\,\beta}{\omega^2 + \beta^2}\,d\omega + \frac{1}{2\pi j}\int_{-j\infty}^{j\infty} Y_2(j\omega)\,Y_2(-j\omega)\,\frac{2\,\overline{\Delta\theta^2}\,\gamma}{\gamma^2 + \omega^2}\,d\omega \qquad (6.14)$$

where

$$Y_1(S) = \frac{1}{S + K_p}$$

$$Y_2(S) = K_p Y_1(S)$$

Evaluating the integral (Ref. 4) yields the result

$$\overline{\theta^2} = \frac{\overline{\epsilon^2}}{K_p(K_p + \beta)} + \frac{\overline{\Delta\theta^2}\,K_p}{K_p + \gamma} \qquad (6.15)$$

This result shows that increasing K_p reduces the effect of random gyro drift, but increases the effect of sensor noise, however the amplification of this latter effect is bounded to unity, for sensor noise with constant spectral density (white noise) so that the effect due to sensor noise is asymptotic to $\Delta\theta^2 \frac{K_p}{\gamma}$.

6.2.2.1 Integral plus Proportional

Suppose that instead of a simple proportional feedback, an integral plus proportional feedback is used. Let

$$T_p = -\left(K_{p1} + \frac{K_{p2}}{S}\right)(\theta + \Delta\theta)$$

The alinement loop is characterized by the second order system

$$(S + K_{p1} + \frac{K_{p2}}{S})\theta = \epsilon_y - (K_{p1} + \frac{K_{p2}}{S}\Delta\theta$$

or

$$\theta = \frac{S}{S^2 + K_{p1}S + K_{p2}} \quad (\epsilon_y - (K_{p1} + \frac{K_{p2}}{S})\Delta\theta \quad)$$

The steady state response is

$$\theta_{SS} = - \Delta\theta$$

Comparing with Eq. 6-8 it is noted that the effect of gyro drift is eliminated. Although a gyro drift is reduced with a proportional gain by increasing K_p, it is possible that the effect from noise can be further reduced with integral control.

6.2.2.2 Mean Squared Error

Assuming the spectral characteristic, Eq. 6.12 and Eq. 6.13, the mean squared steady state pitch error can be obtained by evaluating the noise integrals in Eq 6.14

$$\overline{\theta^2} = \frac{\overline{\epsilon_y^2}\beta}{K_{p1}(K_{p1}^2 + K_{p2} + \beta^2)} + \overline{\Delta\theta^2}\,\frac{K(K_{p1}^2\gamma + (K_{p1}^2\gamma)K_{p2})}{K_{p1}(K_{p1}^2 + K_{p2} + \gamma^2)}$$

6.2.3 Effect of Incorrect Platform Level Torquing Errors

It is appropriate to point out here the effect of the error in torquing the platform to maintain local level. In a local level system nominally alined to the orbital plane and in a planar vehicle trajectory implied by the two-body unperturbed orbit, the pitch gyro axis is driven with orbital frequency.

The pitch attitude error equation, Eq. 6.1, is more correctly written as

$$\dot{\theta} = \epsilon_y + T_y + \Delta\omega_{oy}$$

where $\Delta\omega_o$ is the error in orbital rate. The general analysis of level torquing error is given in a later section. Here, it is desired to examine the effect this error has on the pitch attitude stabilization.

Assuming the proportional control mechanization, the attitude propagation is

$$\dot{\theta} + K_p \theta = \epsilon_y - K_p \Delta\theta + \Delta\omega_{oy}$$

If $\Delta\omega_{oy}$ is a constant, the effect is similar to constant gyro drift rates, the error from $\Delta\omega_o$

$$\theta (t) = \frac{\Delta\omega_{oy}}{K_p} (1 - e^{-K_p t})$$

An error in torquing the platform does not cause an increasing error in the attitude, but has the steady state tilt effect provided that it is constant.

$$\theta_{SS} = \frac{\Delta\omega_{oy}}{K_p}$$

Depending upon how the torquing signals are generated, this error can potentially result in a large attitude error. If the platform is leveled by the direct slaving to the horizon sensor, then the sensor rate errors appear in this form as bias and noise.

If the platform is torqued with the orbital parameter data, then the effect of navigation errors appear in the pitch determination

This case is somewhat more difficult to describe. The pitch component of $\Delta\omega_o$ is shown in a later section be be (for circular orbits)

$$\Delta\omega_{oy} = \delta\dot{\theta}_y = \frac{\Delta\dot{x}}{R}$$

Where $\Delta\dot{x}$ is the inertial downrange velocity error. The expansion of $\Delta\dot{x}$ in terms of initial errors can be shown to yield

$$\delta\dot{\theta}_y = -\omega_o S\theta \frac{\Delta_{xo}}{R_o} - \omega_o (1 - C\theta) \frac{\Delta_{zo}}{R_o}$$

$$+ (-1 + 2 C\theta) \frac{\Delta\dot{}_{xo}}{R_o} - S\theta \frac{\Delta\dot{}_{zo}}{R_o}$$

where

Δ_{xo} is the initial range error

Δ_{zo} is the initial vertical error

$\Delta_{\dot{x}o}$ is the initial inertial downrange velocity error

$\Delta_{\dot{z}o}$ is the initial inertial vertical velocity error

$\theta = \omega_o(t-t_o)$

Substituting $\delta\dot{\theta}_y$ for $\Delta\omega_{oy}$ in the mechanization involving proportional gain, the pitch error is

$$\theta = \int_0^t e^{-K_p(t-\tau)} \delta\dot{\theta}_y(\tau)\, dt$$

This results in periodic response with orbital frequency, and with amplitude response depending upon the gain K_p.

The conclusion is that pitch platform torquing errors tend to give rise to pitch errors which are sinusoidal with orbital frequency. A similar result will be true of other mechanization so long as they are stable.

If the orbit were eccentric, it can be demonstrated that a secular (linear time build-up) effect will occur in the pitch channel. This effect is attenuated by the eccentricity parameter, however.

6.2.4 Summary of Errors

Table 6.1 presents a summary of the transient response characteristics for the pitch axis in the undamped and damped modes of operation. If the feedback gain constant K_p is chosen large (high stiffness), the transient response is improved, the steady state error effect is attenuated for both constant and random gyro drift; while the effect from the sensor bias and noise is increased. If sensor errors can be assumed to be negligible, high gain feedback improves system response. On the other hand, if these errors are large, then the real tradeoff is between the effect of initial errors as against the effect of sensor errors resulting in the closed loop response. If gyro drift is the dominant error source, closed loop mechanization definitely improves system response.

The platform torquing errors are only shown in the table as a bias. However, the random characteristics of this error should be recognized for the general problem. The mean squared errors are similar to the effect of random gyro drift.

Similar considerations apply to the case of integral plus proportional control. As noted in Table 6.1, some improvement over the proportional gain can be noted for errors due to noise. The primary advantage is the elimination of the error from constant gyro drift rate.

Except for the possibility of introducing a shaping filter, the analysis of the pitch channel is a relatively simple problem. No apparent purpose is served, however, by introducing a shaping filter except perhaps to take into account the frequency characteristic of gyro drift and sensor noise. This would not appear to greatly improve performance over a constant gain function or integral plus proportional gain inasmuch as the simple expedient of increasing the gain K_p actually reduces the effect of most of the primary error sources.

6.3 Case 1 - Open Loop Roll-Yaw

6.3.1 Roll Caging Torque as Measure of Yaw

One simple open loop yaw indication is based on the assumption of gyro drift and vehicle roll rate can be held to tolerable levels. This mechanization would correspond to caging the platform frame to the vehicle frame by nulling the gimbal angles via a high gain caging servo with the vehicle vertical stabilized. The nulling torque is a direct measure of vehicle yaw. This configuration is similar to a strap down system with three single axis platforms. The basic equation is obtained from the roll component of platform tilt error equations (eq. (5.33)). A preliminary discussion of the technique given in sections 3.2 and 3.3.

Table 6.1. Summary of Pitch Axis Error Response Characteristics for Undamped and Damped Modes

Error Source	Open-Loop Pitch Axis Response $\theta(t)$	Closed-Loop (Proportional Control) Pitch Axis Response $\theta(t)$	Closed-Loop Integral Plus Proportional Response $\theta(t)$
1. Initial Condition	θ_o	$\theta_o e^{-K_p t}$	$\frac{\theta_o}{\omega_N\sqrt{1-\zeta^2}} e^{-\zeta\omega_N t} \sin \omega_N\sqrt{1-\zeta^2}\, t$ $\zeta\omega_N = \frac{K_{p1}}{2}$ $\omega_N^2 = K_{p2}$
2. Constant Pitch Gyro Drift Rate	$\varepsilon_y t$	$\frac{\varepsilon_y}{K_p}(1-e^{-K_p t})$	$\frac{\varepsilon_y}{\omega_N\sqrt{1-\zeta^2}} e^{-\zeta\omega_N t} \sin \omega_N\sqrt{1-\zeta^2}\, t$
3. Random Gyro Drift Rate $\phi_\varepsilon = \overline{\varepsilon_y}^2 e^{-\beta\|t\|}$	$\sqrt{\overline{\varepsilon_y}^2} \sqrt{\frac{t}{\beta}}$	$\sqrt{\overline{\varepsilon_y}^2} \sqrt{\frac{1}{K_p(K_p+\beta)}}$	$\sqrt{\overline{\varepsilon_y}^2} \sqrt{\frac{\beta}{K_{p1}(K_{p1}^2+K_{p2}+\beta^2)}}$
4. Horizon Sensor Bias $\Delta\theta$	---	$\Delta\theta(1-e^{-K_p t})$	$\Delta\theta(1-\frac{1}{\sqrt{1-\zeta^2}} e^{-\zeta\omega_N t} \sin \omega_N\sqrt{1-\zeta^2}\, t)$
5. Horizon Sensor Noise $\phi_{\Delta\theta} = \overline{\Delta\theta^2}\, e^{-\gamma\|T\|}$	---	$\sqrt{\overline{\Delta\theta^2}} \sqrt{\frac{K_p}{K_p+\gamma}}$	$\sqrt{\overline{\Delta\theta^2}} \sqrt{\frac{(K_{p1}^2\gamma+K_{p2}(K_{p1}+\gamma))}{K_{p1}(K_{p1}^2+K_{p2}+\gamma^2)}}$
6. Platform Torquing Error Slaved to Sensor $\Delta\omega_o$ (Bias)	$(\Delta\omega_o)t$	$\frac{\Delta\omega_o}{K_p}(1-e^{-K_p t})$	$\frac{\Delta\omega_o}{\omega_N\sqrt{1-\zeta^2}} e^{-\zeta\omega_N t} \sin \omega_N\sqrt{1-\zeta^2}\, t$

$$\dot{\phi} + \omega_y \psi = \Delta\omega_x^{pI} \tag{6.16}$$

Re-introducing the superscript notation

$$\dot{\phi} \equiv \dot{\phi}^{po} = \dot{\phi}^{pv} + \dot{\phi}^{vo} \tag{6.17}$$

$$\psi \equiv \psi^{po} = \psi^{pv} + \psi^{vo} \tag{6.18}$$

This equation is written as

$$\dot{\phi}^{pv} + \dot{\phi}^{vo} + \omega_y (\psi^{pv} + \psi^{vo}) = \Delta\omega_x^{pI} \tag{6.19}$$

Re-arranging the measurables $\dot{\phi}^{pv}$ and ϕ^{pv} on one side of the equation, one can write

$$\dot{\phi}^{pv} + \omega_y \psi^{pv} = \Delta\omega_x^{pI} - (\dot{\phi}^{vo} + \omega_y \psi^{vo}) \tag{6.20}$$

The roll axis gimbal output essentially measures the quantity $\dot{\phi}^{pv} + \omega_y \psi^{pv}$; and the caging servo attempts to null this measurable (note that x^{pv} is nulled by the azimuth servo). This condition corresponds to equating the right sine of the equation to zero or

$$\Delta\omega_x^{pI} = \dot{\phi}^{vo} + \omega_y \psi^{vo} \tag{6.21}$$

Where $\Delta\omega_x^{pI}$ corresponds to the caging torque. If $\dot{\phi}^{vo}$ is measurable or can be held to small tolerable levels, the vehicle yaw is given by

$$\psi^{vo} = + \frac{1}{\omega_y} \Delta\omega_x^{pI} \tag{6.22}$$

Note that this mechanization is independent of initial platform errors. Actually, there is always a residual vehicle roll rate. If this rate can be computed then the indicated yaw is more correctly expressed as

$$\psi^{vo} = + \frac{1}{\omega_y} (\Delta\omega_x^{pI} - \dot{\phi}^{vo}) \tag{6.23}$$

where $\dot{\phi}^{vo}$ is computed.

The error in yaw indication is primarily determined by the residual roll rate error and gyro drift.

$$\Delta\psi^{vo} = + \frac{1}{\omega_y} (\Delta\dot{\phi} + \epsilon_x) \tag{6.24}$$

where $\Delta\dot{\phi}$ is the error in determining vehicle roll rate. Other errors which might be included are the effects from the transient characteristic of the servo caging function.

While this mechanization is relatively simple, its primary drawbacks are its dependence upon external roll rate determination via a horizon sensor; and the requirement to slave the platform frame to the vehicle without having specific information on the noise characteristic of horizon sensors, it is difficult to specify the error in the indication of yaw.

To obtain a numerical measure of the yaw error consider the example. A high frequency sensor pointing noise of six mils maximum 3σ peak-to-peak variation with a smoothing time of one second results in a maximum yaw indication error of 4.8 miles.

6.3.2 Roll and Yaw in Free-Inertial Mode

Instead of caging the platform to the vehicle frame, a more practical mechanization is to slave the platform to the orbital frame. The previous case of alining the platform frame to the vehicle frame was subject to motions of the vehicle. The purpose of considering a gimballed system is to achieve isolation from the vehicle motion.

An open loop mechanization would assume that the initial platform level tilt errors relative to the orbital frame ϕ_0^{pv} and θ_0^{pv} are negligible. Since the pitch error was unbounded for gyro drift, the pitch axis is operated in a closed loop mode. The roll-yaw axes are operated in the free inertial mode. Figure 6.2 is an error diagram corresponding to the present mechanization. The transfer functions for the roll-yaw in the free-inertial mode are given by the equations (dropping again the superscripts)

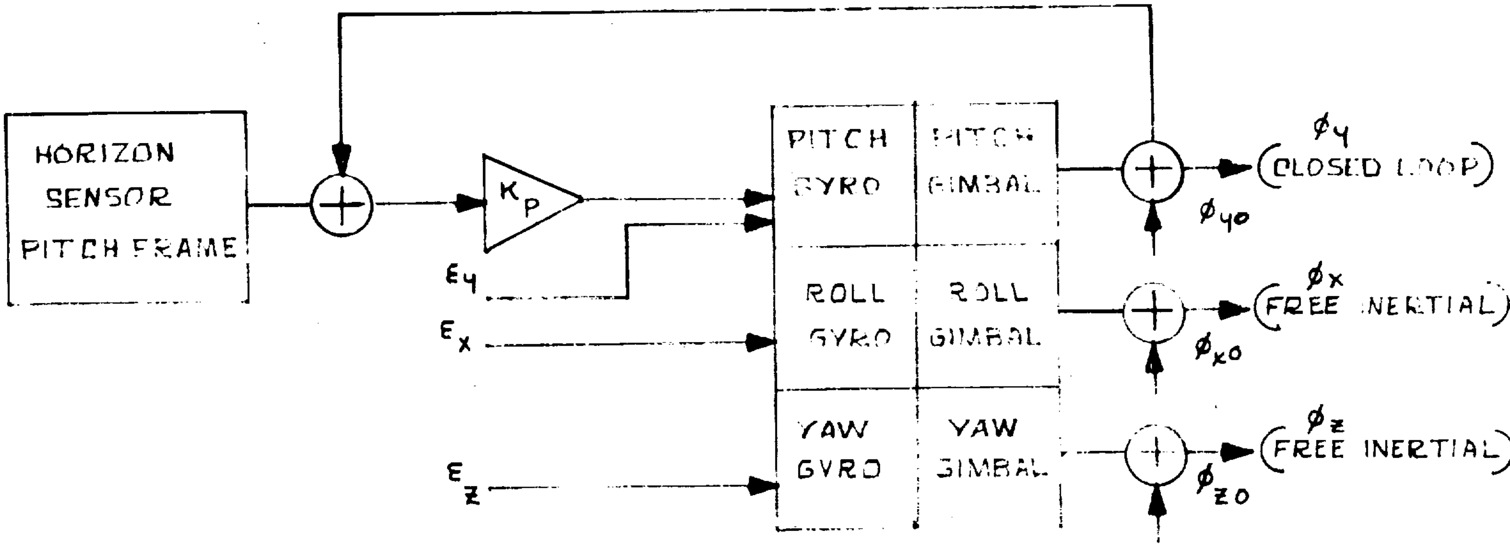
HORIZON SENSOR PITCH FRAME
K_p
ϵ_y
ϵ_x
ϵ_z
PITCH GYRO
PITCH GIMBAL
ROLL GYRO
ROLL GIMBAL
YAW GYRO
YAW GIMBAL
ϕ_y (CLOSED LOOP)
ϕ_{y0}
ϕ_x (FREE INERTIAL)
ϕ_{x0}
ϕ_z (FREE INERTIAL)
ϕ_{z0}

Fig. 6.2

An Error Diagram of an Open Loop Mechanization of Roll and Yaw

$$\phi = \frac{\omega_o \varepsilon_z - S\varepsilon_x + \omega_o \psi_o - S\phi_o}{S^2 + \omega_o^2} \tag{6.25}$$

$$\psi = \frac{S\varepsilon_z + \omega_o \varepsilon_x + S \psi_o + \omega_o \phi_o}{S^2 + \omega_o^2} \tag{6.26}$$

The effect from constant gyro drift and initial errors causes a bounded sinusoidal error propagation along the roll-yaw axes. If these error sources are tolerable, then roll and yaw is obtained directly from the platform gimbals.

The basic time error response associated with the mechanization (Figure 6.2) for constant error sources can be given as

$$\theta^{po} = \frac{\varepsilon_y}{K_p} (1 - e^{-K_p t}) - \Delta\theta (1 - e^{-K_p t}) + \theta_o \; e^{-K_p t}$$

$$\phi^{po} = \frac{1}{\omega_o} (1 - C\, \omega_o t)\, \varepsilon_z + \frac{1}{\omega_o}\, \varepsilon_x\, S\, \omega_o t + \psi_o^{po} \cos \omega_o t \tag{6.27}$$

$$\psi^{po} = -\frac{1}{\omega} S\, \omega_o t\, \varepsilon_z + \frac{1}{\omega_o} (1 - C\, \omega_o t)\, \varepsilon_x + \psi_o^{po}\, C\, \omega_o t + \phi_o^{po}\, S\, \omega_o t$$

The mean squared transient response due to random gyro drift can be derived from equation (6.25) and (6.26). For an undamped system the mean squared error approximately increases linearly with time. It can be shown that the long term (βt 771) errors in roll and yaw is given by

$$\overline{\phi^2} = \frac{\overline{\varepsilon_x^2}\, \beta t}{\omega_o^2 + \beta^2} + \frac{\overline{\varepsilon_z^2}\, \beta t}{\omega_o^2 + \beta^2} = \overline{\psi^2} \tag{6.28}$$

Where the correlation of the roll and yaw gyros are assumed to be the same for gyro drift correlation times greater than the orbital period (about 90 minutes), the mean squared error is approximated by

$$\overline{\phi^2} = \frac{\overline{\epsilon_x^2}\,\beta t}{\omega_o^2} + \frac{\overline{\epsilon_z^2}\,\beta t}{\omega_o^2} = \overline{\psi^2} \tag{6.29}$$

To summarize the system mechanization, the pitch channel is computed with feedback to damp the unbounded effect of gyro drift. The roll-yaw channels are left in open loop which results in conditionally stable but bounded response. It is instructive to consider what basic error limitations are implied by such a mechanization. Table 6.2 presents a **summary** of error sources. In the pitch channel the gain K_p was arbitrarily set to correspond to a 1 minute time constant. The initial yaw error was assumed to be three times as large as the initial level errors which are set by the horizon sensor pointing resolution errors. This assumption is compatible with cruise system gyro compassing where initial azimuth errors always tend larger than level. Random error in the pitch channel was obtained in section 6.2

Error Source	Error Magnitude	Roll ϕ (mil)	Pitch θ (mil)	Yaw ψ (mil)
Pitch Vertical Error $\Delta\theta$ Horizon Sensor	1 mil		Bias 1.0 Noise 1.0	
Initial Platform Pitch Error θ_0	1 mil			
Initial Platform Roll Error	1 mil	$1.0 \cos \omega_0 t$		$1.0 \sin \omega_0 t$
Initial Platform Yaw Error	3 mil	$3.0 \sin \omega_0 t$		$3.0 \cos \omega_0 t$
x-Gyro Drift ε_x Roll	0.1°/hr Bias 0.1°/hr Random			$0.4(1-c\ \omega_0 t)$ $0.4\sqrt{\beta t}$
y-Gyro Drift Pitch ε_y Assume $K_p = 1/60 sec^{-1}$	0.1°/hr Bias 0.1°/hr Random		1.7 1.1 (1 min time constant)	
z-Gyro Drift ε_z Yaw	0.1°/hr Bias 0.1°/hr Random	$0.4(1-c\ \omega_0 t)$ $.4\sqrt{\beta t}$		$0.4 \sin \omega_0 t$ $.4\sqrt{\beta t}$

Table 6.2

Steady State Errors Closed Loop in Pitch Open Loop Roll-Yaw

6.4 Case 2 - Damping the Roll-Yaw Channels

Although the roll-yaw channels have bounded response with orbital frequency, it would still be desirable to stiffen and damp this response so as to eliminate the initial errors and bound the system errors to a lower level by increasing the frequency response. Figure 6.3 is a mechanization in which the roll and yaw response can be damped by a feedback torque to the roll gyro which is proportional to the platform inertial roll error.

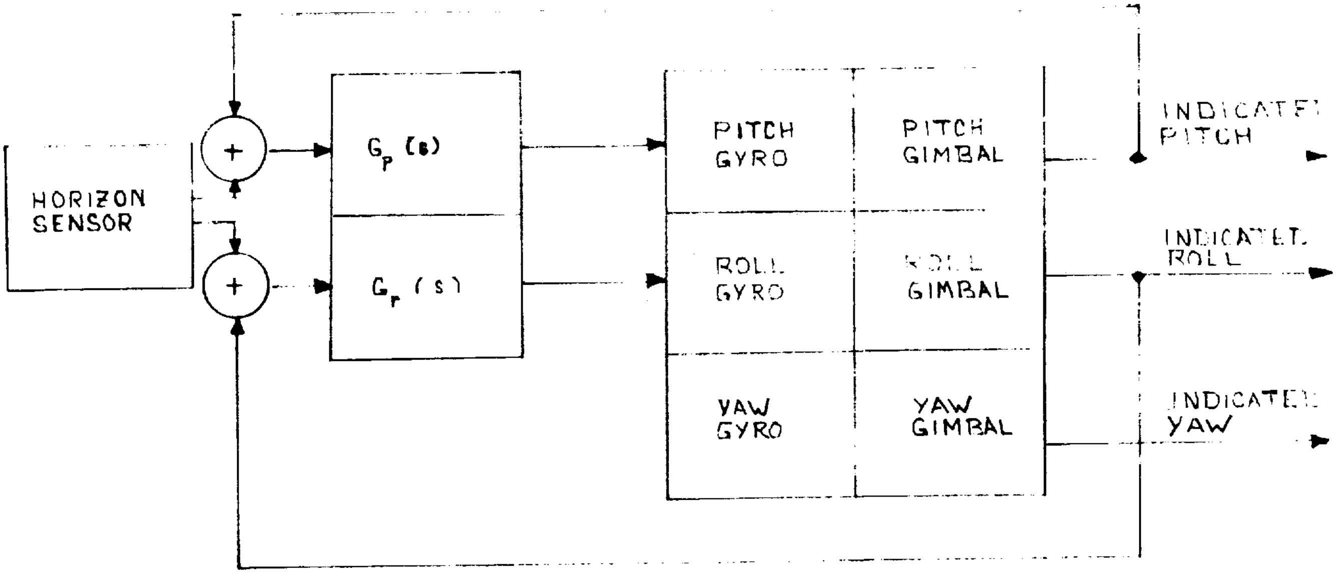
HORIZON SENSOR
+
+
G_p (s)
G_r (s)
PITCH GYRO
PITCH GIMBAL
ROLL GYRO
ROLL GIMBAL
YAW GYRO
YAW GIMBAL
INDICATED PITCH
INDICATED ROLL
INDICATED YAW

Fig. 6.3

Damping the Roll-Yaw Response

The roll gyro torque is generated similar to the pitch using the sum of the roll gimbal and roll horizon sensor error signal

$$T_R = -K_R\,(\phi^{pv} + \phi^{vO} + \Delta\phi) \qquad (6.30)$$

The insight into this roll torquing is that roll error can be damped similarly to the pitch error. The mechanization equations for the three axes are

$$\begin{aligned}
\dot{\phi}^{pO} + K_R\,\phi^{pO} + \omega_0\,\psi^{pO} &= \Delta\omega_x^{pI} - K_R\,\Delta\phi \\
\dot{\theta}^{pO} + K_p\,\theta^{pO} &= \Delta\omega_y^{pI} - K_p\,\Delta\theta \qquad (6.31) \\
\dot{\psi}^{pO} - \omega_0\,\phi^{pO} &= \Delta\omega_z^{pI}
\end{aligned}$$

Considering the roll and yaw channels separately, the solution is:

$$\begin{bmatrix} \phi^{pO} \\ \psi^{pO} \end{bmatrix} = \frac{1}{S^2 + K_R\,S + \omega_0^{\,2}} \begin{bmatrix} S & -\omega_0 \\ +\omega_0 & S + K_R \end{bmatrix} \begin{bmatrix} \Delta\omega_x^{pI} - K_R\,\Delta\phi + \phi_0 \\ \Delta\omega_z^{pI} + \psi_0 \end{bmatrix} \qquad (6.32)$$

The significance of Eq. (6.32) is that the simple expedient of torquing the roll gyro only with proportional roll error signal effects a damped response for both the roll and yaw axes. The natural frequency of the system is unaffected at orbital frequency. To obtain stable response the gain constant K_R is set equal to

$$K_R = 2\zeta\,\omega_0 \tag{6.33}$$

where ζ is the damping ratio which is the parameter to be adjusted. This parameter must satisfy the inequality $0 < \zeta < 1$ in order that the response be stable and that the time constant is sufficiently small. For example, choosing K_R large will amplify the effect of constant gyro drift and yield a long settling time constant. The latter condition is seen from considering the characteristic equation

$$S^2 + K_R S + \omega_0^{\,2} = (S + a)(S + b)$$

If K_R is large, then either a or b is smaller than ω_0 resulting in one of time constants to be large.

From Eq. (6.32) the steady state response to constant errors is

$$\begin{bmatrix} \phi^{pO}_{SS} \\ {}^{pO}_{SS} \end{bmatrix} = \frac{1}{\omega_0^{\,2}} \begin{bmatrix} 0 & -\omega_0 \\ +\omega_0 & K_R \end{bmatrix} \begin{bmatrix} \Delta\omega^{pI}_x - K_R\Delta\psi \\ \Delta\omega^{pI}_z \end{bmatrix} \tag{6.34}$$

The steady state platform tilt is thus independent of initial platform attitude errors

$$\begin{aligned} \phi^{pO}_{SS} &= -\frac{1}{\omega_0}\,\Delta\omega^{pI}_z \\ \psi^{pO}_{SS} &= +\frac{1}{\omega_0}\left(\Delta\omega^{pI}_x - K_R\,\Delta\phi\right) + \frac{K_R}{\omega_0^{\,2}}\,\Delta\omega^{pI}_z \\ \theta^{pO}_{SS} &= \frac{\Delta\omega^{pI}_Y}{K_p} - \Delta\theta^{P} \end{aligned} \tag{6.35}$$

To minimize the effect from sensor bias, K_R on the damping ratio ζ should be chosen to be as small as possible. However, this tends to increase the transient response. By increasing the settling time

$$\frac{1}{\zeta\omega_0} = \frac{2}{K_R}$$

Since ω_0 is about $1.2\text{x}10^{-3}\text{sec}^{-1}$, the time constant is limited to

$$\frac{2}{K_R} = \frac{15 \text{ min}}{\zeta}$$

since ζ is less than unity, this implies that the lower limit of time constant is about 15 min. A damping ratio of $\frac{1}{2}$ implies a time constant of 30 minutes.

The mean squared error response due to random gyro drift and horizon sensor noise can be evaluated from Eq. (6.32) using the noise integrals (Ref. 4). Assuming the spectral density for both gyro drift and sensor noise, Eq. (6.12) and (6.13), the result can be given as

$$\overline{\phi^2} = \frac{\beta\,\overline{\varepsilon_x{}^2}}{K_R(K_R\beta+\omega_0{}^2+\beta^2)} + \frac{\overline{\varepsilon_z{}^2}(K_R+\beta)}{K_R(K_R\beta+\omega_0{}^2+\beta^2)} + \frac{K_R\;\overline{\Delta\phi^2}}{K_R\gamma+\omega_0{}^2+\gamma^2} \qquad (6.36)$$

$$\overline{\psi^2} = \frac{\overline{\varepsilon_x{}^2}(K_R+\beta)}{K_R(K_R\beta+\omega_0{}^2+\beta^2)} + \frac{\overline{\varepsilon_z{}^2}(K_R{}^3+\omega_0{}^2+\beta K_R{}^2)}{K_R\;(K_R\beta+\omega_0{}^2+\beta^2)} + \frac{K_R(K_R+\gamma)}{(K_R\gamma+\omega_0{}^2+\gamma^2)} \qquad (6.37)$$

Qualitatively, while small K_R is desirable for reducing the effect from sensor bias and sensor noise, the error due to random gyro drift rate tends to increase because damping is reduced.

The design problem would optimize K_R against the opposite characteristics of random gyro drift and sensor bias. However, the basic limitation of this system is due to constant gyro drift which is independent of the system gain K_R. Damping the roll and yaw channels results in a steady state tilt which is measured by ϵ / ω_0. For an underdamped system $K_R << 2\omega_0$. Assuming critical damping $K_R = 2\omega_0$ and $K_p = \infty$, the steady platform tilt errors are shown summarized in Table 6.3 for an assumed set of error sources. The gain of the pitch gyro was arbitrarily set equal to ∞. The roll channel gain was set so as to make the roll-yaw loop critically damped. To overdamp the loop will cause the integration of gyro drift in an unbounded manner. (Underdamping is more desirable since the yaw steady state errors will be reduced by the factor ζ.) As noted in the table, the roll mode is limited by the yaw gyro drift rate, while the pitch mode is limited by the pitch error of the horizon sensor. The yaw error is considerably larger because yaw indication so far has been considered in open loop.

The mechanization as given by Eq. (6.31) is analogous to the leveling of a stationary platform using accelerometer outputs. In the present case the accelerometer data is replaced by the horizon sensor data.

Error Source	Error Source Magnitude	Roll ϕ_{SS}	Pitch θ_{SS}	Yaw ψ_{SS}
Pitch Vertical Error $\Delta\theta$	1 mil		1 mil	
Roll Vertical Error $\Delta\phi$ Assume $K_R=2\,\omega_0$	1 mil			2 mil
x-Gyro Drift	0.1°/hr			0.4 mil
y-Gyro Drift	0.1°/hr			
z-Gyro Drift	0.1°/hr	0.4 mil		0.8 mil

Table 6.3

Summary of Steady State Platform Errors
in the Damped Leveling Mode

6.5 Case 3 - Torquing Yaw Gyro With Proportional Roll Error

Consider torquing the yaw gyro only with a signal proportional to the roll error. Reason for considering this case is that, since the steady state roll error is proportional to the steady state yaw error, the torquing of the yaw gyro with proportional roll error may tend to reduce both yaw and roll. However, as will be noted in the following, driving the yaw gyro with only proportional roll signal cannot effect damping. Nevertheless, it is interesting to consider what the response characteristics of such a system will be.

Let the yaw gyro torquing signal be given by

$$T_z = -K_Y(\phi^{po} + \Delta\phi) \tag{6.38}$$

The roll-yaw equations [Eq (35)] will yield the solution

$$\begin{bmatrix} \phi \\ \psi \end{bmatrix} = \frac{1}{s^2 + \omega_o(\omega_o+K_Y)} \begin{bmatrix} s & \omega_o \\ -(\omega_o+K_Y) & s \end{bmatrix} \begin{bmatrix} \epsilon_x + \phi_o \\ \epsilon_z + \psi_o - K_y\Delta\phi \end{bmatrix} \tag{6.39}$$

and the time response of Eq (6.39) for constant errors yields

$$\begin{aligned} \phi &= \frac{1}{\omega^*}\epsilon_x \sin\omega^*t + \phi_o\cos\omega^*t + \psi_o\sin\omega^*t \\ &\quad + \frac{1}{\omega^*}\epsilon_z(1-\cos\omega^*t) - \frac{K_Y}{\omega^*}\Delta\phi(1-\cos\omega^*t) \end{aligned} \tag{6.40}$$

$$\begin{aligned} \psi &= -\frac{(\omega_o+K_Y)}{\omega^*}\epsilon_x(1-\cos\omega^*t) - \frac{(\omega_o+K_Y)}{\omega^*}\sin\omega^*t \\ &\quad \frac{1}{\omega^*}\epsilon_z\sin\omega^*t + \psi_o\cos\omega^*t - \frac{K_Y}{\omega^*}\Delta\phi\sin\omega^*t \end{aligned}$$

where

$$\omega^* = \sqrt{\omega_o(\omega_o+K_Y)}$$

For K_Y positive, it is seen that increasing K_Y has the effect of reducing the amplitude response. Comparing this solution with the open loop mechanization of Case 1, amplitudes of the sinusoidal errors are reduced as the expense of introducing the horizon sensor bias which also increases with K_Y. If the sensor bias were zero, this mechanization would have merit over Case 1 if only because of the attenuation of the amplitude response.

The long term transient effect due to random gyro drift and horizon errors, can be expressed as

$$\overline{\phi^2} \approx \frac{\overline{\epsilon_x^2}\,\beta t}{\beta^2 + \omega_o(\omega_o+K_Y)} + \frac{\overline{\epsilon_z^2}\,\beta t}{\beta^2 + \omega_o(\omega_o+K_Y)} + \frac{\omega_o^{\sim} K_Y^2\gamma\,\overline{\Delta\phi^2}\,t}{\gamma^2 + \omega_o(\omega_o+K_Y)}$$

$$\overline{\psi^2} \approx \frac{(\omega_o+K_Y)^2}{\beta^2 + \omega_o(\omega_o+K_Y)}\,\overline{\epsilon_x^2}\,\beta t + \frac{K_Y^2\,\overline{\Delta\phi^2}\,\gamma t}{\gamma^2 + \omega_o(\omega_o+K_Y)} \qquad (6.41)$$

The effect of increasing K_Y has mixed characteristics. The roll channel tilt, due to gyro drift, is decreased while the sensor noise effect is increased. In the yaw channel, increasing K_Y has the effect of increasing the effect from both error sources.

Decreasing K_Y decreases the natural frequency of the system. This is undesirable from the point of view that it tends to increase the effect from constant gyro drift and sensor bias. In the limit as $\omega_o+K_Y \to o$, gyro drift and sensor bias will be integrated which is highly undesirable.

The difference between this solution and that of Case 3 is noted. In Case 2, the characteristic equation gave rise to a damped response primarily because the roll rate was augmented by a proportional roll signal. The natural frequency of the system is orbital. In the present case, the characteristic equation is conditionally stable with a natural frequency given by $\sqrt{\omega_y(\omega_y+K_Y)}$. Damping is absent because yaw rate is not augmented with a proportional yaw signal.

While Case 3 is not expected to yield a practical mechanization because of its oscillatory characteristics, it does point to an important result. The torquing of the yaw gyro with a roll signal will permit the natural frequency of the system to be altered, but will not provide damping.

6.6 Case 4 - Torque the Roll and Yaw Gyros With Proportional Roll Error

As noted in Cases 2 and 3, torquing just the roll gyro with a proportional roll signal provides a damped roll-yaw system but whose natural frequency is the basic orbital frequency; torquing just the yaw gyro provides no damping possibilities, but provides the possibility of altering the natural frequency. A combined torquing of both the roll and yaw gyro with a proportional roll signal can be expected to provide a characteristic equation which is both damped and of an adjustable natural frequency. Figure 6.4 is a detailed error diagram of this mechanization.

This case can lead to a practical gyrocompass alinement mechanization since two desirable characteristics of adjustable damping constant is available to settle out the initial conditions and the transient response, and stiffness can be provided by adjusting the gain constant to the yaw gyro.

Let the torquing to the roll and yaw gyro be based on proportional roll error signal

$$T_R = -K_R(\phi^{po} + \Delta\phi) \tag{6.42}$$

$$T_Y = +K_Y(\phi^{po} + \Delta\phi) \tag{6.43}$$

Substituting into Eq (35) and solving the roll-yaw equations simultaneously, yields

$$\begin{bmatrix} \phi \\ \psi \end{bmatrix} = \frac{1}{s^2+K_R s+\omega_y(\omega_y+K_Y)} \begin{bmatrix} s & -\omega_y \\ +(\omega_y+K_Y) & s+K_R \end{bmatrix} \begin{bmatrix} \varepsilon_x + \phi_o - K_R\Delta\phi \\ \varepsilon_x + \psi_o + K_Y\Delta\phi \end{bmatrix} \tag{6.44}$$

The characteristic equation for this mechanization is

$$\Delta(s) = s^2+K_R s + \omega_y(\omega_y+K_Y) \tag{6.45}$$

More explicitly, Eq (6.44) can be written as

$$\phi(s) = \frac{s\varepsilon_x-\omega_o\varepsilon_z+s\phi_o-\omega_o\psi_o+(-sK_R-\omega_o K_Y)\Delta\phi}{s^2+K_R s + \omega_o(\omega_o+K_Y)} \tag{6.46}$$

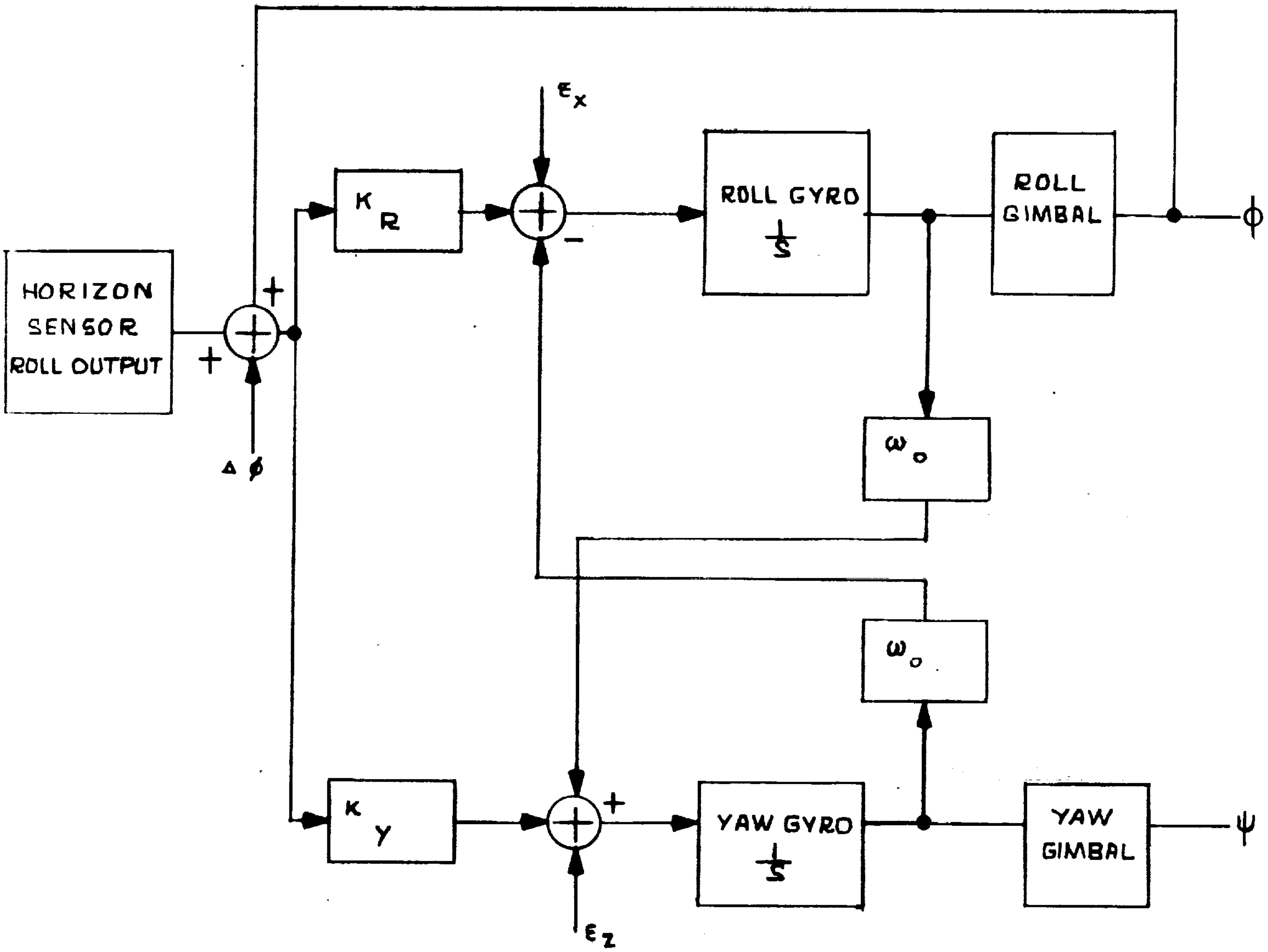
HORIZON SENSOR ROLL OUTPUT
+
+
Δ φ
K R
ε x
+
−
ROLL GYRO
1/S
ROLL GIMBAL
φ
ω o
ω o
K Y
+
YAW GYRO
1/S
YAW GIMBAL
ψ
ε z

Fig. 6.4

Error Diagram of Gyrocompass Loop for Case 4 - Proportional Torque to Roll and Yaw Gyro with Roll Error

$$\psi(s) = \frac{(\omega_o+K_Y)\varepsilon_x + (s+K_R)\varepsilon_z + (\omega_o+K_Y)\phi_o + (s+K_R)\psi_o + (sK_Y-\omega_o K_R)\Delta\phi}{s^2+K_R s+\omega_o(\omega_o+K_Y)} \tag{6.47}$$

The steady state mean squared error due to random gyro drift and sensor bias can be derived from Eq (6.46) and Eq (6.47). Assuming the same spectral characteristics for the noise in the previous cases, Eq (6.12) and Eq (6.13), the mean squared errors are

$$\overline{\phi^2} = \frac{\frac{\beta}{\omega_N}\frac{\overline{\varepsilon_x^2}}{\omega_N^2} + \left(\frac{\omega_o}{\omega_N}\right)^2\left(2\zeta+\frac{\beta}{\omega_N}\right)\frac{\overline{\varepsilon_z^2}}{\omega_N^2}}{2\zeta\left(1+2\zeta\frac{\beta}{\omega_N}+\frac{\beta^2}{\omega_N^2}\right)} + \frac{\overline{\Delta\phi^2}\left[4\zeta^2\frac{\gamma}{\omega_N}+\left(1-\frac{\omega_o^2}{\omega_N^2}\right)^2\left(2\zeta+\frac{\gamma}{\omega_N}\right)\right]}{2\zeta\left(1+2\zeta\frac{\gamma}{\omega_N}+\frac{\gamma^2}{\omega_N^2}\right)}$$

$$\overline{\psi^2} = \frac{\left(\frac{\omega_N^2}{\omega_o^2}\right)\left(2\zeta+\frac{\beta}{\omega_N}\right)\frac{\overline{\varepsilon_x^2}}{\omega_N^2}}{2\zeta\left(1+2\zeta\frac{\beta}{\omega_N}+\frac{\beta^2}{\omega_N^2}\right)} + \frac{\left(\frac{\beta}{\omega_N}+4\zeta^2\left(2\zeta+\frac{\beta}{\omega_N}\right)\right)\frac{\overline{\varepsilon_z^2}}{\omega_N^2}}{2\zeta\left(1+2\zeta\frac{\beta}{\omega_N}+\frac{\beta^2}{\omega_N^2}\right)}$$

$$+ \frac{\overline{\Delta\phi^2}\left[\left(1-\frac{\omega_o^2}{\omega_N^2}\right)^2\frac{\omega_N^2}{\omega_o^2}\frac{\gamma}{\omega_N}+\frac{\omega_o}{\omega_N}(4\zeta^2)\left(2\zeta+\frac{\gamma}{\omega_N}\right)\right]}{2\zeta\left(1+2\zeta\frac{\gamma}{\omega_N}+\frac{\gamma^2}{\omega_N^2}\right)}$$

where

$\omega_N = \sqrt{\omega_o(\omega_o+K_Y)}$ = natural frequency of system

$\zeta = \frac{1}{2\omega_N}K_R$ = damping ratio

In general, it is not desirable to reduce the damping ratio ζ to low values as this tends to increase the effect from noise. The increase of the natural frequency is also limited by the fact that while roll errors are reduced, the yaw sensor errors increase.

For low attitude earth vehicles, the effect of gyro drift is relatively unimportant. Assuming sensor noise to be the dominant error, Eq. (6.48) and (6.49) reduce to the following for the case of white noise ($\gamma \to \infty$)

$$\overline{\phi_{SS}^{2}} = \overline{\Delta\phi^{2}} \; \frac{\omega_N}{\gamma} \; \frac{4\zeta^{2}+\left(1-\frac{\omega_o^{2}}{\omega_N^{2}}\right)^{2}}{2\zeta}$$

$$\overline{\psi_{SS}^{2}} = \overline{\Delta\phi^{2}} \; \frac{\omega_N}{\gamma} \; \frac{\left(1-\frac{\omega_o^{2}}{\omega_N^{2}}\right)^{2}\frac{\omega_N^{2}}{\omega_o^{2}} + 4\zeta^{2}\frac{\omega_o^{2}}{\omega_N^{2}}}{2\zeta}$$

For small values of $\frac{\omega_o}{\omega_N}$ these reduce to

$$\overline{\phi_{SS}^{2}} = \overline{\Delta\phi^{2}} \; \frac{\omega_N}{\gamma} \cdot \frac{1+4\zeta^{2}}{2\zeta} \qquad (6.48)$$

$$\overline{\psi_{SS}^{2}} = \overline{\Delta\phi^{2}} \; \frac{\omega_N}{\gamma} \; \frac{\omega_N^{2}}{\omega_o^{2}} \; \frac{1}{2\zeta}$$

For large values of $\frac{\omega_o}{\omega_N}$ the errors are

$$\overline{\phi_{SS}^{2}} = \overline{\Delta\phi^2} \ \frac{\omega_N}{\gamma} \left(\frac{\omega_o}{\omega_N}\right)^4 \frac{1}{2\zeta}$$

$$\overline{\psi_{SS}^{2}} = \overline{\Delta\phi^2} \ \frac{\omega_N}{\gamma} \ \frac{\omega_o^{\,2}}{\omega_N^{\,2}} \ \frac{(1+4\zeta^{\,2})}{2\zeta} \qquad (6.49)$$

Substituting the normalized form, Eq (6.48) and (6.49), the steady state errors are expressed as

$$\phi_{ss} = -\frac{\omega_o}{\omega_N^2}\,\epsilon_z - \left(1 - \frac{\omega_o^2}{\omega_N^2}\right)\Delta\phi$$

$$\psi_{ss} = \frac{\epsilon_x}{\omega_o} + \frac{2\zeta}{\omega_N}\,\epsilon_z - 2\zeta\,\frac{\omega_o}{\omega_N}\,\Delta\phi \tag{6.50}$$

The effect of the z-gyro drift on the roll and yaw channels and the effect of sensor bias in the yaw channels are decreased by increasing the natural frequency. On the other hand, the sensor bias in the roll channel increases. The effect of the x-gyro on the yaw channel is unaffected. This latter effect has been characteristic with the other mechanizations considered so far (Section 6.1); ϵ_x/ω_o is a limiting yaw error of all gyrocompass alinement schemes.

On the basis the gyro errors are negligible, the steady state errors from the sensor bias become [Eq (6.50 and Eq (6.54)]

$$\phi_{ss} = \left(1 - \frac{\omega_o^2}{\omega_N^2}\right)\Delta\phi = \frac{-K_Y}{\omega_o + K_Y}\,\Delta\phi$$

$$\psi_{ss} = -2\zeta\,\frac{\omega_o}{\omega_N}\,\Delta\phi = -\frac{K_R}{\omega_o + K_Y}\,\Delta\phi \tag{6.51}$$

Increasing the natural frequency (corresponds to increasing K_Y) increases the effect on roll, but the upper bound is limited to unity (i.e., the roll error is one-to-one with the sensor bias). The yaw error, on the other hand, decreases. It is preferable to choose K_R large so as to reduce the settling time.

The steady state sensitivities and the time constant are shown plotted in Fig. 6.5 for several values of the damping ratio. Against the parameter $x = \frac{\omega_O}{\omega_N}$. In general, increasing the natural frequency, ω_N, or decreasing x is desirable for decreasing the effect of bias errors and the time constant. The roll bias error is bounded to unity for small x and approaches zero as x approaches unity. Since the maximum amplification is never more than one-to-one, attenuation on the basis of the roll bias effect can be ignored. This is especially valid when it is recognized the pitch axis is bounded to the same error regardless of the particular mechanization.

Figure 6.6 gives plots of the roll-yaw errors against $x = \frac{\omega_O}{\omega_N}$ for the case where the damping ratio set to $\zeta = 0.5$. Included in this graph are the rms roll and yaw error due to horizon sensor noise which has been assumed to be described by white noise. This figure shows the amplification of white noise in the roll and yaw channels. This amplification is greater than unity for $\frac{\omega_O}{\omega_N}$ greater or less than unity.

On the basis of this figure, if the effect of sensor noise is the dominant error source, the parameter x should be chosen close to unity to minimize the effect of noise. This is to say, the natural frequency of the system should be close to the orbital frequency (i.e., same as case 2). This implies that feedback torque should be provided only to the roll gyro. For this value of x the roll bias error will be zero and the yaw error will be equal to the sensor bias, and the time constant will be about 1.5 hrs. To decrease the time constant, larger errors in the roll-yaw channels due to noise must be tolerated.

The foregoing discussion is intended to briefly outline the basic response characteristics of the system and how to analyze their effects. If the sensor noise has characteristics frequency approaching the orbital frequency the optimum operating value of x would be different. Moreover, a complete analysis would include the effect of gyro errors. In particular, for high altitude vehicles the gyro drift errors may become more important than the sensor errors, In this case the analysis would perhaps center around gyro errors rather horizon sensor errors.

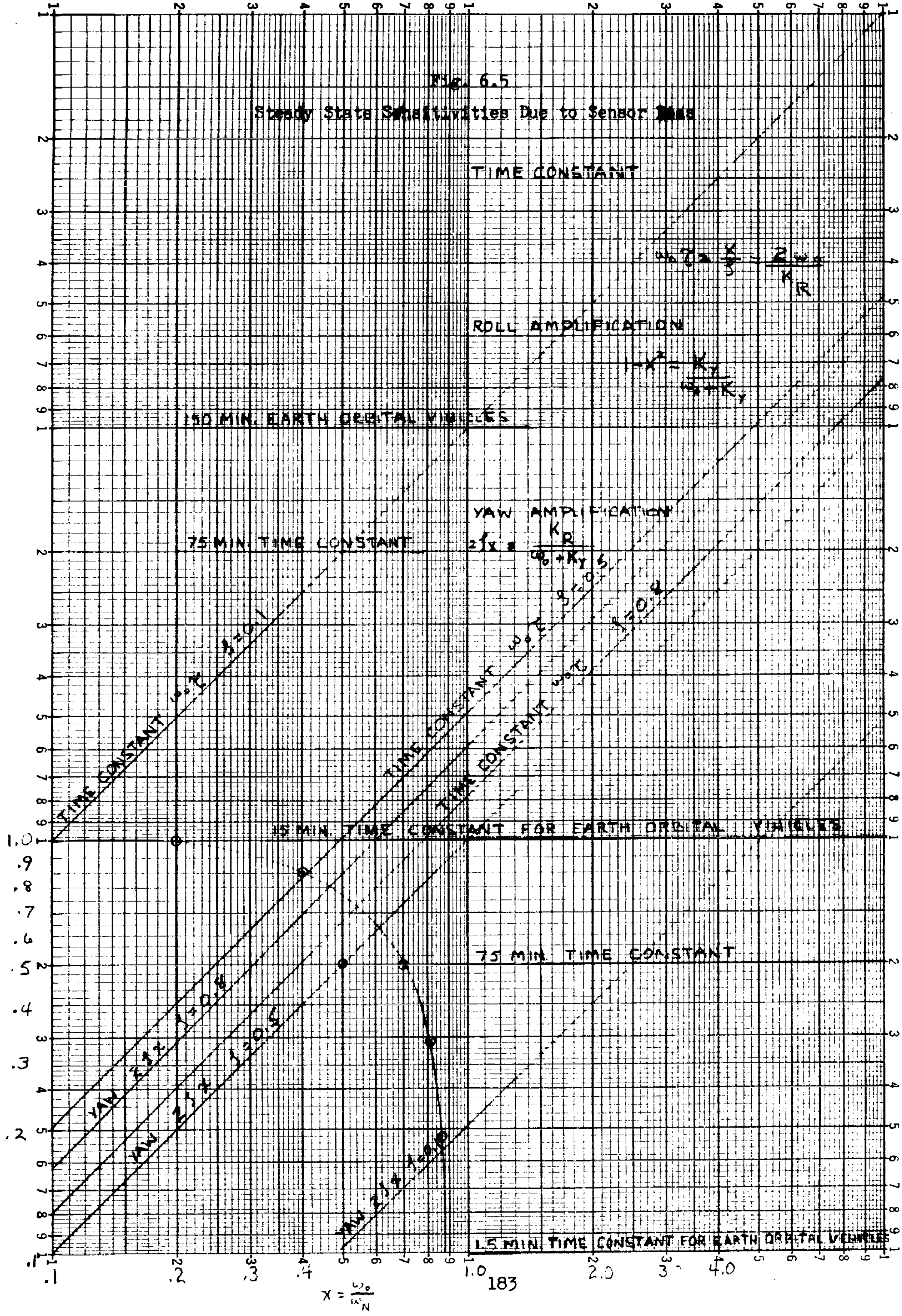

Fig. 6.5

Steady State Sensitivities Due to Sensor Bias

K+E LOGARITHMIC 46 7323
2 X 3 CYCLES MADE IN U.S.A.
KEUFFEL & ESSER CO.

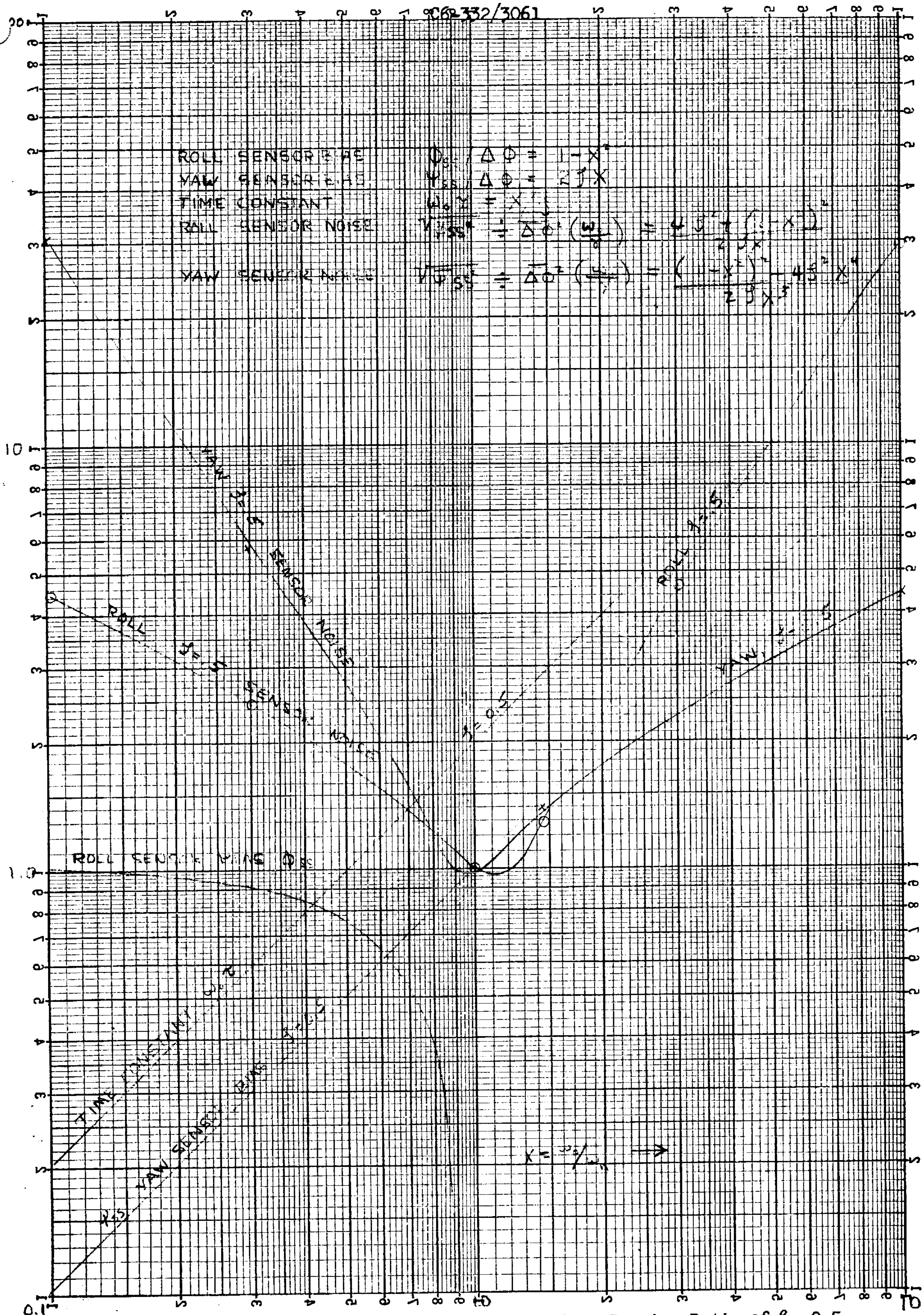

Fig. 6.6 - Roll-Yaw Characteristics of Case 4 at Damping Ratio of $\zeta = 0.5$

6.7 Cases 5 to 7 - Derivative Plus Proportional Control

The three cases considered here are derivative plus proportional control on roll, then yaw, and finally both roll and yaw. This mechanization does not appear to be very promising primarily because the sensor signal must be differentiated. Present sensor pointing data are noisy so that the differentiated signal is extremely poor. The possible advantage is that sensor bias effects will tend to be attenuated. The steady state characteristics are shown in Table 4.1. Further studies are required on the sensor error characteristics, however, before a definitive conclusion can be arrived regarding this scheme.

6.8 Cases 8 and 9 - Torquing With Integral Plus Proportional Roll Error

Torquing just the roll gyro gives rise to a characteristic similar to Case 3. However the sensor bias error and constant gyro drift rates are integrated. While the integration loop is desirable from the point of view of attenuating noise, it is undesirable from the point of view of bias type error sources.

It is interesting to note that Case 9 where just the yaw gyro is torqued gives rise to an unstable characteristic equation similar to Case 3. Table 4.1 includes a summary of the characteristic responses for these two cases. Possibilities exist for compensating the effect of sensor bias. These considerations are discussed in Ref. 1. If indeed bias effects can be compensated, a promising mechanization may be possible. However, the effect of gyro bias would still be present.

Consider Case 8 in more detail. Let the torquing to the roll gyro be given by

$$T_R = (K_{R1} + \frac{K_{R2}}{s}) (\phi + \Delta\phi)$$

This is equivalent to torquing the roll gyro with an integral plus a proportional horizon sensor derived signal. The characteristic equation is

$$\Delta(s) = S^2 + K_{R1}s + K_{R2} + \omega_o^2$$

and the steady state gain is $K_{R2} + \omega_o^2$.

The steady state response is given by

$$\phi_{ss}^{po} = \frac{\omega_o}{\omega_o^2 + K_{R2}} \left[\Delta\omega_x^{pI} - K_{R1}\Delta\phi - K_{R2}\int\Delta\phi \right]$$

$$\psi_{ss}^{po} = \frac{1}{\omega_o^2+K_{R2}}\left[-\omega_o\Delta\omega_x^{pI}+\omega_o K_{R1}\Delta\phi+\omega_o K_{R2}\int\Delta\phi+K_{R2}\int\Delta\omega_x^{pI} + K_{R2}\int\Delta\omega_x^{pI}+K_{R2}\psi_o\right]$$

This result shows that while the effect from the earlier error sources can be reduced in the roll channel by increasing K_{R2}, an integrated horizon sensor error is added into the roll channel. If $\Delta\phi$ is a random variable then its effect may be small. However, if it is a bias increasing K_{R2} increases the roll tilt.

The steady state yaw error includes integrated horizon sensor error, integrated roll gyro drift, and the initial yaw error. It is possible the roll channel error can be reduced by this mechanization. The time constant can be reduced allowing a faster leveling. However, this is accomplished at the expense of introducing an integrated horizon sensor error $\int\Delta\phi$. The improvement in roll leveling therefore depends upon relative improvement due to increased gain K_{R1} against the loss of accuracy due to the addition of the integrated horizon sensor bias.

6.9 Case 10 - Integral Plus Proportional Control on Roll and Yaw Gyro

Assuming that the effect of noise in the sensor and in gyro drift will have a tendency to be attenuated with integral control. Another combination which has interest is to drive both the roll and yaw with integral plus proportional control. As noted in Case 8, the effect of control on only the roll gyro resulted in the sensor bias and constant gyro drift to be integrated in the yaw channel (see Table 4.1, Steady State Solution). This is an undesirable characteristic. Torquing the yaw gyro only resulted in an unstable characteristic equation similar to Case 3.

If both gyros are torqued, the possibility of shaping the response exists. This would be the motivation for considering the present case. As shown in the following, indeed, the integrated effects are removed. The error diagram for this case is similar to Fig. 6.4, except that the gains K_R and K_Y are replaced by the transfer functions

$$T_R = -(K_{R1}+ \frac{K_{R2}}{s})(\phi + \Delta\phi) \tag{6.52}$$

$$T_Y = (K_{Y1} + \frac{K_{Y2}}{s})(\phi + \Delta\phi) \tag{6.53}$$

The error equations can be written as

$$\begin{bmatrix} s+K_{R1}+ \frac{K_{R2}}{s} & \omega_o \\ -(\omega_o+K_{Y1}+ \frac{K_{Y2}}{s}) & s \end{bmatrix} \begin{bmatrix} \phi \\ \psi \end{bmatrix} = \begin{bmatrix} \epsilon_x-(K_{R1}+ \frac{K_{R2}}{s})\Delta\phi \\ \epsilon_z+(K_{Y1}+ \frac{K_{Y2}}{s})\Delta\phi \end{bmatrix} \tag{6.54}$$

The characteristic equation is the third order system

$$\Delta(s) = S^3+S^2K_{R1}+s[\omega_o(\omega_o+K_{Y1})+K_{R2}]+\omega_oK_{Y2} \tag{6.55}$$

and the solution is

$$\begin{bmatrix} \phi \\ \psi \end{bmatrix} = \frac{s}{\Delta(s)} \begin{bmatrix} s & -\omega_o \\ \omega_o+K_{Y1}+\dfrac{K_{Y2}}{s} & s+K_{R1}+\dfrac{K_{R2}}{s} \end{bmatrix} \begin{bmatrix} \varepsilon_x-(K_{R1}+\dfrac{K_{R2}}{s})\Delta\phi \\ \varepsilon_z+(K_{Y1}+\dfrac{K_{Y2}}{s})\Delta\phi \end{bmatrix} \tag{6.56}$$

which can be explicitly expressed as

$$\phi = \frac{s}{\Delta(s)}\left[s\varepsilon_x-\omega_o\varepsilon_z-[s(K_{R1}+\frac{K_{R2}}{s})+\omega_o(K_{Y1}+\frac{K_{Y2}}{s})]\Delta\phi\right] \tag{6.57}$$

$$\psi = \frac{s}{\Delta(s)}\ (\omega_o+K_{Y1}+\frac{K_{Y2}}{s})\varepsilon_x+(s+K_{R1}+\frac{K_{R2}}{s})\varepsilon_z-\omega_o(K_{R1}+\frac{K_{R2}}{s})\Delta\phi \tag{6.58}$$

Note that the integrated effects have been completely eliminated (compare with Section 6.8).

The steady state response can be obtained for constant drift rate and sensor bias

$$\phi_{ss} = -\Delta\phi \tag{6.59}$$

$$\psi_{ss} = \frac{\varepsilon_x}{\omega_o} + \frac{K_{R2}}{\omega_o K_{Y2}}\ \varepsilon_z - \frac{K_{R2}}{K_{Y2}}\ \Delta\phi \tag{6.60}$$

By increasing yaw gyro integral control ($K_{Y2} \to \infty$) and decreasing roll integral control ($K_{R2} \to 0$), the effect of yaw gyro drift and sensor bias in the yaw channel can be eliminated. The steady state error response is then characterized by roll channel being limited by sensor bias and the yaw channel by the roll drift rate.

The above characteristic is very similar to cruise gyrocompass mechanization where an integral control is used on the velocity feedback to the level and azimuth gyros.

6.9.1 Transient Characteristics

Since the system is third order, the transient characteristics of the system is difficult to characterize. However, an approximate result is obtainable using Lin's method if one can arbitrarily assume the roots of the characteristic equation are not close together. On this basis, the following approximate factorization can be obtained.

$$\Delta(S) = S^3 + S^2 K_{R1} + S(\omega_0^2 + \omega_0 K_{y1} + K_{R2}) + \omega_0 K_{y2}$$

$$\approx \left[S^2 + \frac{K_{R1}(\omega_0^2 + \omega_0 K_{y1} + K_{R2}) - \omega_0 K_{y2}}{K_{R1}^2 - \omega_0^2 - \omega_0 K_{y1} - K_{R2}} \right.$$

$$\left. S + \frac{K_{R1} K_{y2} \omega_0}{K_{R1}^2 - \omega_0^2 - \omega_0 K_{y1} - K_{R2}} \right] \times$$

$$\left[S + \frac{K_{R1}^3 - 2K_{R1}(\omega_0^2 + \omega_0 K_{y1} + K_{R2}) + \omega_0 K_{y2}}{K_{R1}^2 - \omega_0^2 - \omega_0 K_{y1} - K_{R2}} \right] \qquad (6.61)$$

This result is obtained with two iterations on Lin's method so that provided the basic assumption on the roots hold, it should be a reasonably accurate factorization.

Some insight on the bounds to place upon the gain parameters is obtained by considering the quadratic ten first. If underdamped condition is assumed then

$$2\zeta\omega_N = \frac{K_{R1}(\omega_0^2 + \omega_0 K_{y1} + K_{R2}) - \omega_0 K_{y2}}{K_{R1}^2 - \omega_0^2 - \omega_0 K_{y1} - K_{R2}} \qquad (6.62)$$

and

$$\omega^2{}_N = \frac{K_{R1} K_{y2} \omega_0}{K_{R1}^2 - \omega_0^2 - \omega_0 K_{y1} - K_{R2}} \qquad (6.63)$$

The increase of K_{y2} reduces the steady state error, however, it must be bounded by the condition that the numerator of $2\zeta\omega_N$ be positive

$$\omega_0 K_{y2} < K_{R1}(\omega_0^2 + \omega_0 K_{y1} + K_{R2}) \qquad (6.64)$$

Also the denominator must be positive

$$K_{R1}^2 > \omega_0^2 + \omega_0 K_{y1} + K_{R2}$$

Relative to the second factor which is written as $S + \alpha$, the constant α is expressed in terms of $2\zeta\omega_N$ as

$$\alpha = K_{R1} - 2\zeta\omega_N \qquad (6.65)$$

Since α must be positive, it follows that

$$K_{R1} - 2\zeta\omega_N > 0$$

or

$$K_{R1} \quad \frac{K_{R1}(\omega_0^2 + \omega_0 K_{y1} + K_{R2}) - \omega_0 K_{y2}}{K_{R1}^2 - \omega_0^2 - \omega_0 K_{y1} - K_{R2}} \qquad (6.66)$$

which implies that

$$\frac{\omega_0^2 + \omega_0 K_{y1} + K_{R2} - \omega_0 \frac{K_{y2}}{K_{R1}}}{K_{R1}^2 - (\omega_0^2 + \omega_0 K_{y1} + K_{R2})} < 1$$

or

$$K_{R1}^2 > 2(\omega_0^2 + \omega_0 K_{y1} + K_{R2}) - \omega_0 \frac{K_{y2}}{K_{R1}}$$

From this equation it is seen a desirable response is obtained if the proportional control gain to the roll gyro K_{R1} is increased. Since this parameter does not affect the steady state response, only the transient characteristic need be considered. The natural frequency can be increased by increasing K_{y2} (yaw gyro integral control) to a certain level and settling time can be decreased provided the condition $\zeta\omega_N > 0$ is held. The increase of K_{R2} is desirable because it increases the natural frequency but decreases the damping ratio. This can be seen from the equation for the damping ratio which is obtained from the $2\zeta\omega_N$ and ω_N^2 equations

$$2\zeta = \frac{\omega_N}{\omega_0 K_{y2}} [\omega_0^2 + \omega_0 K_{y1} + K_{R2} - \frac{\omega_0 K_{y2}}{K_{R1}}] \qquad (6.68)$$

6.9.2 Mean Squared Error Characteristics

The mean squared response due to random gyro drift rate and sensor noise can be obtained from the transient response. However, the system being third order, the noise integrals are complex and results have not been obtained to date. Since this mechanization is an interesting one showing promise, attempts are being made to evaluate the mean squared response.

6.10 Cases 11 to 13 - Torquing With a Bilinear Transfer Function

The most general transfer function one can consider without increasing the order by the system beyond the fourth, is the bilinear form

$$T = G(S)\,(\phi + \Delta\Psi)$$

$$G(s) = \frac{K_1 S + K_2}{K_3 S + K_4} \qquad (6.69)$$

With this form all the cases previously considered can be represented as special cases. The fact that four parameters are available from each control loop would allow shaping the response due to much of the error sources. The basic error sources being about six in number, controlling two channels with this generalized transfer function can lead to attenuating most of the error effects. The effect on the yaw channel, due to constant gyro drift rate however, is unaffected as proven earlier.

Case 11 is a mechanization where just the roll gyro is torqued. The steady state response is very similar to Case 2. To determine the merits of this mechanization it would be necessary to examine the transient response.

Consider the general bilinear form to torque the roll gyro

$$K_R(S) = \frac{aS + b}{cS + a}$$

This leads to a third order transfer function

$$cS^3 + S^2(d + a) + S(b + c\ \omega_0^{\ 2}) + \omega_0^{\ 2}d$$

providing sufficient gain parameters to shape the transient response of the roll channels.

Substituting $K_R(S)$ into the tilt equations the transient response is described by

$$\begin{bmatrix} \phi \\ \psi \end{bmatrix} = \left[\frac{cS + d}{cS^3 + S^2(d+a) + S(b + c\,\omega_0^{\ 2}) + d\,\omega_0^{\ 2}} \right] \begin{bmatrix} S & \omega_0 \\ -\omega_0 & \dfrac{cS^2 + S(d+a) + b}{cS + d} \end{bmatrix}$$

$$\begin{bmatrix} \epsilon_x - \dfrac{aS+b}{cS+d}\,\Delta\phi + \phi_0 \\ \epsilon_x + \psi_0 \end{bmatrix} \qquad (6.70)$$

with steady state given by

$$\begin{bmatrix} \phi_{SS} \\ \psi_{SS} \end{bmatrix} = \frac{1}{\omega_0^{\ 2}} \begin{bmatrix} 0 & \omega_0 \\ -\omega_0 & \dfrac{b}{d} \end{bmatrix} \begin{bmatrix} \epsilon_x - \dfrac{b}{d}\,\Delta\phi \\ \epsilon_x \end{bmatrix} \qquad (6.71)$$

This steady state solution is the same as resulting in Case 4. Comparing with these results, it is seen that while the steady state response is not materially different than Case 4, the transient response can be improved by optimizing the set of constants a, b, c, and d.

The most general case is represented by Case 13. Here both roll and yaw gyros are torqued with the bilinear transfer function. This leads to a fourth order system. Presently, however, there is no requirement for considering a mechanization as high as a fourth order system. Just on the basis of the foregoing cases, it would appear that the lower order cases represented earlier are entirely adequate for proper shaping of the system response.

6.11 Case 14

The reason for considering this special case is that it is identical in all essential respects to the cruise and fixed site gyrocompass mechanizations. Since this mechanization has proven practicable there, it is reasonable to suppose that its application to the orbital case may prove fruitful.

6.11.1 Torquing Transfer Functions

The alinement control torques to the gyros are given as follows:

$$\begin{aligned} T_x &= -\frac{K_R}{s+K}(\phi + \Delta\phi) \\ T_y &= -\frac{K_P}{s+K}(\theta + \Delta\theta) \\ T_z &= +\frac{K_Y}{s+K}(\phi + \Delta\phi) \end{aligned} \tag{6.72}$$

where θ and ϕ are the pitch and roll errors defined by the horizon sensor and the level gimbals and $\Delta\theta$, $\Delta\phi$ are the sensor errors.

It is difficult to assess what final effect these transfer functions will have on the overall stability characteristics of the system. However, some rational basis for selection of this particular form can be obtained by considering the frequency responses of the two following examples shown as Fig. 6.7 and 6.8. Figure 6.7 is a case where the gain is in the feedback loop and Fig. 6.8 is a case where the gain is in the forward loop. The overall transfer function for both cases is of the form $K_1/s+K$. In the former case the bias and noise errors in the horizon sensor are attenuated by increasing K at the expense of also attenuating the signal (i.e., the level deviation). In the latter case the bias errors and the signal (assuming low frequency) are passed with very little attenuation but high frequency noise is attenuated by decreasing K. Thus, while the structure of the transfer functions are the same, the open loop response have opposing characteristics.

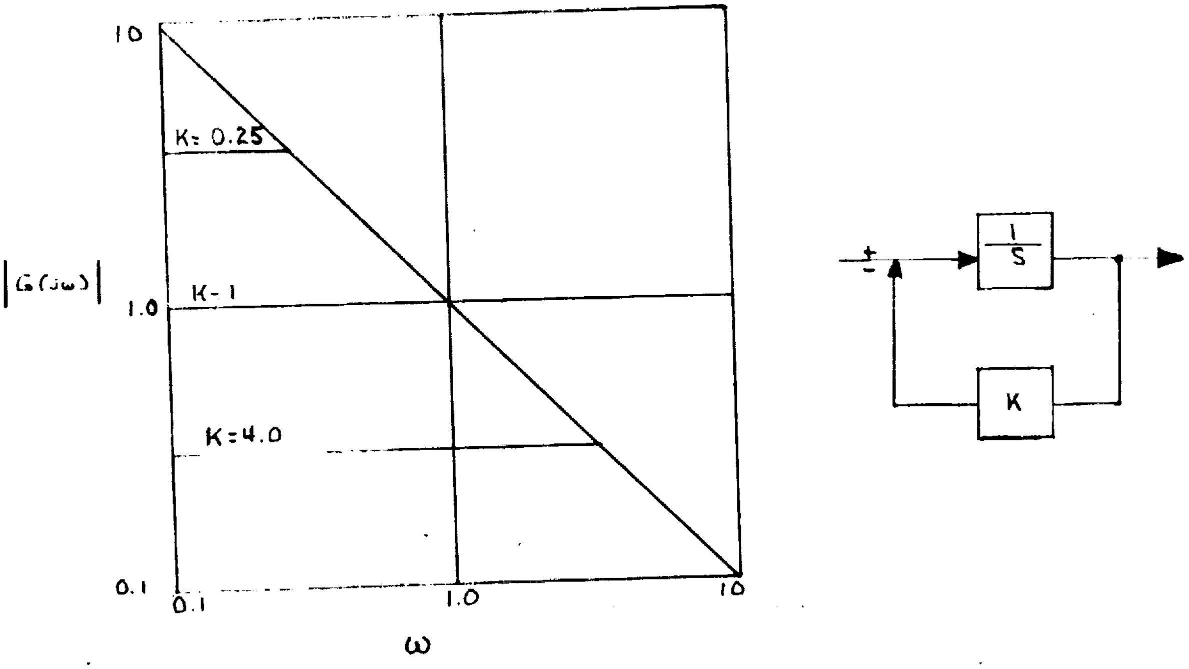

Fig. 6.7

Frequency Response of $G(s) = \frac{1}{s+K}$

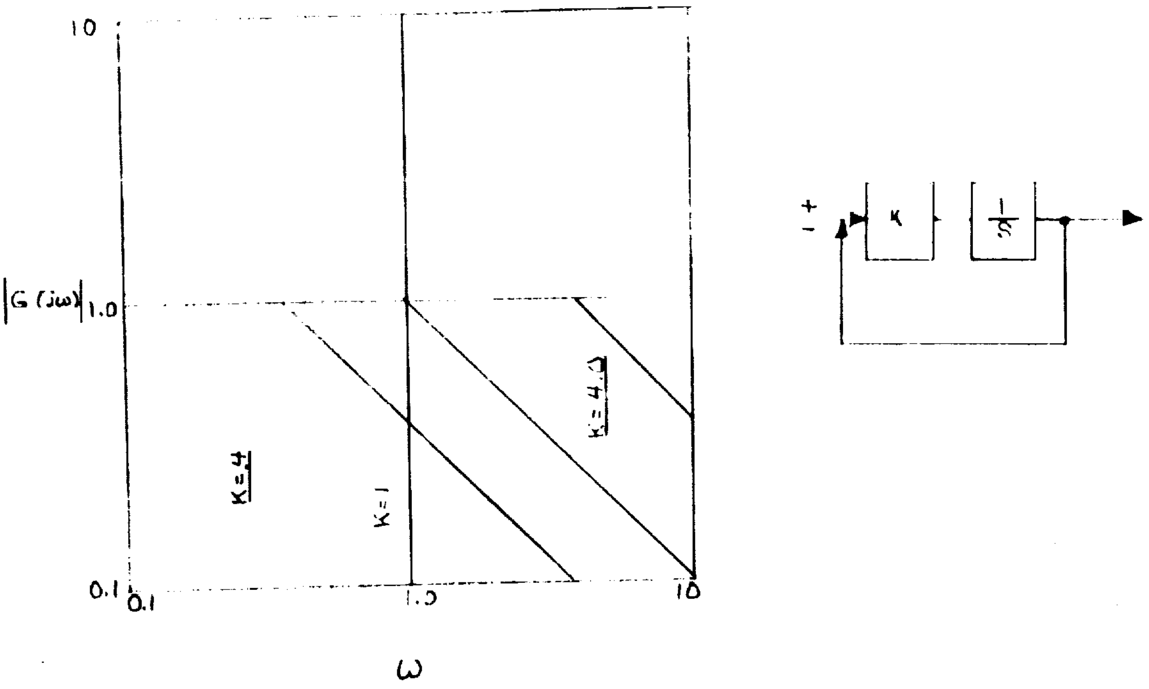

Fig. 6.8

Frequency Response of $G(s) = \dfrac{K}{s+K}$

In the former case, the time constant is decreased with the effect of noise errors by increasing K, while in the latter case these two characteristics change in opposite directions. In a general way it would appear the transfer function 1/s+K would possess more desirable characteristics than the latter lag function K/s+K.

The following analysis will assume the transfer function of Fig. 1. It will be shown in a later section that the second case, where the transfer function is given by K/s+K, can be analyzed with the same equations with a small modification. Therefore, while the analysis will be based on the transfer function being of the form 1/s+K, the same analysis can essentially be applied to the case where K/s+K is the control transfer function.

6.11.2 Mechanization Error Equations

Substituting Eq 6.72 into Eq 5.34 yields the following system error equations:

$$\begin{bmatrix} s+\frac{K_P}{s+K} & 0 & 0 \\ 0 & s+\frac{K_R}{s+K} & \omega \\ 0 & -\omega-\frac{K_Y}{s+K} & s \end{bmatrix} \begin{bmatrix} \theta \\ \phi \\ \psi \end{bmatrix} = \begin{bmatrix} \epsilon_y - \frac{K_P}{s+K}\,\Delta\theta \\ \epsilon_x - \frac{K_R}{s+K}\,\Delta\phi \\ \epsilon_z + \frac{K_Y}{s+K}\,\Delta\phi \end{bmatrix} \qquad (6.73)$$

Inverting this equation with the initial conditions included results in the following

$$\theta = \frac{s+K}{s^2+Ks+K_Y}(\theta_o+\epsilon_y) - \frac{K_P}{s^2+Ks+K_Y}\,\Delta\theta \qquad (6.74)$$

$$\phi = \frac{(s+K)s(\epsilon_X+\phi_o)-(s+K)\omega(\epsilon_Z+\psi_o)-(sK_R+\omega K_Y)\Delta\phi}{s^3+s^2K+s(K_R+\omega^2)+\omega^2K+\omega K_Y} \qquad (6.75)$$

$$\psi = \frac{(\omega(s+k)+K_Y)(\epsilon_X+\phi_o)+(s(s+K)+K_R)(\epsilon_Z+\psi_o)+(sK_Y-\omega K_R)\Delta\phi}{s^3+s^2K+s(K_R+\omega^2)+\omega^2K+\omega K_Y} \qquad (6.76)$$

Figure 6.9 is an error block diagram of this mechanization.

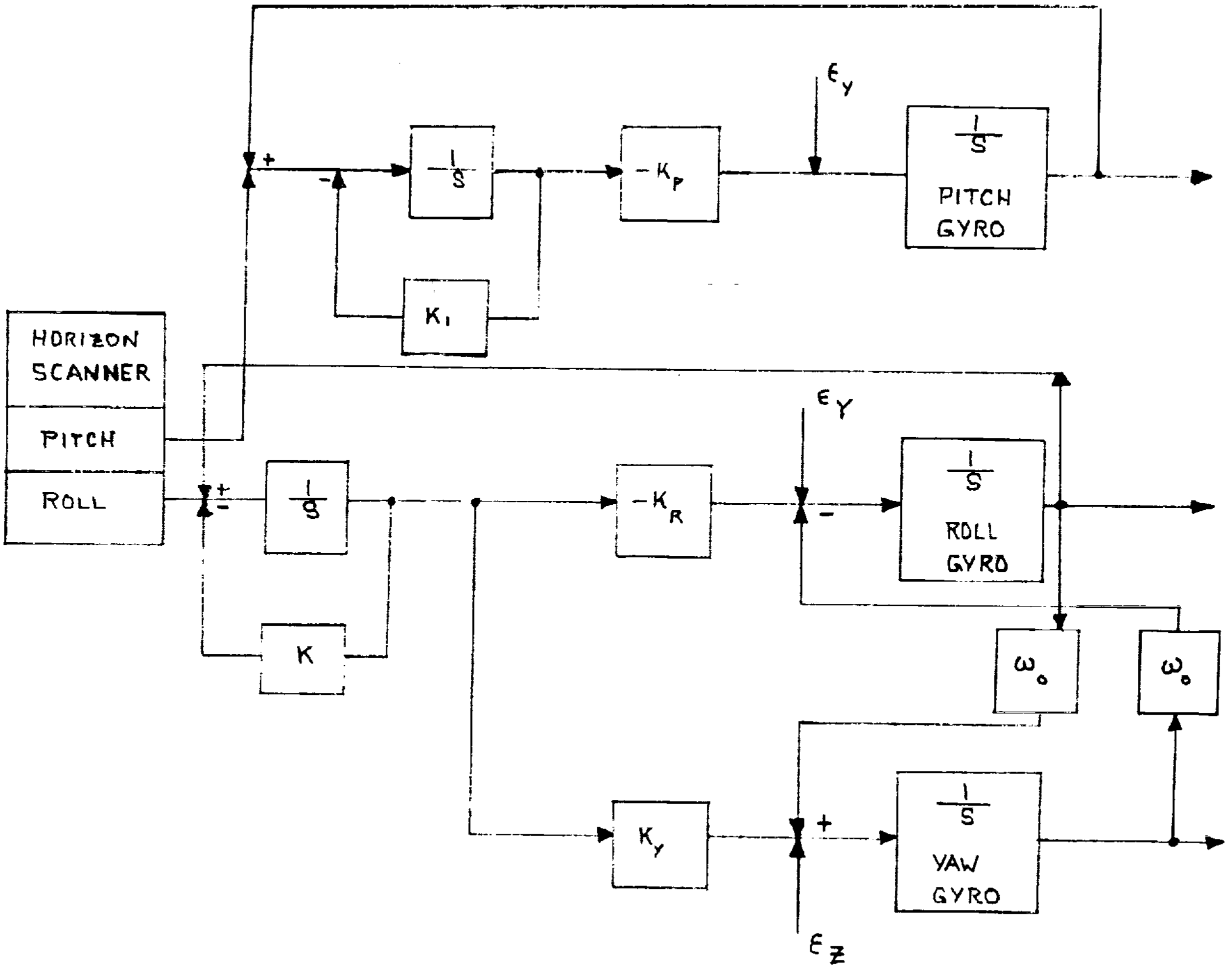
HORIZON SCANNER
PITCH
ROLL
+
−
$\frac{1}{S}$
K_1
$-K_P$
ϵ_Y
$\frac{1}{S}$
PITCH GYRO
±
$\frac{1}{S}$
K
$-K_R$
ϵ_Y
−
$\frac{1}{S}$
ROLL GYRO
ω_o
ω_o
K_Y
+
$\frac{1}{S}$
YAW GYRO
ϵ_Z

Fig. 6.9

Error Block Diagram of Alinement Scheme

The steady state response is given by

$$\theta_{ss} = \frac{K}{K_P} \epsilon_y - \Delta\theta \qquad (6.77)$$

$$\phi_{ss} = -\frac{K\epsilon_Z}{\omega K+K_Y} - \frac{K_Y}{\omega K+K_Y} \Delta\phi \qquad (6.78)$$

$$\psi_{ss} = \frac{\epsilon_X}{\omega} + \frac{K_R}{\omega(\omega K+K_Y)} \epsilon_Z - \frac{K_R}{\omega K+K_Y} \Delta\phi \qquad (6.79)$$

Examining this set of equations it is noted that the pitch error is limited by the sensor bias which cannot be attenuated by the adjustment of system gain. The effect of gyro drift can be attenuated by setting $K/K_P << 1$. For the roll and yaw channels, the effect of gyro drift rates are all bounded below ε/ω. This effect is negligible for most gyro drifts in low earth orbits. Typically a drift rate of 0.1 deg/hr corresponds to 0.42 mil gyrocompass error.

For the purposes of the present analysis, it will be assumed that the effect of gyro drift rates is negligible and that the error sources limiting gyrocompass accuracy are associated with the horizon scanner bias and random noise. For higher altitude vehicles and gyrocompassing relative to other primary bodies with different gravitational mass, this assumption is no longer necessarily valid.

On the basis of the assumption the system response errors are given by the following equation [Eq 6.73-6.79]. The settling time is assumed to be sufficiently fast as to damp out the initial errors

$$\theta = -\frac{K_P}{s^2+Ks+K_P}\,\Delta\theta \tag{6.80}$$

$$\phi = -\frac{(sK_R+\omega K_Y)}{s^3+s^2K+s(K_R+\omega^2)+\omega^2K+\omega K_Y}\,\Delta\phi \tag{6.81}$$

$$\psi = \frac{(sK_Y-\omega K_R)}{s^3+s^2K+s(K_R+\omega^2)+\omega^2K+\omega K_Y}\,\Delta\phi \tag{6.82}$$

and the steady errors

$$\theta_{ss} = -\Delta\theta \tag{6.83}$$

$$\phi_{ss} = -\frac{K_Y}{\omega K+K_Y}\,\Delta\phi \tag{6.84}$$

$$\psi_{ss} = -\frac{K_R}{\omega K+K_Y}\,\Delta\phi \tag{6.85}$$

6.11.3 A Basic Lower Bound to Alinement Accuracy

From Eq 6.83 it is noted that the steady state platform pitch error is related to the horizon error with a unit gain being independent of the system parameters. In general, it can be shown that a feedback mechanization to the pitch channel utilizing only the pitch error signal cannot eliminate or bound the effect of sensor bias. This is proven below. Let a generalized torquing transfer function be assumed for the pitch channel. The mechanization error equation can be written as

$$\dot{\theta} = - G_p(s)(\theta + \Delta\theta) \qquad (6.86)$$

or, solving

$$\theta = - \frac{G_p(s)\Delta\theta}{s + G_p(s)} \qquad (6.87)$$

For a bias error, it follows that in the steady state

$$\theta_{ss} = -\Delta\theta$$

which is independent of the parameters of the transfer function.

Therefore, a basic contraint to gyrocompass alinement accuracy results from the pitch error of the horizon scanner. All analysis on the other axes will have to recognize that the alinement accuracy will be bounded below by the sensor bias error.

Note that this argument is not generally true relative to the roll and yaw axes. In Eq 6.84 and 6.85, ignoring other considerations, it is clear that the effect of the level bias error can be attenuated by increasing the parameter K or by adjustment of K_R or K_Y. This shows, heuristically, that the roll and yaw axes are not necessarily bounded one-to-one by the sensor bias.

A conclusion to be drawn is that in any system mechanization the horizon sensor bias will be a basic lower bound to any alinement accuracy. To improve the alinement accuracy, a primary consideration would initially revolve around ways to reduce the bias errors $\Delta\theta$ and $\Delta\phi$ of the sensor. This consideration would be irrespective of the particular mechanization techniques. A number of studies have been made to reduce the bias errors of horizon sensors. One scheme (Ref. 2) provides for automatic compensation of sensor bias by the rotation of the horizon sensor heads in azimuth relative to the vehicle. This, in effect, averages the bias errors and results in smaller overall bias error.

Figure 6.10 is a comparative summary of the platform pitch error in terms of the sensor errors for several cases of the torquing transfer function. The cases considered are proportional, lag function, and integral plus proportional controls. The characteristics of some of the more fundamental parameters are indicated in this table. For proportional control increasing the gain, decreases the time constant while increasing the effect of random noise. For the simple lag function, increasing the gain K_p increases the effect of noise, increases the natural frequency, and decreases the damping ratio; while increasing the time constant of the filter decreases the effect of noise and the time constant. For the proportional plus integral case, increasing the proportional gain increases the effect of noise, decreases the time constant and increases the damping ratio; while increasing the integral gain, increases the effect of noise, increases the natural frequency, and decreases the damping ratio.

Comparing the three cases, it appears the simple lag function (the second case) would lead to a preferable mechanization because, by the simple increase of the time constant of the lag filter, the effect of noise is attenuated, the time constant is decreased and the damping ratio is increased--all of which are desirable attributes not possessed by the other two.

Fig. 6.10. Pitch Axis Response Characteristics

	$G_p(s) = K_p$	$G(s) = \frac{K_p}{s+K}$	$G_p(s) = K+\frac{K_p}{s}$
Response to Sensor Error	$\theta = -\frac{K_p}{s+K_p}\Delta\theta$	$\theta = -\frac{K_p}{s^2+sK+K_p}\Delta\theta$	$\theta = -\frac{(K_p+Ks)}{s^2+Ks+K_p}\Delta\theta$
Bias	$-\Delta\theta$	$-\Delta\theta$	$-\Delta\theta$
Mean Squared Noise (White)	$\Delta\bar{\theta}^2\frac{K_p}{\beta}$	$\Delta\bar{\theta}^2\frac{K_p}{K\beta}$	$\frac{\Delta\bar{\theta}^2}{\beta}(\frac{K^2+K_p}{K})$
Time Constant	$\frac{1}{K_p}$	$\frac{2}{K}$	$\frac{2}{K}$
Natural Frequency $(\omega_N)^2$	---	K_p	K_p
Damping Ratio	---	$\frac{K}{2\sqrt{K_p}} < 1$	$\frac{K}{2\sqrt{K_p}} < 1$

6.11.4 Roll-Yaw Stabilization

The roll-yaw stabilization problem is more complex because the system is third order. To simplify the analysis, Eq 6.81 and 6.82 are non-dimensionalized. Let the following parameters be defined.

$$\xi = \frac{K}{\omega} \qquad x = \frac{s}{\omega}$$

$$\eta = \frac{K_R}{\omega^2} \tag{6.88}$$

$$\zeta = \frac{K_Y}{\omega^2}$$

Then Eq 6.81 and 6.82 can be written as

$$\phi = -\frac{\eta(x + \frac{\zeta}{\eta})}{x^3 + x^2\xi + x(\eta+1) + \xi + \zeta}\,\Delta\phi \tag{6.89}$$

$$\psi = \frac{\zeta(x - \frac{\eta}{\zeta})}{x^3 + x^2\xi + x(\eta+1) + \xi + \zeta}\,\Delta\phi \tag{6.90}$$

The steady state errors are given by

$$\phi_{ss} = -\frac{\zeta}{\xi+\zeta}\,\Delta\phi \tag{6.91}$$

$$\psi_{ss} = -\frac{\eta}{\xi+\zeta}\,\Delta\phi \tag{6.92}$$

6.11.5 Stability Characteristics

Utilizing Routh's criterion, the stability of the characteristic equation is assured if

$$\xi\eta - \zeta > 1 \qquad \text{or} \qquad \frac{\eta}{\zeta} > \frac{1}{\xi} \qquad \text{or} \qquad \frac{K_R}{K_Y} > \frac{\omega}{K} \tag{6.93}$$

if the roll and yaw gains K_R and K_Y are equal, then Routh's criterion reduces to

$$\xi > 1 \qquad \text{or} \qquad \frac{K}{\omega} > 1 \tag{6.94}$$

In the latter case, stability is insured if the time constant of the torquing filter is selected to be smaller than the orbital period.

In the general case, Eq 6.91, η and ζ the gains to the gyros will be different depending upon the relative weighting from the other error sources in which case the condition reduces to

$$\frac{K_R}{K_Y} > \frac{\omega}{K} .$$

Figures 6.11 and 6.12 show two graphical representations of Routh's criterion against the band pass of the filter. Figure 6.11 defines stability boundaries for ζ and η with parameter variations η and ζ, respectively. Figure 6.12 shows the stability domains of the η/ζ ξ against ξ. For low values of ξ, this figure shows that the ratio of the roll gain to yaw gain should be increased. For example, if $\xi = K/\omega = 1$, $\eta/\zeta = K_R/K_Y$ should be greater than 1. If $\xi = 0.5$, then η/ζ must be greater than 2.

6.11.6 Roots of the Characteristic Equation

Routh's criterion $\xi\eta - \zeta > 0$ provide both a necessary and sufficient condition for stability of the roll-yaw channels. Using this criterion, it is next desired to define the domains of the characteristic roots of the cubic equation. The cubic equation of Eq (19) and (20) has a unique factorization

$$x^3+x^2\xi+x(1+\eta)+\xi+\zeta = \left(x+\frac{\omega_1}{\omega}\right)\left(x^2+2\gamma\,\frac{\omega_2}{\omega}\,x+\frac{\omega_2^2}{\omega^2}\right) \tag{6.95}$$

Because the equation is a cubic, it is difficult to represent the roots and the damping ratio ω_1, ω_2, and γ, explicitly in terms of the system gain parameters ξ, η, and ζ. A literal factorization using Lin's method is possible; however, this yields only an approximate factorization so that without an a priori knowledge of the bounds of the parameters, the factorization may not be unique.

The present section is primarily concerned with defining the stability domains for ω_1, ω_2, and γ.

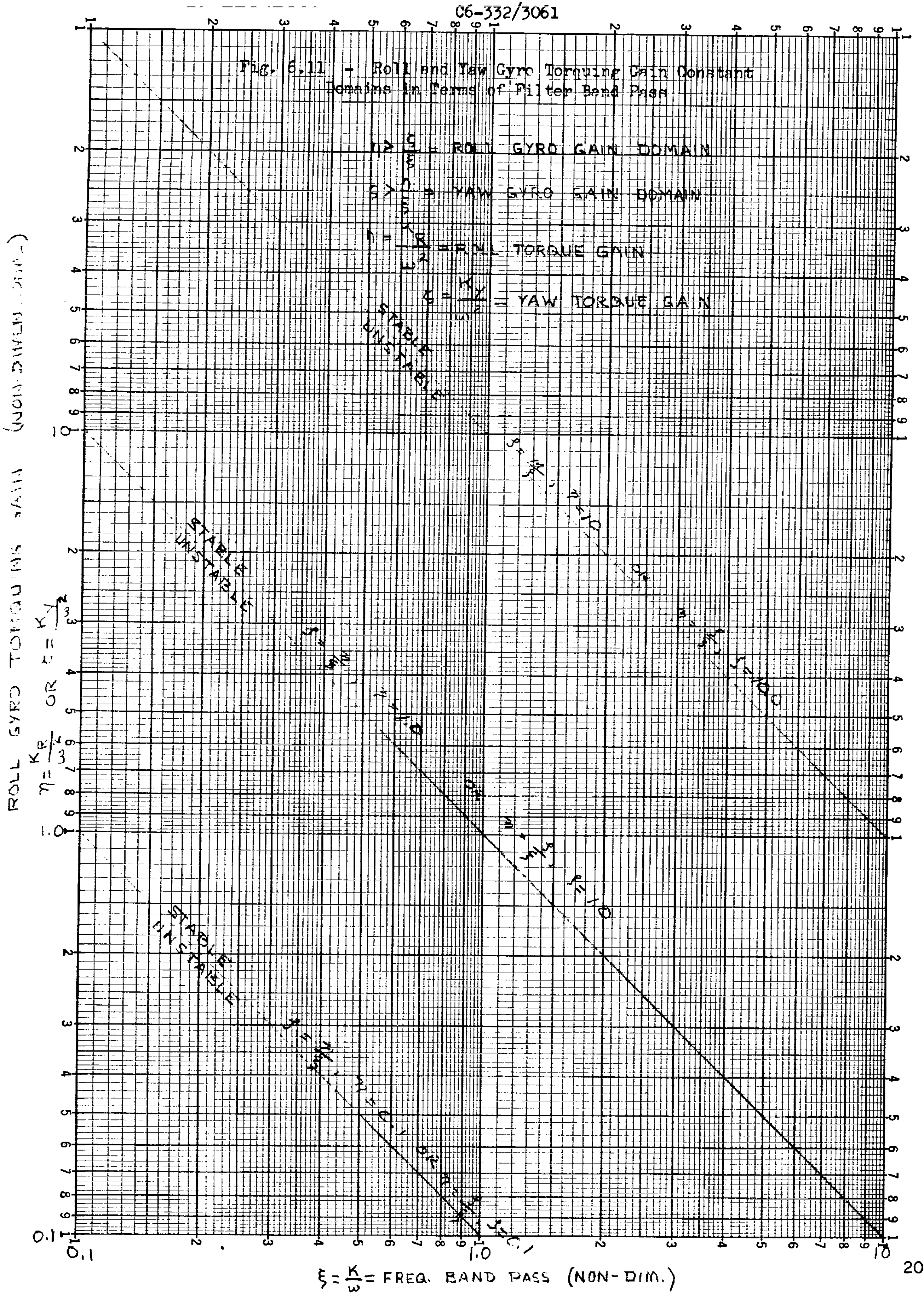

Fig. 6.11 - Roll and Yaw Gyro Torquing Gain Constant Domains in Terms of Filter Band Pass

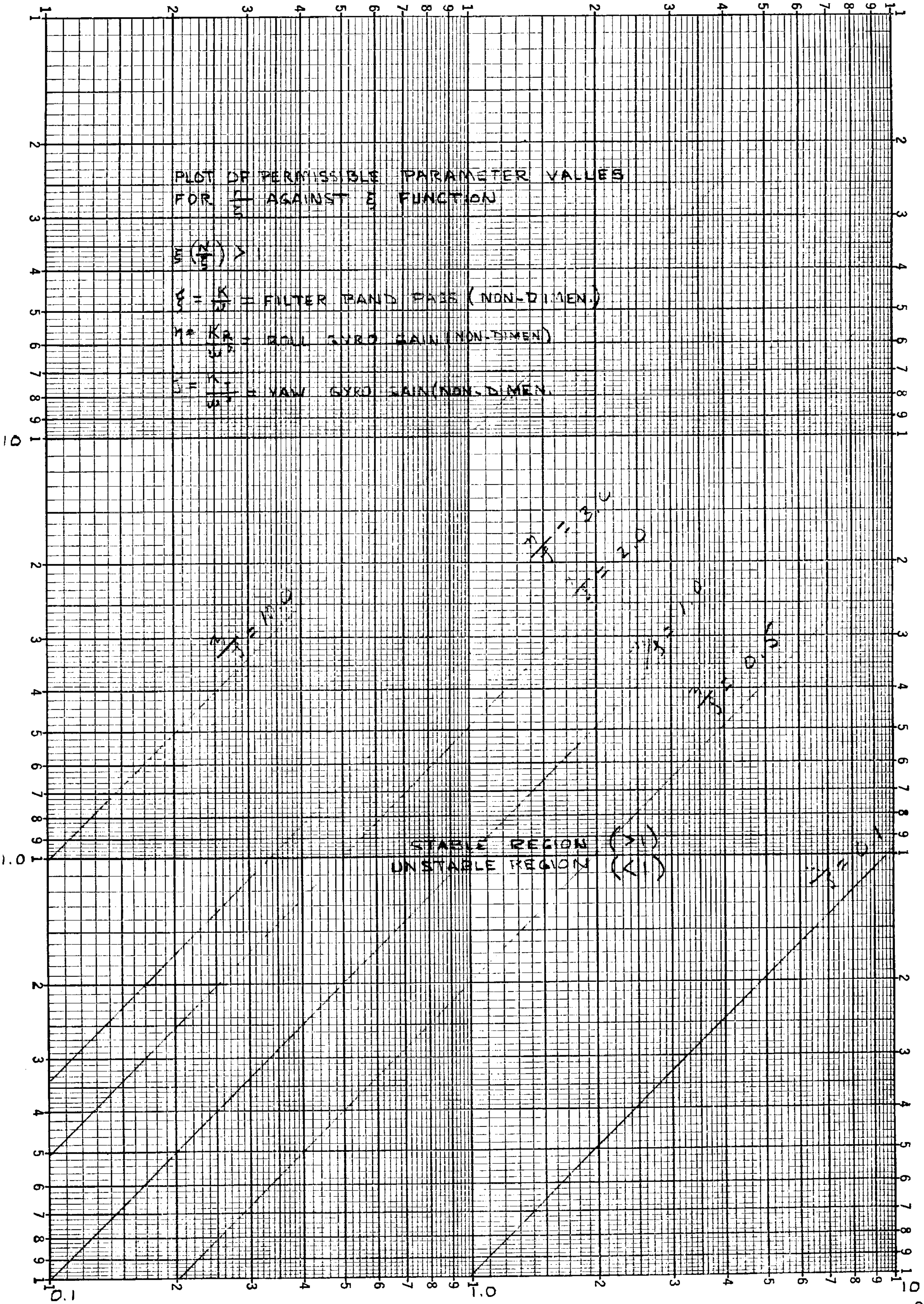

Fig. 6.12 - Routh's Criterion

Multiplying the right side of Eq 6.95 and equating coefficients, the following inequalities can be established. These inequalities are based on the parameter values being all positive as required from stability considerations.

1. Inequality domain for real root

$$\xi > \frac{\omega_1}{\omega} > \frac{\xi+\zeta}{1+\eta} \tag{6.96}$$

2. Inequality domain for natural frequency of the quadratic

$$1+\eta > \frac{\omega_2^2}{\omega^2} > \frac{\xi+\zeta}{\xi} > 1 \tag{6.97}$$

3. Domains for damping ratio of quadratic. Damping ratio defined by lower bound of

$$\xi > 2\gamma \frac{\omega_2}{\omega} \qquad \gamma = \text{damping ratio} \tag{6.98}$$

or

$$\frac{(1+\eta)^2}{4(\xi+\zeta)} > 2\gamma \frac{\omega_2}{\omega} \qquad \gamma = \text{damping ratio} \tag{6.99}$$

4. Representation of natural frequency to real root

$$\frac{\omega_2^2}{\omega^2} = \frac{\omega}{\omega_1} (\xi+\zeta) \tag{6.100}$$

Figure 6.13 gives a plot of the curves defining the boundaries of the inequality Eq 6.96 . This figure yields the bounds on the real root ω_1 as a function of the system parameters. These curves are plotted with the normalized filter band pass ξ as the abscissa. Generally, to achieve stable response for most combinations of the roll and yaw gains η and ζ, K/ω must be selected greater than unity. Furthermore, over the region of ξ shown in the figure $(0.1<\xi<10)$, it appears that η should always be selected such that $\eta \geq \zeta$. That is to say the gain to the roll gyro should always be at least equal to or greater than the gain to the yaw gyro.

C6-332/3061

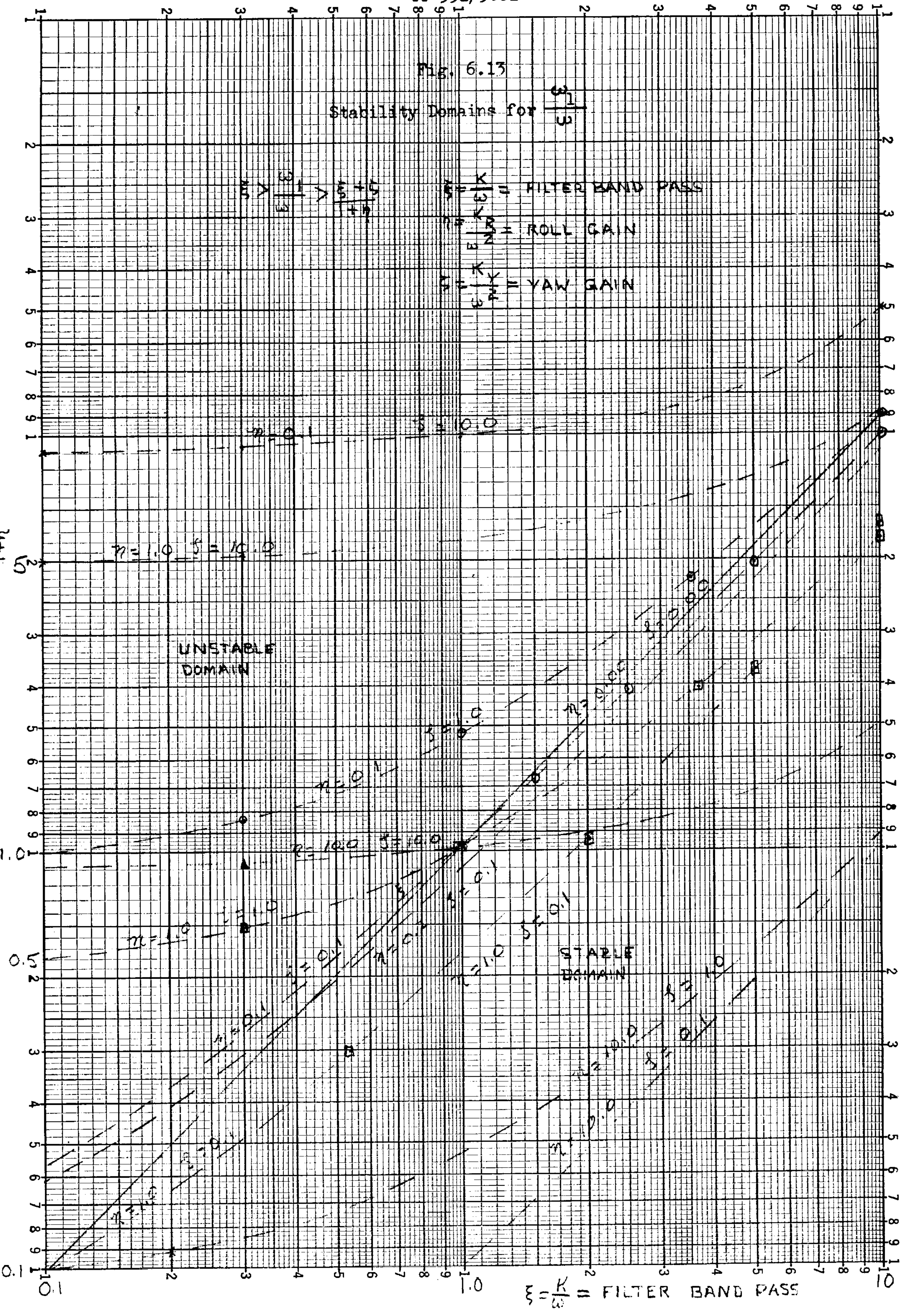

Fig. 6.13

Stability Domains for $\frac{\omega_1}{\omega}$

$\xi > \frac{\omega_1}{\omega} > \frac{\xi+\zeta}{1+\eta}$

$\xi = \frac{K}{\omega}$ = FILTER BAND PASS

$\eta = \frac{K_R}{\omega N}$ = ROLL GAIN

$\zeta = \frac{K_Y}{\omega N}$ = YAW GAIN

If the reverse inequality $\zeta > \eta$ is selected, then ξ must always be greater than one. Typically, if $\eta = 1.0$ and $\zeta = 10.0$, then $\xi > 10$, this implies that ω_1/ω is also bounded close to ten.

In all cases, if $\eta = \zeta$, both gyros being torqued with the same gain, then $\xi > 1$ must always hold. This implies that the real root ω_1/ω is bounded above by unity; the smaller the value of $\eta = \zeta$, the closer the root to unity. Figure 6.14 is a plot of the stability domains for ω_1/ω for the case $\eta = \zeta$.

To insure that $\omega_1/\omega < 1$ it is necessary to bound $\xi < 1$ which is achieved by selecting $\zeta < \eta$. The smaller η is chosen, the narrower is the bound. If a wide latitude is desired on ω_1/ω then η should be chosen larger. Typically, at $\xi = 0.5$ the bound is $0.5 > \omega_1/\omega > 0.3$.

Figures 6.15 and 6.16 show the natural frequency domains of the quadratic [of Eq 6.94] plotted against ξ, respectively, for the cases of arbitrary η, ζ and $\eta = \zeta$. In all cases, ω_2/ω must be greater than unity. To increase the natural frequency of the system, η must be increased.

Figure 6.17 is a plot showing the permissible domain for the combined damping ratio and the natural frequency of the quadratic $2\gamma\ \omega_2/\omega$. The boundaries are defined by the lower bound of the functionals ξ or $\frac{(1+\eta)^2}{4(\xi+\zeta)}$, the time constant by inverting the inequalities.

6.11.7 A Literal Factorization (By Lin's Method)

If the parameter ξ is assumed to be large in relation to $\frac{\zeta}{\xi}$ or $\frac{\eta}{\xi}$ then three iteration on Lin's method yields the factorization

$$(x+\xi)(\xi\, x^2 + \frac{\eta\xi-\zeta}{\xi}\, x + \xi + \zeta) \qquad (6.101)$$

Since $\eta\xi-\zeta > 0$ from Routh's criterion, this yields a factorization which is stable. The characteristics of the quadratic are as follows

$$\frac{\omega_2^2}{\omega^2} = \frac{\xi+\zeta}{\xi} \; ; \; \frac{2\zeta\omega_2}{\omega} = \frac{\eta\xi-\zeta}{\xi^2} \qquad (6.102)$$

Thus, on the assumption of large $\xi = \frac{K}{\omega} >> 1$. The characteristics of the cubic are summarized as follows:

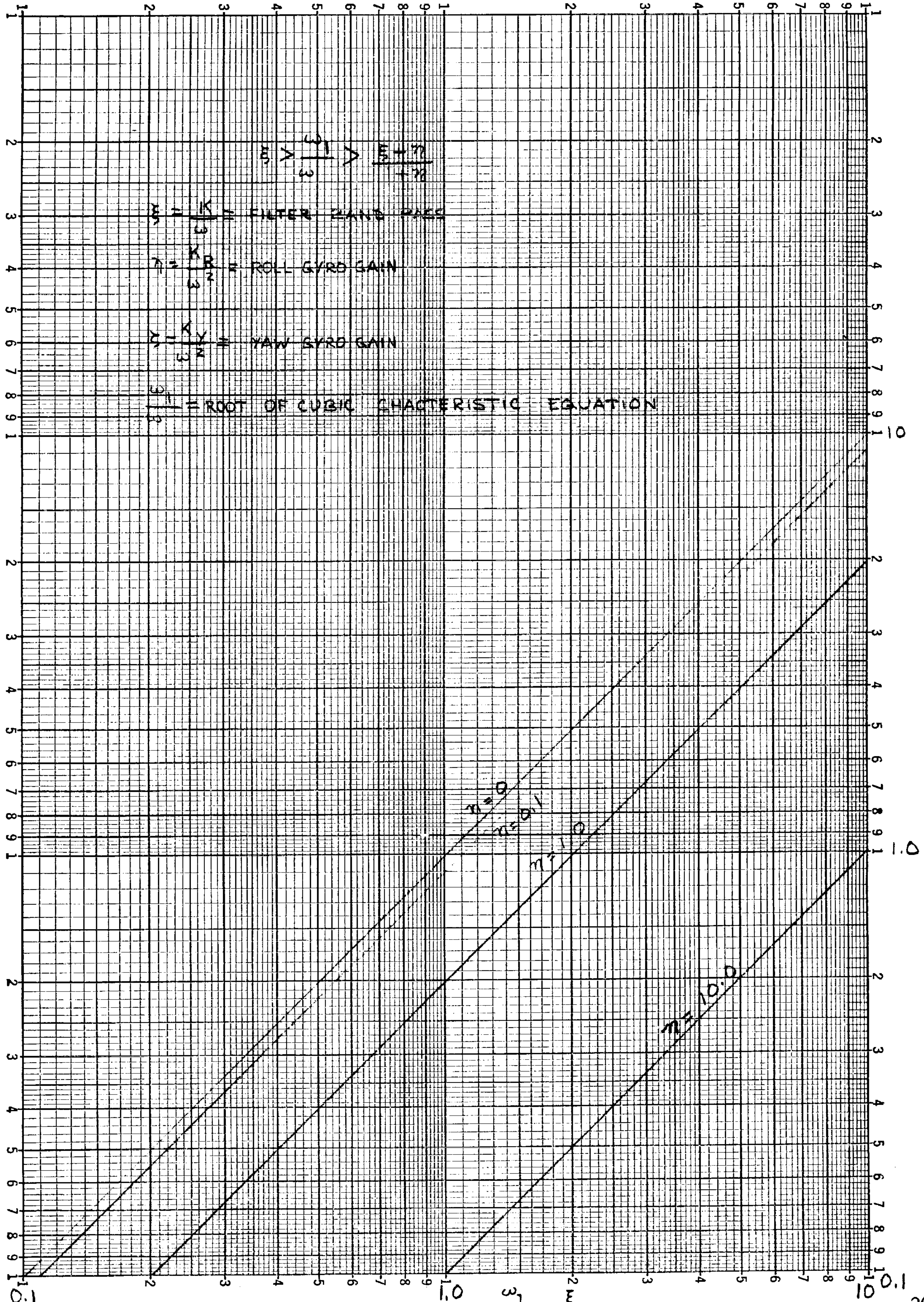

Fig. 6.14 - Stability Domains for $\frac{\omega_1}{\omega}$ when $\eta = \zeta$

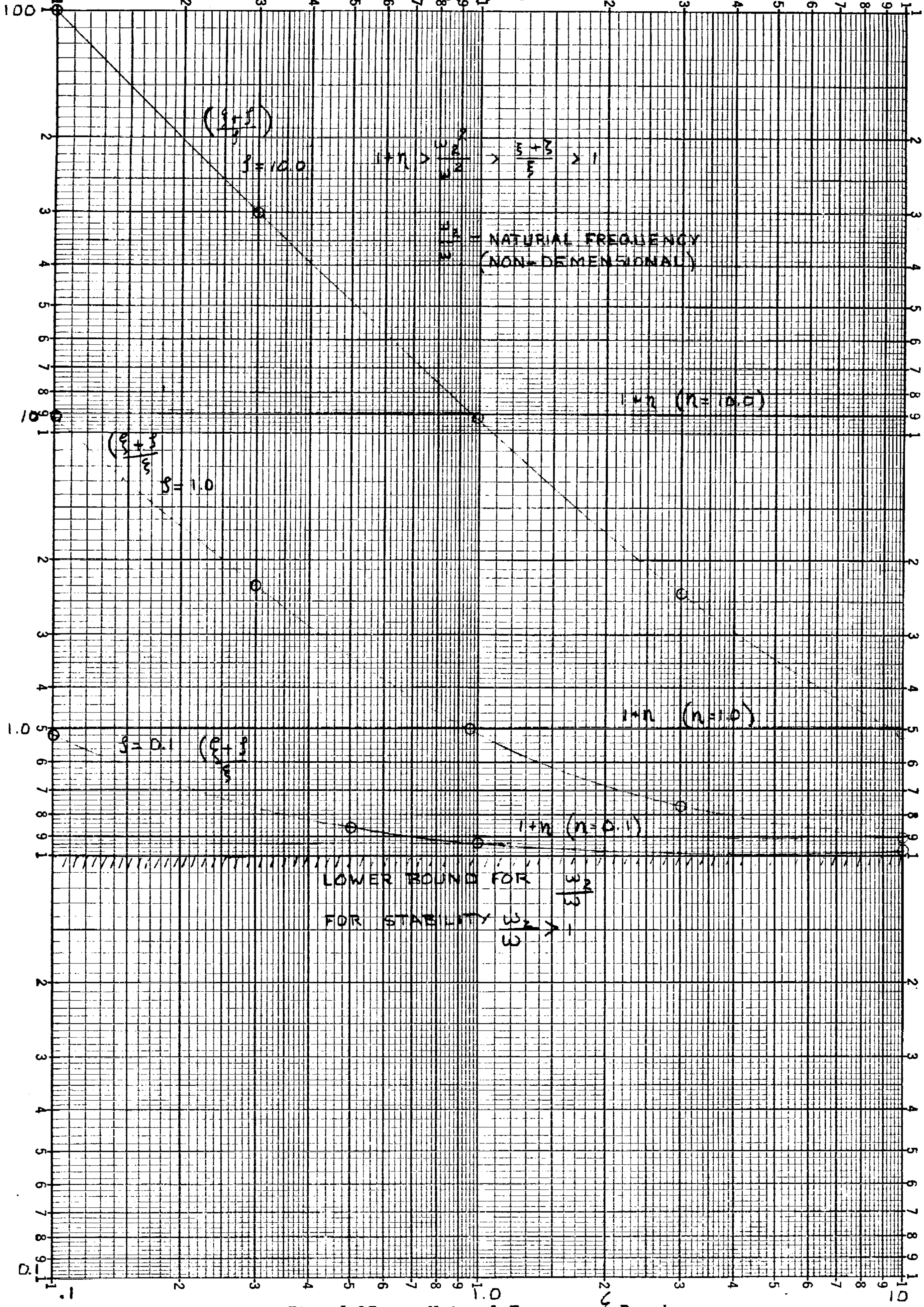

Fig. 6.15 - Natural Frequency ζ Domains

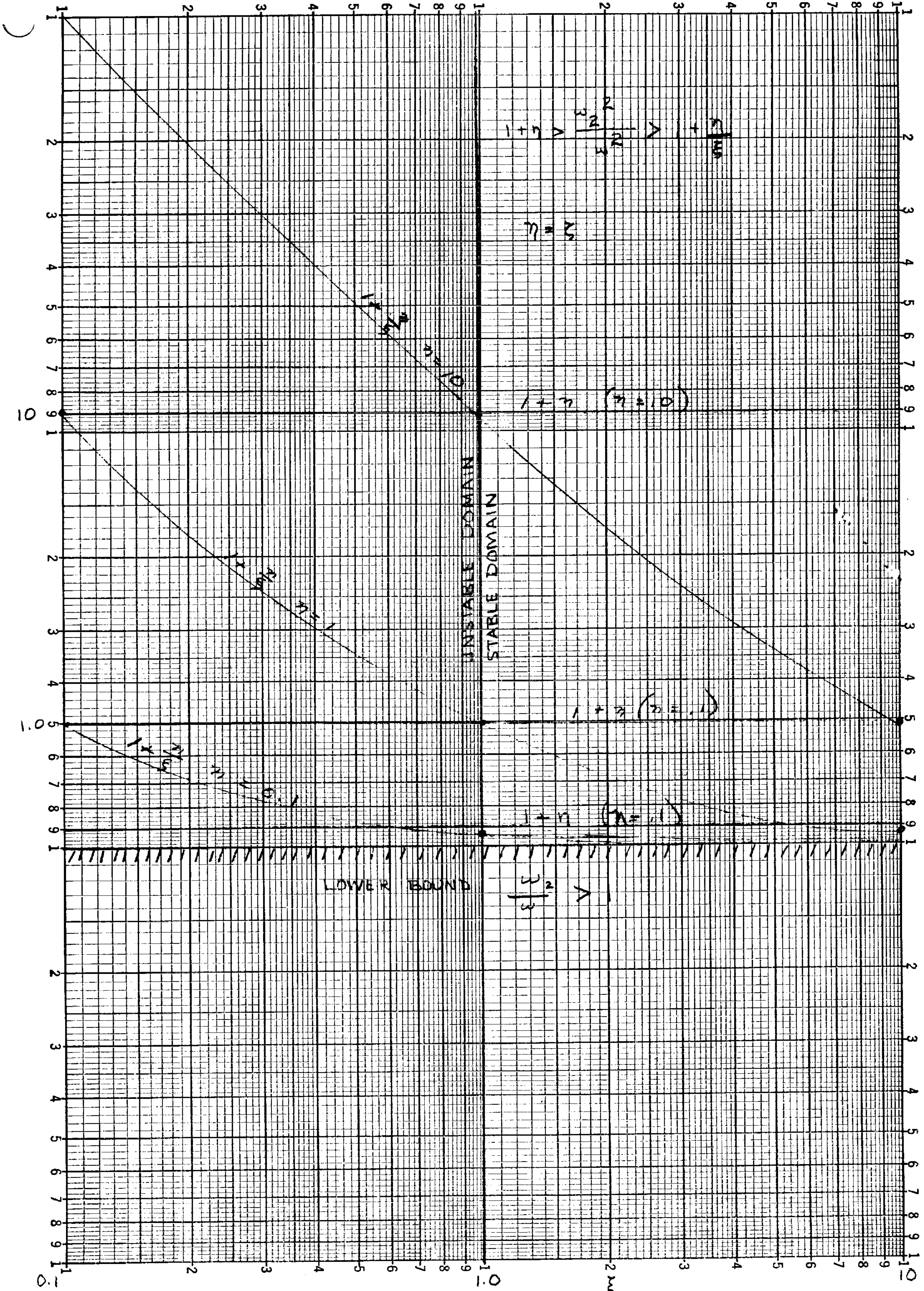

Fig. 6.16 - Natural Frequency Domains for Case $\eta = \zeta$

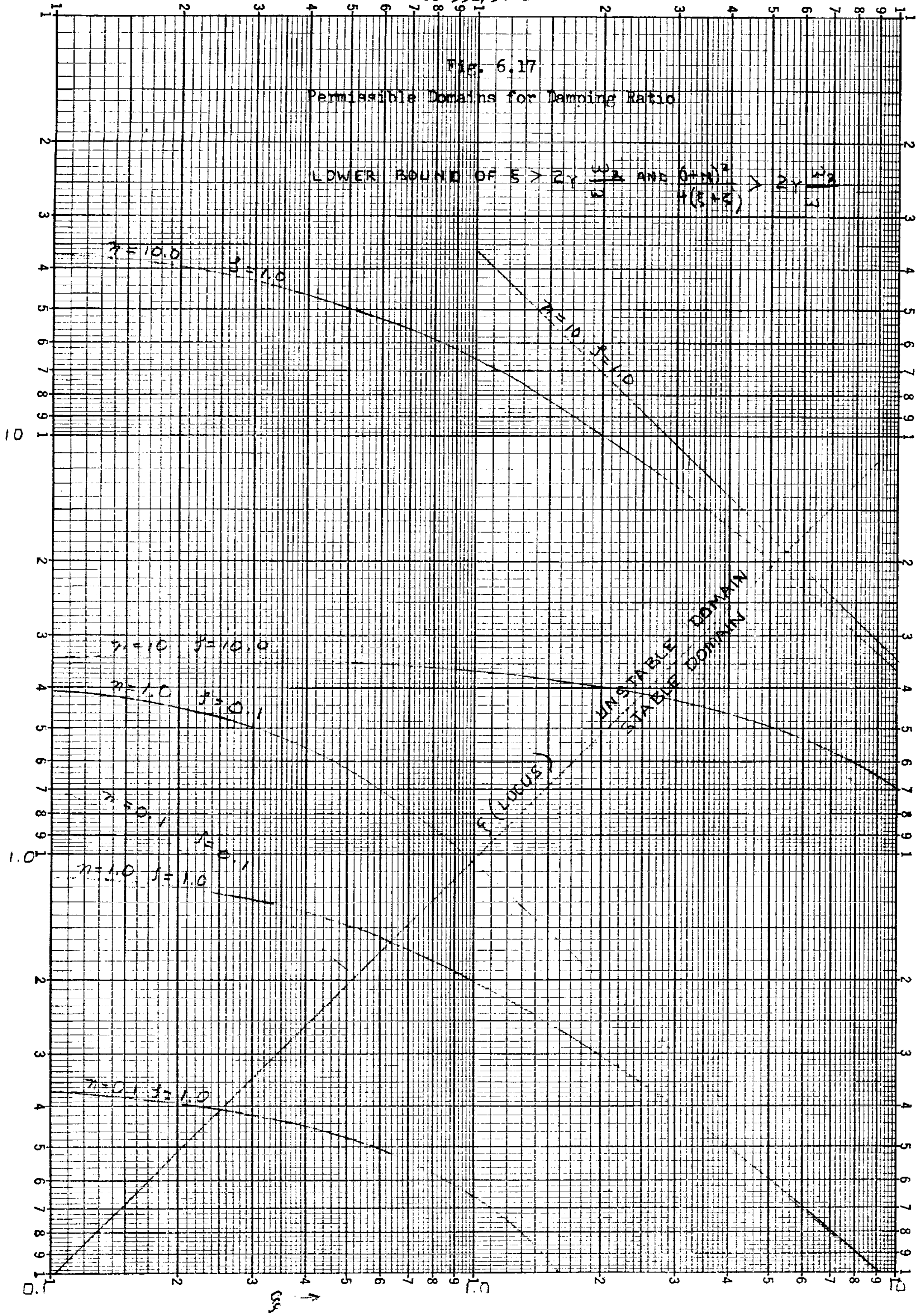

Fig. 6.17

Permissible Domains for Damping Ratio

1. The real root is

   $\omega_1 = K =$ band pass of torquing function

2. Its time constant

$$T_1 = \frac{1}{K} \tag{6.103}$$

3. Natural frequency of quadratic

$$\frac{\omega_2}{\omega} = \frac{\omega K + K_Y}{\omega K} > 1 \text{ (depends only on the yaw gain)} \tag{6.104}$$

4. Damping ratio of quadratic

$$\gamma = \frac{1}{2}\sqrt{\frac{\omega K}{\omega K + K_Y}} \; \frac{K\,K_R - K_Y \omega}{\omega\,K^2} \tag{6.105}$$

   (from Routh's criterion, $K\,K_R - K_Y\omega > 0$)

5. The time constant of the quadratic is

$$\omega T_2 = \frac{\omega}{\omega_2} = \frac{2\omega K^2}{K\,K_R - \omega K_Y} = \frac{2\,\xi^2}{\eta\xi - \zeta} \tag{6.106}$$

To decrease the time constant of the quadratic, either K is decreased or $K\,K_R - K_Y\omega$ is increased. The latter is to be preferred because the time constant associated with the real root is unaffected, thereby providing the possibility of equating the two time constants.

6.11.8 Steady State Characteristics

The steady state roll-yaw errors due to sensor bias can be characterized by the system parameter. From Eq 6.84 and 6.85, the steady state errors can be expressed in terms of the normalized system parameters

$$\phi_{ss} = -\frac{\zeta}{\xi + \zeta}\,\Delta\phi \tag{6.107}$$

$$\psi_{ss} = -\frac{\eta}{\xi + \zeta}\,\Delta\phi \tag{6.108}$$

$$\frac{\psi_{ss}}{\phi_{ss}} = -\frac{\eta}{\zeta} \qquad (6.109)$$

Using the Routh's criterion, it follows that

$$\frac{\psi_{ss}}{\phi_{ss}} = \frac{\eta}{\zeta} > \frac{1}{\xi} \qquad (6.110)$$

This equation gives a condition for setting system parameters in terms of the steady state errors. If the yaw and roll are set equal to each other, then $\frac{\eta}{\zeta} = 1$ and therefore ξ must be > 1. Since the roll or yaw error sensitivity is $\frac{\eta}{\xi+\zeta} = \frac{\zeta}{\xi+\zeta} < 1$, the roll and yaw bias errors can be attenuated below unity gain. However, since the corresponding error in the pitch channel cannot be adjusted, it follows that it is not necessary to place heavy emphasis on attenuating sensor bias errors.

Figures 6.18 and 6.19 are plots of the ratio of yaw and roll errors and the roll error against ξ. Roll error is attenuated by reducing the yaw gyro gain. Cross plots of these curves can be generated from these figures to show the attenuation with variation in yaw gain ζ for particular values of filter band pass ξ.

6.11.9 Mean Squared Error Characteristics

Assuming the sensor noise to be characterized by a Markovian process whose spectral characteristics are given by the function

$$\Phi(\omega) = \frac{2\overline{\Delta\phi}^2\beta}{\omega^2+\beta^2} \qquad (6.111)$$

where

$\Phi(\omega)$ = spectral density function of noise process

$\overline{\Delta\phi}^2$ = mean squared sensor noise

β = reciprocal correlation time of process

ω = angular frequency

The mean squared roll and yaw errors are

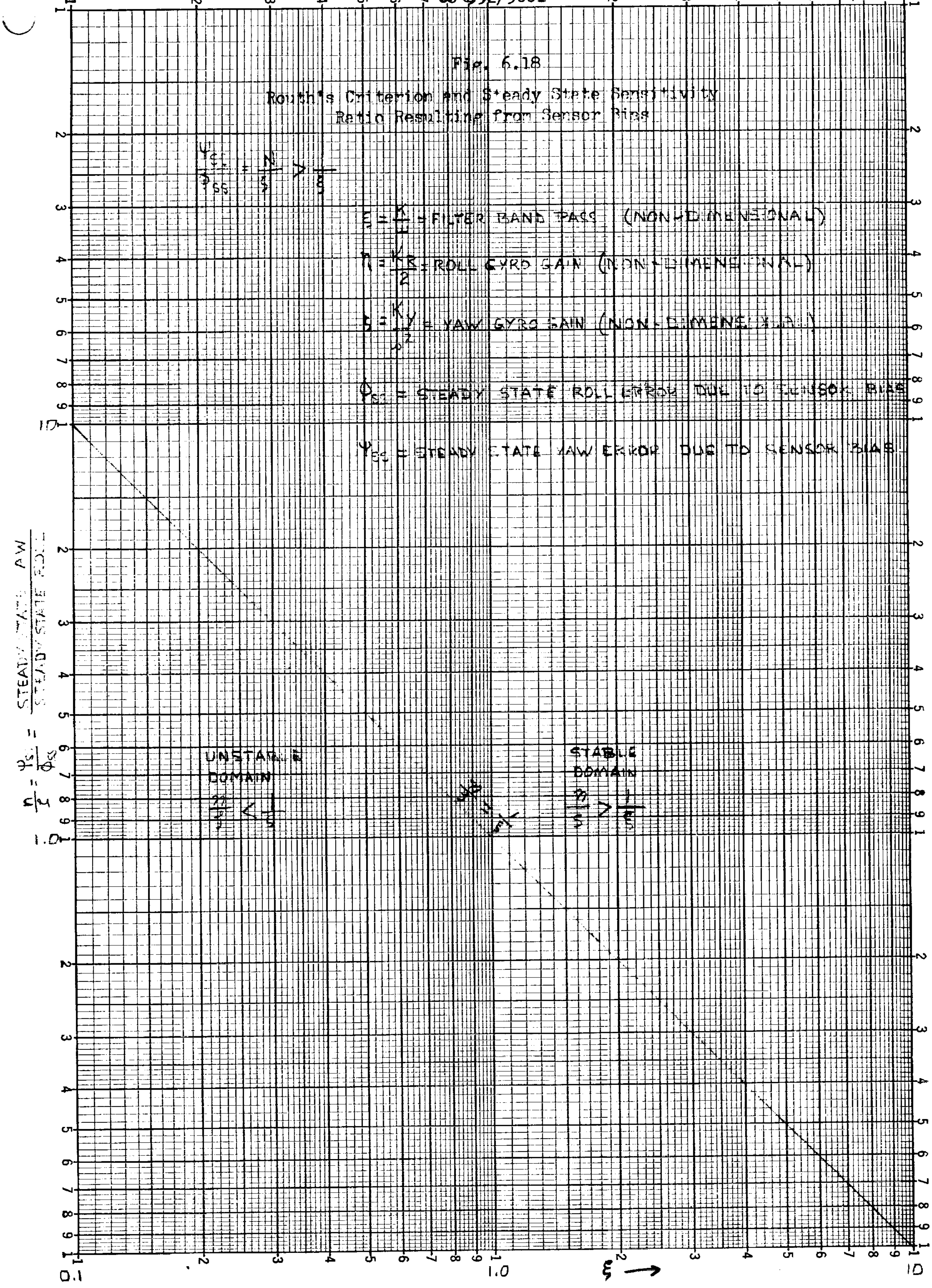

Fig. 6.18

Routh's Criterion and Steady State Sensitivity Ratio Resulting from Sensor Bias

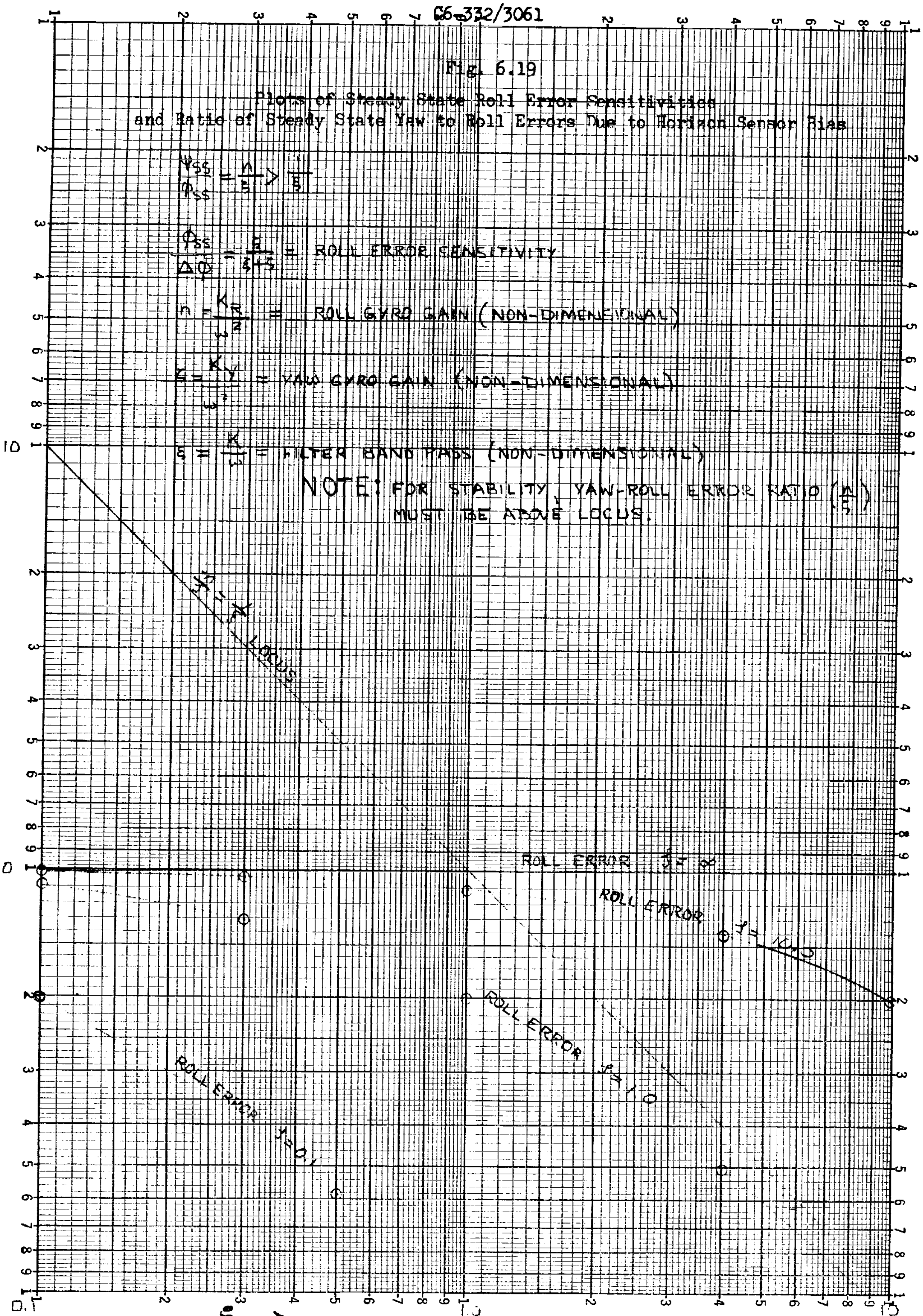

Fig. 6.19

Plots of Steady State Roll Error Sensitivities and Ratio of Steady State Yaw to Roll Errors Due to Horizon Sensor Bias

$$\bar{\phi}_{ss}^{2} = \frac{1}{2\pi j} \int_{-\infty}^{\infty} Y_R(j\omega) T_R(-j\omega) \frac{2\overline{\Delta\phi}^2 \beta}{\omega^2+\beta^2} \phi(j\omega)\, d\omega \tag{6.112}$$

$$\bar{\psi}_{ss}^{2} = \frac{1}{2\pi j} \int_{-\infty}^{\infty} Y_R(j\omega) Y_Y(-j\omega) \frac{2\overline{\Delta\phi}^2 \beta}{\omega^2+\beta^2} \phi(j\omega)\, d\omega \tag{6.113}$$

$$Y_R(j\omega) = Y_R(s=j\omega) = \frac{sK_R+\omega K_Y}{\Delta(s)} \tag{6.114}$$

$$Y_Y(j\omega) = Y_R(s=j\omega) = \frac{sK_Y-\omega K_R}{\Delta(s)} \tag{6.115}$$

$$\Delta(s) = s^3+s^2K+s(K_R+\omega_o^2)+\omega_o^2K+\omega_oK_Y \tag{6.116}$$

$$= (s+\omega_1)(s^2+2\gamma\omega_2 s+\omega_2^2) \tag{6.117}$$

Substituting Eq (45), (46), and (47) into Eq (43) and (44), integrating the result (see Ref. 4), yields

$$\bar{\phi}_{ss}^{2} = \overline{\Delta\phi}^2 \frac{x(\xi+x)[\eta^2(\xi+\zeta)+\xi\zeta^2]+s^2(\xi\eta-\zeta)}{(\xi+\zeta)(\xi\eta-\zeta)(x^3+x^2\xi+x(1+\eta)+\xi+\zeta)} \tag{6.118}$$

$$\bar{\psi}_{ss}^{2} = \overline{\Delta\phi}^2 \frac{x(\xi+x)[\zeta^2(\xi+\zeta)+\xi\eta^2)+\eta^2(\xi\eta-\zeta)}{(\xi+\zeta)(\xi\eta-\zeta)(x^3+x^2\xi+x(1+\eta)+\xi+\zeta)} \tag{6.119}$$

where

$x = \frac{\beta}{\omega}$

$\xi = \frac{K}{\omega}$

$\eta = \frac{K_R}{\omega^2}$

$\zeta = \frac{K_Y}{\omega^2}$

Routh's criterion insures that $\xi\eta-\zeta$ is always positive so there is no ambiguity in the negative sign.

The case when the roll and yaw gyro gains are equal can be obtained from Eq 6.118 and 6.119 upon setting $\eta = \zeta$. The result is

$$\bar{\phi}_{ss}^{2} = \bar{\psi}_{ss}^{2} = \frac{\eta[x(\xi+x)(\eta+2\xi)+\eta(\xi-1)]}{(\xi+\eta)(\xi-1)(x^{3}+x^{2}\xi+x(+\eta)+\xi+\eta)} \qquad (6.120)$$

To attenuate the error, it seems that η should be small and ξ should be large. The case η small is obvious; the case ξ large follows from Eq 6.120 by observing that for finite correlation times, the mean square error is asymptotic to $1/\xi$ for large ξ. This is also noted from Fig. 1, where as K increases (ξ increases) the power as represented by the area decreases.

Note that if the filter K/s+K is used instead of 1/s+K, the error effect [Eq 6.120] is asymptotically independent of ξ for large values. This is a basic difference between the effects of the two torquing functions.

While it is desired to decrease η to reduce the mean squared error, η of course must always be chosen greater than zero for stability and as noted in Fig. 6.16 η must be chosen such that the natural frequency of the quadratic is sufficiently high as to reduce the time constant. From the steady state error point given, reducing η also reduces the effect of bias.

A general design criterion for the case is to increase ξ while setting η to match the desired time constant of the quadratic. In this case, the approximate factorization as provided by Lin's method is nearly valid [Eq 6.101]. However, as noted by Eq 6.103 and 6.106, increasing ξ tends to increase the time constant of the quadratic while decreasing the time constant of the real root of the cubic. A reasonable criterion is to equate the two time constants. This results in the relationship

$$\omega_o T_1 = \omega_o T_2$$

or

$$\frac{\omega_o}{K} = \frac{2\omega_o K^{2}}{K\, K_R - \omega K_T}$$

or

$$\frac{1}{\xi} = \frac{2\xi^{2}}{\eta\xi-\zeta}$$

For large ξ asymptotically, therefore,

$$\frac{1}{\xi} \approx \frac{2\xi}{\eta}$$

or

$$\xi^2 \approx \frac{\eta}{2}$$

This requirement gives rise to a contradictory result. On the one hand, it is desired to increase ξ and keep η small to decrease the mean squared error. On the other hand, the requirement of constant time constants forces ξ to be bounded to η by the above equation. Indeed, the latter requirement of equal time constants imply that the mean squared error increases with large ξ.

If represented in terms of the roots of the exact factorizations as given by Eq 6.117, Eq 6.118 and 6.119 can be written in alternate forms. These forms may provide more insight in the adjustment of the gains. Re-evaluating the integrals, Eq 6.112 and 6.113 with the alternate form Eq 6.117 yields

$$\bar{\theta}_{ss}{}^2 = \frac{\Delta\bar{\theta}^2 \omega_o{}^4}{2\gamma\omega_2{}^3\omega_1} \beta\omega_1\omega_2{}^2 \frac{\eta^2(\beta+\omega_1+2\gamma\omega_2)+\zeta^2\omega_o{}^2(2\gamma\omega_2+\omega_1)[\beta^2+\beta(2\gamma\omega_2+\omega_1)+\omega_2(2\gamma\omega_1+\omega_2)]}{(\omega_1{}^2+\omega_2{}^2+2\gamma\omega_1\omega_2)[\beta^3+\beta^2(\omega_1+2\gamma\omega_2)+\omega_2(\omega_2+2\gamma\omega_1)\beta+\omega_1\omega_2{}^2]} \qquad (6.121)$$

$$\bar{\psi}_{ss}{}^2 = \frac{\Delta\bar{\theta}^2 \omega_o{}^4}{2\gamma\omega_2{}^3\omega_1} \beta\omega_1\omega_2{}^2 \frac{\zeta^2(\beta+\omega_1+2\gamma\omega_2)+\eta^2\omega_o{}^2(2\gamma\omega_2+\omega_1)[\beta^2+\beta(2\gamma\omega_2+\omega_o)+\omega_2(2\gamma\omega_1+\omega_2)]}{(\omega_1{}^2+\omega_2{}^2+2\gamma\omega_1\omega_2)[\beta^3+\beta^2(\omega_1+2\gamma\omega_2)+\omega_2(\omega_2+2\gamma\omega_1)\beta+\omega_1\omega_2{}^2]} \qquad (6.122)$$

In general, the mean square error is reduced by increasing ω_1, ω_2, and γ and decreasing η. However, from the graphs (Fig. 6.13 through 6.18)

1. ω_1 is increased if $\xi = \frac{K}{\omega}$ is increased.
2. ω_2 is increased if $\eta = \frac{K_R}{\omega^2}$ is increased.
3. γ (damping ratio) is increased if ξ is increased and/or η and ξ are increased.
4. Both the increase of γ and ω_2 are desirable also to effect short time constants.

These conclusions are in agreement with the general results obtained by Lin's method [Eq 6.101 through 6.106].

6.11.10 Asymptotic Cases

For long correlation times, x = 0 and the result approaches the steady state value. For small correlation times approaching the characteristics of constant power spectral density (white noise) $x \to \infty$ and the expressions, Eq 6.118 and 6.119, reduce ζ.

$$\overline{\theta}_{ss}^{\,2} = \overline{\Delta\theta}^{2}\,\frac{1}{x}\,\frac{\eta^{2}(\xi+\zeta)+\xi\zeta^{2}}{(\xi+\zeta)(\xi\eta-\zeta)} = \overline{\Delta\theta}^{2}\,\frac{1}{x}\,\frac{\omega_{c}^{\,4}}{2\gamma\omega_{2}^{\,3}\omega_{1}}\left[\frac{\eta^{2}\omega_{1}\omega_{2}^{\,2}+\zeta^{2}\omega_{o}^{\,2}(2\gamma\omega_{2}+\omega_{1})}{\omega_{1}^{\,2}+\omega_{2}^{\,2}+2\gamma\omega_{1}\omega_{2}}\right] \tag{6.123}$$

$$\overline{\psi}_{ss}^{\,2} = \overline{\Delta\theta}^{2}\,\frac{1}{x}\,\frac{\zeta^{2}(\xi+\zeta)+\xi\eta^{2}}{(\xi+\zeta)(\xi\eta-\zeta)} = \overline{\Delta\theta}^{2}\,\frac{1}{x}\,\frac{\omega_{o}^{\,4}}{2\gamma\omega_{2}^{\,3}\omega_{1}}\left[\frac{\zeta^{2}\omega_{1}\omega_{2}^{\,2}+\eta^{2}\omega_{c}^{\,2}(2\gamma\omega_{2}+\omega_{1})}{\omega_{1}^{\,2}+\omega_{2}^{\,2}+2\gamma\omega_{1}\omega_{2}}\right] \tag{6.124}$$

To attenuate the error effect, Routh's criterion $\xi\eta-\zeta > 0$ should be made as large as possible (see Fig. 6.7 and 6.8). In the general equations, Eq 6.118 and 6.119, $(\xi\eta-\zeta)$ is a factor in the denominator. Therefore, this condition $\xi\eta-\zeta \gg 1$ is a general requirement to attenuate the effect of noise.

Assuming further $\eta = \zeta$ and ξ is large, these expressions reduce to

$$\overline{\theta}_{ss}^{\,2} = \overline{\psi}_{ss}^{\,2} = \frac{2\eta}{\xi x}\,\overline{\Delta\theta}^{2} = \frac{2\,K_{R}}{K\omega}\,\frac{\omega}{\beta}\,\overline{\Delta\theta}^{2} \tag{6.125}$$

where $\left(\frac{2\,\overline{\Delta\theta}^{2}}{\beta}\right)$ is the constant power per unit frequency.

Figure 6.20 is a plot of the mean squared error due to white noise of sensor for several values of system gain [Eq 6.122]. Increasing ξ decreases the error. Other conditions can be obtained by considering the alternate form of Eq 6.120 and 6.121.

If the filter K/s+K were used, it can be shown that the errors are given by Eq 6.118 and 6.119 with the small modification of replacing all η and ζ of these equations with ξη* and ξζ* where $\eta^{*} = K_{R}/\omega$ and $\zeta^{*} = K_{Y}/\omega$. For this case, Eq 6.122 will reduce to

$$\overline{\theta}_{ss}^{\,2} = \overline{\psi}_{ss}^{\,2} = 2\,K_{R}\,\frac{\overline{\Delta\theta}^{2}}{\beta}$$

which is independent of the filter band pass K.

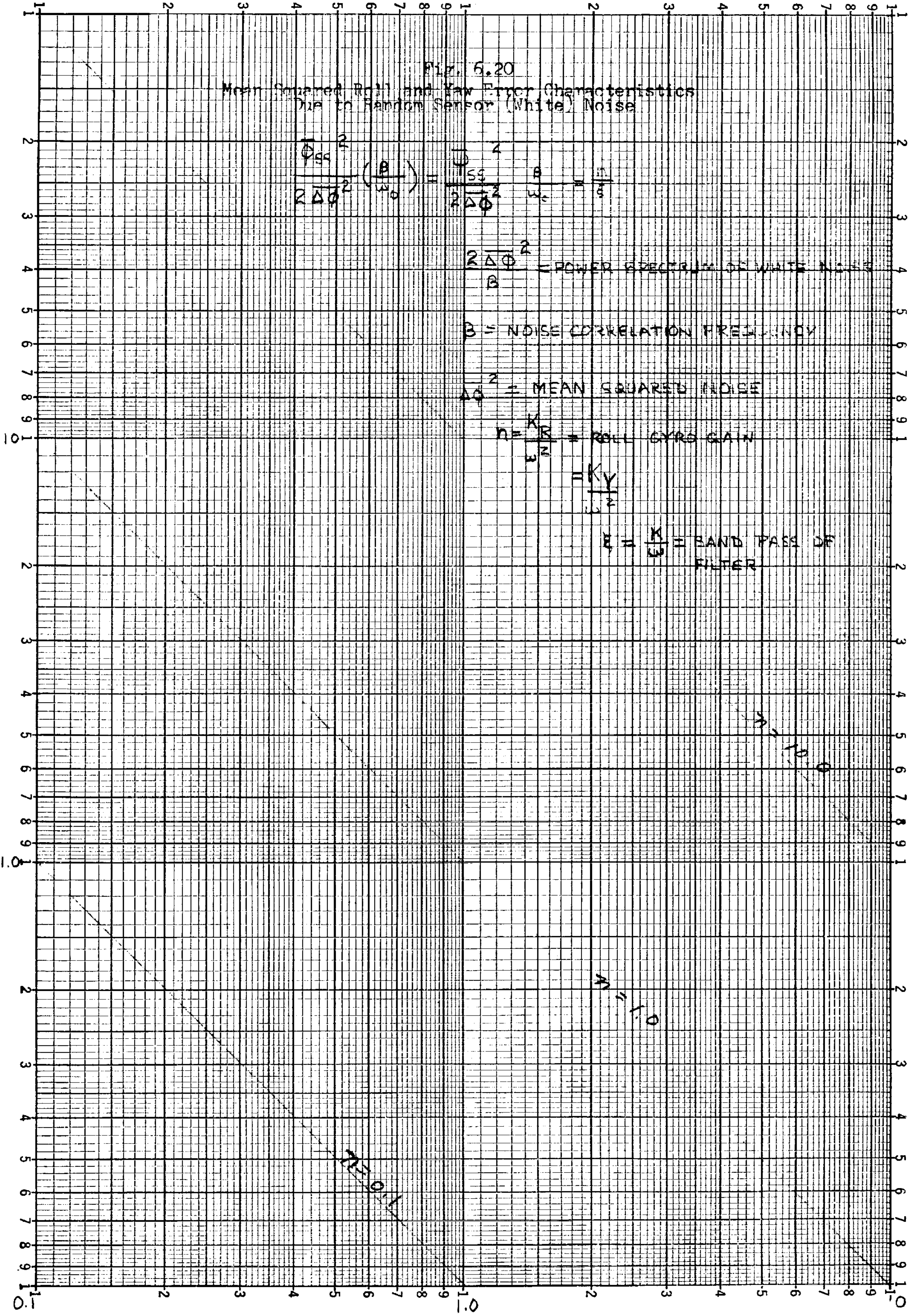

Fig. 6.20
Mean Squared Roll and Yaw Error Characteristics
Due to Random Sensor (White) Noise

7.0 System Mechanization Errors

7.1 General

In the previous sections the gyrocompass mechanizations assumed the basic limitations to high accuracy system alinement was due to instrument associated errors such as gyro drift, sensor errors, and initial condition errors. The purpose for requiring self alinement of a stabilized platform was to periodically re-initialize platform alinement to eliminate the propagated effect of these errors.

The existence of other accuracy limiting error sources must be recognized in a complete mechanization analyses. It is the purpose of the present section to re-examine some of the basic assumptions involved in the earlier analysis and attempt to arrive at a measure of the resulting errors.

The pitch level torquing (orbital) rate error was previously considered in Section 6.2. For a constant rate error it was seen that damping the channel will eliminate the effect of the error. However, if the spectral characteristics of this error were to match the natural frequency of the pitch mode, an error amplification would be possible.

Other effects to be considered are perturbations due to oblateness, other attracting bodies, and air drag. A system completely slaved to the horizon for vertical determination would not be affected by these errors. However, it may be desired to torque the system on the basis of the angular velocity inferred from the orbital parameters and use the sensor to occasionally trim out the effect of the propagated errors. For this case, it would be desired to investigate the effect of navigation on the gyrocompass alinement.

When orbital gyrocompassing is viewed in this way, where it is coupled to the navigational data, indeed then the general problem is identical to the cruise system gyrocompass problem. This problem is more fully explored here.

In a system which is completely slaved to the vertical via the horizon sensor, constant rate errors arising from the sensor will be damped for all of the previously considered stable mechanizations. However, recognizing the transient characteristics of rate torquing via the horizon sensor, the effect on platform tilt from considerations of the associated spectral characteristic must be examined. This problem will be considered in a following study.

7.2 Platform Torquing Mechanization

To maintain platform local level, two basically different torquing mechanizations are possible. The platform level may be maintained by continuously torquing the pitch gyro with the sum of the platform pitch gimbal angle and the horizon scanner error signal. Or the pitch channel may be torqued with the nominal computed orbital rate based on the navigation data with horizon scanner error signals used to update the platform drift. In the first case the platform is completely slaved to the horizon scanner output and consequently, while the system output may be erratic, its level response will be bounded. In the second mechanization the horizon scanner is used to train the system for computed level drift but is subject to the navigation error which may cause an unbounded coupling of errors from the navigation data. For example, a large bias in the horizon sensor will enter directly as a platform attitude error. On the other hand, the trim torques using the horizon error signals will see only a small part of this error since it is a differential effect.

The choice of the particular torquing techniques depends upon the relative accuracy of the horizon sensor to provide the vertical rate information and the navigation data as obtained from orbit determination. Other considerations involve the relative amount of computation. If slaved to the horizon scanner limit, a no computation is required. If slaved to the navigation data, the orbital frame torquing rate must be updated for eccentric orbits; this may involve an undesirable amount of on-board computation.

7.2.1 Generalized Platform Tilt Equations

In either case an error which is associated with the error in determination of rate of change of the vertical is introduced. To accommodate the effect of this error, the basic platform tilt propagation equation (Eq. 5.31) must be modified. From Eq. (5.9) the general platform tilt rate error equation is obtained as in Eq. (5.25), this time including the variation in ω_0. The result is given as the matrix equation

$$\Delta\tilde{\omega}^{pI} = \dot{\tilde{\phi}}^{pO} - \tilde{\phi}^{pO}\,\tilde{\omega}^{pI} + \tilde{\omega}^{pI}\,\tilde{\phi}^{pO} + S^{pO}\,\Delta\tilde{\omega}_0\,S^{Op} \qquad (7.1)$$

which has the vector representation

$$\underline{\dot{\phi}}^{pO} + \underline{\omega}^{pI} + \underline{\phi}^{pO} = \underline{\varepsilon} + \underline{T} - \Delta\underline{\omega}_0 \qquad (7.2)$$

where $S^{pO} = I$ nominally to the first order.

As shown by this equation the additional error $\Delta\underline{\omega}_0$ arises from the requirement to torque the platform (in this case, to local level). If completely slaved to the horizon sensor, $\Delta\underline{\omega}_0$ is a measure of the error of the horizon sensor defined rate of change of the vertical. As noted in previous sections this rate determination is very poor in as much as present day sensor pointing data, even with filtering, has high noise content. The rate determination to torque the platform (pitch gyro) to maintain level will be correspondingly poor which definitely limits capability to achieve accurate gyrocompass alinement.

7.2.2 Coupled Platform Tilt Equations

To avoid reliance on the horizon sensor for the determination of the orbital rate $\underline{\omega}_0$ may be computed provided the orbital parameters (navigation data) of the vehicles center-of-mass were known. Since in most cases where on-board orbit determination requirement is absent and L/M orbit is known to any desired precision, this latter method of torquing the platform would appear to be the more desirable approach.

In conjunction with the foregoing, it is appropriate to note the fundamental difference between celestial alinement and gyrocompass alinement. In celestial alinement no positional information is required since platform alinement is secured with respect to a pair of stellar lines. For gyrocompass alinement, the platform is alined relative to the orbital frame which frame depends upon the trajectory parameters. Consequently, gyrocompass alinement is closely coupled to the navigational data whereas in celestial alinement it is completely decoupled. This dependence on navigational data has a close parallel to the classical cruise gyrocompass alinement. There alinement error equations are coupled to the level position and velocity errors, so that the overall gyrocompass alinement involves both the attitude and the position-velocity error equations. This coupling characteristic is used to level the system by nulling the accelerometer outputs.

To show how position and velocity errors appear in Eq. (6.54) it is necessary to express $\tilde{\omega}_0$ in terms of its elements. From an earlier development

$$\tilde{\omega}_0 = -\dot{S}^{OI} S^{IO} = \begin{bmatrix} 0 & -(\dot{\Omega}\, SuS\gamma + \dot{\gamma}\, Cu) & \dot{u} + \dot{\Omega}\, C\gamma \\ \dot{\Omega}\, SuS\gamma + \dot{\gamma}\, Cu & 0 & 0 \\ -(\dot{u} + \dot{\Omega}\, C\gamma) & 0 & 0 \end{bmatrix} \tag{7.3}$$

Perturbing this equation

$$\Delta\tilde{\omega}_O = -\Delta\dot{S}^{OI} S^{IO} - \dot{S}^{OI} \Delta S^{IO}$$

$$= -\Delta\dot{S}^{OI} S^{IO} - \dot{S}^{OI} S^{IO} S^{OI} \Delta S^{IO} \qquad (7.4)$$

Let

$$\tilde{\phi}^{OI} \equiv -\Delta S^{OI} S^{IO}$$

represent the angular position error of the vehicle center-of-mass. Then

$$\dot{\tilde{\phi}}^{OI} = -\Delta\dot{S}^{OI} S^{IO} - \Delta S^{OI} \dot{S}^{IO}$$

$$= -\Delta\dot{S}^{OI} S^{IO} - \Delta S^{OI} S^{IO} S^{OI} \dot{S}^{IO}$$

$$= -\Delta\dot{S}^{OI} S^{IO} + \tilde{\phi}^{OI} (\dot{S}^{OI} S^{IO})^T$$

$$= -\Delta\dot{S}^{OI} S^{IO} + \tilde{\phi}^{OI} (-\tilde{\omega}_O)^T \qquad (7.5)$$

from which

$$-\Delta\dot{S}^{OI} S^{IO} = \dot{\tilde{\phi}}^{OI} - \tilde{\phi}^{OI} \tilde{\omega}_O \qquad (7.6)$$

Substituting into Eq. (6.57) the following expansion for $\Delta\tilde{\omega}_O$ is obtained

$$\Delta\tilde{\omega}_O = \dot{\tilde{\phi}}^{OI} - \tilde{\phi}^{OI} \tilde{\omega}_O + \tilde{\omega}_O \tilde{\phi}^{OI} \qquad (7.7)$$

The angular position error matrix $\tilde{\phi}^{OI} \equiv -\Delta S^{OI} S^{IO}$ can be expanded further in terms of the orbital parameters. Let the components of the matrix $\tilde{\phi}^{IO}$ be expressed as

$$\underline{\phi}^{OI} = \delta\theta_x \underline{1}_x + \delta\theta_y \underline{1}_y + \delta\theta_z \underline{1}_z = \delta\underline{\theta} \qquad (7.8)$$

Substituting Eq. (7.8) into Eq. (7.7) and expanding the result, the following equation is obtained

$$\Delta\underline{\omega}_0 = \delta\dot{\underline{\theta}} + \underline{\omega}_0 \times \delta\underline{\theta}$$

$$\delta\dot{\theta}_x + \omega_0\,\delta\theta_z = \Delta\omega_{0x}$$

$$\delta\dot{\theta}_y = \Delta\omega_{0y}$$

$$\delta\dot{\theta}_z - \omega_0\,\delta\theta_x = \Delta\omega_{0z}$$

Here

$$\tilde{\delta\theta} = \tilde{\phi}^{0I} = \begin{bmatrix} 0 & -\delta\theta_z & \delta\theta_y \\ \delta\theta_z & 0 & -\delta\theta_x \\ -\delta\theta_y & \delta\theta_x & 0 \end{bmatrix}$$

Provided that the components of $\Delta\underline{\omega}_0$ above are constants, the mechanizations discussed in the earlier sections will bound their effects provided the system is stable. In general, the representation as given is not constant but varies with time. For example, the propagation of initial errors give rise to unbounded effects in $\delta\theta_y$ and $\delta\theta_x$ (roll and azimuth navigation errors); therefore, the mechanization can also yield unbounded errors. The matrix $\tilde{\phi}^{0I}$ represents the angular position error of the orbital triad. This can be seen by referring to the following development. The position vector in the orbital triad is expressed as

$$\bar{R}^0 = S^{0I}\,\bar{R}^I \tag{7.9}$$

and the position error is obtained by perturbing this equation

$$\Delta \bar{R}^{O} = \Delta S^{OI}\, \underline{R}^{I} + S^{OI}\Delta \bar{R}^{I}$$

$$= \Delta S^{OI}\, S^{IO}\, \underline{R}^{O} + S^{OI}\Delta R^{I} = -\tilde{\phi}^{OI}\, \underline{R}^{O} + S^{OI}\Delta \underline{R}^{I} \quad (7.10)$$

from which the inertial position error in the orbital frame is

$$S^{OI}\ \Delta \underline{R}^{I} = \Delta \bar{R}^{O} + \tilde{\phi}^{OI}\, \underline{R}^{O} \quad (7.11)$$

From this equation it is seen that $\tilde{\phi}^{OI}$ represents the angular position error resulting from the orbital triad being tilted relative to the desired orientation.

The expansion of $\tilde{\phi}^{OI} = -\Delta S^{OI}\, S^{IO}$ using the representation for S^{OI} on the previous page

$$\delta\theta = \begin{bmatrix} 0 & -(\Delta\Omega Su\ S\gamma + \Delta\gamma Cu) & \Delta u + \Delta\Omega C\gamma \\ \Delta\Omega Su\ S\gamma + \Delta\gamma Cu & 0 & -(\Delta\Omega Cu\ S\gamma - \Delta\gamma Su) \\ \Delta u + \Delta\Omega C\gamma & (\Delta\Omega Cu\ S\gamma - \Delta\gamma Su) & 0 \end{bmatrix} \quad (7.12)$$

where the second matrix represents the navigation error

$$r\,\delta\theta_x = r(\Delta\Omega Cu\ S\gamma - \Delta\gamma Su) = \text{cross track navigation error} = \Delta_y \quad (7.13)$$

$$r\,\delta\theta_y = r(\Delta u + \Delta\Omega C\gamma) \quad = \text{range navigation error} = \Delta_x \quad (7.14)$$

$$\delta\theta_z = \quad = \text{heading navigation error} = \frac{\dot{R}}{RV}\frac{\Delta_y}{R} + \frac{\dot{\Delta}_y}{RV} \quad (7.15)$$

The rate errors $\delta\dot{\theta}_x$, $\delta\dot{\theta}_y$, $\delta\dot{\theta}_z$ are obtained from Eqs. (7.13), (7.13), and (7.15) upon differentiation, and representing the results in terms of $\Delta_{\dot{x}}$, $\Delta_{\dot{y}}$, $\Delta_{\dot{z}}$ and the nominal orbit parameters.

Substituting Eq. (7.7) into (7.1) the complete attitude error equation with navigation error coupling is given as

$$\Delta\tilde{\omega}_I^p = \dot{\tilde{\phi}}_0^p - \tilde{\phi}_0^p \; \tilde{\omega}_I^p + \tilde{\omega}_I^p \, \tilde{\phi}_0^p + S^{p0} \left\{ \dot{\tilde{\phi}}^{0I} - \tilde{\phi}^{0I} \; \tilde{\omega}_0 + \tilde{\omega}_0 \; \tilde{\phi}^{0I} \right\} \; S^{0p}$$

This equation can be given the equivalent vector representation

$$\Delta\underline{\omega} = \dot{\underline{\phi}} + \underline{\omega} \times \underline{\phi} + \delta\dot{\underline{\theta}} + \underline{\omega} \times \delta\underline{\theta} = \dot{\underline{\phi}} + \delta\dot{\underline{\theta}} + \underline{\omega} \times (\underline{\phi} + \delta\underline{\theta}) \qquad (7.17)$$

where both superscripts and subscripts have been removed, $\delta\underline{\theta}$ is the navigation error in the platform frame; and the vector representation is in the platform frame.

Equation (7.17) is the final form of the complete platform attitude error propagation equations which includes the effect of the navigation error $\delta\underline{\theta}$. The form of Eq. (7.17) is the same as the platform attitude error propagation equation of Section 5.3; and therefore, the free-inertial integral solution has the same form as that given in Section 5.4. This equation suggests that in the presence of navigation errors, the platform attitude error cannot be separated from the navigation errors for an open loop type mechanization. To separate the two errors, the navigation error $\delta\underline{\theta}$ must somehow be independently damped out; for example, with orbit redetermination.

To summarize the results of this section, orbital gyrocompass mechanization must take into account the intrinsic coupling of platform attitude errors with navigation errors. In an open loop mechanization the gyrocompass attitude errors cannot be separated from the navigation errors. In a closed loop mechanization separate measures must be taken to damp out the navigation errors.

7.2.3 The Effect of Navigation Errors in the Mechanization

To show how the effect of orbit determination can propagate in the alinement equations, consider the following example for circular orbits. Expanding Eq. (7.17) assuming the mechanization of Case 4 (porportional control and roll and yaw), the roll and yaw mechanization error due to navigation errors can be expressed as

$$\begin{bmatrix} \phi \\ \psi \end{bmatrix} = \frac{1}{S^2 + K_R S + \omega_0(\omega_0 + K_y)} \begin{bmatrix} S & -\omega_0 \\ \omega_0 + K_y & S + K_R \end{bmatrix} \begin{bmatrix} -\delta\dot{\theta}_x - \omega_0 \delta\theta_z \\ -\delta\theta_z + \omega_0 \delta\theta_x \end{bmatrix} \qquad (7.18)$$

As noted earlier the pitch axis error $\delta\theta_y$ presents no problems because its amplitude can be bounded. A similar result can be shown to hold for the roll-yaw channels. Considering only the effect of the navigation errors, one obtains

$$\phi = \frac{1}{\Delta(s)} [-s\,\delta\dot{\theta}_x - \omega_0^2\,\delta\theta_x] \qquad (7.19)$$

$$\psi = \frac{1}{\Delta(s)} [-\omega_0 / \omega_0 + K_y / \delta\theta_x - (s + K_R)\,\delta\dot{\theta}_z) = \delta\theta_z \qquad (7.20)$$

Note that the error in yaw propagates as the navigation heading error.

For circular orbit the error $\delta\theta_x$ and $\delta\theta_z$ can be expressed as (for any two-body conical orbits)

$$\delta\theta_x = C(v - v_0)\,\delta\theta_{x0} - s(v - v_0)\,\delta\theta_{z0}$$

$$\delta\theta_z = s(v - v_0)\,\delta\theta_{x0} + C(v - v_0)\,\delta\theta_{z0}$$

$$\delta\dot{\theta}_x = -\sqrt{\frac{\mu}{p^3}}\;\frac{p^2}{R^2}\;s(v-v_0)\,\delta\theta_{x0} - \sqrt{\frac{\mu}{p^3}}\;\frac{p^2}{R^2}\;c(v-v_0)\,\delta\theta_{z0}$$

$$\delta\dot{\theta}_z = \sqrt{\frac{\mu}{p^3}}\;\frac{p^2}{R^2}\;c(v-v_0)\,\delta\theta_{x0} - \sqrt{\frac{\mu}{p^3}}\;\frac{p^2}{R^2}\;s(v-v_0)\,\delta\theta_{z0} \qquad (7.21)$$

where $v-v_0$ is the relative central angle between the two epochs.

Substituting the above set (Eq. 7.21) into Eq. (7.19) and (7.20), it can be easily established that the steady state error response in the roll and yaw channels are at most periodic for both circular and elliptic orbits.

To summarize, the basic conclusion reached regarding the error in platform level torquing due to the navigation error coupling is that, stable mechanizations yield sinusoidal roll and yaw platform errors of orbital frequency for both circular and eccentric orbits; while in the pitch mode (see Section 6.2) periodic errors occur for circular orbits, and secular errors to the order of the eccentricity occur for non-circular orbits.

Since the navigation errors will essentially be damped or bounded by periodic orbit determination, the alinement errors can be bounded. It is appropriate to discuss here again the similarity of the present case of incorrect torquing in the orbital case with the cruise mechanization. In the cruise case the navigation errors are damped with an external velocity measurable (a doppler radar). In the orbital case these errors are damped via orbit determination. In the cruise case the navigation errors can be damped in real time by analogue mechanization. In the orbital case real time mechanization of orbit determination involves complex computation, and may be difficult to inplement on a real time basis; hence navigation errors will be bounded by periodic orbit determination at discrete intervals. To this extent navigation errors propagate in open loop, while for the cruise case, it propagates in closed loop.

7.2.4 The Effect of Perturbations

Orbital perturbations can affect the accuracy of gyrocompass alinement in various ways. If the system is torqued to level by slaving to the sensor, then the shape of the earth must be taken into account. The horizon sensor derived vertical must be modified for the oblate earth. Reference 6 derives the oblateness connection equations which might be used to correct the vertical.

If, on the other hand, the system is torqued with the orbital parameters, thse parameters must be updated for the perturbative acceleration effects due to the oblateness of the earth. Also, for low altitude orbits the effect of air drag must be compensated for. The correction for these errors will depend upon such factors as the system accuracy requirements and the frequency of orbit parameter re-initialization for a given mission. First order error equations for various perturbation forces are developed in reference 7.

The effect of perturbation on the alinement accuracy can be developed in terms of variations in the orbit parameters. The general tilt equation is given as

$$\dot{\underline{\phi}} + \underline{\omega} \times \underline{\phi} = \underline{\epsilon} + \underline{T} + \Delta\underline{\omega}_0$$

where $\Delta\underline{\omega}_0$ is the error in torquing which results from perturbation. In Eq. (7.12) $\Delta\underline{\omega}_0$ is expressed in terms of the orbital parameter errors $\Delta\Omega$, $\Delta\gamma$, Δu. These in turn can be related to the perturbations via the variation of constant equations (see Ref. 7).

8.0 High Precision Gyrocompass Mechanization

Recognizing the dependence of high accuracy gyrocompass alinement to the navigational data, a mechanization can be devised which simultaneously performs orbit determination and gyrocompass alinement using the horizon sensor data. Such a mechanization would be computational and might include optimal parameter estimation procedures taking into account the a priori statistics of the noise processes of the sensor and the gyro drift. A Kalman type mechanization which includes a recursive type estimation algorithm is described in Ref. 5. Needless to say, a considerable amount of on-board data processing capability is required.

REFERENCES

1. "Inertial Guidance," Edited by G. A. Pitman, Jr., John Wiley & Sons, New York

2. "An Orbital Gyrocompass Heading Reference for Satellite Vehicles," AIAA Preprint 64-238, July 1964

3. "Control, Guidance, and Navigation of Spacecraft," NASA-SP-17 December 1962, Office of Scientific and Technical Information

4. H. M. James, N. B. Nichols, and R. S. Philips, "Theory of Servo Mechanisms," McGraw-Hill, New York, 1947

5. A. L. Knoll, and M. M. Epelstein, "Estimation of Local Vertical and Orbital Parameters for an Earth Satellite on the Basis of Horizon Sensor Measurements," January 20, 1964.

6. R. E. Roberson, "Optical Determination of Orientation and Position Near a Planet," ARS Preprint, August 11, 1958

7. Wadd TR 60-214 "Methods for Analysis by Satellite Trajectories," September 1960 (Autonetics Report EM-2075)

CHAPTER VIII

MEASUREMENT GYROCOMPASSING IN ORBIT

1. Introduction

The present chapter contains a study on orbital gyrocompass alinement mechanization techniques for strapdown systems. The mechanizations are discussed in a general way being applicable to rotation sensors which include rate gyro, single axis platform, and ESG packages. Because the output data of ESG systems requires processing of a nature considerably different than the other two, a separate section is devoted to its discussion. Gyro packages which includes two body mounted free-rotor gyros or two two-axis gyros are similar in their output characteristics to rate gyro and single axis platform packages; and for this reason are not considered.

On a conceptual basis the gyrocompass alinement of strapdown systems is no different then for the gimballed platform. Indeed the orbital gyrocompass alinement equations are identical. The only difference is one of emphasis to be placed on the role of the hardware and the computer (software) participation in the alinement problem. For the gimballed case, servo controllers bring the platform into physical alinement with the desired frame of reference. For the strapdown system the same function of stabilizing the error is performed in the computer. Both systems would process the same kind of error observables from the horizon sensors. However, there are fundamental differences involved in gyrocompassing strapdown systems; whereas the gimballed platform may be rotated to the desired initial alinement while undesired vehicle rotations are compensated automatically (vehicle angular rate isolation, Ref. 1), the initial gyrocompass alinement for strapdown inertial packages must be accepted in whatever attitude state the vehicle (platform) frame finds itself in, and the initial conditions for the direction cosine transformation computer must be determined in the presence of this undesired vehicles motion. Since the computer is essentially following the vehicle rotations via the gyro outputs, the initial conditions must be determined and utilized instantaneously if the attitude determination is to be precise. Any delay in initializing the system relative to the epoch at which the state of the system was determined introduces a bias error in the rotation rate of the system. This appears as an integrated effect when the direction cosine attitude matrix is updated.

When a strapdown ESG package is considered, other difficulties arise. The direction cosines determined from the two or three readout parts are actually computed for different times. In the presence of high body rates, it is necessary to interpolate the direction cosines and the vehicle angular rates so that they will represent their actual values for the same instant of time.

The coupling of unstabilized vehicle angular rates into the gyrocompass alinement loop is perhaps the principal limitation to achieving highly accurate alinement with a minimal amount of computation. It is possible to minimize the coupling with tighter attitude control during the gyrocompass mode; this, however, is achieved at the expense of greater fuel expenditures. Another way, achieved at the expense of increased computation, is to estimate the effect of vehicle rates and subtract its effect out from the basic gyrocompass equations. If the direction cosine equations are being continuously integrated, the computed rates will always be available, and this computation poses no real difficulty. On the other hand, in a minimal computation system where the direction cosine equations may not be integrated, vehicle rate coupling becomes an important consideration.

Even if the vehicle rates are computed via the direction cosine equations, it should be recognized that vehicle rate coupling can occur. In the gimballed case this coupling is totally absent while in the strapdown case it is absent only to the degree that the rates can be accurately computed. Thus in the presence of high body rates and depending upon the computer and gyro data rates, computational errors associated with the isolation of vehicle rates will occur, in turn, causing errors in initializing the direction cosine matrix. This error will then be integrated causing the direction cosines to drift.

2. Preliminary Mechanization Considerations for Strapdown In-orbit Gyrocompass Alinement

2.1 Definition of Gyrocompass Alinement Modes

The gyrocompass alinement of strapdown systems may be considered in two specific modes. Either, or both modes, may be operating for a given mission. One mode involves gyrocompassing the vehicle frame in a physical sense to aline with the orbital frame. The second mode would involve the analytical gyrocompassing the vehicle frame transformation matrix in the on-board computer. The former may be thought of as a coarse alinement mode; the latter as a fine mode.

Gyrocompassing the vehicle physically is analogous to the problem of gyrocompass alinement of a gimballed local level platform. One can imagine the vehicle - attitude control system - strapdown gyro package in orbit as a huge gimballed platform with the attitude controllers serving the function of platform servoes. There are, however, several important differences which are to be noted. First, the attitude control system is non-linear with deadband limits, and insofar as accurate alinement of the reference system is concerned can only serve the function of coarse alinement. Second, the stability analysis considerations depend upon the vehicle dynamics and the control system. For the gimballed platform stability analysis, it is only necessary to consider angular velocities (kinematics) because the motion of the platform is largely described in terms of its gyroscopic effect, i.e., torquing the gyros; while in the other case, the principal inertias of the vehicle are being torqued and gyro coupling is nil. Finally, for low earth vehicles in particular, the accuracy of gyrocompass alinement will be limited by the residual unstablized vehicle angular rates while for the gimballed platform the equivalent effect would result from gyro drift rates the effect of which are negligible by comparison. Thus, for the gimballed platform, horizon sensor errors would limit alinement accuracy while for gyrocompassing the vehicle unstabilized angular rate coupling would limit accuracy.

To reference basic accuracy capabilities of computational alinement schemes, consider the basic errors associated with gyrocompassing the vehicle. Suppose the vehicle frame is stabilized in level with a horizon scanner. In the steady state the level alinement of the vehicle frame is governed by the horizon sensor errors (typically about one mil), or by the deadband (typically $.1^\circ = 2$ mil). In the case of yaw alinement, the accuracy is limited by a gyrocompass type error. This error in steady state is Ψ(yaw error) $\approx \dot{\phi}/\omega_o$ where $\dot{\phi}$ is the vehicle roll rate coupling and ω_o is the orbital rate. Roll rate coupling of the vehicle results from the unstabilized motion associated with limit cycle oscillations. For Voyager and Agena typically $\dot{\phi}$ is about 2°/hr. On the basis this is a dc type error yaw alinement accuracy for low earth vehicles is about 8 mils.

The principal objective of the present study is to consider the second mode of computational gyrocompass alinement of the vehicle frame transformation matrix. The mechanization schemes considered do not involve the vehicle attitude control system in a direct way; however, as noted earlier, the alinement accuracy is dependent upon the characteristics of the unstabilized vehicle rates in a subtle way.

Several different configurations can be envisioned for computationally performing the gyrocompass alinement of strapdown systems. Table 1 is a summary of the gross characteristics of some of the various schemes considered. Depending upon the alinement accuracy requirement, real time data processing requirement, the on-board computer capabity, and the unstabilized rotation rate of the vehicles, the alinement mechanization equations can have varying degrees of sophistication.

To update the attitude matrix, strapdown systems typically require the integration of the direction cosine equations. The integration and the associated algorithm can place a heavy demand upon the computer capacity. If two measurable non-collinear vectors (such as the vertical and the orbital pole) can be processed in real time, then it may not be necessary to perform this updating computation; or if the computation is required, the direction cosines can be updated at a slower pace. The alinement accuracy will depend upon the coupling of the unstabilized vehicle angular rate.

On the other hand if the direction cosine equations are computed onboard then it is possible to follow the vehicle motion with the gyros, so that on integration the unstabilized vehicle rates will be included in the estimate of the transformation matrix. As a result the alinement will be more accurate because the effect of the undesired vehicle motion about its center-of-mass will have been included in the gyrocompass alinement equations.

To determine a unique three-axis transformation matrix it is necessary to determine the directions of at least two well-defined non-collinear lines relative to the body frame. These lines may be defined in a number of different ways. Figures 1 and 2 show two schemes which are called "one-point" and "two-point" gyrocompass schemes.

In a one point gyrocompass scheme (Fig. 1) the two vectors are instantaneously specified; typically, the direction to the local vertical and the direction to the orbital pole. Other directions that may be utilized in earth's orbits might be the sun line. The local vertical in the vehicle frame might be defined by the direction of the horizon sensor axis, and the orbital pole direction might be defined by measuring the rate outputs of the gyro package. This is essentially the technique used in the fixed site gyrocompass problem. There local vertical is defined by the direction of local gravity vector; which is measured via the accelerometers; and the gyro outputs measure the direction of the rotation of the earth in the vehicle frame. Because of the relative simplicity of the alinement equations, for the orbital problem, this one point scheme might be used to coarse initialize the direction cosine equations.

In a two-point gyrocompass scheme (Fig. 2), the direction of the local vertical might be measured in the vehicle frame for two different instants of time. In this sequential scheme the history of the relative vehicle angular motion must be known between the two instants of time. This can be achieved by integration of the direction cosine equations using the rate outputs from the gyro package.

In the one point scheme geometric sensitivity to error in the measurement is minimized because the two vectors are orthogonal. In the two-point scheme, because the two lines must be closely spaced if real time determination is to be realized; alinement accuracy is extremely sensitive to the geometry of the two lines. In particular, if just two verticals are processed the alinement accuracy sensitivity is proportional to the reciprocal of the square of the line of the angle between the two verticals. On the other hand, the one point scheme is sensitive to unstabilized vehicle angular rate coupling into the alinement equation; the gyrocompass error being essentially that associated with gyrocompassing the vehicle. Because the two-point scheme processes only horizon sensor data the alinement accuracy is largely governed by the sensor errors (provided vehicle rotation rates are computed).

Computation requirements associated with the one-point scheme tends to be minimal. On the other hand it tends to be maximal for two point schemes because of the requirement to compute the attitude matrix between the two points. However, if vehicle rates are computed and compensated in the one point scheme, the computational requirements are comparable.

Table 1

Summary of Gross Errors of Gyrocompassing Techniques

Gyrocompass Scheme	Level Errors Defined By	Yaw Errors Defined By	Comments
1. Gyrocompassing the vehicle	1. Attitude control deadband; typically 0.1° ≈ 2 mils 2. Horizon sensor resolution Error; typically 1 mil	1. Vehicle roll rate coupling, typically limit cycle rate 2°/hr corresponds to 8 mils 2. Horizon sensor errors	1. Coarse alinement to local level
2. Computational gyrocompass alinement of attitude matrix			1. Both coarse and fine
A. Open-loop	1. Attitude control deadband; typically 0.1° ≈ 2 mils	1. Vehicle roll rate coupling 2°/hr limit cycle corresponds to 8 mils	1. Essentially no computation 2. Coarse alinement
B. One-point scheme No estimate of unstabilized rates	1. Attitude control deadband typically 0.1° ≈ 2 mils 2. Horizon sensor resolution error; typically 1 mil	1. Vehicle roll rate coupling 2°/hr limit cycle corresponds to 8 mils 2. Horizon sensor errors	1. Direction cosine equations not computed 2. Possibly fine alinement
C. One-point scheme Estimate (compute) vehicle rates	1. Horizon sensor resolution error; typically 1 mil	1. Roll gyro drift rate coupling .01°/hr gyro drift rate corresponds to 0.04 mils 2. Horizon sensor errors	1. Direction cosine equations computed to estimate vehicle rates 2. Coarse alinement
D. Two-point scheme no computation 10° separation	1. Attitude control deadband; typically 0.1° ≅ 2 mils 2. Horizon sensor resolution error; typically 1 mil corresponds to 25 mil	1. Roll vehicle rate coupling 2°/hr limit cycle ≈ 8 mils 2. Horizon sensor errors	1. Direction cosine equations not computed 2. Coarse alinement

able 1 (Cont'd)

E. Two-point scheme computation 10° separation	1. Horizon sensor resolution error; 1 mil corresponds to 25 mil geometric error	1. Roll gyro drift rate; $.01^\circ/\text{hr} \approx 0.4$ mils 2. Horizon sensor errors	1. Direction cosine equation computed 2. Possible fine alinement
F. Multi-point scheme computation	1. Horizon sensor resolution; asymptotic error 2. Bias errors estimated out $\frac{1}{\sqrt{n}}$ (random)	1. Roll gyro drift rate; $.01^\circ/\text{hr} \approx .04$ mils 2. Horizon sensor error proportional to $\frac{1}{\sqrt{n}}$ (random) 3. Bias errors estimated out	1. Assume correlation time of sensor "bias" smaller than averaging time 2. High precision alinement 3. For Kalman procedure require a priori statistics of noise in sensors to yiel optimal data process filter
G. Continuous self-alinement	1. Horizon sensor resolution error 1 mil	1. Roll gyro drift rate; $.01^\circ/\text{hr} \approx .04$ mils 2. Horizon sensor errors	1. Depends upon assumed gains. However, assume proportiona feedback control. 2. Essentially fine problem as alinement of gimballed platform 3. Fine alinement 4. Less accurate than

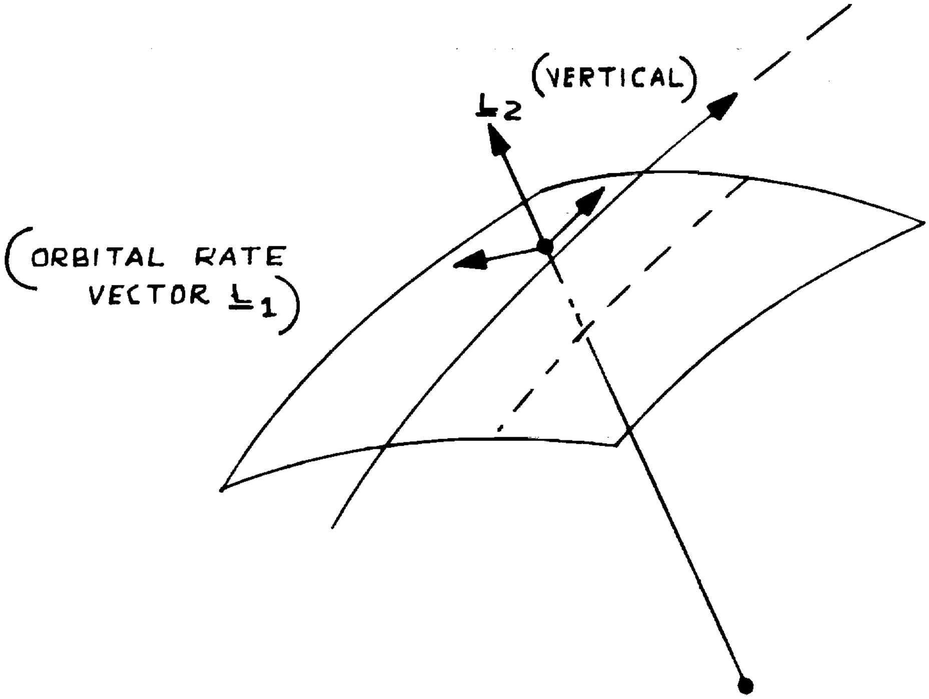
$\underline{L}_2$ (VERTICAL)
(ORBITAL RATE VECTOR $\underline{L}_1$)

Fig. 1

One-Point Gyrocompass Mode

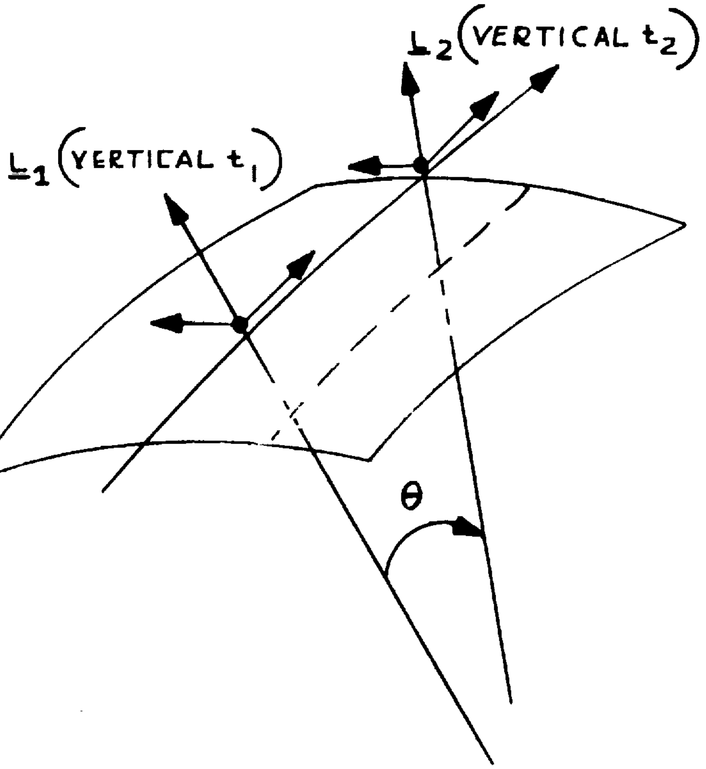
$\underline{L}_2$ (VERTICAL t_2)
$\underline{L}_1$ (VERTICAL t_1)
θ

Fig. 2

Two-Point Gyrocompass Mode

Both of these schemes can be extended into sequential procedures in which optimal parameter estimation algorithms are used to estimate and update the vehicle frame attitude state. One scheme which is an extension of the two point scheme is considered in the present study. A series of horizon sensor data are processed sequentially to update the vehicle attitude matrix using Kalman's estimation algorithm. These schemes would be utilized for high precision gyrocompass alinement.

A limiting case of the foregoing multipoint scheme is the case where the series of verticals are continuously measured and processed. An insight on how to correct the attitude error matrix is provided by the orbital self-alinement of the gimballed platform (Ref. 1). There the level deviation errors defined by the horizon sensors are used to torque the level gyros, thereby stabilizing all three axes. Since the attitude error propagation equations are identical for both cases, the same technique of feedback corrections, applied computationally might effect a "computational self-alinement" of the attitude matrix. This problem is considered in detail in a following section.

2.2 Systems Considerations

The overall system diagram of the gyrocompass alinement with a strapdown system is shown in Fig. 3. The vehicle dynamics include the attitude control system. Typically, a horizon scanner and gyro rate outputs will provide signals to drive and hold the vehicle to the local level orientation. The error signals provide the feedback signals to the vehicle attitude controllers. Assuming the vehicle is stabilized in the local level configuration, the direction cosine matrix S^{po} is initialized by processing the directions of the local vertical and the orbital hole in the vehicle frame. On the basis of the estimated value of S^{po}, the two directions are in turn computed in the platform frame, compared with their measured counterparts; and feedback corrections to S^{po} are determined. Continuous feedback corrections to the current estimate, in real time, while at the same time computing the elements with the gyro outputs, provides the corrected updated direction cosine transformation matrix. This feedback correction can be handled on the basis of an analog or a discrete sampled data mechanization. The apparent large amount of computation and the presence of a noisy environment would probably imply that the feedback corrections be mechanized on the basis of sampled data. Sampled data techniques would permit smoothing (prefiltering) the residuals before determining the corrections; maintain real time; update albeit at the expense of the information being available at discrete times; and be suited for digital computation.

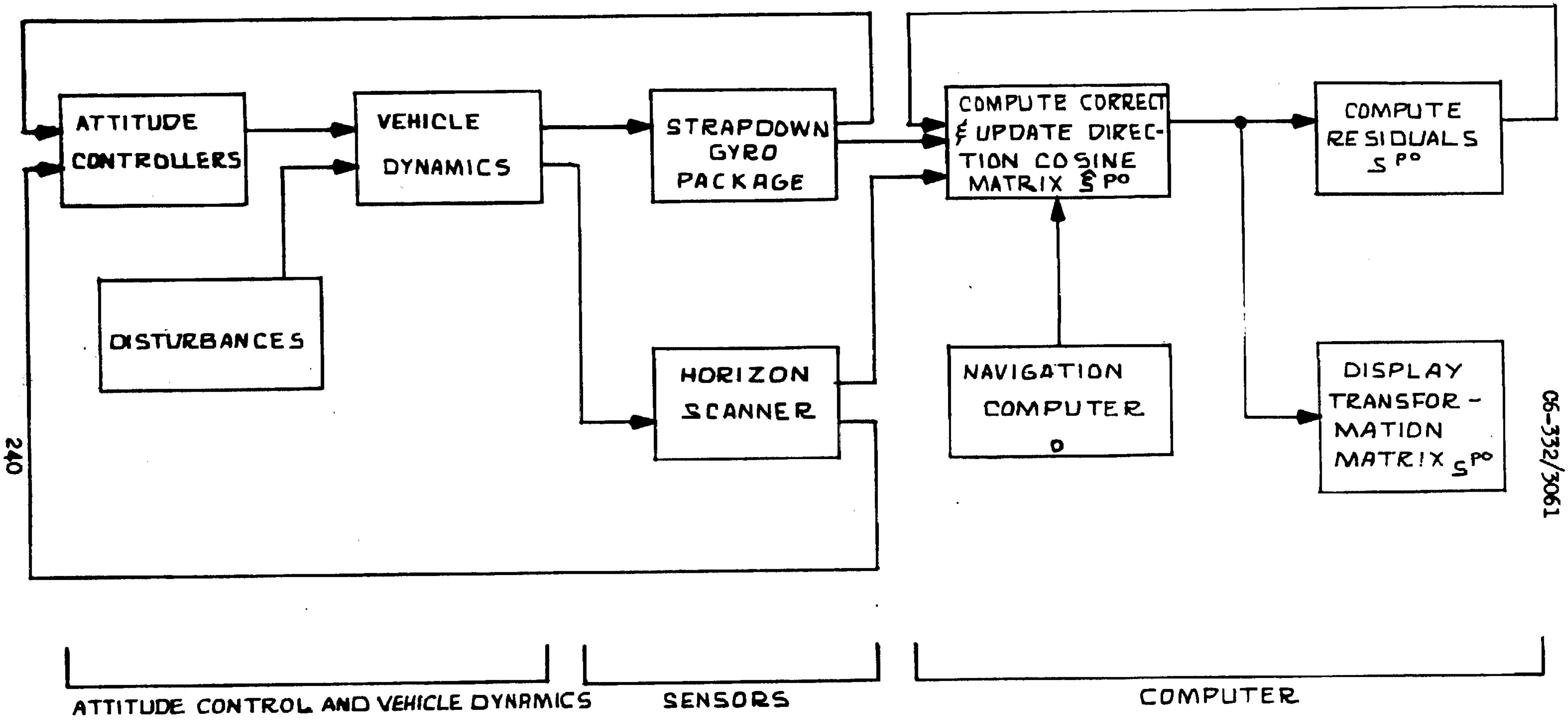
ATTITUDE CONTROLLERS
DISTURBANCES
VEHICLE DYNAMICS
STRAPDOWN GYRO PACKAGE
HORIZON SCANNER
COMPUTE CORRECT & UPDATE DIRECTION COSINE MATRIX S^{PO}
NAVIGATION COMPUTER
COMPUTE RESIDUALS S^{PO}
DISPLAY TRANSFORMATION MATRIX S^{PO}
ATTITUDE CONTROL AND VEHICLE DYNAMICS
SENSORS
COMPUTER

Fig. 3

Overall System Diagram of In-Orbit Strapdown Computational Gyrocompass Mode

As noted in Fig. 3, while the vehicle rotation rates couple into the alinement mode, the rates in turn are governed by the sensors which control the vehicle. Thus drift rates in the gyro package, bias, and noise errors in the horizon sensor act as driving inputs to the vehicle control system. To characterize the error inputs to the gyrocompass loop, the transfer functions between the sensor outputs to the input point of the vehicle attitude controllers are required to be known. These transfer functions are dependent upon the particular vehicle and attitude control systems. The present study will not consider this problem further, except as to indicate its importance for a complete analysis of a strapdown alinement mechanization.

2.3 Strapdown Platforms

A strapdown platform is a natural system for providing vehicle attitude relative to the orbital frame. The primary reason stems from the fact that the system output yields the total inertial vehicle body rates in the vehicle frame. For a vehicle whose axes are nominally oriented with the local level orbital frame, continuous yaw can be obtained directly with little or no computation.

The strapdown platform can be characterized by three specific configurations. Figure 4 shows a configuration which is made up of three single axis platforms. Each gyro is a single degree of freedom integrating gyro with a gimbal follow-up. The input axis of the gyro defines the axis of stabilization. The output axis pickoff on the gyro controls the servo motor which torques the input axis of the gyro in order to null the gyro output axis angle (precession angle). In this way, the servo torquer performs the usual platform function of cancelling out disturbance torques appearing about the input axis of the gyro (the stabilization axis). When the vehicle axes rotates about the gyro output axis, the servo torquer performs the additional function of applying a precession torque (follow-up) to the gyro so that it will follow the vehicle frame. Digital encoders or gimbal angle transducer outputs are used to measure the gimbal angle and gimbal angle rate between the gyro case and the vehicle frame. The three platforms measure rotations about pitch, roll, and yaw axes of the missile. A gimballed platform can be considered strapdown in the above sense where the gimbals are all held nominally orthogonal, (i.e., caged to the vehicle frame).

Figure 5 depicts a second type of a strapdown package. The gyro package includes three single axis spring restrained rate gyros. The spring restrained output axis angle is a direct measure of the total angular rate appearing about the input axis. This system is simpler than the integrating platform because it requires no gimbal follow-up, servoes, and angle readouts.

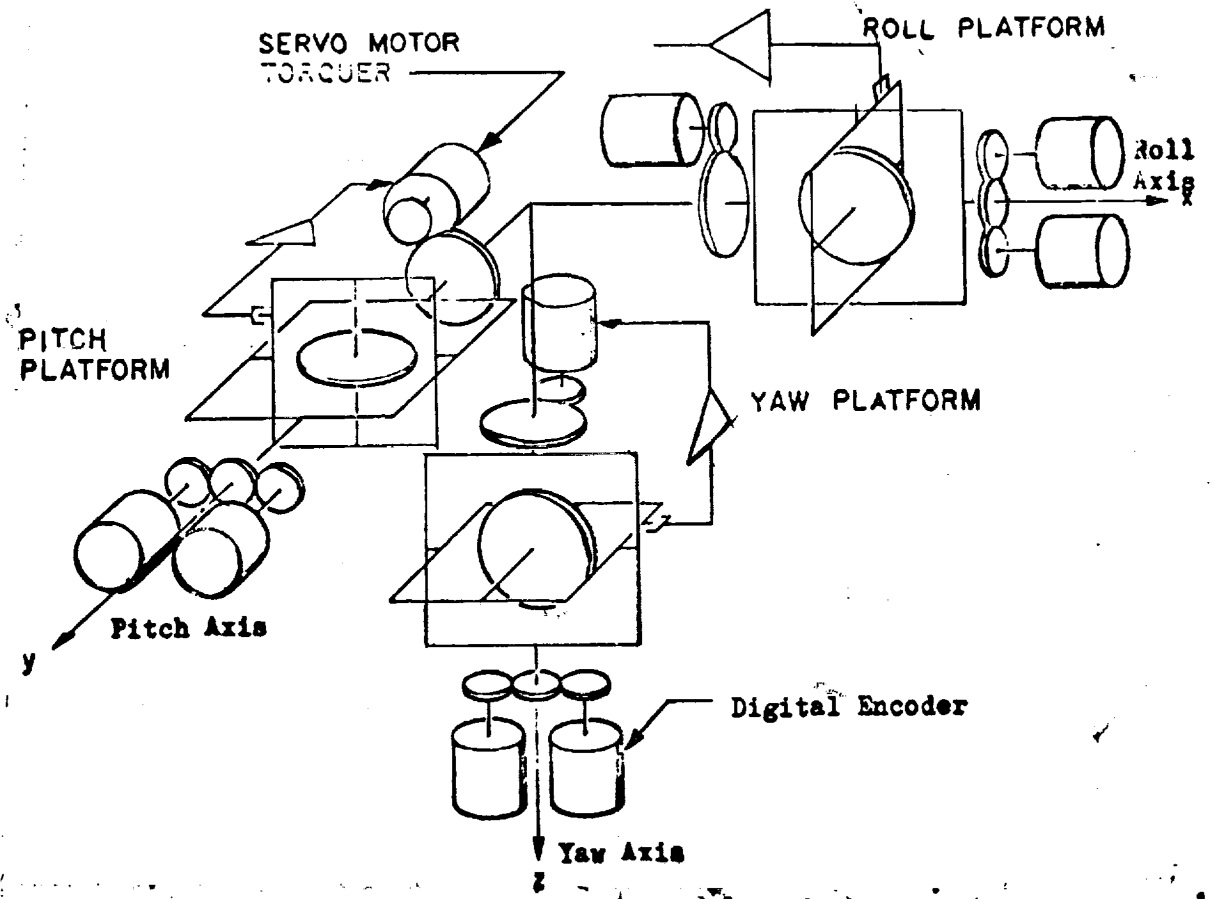
SERVO MOTOR
TORQUER
ROLL PLATFORM
Roll
Axis
x
PITCH
PLATFORM
YAW PLATFORM
Pitch Axis
y
Digital Encoder
Yaw Axis
z

Fig. 4

Three Single Axis Platforms

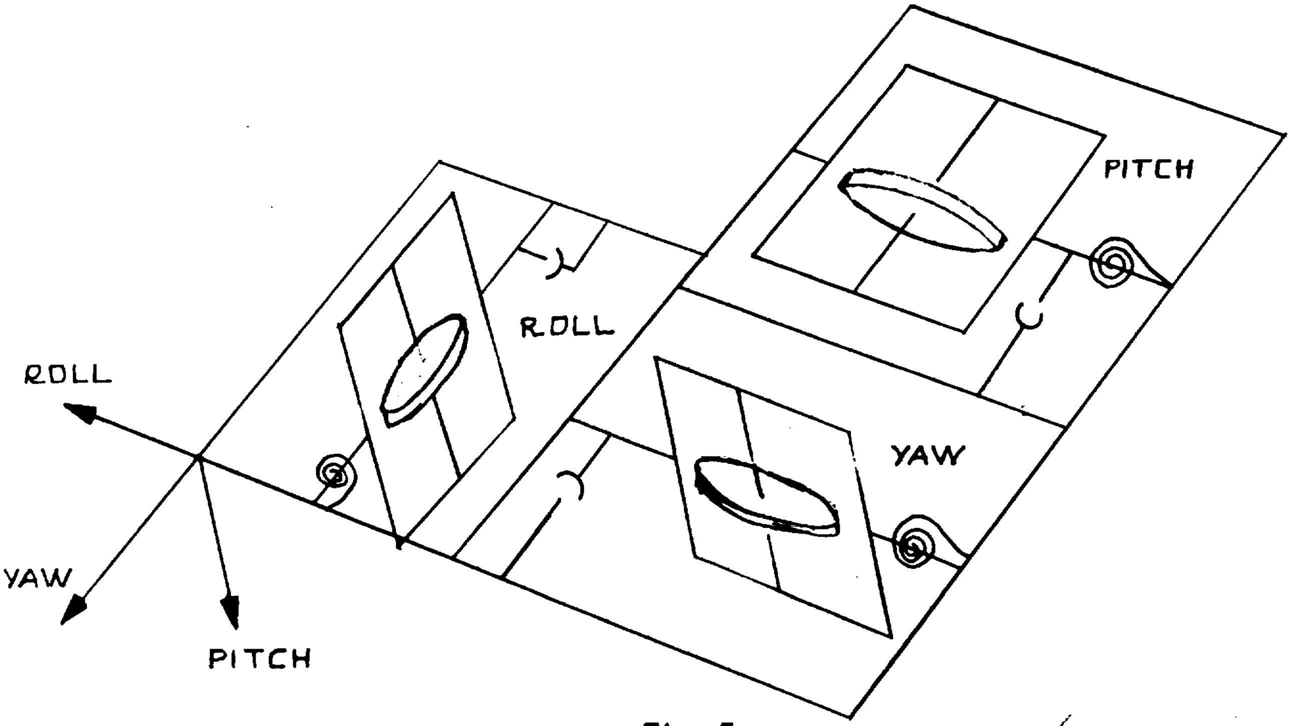
PITCH
ROLL
ROLL
YAW
YAW
PITCH

Fig. 5

Rate Gyro Package

From a computational point of view the single axis platform leads to a simpler mechanization than the rate gyro system. Small angle deviation indication is directly available at the readout, whereas for rate gyro systems the attitude must be determined by integration. For the local level orbital frame configuration the yaw indication for the single axis platform is available as the output of the yaw gyro angle transducer, while for the rate gyro platform, it is available as the rate output of the roll gyro.

A third type of strapdown system utilizes the electrostatically suspended gyro (ESG). Two free spinning gyros with the rotor cases mounted directly to the vehicle frame provide the body axes attitude information. Optical readout data are used to compute the spin direction of the rotor relative to the body frame. Thus, it is possible to obtain real time direction cosines of the body frame transformation matrix without the integration of the direction cosine equations (as required for the other systems to update attitude). The processing of the readout data to obtain direction cosines involve a considerable amount of digital computation (as shown in Appendix A). Thus, this gyro system requires a high speed digital computer with a large capacity.

3. Open Loop Attitude Determination and Error Characteristics

3.1 General

To gain insight into the kind of errors involved with strapdown systems, it is initially instructive to consider two basically different open loop attitude determination mechanizations. One mechanization processes the roll gyro rate output directly to obtain yaw; the other integrates the rate outputs from the gyro package to determine the attitude. Both of these cases are considered separately in the present section. These cases are designated respectively as Case 1 and Case 2. In essence, these cases are respectively the open loop analogue of the one-point and the multipoint alinement schemes discussed in section 2.2.

3.2 Case 1 - Open Loop Yaw From Roll Gyro Rate Output

Suppose the vehicle frame is nominally alined to the orbital frame. As shown in Ref. 1 the vehicle frame rate error propagation equation is given to the first order by

$$\dot{\underline{\phi}} + \underline{\omega}_x^{pI} \underline{\phi} = \underline{\omega}^{pI} - S^{pe} \underline{\omega}_e - \underline{\omega}^{vo} \qquad (3.1)$$

where $\boldsymbol{\omega}^{pI}$ is total inertial vehicle frame rate which is measurable by the gyro package, $\boldsymbol{\omega}_o$ is the orbital rate of the vehicle center-of-mass and $\boldsymbol{\phi} = \boldsymbol{\phi}^{po}$ is the alinement error vector (assume small deviations) of the vehicle frame relative to the desired orbital frame. For two-body orbits and a locally vehicle configuration, the components of this equation are written as

$$
\begin{aligned}
\dot{\phi} + \omega_y \psi &= \omega_x^{vI} &&= \text{vehicle roll rate} \\
\dot{\theta} &= \omega_y^{vI} - \omega_y &&= \text{vehicle pitch rate} \qquad (3.2) \\
\dot{\psi} - \omega_y \phi &= \omega_z^{vI} &&= \text{vehicle yaw rate}
\end{aligned}
$$

where $\dot{\phi}$, $\dot{\theta}$, and $\dot{\psi}$ are respectively the roll, pitch, and yaw vehicle frame angular rate deviations relative to the orbital frame the vehicle frame attitude deviation which is required to be determined is ϕ, θ, and ψ.

The angular rates as sensed by the gyros include the effect of the orbital motion and the vehicle rotation about the orbital frame. If the vehicle frame were perfectly alined, then

$$
\begin{aligned}
\omega_x^{vI} &= 0 &&= \text{roll inertial rate} \\
\omega_y^{vI} &= \omega_o &&= \text{orbital rate along pitch axis} \\
\omega_z^{vI} &= 0 &&= \text{yaw inertial rate}
\end{aligned}
$$

Since the vehicle is slaved to the horizon sensor, the roll-pitch vehicle angle and rate deviations relative to the vertical are nominally equal to zero. Assuming this to be the case, the gyro rate outputs are

$$
\begin{aligned}
\omega_y \psi &= \omega_x^{vI} \\
\omega_y^{vI} &= \omega_o \qquad (3.3) \\
\dot{\psi} &= \omega_z^{vI}
\end{aligned}
$$

The yaw gyro rate output ω_z^{vI} can be used to hold the yaw deviation to its steady state value (at $\dot{\psi} = 0$). Measuring the roll gyro output, ω_x^{vI}, yields a direct measure of yaw via the equation

$$\psi = \frac{1}{\omega_y} \omega_x^{vI} \tag{3.4}$$

This is one way in which the yaw deviation can be sensed. Notice that no integration computation is required, and the result does not depend upon initial conditions. Yaw is obtained by the simple scaling of the roll gyro output with the orbital rate. For large angle yaw, yaw indication can be obtained by taking the ratio of the roll and pitch gyro rate outputs. This yields the result

$$\tan \psi = \frac{\omega_x^{vI}}{\omega_y^{vI}} \tag{3.5}$$

In the general case, the vehicle roll rate coupling must be taken into account. Thus, the more correct expression for yaw is obtained from the roll rate equation.

$$\psi = \frac{1}{\omega_y} (\omega_x^{vI} - \dot{\phi}) \tag{3.6}$$

If $\dot{\phi}$ is negligible, yaw is simply obtained. If $\dot{\phi}$ is a random rate fluctuation, as might be associated with the limit cycle oscillations, then a time average may smooth out its effect so that

$$\psi(\text{average}) = \frac{1}{\omega_o T} \int_0^T \omega_x^{vI} \, d\tau \tag{3.7}$$

where $\bar{\dot{\phi}} \cong 0$. The accuracy of this average depends upon the smoothing time and the correlation time of the drift rate process. It is expected that the high frequency components, if they exists, can be smoothed in this fashion. For low frequency modes, such as resulting from the limit cycle oscillations, longer smoothing times are required to attenuate their effects.

Another way to reduce the effect of roll rate coupling is to compensate for $\dot{\phi}$ using the horizon sensor data. Here $\dot{\phi}$ is computed from the horizon data and subtracted from the roll gyro rate output. One such mechanization is described in Ref. 6. The principal drawback is that horizon sensor data must be differentiated. As indicated in the reference, the noise in the sensor data limits obtaining accurate rate information. Figure 6 is a block diagram of a yaw indication system with roll rate compensation.

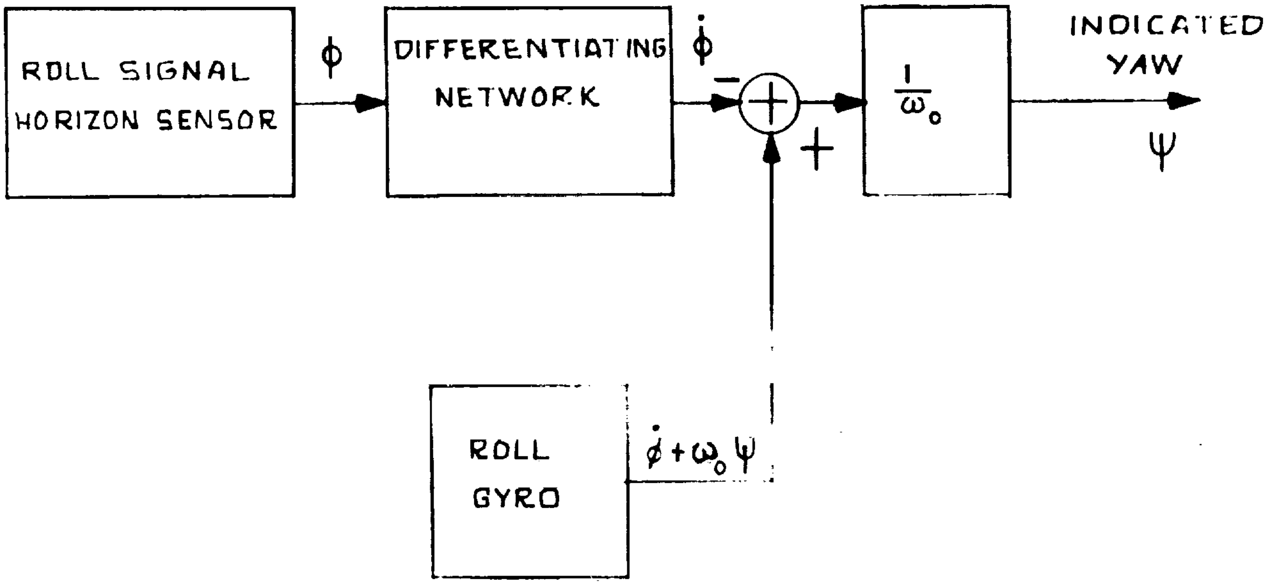
ROLL SIGNAL HORIZON SENSOR
ϕ
DIFFERENTIATING NETWORK
$\dot{\phi}$
−
+
$\frac{1}{\omega_0}$
INDICATED YAW
ψ
ROLL GYRO
$\dot{\phi}+\omega_0\psi$

Fig. 6

Roll Rate Compensation

A network which effects roll rate from roll signal might include comparing the roll signal with the output of a lag filter. One mechanization is given in Ref. 6 is shown as Fig. 7.

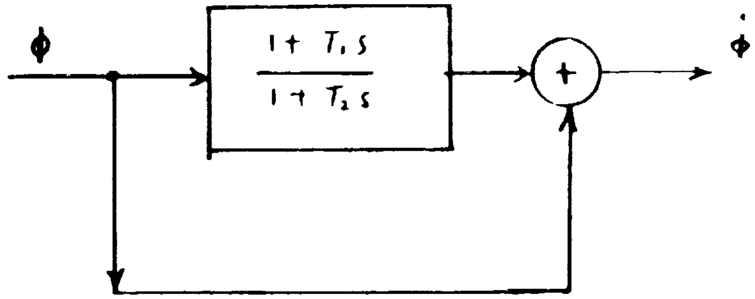

Fig. 7 - Roll Rate Network

If ϕ is noisy then differentiating this way will yield poor measures of $\dot{\phi}$ since a lag network is involved.

3.2.1 Error Characteristics

To obtain measures of the accuracy of attitude determination of the foregoing case, it suffices to note that the level errors are essentially bounded to the horizon sensor error. Thus a 1 mil sensor resolution error corresponds to level errors of the same magnitude. Ignoring the level errors, the following is a discussion of yaw indication errors for the various mechanization of roll rate considered in the previous section. Table 2 is a summary of yaw indication error for various conditions of smoothing and various correlation times of the noise process.

If $\dot{\phi}$ is not mechanized then the error in the indicated yaw is

$$\psi(\text{error}) = \frac{1}{\omega_o}(\Delta\omega_x + \dot{\phi}) \tag{3.8}$$

Table 2

Summary of Open Loop Gyrocompass Errors

Error Source	Error Magnitude	Case 1 No Smoothing No Compensation	Case 2 Smoothing Roll Gyro Output 1200 sec Smoothing No Compensation	Case 3 Smoothing Roll Gyro Output 200 sec Smoothing No Compensation	Case 4 Compensation 100 sec Smoothing Horizon Sensor Data	Case 5 Compensation 500 sec Smoothing Horizon Sensor Data
Vehicle roll rate coupling due to limit cycle oscillations	Assume dc 2°/hr	8 mils	8 mils	8 mils		
	Assume random 2°/hr rms with 200 sec period	8 mils	4 mils	6 mils		
	Assume random 2°/hr rms with 20 sec period	8 mils	0.2 mils	4 mils		
Compensated Roll Rate	RMS 2 mil peak-to-peak horizon sensor error				15 mils	3 mils

where $\Delta\dot{\omega}_x$ is the drift rate in the roll channel due to instrument errors and $\dot{\phi}$ is the vehicle roll rate. Pitch and roll errors are associated with the steady state horizon sensor errors (Note: this is a heuristic result).

$$\theta \text{ (pitch error)} = \Delta\theta \text{ (pitch horizon scanner error)}$$

$$\phi \text{ (roll error)} = \Delta\phi \text{ (roll horizon scanner error)}$$

It is expected that the roll rate error $\dot{\phi}$ is, by far, the limiting error source. Typically, a roll rate of 2°/hr (limit cycle oscillation) implies an 8 mils gyrocompass error in yaw.

3.2.2 Smoothing Errors

If the vehicle limit cycle oscillations are random, the foregoing error in yaw may be attenuated to a certain extent by averaging the roll gyro rate output

$$\Psi(\text{average}) = E(\Psi) = \frac{1}{\omega_o}\left(E(\omega_x^{vI}) - \bar{\dot{\phi}}\right)$$

and if $\bar{\dot{\phi}} \approx 0$, then (average) gives a good indication of yaw. Actually, $\bar{\dot{\phi}}$ is not equal to zero because of finite smoothing times. The error in yaw indication is then

$$\Psi(\text{error}) = \frac{1}{\omega_e}\,\frac{1}{T}\int_0^T \dot{\phi}\, d\tau \tag{3.9}$$

It is instructive to characterize the variance of this error in terms of the spectral characteristics of the $\dot{\phi}$. Suppose for the purpose of analysis, the closed loop vehicle roll motion in the presence of a stochastic perturbation torques on the vehicle can be characterized by the spectral density function

$$\Phi(\omega) = \frac{2\,\overline{\dot{\phi}^2}\beta}{\omega^2+\beta^2} \tag{3.10}$$

Then the mean squared error in yaw indication is

$$\overline{\psi^2} = \frac{2}{\omega_o^2}\,\frac{1}{T^2}\int_0^T du\int_0^u \overline{\dot{\phi}^2}\,e^{-\beta(u-v)}\,dv$$

$$= 2\,\frac{\overline{\dot{\phi}^2}}{\omega_o^2}\,\left[\frac{1}{\beta T} - \frac{1}{(\beta T)^2}\,(1-e^{-\beta T})\right]$$

Figure 8 is a plot of the square root of this function and shows the attenuation possible with smoothing and with the combined parameter βT. In all cases smoothing improves performance. However, a penalty is incurred to the extent that indicated yaw lags the actual yaw. In the presence of high body rates, therefore, this lag can limit system accuracy.

The asymptotes of the plot in Fig. 8 are worth discussing. If smoothing times are larger then the noise correlation time, $\beta T << 1$, the mean squared error is asymptotic to

$$\overline{\psi^2} \cong \frac{2\overline{\dot{\phi}^2}}{\omega_o^2}\,\frac{T_\beta}{T} \qquad \text{where } T_\beta = \frac{1}{\beta} \tag{3.12}$$

If the correlation times of the limit cycle oscillations are larger than the smoothing time $\beta T << 1$, the asymptotic error is

$$\overline{\psi^2} = \frac{\overline{\dot{\phi}^2}}{\omega_y^2}\,\frac{T}{T_\beta}$$

This shows that increasing smoothing time T increases the effect of low frequency noise.

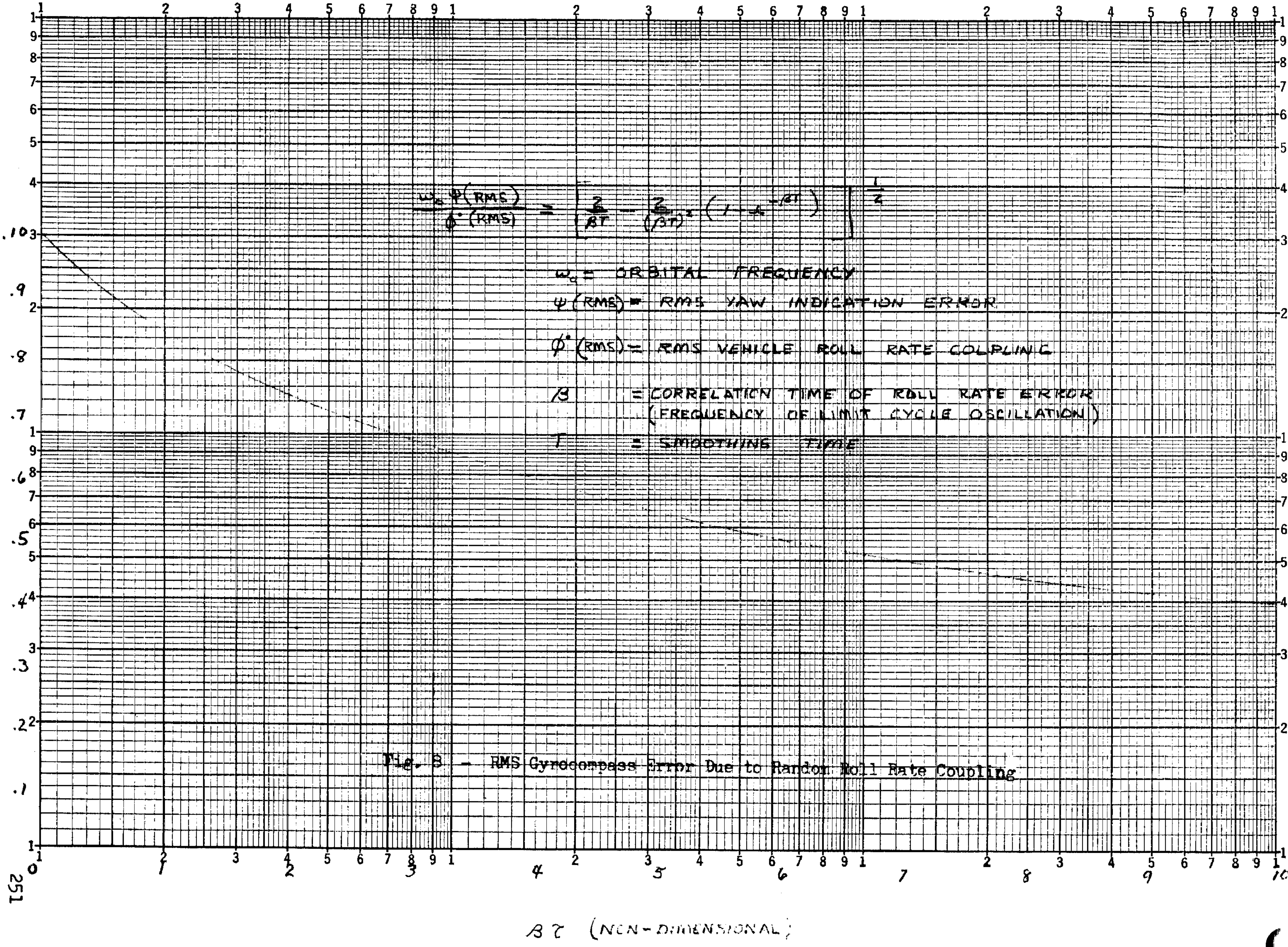

$$\frac{\omega_o \psi(RMS)}{\dot{\phi}(RMS)} = \left[\frac{2}{\beta T} - \frac{2}{(\beta T)^2}\left(1 - e^{-\beta T}\right)\right]^{\frac{1}{2}}$$

ω_o = ORBITAL FREQUENCY

$\psi(RMS)$ = RMS YAW INDICATION ERROR

$\dot{\phi}(RMS)$ = RMS VEHICLE ROLL RATE COUPLING

β = CORRELATION TIME OF ROLL RATE ERROR (FREQUENCY OF LIMIT CYCLE OSCILLATION)

T = SMOOTHING TIME

Fig. 8 - RMS Gyrocompass Error Due to Random Roll Rate Coupling

The averaging enhances the accuracy provided the correlation time of the noise process is shorter than the smoothing time. Considering the former case, a .01°/sec roll rate with a 200 sec period (not unreasonable) corresponding to a 1° deadband implies that 200 sec smoothing time is required to attenuate the error effect by a factor of 2 (Fig. 7).

Further reduction of this error can be achieved if the deadband limits are lowered during the gyrocompass mode, thereby decreasing the correlation time. The approximate equation giving the correlation time, in terms of the vehicle control system deadband, is

$$\tau_\phi = \frac{2(\text{deadband})}{\text{limit cycle rate}} \qquad (3.14)$$

thus the rms yaw indication error is proportional to the square root of the ratio of the control system deadband and the smoothing time

$$\overline{\psi^2} = \frac{2\dot{\phi}^2}{\omega_y^2} \quad \frac{2(\text{deadband})}{\text{limit cycle rate}} \qquad (3.15)$$

3.2.3 Compensation Errors

To estimate the effect of compensation, suppose a 2 mil rms peak-to-peak horizon scanner resolution error is assumed. A one second smoothing in the network implies a 0.1°/sec roll rate determination error. A 100 second smoothing time constant implies a 0.001°/sec drift rate. Table 1 tabulates the yaw error for several cases of smoothing times.

3.3 Case 2 - Integration of Attitude Deviation Equation

Since the attitude error equations correspond to the rotation equations of motion of the vehicle, and since the angular rates of $\underline{\omega}^{PI}$ are available, the integration of these equations in the computer is another way to determine the attitude. Suppose the vehicle is in a circular orbit, then $\omega_y = \omega_o$ = constant (mean motion), and the equations can be integrated to yield

$$\phi(t) = \phi_o \, C\omega_o(t-t_o) - \psi_o \, S\omega_o(t-t_o) + \int_{t_o}^{t} C\omega_o(t-\tau)\,\omega_x(\tau)d\tau$$

$$- \int_{t_o}^{t} S\omega_o(t-\tau)\,\omega_z(\tau)d\tau$$

$$\psi(t) = \psi_o \, C\omega_o(t-t_o) + \phi_o \, S\omega_o(t-t_o) + \int_{t_o}^{t} S\omega_o(t-\tau)\;\omega_x(\tau)d\tau$$

$$+ \int_{t_o}^{t} C\omega_o(t-\tau)\;\omega_z(\tau)d\tau$$

$$\theta(t) = \theta_o + \int_{t_o}^{t} (\omega_y - \omega_o)d\tau$$

thus, if the initial condition θ_o, ϕ_o, ψ_o, can be fixed at a prior epoch t_o, or if the magnitudes can be bounded to negligible values, the integration of the gyro rates will yield the vehicle deviation as a function of time and, therefore, provide an updated attitude matrix S^{vo} or S^{po}.

The primary drawback to this mechanization is that while the initial level errors can be bounded with the horizon scanner, no such bound is possible for the initial yaw deviation. To insure that yaw deviation can be bounded implies a gyrocompass alinement. Thus the integration scheme considered in the above is just another of keeping S^{po} updated assuming a prior gyrocompass mode had reduced the initial errors in both level and azimuth to bounded tolerable levels.

The foregoing is another way of obtaining an updated estimate of the vehicle frame attitude relative to the orbital frame. Both of these schemes are typical of open loop attitude indication schemes.

3.3.1 Updating the Attitude Error Matrix

For the two-point or the multipoint scheme, the attitude error between two epochs can be characterized as the integral of Eq. (3.1). Suppose that it is possible to compute the total vehicle rate via the direction cosine equations. Then the computed value is

$$\hat{\omega}^{pI} = \underline{\omega}^{vo} + \hat{S}^{po}\underline{\omega}_o \qquad (3.17)$$

where $\hat{S}^{po}$ is the computed value and $\underline{\omega}^{vo}$ is obtained from $\hat{S}^{po}\hat{S}^{po}$. Then the difference between the measured and the computed is essentially the gyro drift rate

$$\omega^{pI} - \hat{\omega}^{pI} = \underline{\varepsilon} \qquad (3.18)$$

If $\underline{\varepsilon}$ can be taken to be zero between the two times then Eq. (3.1) yields

$$\dot{\underline{\phi}} + (\hat{S}^{po}\underline{\omega}_o) \times \underline{\phi} = 0 \qquad (3.19)$$

Furthermore, if $\dot{S}^{po} S^{po}$ is very small then S^{po} is nearly constant. The solution to this equation at any attitude S^{po} and relative to circular orbits is

$$\underline{\phi}(t) = \left[\cos\omega_o t \; I - \frac{\tilde{\underline{\omega}}^{pI}}{\omega_o}\sin\omega_o t + \frac{\underline{\omega}^{pI}(\underline{\omega}^{pI})^T}{\omega_o^2}(1-\cos\omega_o t)\right]\underline{\phi}_o \qquad (3.20)$$

where

$$\underline{\omega}^{pI} = S^{po}\underline{\omega}_o$$

This equation can be used to represent the attitude deviation at one epoch in terms of another.

3.3.2 Error Analysis

In the mechanization involving integration, the errors are dependent on initial errors and drift rates. These errors oscillate with orbital period in the roll and yaw channels, while the pitch channel increases with time from constant drift rate errors. A constant error in orbital torquing rate causes the pitch indication error to increase with time.

Typically initial conditions errors in the level channels would be set by the horizon sensor error. Therefore, a 1 mil level error corresponds to level attitude errors with 1 mil amplitude. A .01°/hr rate error corresponds to a .042 mil roll and yaw error while the pitch error increases as .01°/hr (t hrs). These are the open loop errors. A closed loop response with attitude control feedback would, however, bound the pitch axis error build-up. This problem will receive consideration in a following section.

4. General Theory of Computational Strapdown Gyrocompass Alinement

4.1 General

This section is concerned primarily with the problem of computation of gyrocompass alinement of strapdown systems. As noted in the earlier sections of this study, the gyrocompass alinement problem for strapdown system is essentially a problem of initializing the direction cosine matrix of the vehicles frame relative to the orbital frame in the presence of extraneous vehicle angular motions.

Basic mechanization equations associated with the one-point and the two-point schemes which were briefly described in Section 2.1 are more fully described in the present section.

4.2 Attitude Determination Equations

4.2.1 Direction Cosine Equations

The direction cosine matrix of the platform or vehicle frame relative to inertial space is given by

$$S^{pI} = S^{vI} = S^{vo} S^{oI} \qquad (4.1)$$

where $S^{vo} = S^{po}$ is the transformation matrix (Euler angles) between the vehicle and orbital frame, and S^{oI} is the transformation between orbital and inertial. The system output measures the total inertial angular velocity of the vehicle frame

$$\begin{aligned}\tilde{\omega}^{vI} &= -\dot{S}^{vI} S^{vI} = -\dot{S}^{vo} S^{ov} - S^{vo} \dot{S}^{oI} S^{oI} S^{ov} \\ &= \tilde{\omega}^{vo} + S^{vo} \tilde{\omega}_o S^{ov}\end{aligned} \tag{4.2}$$

Solving for S^{vo} from Eq. (4.2) the following differential equation is obtained.

$$\dot{S}^{vo} = -\tilde{\omega}^{vI} S^{ov} + S^{vo} \tilde{\omega}_o \tag{4.3}$$

In this equation $\tilde{\omega}^{vI}$ represents the three components of the total vehicle angular rate with respect to inertial space available as outputs of the gyro package, and $\tilde{\omega}_o$ is the orbital rate of the vehicle center-of-mass which is computed on the basis of the orbital parameters (navigation data).

The integral of Eq. (4.3) can be written as

$$S^{vo} = S^{vo}(t_o) + \int_{t_o}^{t} (-\tilde{\omega}^{vI} S^{ov} + S^{vo} \tilde{\omega}_o) d\tau$$

Thus, if $S^{vo}(t_o)$, the initial condition matrix, can be specified at t_o, the attitude matrix S^{po} can be updated for any arbitrary vehicle motion.

The initialization of the matrix S^{po} constitutes the in-orbit gyrocompass problem. The objective is to determine the orientation of the platform or vehicle frame relative to specifically the orbital frame by processing measurable data (e.g., such as angular rates via the gyros, and direction to the vertical via the horizon sensor).

4.2.2 Attitude Error Propagation Equation (The Gyrocompass Equation)

From Eq. (4.3) the attitude error propagation equation can be developed. Let $\hat{S}^{vo}$ represent the computed estimate of the vehicle frame attitude matrix. The actual vehicle frame matrix is given by

$$S^{vo} = \hat{S}^{vo} + \Delta S^{vo}$$

where ΔS^{vo} is computed error matrix which is to be determined.

The actual direction cosine equation which characterizes the rate of change of S^{po} is

$$\dot{\hat{S}}^{vo} + \Delta \dot{S}^{vo} = -(\tilde{\omega}^{vI} + \Delta\tilde{\omega})(\hat{S}^{ov} + \Delta S^{ov}) + (\hat{S}^{vo} + \Delta S^{vo})\,\tilde{\omega}_o$$

where $\Delta\tilde{\omega}$ is the drift rate matrix. The computed direction cosine equation is governed by

$$\dot{\hat{S}}^{vo} = -\tilde{\omega}^{vI}\,\hat{S}^{ov} + \hat{S}^{vo}\,\tilde{\omega}_o$$

Subtracting the two equations (to the first order)

$$\Delta\dot{S}^{vo} = -\tilde{\omega}^{vI}\,\Delta S^{ov} + \Delta S^{vo}\,\tilde{\omega}_o - \Delta\tilde{\omega}\,\hat{S}^{ov} \qquad (4.4)$$

This is the direction cosine error propagation equation. A vector representation can be given to this equation which is more convenient.

Suppose the only error in the system is the deviation in the specification of the attitude matrix. Denote this deviation by ΔS^{po}. Then, assuming small angular errors (such as for example the errors in the angles of the canonical Euler rotation matrix), the attitude error of the platform or vehicle frame can be given as a vector which is represented as an anti-symmetric matrix

$$\tilde{\phi} = -\Delta S^{po}\, S^{op} = \begin{bmatrix} 0 & -\phi_z & \phi_y \\ \phi_z & 0 & -\phi_x \\ -\phi_y & \phi_x & 0 \end{bmatrix} \qquad (4.5)$$

This representation is always possible for expressing the attitude deviation of an orthogonal tried.

If

$$\tilde{\phi} = -\Delta S^{vo} S^{ov}$$

then

$$\begin{aligned}\dot{\tilde{\phi}} &= -\Delta\dot{S}^{vo} S^{ov} - \Delta S^{vo} \dot{S}^{ov} \\ &= -\Delta\dot{S}^{vo} S^{ov} - \Delta S^{vo} S^{ov} S^{vo} \dot{S}^{ov} \\ &= -\Delta\dot{S}^{vo} S^{ov} + \tilde{\phi}\, \tilde{\omega}^{vo} \qquad (4.6)\end{aligned}$$

Substituting into Eq. (4.4) and post multiplying by S^{vo}, there results the following equation

$$\dot{\tilde{\phi}} - \tilde{\omega}^{pI} \tilde{\phi} + \tilde{\phi}\, \tilde{\omega}^{pI} = S^{po} \Delta\tilde{\omega}\, S^{op} \qquad (4.7)$$

or in vector form

$$\dot{\underline{\phi}} + \underline{\omega}^{pI} \times \underline{\phi} = S^{po}\, \Delta\underline{\omega} = \underline{\epsilon} \qquad (4.8)$$

This equation is identical to the one used as a basis for gyrocompass alinement of a gimballed platform.

Note, however, that if the computed rate ignores the effect of the vehicle rate ω^{vo}, a considerably simpler equation results. On the basis of the estimated S^{po} the rate computed in the vehicle frame is

$$\tilde{\omega}^{vI} = S^{vo}\, \tilde{\omega}_o\, S^{ov} \qquad (4.9)$$

This equation ignores the effect of vehicle motion $\tilde{\omega}^{vo} = \dot{S}^{vo} S^{ov}$ and the neglect of this term is justified only if ω^{vo} can be held to small values. Otherwise the computed value must include this term.

The inclusion of this term is achieved at the expense of more computation. Therefore, if the vehicle rates can be stabilized to low values, it is desirable to neglect this term in the computation. The attitude error equation corresponding to Eq. (4.9) becomes

$$\Delta\underline{\omega}^{vI} - \underline{\omega}^{vo} = \dot{\underline{\phi}} + (S^{vo}\, \underline{\omega}_o) \times \underline{\phi} \qquad (4.10)$$

where $\underline{\omega}^{vo}$ is the effect of the vehicle rates. Comparing this equation with Eq. (4.9), it is seen that the latter case is limited by gyro drift and the former is limited by vehicle rates.

In the general case, the residual vehicle rates are by far the larger; therefore, if drift rates do limit the accuracy of gyrocompass alinement (e.g., as against the horizon sensor errors) then the more complex form is required to be computed. On the other hand, if horizon sensor errors are larger than the unstablized vehicle rates, then the simpler formulation would be more desirable.

4.2.3 Horizon Error Equation

To show how the horizon sensor output is used in the alinement problem. Let $\underline{1}_H$ represent the unit vector of the local vertical as represented in the vehicle frame. The true local vertical is given by the radial unit vector $\underline{1}_z$ of the orbital triad. Then

$$\underline{1}_H = S^{po}\,\underline{1}_z = S^{po}\begin{bmatrix} 0 \\ 0 \\ 1 \end{bmatrix}$$

In the presence of an error ΔS^{po}

$$\begin{aligned} \underline{1}_H + \Delta\underline{1}_H &= (S^{po} + \Delta S^{po})\underline{1}_z \\ &= (I + \Delta S^{po}\, S^{op})S^{po}\,\underline{1}_z \end{aligned}$$

From which it follows that

$$\Delta\underline{1}_H = -\tilde{\phi}\, S^{po}\begin{bmatrix} 0 \\ 0 \\ 1 \end{bmatrix} = -\underline{\phi} \times (S^{po}\,\underline{1}_z) \tag{4.11}$$

This equation gives the relationship of the vehicle frame attitude error to the deviation of the vertical as observed in the vehicle frame. Although the equation is given as a set of three equations (the components of the vector), there are only two equations which are independent. These correspond to the two observables which are the residuals of the observed tilt in the vertical arising from the error S^{po}. That is, the residuals which are observable from the line-of-sight to the vertical are perpendicular to the line-of-sight (e.g., the pitch and roll error of the vertical). An error about the line-of-sight is unobservable and, therefore, the corresponding equation is unusable.

4.3 Mechanisation Schemes

4.3.1 Basic Equations

To summarize, the basic equations associated with gyrocompass alinement of a strapdown system are

$$\Delta \underline{\omega} = +\dot{\underline{\phi}} + (S^{vo} \underline{\omega}_o) \times \underline{\phi} \qquad (4.12)$$

$$\Delta \underline{1}_H = -\underline{\phi} \times S^{vo} \underline{1}_z \qquad (4.13)$$

Equation (4.12) gives the measurable angular rate error due to alinement error of the direction cosine matrix, and Eq. (4.13) gives the observed verticality error in terms of the same direction cosine matrix error. These two equations represent a set of five equations in six unknowns $(\dot{\underline{\phi}}, \underline{\phi})$. Three of the equations are associated with the outputs of the gyro package, and two of these equations are associated with the measured deviations of the local vertical.

If the set (4.12) and (4.13) can be inverted, the gyrocompass alinement mechanization would be a relatively simple problem for strapdown systems in any attitude. The gyro outputs and the horizon sensor deviations are monitored continuously providing measures of $\underline{\phi}$ and $\dot{\underline{\phi}}$ which in turn are used to correct S^{po}. The fact that six parameters need to be determined, whereas only five equations are available, presents the essential difficulty of the orbital gyrocompass alinement problem and forces certain simplifying configurations.

It is easy to demonstrate why the set (4.12) and (4.13) is insoluble for a general one-point attitude configuration. Assuming that $\underline{\omega}^{vo}$ is known as a function of time, Eq. (4.12) can be integrated to yield the following functional solution

$$\underline{\phi} = \underline{\phi}_o + \int (\Delta\underline{\omega} - S^{vo}\,\underline{\omega}_v \times \underline{\phi})d\tau$$

Here, $\bar{\phi}_o$, the initial deviation, is unknown and is composed of three parameters; ϕ_{xo}, ϕ_{yo}, and ϕ_{zo}. Substituting the solution into Eq. (4.13), results in two equations in the unknowns ϕ_{xo}, ϕ_{yo}, and ϕ_{zo}. Thus, in a general configuration the set (4.12) and (4.13) is insoluble.

4.3.2 Continuous Computational Self-Alinement Gyrocompass Techniques

As noted by Eq. (4.12) and (4.13), the basic equations governing the gyrocompass alinement of strapdown systems is completely equivalent to the gimballed platform (Ref. 1). It is appropriate to consider here the possibilities of implementing the same feedback mechanization schemes considered in Ref. 1 for strapdown systems.

For a comparative discussion consider the corresponding Eqs. (4.12) and (4.13) for the gimballed local level platform. In this case $S^{po} = I$ and gimbal isolation eliminates the effect of the vehicle motion. The basic equations are re-written

$$\underline{T} + \Delta\underline{\omega} = \dot{\underline{\phi}} + \underline{\omega}_o \times \underline{\phi} \tag{4.14}$$

$$\Delta\underline{1}_H = -\underline{\phi} \times \underline{1}_z \tag{4.15}$$

where $\underline{T}$ has been added to denote the control torques. This set is still insoluble for the open loop problem because there are six parameters to be determined ($\dot{\underline{\phi}}$ and $\underline{\phi}$) and only five independent equations.

Equations (4.14) and (4.15) are solved for the gimballed system by forcing self-alinement of the system; thereby damping out the initial errors $\bar{\phi}_o$. The techniques by which, in effect, the solution (4.14) and (4.15) is damped is to drive the gyros with a signal proportional to the horizon sensor deviation $\underline{\Delta 1_H}$. This effected damping of the system response, and the steady state solution was such that the deviation ϕ could be bounded automatically to tolerable levels, and at the same time damp out the initial errors ϕ_0 (which, in effect, reduces the order of the system).

The natural question to ask is whether the same technique can be implemented for strapdown systems. Returning to Eq. (4.12) and Eq. (4.13), it is seen that the basic equations associated with the gyrocompass problem are completely equivalent to that for the gimballed system, Eq. (4.14) and (4.15). Indeed damping out of the error ϕ is conceivable by the application of the same technique of driving the system with horizon sensor derived error signals.

Heuristically, one might conceive of a continuous self-alinement mechanization for strapdown systems which "computationally" gyrocompass alines the attitude matrix in just the same way in which a gimballed platform is "physically" gyrocompassed. If, indeed, this were possible then the analysis given for local level platforms (Ref. 1) is directly applicable to the strapdown systems. Furthermore, the error sources which limit the accuracy are essentially the same for both cases.

The difference between these two mechanizations is that in the gimballed case the platform is being torqued physically to alinement. The present scheme for strapdown systems would perform the equivalent function in the computer and in such a way as to cause the computed ϕ to damp to null by the application of feedback signals based on the horizon sensor errors. In the gimballed case, a dynamical system is involved and the notion of damping has meaning. In the computational case damping has meaning only in the mathematical sense. Yet, in both cases, the end result should be the same; that of driving the error vector ϕ to null or to bounded tolerable values. Stated in still another way, computational gyrocompassing is analogous to an on-board computer simulation, in real time, of the gimballed platform system. The simulation of the gimballed system is, itself, the mechanization model relative to which the strapdown gyrocompass alinement is secured. Closed loop operation takes place by augmenting the tilt equation with a simulated feedback model which in the gimballed case is simply the feedback control torques to the gyros.

4.3.3 One-Point Mechanization Schemes for Initial Attitude Determination

The present section considers mechanization techniques for initial attitude determination utilizing the one-point scheme. In general, this scheme would be utilized to quick gyrocompass the system without processing too many observables. The fact that residual vehicle stabilization rate coupling limits the accuracy of alinement would appear to preclude its application for high precision alinement. On the other hand, if the vehicle can be stabilized to low level rates, simple smoothing techniques can result in simple mechanizations which are also reasonably precise. A more sophisticated approach achieved at the expense of more computation is to compute the vehicle rate from the direction cosine equations and subtract the extraneous rates out so that a true measure of the orbital rate can be obtained relative to the vehicle frame.

The close similarity of the one-point orbital gyrocompass scheme to the fixed site gyrocompass problem is clearly evident. In the fixed site case the gravity vector and the true north were the two basic vectors used for alinement. In the present case "gravity" is replaced by the "vertical" and "true north" by the "orbital pole". In the fixed site case swaying motion of the vehicle is a primary error source to the alinement accuracy. In the orbital case the unstabilized vehicle angular rate about its center-of-mass is the limiting error source.

As noted earlier, to update the attitude matrix S^{po} or S^{vo} as a function of time, it is necessary to initialize this matrix at an arbitrarily chosen epoch. With the initial matrix S^{po} (t_0) specified the direction cosine equations are integrated using the rate output of the gyros. Figure 9 shows a general block diagram in a way in which the vehicle or platform frame attitude will be updated relative to the orbital frame. For ESG strapdown systems, attitude update is not required, since the attitude is directly available by way of the information obtained from the pickoffs; however, angular rate must be computed for gyrocompass alinement.

The initialization of the matrix S^{po} constitutes the gyrocompass problem for strapdown systems. If the vehicle frame is to remain earth pointing (local level attitude), the updating S^{po} is a relatively simple problem of measuring rate outputs from the gyros to determine yaw, and is independent of the initial determination of S^{po}.

For an arbitrary vehicle attitude, the gyrocompass alinement problem is somewhat more complicated. The vertical must first be established relative to the vehicle frame, and the vehicle frame must be stablized relative to this vertical (i.e., the orbital frame). This is the only way in which the two basic measurables (the local vertical, and the direction of the orbital rate) can be obtained for referencing to the orbital frame. The following is a discussion on the initialization of S^{po} for an arbitrary vehicle attitude (i.e., not necessarily local level oriented). The one point mode (gyrocompass mode Fig. 2) is considered initially.

Let $\underline{L}_1$ represent a unit vector in the direction of the total vehicle orbital rate vector. Then

$$\underline{L}_1 = \frac{\underline{\omega}_y}{|\omega_y|} = L_{1x}\,\underline{1}_x + L_{1y}\,\underline{1}_y + L_{1z}\,\underline{1}_z$$

$$= L^P_{1x}\,\underline{1}_{px} + L^P_{1y}\,\underline{1}_{py} + L^P_{1z}\,\underline{1}_{pz} \qquad (4.16)$$

where L_{1x}, L_{1y}, L_{1z} are the components of $\underline{L}_1$ in the orbital frame which are known based upon the vehicle orbital parameters; and L^P_{1x}, L^P_{1y}, L^P_{1z} are the components as measured on the vehicle or platform frame by the gyros (assume vehicle is local level stabilized so that vehicle attitude rate relative to orbital frame is zero).

In a similar way let $\underline{L}_2$ represent a unit vector in the direction of the local level. One can write the components of $\underline{L}_2$ in the orbital and the vehicle frame

$$\underline{L}_2 = L_{2x}\,\underline{1}_x + \underline{L}_{2y}\,\underline{1}_y + \underline{L}_{2z}\,\underline{1}_z$$

$$= L^P_{2x}\,\underline{1}_{px} + \underline{L}^P_{2y}\,\underline{1}_{py} + \underline{L}^P_{2z}\,\underline{1}_{pz} \qquad (4.17)$$

Here again the components in the orbital frame are known on the basis of the orbital parameters, and the components in the platform frame are measured.

Both equations for $\underline{L}_1$ and $\underline{L}_2$ of course assume that the vehicle is stabilized relative to the orbital frame. That is to say, there is no angular rate about the center-of-mass relative to the local vertical. In Eq. (4.16) the components of $\underline{L}_1$ in the orbital frame are nominally $L_{1x} = L_{1z} = 0$, and $L_{1y} = 1$; and for $\underline{L}_2$, $L_{2x} = L_{2y} = 0$, $L_{2z} = 1$. Thus, in the absence of errors $\underline{L}_1$ and $\underline{L}_2$ are expressed in the vehicle frame as

$$\underline{L}_1 = \begin{bmatrix} L^p_{1x} \\ L^p_{1y} \\ L^p_{1z} \end{bmatrix} = S^{po} \begin{bmatrix} 0 \\ 1 \\ 0 \end{bmatrix} \qquad (4.18)$$

$$\underline{L}_2 = \begin{bmatrix} L^p_{2x} \\ L_{2y} \\ L_{2z} \end{bmatrix} = S^{po} \begin{bmatrix} 0 \\ 0 \\ 1 \end{bmatrix} \qquad (4.19)$$

As shown here $\underline{L}_1$ and $\underline{L}_2$ are orthogonal. The general case will assume $\underline{L}_1$ and $\underline{L}_2$ to be non-orthogonal (so that the effect of errors in the nominal can be included later). The non-orthogonal case can arise when the measurables are other than local level and orbital rate. The more general transformations for $\underline{L}_1$ and $\underline{L}_2$ are therefore given as

$$\underline{L}_1 = \begin{bmatrix} L^p_{1x} \\ L^p_{1y} \\ L^p_{1z} \end{bmatrix} = S^{po} \begin{bmatrix} L_{1x} \\ L_{1y} \\ L_{1z} \end{bmatrix} \qquad (4.20)$$

$$\underline{L}_2 = \begin{bmatrix} L^p_{2x} \\ L^p_{2y} \\ L^p_{2z} \end{bmatrix} = S^{po} \begin{bmatrix} L_{2x} \\ L_{2y} \\ L_{2z} \end{bmatrix} \qquad (4.21)$$

The problem is to determine the direction cosine matrix S^{po} from these two equations. To facilitate this computation the vectors $\underline{L}_1$, $\underline{L}_2$, and $\underline{L}_1 \times \underline{L}_2$ which span the three-dimensional vector space of the platform triad are orthogonalized using Schmidt's orthogonalization process. It is easy to show that the set

$$\underline{L}_1, \quad \frac{\underline{L}_1 \times \underline{L}_2}{|\underline{L}_1 \times \underline{L}_2|}, \text{ and } \frac{\underline{L}_1 \times (\underline{L}_1 \times \underline{L}_2)}{|\underline{L}_1 \times \underline{L}_2|} \tag{4.22}$$

represent a mutually orthogonal set of unit vectors. One can, therefore, write the following matrix equation

$$\left[\underline{L}_1^P \;\vdots\; \frac{\underline{L}_1^P \times \underline{L}_2^P}{|\underline{L}_1^P \times \underline{L}_2^P|} \;\vdots\; \frac{\underline{L}_1^P \times (\underline{L}_1^P \times \underline{L}_2^P)}{|\underline{L}_1^P \times \underline{L}_2^P|} \right] = S^{po} \left[\underline{L}_1 \;\vdots\; \frac{\underline{L}_1 \times \underline{L}_2}{|\underline{L}_1 \times \underline{L}_2|} \;\vdots\; \frac{\underline{L}_1 \times (\underline{L}_1 \times \underline{L}_2)}{|\underline{L}_1 \times \underline{L}_2|} \right] \tag{4.23}$$

Each of these matrices are orthonormal, therefore, inverting by transposing one can solve for S^{po}

$$S^{po} = \left[\underline{L}_1^P \;\vdots\; \frac{\underline{L}_1^P \times \underline{L}_2^P}{|\underline{L}_1^P \times \underline{L}_2^P|} \;\vdots\; \frac{\underline{L}_1^P \times (\underline{L}_1^P \times \underline{L}_2^P)}{|\underline{L}_1^P \times \underline{L}_2^P|} \right] \left[\underline{L}_1 \;\vdots\; \frac{\underline{L}_1 \times \underline{L}_2}{|\underline{L}_1 \times \underline{L}_2|} \;\vdots\; \frac{\underline{L}_1 \times (\underline{L}_1 \times \underline{L}_2)}{|\underline{L}_1 \times \underline{L}_2|} \right]^T \tag{4.24}$$

As a check, if the platform frame is perfectly alined to the orbital frame $S^{po} = I$, then it is desired to show the equivalence

$$\underline{L}_1 \underline{L}_1^T + \frac{(\underline{L}_1 \times \underline{L}_2)(\underline{L}_1 \times \underline{L}_2)^T}{(\underline{L}_1 \times \underline{L}_2) \cdot (\underline{L}_1 \times \underline{L}_2)} + \frac{(\underline{L}_1 \times (\underline{L}_1 \times \underline{L}_2)(\underline{L}_1 \times (\underline{L}_1 \times \underline{L}_2))^T}{(\underline{L}_1 \times \underline{L}_2) \cdot (\underline{L}_1 \times \underline{L}_2)} = I \tag{4.25}$$

First it can be shown that

$$L_1 x (L_1 x L_2) = (\underline{L}_1 \cdot \underline{L}_2)\underline{L}_1 - \underline{L}_2$$

and

$$(\underline{L}_1 x(\underline{L}_1 x \underline{L}_2))(\underline{L}_1 x(\underline{L}_1 x \underline{L}_2))^T = (\underline{L}_1 \cdot \underline{L}_2)^2(\underline{L}_1\underline{L}_1^T) - (\underline{L}_1 \cdot \underline{L}_2)(\underline{L}_1\underline{L}_2^T)$$

$$- (\underline{L}_1 \cdot \underline{L}_2)\,(\underline{L}_2\underline{L}_1^T) + (\underline{L}_2\underline{L}_2^T)$$

Next it can be shown that

$$(\underline{L}_1 x \underline{L}_2)(\underline{L}_1 x \underline{L}_2)^T = (1 - (\underline{L}_1 \cdot \underline{L}_2)^2)\; I - (\underline{L}_1\underline{L}_1^T) - (\underline{L}_2\underline{L}_2^T)$$

$$+ (\underline{L}_1 \cdot \underline{L}_2)(\underline{L}_1\underline{L}_2^T) + (\underline{L}_1 \cdot \underline{L}_2)(\underline{L}_2\underline{L}_1^T)$$

Substituting into Eq. (4.25), the equivalence can be established.

Equation (4.24) can be used as a basis for the initialization mechanization. First note that the magnitude of the cross product $\underline{L}_1 x \underline{L}_2$ computed in the vehicle frame is equal to that computed in the orbital frame (provided there are no errors in measurement and no relative angular motion of vehicles relative to the vertical)

$$\left|\underline{L}_1^P \; x \; \underline{L}_2^P\right| = \left|\underline{L}_1 \; x \; \underline{L}_2\right| = \sin(\text{angle } \underline{L}_1,\ \underline{L}_2) \qquad (4.26)$$

Introducing this condition into Eq. (4.24) S^{PO} can be written as

$$S^{PO} = [L_1^P \;\vdots\; \underline{L}_1^P x \underline{L}_2^P \;\vdots\; \underline{L}_1^P x(\underline{L}_1^P x \underline{L}_2^P)][\underline{L}_1 \;\vdots\; \frac{\underline{L}_1 x \underline{L}_2}{(\underline{L}_1 x \underline{L}_2)(\underline{L}_1 x \underline{L}_2)} \;\vdots\; \frac{\underline{L}_1 x(\underline{L}_1 x \underline{L}_2)}{(\underline{L}_1 x \underline{L}_2)\cdot(\underline{L}_1 x \underline{L}_2)}]^T$$

(4.27)

To compute S^{pe}, the components of $\underline{L}_1^p$ are obtained by normalizing the gyro rate outputs; the components of L_2^p are obtained as the direction cosines of the vertical as defined by the horizon sensor relative to the vehicle frame, and the first matrix is formed. The second matrix is known beforehand representing the orbital frame relative to which the vehicle frame attitude is to be measured.

If the basic measurables are the directions of the true local vertical and the true orbital rate, then Eq. (4.18) and (4.19) can be substituted for $\underline{L}_1$ and $\underline{L}_2$. Then

$$|\underline{L}_1 \times \underline{L}_2| = 1$$

and Eq. (4.27) can be expanded in terms of its elements (using the components of (4.18) and (4.19).

$$\begin{bmatrix} S_{11} & S_{12} & S_{13} \\ S_{21} & S_{22} & S_{23} \\ S_{31} & S_{32} & S_{33} \end{bmatrix} = \begin{bmatrix} a_x & b_x & c_x \\ a_y & b_y & c_y \\ a_z & b_z & c_z \end{bmatrix} \begin{bmatrix} 0 & 1 & 0 \\ 1 & 0 & 0 \\ 0 & 0 & 1 \end{bmatrix} \qquad (4.28)$$

Expanding this equation

$$\begin{matrix} S_{11} = b_x & S_{12} = a_x & S_{13} = c_x \\ S_{21} = b_y & S_{22} = a_y & S_{32} = c_y \\ S_{31} = b_z & S_{32} = a_z & S_{33} = c_z \end{matrix} \qquad (4.29)$$

where

$$\underline{a} = \underline{L}_1^p = \frac{\underline{\omega}}{\omega}$$

$$\underline{b} = \underline{L}_1^P \times \underline{L}_2^P$$

$$\underline{c} = \underline{L}_1^P \times (\underline{L}_1^P \times \underline{L}_2^P) = \frac{\underline{\omega}}{\omega} \times \left(\frac{\underline{\omega}}{\omega} \times \underline{1}_H\right) \tag{4.30}$$

and $\underline{1}_H$ is the vertical as observed in the platform (vehicle) frame. Equation (4.29) is the basic algorithm to use in determining S^{PO} with the elements of $\underline{a}$, $\underline{b}$, and $\underline{c}$ computed via Eq. (4.30).

4.3.4 An Alternate Scheme

The representation as shown by Eq. (4.24) is based on orthogonalizing $\underline{L}_1$, $\underline{L}_2$ and $\underline{L}_1 \times \underline{L}_2$. This leads to the requirement for computing $\underline{L}_1^P \times (\underline{L}_1^P \times \underline{L}_2^P) = (\underline{L}_1 \cdot \underline{L}_2)\underline{L}_1^P - \underline{L}_2^P$. Which is really superfluous as the following development shows. Equation (4.25) can be written as

$$[\underline{L}_1^P \;\vdots\; \underline{L}_2^P \;\vdots\; \underline{L}_1^P \times \underline{L}_2^P] = S^{PO}\,[\underline{L}_1 \;\vdots\; \underline{L}_2 \;\vdots\; \underline{L}_1 \times \underline{L}_2] \tag{4.31}$$

The matrix on the right side will always have an inverse provided $\underline{L}_1$ and $\underline{L}_2$ are not collinear. Solving for S^{PO} there results .

$$S^{PO} = [L_1^P \;\vdots\; L_2^P \;\vdots\; L_1^P \times L_2^P][L_1 \;\vdots\; L_2 \;\vdots\; L_1 \times L_2]^{-1} \tag{4.32}$$

Since the matrix is not orthonormal, the inverse operation must be used. This inverse matrix, however, is known via the reference parameters and can, therefore, be pre-computed. Again, for the particular case where $\underline{L}_1$ = orbital rate direction, $\underline{L}_2$ = local vertical direction

$$[\underline{L}_1 \;\vdots\; \underline{L}_2 \;\vdots\; \underline{L}_1 \times \underline{L}_2]^{-1} = \begin{bmatrix} 0 & 1 & 0 \\ 0 & 0 & 1 \\ 1 & 0 & 0 \end{bmatrix} \tag{4.33}$$

Substituting Eq. (4.33) into (4.32), the elements can be represented as

$$\begin{aligned} S_{11} &= b_x & S_{12} &= a_x & S_{13} &= c_x \\ S_{21} &= b_y & S_{22} &= a_y & S_{23} &= c_y \\ S_{31} &= b_z & S_{32} &= a_z & S_{33} &= c_z \end{aligned} \tag{4.34}$$

where

$$\begin{aligned} \bar{a} &= \underline{L}_1^p \\ \underline{b} &= \underline{L}_1^p x \underline{L}_2^p \\ \underline{c} &= \underline{L}_2^p \end{aligned} \tag{4.35}$$

The inverse can be given for the more general case. Let L_1, L_2 be represented in an arbitrary frame $\underline{I}$, $\underline{J}$, $\underline{K}$. Then it is easy to show that

$$[\underline{L}_1 \vdots \underline{L}_2 \vdots \underline{L}_1 x \underline{L}_2]^{-1} = \left[\frac{\underline{L}_2 x(\underline{L}_1 x \underline{L}_2)}{(\underline{L}_1 x \underline{L}_2)\cdot(\underline{L}_1 x \underline{L}_2)} \vdots \frac{-\underline{L}_1(\underline{L}_1 x \underline{L}_2)}{(\underline{L}_1 x \underline{L}_2)\cdot(\underline{L}_1 x \underline{L}_2)} \vdots \frac{\underline{L}_1 x \underline{L}_2}{(\underline{L}_1 x \underline{L}_2)\cdot(\underline{L}_1 x \underline{L}_2)} \right] \tag{4.36}$$

Comparing Eq. (4.32) with Eq. (4.24), it is seen that the former is simpler in that only $\underline{L}_2^p$ is used in place of $\underline{L}_1^p x(\underline{L}_1^p x \underline{L}_2^p)$. The inverse matrix can also be analytically represented in terms of its direction cosine.

4.3.5 Alinement Relative to Arbitrary Frames of Reference

It should be recognized that Eq. (4.27) is a general alinement equation. If it is desired to aline relative to another frame of reference, then the components of $\underline{L}_1$ and $\underline{L}_2$ are determined relative to this frame, and the computation implied by Eq. (4.27) is performed. For example, to determine the matrix S^{pI} of the vehicle relative to the inertial frame, the direction cosines of $\underline{L}_1$ and $\underline{L}_2$ (directions of orbital rate and local vertical) are expressed in the celestial frame, with $\underline{L}_1^*$ and $\underline{L}_2^*$ determined in the same way relative to the vehicle frame, and S^{pI} is determined from an equation similar to 19. For this particular case note that $\underline{L}_1$ and $\underline{L}_2$ must be updated with the orbital motion. Relative to the orbital frame, the only components needed to be updated are $\underline{L}_1^*$ and $\underline{L}_2^*$ which are nearly constant for low vehicle angular motion.

4.3.6 Two-Point Gyrocompass Mode

One special case of gyrocompass alinement of a strapdown system follows from Eq. (4.27). Suppose that a vehicle stationary relative to inertial space is required to be gyrocompass alined. The gyros would hold the vehicle essentially fixed with respect to inertial space. The direction to the local inertial will be measured relative to the body frame for two different epochs (corresponding to $\underline{L}_1^p$ and $\underline{L}_2^p$). Then

$$\underline{L}_1^p = S^{pI}\,\underline{L}_1$$

$$\underline{L}_2^p = S^{pI}\,\underline{L}_2$$

$$\underline{L}_1 = S_1^{Ie}\,\underline{L}_1^*$$

$$\underline{L}_2 = S_2^{Io}\,\underline{L}_2^*$$

$$L_1^* = \begin{bmatrix} 0 \\ 0 \\ 1 \end{bmatrix} = \text{vertical at epoch 1}$$

$$\underline{L}_2^* = \begin{bmatrix} 0 \\ 0 \\ 1 \end{bmatrix} = \text{vertical at epoch 2}$$

Knowing the orbital parameters and the time the elements of S_1^{Io} and S_2^{Io} can be computed. The matrix S^{pI} of the platform relative to a celestial reference frame can be obtained using an equation similar to Eq. (4.19). In this scheme the gyros are used only to hold the vehicle fixed in inertial space, and the only external measurable used are the direction cosines of the vertical as measured at two different times. The direction of the orbital rate is implied by the time difference and the orbital parameters.

The foregoing scheme can be sensitive to noise errors. The angle between $\underline{L}_1$ and $\underline{L}_2$ is necessarily limited to small values because of the requirement to initialize S^{po} in real time. Consequently, errors in $\underline{L}_1$ and $\underline{L}_2$ are amplified by the reciprocal of $(\underline{L}_1 \times \underline{L}_2 \cdot \underline{L}_1 \times \underline{L}_2) = \sin^2\theta$ where θ is the angle between $\underline{L}_1$ and $\underline{L}_2$. For example, a 10° separation between the measurement of the two verticals imply a thirty to one amplification of noise errors in the determination of attitude. Going to larger separation angles defeats the purpose of gyrocompass alinement. In the first case where $\underline{L}_1$ and $\underline{L}_2$ correspond to orbital rate and local vertical directions the angle between them is 90° so that there is essentially no error amplification; however, a 90° separation implies approximately a 20 minute delay in the determination (for low earth vehicles) of the attitude.

This scheme has value to the extent that a gyro package is not required. The only requirement is that the vehicle can be held stationary relative to the orbital frame.

4.3.7 Updating the Attitude Matrix

Having determined S^{po} or S^{vo} in the foregoing way for a given instant of time, S^{po} can be updated by processing the angular rate information obtained from the gyros and integrating equation (4.3). The important point to recognize is that the initial matrix can only be determined in the absence of all angular motion of the vehicle relative to the local level.

If the components of $\underline{a}$, $\underline{b}$ and $\underline{c}$ were available in the vehicle frame in real time, then Eq. (4.32) is a basis for real time determination of S^{po}. This would not require the integration of the direction cosine equation, Eq. (4.3). The only requirement would be that the vehicle angular motion be sufficiently low so that the error in $\underline{a}$ and $\underline{c}$ will be tolerable.

In the presence of high vehicle angular rates, it would be difficult to compute $\underline{a}$ and $\underline{b}$ in real time. In this case, S_0^{po} is determined when the angular rates are low and the direction cosine equations are integrated with the initialized S_0^{po} determined by the gyrocompass alinement procedure described above.

In a general gyrocompass alinement problem, the vehicle angular motion must be included as error sources. The alinement must be accomplished in the presence of small residual vehicle rates such as the presence of the limit cycle oscillations resulting from the three axes vehicle attitude control loops.

For an arbitrary vehicle frame orientation, there is no way in which to separate the angular rates resulting from the motion of the center-of-mass in orbit from the motion of the vehicles about its center-of-mass. This difficulty has been discussed earlier and it is the primary reason for the requirement to stabilize the vehicle motion relative to the vertical.

4.4 Fine Alinement Schemes (Closed Loop Modes)

The alinement schemes discussed in the previous sections was based on the assumption that the vehicle angular rate about the local level axes were negligible. Actually small residual motions of the vehicle are present. These may be associated with the limit cycle oscillation resulting from the deadband of the attitude control system. In the presence of rotational motion, other than the orbital, the computation of the S^{po} via Eq. (4.16) will be subject to error because the $\underline{L}_1^p$ and $\underline{L}_2^p$ cannot be defined accurately relative to a rotating vehicle frame reference simultaneously at a specific instant of time. Furthermore, the vector $\underline{L}_1^p$ will include the effect of the undesired motion of the vehicle.

One scheme in which the system can be alined with higher precision is to average the angular rate output of the gyro package. This is best handled on the basis of linear equations. Figure 10 is an overall block diagram of this closed loop mode.

Suppose an estimate of $\hat{S}^{po}$ ($\wedge$ = estimate) is available from the alinement scheme as described by Eq. (4.16). Then transforming the measurables $\underline{L}_1^p$ and $\underline{L}_2^p$ back to the orbital frame with the estimated matrix

$$\begin{aligned} \hat{\underline{L}}_1 &= \hat{S}^{op} \underline{L}_1^p \\ \hat{\underline{L}}_2 &= \hat{S}^{op} \underline{L}_2^p \end{aligned} \qquad (4.38)$$

Compare $\underline{L}_1$ and $\underline{L}_2$ which are expressed in the orbital frame with the desired nominal $\underline{L}_1$ and $\underline{L}_2$. A difference in these vectors is ascribed to an error in the direction cosine matrix.

Let

$$S^{po} = \hat{S}^{po} - \Delta S^{po} \tag{4.39}$$

where $\hat{S}^{po}$ is the estimated (or computed) matrix, then

$$\begin{aligned} \hat{S}^{po} \underline{L}_1 &= \hat{\underline{L}}_1^p \\ \hat{S}^{po} \underline{L}_2 &= \hat{\underline{L}}_2^p \end{aligned} \tag{4.40}$$

and

$$S^{po} \underline{L}_1 - \hat{S}^{po} \underline{L}_1 = \Delta S^{po} \underline{L}_1 = \underline{L}_1^p - \hat{\underline{L}}_1^p = \Delta \underline{L}_1^p$$

similarly

$$\Delta S^{po} \underline{L}_2 = \Delta \underline{L}_2^p$$

where both $\Delta \underline{L}_1^p$ and $\Delta \underline{L}_2^p$ can be computed, then

$$\Delta S^{po} = [\Delta \underline{L}_1^p \,\vdots\, \Delta \underline{L}_2^p \,\vdots\, \Delta(\underline{L}_1^p x \underline{L}_2^p)] \, [\underline{L}_1 \,\vdots\, \underline{L}_2 \,\vdots\, \underline{L}_1 x \underline{L}_2] \tag{4.41}$$

This equation can be the basis for a continuous closed loop gyrocompass alinement mechanization. The components of the deviations $\Delta \underline{L}_1^p$ $\Delta \underline{L}_2^p$ are continuously measured; the elements of S^{po} are computed; the initial estimate of S^{po} is updated; and if the relative vehicle motion characteristics be sever, the direction cosine equations are integrated for a continuous attitude update with the new initial conditions.

To further detail the mechanization equations, consider again the case where $\underline{L}_1$ and $\underline{L}_2$ are respectively the directions to the orbital pole and local level; then Eq. (4.41) can be written as

$$\begin{bmatrix} S_{11} & S_{12} & S_{13} \\ S_{21} & S_{22} & S_{23} \\ S_{31} & S_{32} & S_{33} \end{bmatrix} = \begin{bmatrix} L^P_{1x} & L^P_{2x} & (\underline{L}^P_1 x \underline{L}^P_2)_x \\ L^P_{1y} & L^P_{2y} & (\underline{L}^P_1 x \underline{L}^P_2)_y \\ L^P_{1z} & L^P_{2z} & (\underline{L}^P_1 x \underline{L}^P_2)_z \end{bmatrix} \begin{bmatrix} 0 & 0 & 1 \\ 1 & 0 & 0 \\ 0 & 1 & 0 \end{bmatrix}$$

The components of $\Delta\underline{L}^P_1$ and $\Delta\underline{L}^P_2$ are obtained as follows. On the basis of the current estimate of $\hat{S}^{po}$ (denoted by ($\hat{}$)), $\hat{\underline{L}}^P_1$ and $\hat{\underline{L}}^P_2$ computed are

$$\underline{L}^P_1 = \hat{S}^{po} \begin{bmatrix} 0 \\ 1 \\ 0 \end{bmatrix} = \begin{bmatrix} \hat{S}_{12} \\ \hat{S}_{22} \\ \hat{S}_{23} \end{bmatrix}$$

$$\underline{L}^P_2 = \hat{S}^{po} \begin{bmatrix} 0 \\ 0 \\ 1 \end{bmatrix} = \begin{bmatrix} \hat{S}_{13} \\ \hat{S}_{23} \\ \hat{S}_{33} \end{bmatrix}$$

The measured values are correspondingly

$$\underline{L}_1^p = \frac{\omega^p}{|\omega|} = \begin{bmatrix} \frac{\omega_x^p}{|\omega|} \\ \\ \frac{\omega_y^p}{|\omega|} \\ \\ \frac{\omega_z^p}{|\omega|} \end{bmatrix} = \begin{bmatrix} \text{normalised x-gyro output} \\ \\ \text{normalised y-gyro output} \\ \\ \text{normalised z-gyro output} \end{bmatrix}$$

$$\underline{L}_2^p = \underline{l}_H = \begin{bmatrix} l_{Hx} \\ \\ l_{Hy} \\ \\ l_{Hz} \end{bmatrix} \quad \begin{bmatrix} \text{direction cosine horizon sensor} \\ \text{axis relative to x-body axis} \\ \\ \text{direction cosine horizon sensor} \\ \text{axis relative to y-body axis} \\ \\ \text{direction cosine horizon sensor} \\ \text{axis relative to z-body axis} \end{bmatrix}$$

Then,

$$\Delta\underline{L}_1^p = \underline{L}_1^p - \hat{\underline{L}}_1^p = \begin{bmatrix} \frac{\omega_x^p}{|\omega|} - \hat{S}_{12} \\ \\ \frac{\omega_y^p}{|\omega|} - \hat{S}_{22} \\ \\ \frac{\omega_z^p}{|\omega|} - \hat{S}_{33} \end{bmatrix}$$

$$\Delta \underline{L}_2^P = \underline{L}_2^P - \underline{L}_2^P = \begin{bmatrix} l_{Hx} - \hat{S}_{13} \\ l_{Hy} - \hat{S}_{23} \\ l_{Hz} - \hat{S}_{33} \end{bmatrix}$$

Provided these measures of $\Delta \underline{L}_1^P$ and $\Delta \underline{L}_2^P$ are true measures of the deviation in the transformation matrix S^{po} and are free of errors, the expressions for the elements of ΔS^{po} when added to the estimated value will yield the corrected matrix which is itself orthonormal. In general, the presence of errors in these two vectors will cause the corrected value to be non-orthonormal.

Note that the foregoing computations involve transformation to the vehicle frame. In practice, it may be more appropriate to compute in the orbital frame for ΔS^{op} rather than in the vehicle frame for ΔS^{po}.

4.4.1 Orthonormality Constraint

If the vehicle motion has been stabilised, the components of $\Delta \underline{L}_1^P$, $\Delta \underline{L}_2^P$ are constants and yield a direct measure of the error in the estimate of S^{po}. In the presence of small oscillatory vehicle motions $\Delta \underline{L}_1^P$ and $\Delta \underline{L}_2^P$ may be averaged yielding an average value for ΔS^{po}. In the presence of dc motion, however, $\Delta \underline{L}$ would include the effect of the vehicle motion and, therefore, ΔS^{po} would be in error. These error sources will all be such as to cause S^{po} to deviate from its orthonormal property.

In the following it is demonstrated that the corrected value of S^{po} will always remain orthonormal to the first order provided that $\Delta \underline{L}_1^P$ and $\Delta \underline{L}_2^P$ include only the measures of the tilt of the platform frame. The problem is to show that $\Delta S^{po} S^{op}$ leads to an antisymmetric matrix with a vector representation. This deviation has value since it will also lead to a simpler mechanization involving a three angle Euler rotation matrix.

Suppose the residuals represented by $\Delta \underline{L}_1^P$ and $\Delta \underline{L}_2^P$ result from platform frame tilt errors only, then Eq. (4.32) can be represented in a more simple way. Alinement errors represented by the error matrix ΔS^{po} as a perturbation on S^{po} will always be such that $S^{po} + \Delta S^{po}$ is an orthonormal matrix. Consequently $\Delta S^{po} S^{op}$ is antisymmetric matrix representing tilt errors (this will be demonstrated)

$$\Delta S^{po}S^{op} = \begin{bmatrix} 0 & \phi_z & -\phi_y \\ -\phi_z & 0 & \phi_x \\ \phi_y & -\phi_x & 0 \end{bmatrix} = -\tilde{\phi} \qquad (4.42)$$

and it follows that the tilt

$$-\tilde{\phi} = \Delta S^{po}S^{op} = [\Delta \underline{L}_1^p \;\; \Delta \underline{L}_2^p \;\; \Delta(L_1^p \times L_2^p)][\underline{L}_1^p \;\; L_2^p \;\; L_1^p \times L_2^p]^{-1}$$

where the residuals $\Delta \underline{L}_1^p$ and $\Delta \underline{L}_2^p$ result only from platform frame tilt errors (i.e., no sensor errors). This result can lead to a simpler algorithm than that of Eq. (4.41). Only three elements of $\Delta S^{po}S^{op}$ need be computed. Since each component can be analytically represented, this may be a simpler way to update S^{po}.

To prove that the right side of Eq. (4.43) is antisymmetric with a vector representation first note that the residuals can be represented in terms of the platform tilt vector $\underline{\phi}$

$$\Delta \underline{L}_1^p = \underline{\phi} \times \underline{L}_1^p \qquad = -\tilde{\phi}\, \underline{L}_1^p \qquad (4.44)$$

$$\Delta \underline{L}_2^p = \underline{\phi} \times \underline{L}_2^p \qquad = -\tilde{\phi}\, \underline{L}_2^p \qquad (4.45)$$

$$\Delta(\underline{L}_1^p \times \underline{L}_2^p) = \underline{\phi} \times (\underline{L}_1^p \times \underline{L}_2^p) = -\tilde{\phi}\, (\underline{L}_1^p \times \underline{L}_2^p) \qquad (4.46)$$

Equation (4.46) is derived as follows (remove superscript)

$$\Delta(\underline{L}_1 \times \underline{L}_2) = \Delta \underline{L}_1 \times \underline{L}_2 + \underline{L}_1 \times \Delta \underline{L}_2$$

$$= -(\underline{\phi} \times \underline{L}_1) \times \underline{L}_2 - \underline{L}_1 \times (\underline{\phi} \times \underline{L}_2)$$

$$= -[(\underline{L}_1\underline{L}_2{}^T) - (\underline{L}_2\underline{L}_1{}^T)]\underline{\phi}$$

$$= -\tilde{\phi}\ (\underline{L}_1 x \underline{L}_2)$$

Substituting Eqs. (4.44), (4.45), (4.46) into (4.43), there results the equivalence

$$\Delta S^{po} S^{op} = -\tilde{\phi} \tag{4.47}$$

This result shows that if $\Delta\underline{L}_1^p$ and $\Delta\underline{L}_2^p$ truely measure the alinement error of the platform triad, then Eq. (4.43) will yield the tilt error vector whose components are ϕ_x, ϕ_y, and ϕ_z. This vector $\tilde{\phi}$ is then used to correct the attitude matrix to obtain the more correct matrix $\hat{S}^{po}$ by the equation

$$\hat{S}^{po} = S^{po} + \Delta S^{po} = (I + \Delta S^{po} S^{op}) S^{po}$$

$$= S^{po} - \tilde{\phi}\ S^{po} \tag{4.48}$$

In general the matrix represented by the right side of Eq. (4.43) will not be antisymmetric because the residuals $\Delta\underline{L}_1^p$ and $\Delta\underline{L}_2^p$ will include the uncorrelated effect of sensor errors and gyro drift. The gyro errors will cause $\Delta\underline{L}_1^p$ to vary in a different way from the horizon sensor errors associated with $\Delta\underline{L}_2^p$.

4.4.2 A Psuedo Inverse Scheme

Another example of a fine alinement scheme employing differental correction is presented here. This scheme is similar to that associated with Eq. (4.43), and is presented here primarily because the platform tilt can be analytically represented in terms of the residuals. Further details of this scheme and the determination of attitude rate is given in Ref. 7.

Let $\underline{L}_1$ and $\underline{L}_2$ respectively, define the direction to the orbital pole and the local vertical. Representing $\underline{L}_1$, in terms of the platform axes, one can write

$$\underline{L}_1^p = (\underline{L}_1 \cdot \underline{1}_{xp})\underline{1}_{xp} + (\underline{L}_1 \cdot \underline{1}_{yp})\underline{1}_{yp} + (\underline{L}_1 \cdot \underline{1}_{zp})\underline{1}_{zp} \tag{4.49}$$

Each of the direction cosines in this equation are measured as normaluzed gyro rate outputs. From these three components an orbitrary orthogonal rotation triad can be defined. Letting the triad of unit vectors be defined as $\underline{L}_1^p$, $\underline{A}_1^p$, $\underline{D}_1^p$ one can write (dropping the subscript p)

$$\begin{bmatrix} \underline{L}_1 \\ \underline{A}_1 \\ \underline{D}_1 \end{bmatrix} = \begin{bmatrix} \underline{L}_1 \cdot \underline{1}_{xp} & \underline{L}_1 \cdot \underline{1}_{xp} & \underline{L}_1 \cdot \underline{1}_{zp} \\ \underline{A}_1 \cdot \underline{1}_{xp} & \underline{A}_1 \cdot \underline{1}_{yp} & \underline{A}_1 \cdot \underline{1}_{zp} \\ \underline{D}_1 \cdot \underline{1}_{xp} & \underline{D}_1 \cdot \underline{1}_{yp} & \underline{D}_1 \cdot \underline{1}_{zp} \end{bmatrix} \begin{bmatrix} \underline{1}_{xp} \\ \underline{1}_{yp} \\ \underline{1}_{zp} \end{bmatrix} \tag{4.50}$$

Since the vector $\underline{L}_1$ can be described relative to the platform axes by two rotation angles, a particular rotation matrix can be typically given as

$$\begin{bmatrix} \underline{L}_1 \\ \underline{A}_1 \\ \underline{D}_1 \end{bmatrix} = \begin{bmatrix} c\alpha_1 \, c\delta_1 & s\alpha_1 \, c\delta_1 & s\delta_1 \\ -s\alpha_1 & c\alpha_1 & 0 \\ -c\alpha_1 \, s\delta_1 & -s\alpha_1 \, s\delta_1 & c\delta_1 \end{bmatrix} \begin{bmatrix} \underline{1}_{xp} \\ \underline{1}_{yp} \\ \underline{1}_{zp} \end{bmatrix} \tag{4.51}$$

where α_1 and δ_1 are the rotation angles respectively about the z and y axis. Knowing the components of $\underline{L}_1$ in the platform triad, the complete rotation matrix can be specified. For example, let

$$\underline{L}_1 \cdot \underline{1}_{xp} = a \qquad \underline{L}_1 \cdot \underline{1}_{yp} = b \qquad \underline{L}_1 \cdot \underline{1}_{zp} = c \tag{4.52}$$

then

$$s\delta = c; \qquad c\delta = \pm \sqrt{1 - c^2} \tag{4.53}$$

$$s\alpha = \pm \frac{b}{\sqrt{1 - a^2}} \; ; \qquad c\alpha = \pm \frac{c}{\sqrt{1 - a^2}} \tag{4.54}$$

the quadrant problem can be resolved by the signs on a, b, and c. In a similar way a triad can be defined with $\underline{L}_2$ (horizon sensor axis direction in the vehicle frame) with a corresponding direction cosine matrix.

Next, using these two direction cosine matrix and the estimated attitude matrix $\hat{S}^{po}$, these two directions are computed in the platform frame, compared with the measured values, and their residuals are computed. Using just the residuals seen in the directions perpendicular to $\underline{L}_1$ and $\underline{L}_2$ respectively, and ascribing all deviations or a rotation error in $\hat{S}^{po}$, the following equation can be written

$$\begin{bmatrix} \phi_{A1} \\ \phi_{D1} \\ \phi_{A2} \\ \phi_{D2} \end{bmatrix} = \begin{bmatrix} \underline{A}_1 \cdot \underline{1}_{xp} & \underline{A}_1 \cdot \underline{1}_{yp} & \underline{A}_1 \cdot \underline{1}_{zp} \\ \underline{D}_1 \cdot \underline{1}_{xp} & \underline{D}_1 \cdot \underline{1}_{yp} & \underline{D}_1 \cdot \underline{1}_{zp} \\ \underline{A}_2 \cdot \underline{1}_{xp} & \underline{A}_2 \cdot \underline{1}_{yp} & \underline{A}_2 \cdot \underline{1}_{zp} \\ \underline{D}_2 \cdot \underline{1}_{xp} & \underline{D}_2 \cdot \underline{1}_{yp} & \underline{D}_2 \cdot \underline{1}_{zp} \end{bmatrix} \begin{bmatrix} \phi_x \\ \phi_y \\ \phi_z \end{bmatrix} \tag{4.55}$$

where ϕ_{A1}, ϕ_{D1}, ϕ_{A2}, and ϕ_{D2} are the angular residuals perpendicular to $\underline{L}_1$ and $\underline{L}_2$ respectively.

Inverting this equation by pseudo inverse techniques yields the solution

$$\begin{bmatrix} \phi_x \\ \phi_y \\ \phi_z \end{bmatrix} = (M^T M)^{-1} M^T \begin{bmatrix} \phi_{A1} \\ \phi_{D1} \\ \phi_{A2} \\ \phi_{D2} \end{bmatrix} \qquad (4.56)$$

where M is the matrix given above.

$$(M^T M)^{-1}\ M^T =$$

$$\left[\begin{matrix} \frac{2(\underline{L}_2\cdot\underline{l}_{xp})(\underline{L}_2\cdot\underline{A}_1)+(\underline{L}_1 x\underline{L}_2\cdot\underline{l}_{xp})(\underline{L}_1 x\underline{L}_2\cdot\underline{A}_1)}{2(\underline{L}_1 x\underline{L}_2)\cdot(\underline{L}_1 x\underline{L}_2)} & \qquad \frac{2(c_2\cdot\underline{l}_{xp})(\underline{L}_2\cdot\underline{D}_1)+(}{2(\underline{L}_1 x\underline{L}_2)} \\ \\ \frac{2(\underline{L}_2\cdot\underline{l}_{yp})(\underline{L}_2\cdot\underline{A}_1)+(\underline{L}_1 x\underline{L}_2\cdot\underline{l}_{yp})(\underline{L}_1 x\underline{L}_2\cdot\underline{A}_1)}{2(\underline{L}_1 x\underline{L}_2)\cdot(\underline{L}_1 x\underline{L}_2)} & \qquad \frac{2(\underline{L}_2\cdot\underline{l}_{yp})(\underline{L}_2\cdot\underline{D}_1)+(}{2(\underline{L}_1 x\underline{L}_2)} \\ \\ \frac{2(\underline{L}_2\cdot\underline{l}_{zp})(\underline{L}_2\cdot\underline{A}_1)+(\underline{L}_1 x\underline{L}_2\cdot\underline{l}_{zp})(\underline{L}_1 x\underline{L}_2\cdot\underline{A}_1)}{2(\underline{L}_1 x\underline{L}_2)\cdot(\underline{L}_1 x\underline{L}_2)} & \qquad \frac{2(\underline{L}_2\cdot\underline{l}_{zp})(\underline{L}_1\cdot\underline{D}_1)+(}{2(\underline{L}_1 x\underline{L}_2\cdot} \end{matrix}\right.$$

$$\frac{{}_1 \times \underline{L}_2 \cdot \underline{1}_{xp})(\underline{L}_1 \times \underline{L}_2 \cdot \underline{D}_1)}{(\underline{L}_1 \times \underline{L}_2)}$$

$$\frac{2(\underline{L}_1 \cdot \underline{1}_{xp})(\underline{L}_1 \cdot \underline{A}_2) + (\underline{L}_1 \times \underline{L}_2 \cdot \underline{1}_{xp})(\underline{L}_1 \times \underline{L}_2 \cdot \underline{A}_2)}{2(\underline{L}_1 \times \underline{L}_2) \cdot (\underline{L}_1 \times \underline{L}_2)}$$

$$\frac{{}_1 \times \underline{L}_2 \cdot \underline{1}_{yp})(\underline{L}_1 \times \underline{L}_2 \cdot \underline{D}_1)}{(\underline{L}_1 \times \underline{L}_2)}$$

$$\frac{2(\underline{L}_1 \cdot \underline{1}_{yp})(\underline{L}_1 \cdot \underline{A}_2) + (\underline{L}_1 \times \underline{L}_2 \cdot \underline{1}_{yp})(\underline{L}_1 \times \underline{L}_2 \cdot \underline{A}_2)}{2(\underline{L}_1 \times \underline{L}_2) \cdot (\underline{L}_1 \times \underline{L}_2)}$$

$$\frac{{}_1 \times \underline{L}_2 \cdot \underline{1}_{zp})(\underline{L}_1 \times \underline{L}_2 \cdot \underline{D}_1)}{(\underline{L}_1 \times \underline{L}_2)}$$

$$\frac{2(\underline{L}_1 \cdot \underline{1}_{zp})(\underline{L}_1 \cdot \underline{A}_2) + (\underline{L}_1 \times \underline{L}_2 \cdot \underline{1}_{zp})(\underline{L}_1 \times \underline{L}_2 \cdot \underline{A}_2)}{2(\underline{L}_1 \times \underline{L}_2) \cdot (\underline{L}_1 \times \underline{L}_2)}$$

3

$$\left.\begin{matrix}
\dfrac{2(\underline{L}_1\cdot\underline{1}_{xp})(\underline{L}_1\cdot\underline{D}_1)+(\underline{L}_1 x\underline{L}_2\cdot\underline{1}_{xp})(\underline{L}_1 x\underline{L}_2\cdot\underline{D}_2)}{2(\underline{L}_1 x\underline{L}_2)\cdot(\underline{L}_1 x\underline{L}_2)} \\[2em]
\dfrac{2(\underline{L}_1\cdot\underline{1}_{yp})(\underline{L}_1\cdot\underline{D}_2)+(\underline{L}_1 x\underline{L}_2\cdot\underline{1}_{yp})(\underline{L}_1 x\underline{L}_2\cdot\underline{D}_2)}{2(\underline{L}_1 x\underline{L}_2)\cdot(\underline{L}_1 x\underline{L}_2)} \\[2em]
\dfrac{2(\underline{L}_1\cdot\underline{1}_{zp})(\underline{L}_1\cdot\underline{D}_2)+(\underline{L}_1 x\underline{L}_2\cdot\underline{1}_{zp})(\underline{L}_1 x\underline{L}_2\cdot\underline{D}_2)}{2(\underline{L}_1 x\underline{L}_2)\cdot(\underline{L}_1 x\underline{L}_2)}
\end{matrix}\right] \qquad (4.57)$$

③

In a special case where the vehicle is alined to the orbital frame, one configuration is to select

$$
\begin{aligned}
\underline{1}_{xp} &= \underline{1}_x = \underline{L}_1 = \underline{D}_2 \\
\underline{1}_{zp} &= \underline{1}_z = \underline{L}_2 = \underline{A}_1 \\
\underline{1}_{yp} &= \underline{1}_y = \underline{A}_2 = \underline{D}_1 = \underline{L}_1 \times \underline{L}_2
\end{aligned}
\qquad (4.58)
$$

Then the pseudo inverse yields the result

$$
\begin{aligned}
\phi_x &= 1/2(\phi_{D1} + \phi_{A2}) \\
\phi_y &= \phi_{D2} \\
\phi_z &= \phi_{A1}
\end{aligned}
\qquad (4.59)
$$

In this result the azimuth deviation is given by the azimuth residual of the deviation in the measured angular velocity, the pitch by the measured horizon sensor defined pitch, and the roll by one-half the sum of the horizon and gyro measured residuals.

5. High Precision Gyrocompass Alinement

5.1 Preliminary Considerations

As noted on several occasions, the primary limitation to achieving high accuracy gyrocompass alinement of strapdown systems results from the coupling of vehicle angular rate into the alinement equations. If indeed vehicle angular rates can be detected, computed, and separated from the orbital rates, the alinement problem would be no different then for gimballed platforms.

On way in which the alinement problem can be made more accurate is to utilize parameter estimation techniques in which the effect of angular rates are estimated on the basis of its a priori stochastic characteristics. These techniques are discussed using stellar observables for the celestial alinement of a coordinate reference system in References 5, 8, and 7. Reference 4 considers the orbital determination problem (which is similar to the attitude determination problem of using horizon scanner data. The use of optimal parameter estimation techniques as an on-board computational algorithm improves accuracy from another point of view. The horizon sensor data is inherently noisy including both a random bias and gaussian noise. These errors are associated with the instrument and the atmospheric phenomena both of which limit high accuracy attitude determination. If a stochastic model characterizing the errors can be developed, its use in the estimation algorithm will improve the accuracy of the attitude determination. Reference 4 concludes a ten-to-one improvement of orbit determination accuracy if a Kalman estimation algorithm (Ref. 4) is used over a deterministic procedure in which horizon data are processed.

It is well to review here, some of the basic difficulties associated with the gyrocompass alinement of strapdown systems.

In the one point gyrocompass mode, the two vectors used for alinement are the local vertical and the total angular rate vectors. As long as angular rates remain the basic source of data, the alinement accuracy will be limited by the inclusion of extraneous vehicle angular motion. Thus, during the gyrocompass mode the vehicle frame stabilization would be an important consideration.

On the other hand, if the one-point scheme can be staged in a sequential fashion, and angular rates compensated by computation, an optimal parameter estimation procedure can be developed in which constant gyro drift rate and sensor bias errors can be estimated and their effects eliminated in the direction cosine determination, thereby enhancing accuracy.

The intrinsic difference of one-point alinement modes which processes two stellar lines as against the gyrocompass problem which processes the vertical and the angular rate data is to be noted In the former case alinement is possible whether or not the vehicle is undergoing angular motion. The integration of the direction cosine equations will keep the attitude updated and the stellar lines can be used as the basis for continuously re-initializing the direction cosine matrix. In the latter gyrocompass problem, while measuring the direction of the vertical is identical to measuring the direction of the stellar line, the measuring of angular rates is intrinsically different. This difference results from the fact that the angular rate data from the gyro package reflects the effect of undesired vehicle motion. Since the primary data required of the gyro package is the direction of the orbital pole, it follows that the alinement suffers by the inability to compute the rates accurately.

In comparing the two alinement techniques, it is clear that gyrocompass alinement accuracy is inherently degraded by the effect of the unstabilized vehicle rotation rates. To eliminate the effect of rotation rates, a solution would avoid use of the gyro outputs and, therefore, rather than a one-point alinement mode, consider a sequential type alinement procedure in which the data obtained from the measurement of the vertical only are processed. Between successive measurements, the direction cosine matrix can be integrated using the gyro outputs. This technique will lead to high accuracy gyrocompass alinement procedures because the integral of the rates are the basic measurables, thus yielding "smoothed" residuals as against processing the rate data directly. For this reason, although perhaps more subject to geometric poor conditioning, the two-point scheme is considered in the following as a basis for high precision alinement.

In a two-point mode, or for that matter, a multi-point mode, a series of verticals is a basis for alinement. In this case the measurables are the directions of the vertical as defined in the vehicle frame. The accuracy of the alinement in this case is limited by the horizon scanner accuracy capability. Therefore, if a smoothing procedure that pre-filters the measurables is employed, high accuracy residuals can be obtained, and gyrocompass alinement can be secured despite the presence of vehicle motion.

5.2 A Multi-point Gyrocompass Alinement Scheme

In this section a multi-point gyrocompass alinement scheme which utilizes a recursive optimal parameter estimation algorithm is described. A Kalman filter is used to process a series of residuals from the horizon scanner derived vertical which are measured in the vehicle frame. This is combined with an updated estimate of the attitude as obtained by integration of the direction cosine equations.

The following developments are based on the linear gyrocompass equations of Section 4.3. The basic equations are re-written below for convenience.

$$\dot{\underline{\phi}} + (s^{vo}\,\underline{\omega}_o) \times \underline{\phi} = \Delta\underline{\omega} \tag{5.1}$$

$$-\underline{\phi} \times (S^{vo}\underline{1}_z) = \Delta\underline{1}_H \qquad (5.2)$$

$$\Delta\underline{\omega} = \underline{\omega}^{vI} - \hat{\underline{\omega}}^{vI}$$

$\Delta\underline{\omega} = \Delta\underline{\omega}^{vI} = \underline{\omega}^{vI} - \hat{\underline{\omega}}^{vI}$ = Difference between actual measured angular rate and nominal orbital rate in the vehicle frame

S^{vo} = Estimated direction cosine matrix

$\underline{\phi}$ = Vehicle frame tilt error vector relative to estimated S^{vo}

$\tilde{\phi} = -\Delta S^{vo} S^{ov}$

$\underline{1}_z = \begin{bmatrix} 0 \\ 0 \\ 1 \end{bmatrix}$ True orbital vertical in the orbital frame

$\Delta\underline{1}_H$ = Error (residual) of vertical as observed in the vehicle frame

$\hat{\underline{\omega}}^{vI}$ = Computed vehicle angular velocity

$\underline{\omega}^{vI}$ = Measured vehicle angular velocity

Assuming for the moment the vehicle rates are stabilized $\underline{\omega}^{vo} = 0$, Eq. (5.1) and (5.2) are written in the state vector form

$$\dot{x} = F_x + u \qquad (5.3)$$

$$y = M_x + u \qquad (5.4)$$

where

$x = \phi$

$y = \Delta l_H$

M = The equivalent matrix of Eq. (5.2)

F = The equivalent matrix of Eq. (5.1)

$u = \Delta\omega$

n = Additive gaussian noise of sensor and associated phenomenology

These equations assume that there are no bias errors in y.

In general, the horizon scanner derived residuals $y = \Delta l_H$ tends to be noisy, and furthermore, the data rates may be relatively high in comparison to the basic computation cycle of the computer. To reduce the data rates, and still process all of the measurables, y as represented by Eq. (5.4) might represent a smoothed value at a discrete time. In any case, at a specific discrete time, y is measured. The Kalman algorithm Ref. (9) provides for estimating x continuously by integration of Eq. (5.3) between the discrete times at which y are measured. When y is available the current estimate x is combined with the newly available data y.

The update of Eq. (5.3) is handled numerically in the following way. Let the transition matrix of the homogeneous part of Eq. (5.3) be defined as $\phi(t_n, t_{n-1})$. Then

$$\dot{x} = F_x$$

$$\dot{\Phi} = F\,\Phi \qquad \Phi(t_{n-1}, t_{n-1}) = I \tag{5.5}$$

and

$$x_n = \Phi(t_n, t_{n-1})x_{n-1} + \int_{t_{n-1}}^{t_n} \Phi(t_n, \tau)\underline{u}(\tau)d\tau \qquad (5.6)$$

is the general solution.

Let (^) designate the optimum estimate of x. Then the estimation algorithm is given as

$$\hat{x}(t_n) = \hat{x}'(t_n) + \omega_n(y(t_n) - \hat{y}'(t_n)) \qquad (5.7)$$

where

$\hat{x}(t_n)$ = optimum estimate at t_n

$\hat{x}'(t_n)$ = predicted estimate at t_n

ω_n = optimal Kalman filter

$\hat{y}'(t_n)$ = $M_n \hat{x}'_n$ = predicted estimate of residual

$y(t_n)$ = measured residuals of horizon scanner at t_n

The predicted estimate $\hat{x}'(t_n)$ is obtained from Eq. (5.6)

$$\hat{x}'(t_n) = \Phi(t_n, t_{n-1})\,\hat{x}(t_{n-1}) + N(t_n) \qquad (5.9)$$

where

$$N(t_n) = \int_{t_{n-1}}^{t_n} \Phi(t_n, \tau)\, u(\tau)d\tau \qquad (5.10)$$

The Kalman algorithm for the optimal weighting filter reduces to the following sets of matrix equations

$$\omega_n = P_n' M_n^T [M_n P_n' M_n^T + C_n]^{-1} \tag{5.11}$$

$$P_n' = \phi(n, n-1) P_{n-1} \phi(n, n-1)^T + R_n \tag{5.12}$$

$$P_{n-1} = P_{n-1}' (I - M_{n-1}^T \omega_{n-1}^T) \tag{5.13}$$

where

$$P_n' = \mathrm{cov}(x(t_n) - \hat{x}'(t_n)) \tag{5.14}$$

$$P_n = \mathrm{cov}(x(t_n) - \hat{x}(t_n)) \tag{5.15}$$

$$R_n = \mathrm{cov}(N(t_n)) \tag{5.16}$$

$$C_n = \mathrm{cov}(n) \tag{5.17}$$

Equation (5.7) can be written in a simpler form

$$\hat{x}_n = (I - \omega_n M_n)\hat{x}_n' + \omega_n y_n \tag{5.18}$$

To compute this estimate the Kalman filter $_n$ is computed in recursive manner via Eq. (5.11) to (5.13). To start the process a set of initial conditions are assumed for x and C_n.

Using the current estimate $\hat{x}_n$ the attitude is immediately updated as follows

$$\hat{x}_n = \begin{bmatrix} \hat{\phi}_{xn} \\ \hat{\phi}_{yn} \\ \hat{\phi}_{zn} \end{bmatrix} = \hat{\boldsymbol{\phi}}_n \tag{5.19}$$

$$\hat{S}^{po}_{n} = \hat{S}^{po}_{n-1} + \Delta\hat{S}^{po}_{n-1} = \hat{S}^{po}_{n-1} = \tilde{\phi}_{n}\ \hat{S}^{po}_{n-1} \qquad (5.20)$$

Having re-set S^{PO}, $\hat{x}_n(t_n+)$ is presumed equal to zero and procedure is iterated for the next measurable y_{n+1} that becomes available. Thus, the predicted estimate $\hat{x}'$ can be assumed to be equal to zero after the first term iterations. Equation (5.18) can then be expressed as

$$\hat{x}_n = \omega_n y_n \qquad (5.21)$$

5.3 Analytical Transition Matrix

Assuming that S^{PO} is nearly constant and gyro drift rate is negligible, Eq. (5.1) and (5.5) can be analytically represented for nearly circular orbits.

$$\underline{\phi} = \begin{bmatrix} \phi_x \\ \phi_y \\ \phi_z \end{bmatrix} = \left[\cos \omega_o \tau I - \frac{\tilde{\underline{\omega}}^{pI}}{\omega_o} \sin \omega_o \tau + \frac{\underline{\omega}^{pI}(\underline{\omega}^{pI})^T}{\omega_o^2} (1-\cos \omega_o \tau)\right] \begin{bmatrix} \phi_{xo} \\ \phi_{yo} \\ \phi_{zo} \end{bmatrix}$$

For an aribtrary vehicle attitude, therefore, the transition matrix $\underline{\Phi}$ is the inner bracketed expression. Where the angular velocity matrix is obtained from

$$\underline{\omega}^{pI} = S^{po}\ \underline{\omega}_o$$

5.4 Discussion

In the presence of the constant unknown vehicle motion, such as resulted from gyro drift, the state vector can be augmented to include this vector as another set of parameters to be estimated

$$x = \begin{bmatrix} \underline{\phi} \\ \Delta \underline{\omega} \end{bmatrix}$$

The state transition matrix is expanded and this higher dimension system solved in essentially the same way. Having estimated $\Delta \underline{\omega}$, the estimate ϕ would necessarily be more accurate.

To accommodate the effect of bias in the sensor residuals, further augmentation can be made on the state vector; and this higher order system solved in the same manner. Estimating out the sensor bias will enhance even further the accuracy of the estimate.

There is, of course, an upper limit to the dimensionality of the parameters-to-be-determined. This is limited by the data rate at which $y(t_n)$ is available, the allowable accuracy in the estimate $\hat{x}$, the computer capacity, the quality of the measurables, the characteristics of vehicle rate coupling, and its error model representation. These considerations require further study. Needless to say, parameter estimation techniques require a considerable amount of computer capacity and speed.

6. Strapdown ESG Orbital Gyrocompass Alinement

The mechanization of the orbital gyrocompass alinement problem for strapdown ESG systems is very similar to the conventional strapdown systems. An ESG system description and a mechanization is briefly described below (Ref. 10 and 11).

The strapdown ESG gyro package consists of two free-rotor ESG gyros. Optical pickoffs on each gyro permit the determination of the rotor spin vector (the rotor angular momentum vector) relative to the vehicle frame. The orientation of the two gyros whose angular momentum vectors are separated by about ninety degrees are also known or computable relative to the orbital or inertial frame. The vehicle frame attitude is determined using an equation similar to Eq. (4.32)

With ESG systems there is no requirement for updating the transformation matrix by integration of the direction cosine equations. The pickoffs yield direct measures of the direction cosine of the spin axis relative to the body or platform axes.

6.1 Attitude Determination

Let $\underline{H}_1$ and $\underline{H}_2$ define the angular momentum vector of gyros 1 and 2. Then represented in the vehicle frame and the inertial reference frame one can write

$$\underline{H}_1 = H^p_{1x}\,\underline{1}_{px} + H^p_{1y}\,\underline{1}_{py} + H^p_{1z}\,\underline{1}_{pz}$$

$$= H_{1X}\,\underline{1}_X + H_{1Y}\,\underline{1}_Y + H_{1Z}\,\underline{1}_Z \qquad (6.1)$$

$$\underline{H}_2 = H^p_{2x}\,\underline{1}_{px} + H^p_{2y}\,\underline{1}_{py} + \underline{H}^p_{2z}\,\underline{1}_{pz}$$

$$= H_{2X}\,\underline{1}_X + H_{2Y}\,\underline{1}_Y + H_{2Z}\,\underline{1}_Z \qquad (6.2)$$

where the H's are all normalized and read as direction cosines. If the vector represented in the platform frame is denoted by the superscript p, the relationship of the components of $\underline{H}_1$ and $\underline{H}_2$ represented in these two frames are given by the matrix equation

$$[\underline{H}^p_1\ \underline{H}^p_2\ \underline{H}^p_1 \times \underline{H}^p_2] = S^{pI}\,[\underline{H}_1\ \underline{H}_2\ \ \underline{H}_1 \times \underline{H}_2] \qquad (6.3)$$

The components of $\underline{H}$ as measured in the platform frame are available as direction cosines of the spin axis relative to the three pickoffs resolved along to three orthogonal platform frame axes. The components expressed in the inertial reference frame are pre-computed constants.

The direction cosine transformation matrix is obtained by solving for S^{po}

$$S^{pI} = [\underline{H}^p_1\ \underline{H}^p_2\ \underline{H}^p_1 \times \underline{H}^p_2]\,[\underline{H}_1\ \underline{H}_2\ \underline{H}_1 \times \underline{H}_2]^{-1} \qquad (6.4)$$

Relative to the orbital frame, the platform frame is given by

$$S^{po} = S^{pI} S^{Io} \tag{6.5}$$

where S^{Io} is computed on the basis of the orbital parameters. The details of this computation is presented in Ref. 10 and 11.

Attitude determination for ESG strapdown systems is a fairly straight forward computational problem. Knowing the matrix $[\underline{H}_1 \; \underline{H}_2 \; \underline{H}_1 \times \underline{H}_2]$ and measuring $[\underline{H}_1^p \; \underline{H}_2^p \; \underline{H}_1^p \times \underline{H}_2^p]$ in the platform frame, S^{pI} is determined from which S^{po} is determined from the trajectory parameters. In this computation it is necessary to determine S^{pI} initially inasmuch as the vectors $\underline{H}_1$ and $\underline{H}_2$ have constant directions only in the inertial frame. To ease this computation somewhat, it may be possible to form the product

$$[\underline{H}_1 \; \underline{H}_2 \; \underline{H}_1 \times \underline{H}_2]^{-1} \; [S^{Io}]$$

directly. This matrix, however, will be time varying thereby requiring a continuous update for the gyrocompass problem.

6.2 Gyrocompass Alinement

The technique for gyrocompass alinement is similar to the fine alinement scheme discussed in the previous sections for the conventional strapdown systems. With the computed estimates of S^{po} or S^{pI} available, the directions to the local vertical and the orbital pole are computed and compared with the corresponding measured values. The resulting residuals are used as a basis to re-determine the spin directions $\underline{H}_1$ and $\underline{H}_2$ relative to the inertial reference system. Having re-determined these directions the attitude is computed by measuring $\underline{H}_1^p$ and $\underline{H}_2^p$.

The present section describes a one-point and a two-point gyrocompass alinement scheme.

In common, ESG strapdown alinement mechanizations are exceedingly complex and involve a considerable amount of on-board computation. The difficulty is primarily associated with the fact that the pickoff data do not provide rate information directly, but must be computed via an algorithm. There is no apparent way in which a simple algorithm can be developed to obtain rates along three axes by data processing a series of direction cosine measurements.

6.2.1 One-Point Scheme

Let (^) denote the computed value, then the computed vertical is given by

$$\hat{\underline{1}}_H = \hat{S}^{po} \begin{bmatrix} 0 \\ 0 \\ 1 \end{bmatrix} = \hat{S}^{pI} S^{Io} \begin{bmatrix} 0 \\ 0 \\ 1 \end{bmatrix} \tag{6.6}$$

and the computed orbital rate in the platform frame is

$$\hat{\underline{\omega}}_o^p = \hat{S}^{po} \begin{bmatrix} 0 \\ \omega_o \\ 0 \end{bmatrix} = \hat{S}^{pI} S^{Io} \begin{bmatrix} 0 \\ \omega_o \\ 0 \end{bmatrix} \tag{6.7}$$

The measured vertical in the platform frame is

$$\underline{1}_H = \begin{bmatrix} 1_{Hx} \\ 1_{Hy} \\ 1_{Hz} \end{bmatrix} \tag{6.8}$$

The measured platform rate in the platform frame is computed from

$$\underline{\omega}^P = \dot{S}^{pI} S^{Ip} = [\dot{H}_1^P\ \dot{H}_2^P\ (\dot{H}_1^P x H_2^P + \underline{H}_1^P x \dot{H}_2^P)]\ [\underline{H}_1^P\ \underline{H}_2^P\ \underline{H}_1^P x H_2^P]^{-1} \tag{6.9}$$

Provided that $\dot{H}_1$ and $\dot{H}_2$ are true rate errors of a rotating coordinate system $\underline{\omega}^P$ will be hence in vector representation. The components of $\dot{\underline{H}}_1$ and H_2 are assumed to be measurable.

Let $\Delta\underline{1}_H = \underline{1}_H - \hat{\underline{1}}_H$ and $\Delta\underline{\omega}^P = \underline{\omega}^P - \hat{\underline{\omega}}_o^P$ (6.10)

then ascribing all deviations to an uncertainty in the directions $\underline{H}_1$ and $\underline{H}_2$ in the inertial frame

$$\Delta S^{PI} = [\underline{H}_1^P \; \underline{H}_2^P \; \underline{H}_1^P x \underline{H}_2^P] \, [\Delta\underline{H}_1 \; \Delta\underline{H}_2 \; \Delta(\underline{H}_1 x \underline{H}_2)]^{-1} \tag{6.11}$$

$$\Delta S^{PO} = \Delta S^{PI} \, S^{IO}$$

and

$$[\Delta\underline{1}_H \;\; \Delta\underline{\omega}^P \;\; \Delta(\underline{1}_H \, x \, \underline{\omega}^P) = \Delta S^{PO} \begin{bmatrix} 0 & 0 & \omega_o \\ 0 & \omega_o & 0 \\ 1 & 0 & 0 \end{bmatrix} \tag{6.12}$$

or

$$\Delta S^{PO} = [\Delta\underline{1}_H \;\; \Delta\underline{\omega}^P \;\; \Delta(\underline{1}_H \, x \, \underline{\omega}^P)] \begin{bmatrix} 0 & 0 & 1 \\ 0 & \frac{1}{\omega_o} & 0 \\ \frac{1}{\omega_o} & 0 & 0 \end{bmatrix} \tag{6.13}$$

The elements of ΔS^{PO} are given directly in terms of the deviations in the local vertical and the orbital rate. From a knowledge of ΔS^{PO} the correction $[\Delta H_1 \;\; \Delta H_2 \;\; \Delta(H_1 \, x \, H_2)]$ can be obtained to re-set the direction of the spin axes in the inertial frame in the computer. This constitutes the gyrocompass alinement for ESG strapdown systems.

6.2.2 Two-Point or Multi-Point Schemes

In a two-point or a multi-point gyrocompass alinement scheme, the basic residuals which are used to re-determine $\underline{H}_1$ and $\underline{H}_2$ are a series of vertical measurement errors. In the presence of unstabilized vehicle motion, it is necessary to connect the vehicle attitude at the two different times of measurement of the vertical. If the vehicle rate is stabilized then the alinement technique is similar to the one-point scheme. Using a subscript 1 and 2 to denote the two different times of measurements of the vertical. If the vehicle rate is stabilized then the alinement technique is similar to the one-point scheme. Using a subscript 1 and 2 to denote the two different times of measurements the deviation in the estimate of S^{pI} is obtained in the following way. Let the computed residuals of the vertical at two different instants of time be given as in Eq. (6.10)

$$\Delta \underline{1}^{P}_{H1} = \Delta \hat{S}^{pI}\, S_1^{Io} \begin{bmatrix} 0 \\ 0 \\ 1 \end{bmatrix}$$

$$\Delta \underline{1}^{P}_{H2} = \Delta \hat{S}^{pI}\, S_2^{Io} \begin{bmatrix} 0 \\ 0 \\ 1 \end{bmatrix}$$

where S_1^{Io} and S_2^{Io} are the direction cosine matrix computed on the basis of the orbital parameters. Then one can write

$$[\Delta \underline{1}^{P}_{H1} \quad \Delta \underline{1}^{P}_{H2} \quad \Delta(\underline{1}^{P}_{H1} \times \underline{1}^{P}_{H2})] = \Delta \hat{S}^{pI} \left[\begin{array}{c|c|c} S_1^{Io} \begin{bmatrix} 0 \\ 0 \\ 1 \end{bmatrix} & S_2^{Io} \begin{bmatrix} 0 \\ 0 \\ 1 \end{bmatrix} & S_1^{Io} \begin{bmatrix} 0 \\ 0 \\ 1 \end{bmatrix} \times S_2^{Io} \begin{bmatrix} 0 \\ 0 \\ 1 \end{bmatrix} \end{array} \right]$$

from which $\Delta \hat{S}^{pI}$ is obtained by inversion.

To account for the effect of motion between the two times, to a first order the direction cosine equations must be integrated. This requires that $\underline{\omega}^{vI}$ be computable which, in turn, implies that this rate be determinable from the pickoff data (see Appendix C)

7. Gyrocompass Error Equations

For the multipoint gyrocompass mechanization discussed in Section 5, the error analysis can be developed around the covariance matrix of the estimation error. Since this covariance matrix is part of the estimation algorithm which is computed, its printout will yield a measure of the alinement accuracy. A sensitivity analysis study can be made by computing this matrix for each of the dominant error sources.

The error equations for the deterministic cases such as the one-point and two-point schemes can be developed analytically as outlined in the following.

The general alinement error equation can be developed from either Eq. (4.24) or (4.32). Using the latter equation, if the measurables $\underline{L}_1^p$ and $\underline{L}_2^p$ are perturbed the error in S^{po} is represented as

$$\Delta S^{po} = [\Delta\underline{L}_1^p \vdots \Delta\underline{L}_2^p \vdots \Delta(\underline{L}_1^p \times \underline{L}_2^p)][\underline{L}_1 \vdots \underline{L}_2 \vdots \underline{L}_1 \times \underline{L}_2]^{-1}$$

The equation is detailed for the one-point gyrocompass mode from Eq. (416)

$$\underline{L}_1^p = \frac{\underline{\omega}_y^{pI}}{|\omega_y^{pI}|} = L_{1x}^p \underline{1}_{px} + L_{1y}^p \underline{1}_{py} + L_{1z}^p \underline{1}_{pz}$$

therefore,

$$\Delta\underline{L}_1^p = \frac{\Delta\underline{\omega}_y^{pI}}{|\omega_y^{pI}|} - \frac{\underline{\omega}_y^{pI}}{\omega_y^2}\,\frac{\underline{\omega}_y^{pI}\cdot\Delta\underline{\omega}_y^{pI}}{|\omega_y|} = \left[I - \frac{\underline{\omega}_y^{pI}(\underline{\omega}_y^{pI})^T}{\underline{\omega}_y^T\,\underline{\omega}_y}\right]\frac{\Delta\underline{\omega}_y^{pI}}{|\omega_y|}$$

But $\underline{\omega}_y^{pI} = S^{po}\underline{\omega}_o$ nominally, therefore,

$$\Delta\underline{L}_1^p = [I - \frac{S^{po}\underline{\omega}_o\underline{\omega}_o^T S^{op}}{\omega_o^2}] \frac{\Delta\underline{\omega}^{pI}}{\omega_o}$$

and from Eq. (4.9)

$$\Delta\underline{\omega}^{pI} = \underline{\omega}^{po} + \dot{\underline{\phi}} + S^{po}\underline{\omega}_o \times \underline{\phi}$$

where $\underline{\omega}^{vo}$ is the residual vehicle rate, $\underline{\phi}$ the alinement error of the system and $\dot{\underline{\phi}}$ the drift rate. The error in $\Delta\underline{L}_1^p$ is finally expressed as

$$\Delta\underline{L}_1^p = [I - \frac{S^{po}\underline{\omega}_o\underline{\omega}_o^T S^{op}}{\omega_o^2}] [\frac{\underline{\omega}^{po} + \dot{\underline{\phi}} + S^{po}\underline{\omega}_o \times \underline{\phi}}{\omega_o}]$$

In a similar way the error in the vertical is obtained from $\underline{L}_2^p$. This error is given directly as $\Delta\underline{L}_2^p$. Whose components in the vehicle frame can be directly related to the pointing resolution error of the horison sensor.

Note that in general the error equation cannot be expressed as a vector equation. The reason for this is that the measurables $\underline{L}_1^p$ and $\underline{L}_2^p$ are not rigidly fixed relative to each other, and, therefore, the errors associated with these vectors are not constrained so that one can write

$$\Delta\underline{L}_1^p = \underline{\phi} \times \underline{L}_1^p \quad \text{and} \quad \Delta\underline{L}_2^p = \underline{\phi} \times \underline{L}_2^p$$

As noted earlier, this is the only condition under which $\Delta S^{po}S^{op}$ becomes the antisymmetric matrix sith a vector equivalent.

Suppose one considers the special case where the vehicle is nominally alined to the orbital frame. Then $S^{po} = I$, and

$$\Delta \underline{L}_1^p = \left[\begin{pmatrix} 1 & 0 & 0 \\ 0 & 1 & 0 \\ 0 & 0 & 1 \end{pmatrix} - \begin{pmatrix} 0 & 0 & 0 \\ 0 & 1 & 0 \\ 0 & 0 & 0 \end{pmatrix} \right] \left[\frac{\Delta \underline{\omega}^{pI}}{\omega_o} \right]$$

$$= \begin{bmatrix} 1 & 0 & 0 \\ 0 & 0 & 0 \\ 0 & 0 & 1 \end{bmatrix} \left[\frac{\Delta \underline{\omega}^{pI}}{\omega_o} \right]$$

$$= \begin{bmatrix} \dfrac{\Delta \omega_x^{pI}}{\omega_o} \\ 0 \\ \dfrac{\Delta \omega_z^{pI}}{\omega_o} \end{bmatrix} = \begin{bmatrix} \text{rate error along roll axis} \\ \text{rate error along pitch axis} \\ \text{rate error along yaw axis} \end{bmatrix}$$

and

$$\Delta \underline{L}_2^p = \begin{bmatrix} \Delta\theta \\ \Delta\phi \\ 0 \end{bmatrix} = \begin{bmatrix} \text{horizon sensor error along roll} \\ \text{horizon sensor error along pitch} \\ \text{yaw sensor error undefined} \end{bmatrix}$$

$$\Delta(\underline{L}_1^p \times \underline{L}_2^p) = \Delta\underline{L}_1^p \times L_2^p + \underline{L}_1^p \times \Delta L_2^p$$

$$= \begin{bmatrix} \underline{l}_{px} & \underline{l}_{py} & \underline{l}_{pz} \\ \frac{\Delta\omega_x^{pI}}{\omega_o} & 0 & \frac{\Delta\omega_z^{pI}}{\omega_o} \\ 0 & 0 & 1 \end{bmatrix} + \begin{bmatrix} \underline{l}_{px} & \underline{l}_{py} & \underline{l}_{pz} \\ 0 & 1 & 0 \\ \Delta\theta & \Delta\phi & 0 \end{bmatrix}$$

$$= \begin{bmatrix} 0 \\ -\frac{\Delta\omega_x^{pI}}{\omega_o} \\ -\Delta\theta \end{bmatrix}$$

$$\Delta S^{po} = \begin{bmatrix} \frac{\Delta\omega_x^{pI}}{\omega_o} & \Delta\theta & 0 \\ 0 & \Delta\phi & -\frac{\Delta\omega_x^{pI}}{\omega_o} \\ \frac{\Delta\omega_z^{pI}}{\omega_o} & 0 & -\Delta\theta \end{bmatrix} \begin{bmatrix} 0 & 0 & 1 \\ 1 & 0 & 0 \\ 0 & 1 & 0 \end{bmatrix}$$

$$= \begin{bmatrix} \Delta\theta & 0 & \frac{\Delta\omega_x^{pI}}{\omega_o} \\ \Delta\phi & -\frac{\Delta\omega_x^{pI}}{\omega_o} & 0 \\ 0 & -\Delta\theta & \frac{\Delta\omega_z^{pI}}{\omega_o} \end{bmatrix}$$

REFERENCES

1. Autonetics T5-1877/3061, "Principles of Orbital Gyrocompass Alinement of a Gimballed Locally Level Platform", dated November, 1965.

2. "Attitude Control of Satellites Using Integrating Gyroscopes", J. E. DeLisle, G. Ogeltree, and B. M. Hildebrant, M.I.T.

3. "The Control Moment Gyro (MOD II), A New Development in Satellite Stabilization", by R. J. Haagens AIAA Preprint, 63-316, dated August, 1963.

4. "Estimation of Local Vertical and Orbital Parameters for Earth Satellite on the Basis of Horizon Sensor Measurements", by Dr. A. L. Knoll, and M. M. Edelstein, dated January 20, 1965.

5. Autonetics TM-AAE00NI-18, "Precision Attitude Determination by Means of Optical Tracking of Stars", by B. B. Gragg, Jr. dated August 24, 1965.

6. "Control, Guidance, and Navigation of Spacecraft", NASA SP-17 Report, NASA Washington, D.C., dated December 1962.

7. "Some Considerations for Precision, High Speed, Attitude and Attitude Rate Determination and Correction for Space Systems", Autonetics TM-31-061-2, dated April 13, 1964, by K. C. Kochi.

8. "An Optimum Stellar-Inertial Navigation System", Journal of the Institute of Navigation, Vol. 12, by B. E. Bona and C. E. Hutchinson, dated Summer 1965.

9. "A New Approach to Linear Filtering and Prediction Problems", Journal of Basic Engineering Vol. 82, Transactions ASM Series D, dated 1960, by R. E. Kalman.

10. AD 336-015 (ASD-TDR-63-216), "Research and Development of a Body-Mounted Inertial Navigation System Using Electrostatically Supported Pendulous Gyro Accelerometers", General Electric Co., dated April 1963, (Secret).

11. AD 336-792 (ASD-TDR-62-750), "Air Borne Electrically Suspended Gyro", Minneapolis-Honeywell, dated September 25, 1962, (Secret).

CHAPTER IX

SPECIAL SITUATIONS AND TECHNIQUES

1. Introduction

The foregoing discussions have presented the gyrocompassing systems of significance for space applications, under the constraint of minimum on-board computer capability. Thus, some of the sophisticated filtering techniques such as Kalman and others have not been covered. Similarly, low accuracy passive techniques such as the use of single gyroscopes with mechanical damping and twin gyroscopes with mechanical coupling have been overlooked as being too inaccurate.

Variations on the general approach to direct and indirect gyrocompassing may be expected to appear in the literature.[1] It is firmly believed that analysis of such systems cannot vary greatly from those developed in this document. There are essentially only two possible philosophies applicable to gyrocompassing, direct measurement and indirect measurement.

Some special situations and associated special techniques, however, are worthy of consideration here.

2. Gyrocompassing During Powered Lift Into Orbit

During the initial boost phase of flight from the earth's surface into parking orbit, some possibility for gyrocompassing exists, provided that the trajectory is confined to a plane. Two difficulties are associated with this effort. One is the high pitch rate required of the platform, perhaps 90 deg in 10 min. The second is the absence of a good vertical reference during boost.

2.1 High Pitch Rate

The problem associated with large pitch rates is that of precessing the gyros rapidly enough to keep up. In this case, pitch rate refers to platform pitch rate rather than vehicle pitch rate. During a 10 min boost into orbit, the vehicle may pitch through 180 deg, while the locally level platform may be required to pitch through onl6 90 deg. Still, this may exceed the capabilities of the gyroscopes employed.

---

[1] For example of one inventive system see Chatkoff, Marvin L. and Lynch, Lewis G., "Attitude Control of a Space Vehicle by a Gyroscopic Reference Unit", Aero/Space Engineering, May 1960

If the system is strapped down, there is no remedy for the situation. Failure of the gyroscopes to precess rapidly enough will result in nonlinear operation of the instrument with attendant loss of attitude information.

If the platform gyrocompassing (indirect) is employed, the problem of excessive pitch rates may be side-stepped by locking the platform pitch gimbals to the vehicle. This presupposes that the vehicle will be attitude controlled. Previous investigation into the equations of motion for the locally level platform mechanization indicated that the pitch channel was completely (for small angular errors) decoupled from the roll-yaw channel. If this is the case, then there literally is no need to place the burden of platform rotation in pitch upon the pitch gyro. Analysis of errors in the roll-yaw channels proceeds identically to that described in Chapter 7.

If a full inertial platform is not required for any phases of vehicle navigation, then the pitch gyro may be eliminated and a two-axis platform may be substituted for the full inertial platform. Such a device has been designed and laboratory tested by MIT[1]. It supplies only roll-yaw information. Pitch information may be supplied by the vehicle attitude control system.

While the roll-yaw channels may be uncoupled from errors in pitch, they are not unaffected by variations in pitch rate. It will be recalled that W_y (the platform angular rotation rate about the y-axis) provided cross-coupling between yaw and roll errors. This angular rate appears in the dynamical error equations. If it is a variable rather than a constant, the effect of such variation on the dynamic response of the roll-yaw feedback system must be studied. However, there is no reason to believe that the nonuniform pitch rate profile associated with the boost trajectory would result in instability of any form. If transients in pitch rate occurring during the early stages of boost introduce undesirable disturbances in the roll-yaw mechanization, gyrocompassing could be delayed until the final state.

This roll-yaw mechanization might be usefully employed during the orbital phase of a space mission. Again, this obviates the requirement of high precession rates for the pitch gyro. The only essential requirements are attitude control of the vehicle in pitch and some indication of the local vertical which will supply a measure of platform roll.

2.2 Vertical Reference

The requirement for a vertical reference suggests that gyrocompassing during boost must be restricted to such time as the horizon sensor may be operative. Actually, if the vehicle is in a controlled trajectory, then the guidance control system must have resonably accurate knowledge of the local vertical. Such knowledge may even be preprogrammed, but it must be present either explicitly or implicitly. This information could be transmitted for use by the gyrocompassing system. The system being gyrocompassed cannot be the system providing steering control.

---

[1] Final Technical Documentary Report for Contract AF04(695)-289, MIT R-441, MIT Instrumentation Laboratory, 10 March 1964 (Confidential)

Such an effort on behalf of early gyrocompassing is undoubtedly unjustified. The most reasonable approach would seem to be to utilize knowledge of vehicle attitude during the very last portion of powered flight to erect the gyrocompass platform in approximately the proper attitude. Closed loop gyrocompassing may or may not be possible prior to injection. Certainly, if the vehicle may be expected to tumble at injection, continuous closed loop gyrocompassing will be impossible because inability of the horizon sensor to function. In this event, open loop gyrocompassing operation may be employed until the vehicle is attitude stabilized. Open loop behavior of platform systems is discussed in Chapter 7. During the time that the vehicle was tumbling, it would not be possible to continue gyrocompassing unless a three-gimbal platform were used.

Gyrocompassing may be initiated prior to injection equally well with strapped down systems. However, there is probably no justification for doing so. If the vehicle tumbles upon injection, the rapid angular rates may produce sufficient commutation errors and instrument errors during the open loop updating period to negate the advantages of an early start.

3. Spin Stabilized Vehicles

It is possible to stabilize a vehicle in orbit gyroscopically by spinning it about its pitch axis. If this were done, it would be preferable to mount the horizon sensor at one end so that it might rotate counter to the vehicle spin and always present its input axis to the earth. If this is not done, then horizon sensor information will be available for only a portion of the spin period. During this time, closed loop gyrocompassing may be employed. While local vertical reference information is unavailable, it will be necessary to open loop gyrocompass; i.e., torque the platform according to the best information available so as to maintain it close to locally level. Obviously, the effectiveness of gyrocompassing will depend upon the ratio of improvement achieved during the open loop period to the degradation occurring during the open loop period. If this is not greater than unity in an r.m.s. sense, then gyrocompassing will probably not be possible. It certainly will not be possible without resort to more sophisticated means. If some knowledge of the vehicle motion may be inferred from orbital information or other sources, it may be possible to devise an optimum control law for platform motion (or for updating the direction cosine matrix in the strapped down case) between the times at which local vertical reference information is available. The study of such a problem appears quite involved as well as quite interesting. But, it is perhaps academic in nature inasmuch as the time required to obtain useful gyrocompassing alinement would undoubtedly be quite excessive under such circumstances.

In the more general case, the period of horizon sensor operation will be an appreciable portion of the spin period and very little degradation of alinement will take place during the open loop operation. The effective settling time may be approximated by dividing the settling time for continuous operation by the ratio of horizon sensor operating time to spin period.

4. Operation on Interplanetary Orbits

The basic limitation on gyrocompassing feasibility during interplanetary transit is simply the roll gyro drift rate divided by the orbital rotation rate. This represents the theoretical minimum azimuth error in radians. Unfortunately, vehicles en route to Mars will rotate about the sun at a rate comparable to .04 deg/hr. In order to achieve an r.m.s. accuracy of 1 deg in azimuth, the r.m.s. gyro drift rate would have to be at least as small as .0007 deg/hr. While this is a little beyond the capabilities of present day space gyros, it is by no means infeasible for the next ten years.

4.1 Utilization of Arbitrary Vertical References

It is clear that higher accuracy gyrocompassing can be achieved by increasing the orbital rotation rate. The same effect may be obtained for short time periods by using some close object in the orbit plane for a vertical line-of-sight reference. The horizon sensor (or other body sensor) tracking the close body will indicate a rapid rotation rate to the gyrocompassing system. There are two principle difficulties associated with this scheme. One is that the level reference for the vehicle is now established with respect to the near body and not the orbit. The second is that the rotation rate about the arbitrary body will change rapidly.

The former difficulty is not a very great one since it is usually not difficult to reacquire the sun and re-establish the proper level reference without altering the azimuth alinement. The latter depends upon how greatly the rotation rate changes. This is the parameter ω_0 in the mechanization equations of Chapters 7 and 8. If ω_0 varies appreciably over the interval of the longest system time constant, then system behavior is not well described by the equations of the previous chapters.

The conclusion is that gyrocompassing around bodies within the orbital plane, but not at the orbit center, may indeed prove useful as a means of improving azimuth alinement.

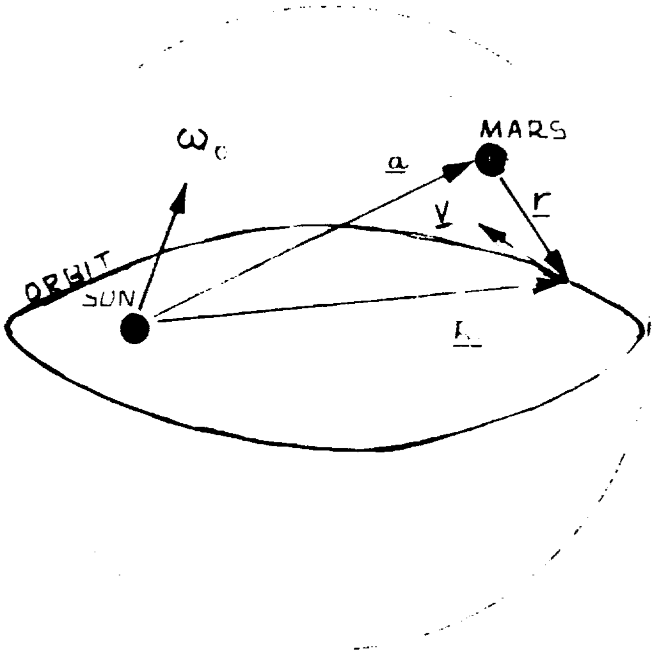

Fig. 4.1

Representation of lines-of-sight from the sun to vehicle and to out-of-plane object at Point a.

4.2 Out-of-Plane Objects

If gyrocompassing around in-plane objects is possible, what about out-of-plane objects? Let the situation be described by Fig. 4.1. The vehicle is in orbit around the sun. The out-of-plane object might be Mars, located by the vector $\underline{a}$ from the sun. The vector distance from Mars to the vehicle is $\underline{r}$ and from the sun to the vehicle is $\underline{R}$. Vehicle velocity tangential to the orbit is given by $\underline{V}$. This is the total velocity vector and is constant only in the special case of a circular orbit. However, for short periods of time, it may be assumed constant, as also may $\underline{R}$.

Orbital rotation rate is ω_o. The rotation rate about Mars is

$$\omega_{\text{Mars}} = \frac{\underline{r} \times \underline{v}}{r \cdot r} \qquad (4.1)$$

The vector $\underline{r}$ may be broken into in-plane and out-of-plane components, $\underline{r_i}$ and $\underline{r_o}$. Equation 4.1 then becomes:

$$\frac{\underline{r} \times \underline{v}}{r \cdot r} = \frac{\underline{r_i} \times \underline{v} + \underline{r_o} \times \underline{v}}{r_i^2 + r_o^2} = \frac{\underline{r_i} \times \underline{v} + \underline{r_o} \times \underline{v}}{r_i^2 \, (1 + \frac{r_o^2}{r_i^2}}$$

$$= \frac{\underline{r_i} \times \underline{v}}{r_i^2} \left(1 - \frac{r_o^2}{r_i^2} + \frac{r_o^4}{r_i^4} \quad \ldots \right)$$

$$+ \frac{\underline{r_o} \times \underline{v}}{r_i^2} \left(1 - \frac{r_o^2}{r_i^2} + \frac{r_o^4}{r_i^4} \quad \ldots \right)$$

$$\frac{\underline{r_i} \times \underline{v}}{r_i^2} + \frac{\underline{r_o} \times \underline{v}}{r_i^2} \qquad \frac{r_o}{r_o} \qquad 1 \qquad (4.2)$$

The first term to the right of the approximately equal sign is an angular rotation perpendicular to the plane of the orbit. This is the desired direction for an azimuth reference. The second term is an angular rotation lying wholly within the plane of the orbit. This contributes to an azimuth reference which is not true orbital north. Furthermore, this cannot be corrected unless the exact values of r_i and r_o are known. But, r_i can only be known if the exact vehicle position is known. If such knowledgs is available, correction for out-of-plane reference objects may be made. Otherwise, the ratio of r_o to r_i must be sufficiently small so as to satisfy the gyrocompassing accuracy requirements without correction.

APPENDIX A

TIME HISTORY OF ALINEMENT ERRORS FOR ONE EXAMPLE OF INDIRECT TERRESTRIAL GYROCOMPASSING

The following graphs show a time history of attitude errors resulting from selected error sources. They may be thought of as error sensitivities. Attitude errors are in rms seconds of arc along the axis of ordinates and time in seconds is plotted along the axis of abscissas. The error source for each curve is labeled at top left. Magnitudes are rms.

In some instances the error sources could equally well be deterministic. The attitude errors plotted would then be absolute value of seconds of arc rather than rms seconds.

Whether considered deterministic or rms, the attitude error associated with each error source scales directly with the magnitude of the error source, with the exception of correlated noise. The effect of variation in correlation time does not scale.

Instrument configuration is shown in Fig. 5.1 of Chapter IV. The actual characteristic equation is Eq. (5.2) of the same chapter. Figure A-1 is a block diagram for the system whose response is characterized by the graphs of the following pages.

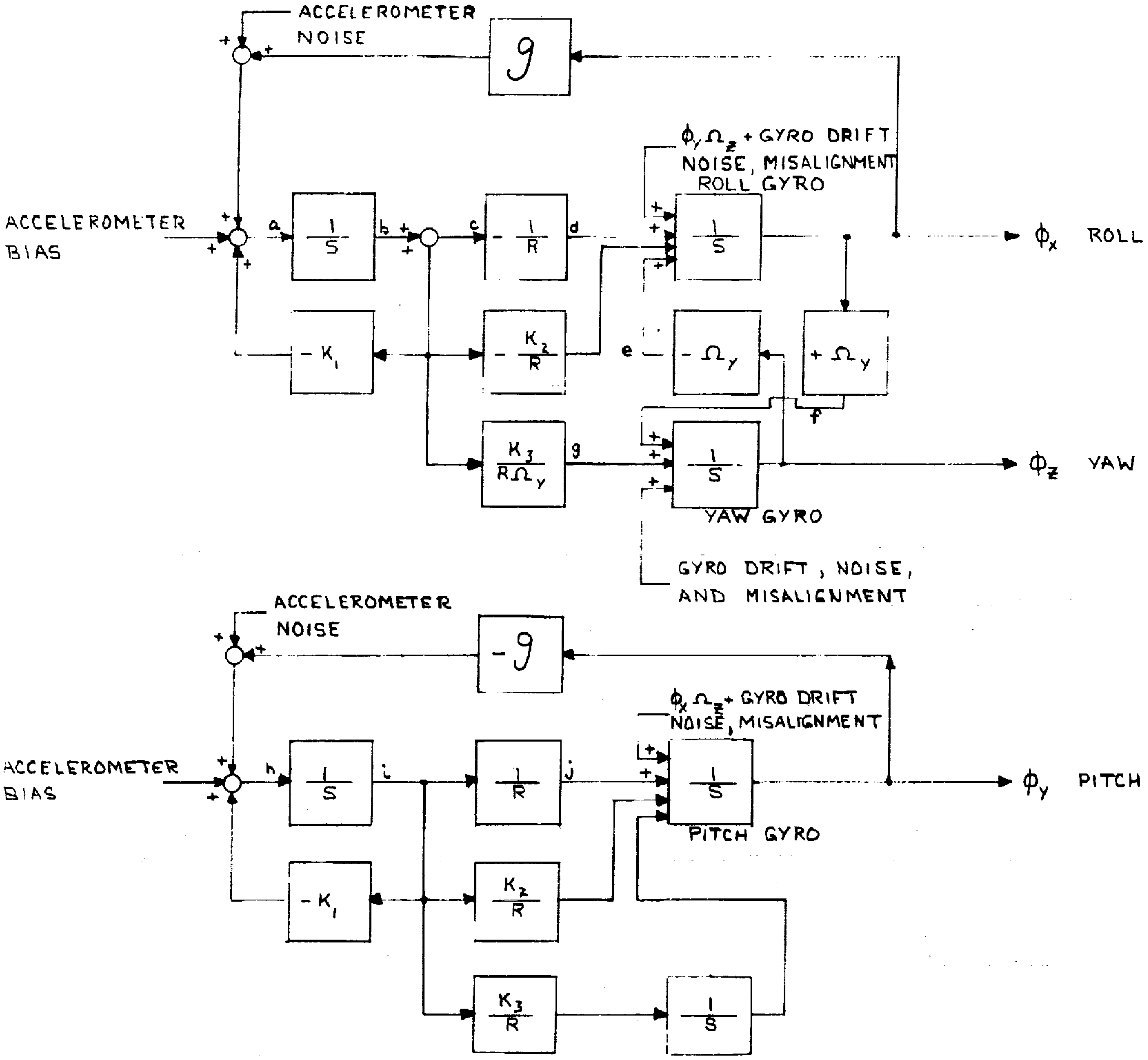
ACCELEROMETER NOISE
g
$\phi_y \Omega_z$ + GYRO DRIFT NOISE, MISALIGNMENT
ROLL GYRO
ACCELEROMETER BIAS
a
$\frac{1}{S}$
b
c
$-\frac{1}{R}$
d
$\frac{1}{S}$
ϕ_x ROLL
$-K_1$
$-\frac{K_2}{R}$
e
$-\Omega_y$
$+\Omega_y$
f
$\frac{K_3}{R\Omega_y}$
g
$\frac{1}{S}$
ϕ_z YAW
YAW GYRO
GYRO DRIFT, NOISE, AND MISALIGNMENT
ACCELEROMETER NOISE
$-g$
$\phi_x \Omega_z$ + GYRO DRIFT NOISE, MISALIGNMENT
ACCELEROMETER BIAS
h
$\frac{1}{S}$
i
$\frac{1}{R}$
j
$\frac{1}{S}$
ϕ_y PITCH
PITCH GYRO
$-K_1$
$\frac{K_2}{R}$
$\frac{K_3}{R}$
$\frac{1}{S}$
+

Fig. A-1

Error Block Diagram of Gyrocompassing System

R =	radius of earth	K_1 =	
g =	acceleration of gravity	K_2 =	
Ω =	earth's rotation rate	K_3 =	

A1

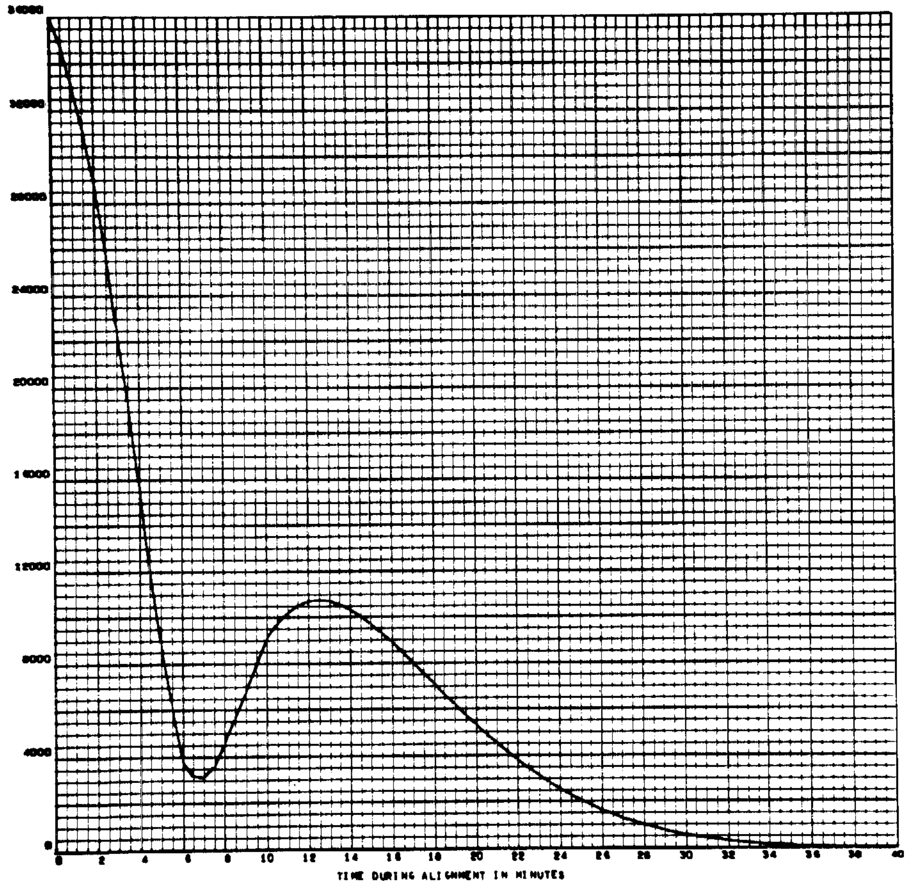
LEVEL TILT IN ARCSECONDS - GROUND GYROCOMPASSING
TOTAL RMS Y TILT

A2

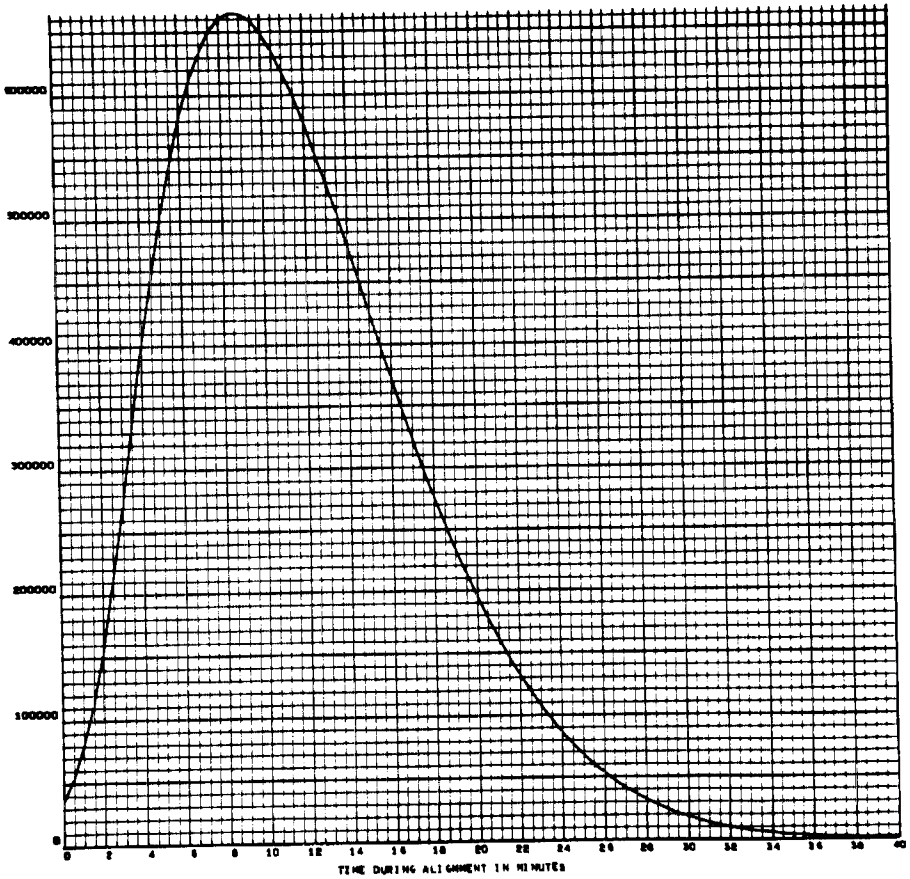
AZIMUTH MISALIGNMENT IN ARCSECONDS - GROUND GYROCOMPASSING
TOTAL RMS AZIMUTH MISALIGNMENT

1A3

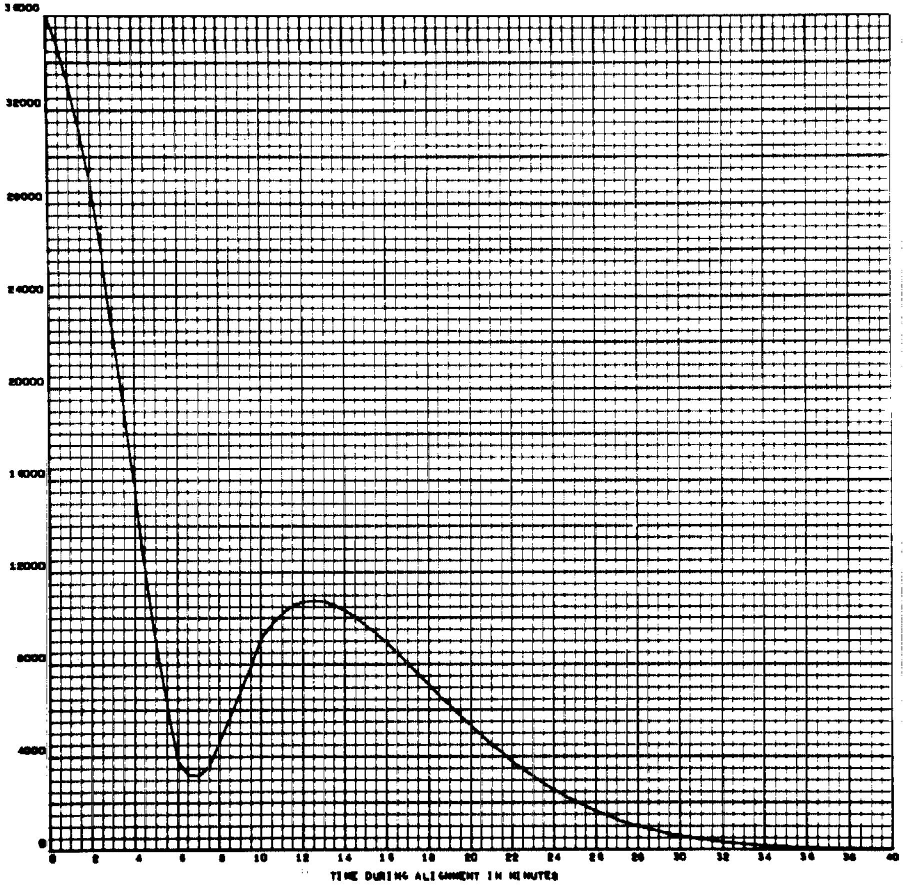

LEVEL TILT IN ARCSECONDS - GROUND GYROCOMPASSING
TOTAL RMS X TILT

1A4

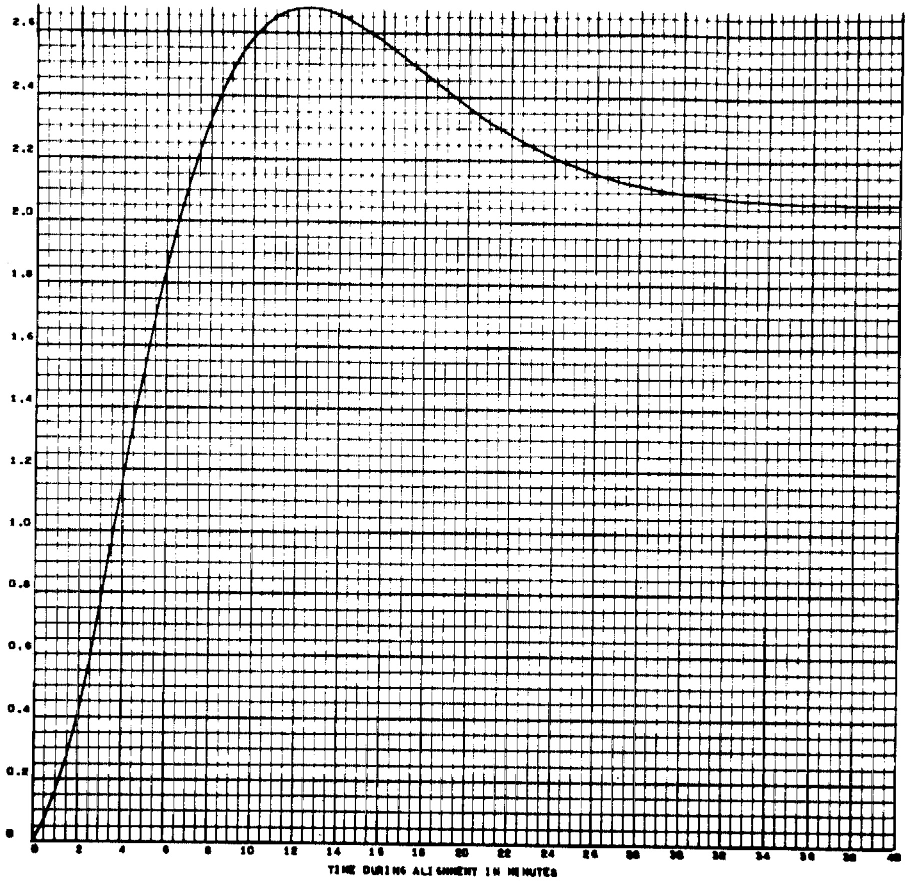

LEVEL TILT IN ARCSECONDS - GROUND GYROCOMPASSING
X TILT DUE TO Y ACCELEROMETER "F" TERM - 10 PPM

A5

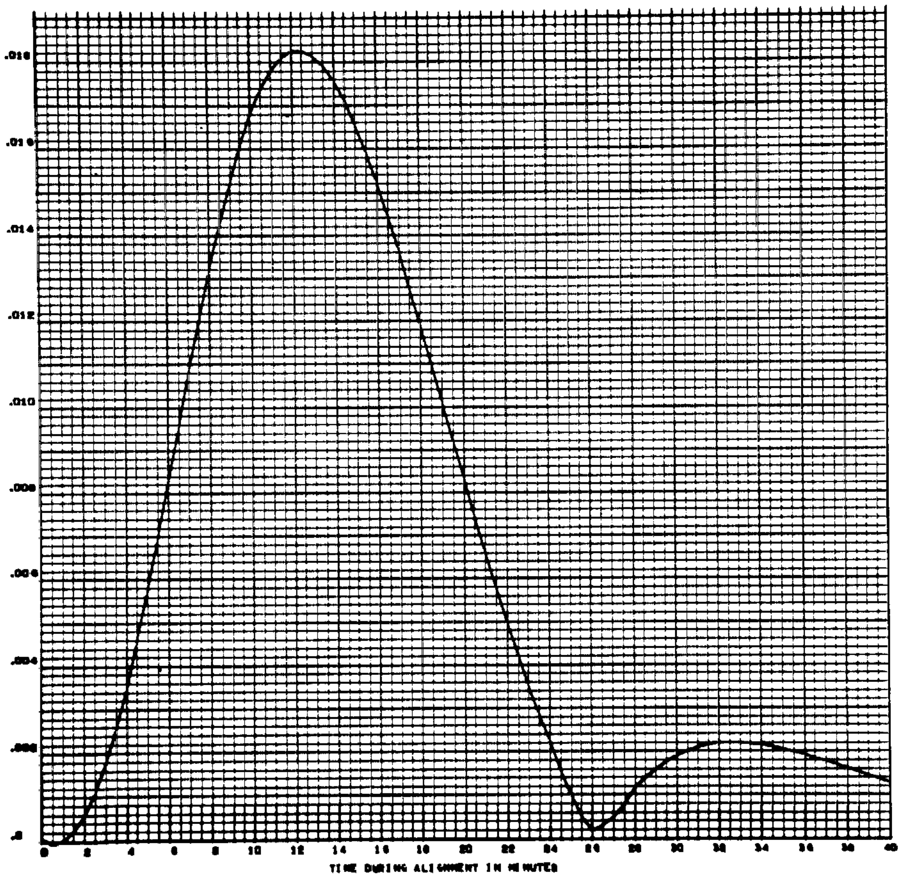
LEVEL TILT IN ARCSECONDS - GROUND GYROCOMPASSING
X TILT DUE TO X ACCELEROMETER "F" TERM - 10 PPM

A6

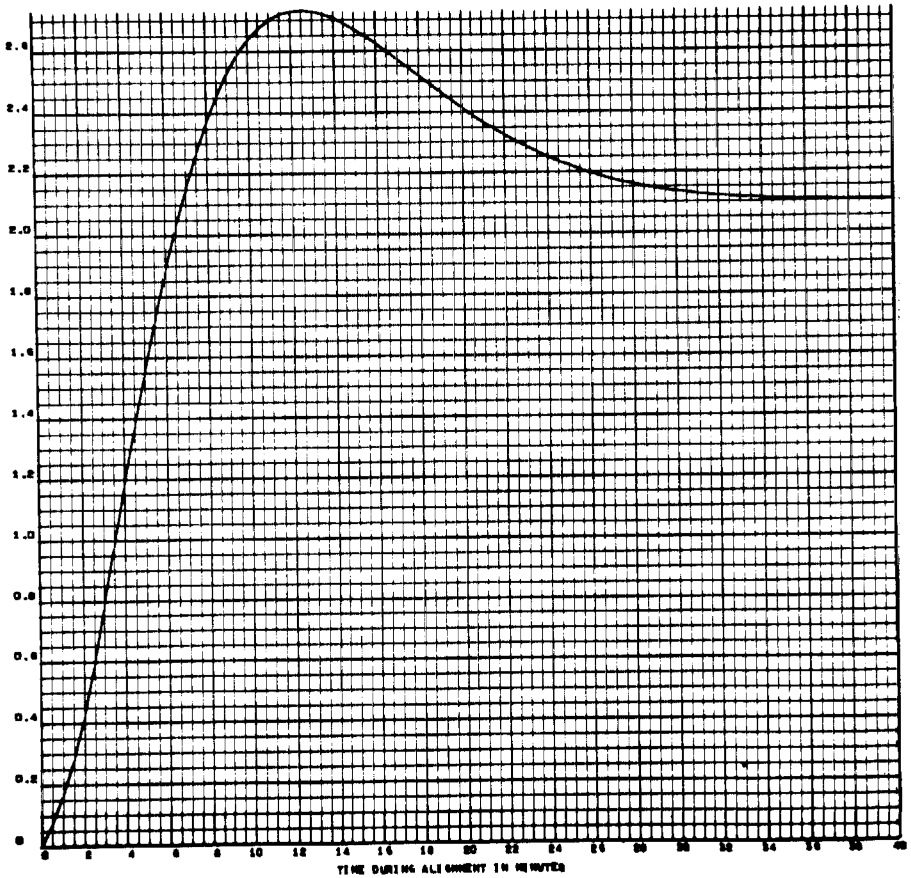
LEVEL TILT IN ARCSECONDS - GROUND GYROCOMPASSING
X TILT DUE TO Y ACCELEROMETER ERROR - .0001 METERS/SECOND SQUARED

7

LEVEL TILT IN ARCSECONDS - GROUND GYROCOMPASSING
X TILT DUE TO X ACCELEROMETER ERROR - .0001 METERS/SECOND SQUARED

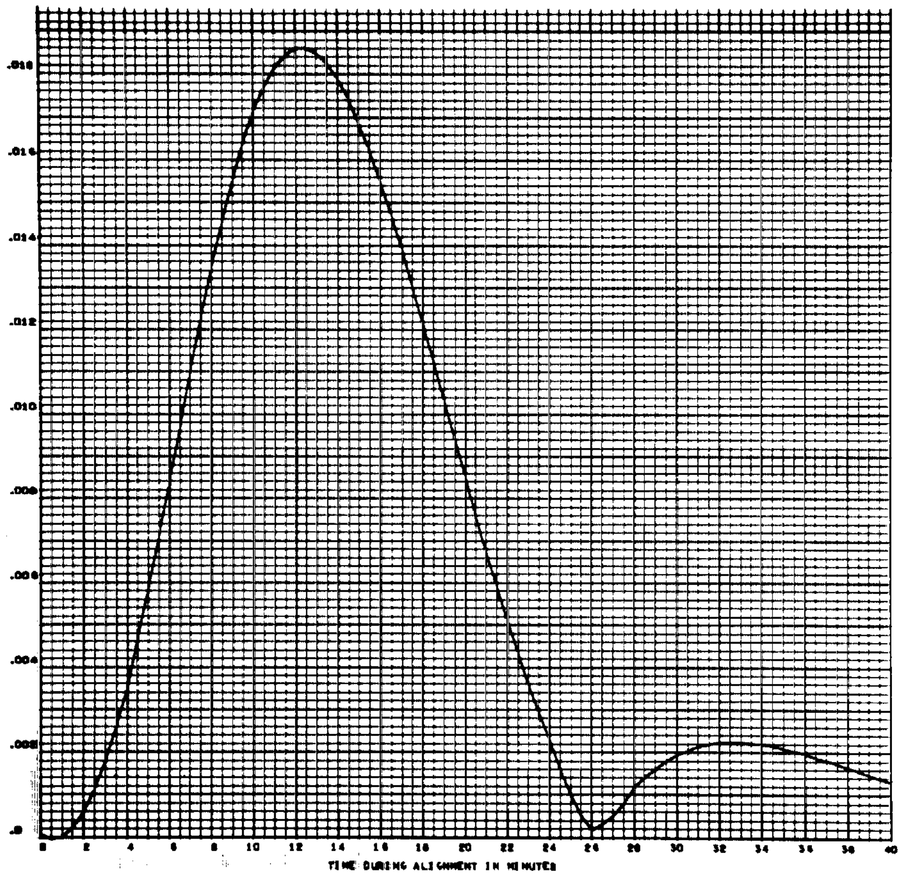

8

LEVEL TILT IN ARCSECONDS - GROUND GYROCOMPASSING
X TILT DUE TO Z GYRO MISALIGNMENT (Y AXIS) - 10 ARCSECONDS

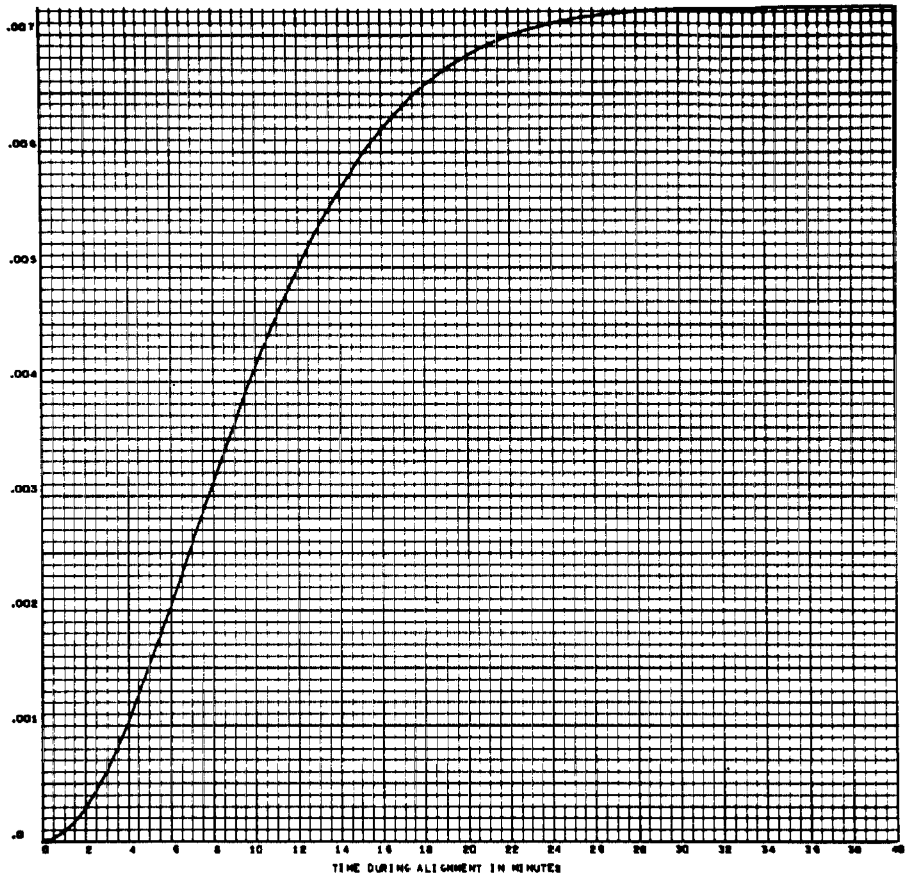

9

LEVEL TILT IN ARCSECONDS - GROUND GYROCOMPASSING
X TILT DUE TO Y GYRO MISALIGNMENT (Z AXIS) - 10 ARCSECONDS

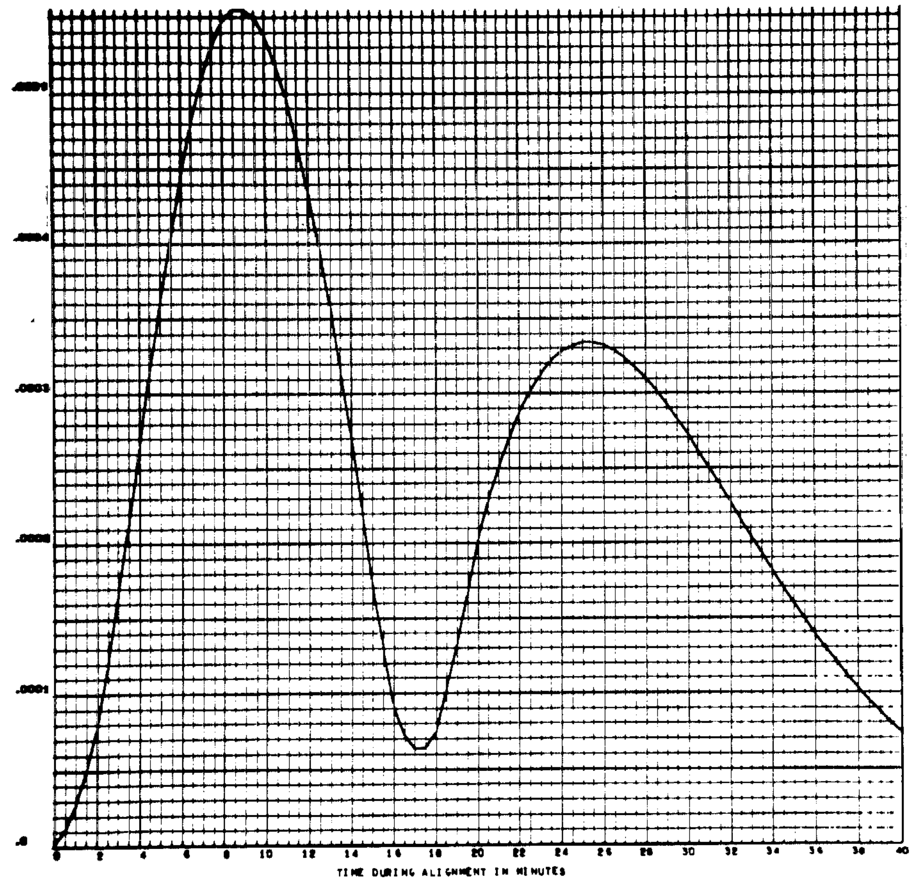

A/10

LEVEL TILT IN ARCSECONDS - GROUND GYROCOMPASSING
X TILT DUE TO X GYRO MISALIGNMENT (Z AXIS) - 10 ARCSECONDS

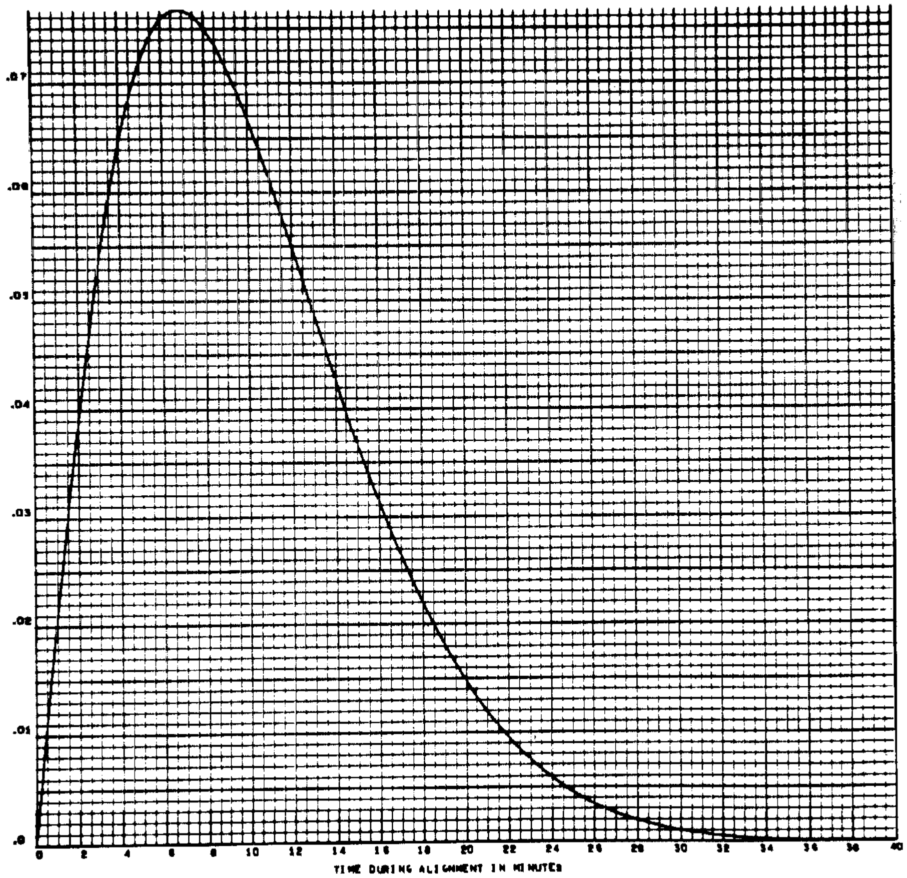

A11

LEVEL TILT IN ARCSECONDS - GROUND GYROCOMPASSING
X TILT DUE TO X GYRO MISALIGNMENT (Y AXIS) - 10 ARCSECONDS

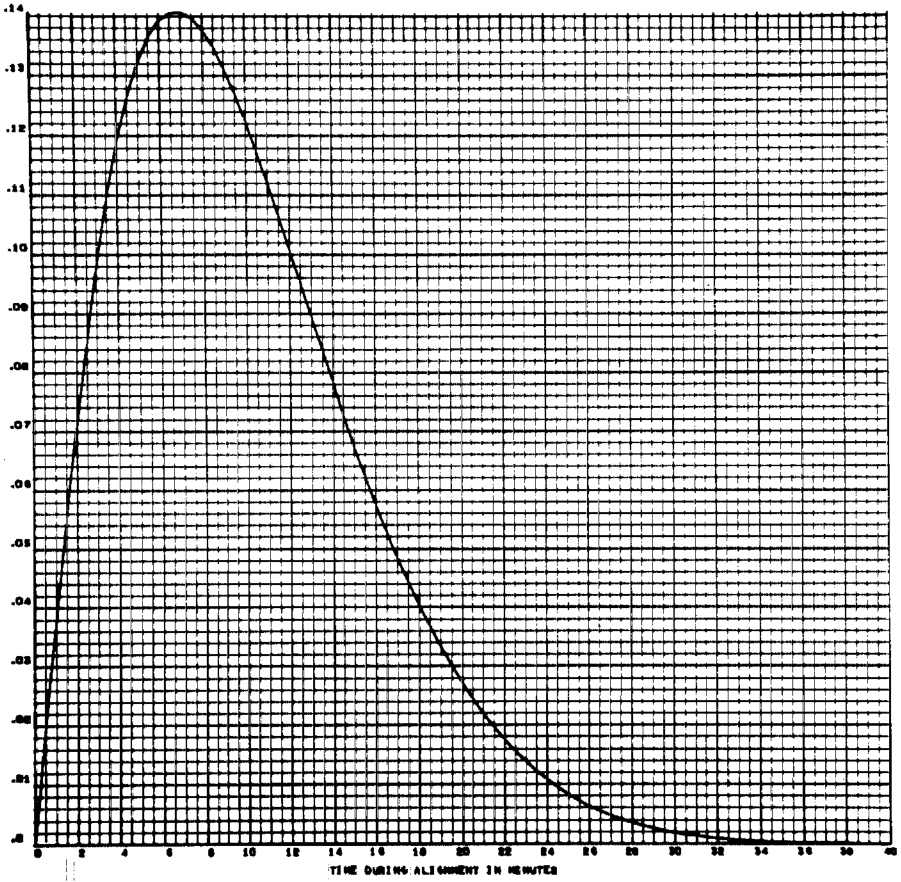

A12

LEVEL TILT IN ARCSECONDS - GROUND GYROCOMPASSING
X TILT DUE TO Z GYRO SCALE FACTOR ERROR - 100 PPM

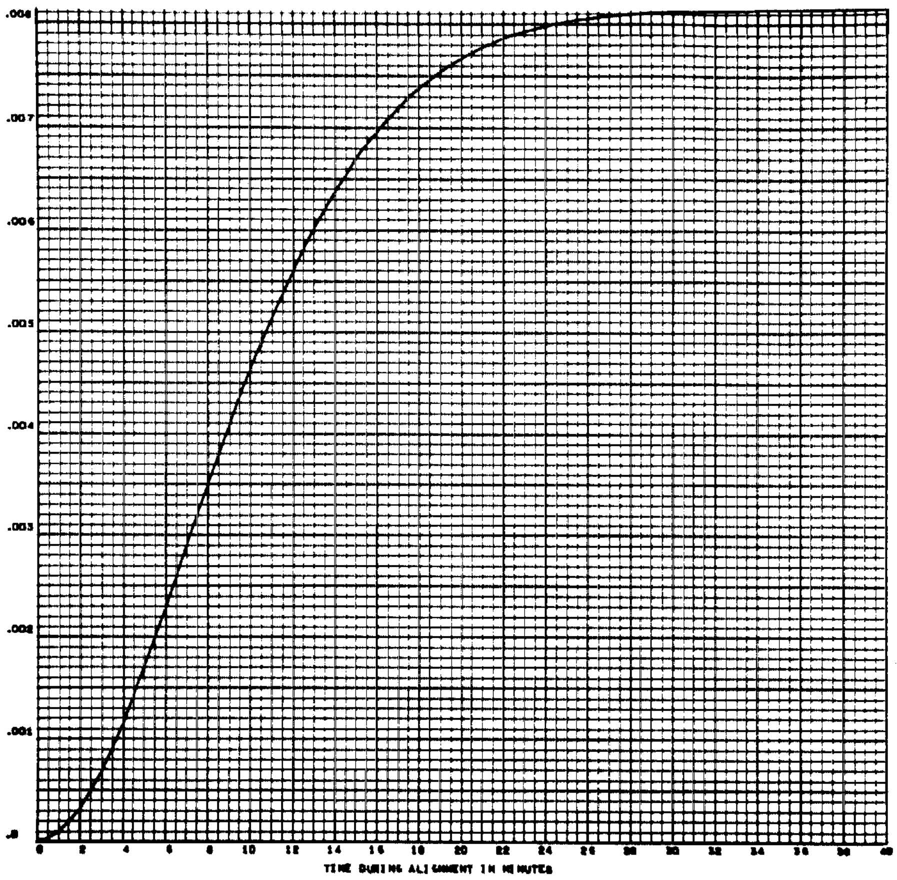

13

LEVEL TILT IN ARCSECONDS - GROUND GYROCOMPASSING
X TILT DUE TO Y GYRO SCALE FACTOR ERROR - 100 PPM

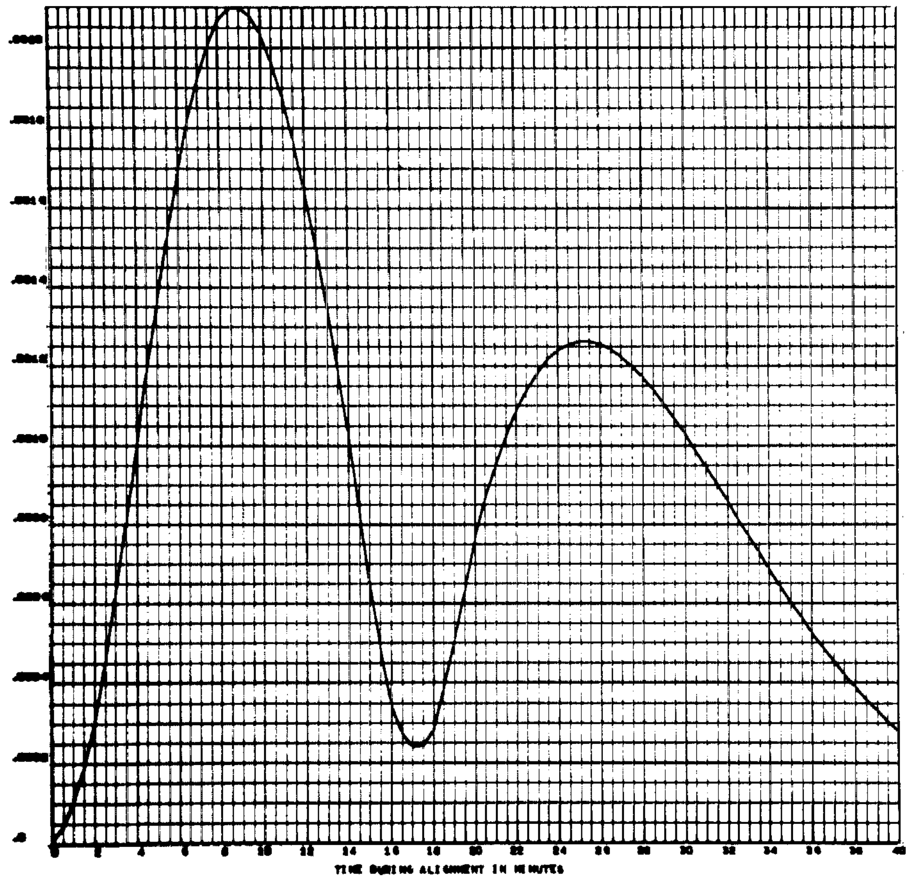

14

LEVEL TILT IN ARCSECONDS - GROUND GYROCOMPASSING
X TILT DUE TO INITIAL AZIMUTH MISALIGNMENT - 10 DEGREES

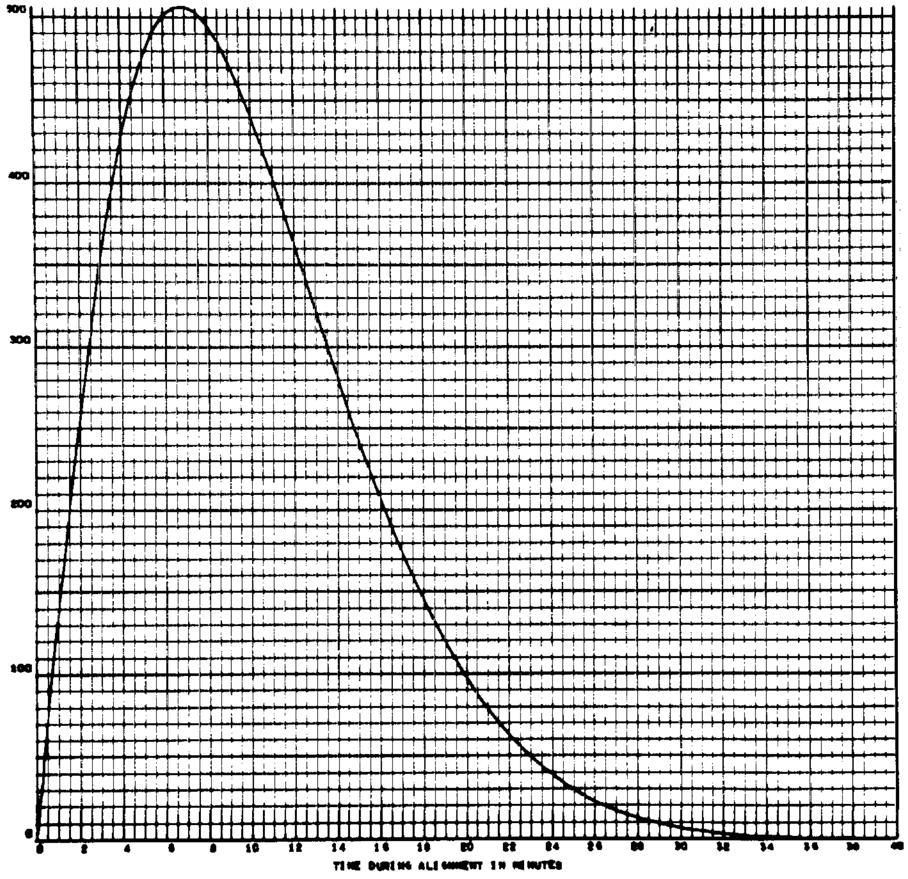

J/15

LEVEL TILT IN ARCSECONDS - GROUND GYROCOMPASSING
X TILT DUE TO INITIAL X TILT - 10 DEGREES

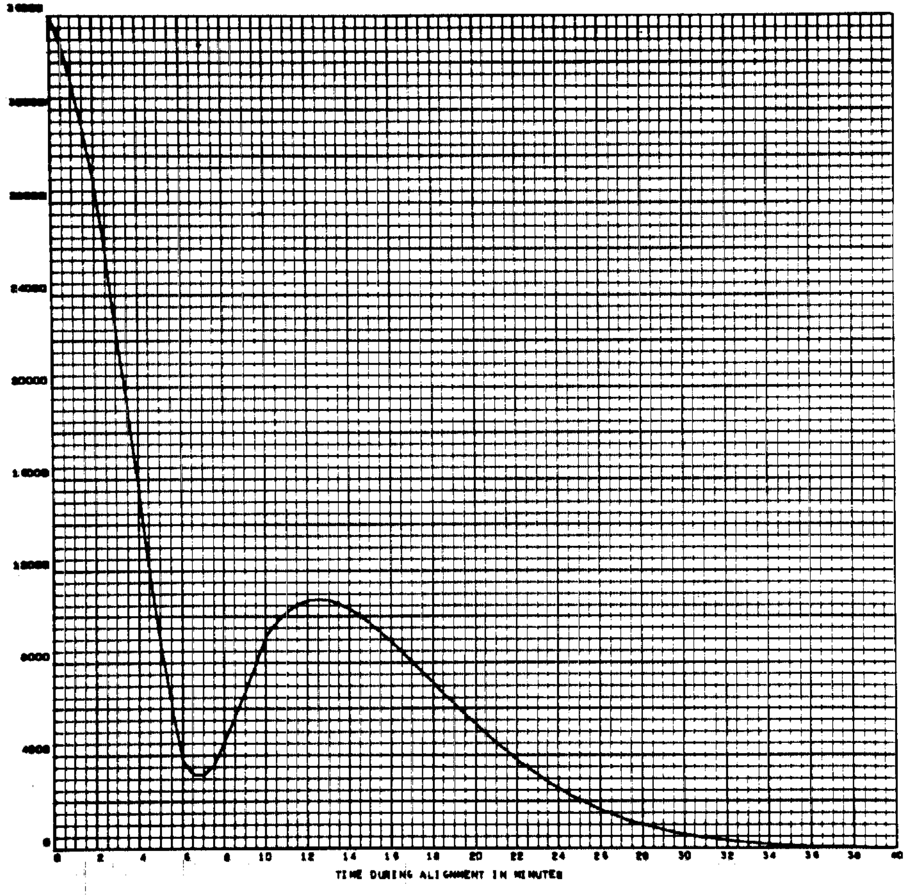

J/16

LEVEL TILT IN ARCSECONDS - GROUND GYROCOMPASSING
Y TILT DUE TO INITIAL Y TILT - 10 DEGREES

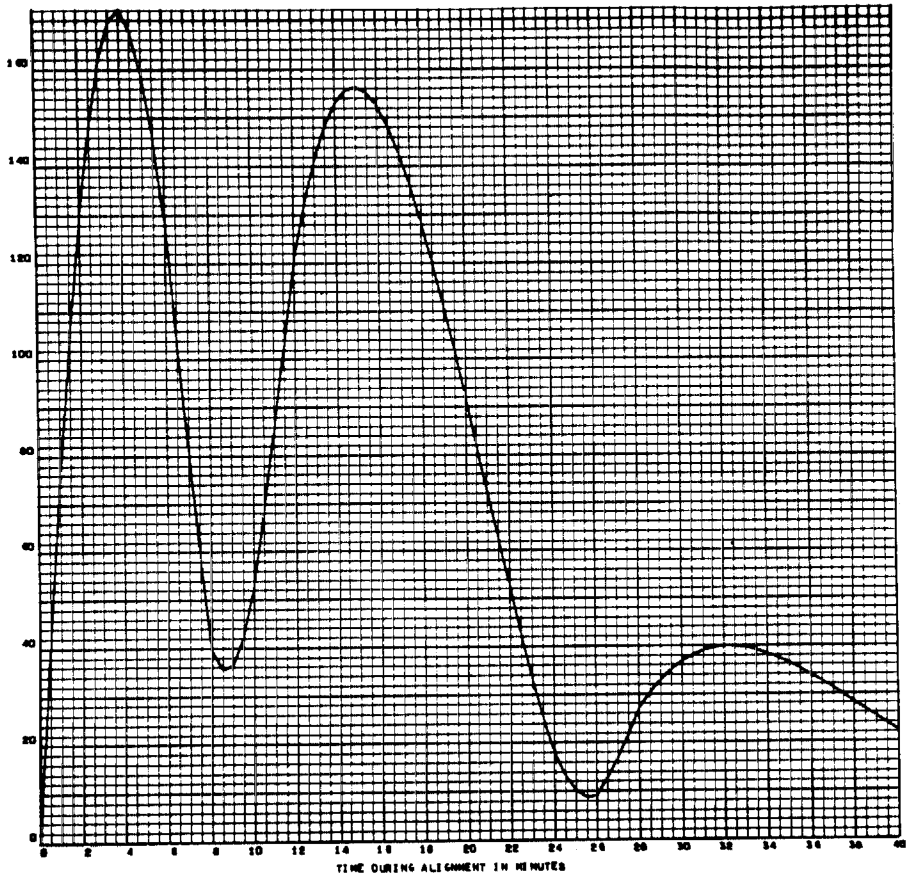

A17

LEVEL TILT IN ARCSECONDS - GROUND GYROCOMPASSING
X TILT DUE TO Z GYRO "P" TERM - .01 DEG/HR/G

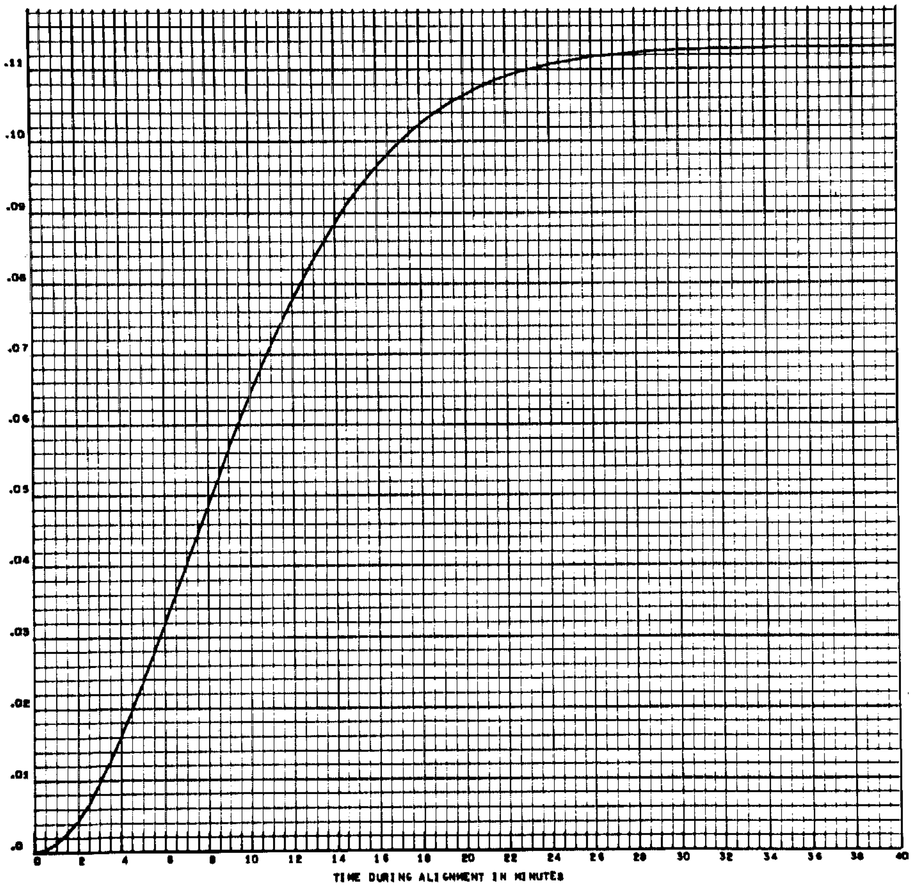

A18

LEVEL TILT IN ARCSECONDS - GROUND GYROCOMPASSING
X TILT DUE TO X GYRO "P" TERM - .01 DEG/HR/G

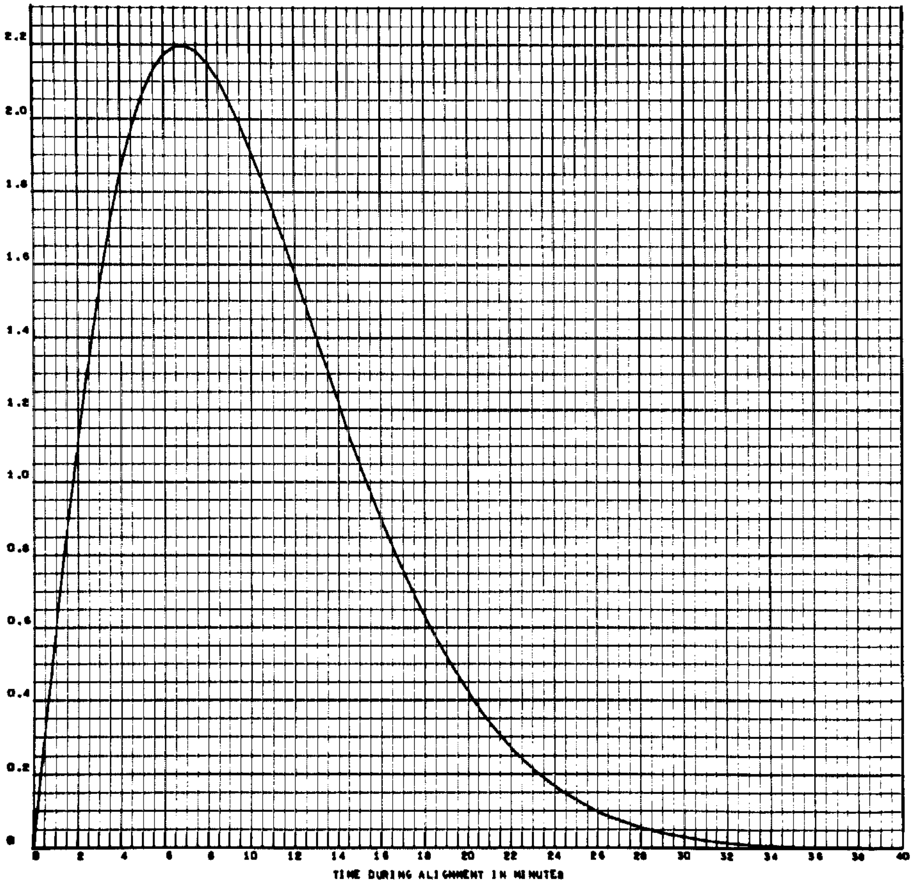

B19

LEVEL TILT IN ARCSECONDS - GROUND GYROCOMPASSING
X TILT DUE TO Y GYRO "F" TERM - .01 DEG/HR/G

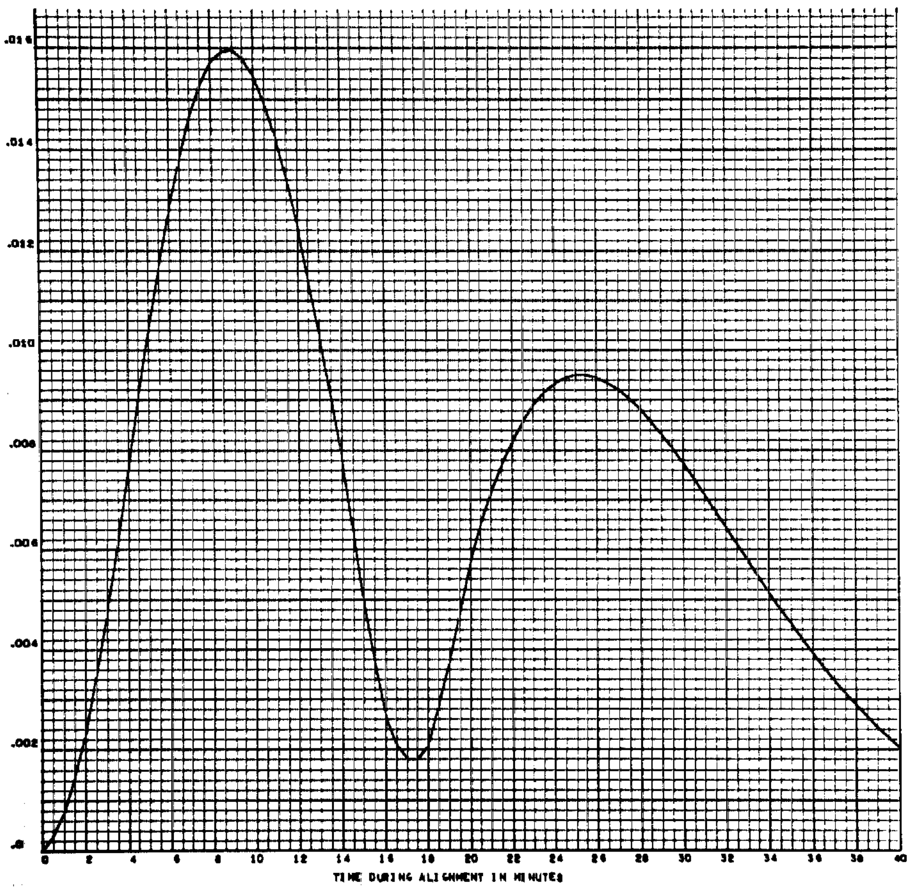

A20

LEVEL TILT IN ARCSECONDS - GROUND GYROCOMPASSING
X TILT DUE TO Z GYRO DRIFT - .01 DEG/HR

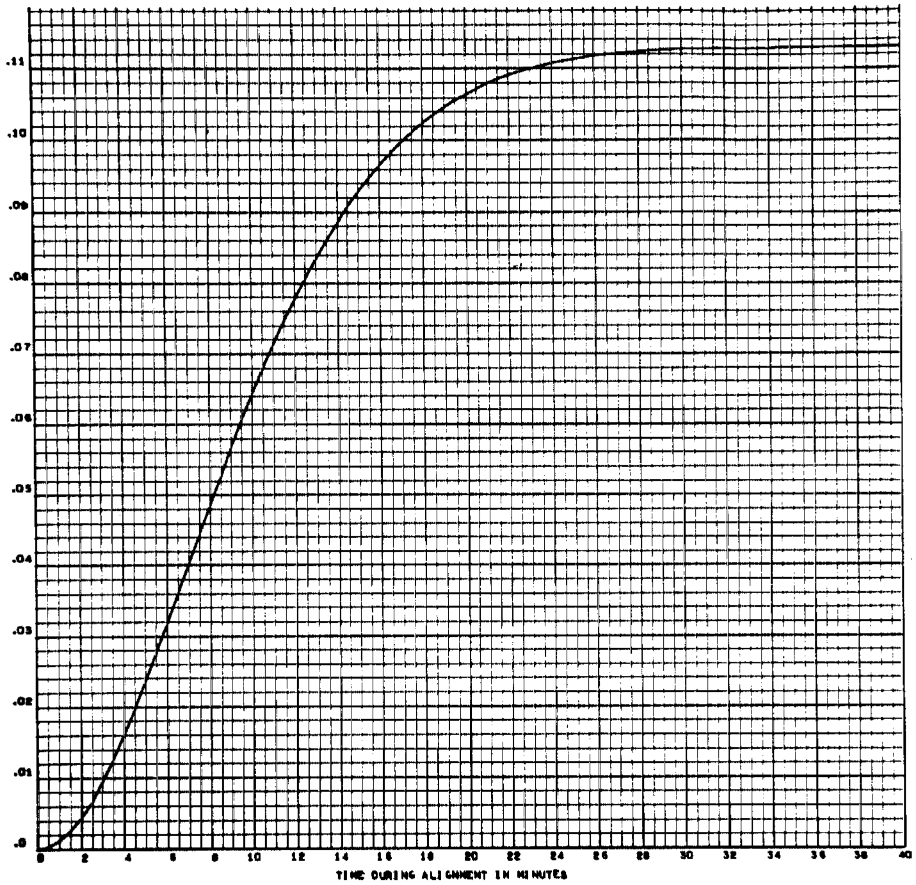

A21

LEVEL TILT IN ARCSECONDS - GROUND GYROCOMPASSING
X TILT DUE TO X GYRO DRIFT - .01 DEG/HR

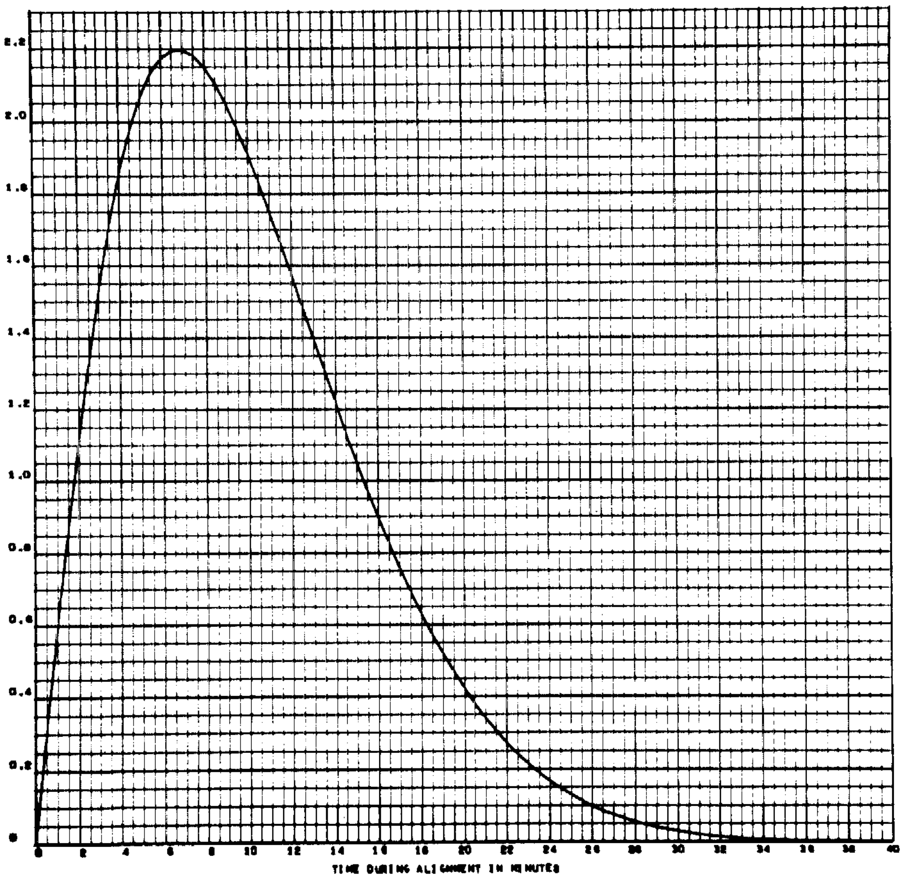

A22

LEVEL TILT IN ARCSECONDS - GROUND GYROCOMPASSING
X TILT DUE TO Y GYRO DRIFT - .01 DEG/HR

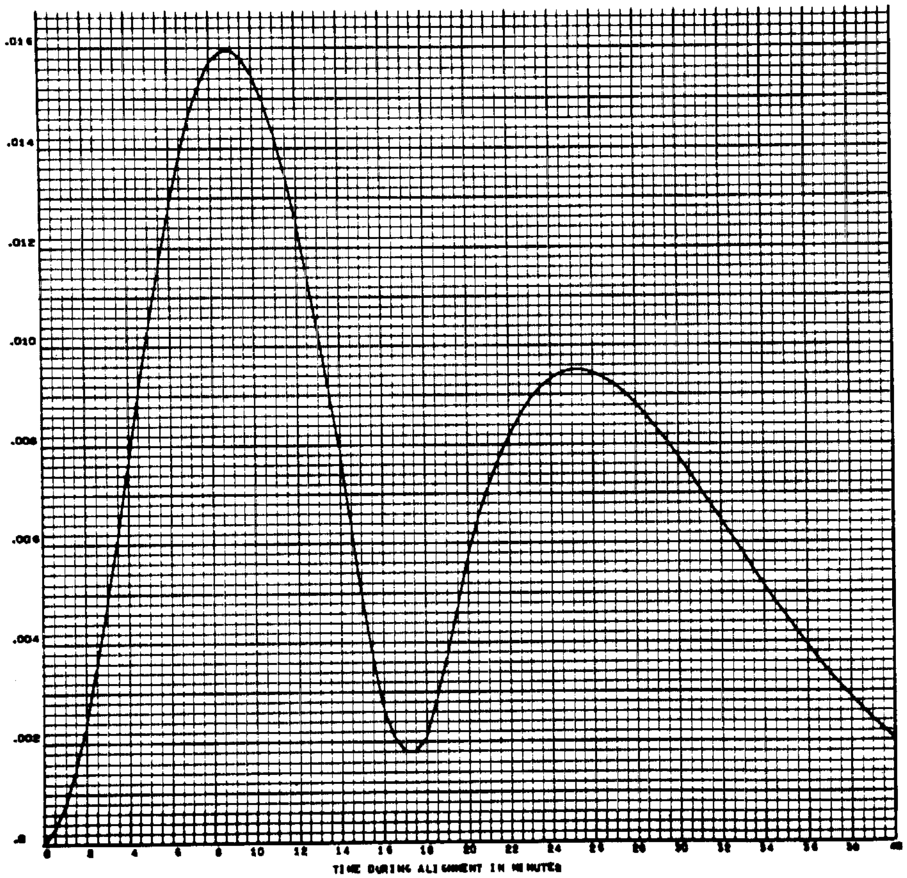

23

LEVEL TILT IN ARCSECONDS - GROUND GYROCOMPASSING
X TILT DUE TO Y ACCELEROMETER MISALIGNMENT - 10 ARCSECONDS

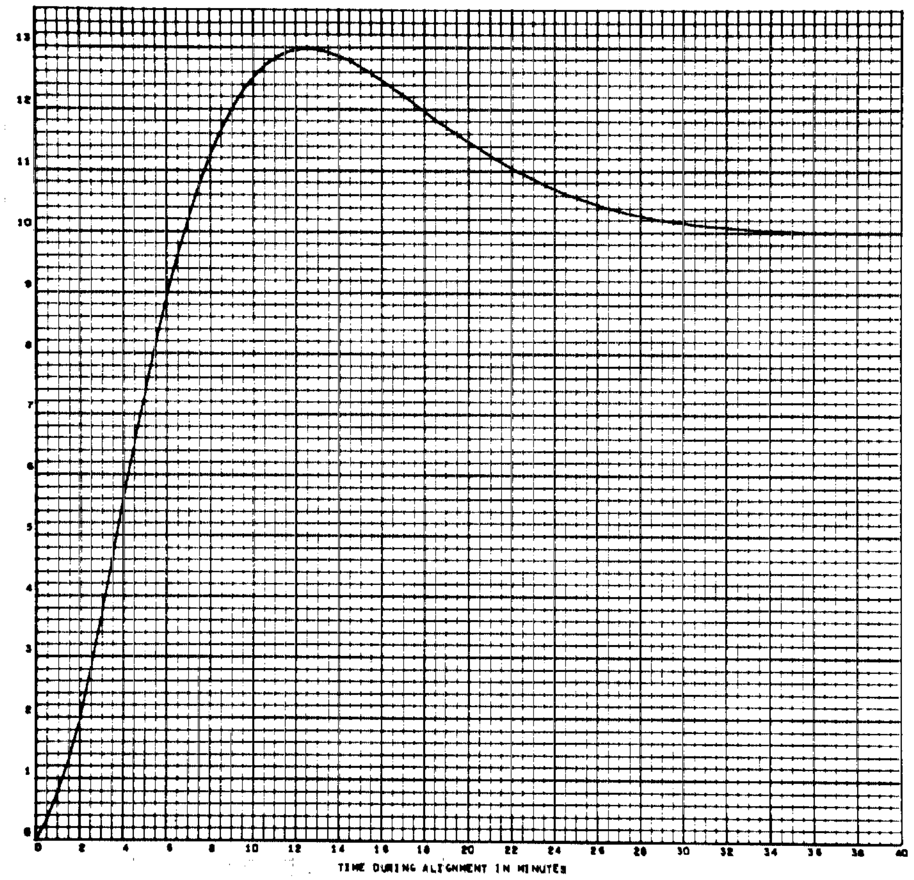

24

LEVEL TILT IN ARCSECONDS - GROUND GYROCOMPASSING
X TILT DUE TO X ACCELEROMETER MISALIGNMENT - 10 ARCSECONDS

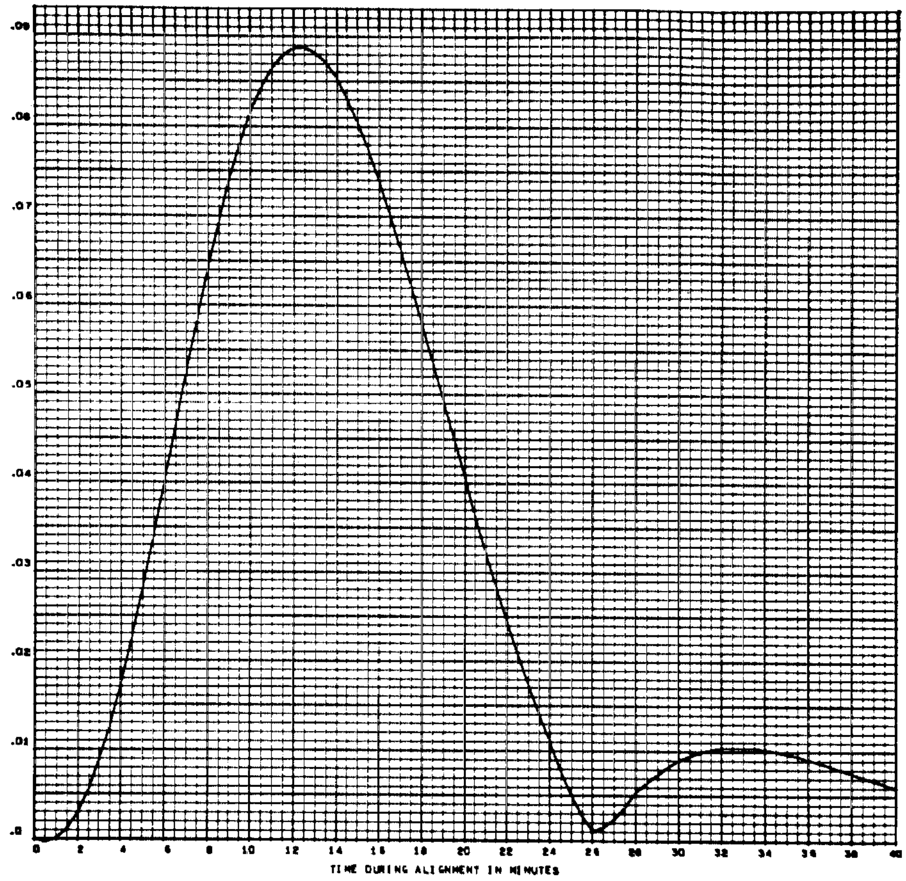

A25

AZIMUTH MISALIGNMENT IN ARCSECONDS - GROUND GYROCOMPASSING
ERROR DUE TO Y ACCELEROMETER "F" TERM - 10 PPM

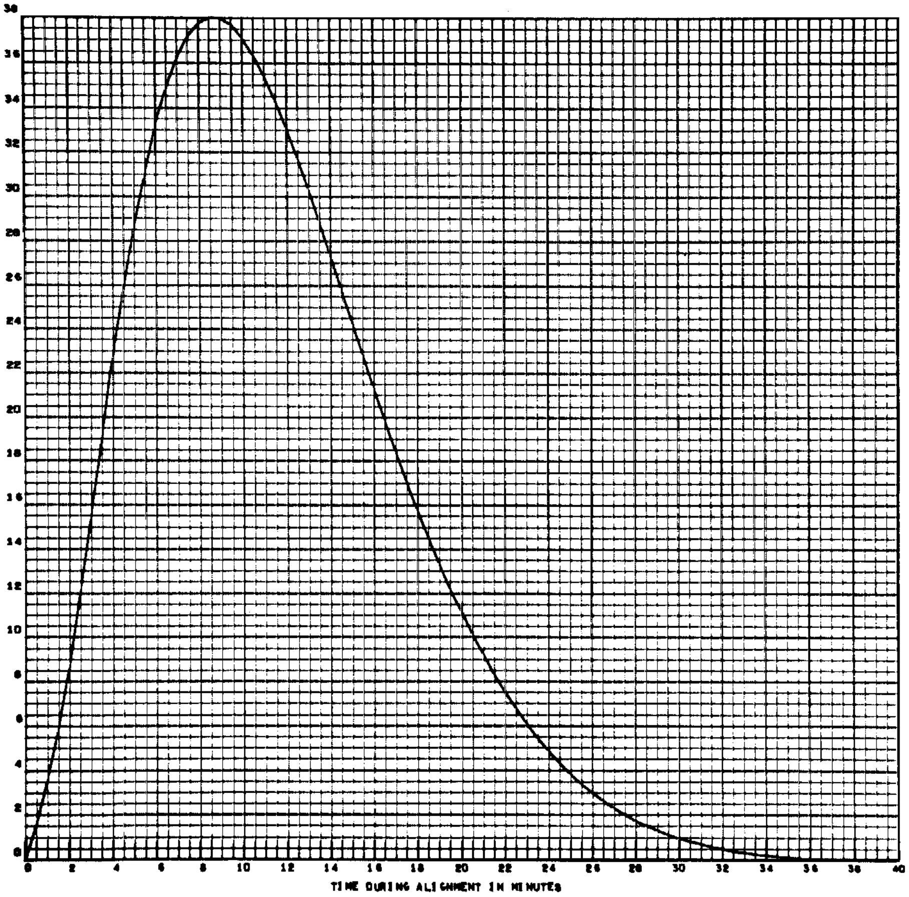

A26

AZIMUTH MISALIGNMENT IN ARCSECONDS - GROUND GYROCOMPASSING
ERROR DUE TO X ACCELEROMETER "F" TERM - 10 PPM

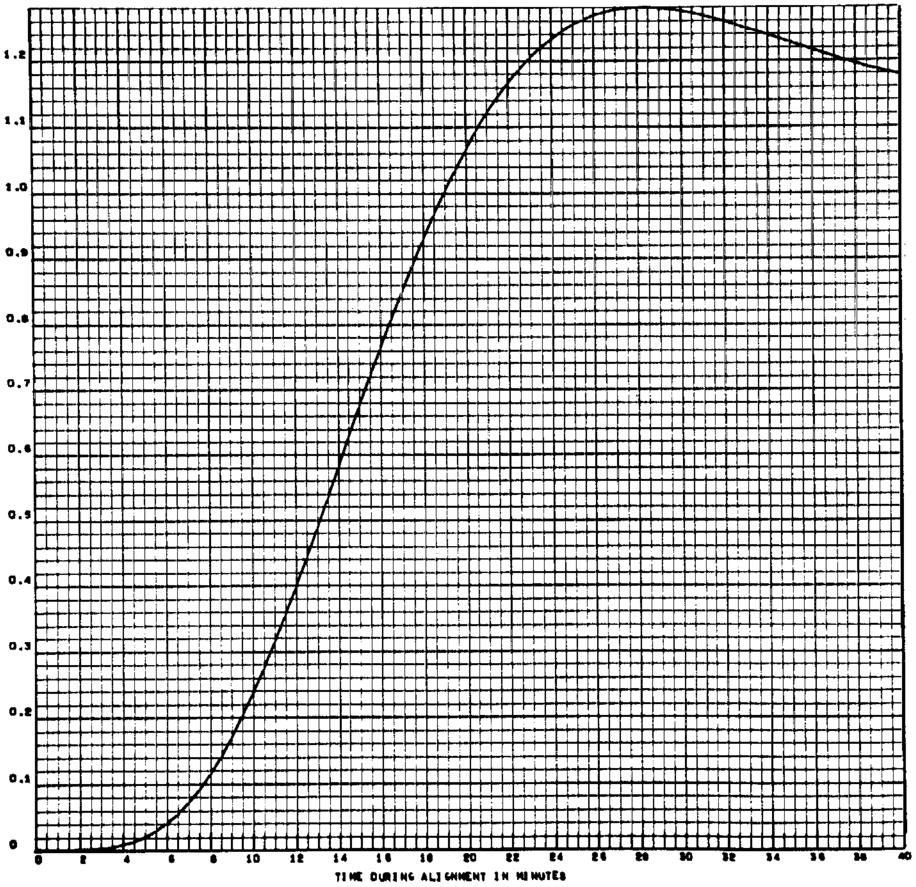

A27

AZIMUTH MISALIGNMENT IN ARCSECONDS - GROUND GYROCOMPASSING
ERROR DUE TO Y ACCELEROMETER ERROR - .0001 METERS/SECOND SQUARED

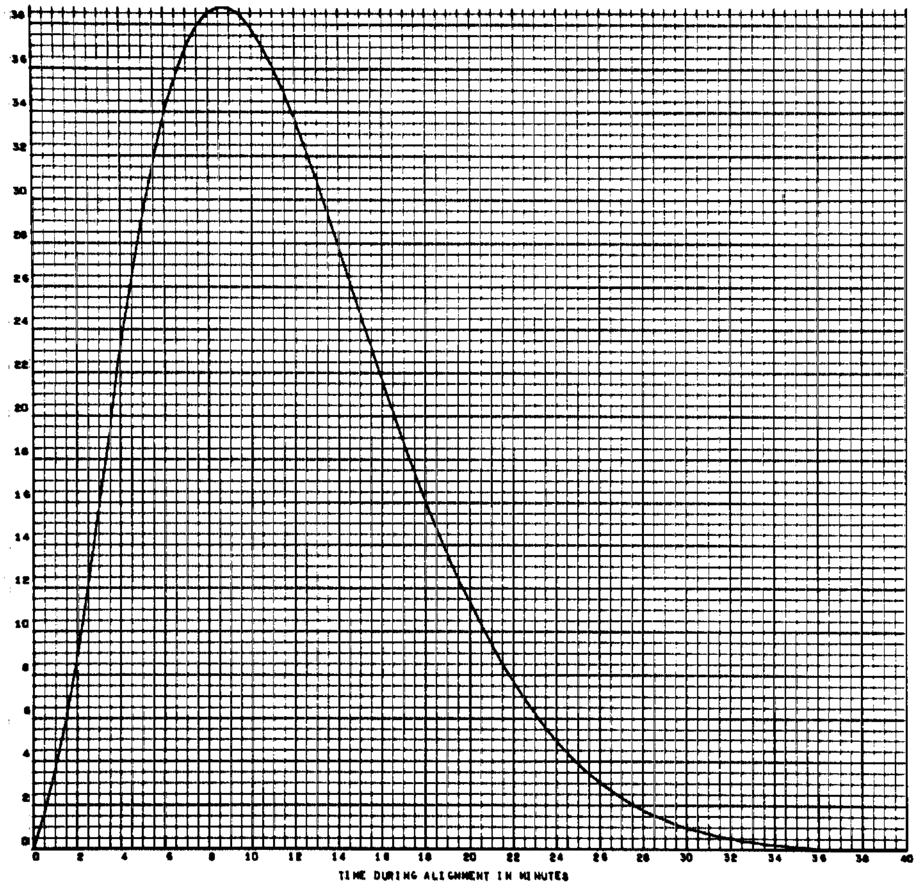

A28

AZIMUTH MISALIGNMENT IN ARCSECONDS - GROUND GYROCOMPASSING
ERROR DUE TO X ACCELEROMETER ERROR - .0001 METERS/SECOND SQUARED

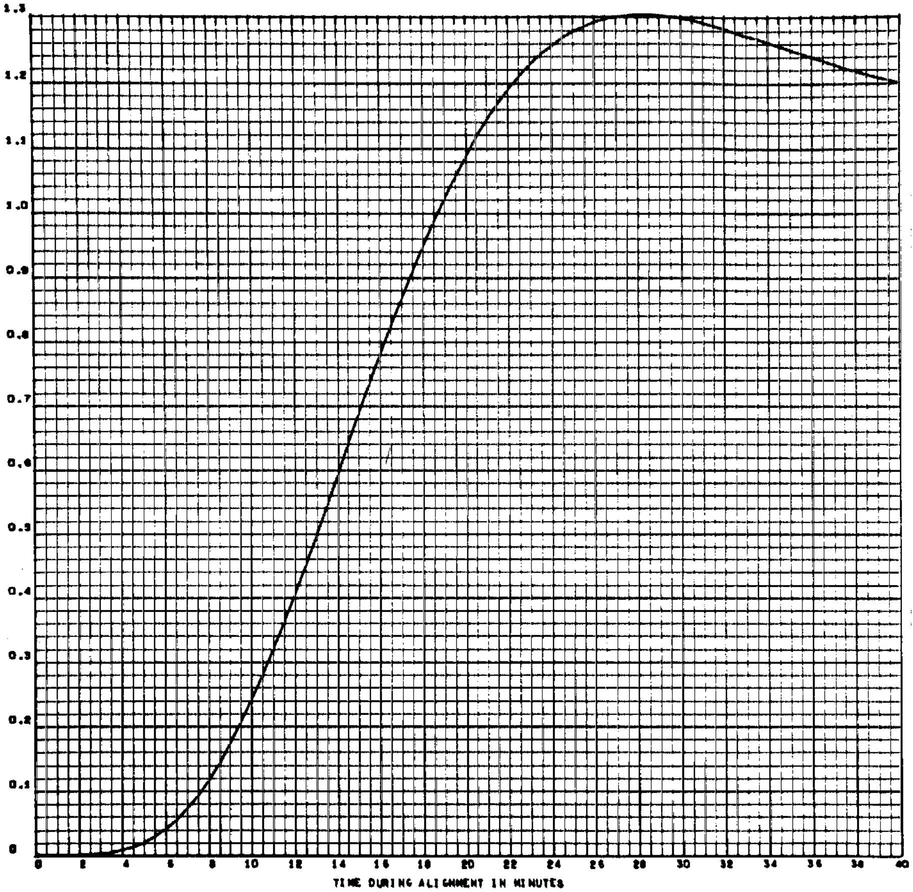

A29

AZIMUTH MISALIGNMENT IN ARCSECONDS - GROUND GYROCOMPASSING
ERROR DUE TO Z GYRO MISALIGNMENT (Y AXIS) - 10 ARCSECONDS

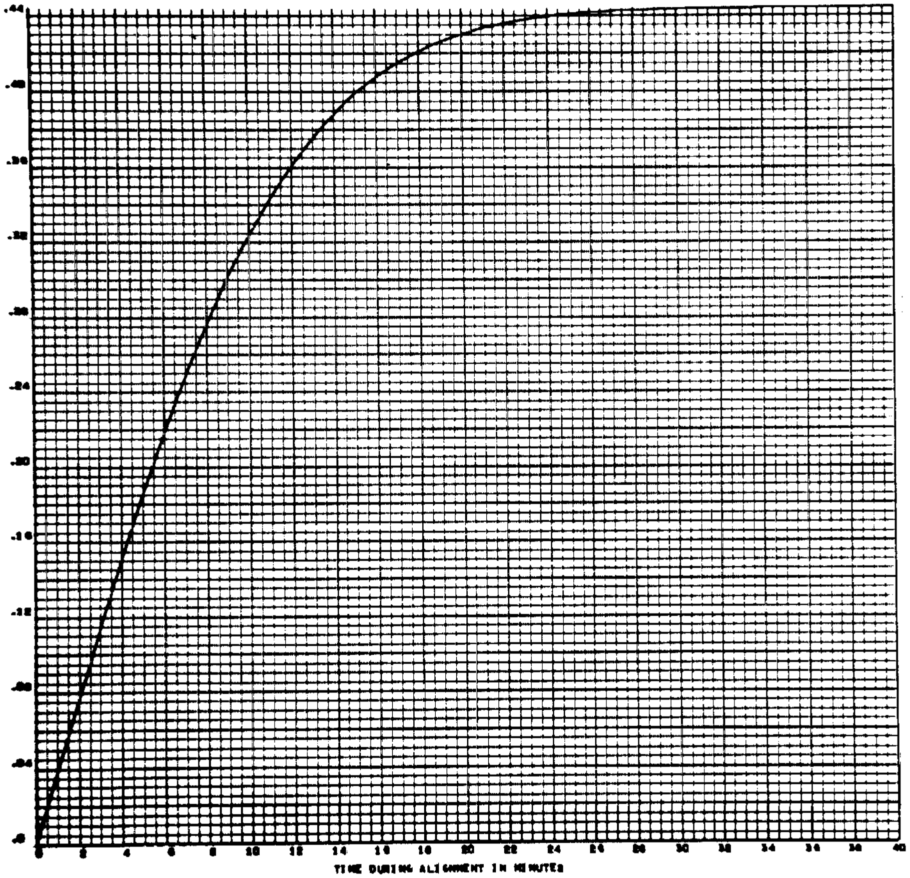

A30

AZIMUTH MISALIGNMENT IN ARCSECONDS - GROUND GYROCOMPASSING
ERROR DUE TO Y GYRO MISALIGNMENT (Z AXIS) - 10 ARCSECONDS

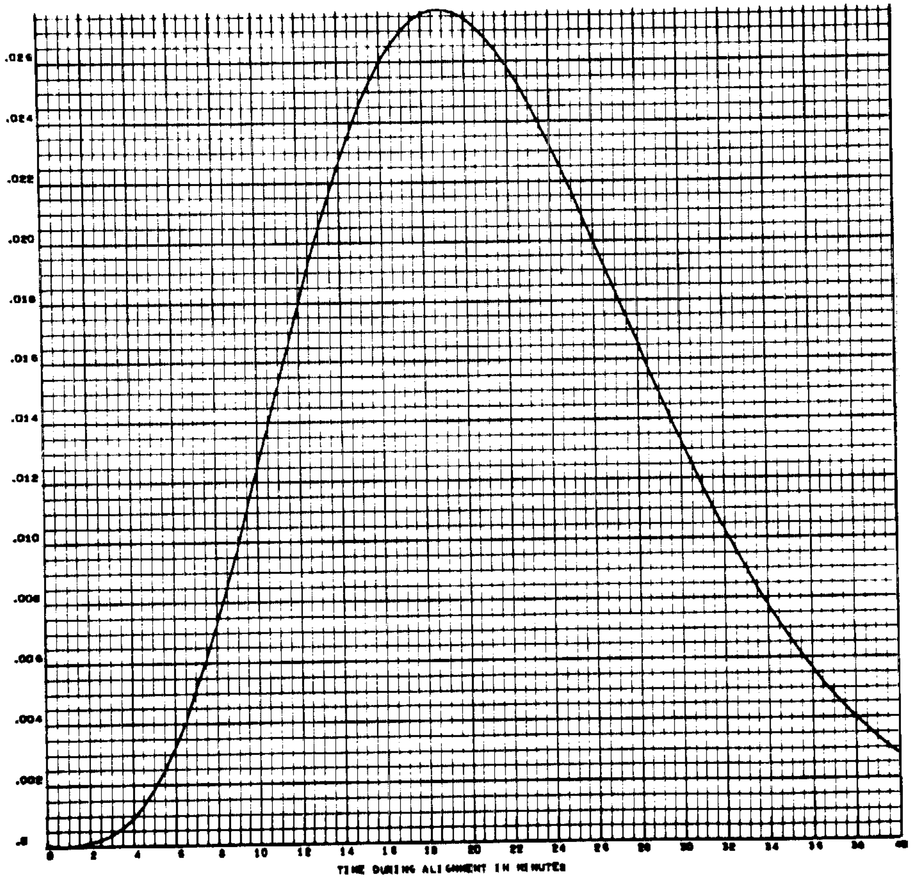

A31

AZIMUTH MISALIGNMENT IN ARCSECONDS - GROUND GYROCOMPASSING
ERROR DUE TO Z GYRO MISALIGNMENT (Z AXIS) - 10 ARCSECONDS

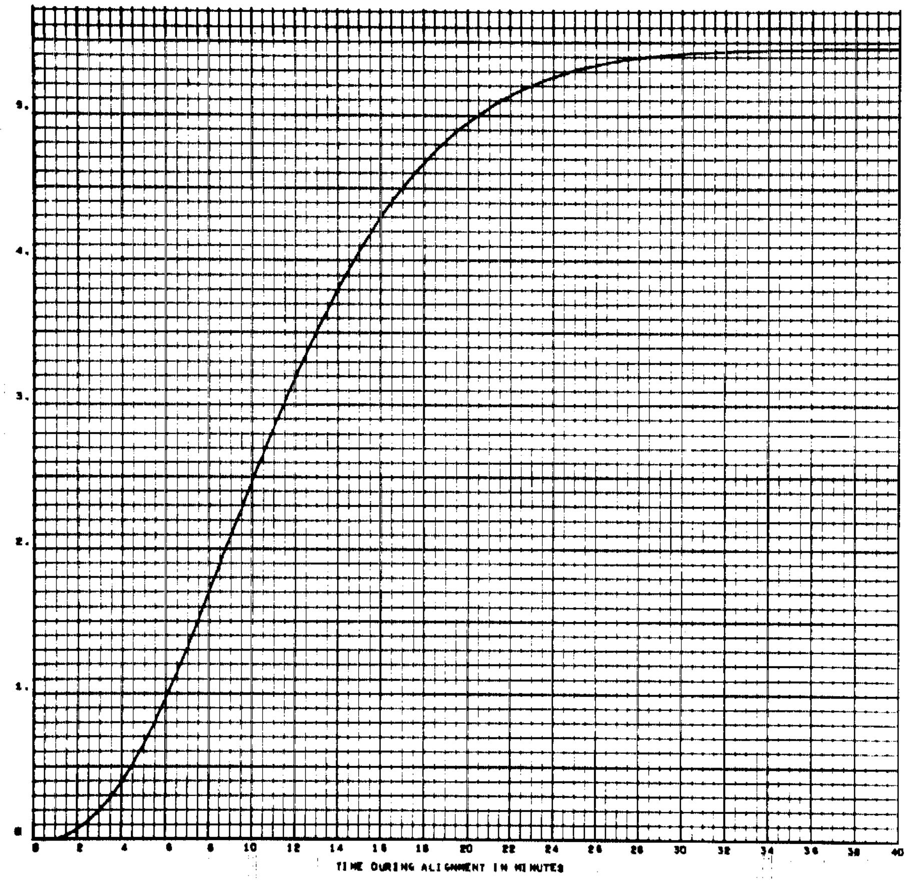

A32

AZIMUTH MISALIGNMENT IN ARCSECONDS - GROUND GYROCOMPASSING
ERROR DUE TO X GYRO MISALIGNMENT (Y AXIS) - 10 ARCSECONDS

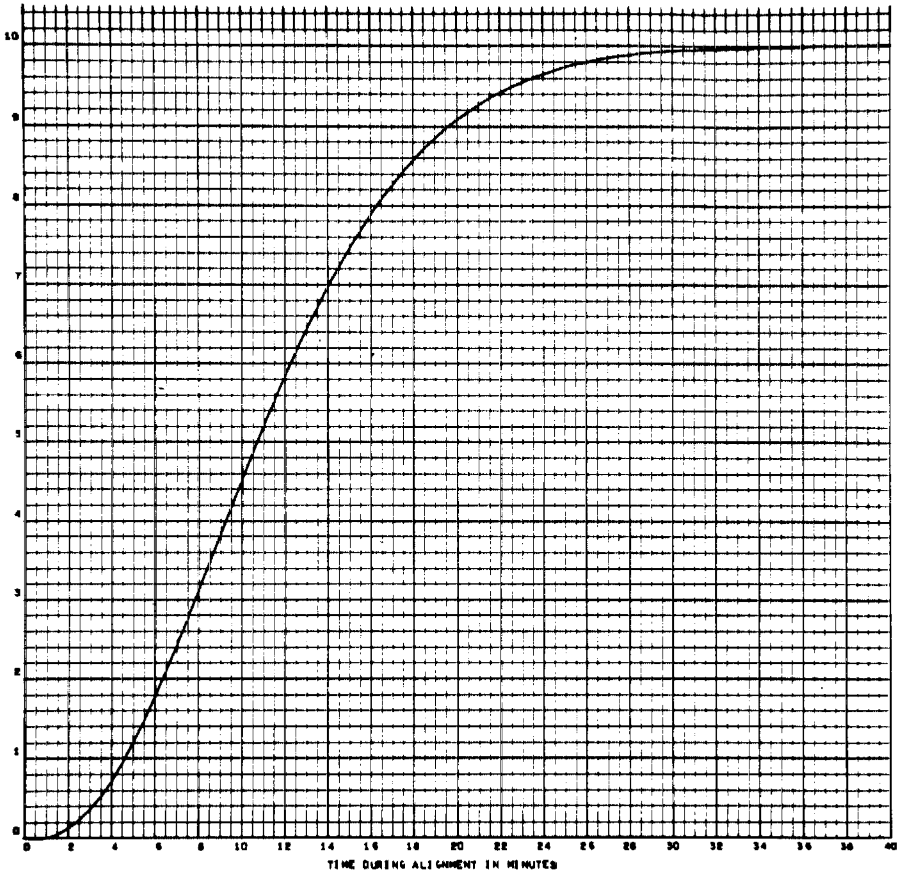

A33

AZIMUTH MISALIGNMENT IN ARCSECONDS - GROUND GYROCOMPASSING
ERROR DUE TO Z GYRO SCALE FACTOR ERROR - 100 PPM

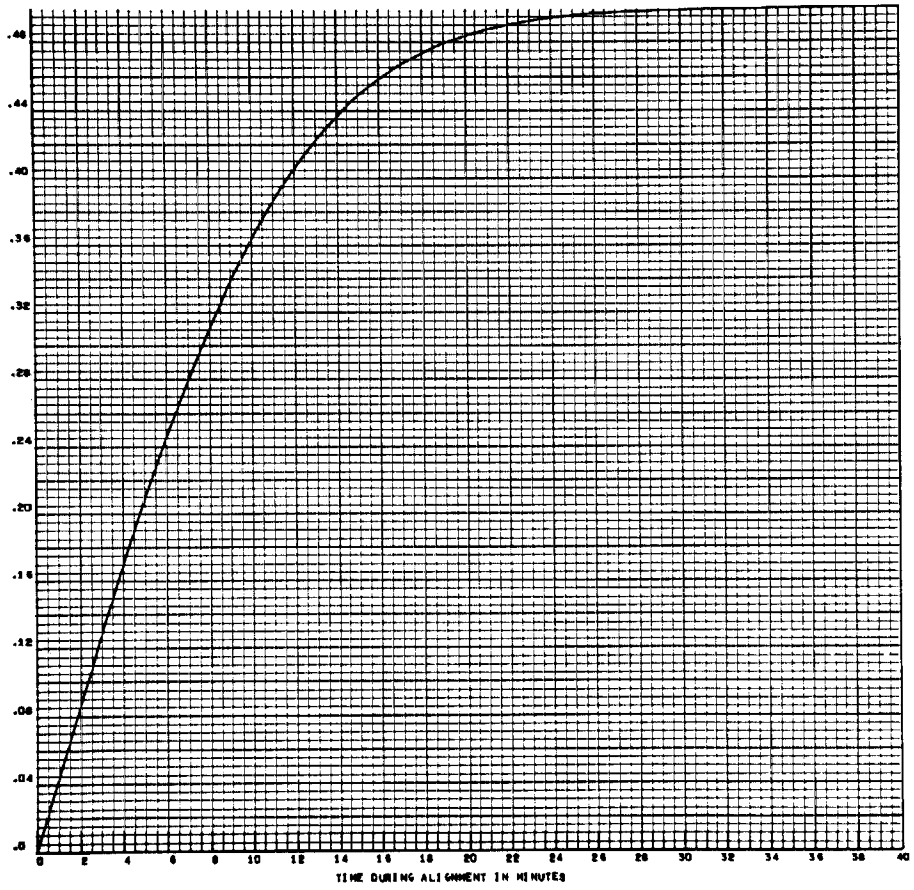

A34

AZIMUTH MISALIGNMENT IN ARCSECONDS - GROUND GYROCOMPASSING
ERROR DUE TO Y GYRO SCALE FACTOR ERROR - 100 PPM

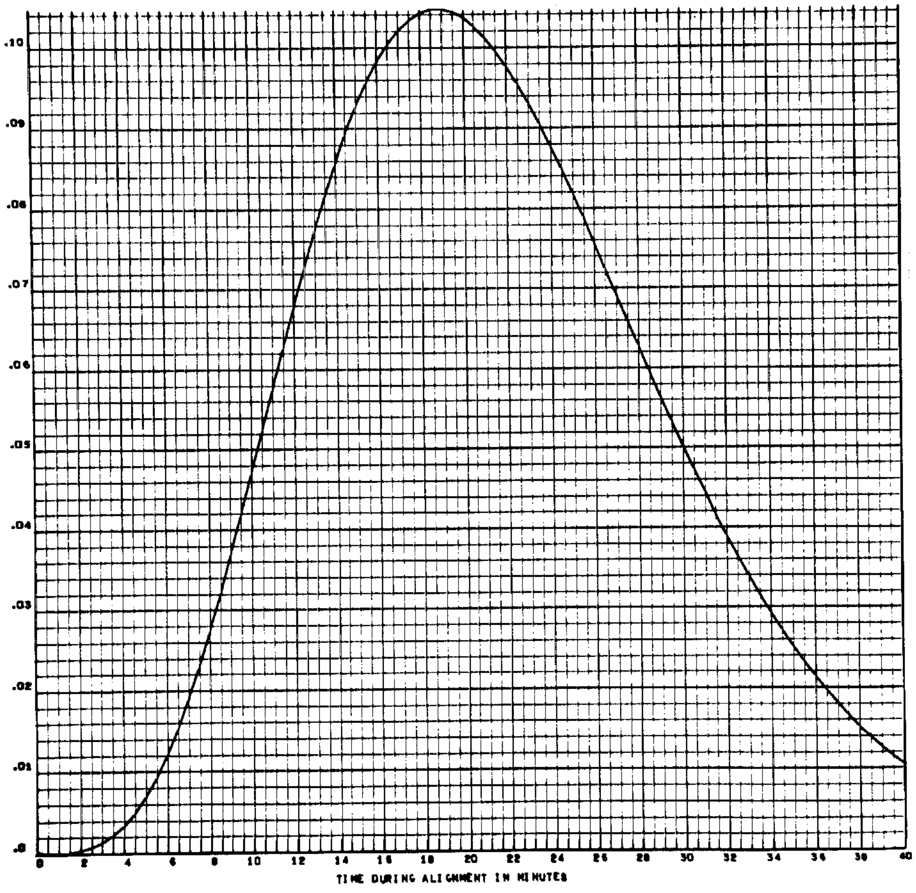

1935

AZIMUTH MISALIGNMENT IN ARCSECONDS - GROUND GYROCOMPASSING
ERROR DUE TO INITIAL AZIMUTH MISALIGNMENT - 10 DEGREES

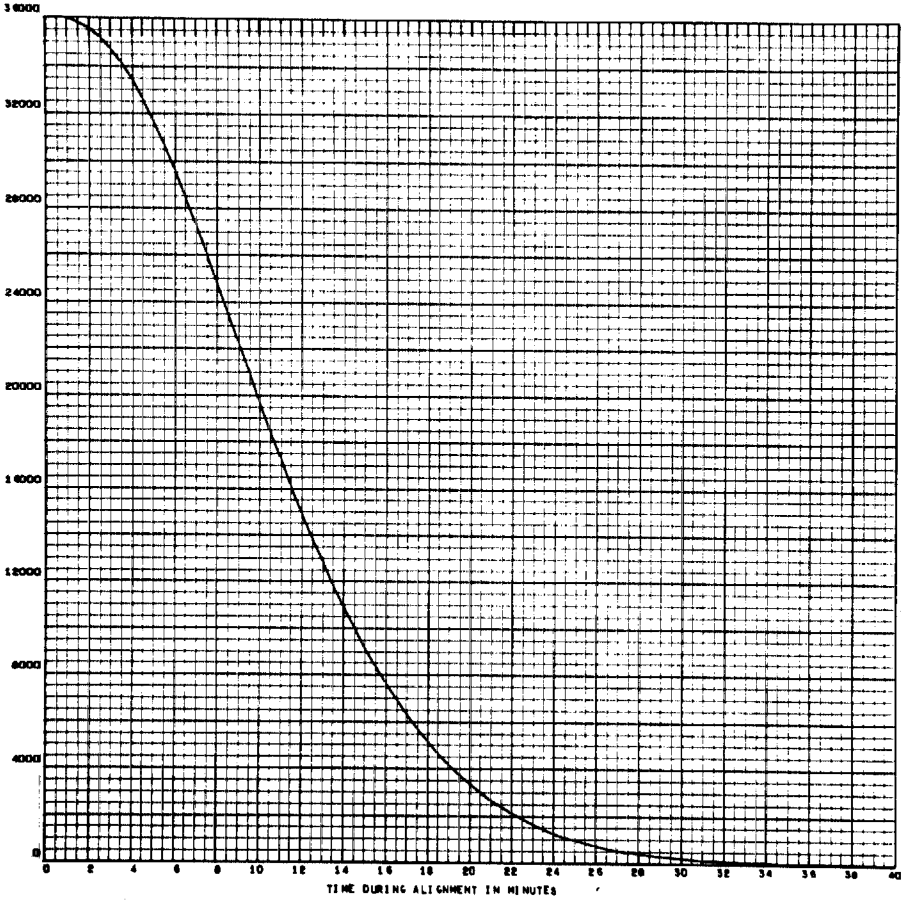

1936

AZIMUTH MISALIGNMENT IN ARCSECONDS - GROUND GYROCOMPASSING
ERROR DUE TO INITIAL X TILT - 10 DEGREES

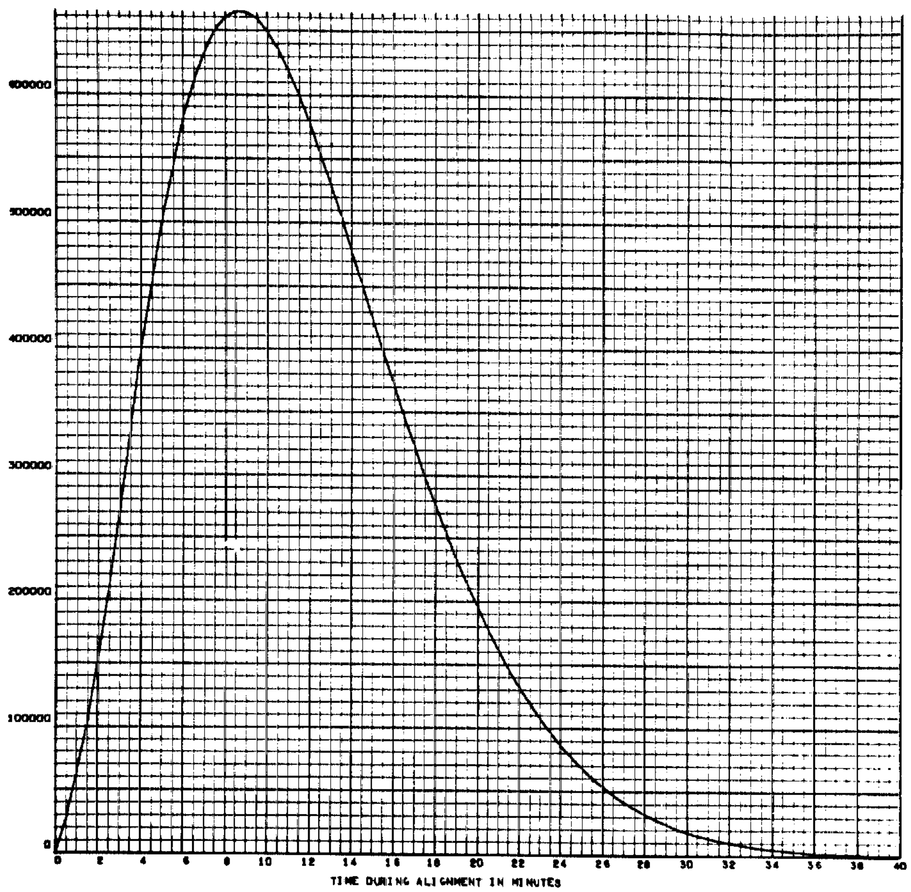

A37

AZIMUTH MISALIGNMENT IN ARCSECONDS - GROUND GYROCOMPASSING
ERROR DUE TO INITIAL Y TILT - 10 DEGREES

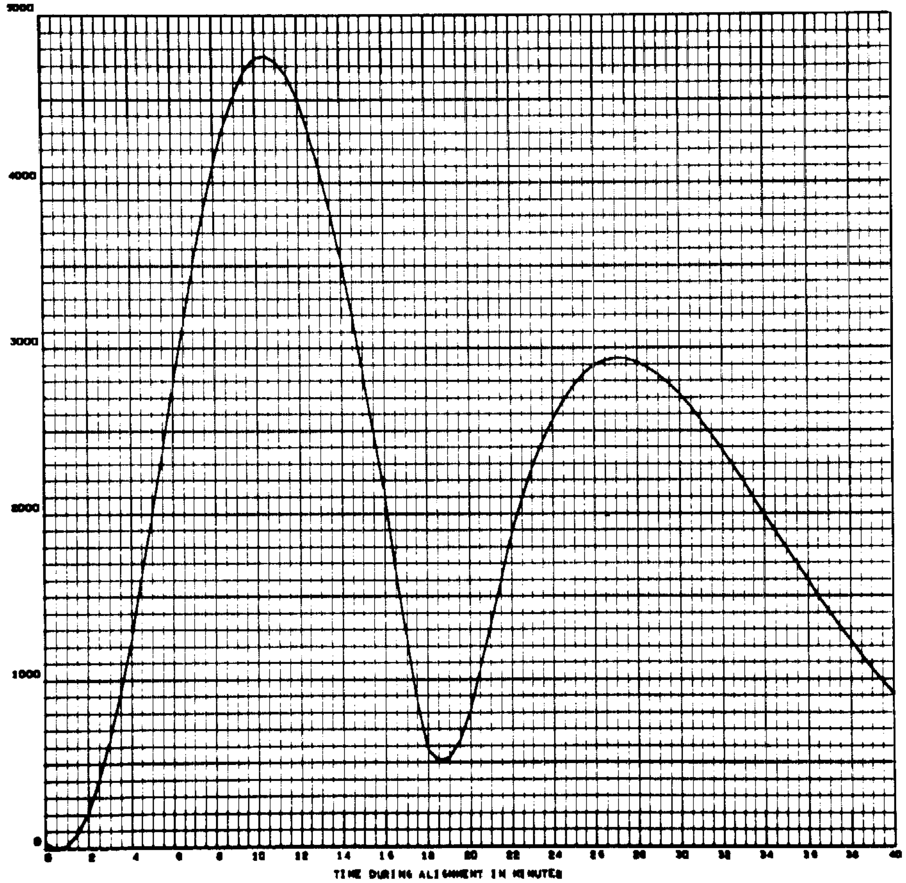

A38

AZIMUTH MISALIGNMENT IN ARCSECONDS - GROUND GYROCOMPASSING
ERROR DUE TO Z GYRO "F" TERM - .01 DEG/HR/G

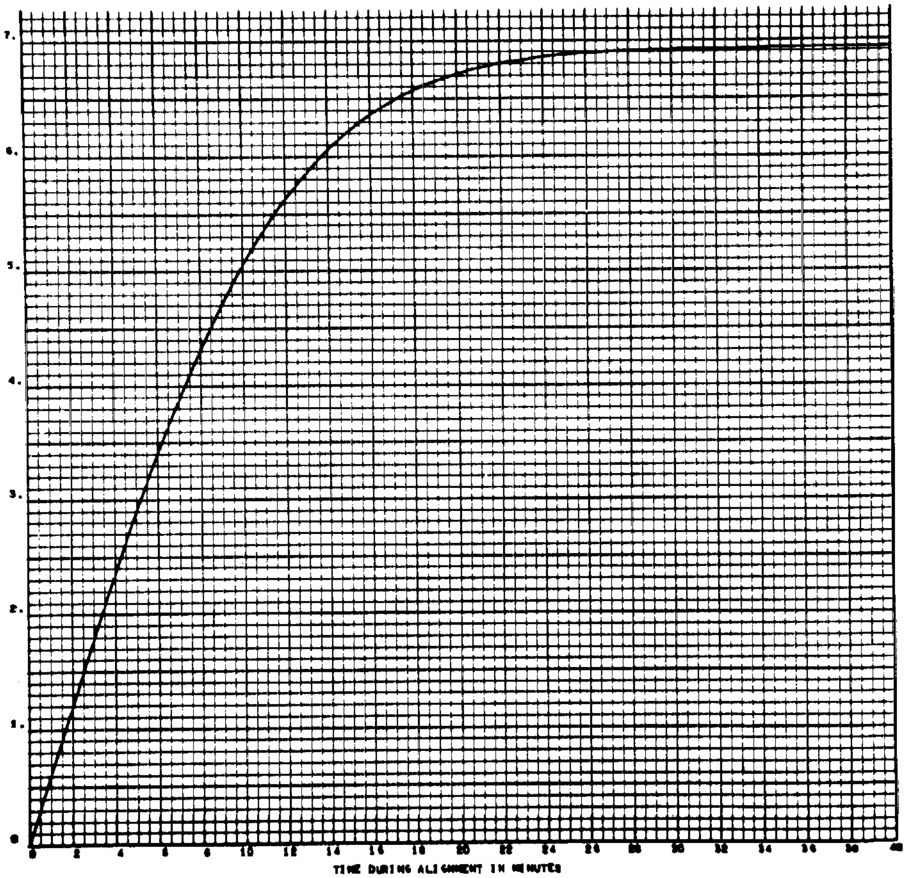

939

AZIMUTH MISALIGNMENT IN ARCSECONDS - GROUND GYROCOMPASSING
ERROR DUE TO X GYRO "P" TERM - .01 DEG/HR/G

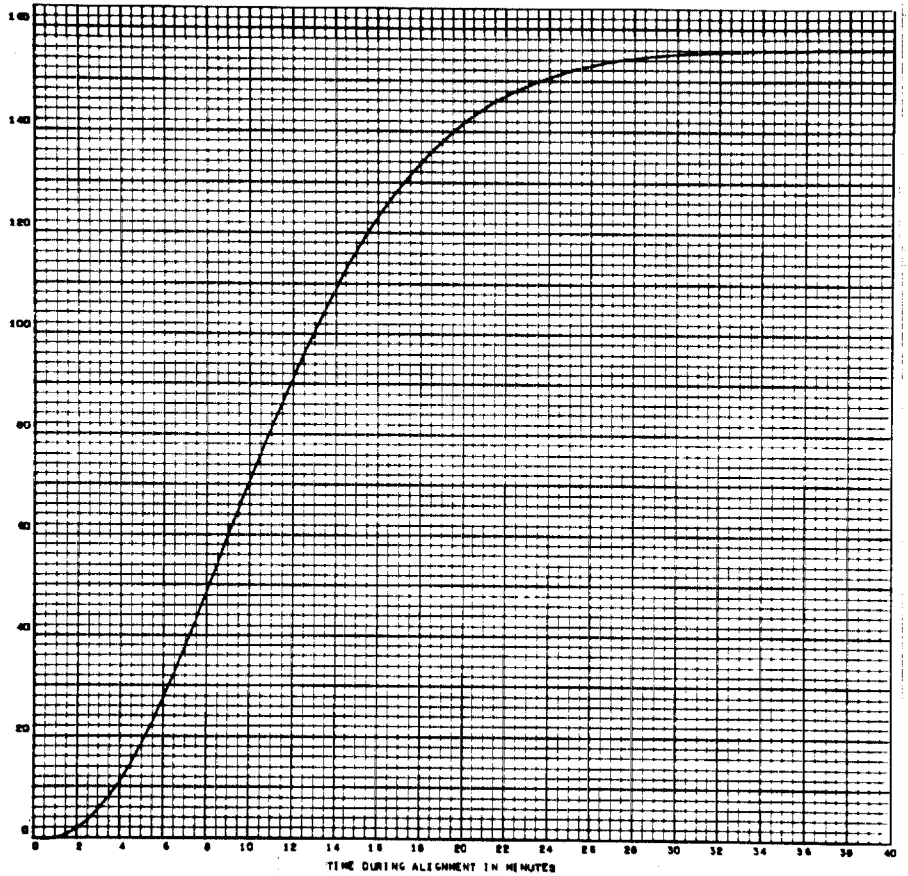

940

AZIMUTH MISALIGNMENT IN ARCSECONDS - GROUND GYROCOMPASSING
ERROR DUE TO Y GYRO "P" TERM - .01 DEG/HR/G

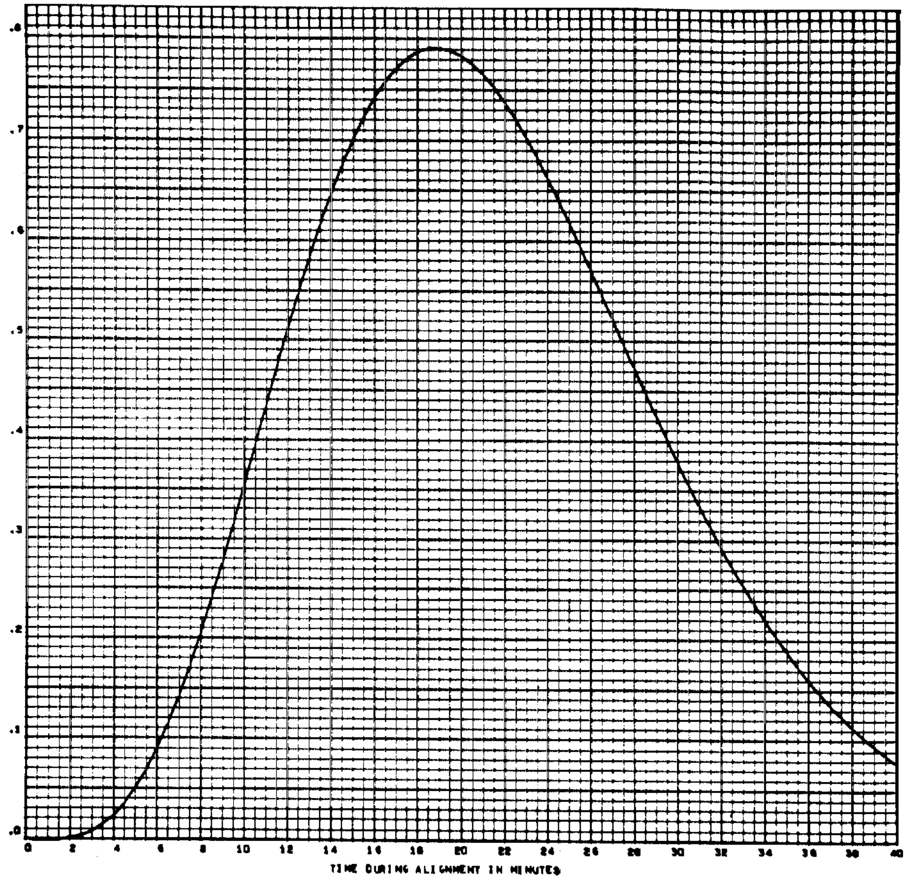

B41

AZIMUTH MISALIGNMENT IN ARCSECONDS - GROUND GYROCOMPASSING
ERROR DUE TO Z GYRO DRIFT - .01 DEG/HR

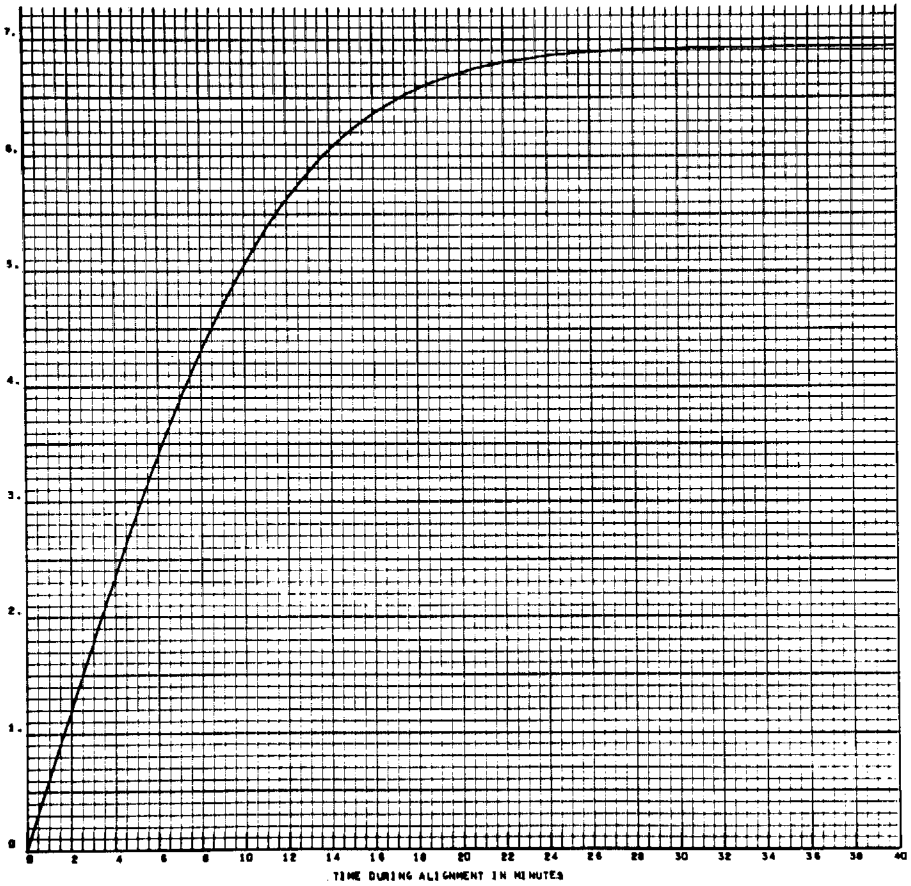

B42

AZIMUTH MISALIGNMENT IN ARCSECONDS - GROUND GYROCOMPASSING
ERROR DUE TO X GYRO DRIFT - .01 DEG/HR

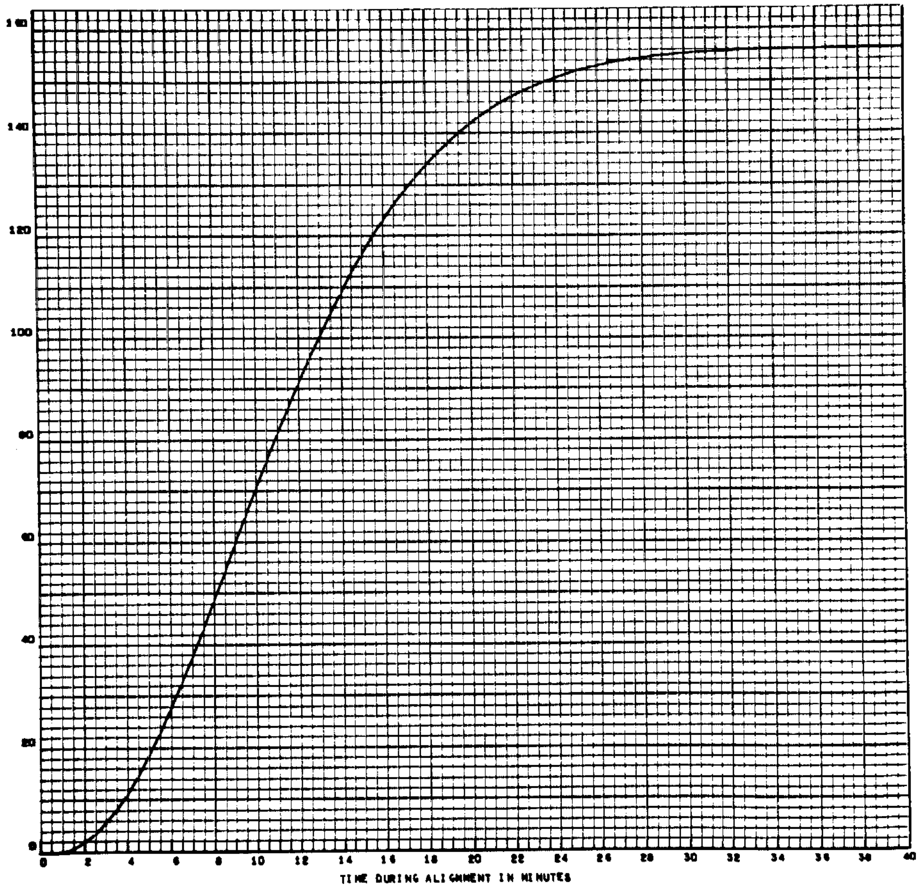

#43

AZIMUTH MISALIGNMENT IN ARCSECONDS - GROUND GYROCOMPASSING
ERROR DUE TO Y GYRO DRIFT - .01 DEG/HR

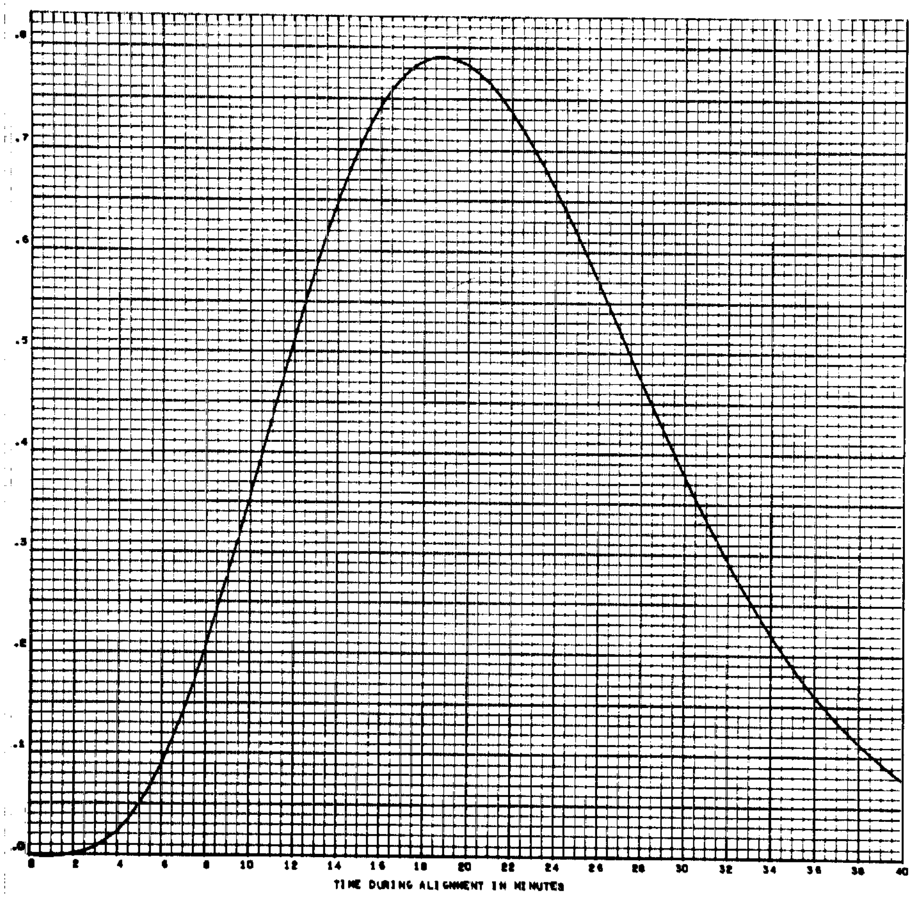

#44

AZIMUTH MISALIGNMENT IN ARCSECONDS - GROUND GYROCOMPASSING
ERROR DUE TO Y ACCELEROMETER MISALIGNMENT - 10 ARCSECONDS

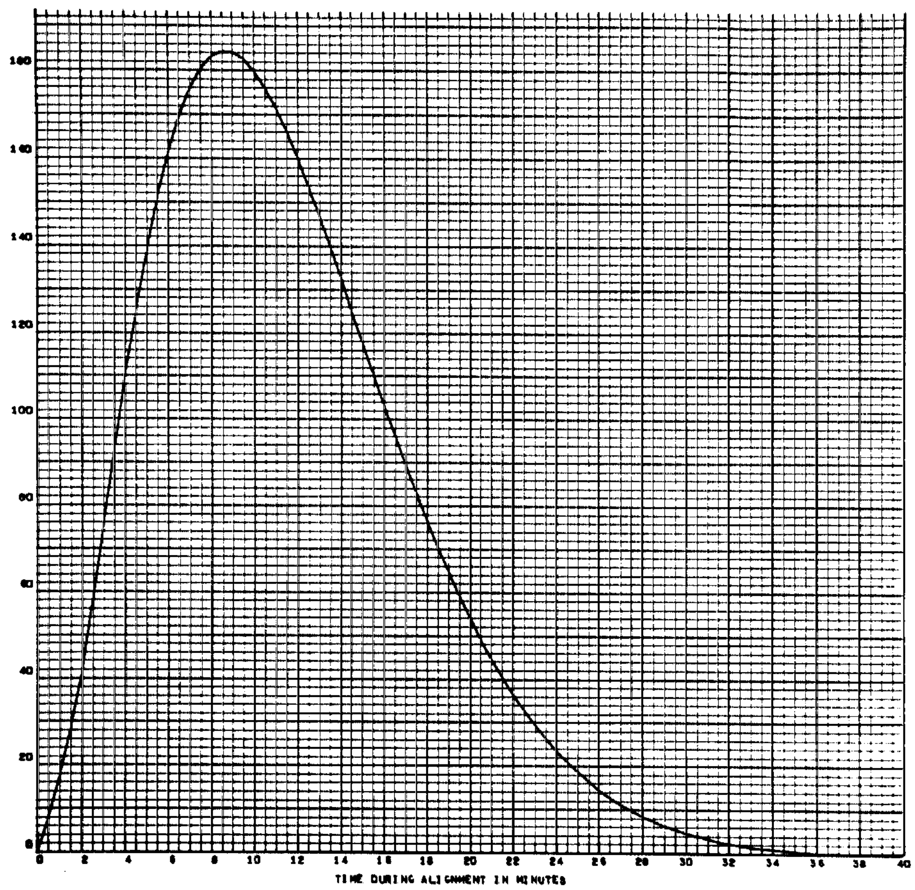

A45

AZIMUTH MISALIGNMENT IN ARCSECONDS - GROUND GYROCOMPASSING
ERROR DUE TO Y ACCELEROMETER MISALIGNMENT - 10 ARCSECONDS

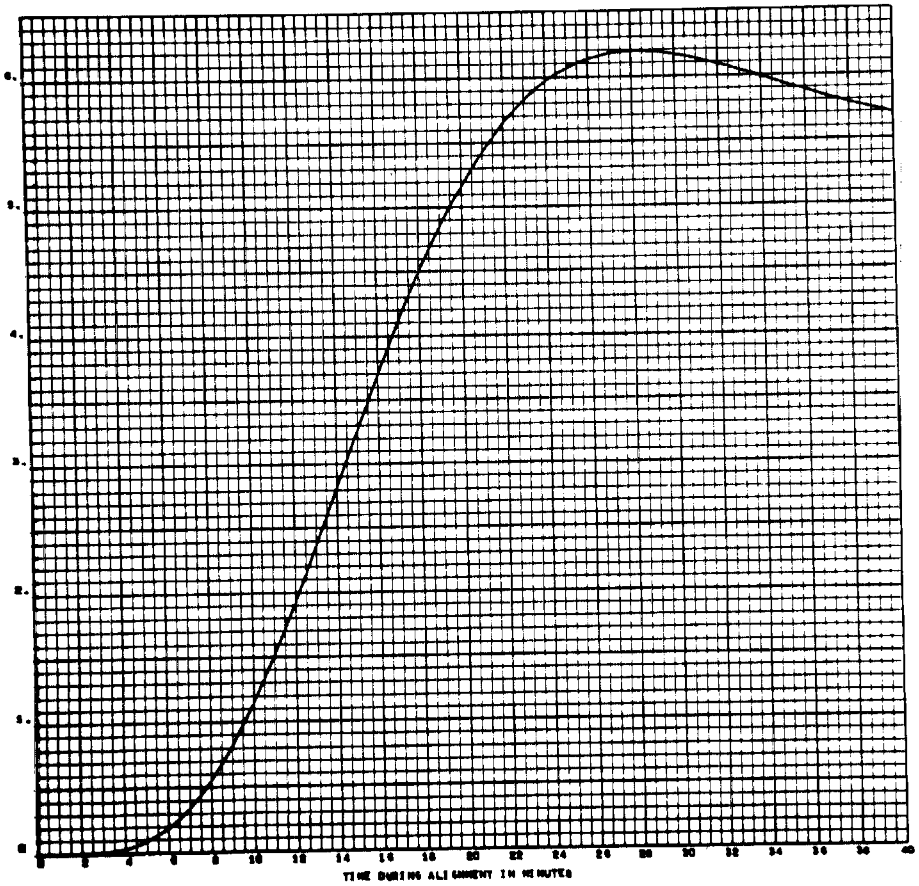

A46

LEVEL TILT IN ARCSECONDS - GROUND GYROCOMPASSING
Y TILT DUE TO Y ACCELEROMETER "F" TERM - 10 PPM

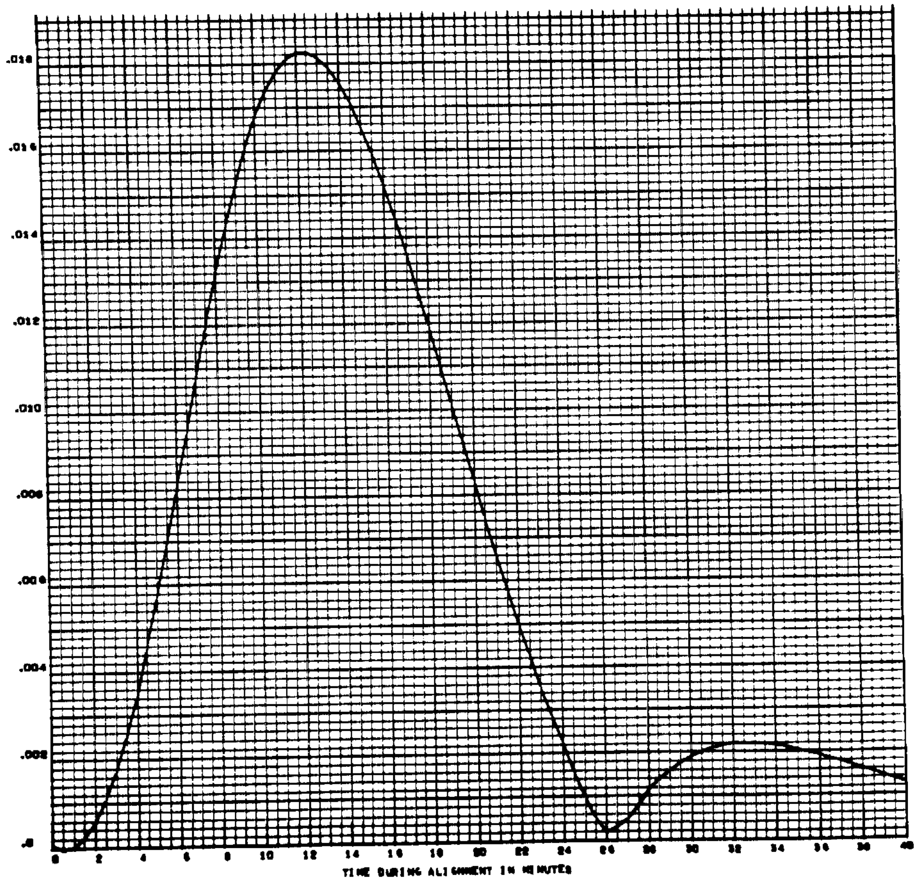

#47

LEVEL TILT IN ARCSECONDS - GROUND GYROCOMPASSING
Y TILT DUE TO X ACCELEROMETER "F" TERM - 10 PPM

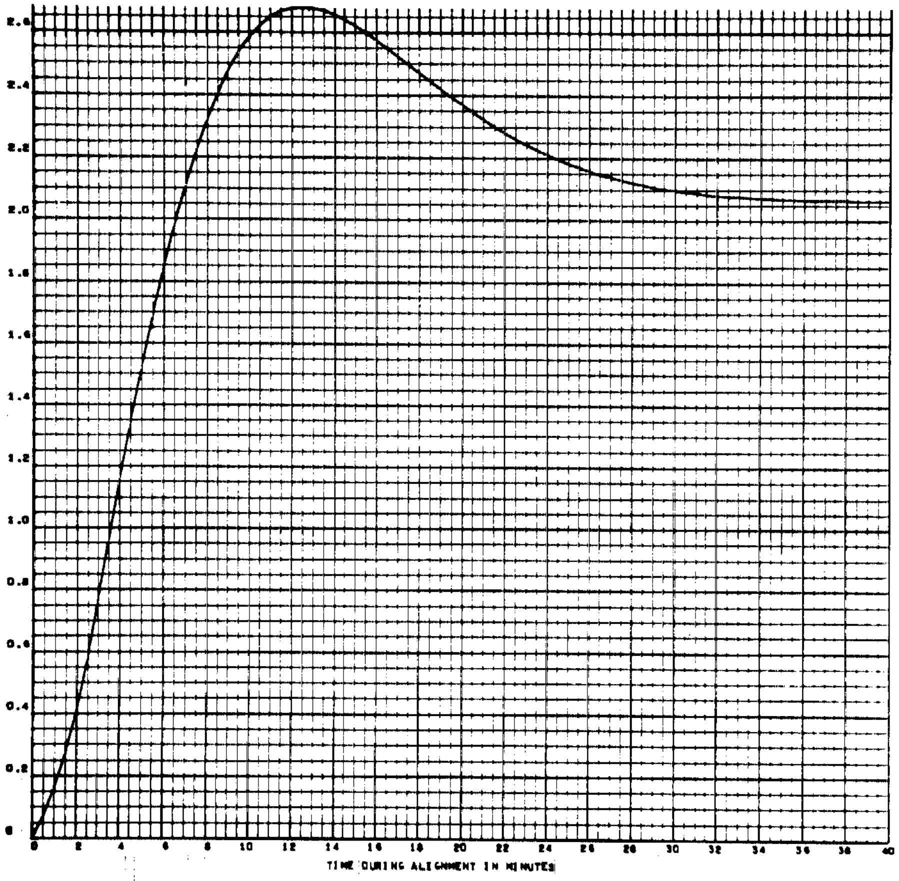

#48

LEVEL TILT IN ARCSECONDS - GROUND GYROCOMPASSING
Y TILT DUE TO Y ACCELEROMETER ERROR - .0001 METERS/SECOND SQUARED

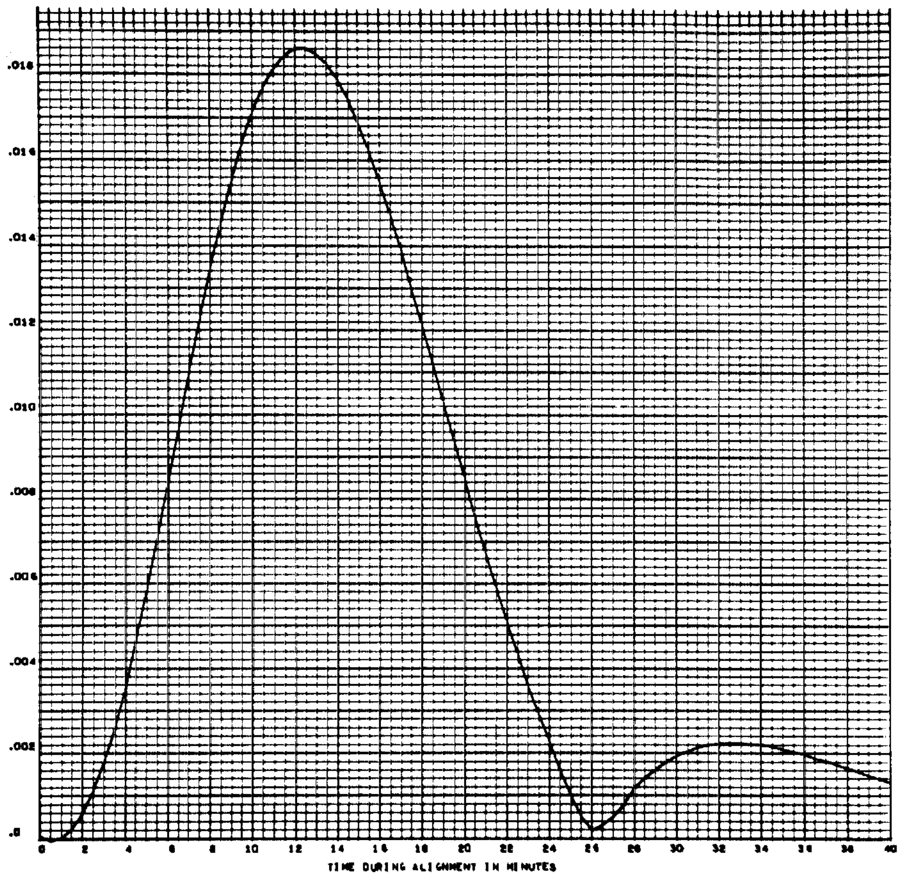

A49

LEVEL TILT IN ARCSECONDS - GROUND GYROCOMPASSING
Y TILT DUE TO X ACCELEROMETER ERROR - .0001 METERS/SECOND SQUARED

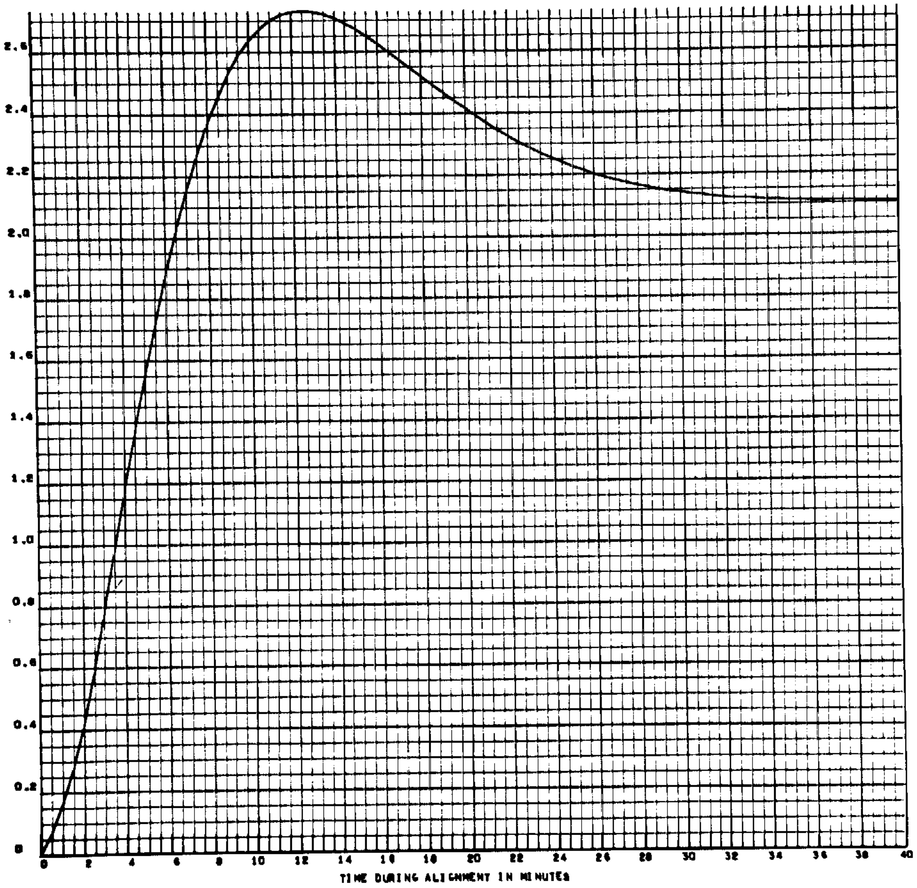

A50

LEVEL TILT IN ARCSECONDS - GROUND GYROCOMPASSING
Y TILT DUE TO Z GYRO MISALIGNMENT (Y AXIS) - 10 ARCSECONDS

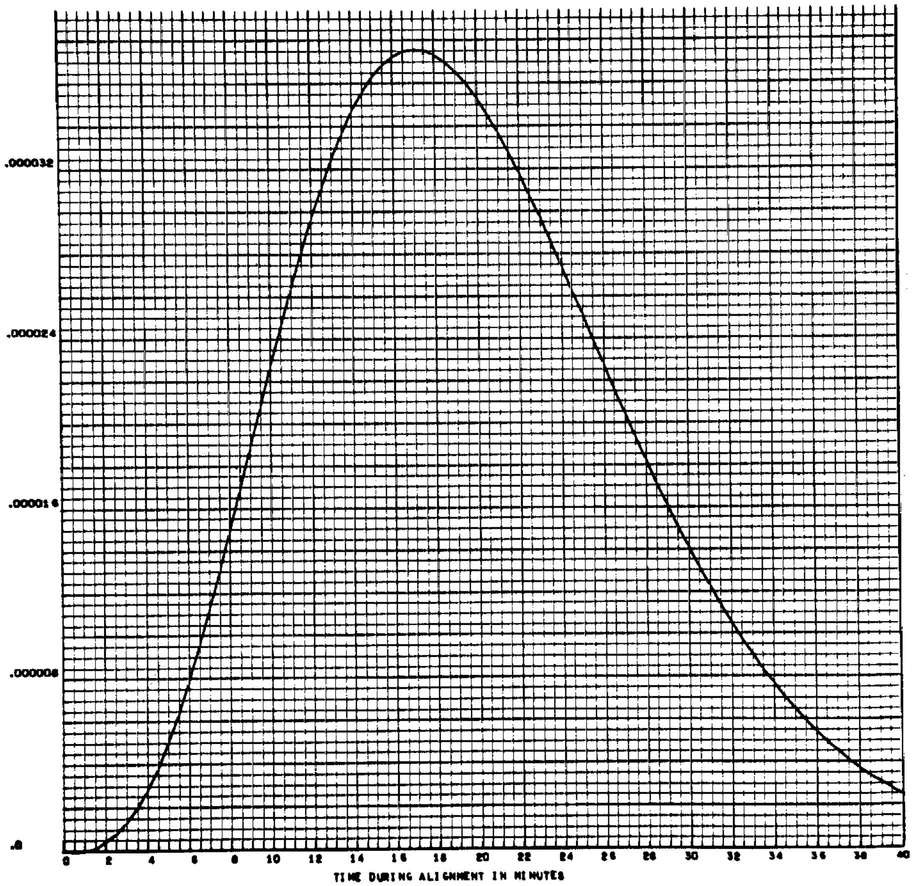

$\mathrm{J}^{A}51$

LEVEL TILT IN ARCSECONDS - GROUND GYROCOMPASSING
Y TILT DUE TO Y GYRO MISALIGNMENT (Z AXIS) - 10 ARCSECONDS

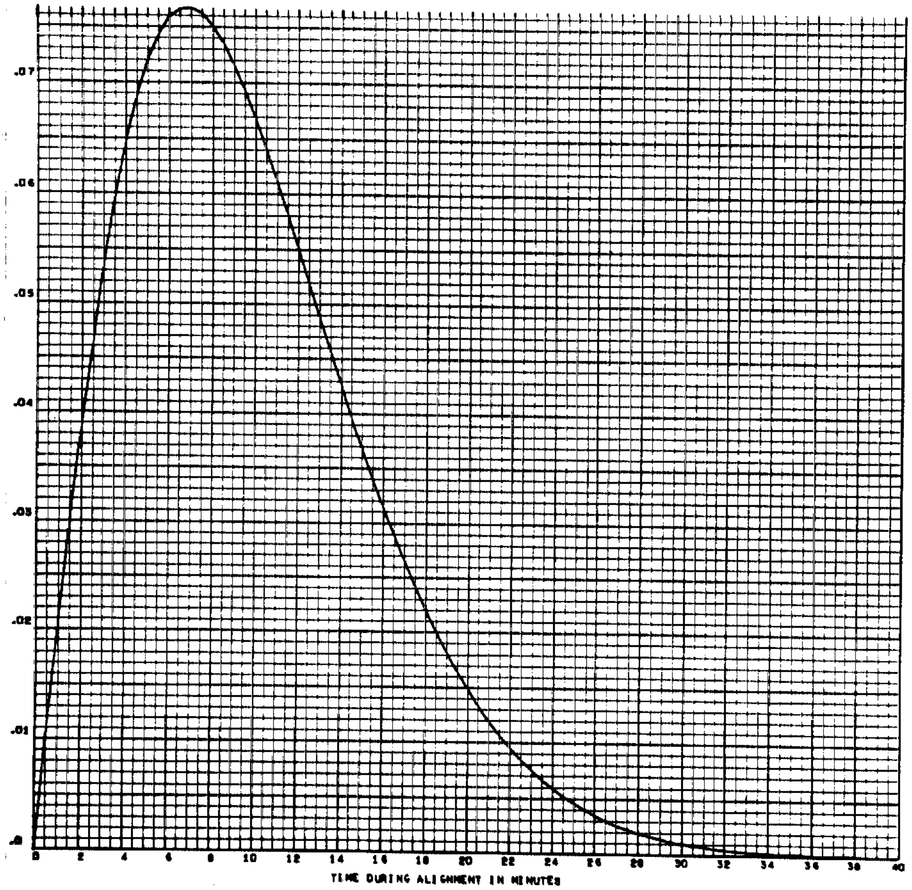

$\mathrm{J}^{B}52$

LEVEL TILT IN ARCSECONDS - GROUND GYROCOMPASSING
Y TILT DUE TO X GYRO MISALIGNMENT (Z AXIS) - 10 ARCSECONDS

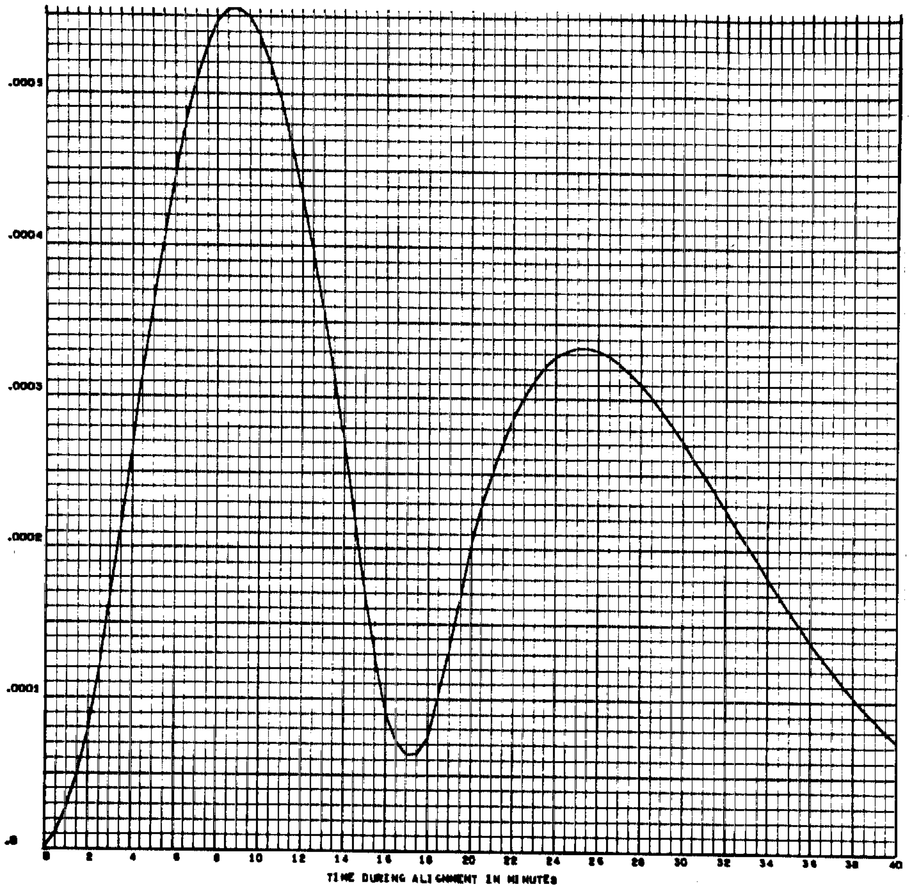

A53

LEVEL TILT IN ARCSECONDS - GROUND GYROCOMPASSING
Y TILT DUE TO X GYRO MISALIGNMENT (Y AXIS) - 10 ARCSECONDS

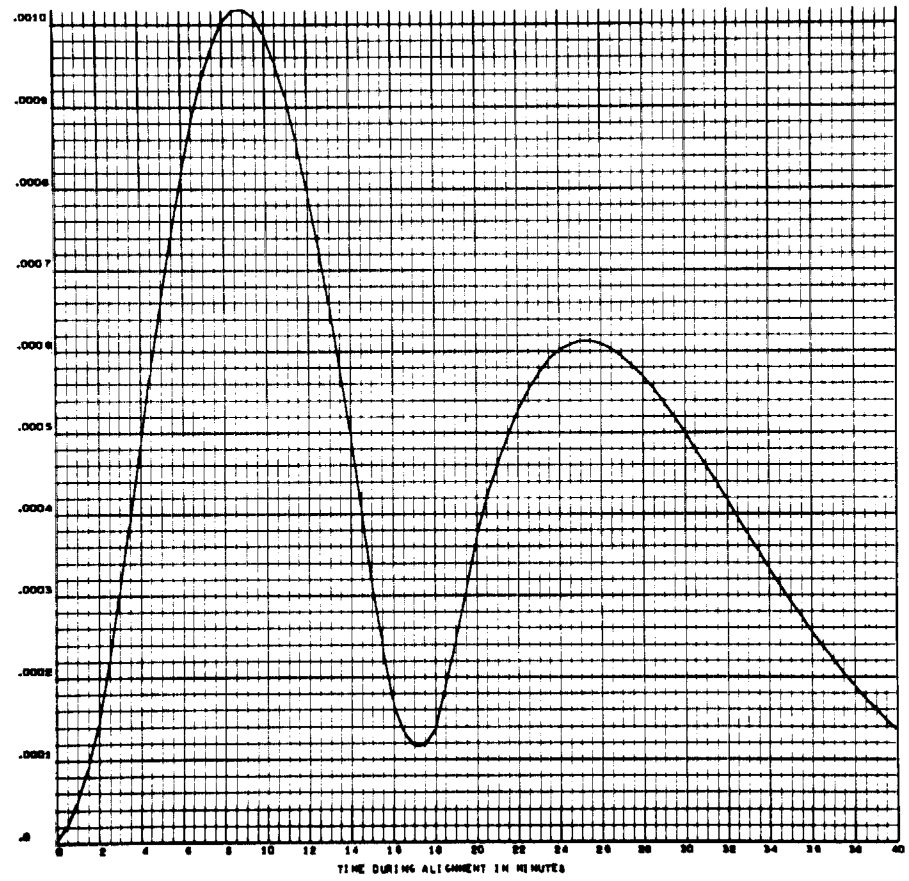

A54

LEVEL TILT IN ARCSECONDS - GROUND GYROCOMPASSING
Y TILT DUE TO Z GYRO SCALE FACTOR ERROR - 100 PPM

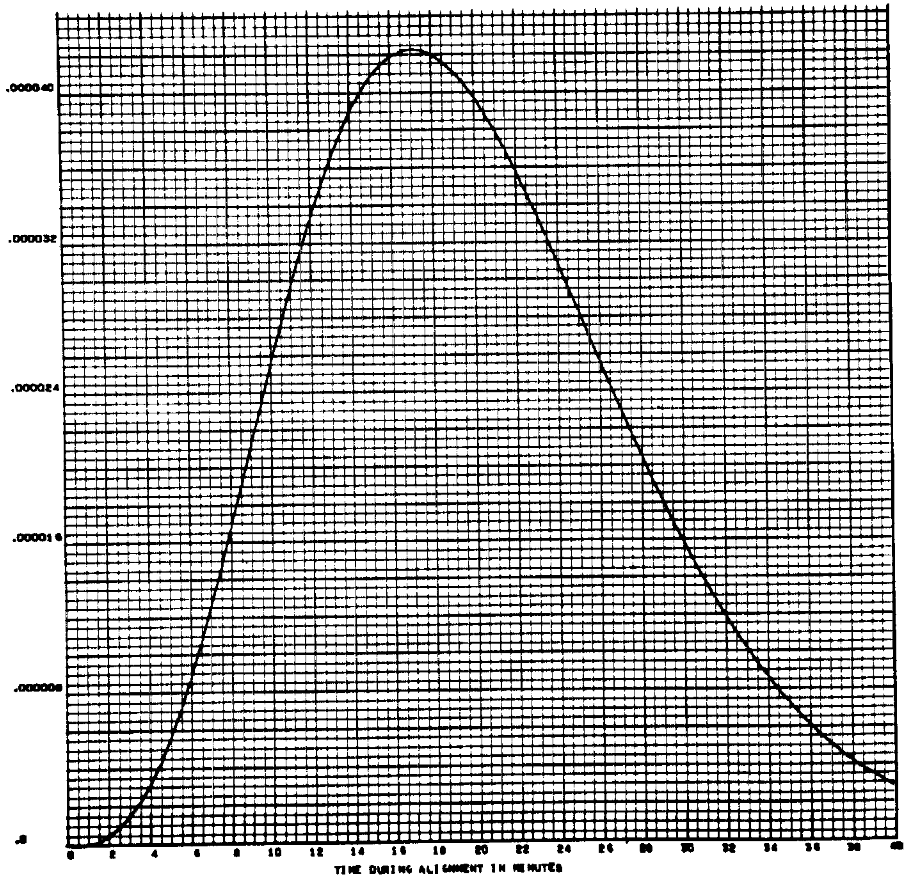

535

LEVEL TILT IN ARCSECONDS - GROUND GYROCOMPASSING
Y TILT DUE TO Y GYRO SCALE FACTOR ERROR - 100 PPM

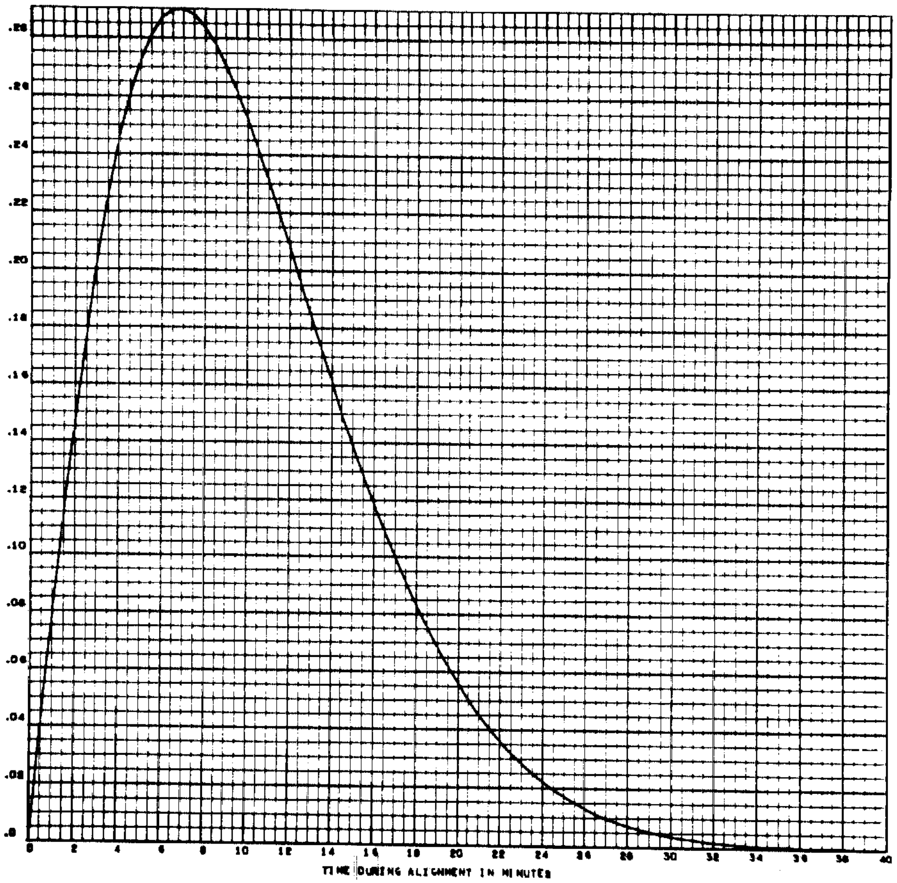

536

LEVEL TILT IN ARCSECONDS - GROUND GYROCOMPASSING
Y TILT DUE TO INITIAL AZIMUTH MISALIGNMENT - 10 DEGREES

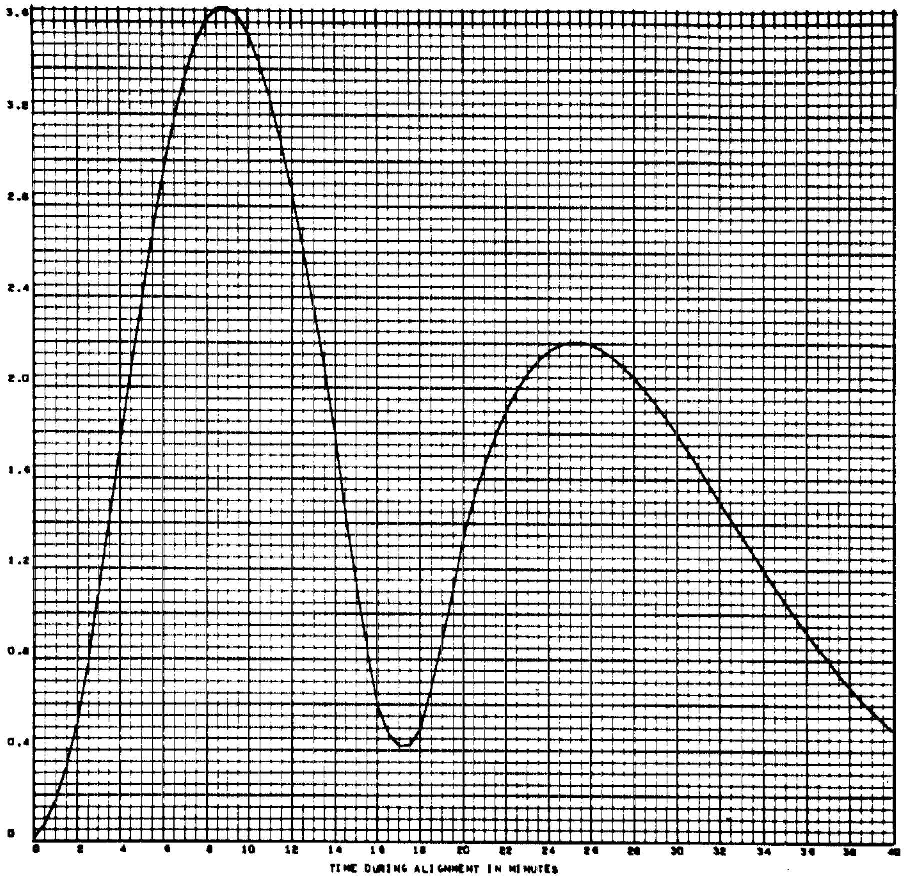

A57

LEVEL TILT IN ARCSECONDS - GROUND GYROCOMPASSING
Y TILT DUE TO INITIAL X TILT - 10 DEGREES

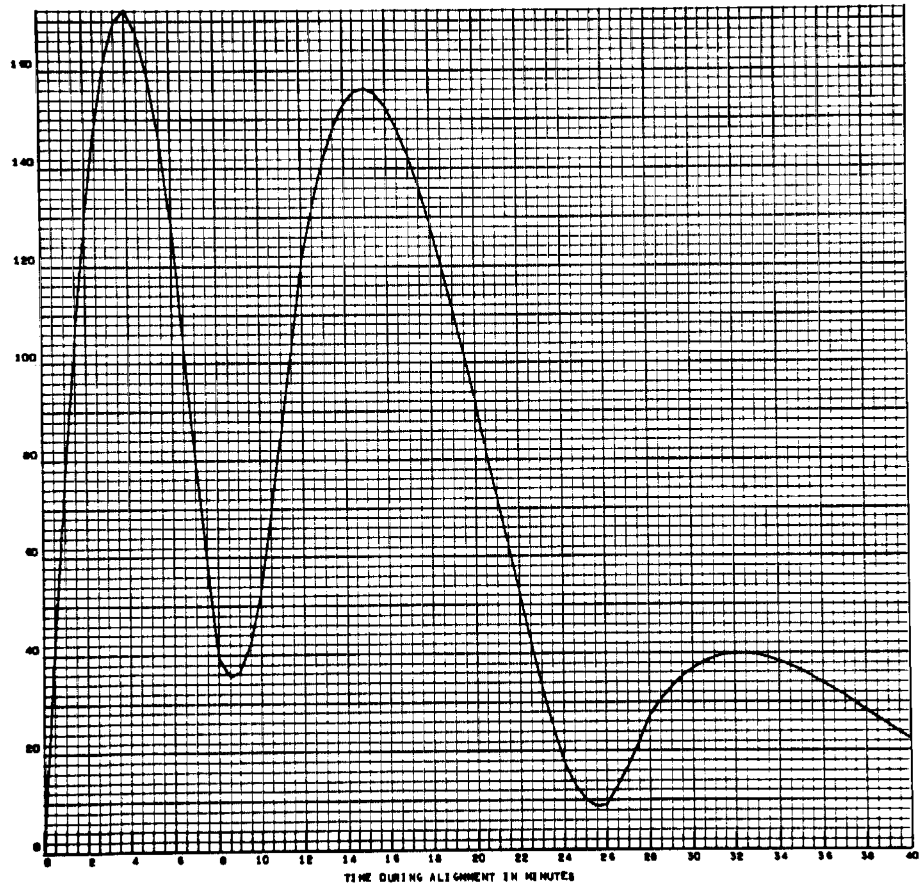

A58

LEVEL TILT IN ARCSECONDS - GROUND GYROCOMPASSING
Y TILT DUE TO INITIAL Y TILT - 10 DEGREES

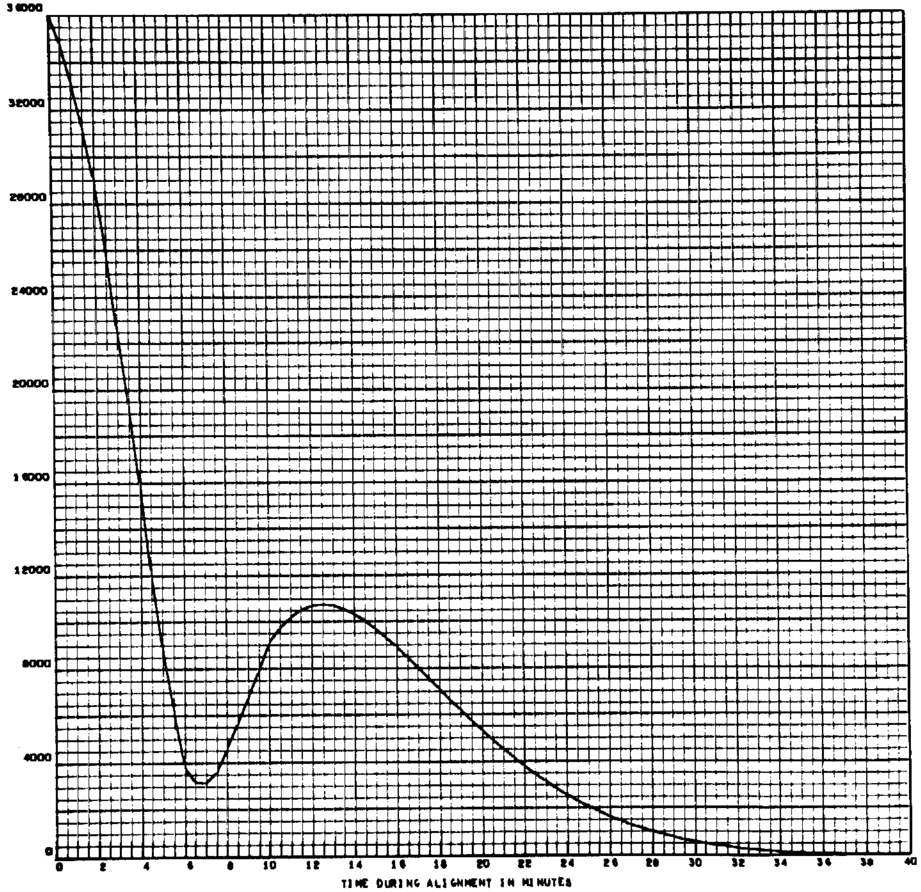

959

LEVEL TILT IN ARCSECONDS - GROUND GYROCOMPASSING
Y TILT DUE TO Z GYRO "P" TERM - .01 DEG/HR/G

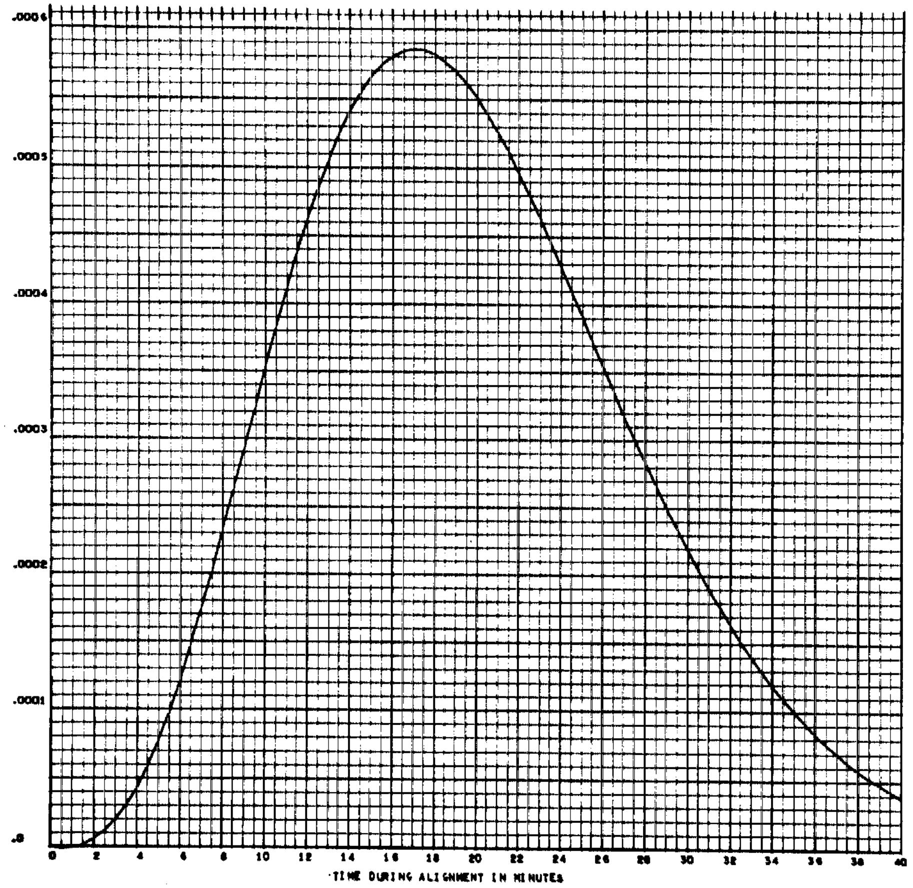

960

LEVEL TILT IN ARCSECONDS - GROUND GYROCOMPASSING
Y TILT DUE TO X GYRO "P" TERM - .01 DEG/HR/G

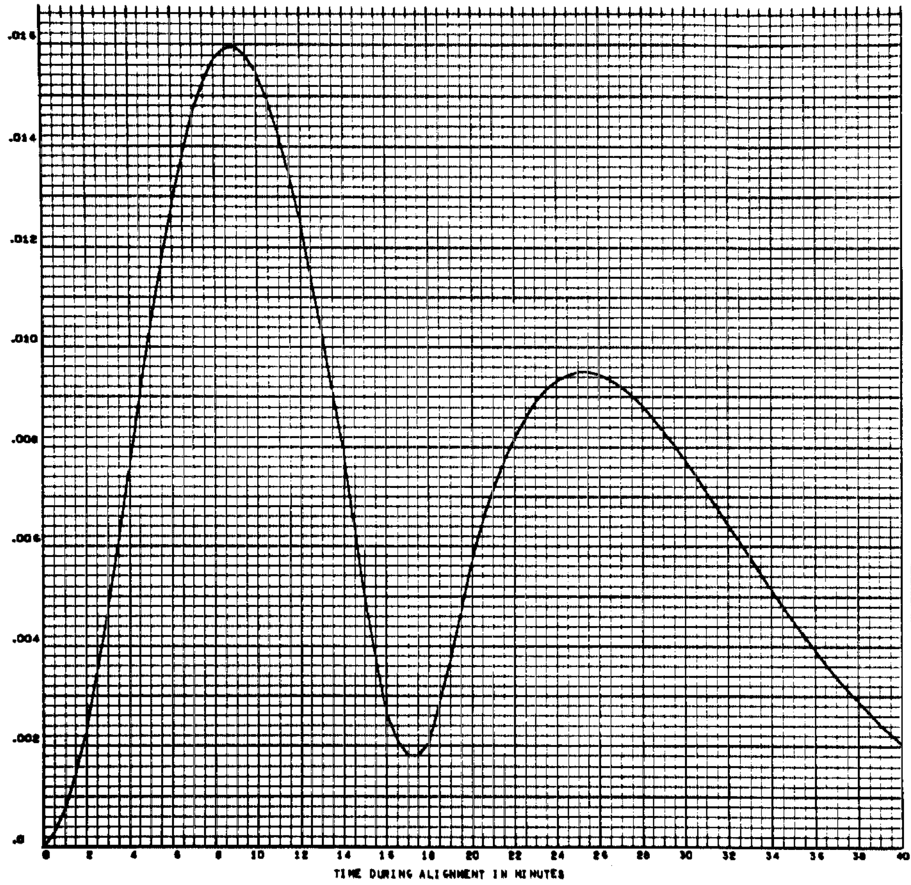

61

LEVEL TILT IN ARCSECONDS - GROUND GYROCOMPASSING
Y TILT DUE TO Y GYRO "P" TERM - .01 DEG/HR/G

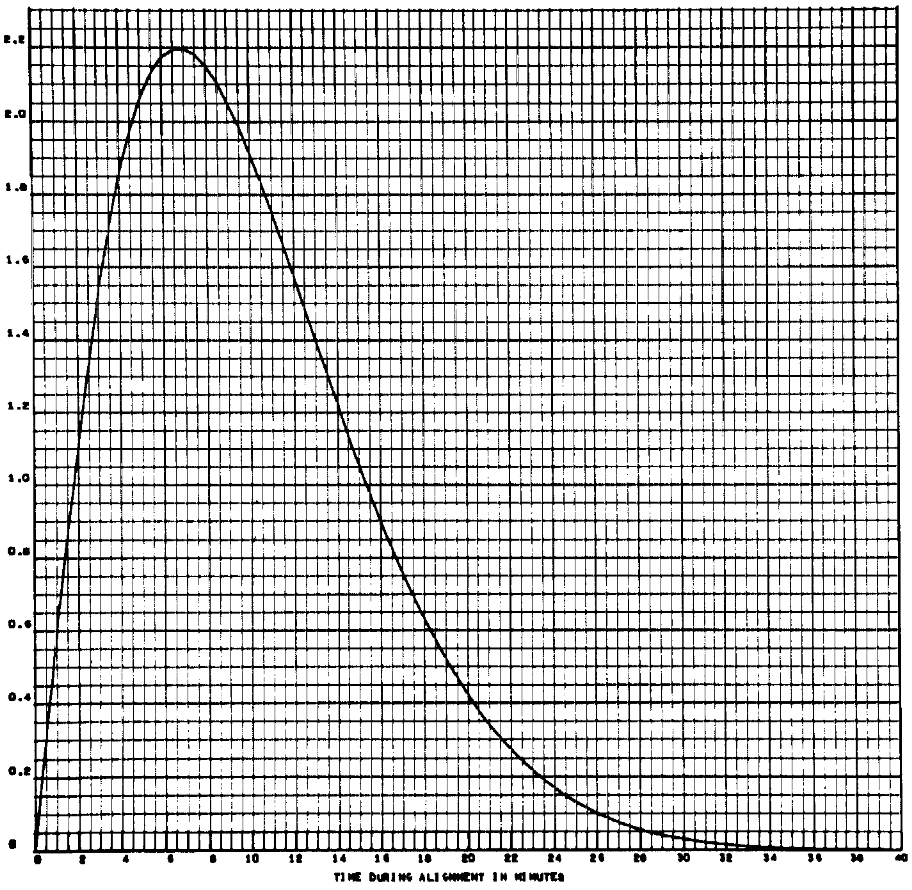

62

LEVEL TILT IN ARCSECONDS - GROUND GYROCOMPASSING
Y TILT DUE TO Z GYRO DRIFT - .01 DEG/HR

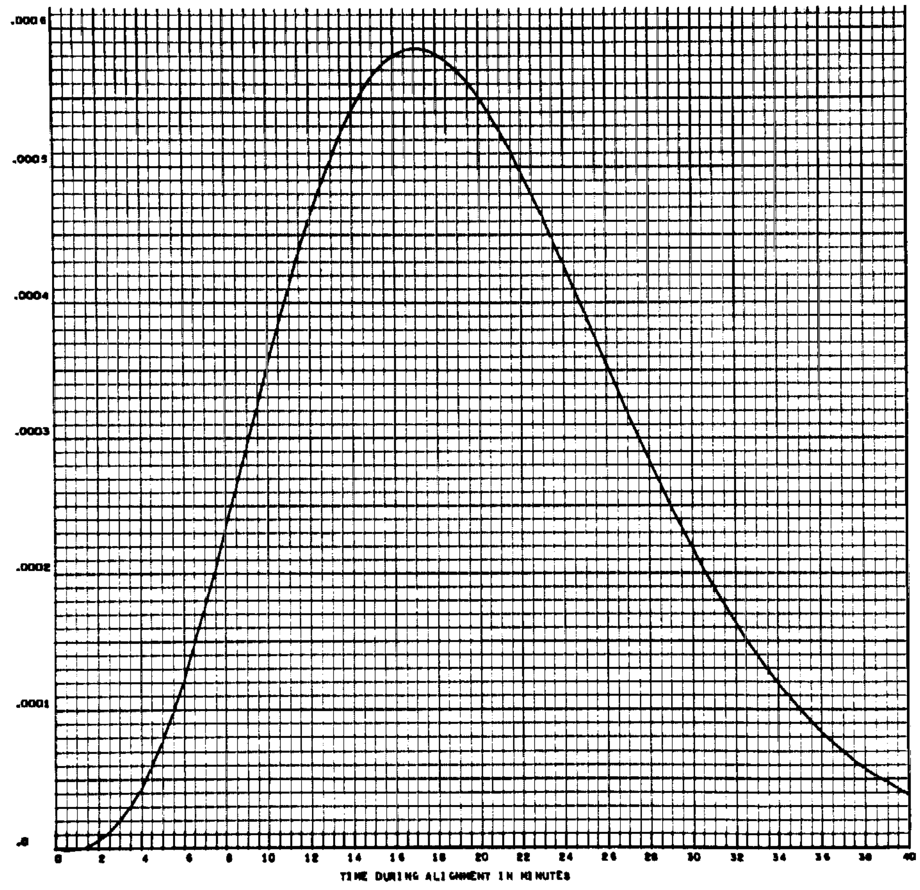

A63

LEVEL TILT IN ARCSECONDS - GROUND GYROCOMPASSING
Y TILT DUE TO X GYRO DRIFT - .01 DEG/HR

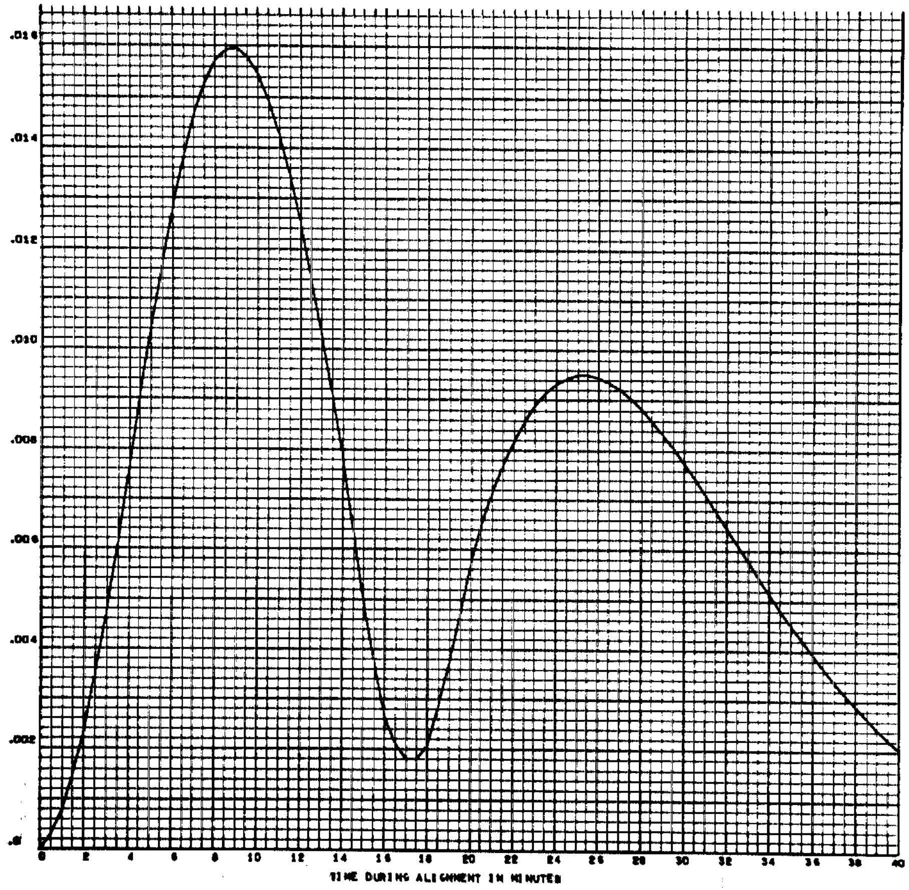

A64

LEVEL TILT IN ARCSECONDS - GROUND GYROCOMPASSING
Y TILT DUE TO Y GYRO DRIFT - .01 DEG/HR

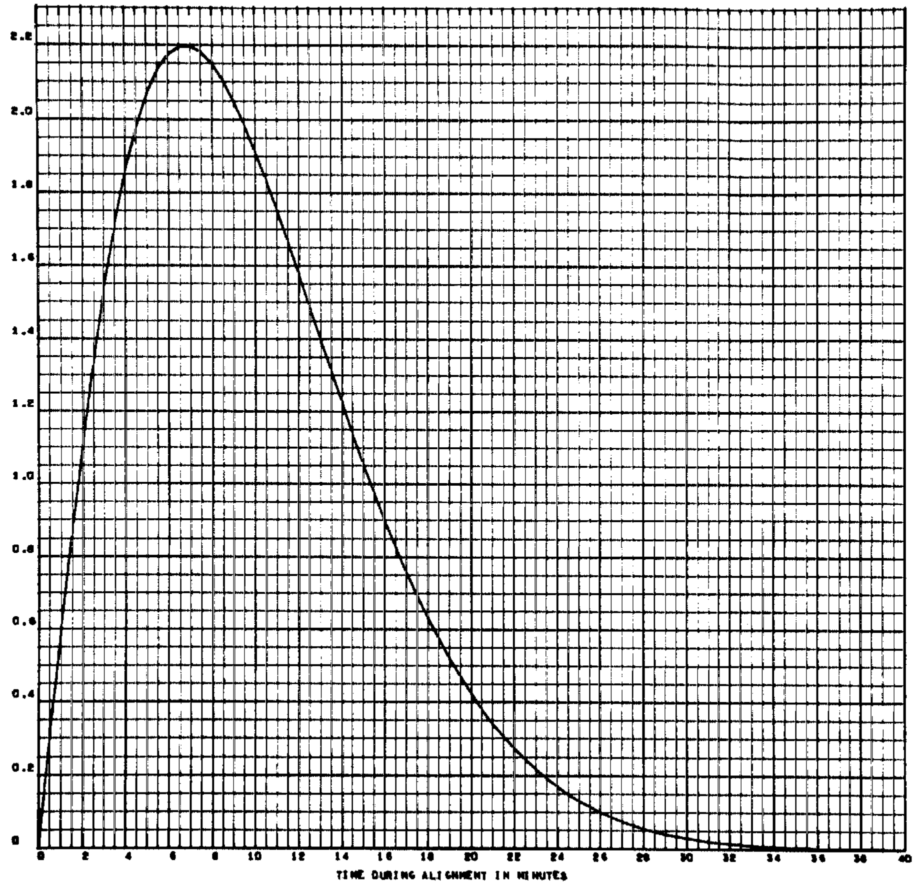

365

LEVEL TILT IN ARCSECONDS - GROUND GYROCOMPASSING
Y TILT DUE TO Y ACCELEROMETER MISALIGNMENT - 10 ARCSECONDS

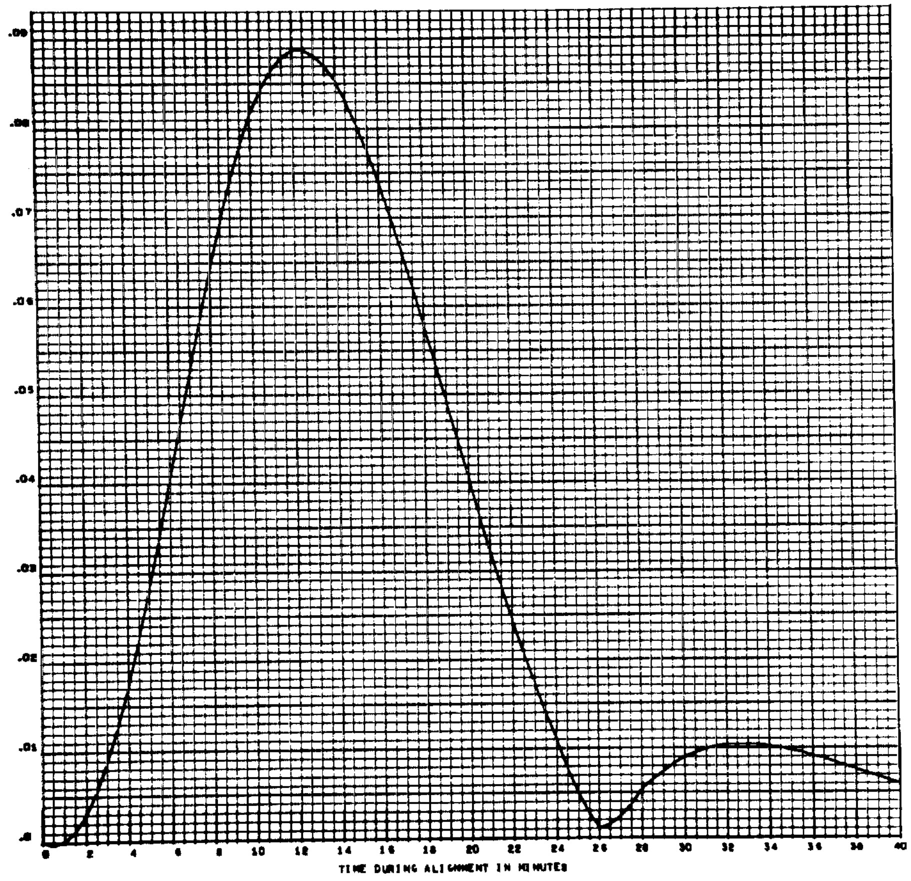

366

LEVEL TILT IN ARCSECONDS - GROUND GYROCOMPASSING
Y TILT DUE TO X ACCELEROMETER MISALIGNMENT - 10 ARCSECONDS

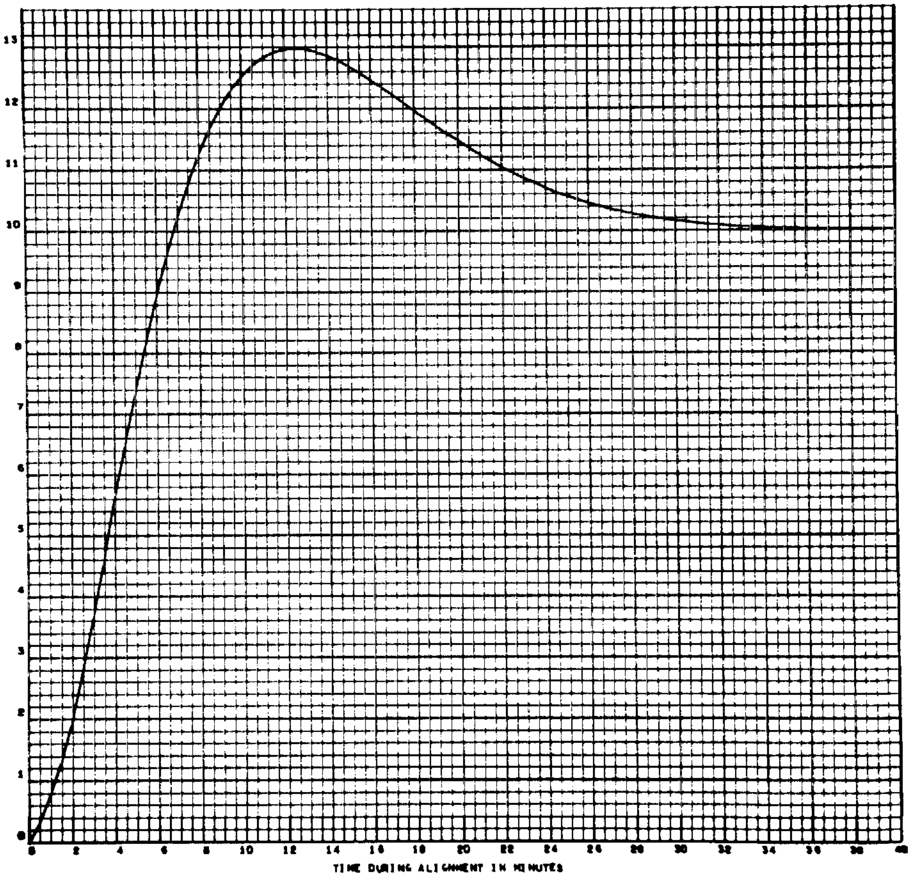

APPENDIX B

TIME HISTORY OF ALINEMENT ERRORS FOR THREE EXAMPLES OF INDIRECT ORBITAL GYROCOMPASSING

The following graphs show a time history of attitude errors resulting from selected error sources for three candidate systems, each with two choices of system time constants. Each graph may be thought of as an error sensitivity as a function of time. Attitude errors are in rms seconds of arc along the axis of ordinates. Time in seconds is plotted along the axis of abscissas. The error source for each curve is labeled at top left. Magnitudes are understood to be rms.

In some instances the error sources could equally well be deterministic rather than random in nature. The resultant attitude errors, as plotted, would then be the absolute magnitude of arc seconds of error rather than rms seconds.

In all cases the attitude errors scale directly with the amplitude of the error source except where correlated noise is concerned. The effect of correlation time variation does not scale.

Figures B-1, B-2, and B-3 show the block diagrams associated with each of the cases studied. Case numbers correspond to the candidate system cases listed in Table 4.1 of Chapter VII.

Two computer runs were made with each system in order to demonstrate the variation in dynamic results associated with variation of system time constants. The runs are labeled 1 and 2. System gains and associated characteristic equations are listed below:

Case 4: Run 1 $K_d = 6.66 \times 10^{-3}$

$K_g = 1.078 \times 10^{-2}$

$K_j = 3.33 \times 10^{-3}$

Characteristic equation for pitch : $S + .0033 = 0$

for roll-yaw : $(S + .0033 - j\ .0017)\ (S + .0033 + j\ .0017) = 0$

Run 2

$K_d = 2.22 \times 10^{-3}$

$K_g = 1.57 \times 10^{-4}$

$K_j = 1.11 \times 10^{-3}$

Characteristic equation for pitch : $(S + .00111) = 0$

for roll-yaw : $(S + .00111 + j\ .000553)\ (S + .00111 - j\ .000553) = 0$

Case 10: Run 1

$K_d = 3.74 \times 10^{-5}$

$K_b = 264$

$K_j = 1.38 \times 10^{-5}$

$K_i = 480$

$K_g = 4.78 \times 10^{-5}$

Characteristic equation for pitch : $(S + .00333 + j\ .00167)\ (S + .00333 - j\ .00167) = 0$

for roll-yaw : $(S + .00132)(S + .00428 + j\ .00488)(S + .00428 - j\ .00488) = 0$

Run 2

$K_d = 2.56 \times 10^{-6}$

$K_b = 1285$

$K_j = 1.54 \times 10^{-6}$

$K_i = 1440$

$K_g = 1.42 \times 10^{-6}$

Characteristic equation for pitch : $(S + .00111 + j\ .000557)\ (S + .00111 - j\ .000557) = 0$

for roll-yaw : $(S + .000325)(S + .00111 + j\ .00169)\ (S + .00111 - j\ .00169) = 0$

Case 14: Run 1

$K_b = 9.88 \times 10^{-3}$

$K_d = 3.74 \times 10^{-5}$

$K_g = 3.64 \times 10^{-5}$

$K_i = 6.66 \times 10^{-3}$

$K_j = 1.38 \times 10^{-5}$

Characteristic equation for pitch : $(S + .00333+j\ .00167)(S + .00333-j\ .00167) = 0$
for roll-yaw : $(S + .0032)(S + .00334+j\ .0025)(S + .00334-j\ .0025) = 0$

Run 2

$K_b = 3.30 \times 10^{-3}$
$K_d = 2.56 \times 10^{-6}$
$K_g = -2.415 \times 10^{-6}$
$K_i = 2.22 \times 10^{-3}$
$K_j = 1.54 \times 10^{-6}$

Characteristic equation for pitch : $(S + .00111+j\ .000555)(S + .00111-j\ .000555) = 0$
for roll-yaw : $(S + .00109)(S + .00112+j\ .000542)(S + .00112-j\ .000542) = 0$

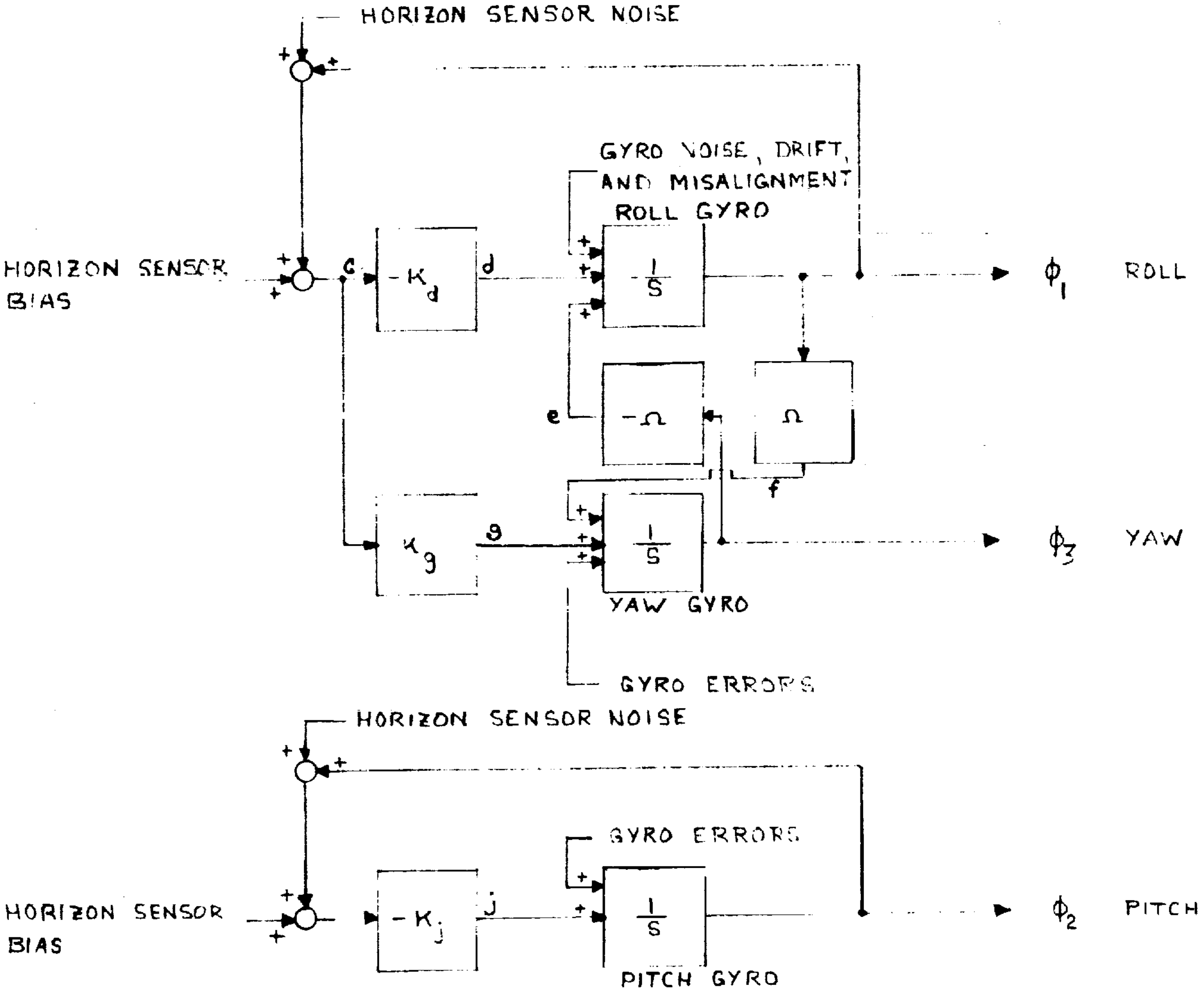
HORIZON SENSOR NOISE
HORIZON SENSOR BIAS
c
$-K_d$
d
GYRO NOISE, DRIFT, AND MISALIGNMENT
ROLL GYRO
$\frac{1}{S}$
ϕ_1
ROLL
e
$-\Omega$
Ω
f
K_g
g
$\frac{1}{S}$
ϕ_3
YAW
YAW GYRO
GYRO ERRORS
HORIZON SENSOR NOISE
GYRO ERRORS
HORIZON SENSOR BIAS
$-K_j$
j
$\frac{1}{S}$
ϕ_2
PITCH
PITCH GYRO
+

Fig. B-1

Error Block Diagram for Case 4

$\Omega = 1.164 \times 10^{-3}$ rad/sec

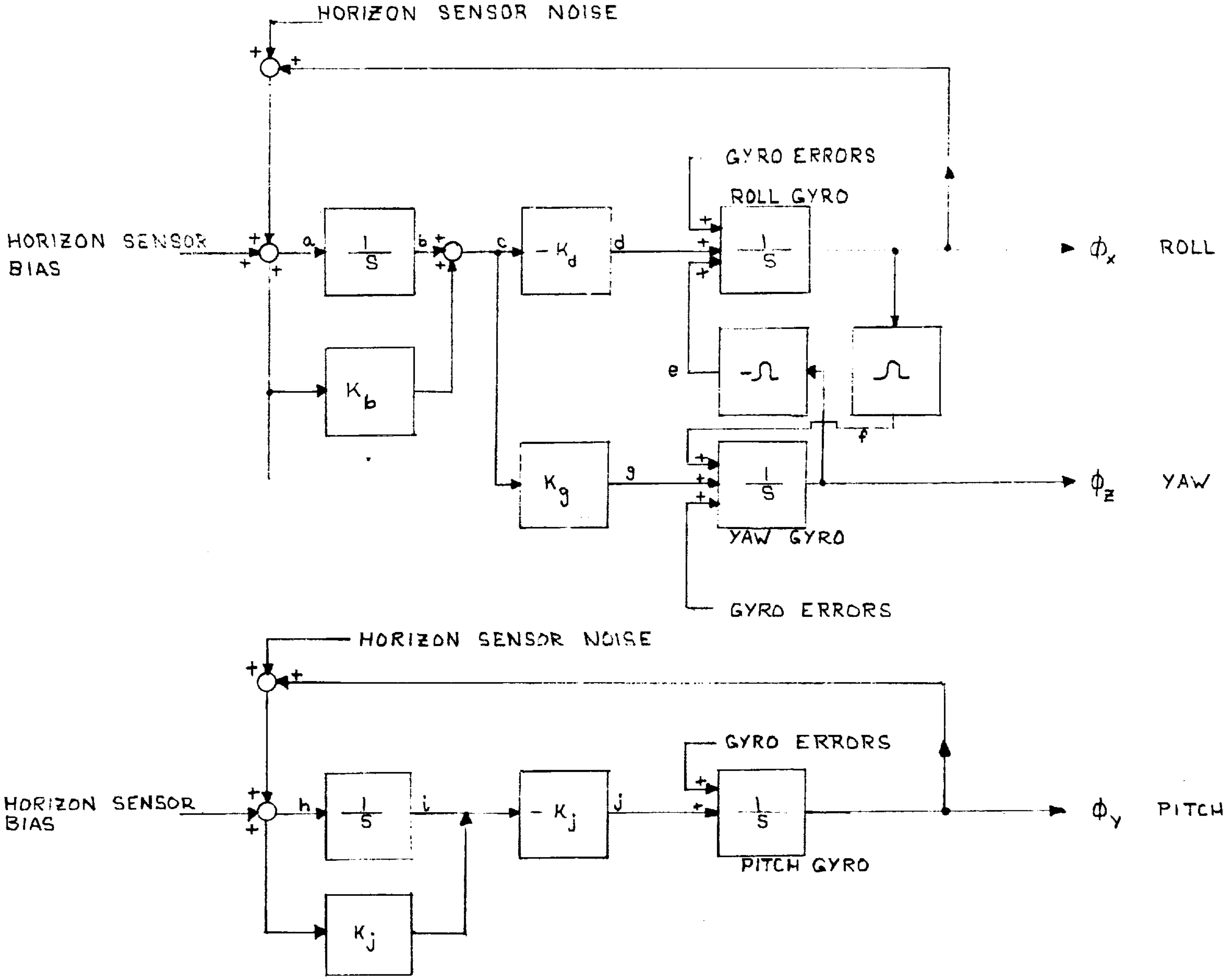
HORIZON SENSOR NOISE
HORIZON SENSOR BIAS
a
$\frac{1}{S}$
b
c
$-K_d$
d
GYRO ERRORS
ROLL GYRO
$\frac{1}{S}$
ϕ_x
ROLL
K_b
e
$-\Omega$
Ω
f
K_g
g
$\frac{1}{S}$
YAW GYRO
ϕ_z
YAW
GYRO ERRORS
HORIZON SENSOR NOISE
HORIZON SENSOR BIAS
h
$\frac{1}{S}$
i
$-K_j$
j
GYRO ERRORS
$\frac{1}{S}$
PITCH GYRO
ϕ_y
PITCH
K_j

Fig. B-2

Error Block Diagram for Case 10

$\Omega = 1.164 \times 10^{-3}$ rad/sec

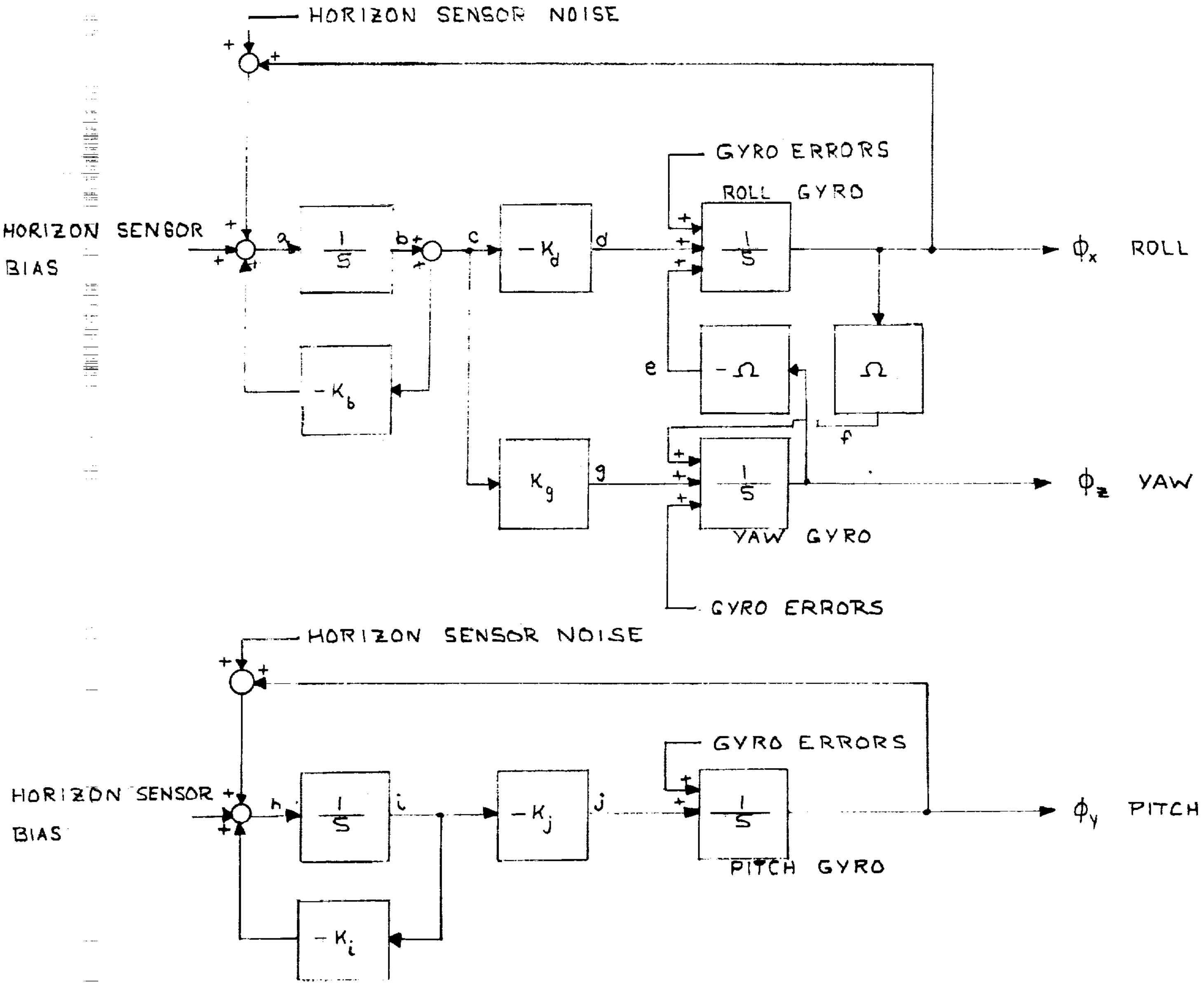
HORIZON SENSOR NOISE
HORIZON SENSOR BIAS
a
$\frac{1}{S}$
b
c
$-K_d$
d
GYRO ERRORS
ROLL GYRO
$\frac{1}{S}$
ϕ_x ROLL
$-K_b$
e
$-\Omega$
Ω
f
K_g
g
$\frac{1}{S}$
ϕ_z YAW
YAW GYRO
GYRO ERRORS
HORIZON SENSOR NOISE
HORIZON SENSOR BIAS
h
$\frac{1}{S}$
i
$-K_j$
j
GYRO ERRORS
$\frac{1}{S}$
ϕ_y PITCH
PITCH GYRO
$-K_i$
+

Fig. B-3

Error Block Diagram for Case 14

$\Omega = 1.164 \times 10^{-3}$ rad/sec

B1

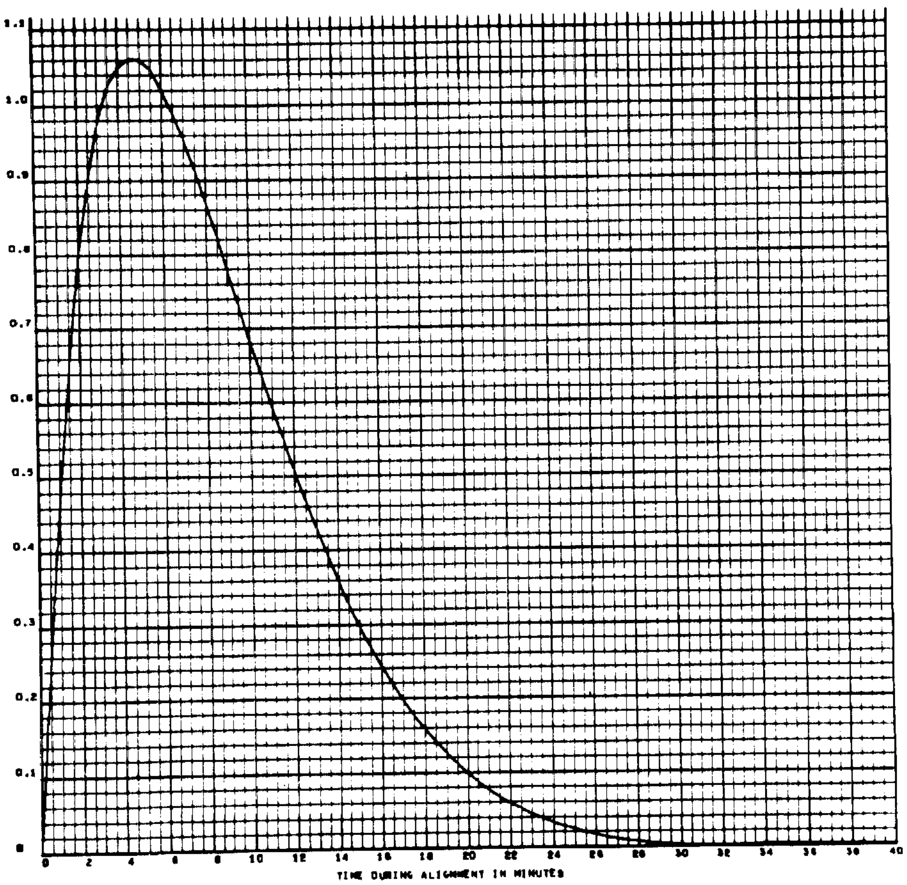

LEVEL TILT IN ARCSECONDS - ORBITAL GYROCOMPASSING, CASE 4, RUN 1
X TILT DUE TO X GYRO DRIFT - .01 DEGREES/HOUR

B2

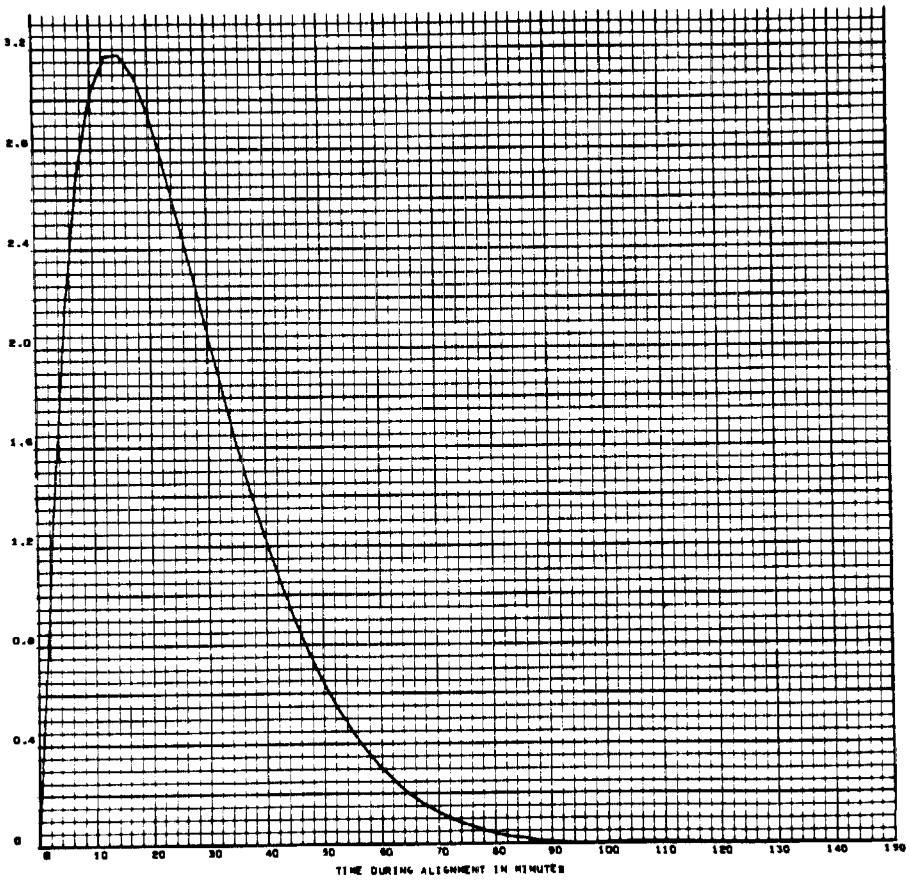

LEVEL TILT IN ARCSECONDS - ORBITAL GYROCOMPASSING, CASE 4, RUN 2
X TILT DUE TO X GYRO DRIFT - .01 DEGREES/HOUR

B3

LEVEL TILT IN ARCSECONDS - ORBITAL GYROCOMPASSING, CASE 10, RUN 1
X TILT DUE TO X GYRO DRIFT - .01 DEGREES/HOUR

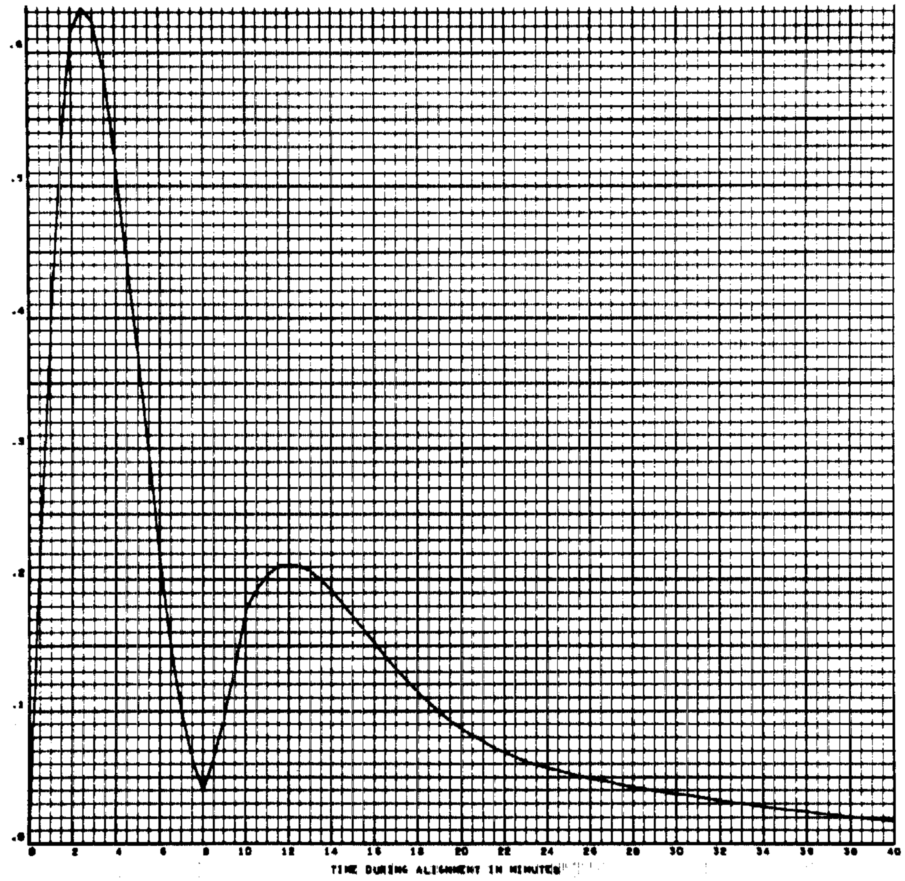

B4

LEVEL TILT IN ARCSECONDS - ORBITAL GYROCOMPASSING, CASE 10, RUN 2
X TILT DUE TO X GYRO DRIFT - .01 DEGREES/HOUR

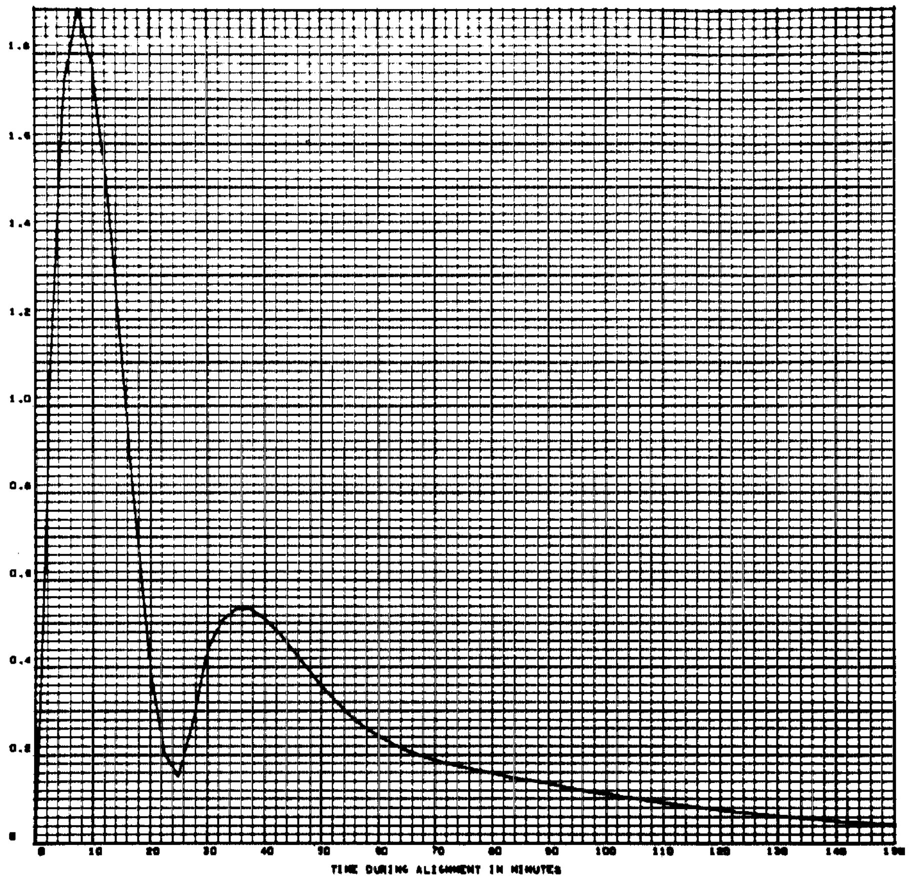

B-5

LEVEL TILT IN ARCSECONDS - ORBITAL GYROCOMPASSING, CASE 14, RUN 1
X TILT DUE TO X GYRO DRIFT - .01 DEGREES/HOUR

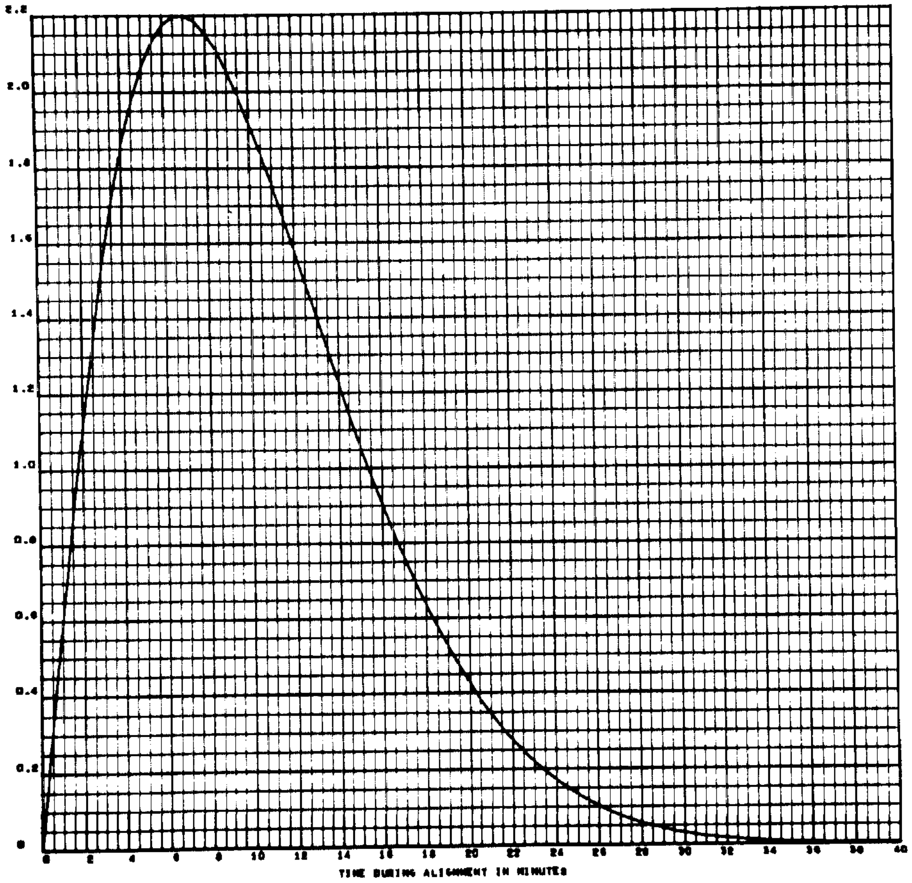

B6

LEVEL TILT IN ARCSECONDS - ORBITAL GYROCOMPASSING, CASE 14, RUN 2
X TILT DUE TO X GYRO DRIFT - .01 DEGREES/HOUR

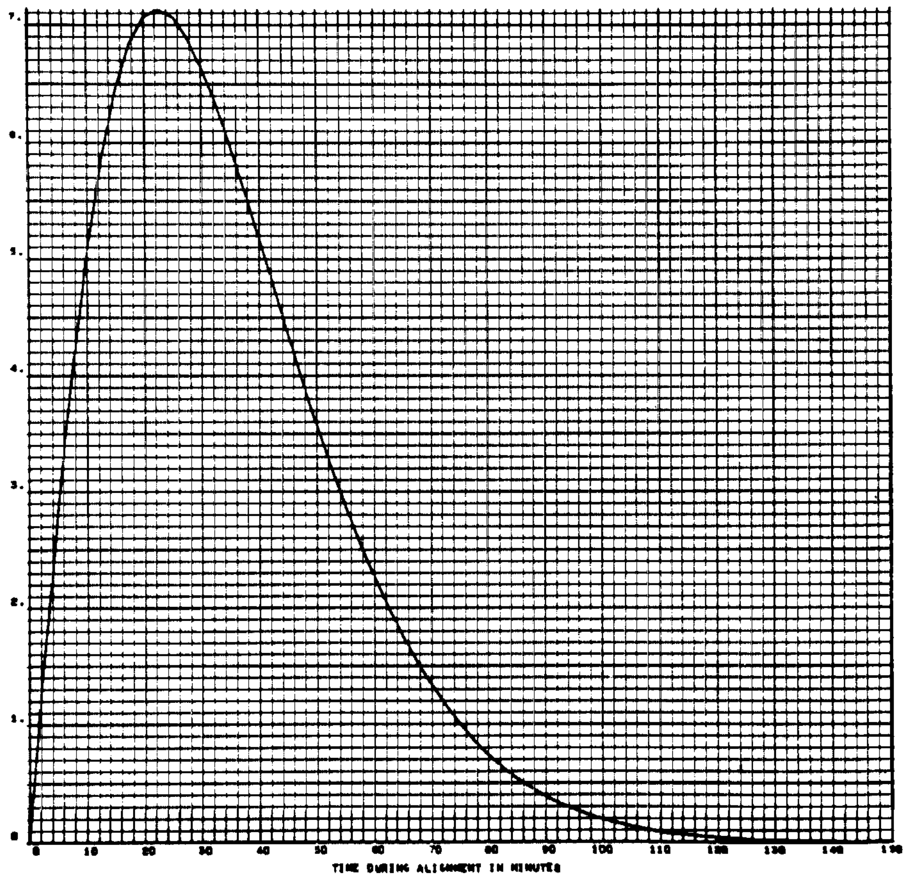

B7

LEVEL TILT IN ARCSECONDS - ORBITAL GYROCOMPASSING, CASE 4, RUN 3
X TILT DUE TO Z GYRO DRIFT - .01 DEGREES/HOUR

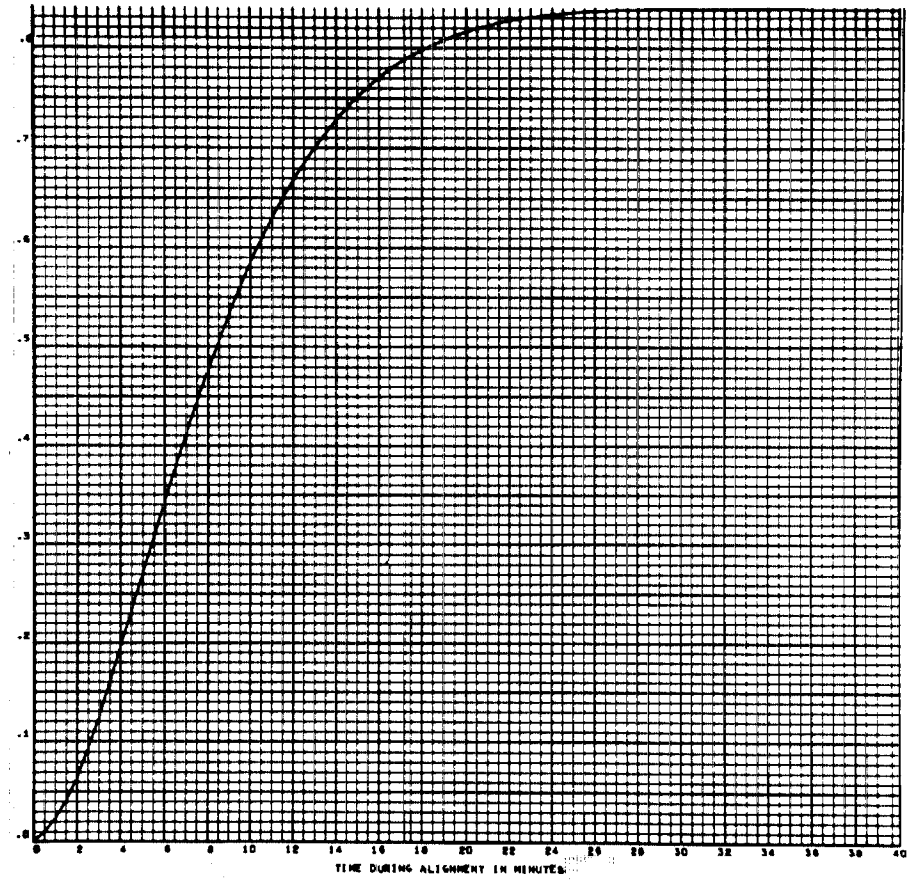

B8

LEVEL TILT IN ARCSECONDS - ORBITAL GYROCOMPASSING, CASE 4, RUN 8
X TILT DUE TO Z GYRO DRIFT - .01 DEGREES/HOUR

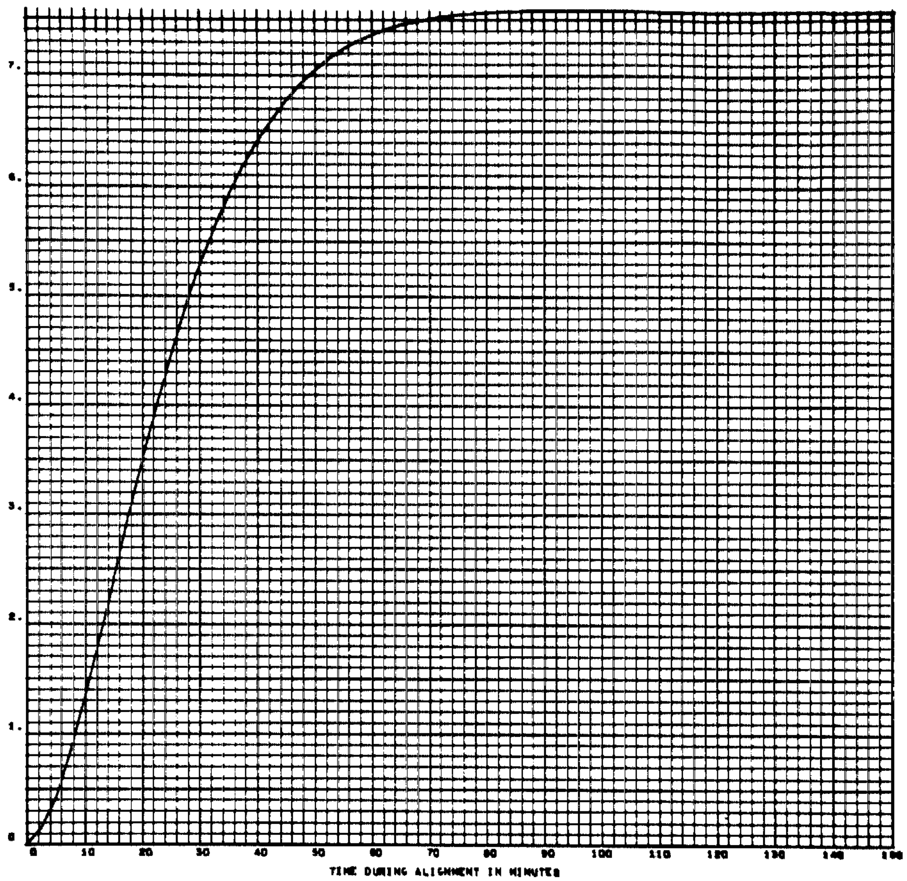

B9

LEVEL TILT IN ARCSECONDS - ORBITAL GYROCOMPASSING, CASE 10, RUN 1
X TILT DUE TO Z GYRO DRIFT - .01 DEGREES/HOUR

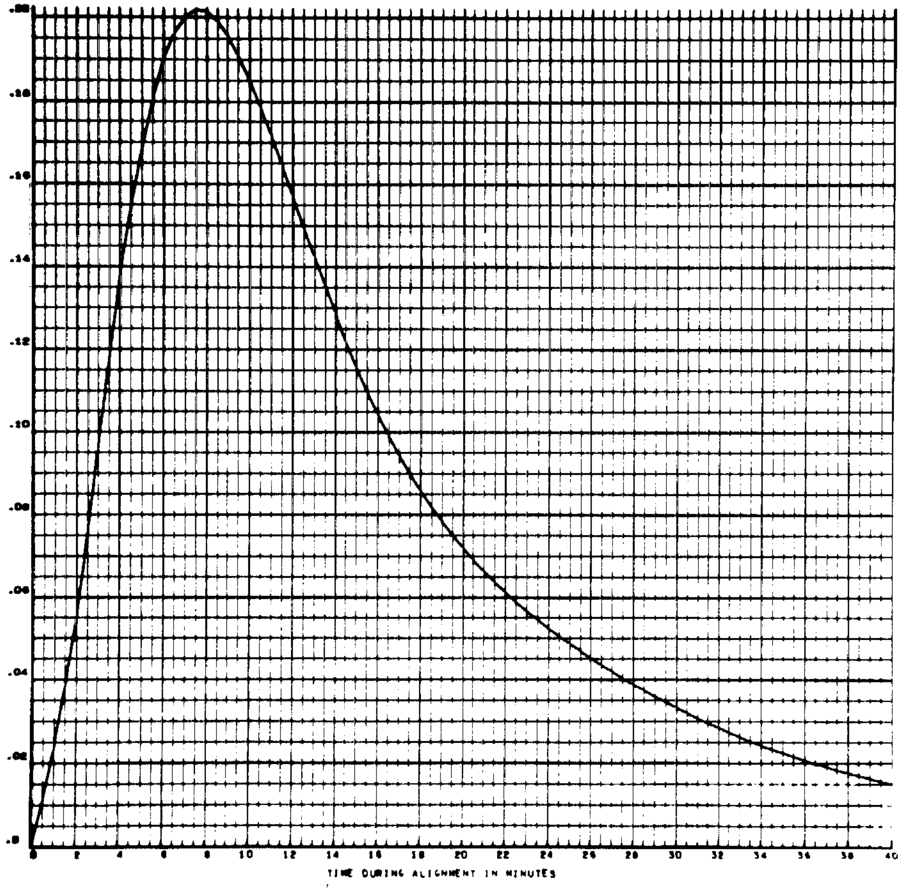

B10

LEVEL TILT IN ARCSECONDS - ORBITAL GYROCOMPASSING, CASE 10, RUN 2
X TILT DUE TO Z GYRO DRIFT - .01 DEGREES/HOUR

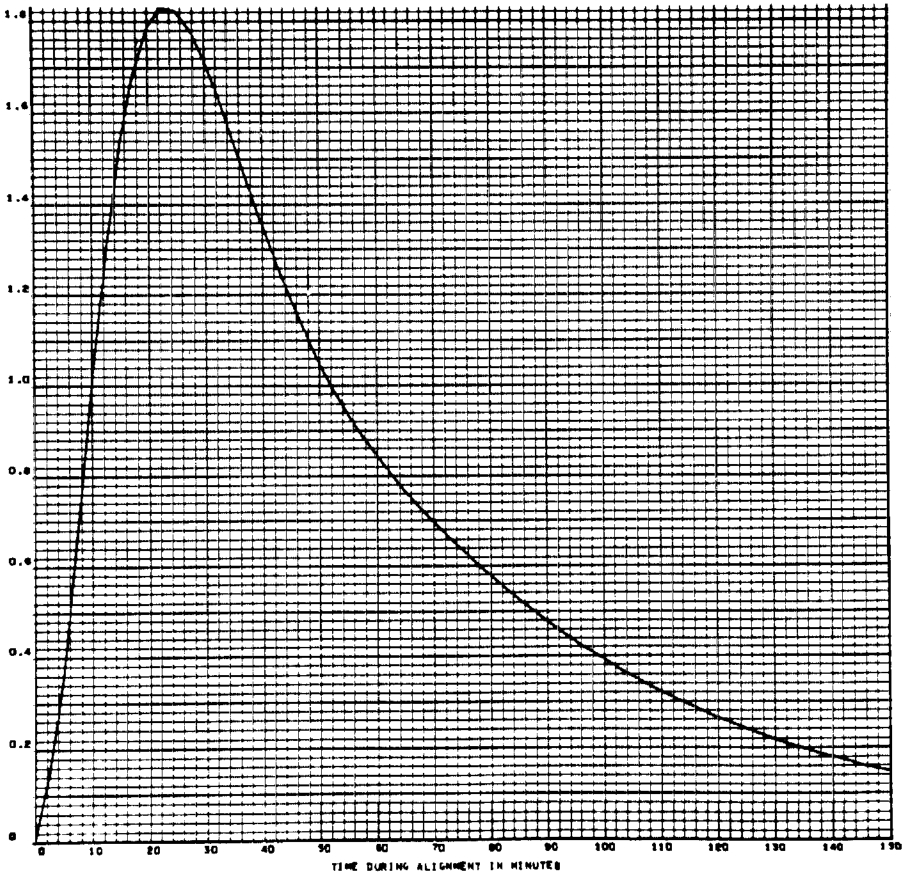

B11

LEVEL TILT IN ARCSECONDS - ORBITAL GYROCOMPASSING, CASE 14, RUN 1
X TILT DUE TO Z GYRO DRIFT - .01 DEGREES/HOUR

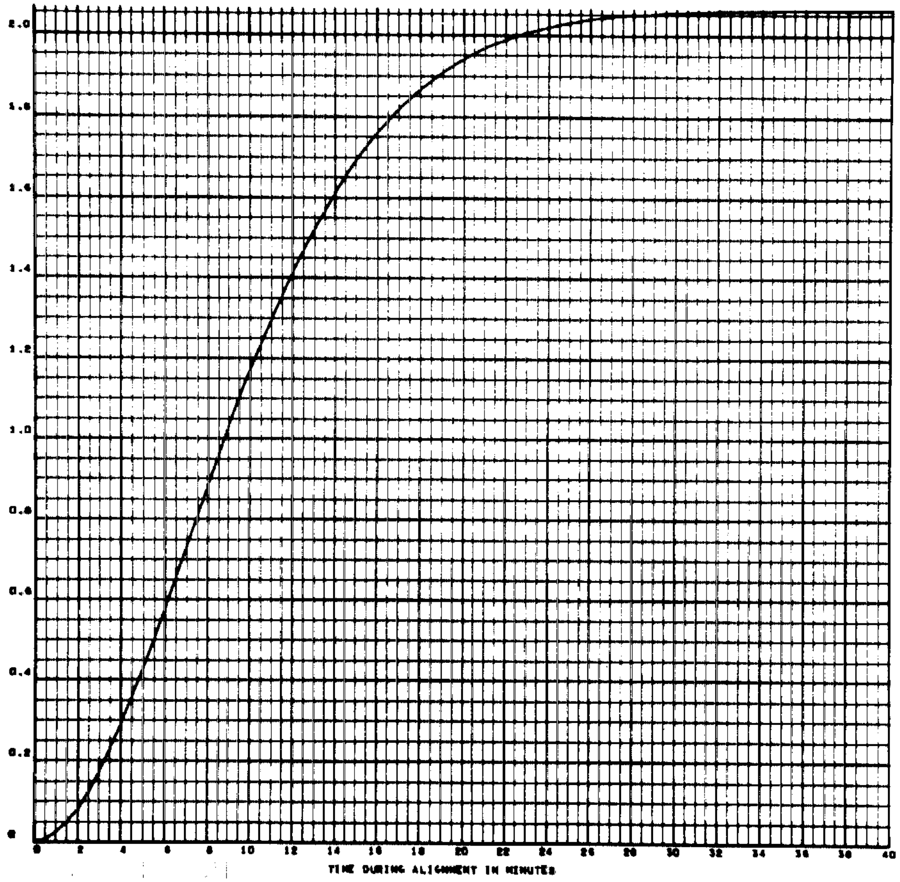

B12

LEVEL TILT IN ARCSECONDS - ORBITAL GYROCOMPASSING, CASE 14, RUN 2
X TILT DUE TO Z GYRO DRIFT - .01 DEGREES/HOUR

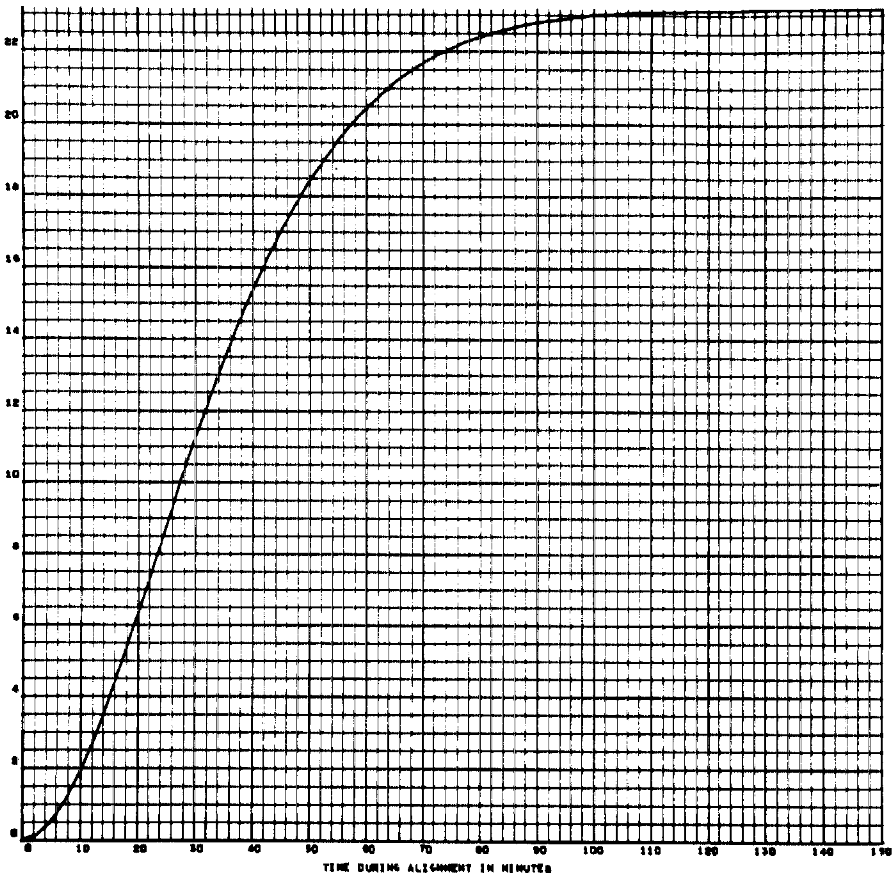

B13

LEVEL TILT IN ARCSECONDS - ORBITAL GYROCOMPASSING, CASE 4, RUN 1
X TILT DUE TO X GYRO NOISE - .01 DEGREES/HOUR, C.T. = 1 HOUR

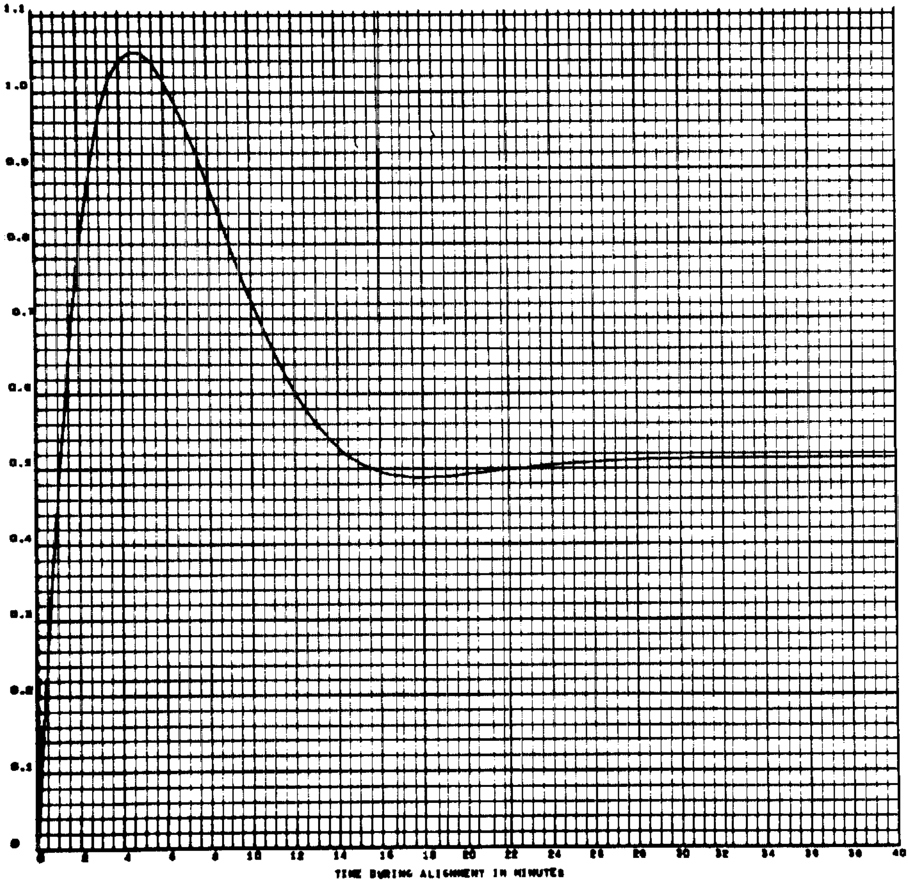

B14

LEVEL TILT IN ARCSECONDS - ORBITAL GYROCOMPASSING, CASE 4, RUN 2
X TILT DUE TO X GYRO NOISE - .01 DEGREES/HOUR, C.T. = 1 HOUR

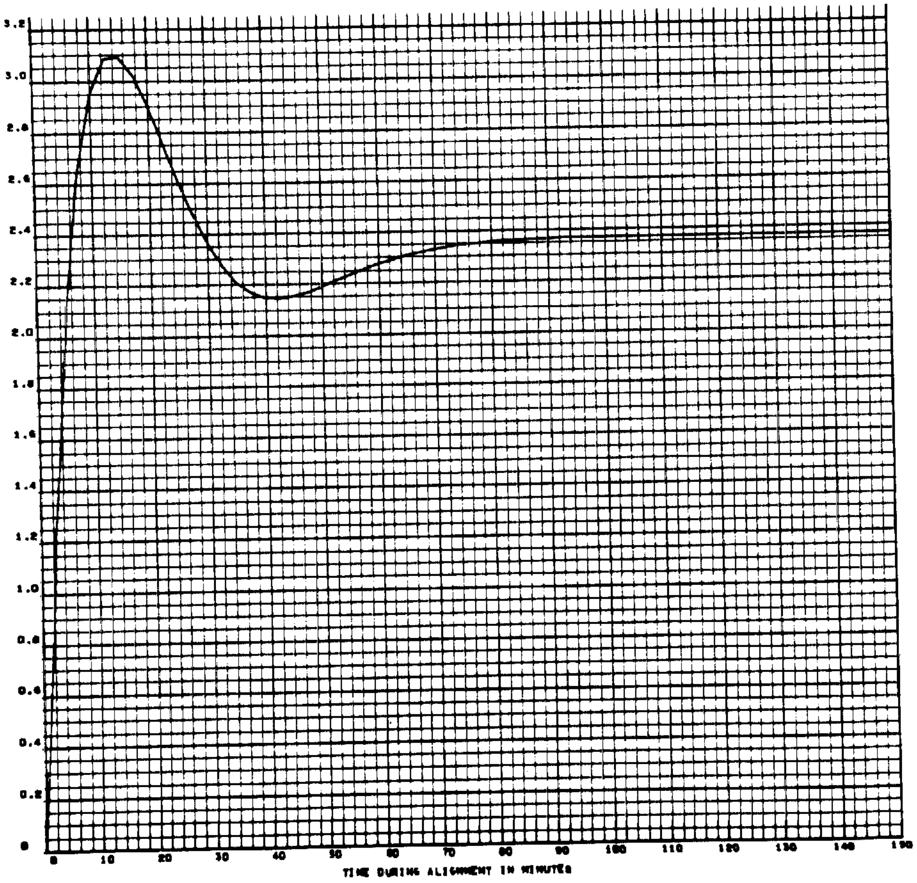

B/5

LEVEL TILT IN ARCSECONDS - ORBITAL GYROCOMPASSING, CASE 10, RUN 1
X TILT DUE TO X GYRO NOISE - .01 DEGREES/HOUR, C.T. = 1 HOUR

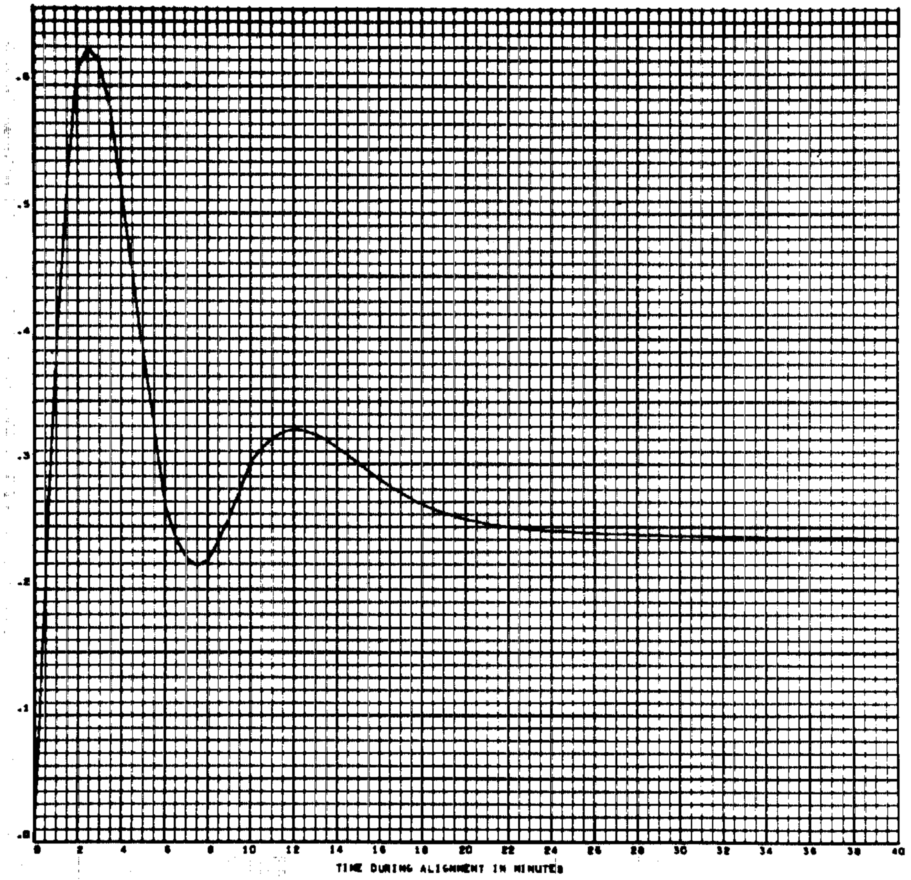

B/6

LEVEL TILT IN ARCSECONDS - ORBITAL GYROCOMPASSING, CASE 10, RUN 2
X TILT DUE TO X GYRO NOISE - .01 DEGREES/HOUR, C.T. = 1 HOUR

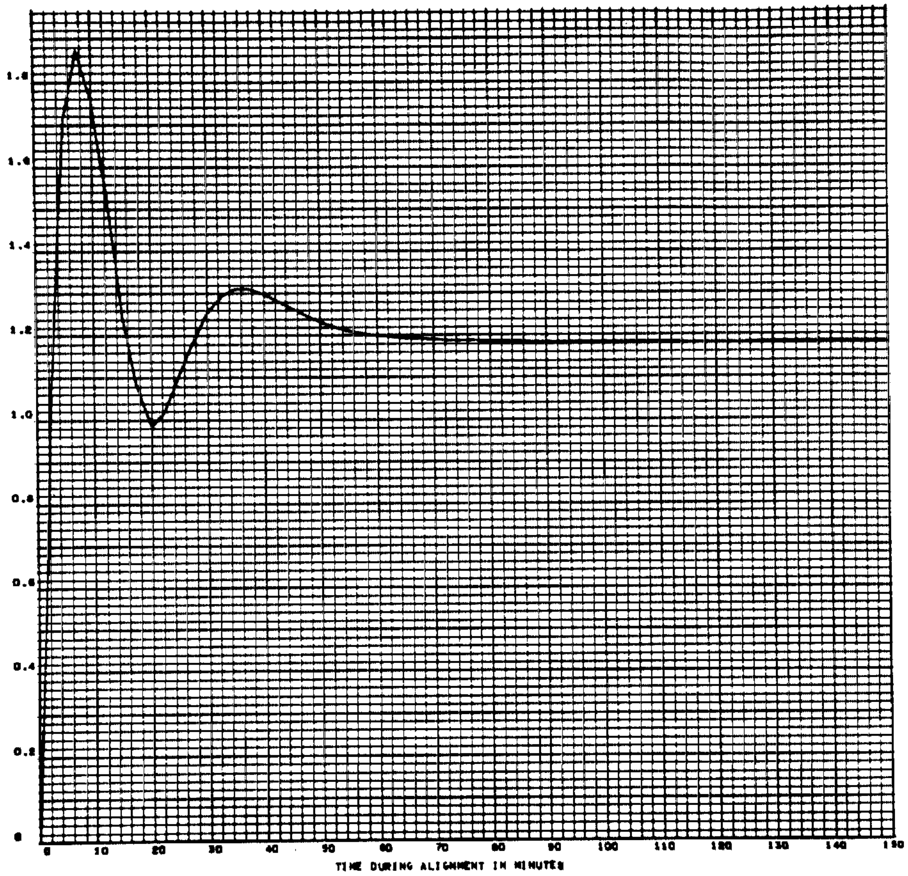

B17

LEVEL TILT IN ARCSECONDS - ORBITAL GYROCOMPASSING, CASE 14, RUN 1
X TILT DUE TO X GYRO NOISE - .01 DEGREES/HOUR, C.T. = 1 HOUR

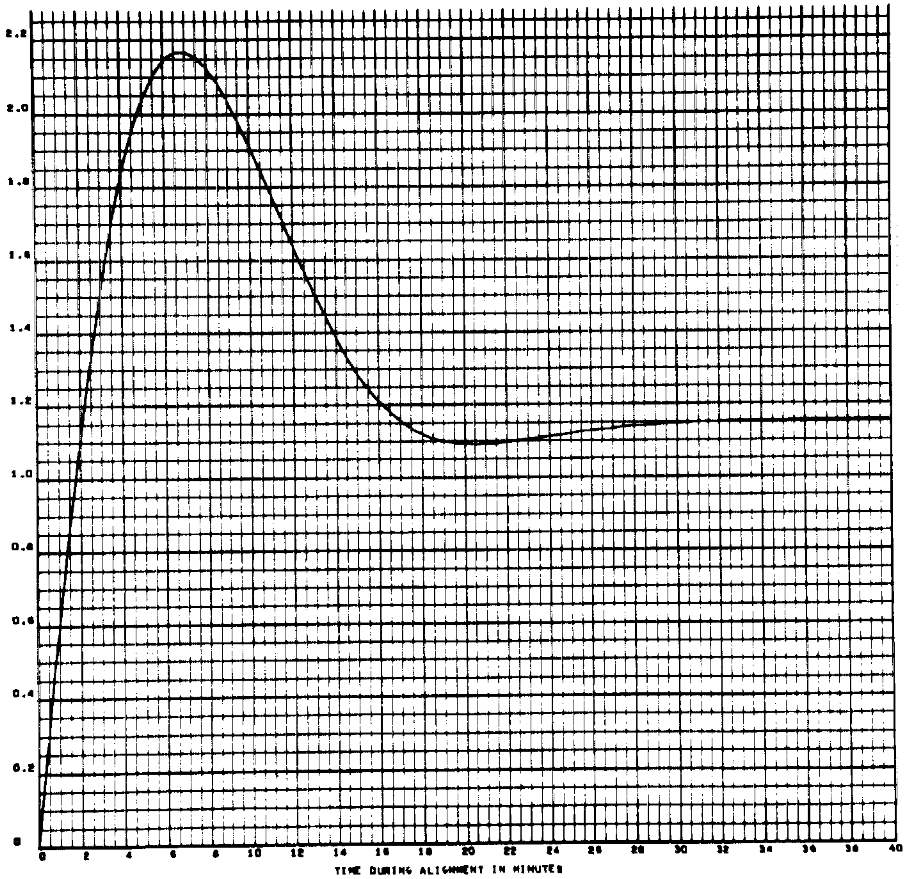

B18

LEVEL TILT IN ARCSECONDS - ORBITAL GYROCOMPASSING, CASE 14, RUN 2
X TILT DUE TO X GYRO NOISE - .01 DEGREES/HOUR, C.T. = 1 HOUR

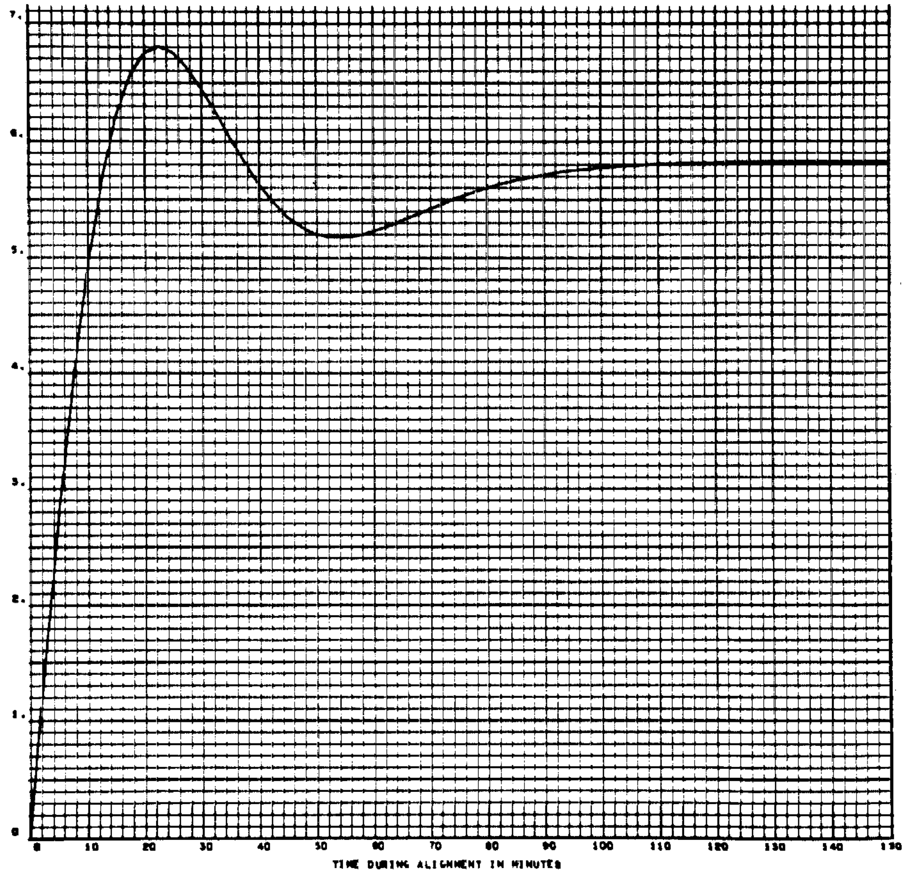

1B19

LEVEL TILT IN ARCSECONDS - ORBITAL GYROCOMPASSING, CASE 4, RUN 1
X TILT DUE TO Z GYRO NOISE - .01 DEGREES/HOUR, C.T. = 1 HOUR

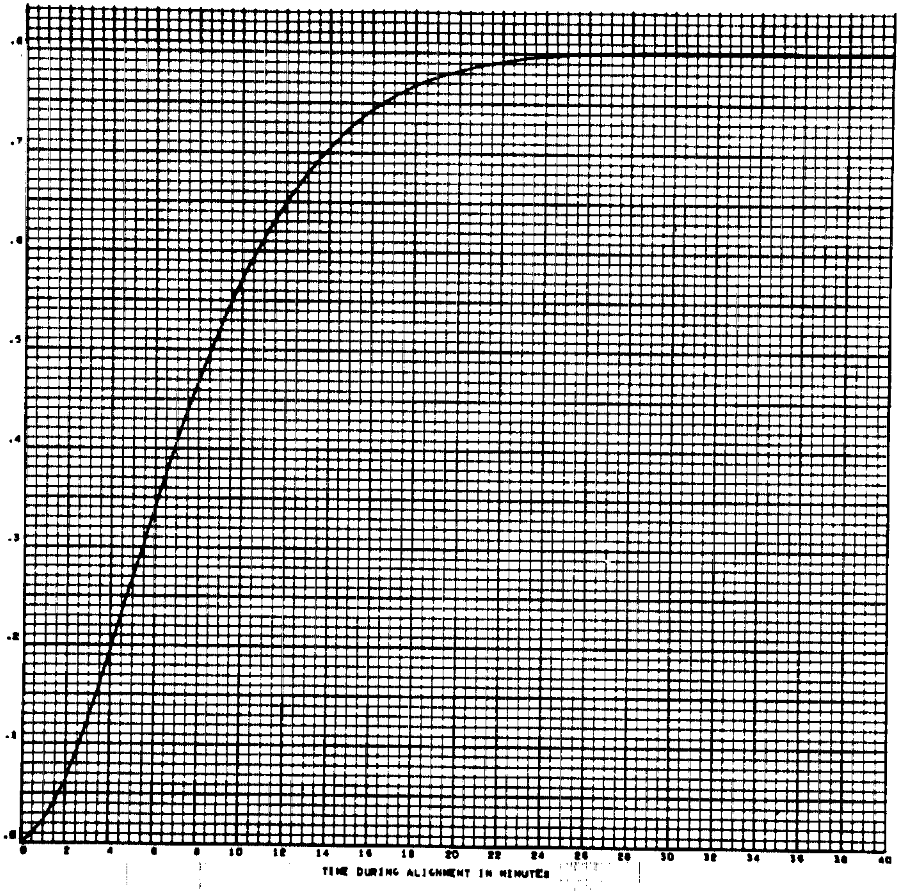

1B20

LEVEL TILT IN ARCSECONDS - ORBITAL GYROCOMPASSING, CASE 4, RUN 2
X TILT DUE TO Z GYRO NOISE - .01 DEGREES/HOUR, C.T. = 1 HOUR

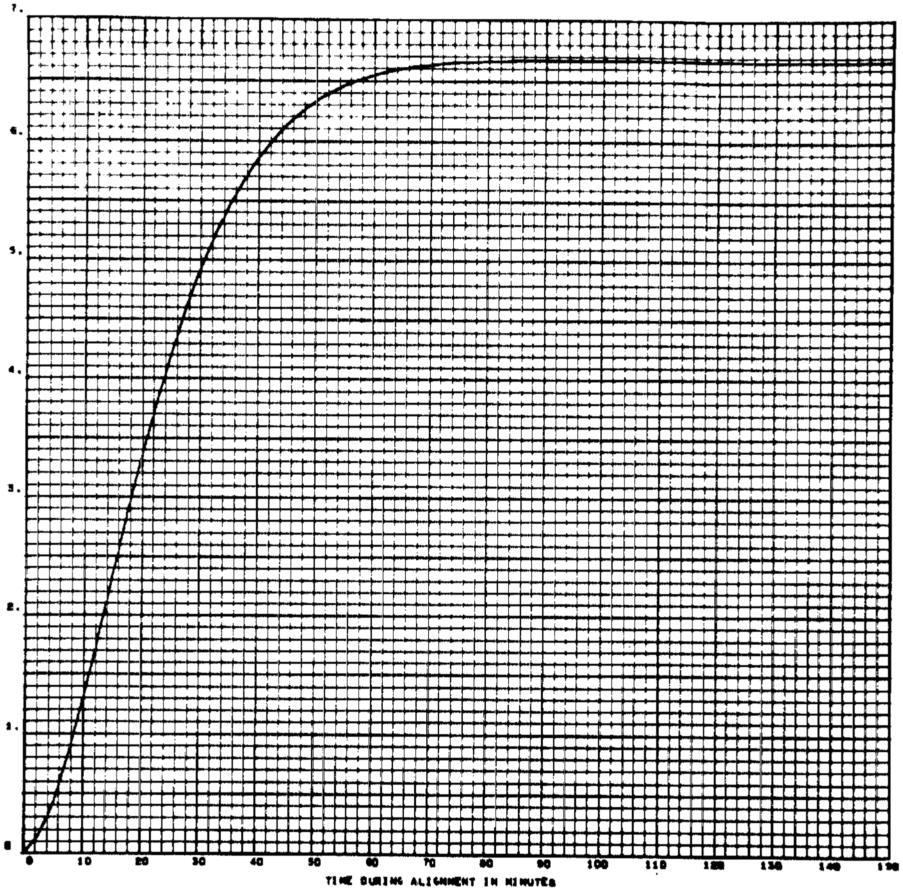

B21

LEVEL TILT IN ARCSECONDS - ORBITAL GYROCOMPASSING, CASE 10, RUN 1
X TILT DUE TO Z GYRO NOISE - .01 DEGREES/HOUR, C.T. = 1 HOUR

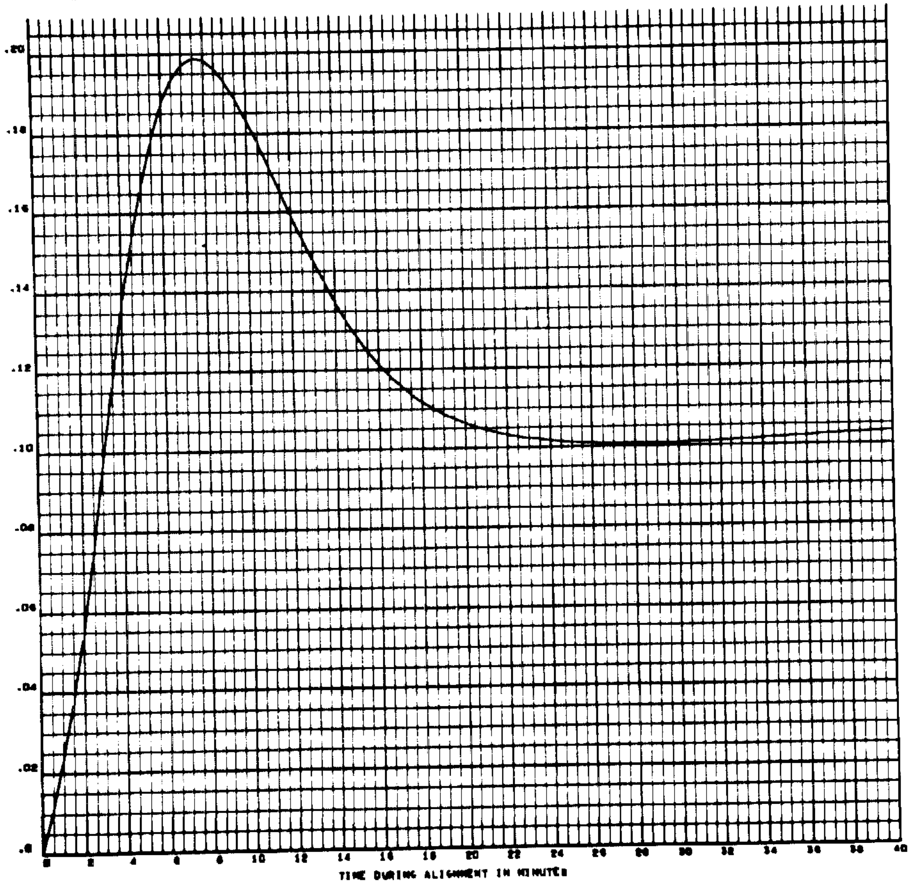

B22

LEVEL TILT IN ARCSECONDS - ORBITAL GYROCOMPASSING, CASE 10, RUN 2
X TILT DUE TO Z GYRO NOISE - .01 DEGREES/HOUR, C.T. = 1 HOUR

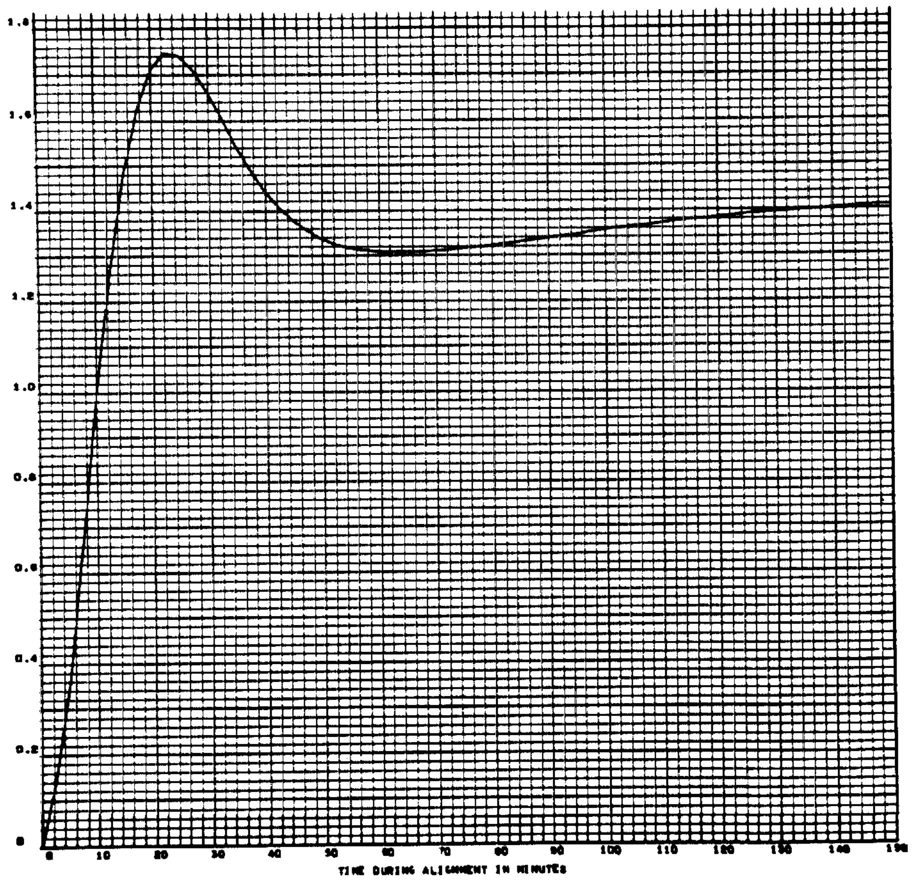

B23

LEVEL TILT IN ARCSECONDS - ORBITAL GYROCOMPASSING, CASE 14, RUN 1
X TILT DUE TO Z GYRO NOISE - .01 DEGREES/HOUR, C.T. = 1 HOUR

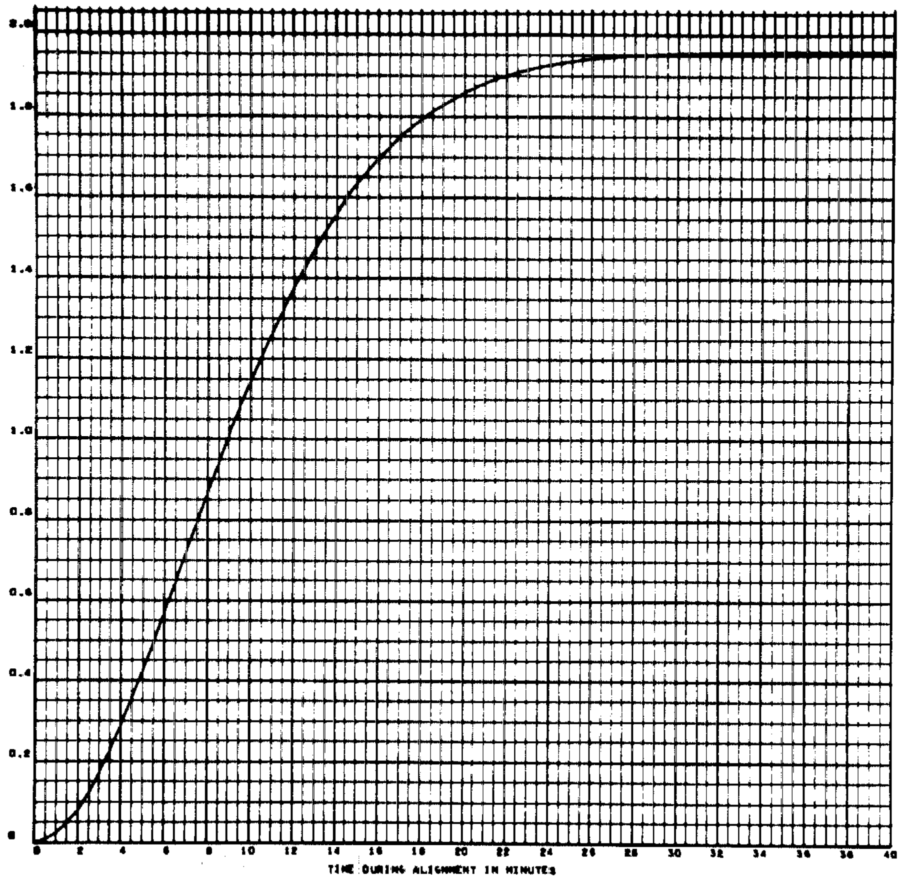

B24

LEVEL TILT IN ARCSECONDS - ORBITAL GYROCOMPASSING, CASE 14, RUN 2
X TILT DUE TO Z GYRO NOISE - .01 DEGREES/HOUR, C.T. = 1 HOUR

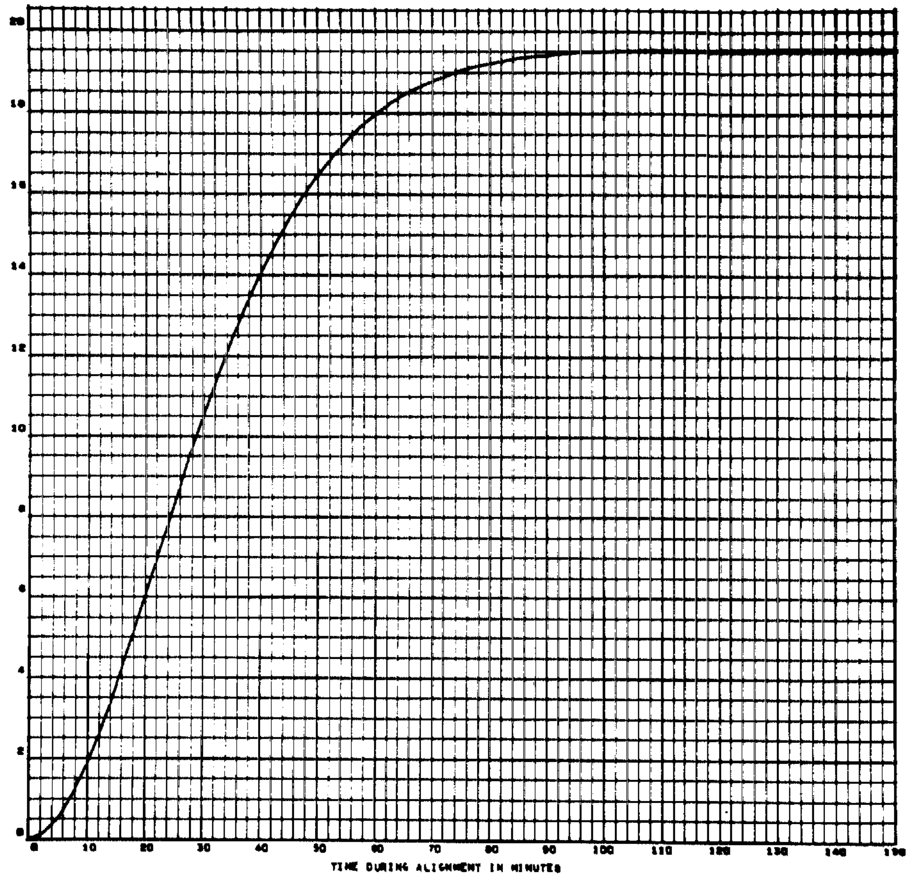

B25

LEVEL TILT IN ARCSECONDS - ORBITAL GYROCOMPASSING, CASE 4, RUN 1
X TILT DUE TO X GYRO MISALIGNMENT - 1 ARCSECOND

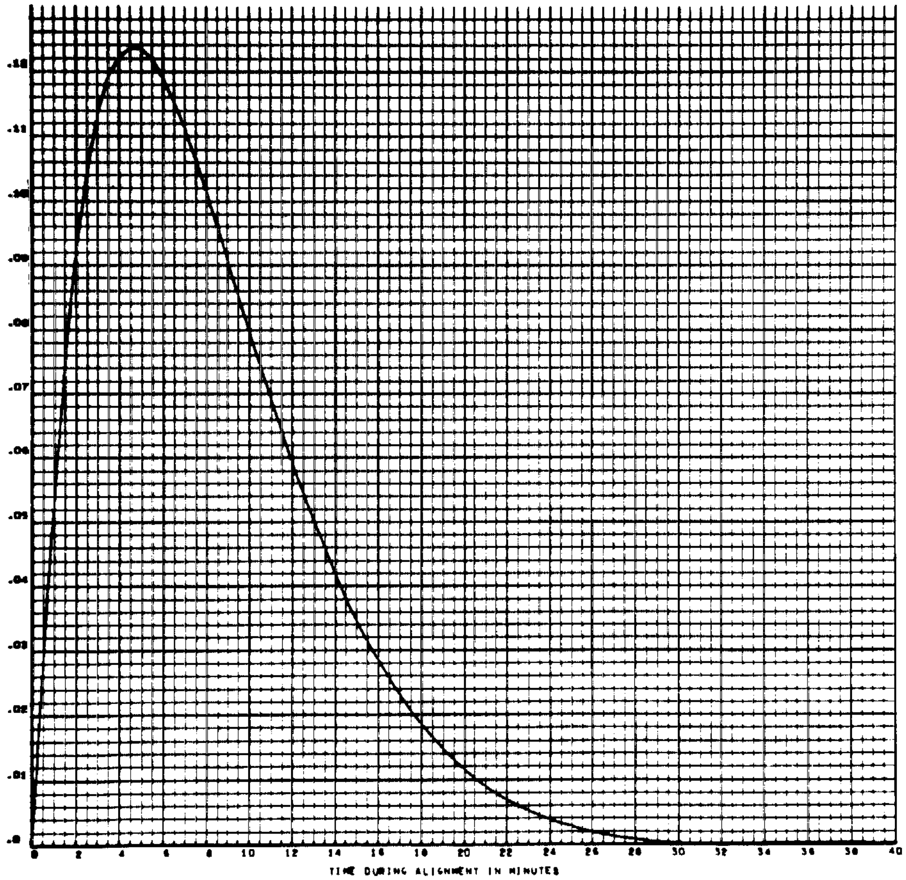

B26

LEVEL TILT IN ARCSECONDS - ORBITAL GYROCOMPASSING, CASE 4, RUN 2
X TILT DUE TO X GYRO MISALIGNMENT - 1 ARCSECOND

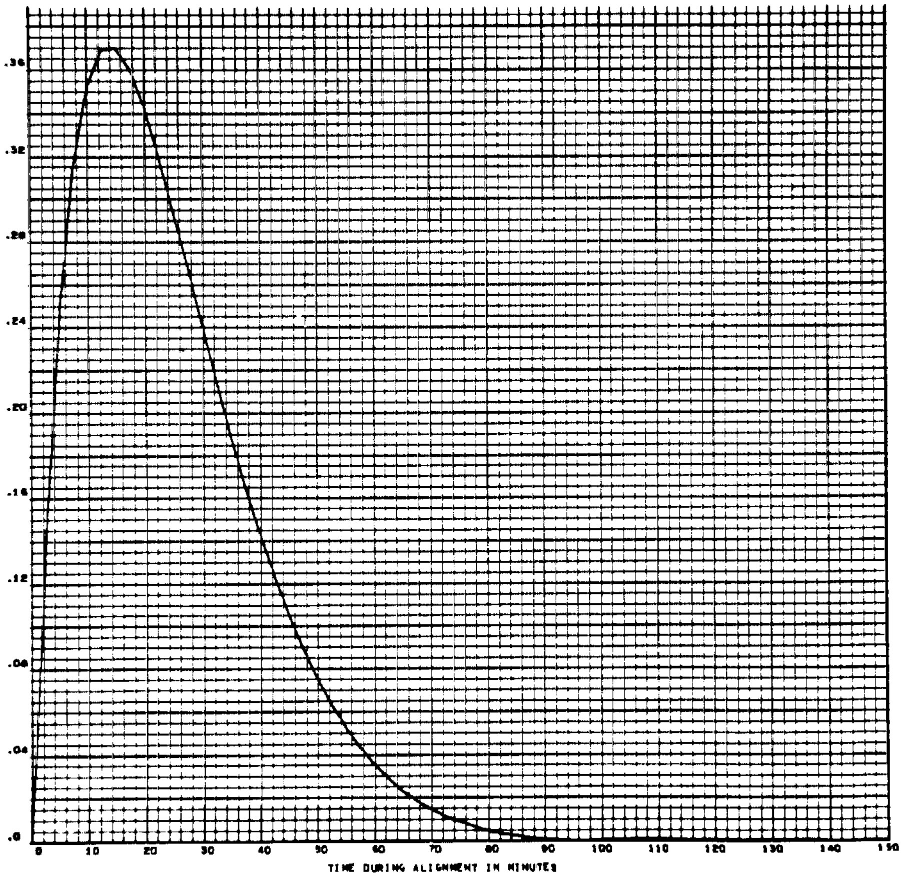

B27

LEVEL TILT IN ARCSECONDS - ORBITAL GYROCOMPASSING, CASE 10, RUN 1
X TILT DUE TO X GYRO MISALIGNMENT - 1 ARCSECOND

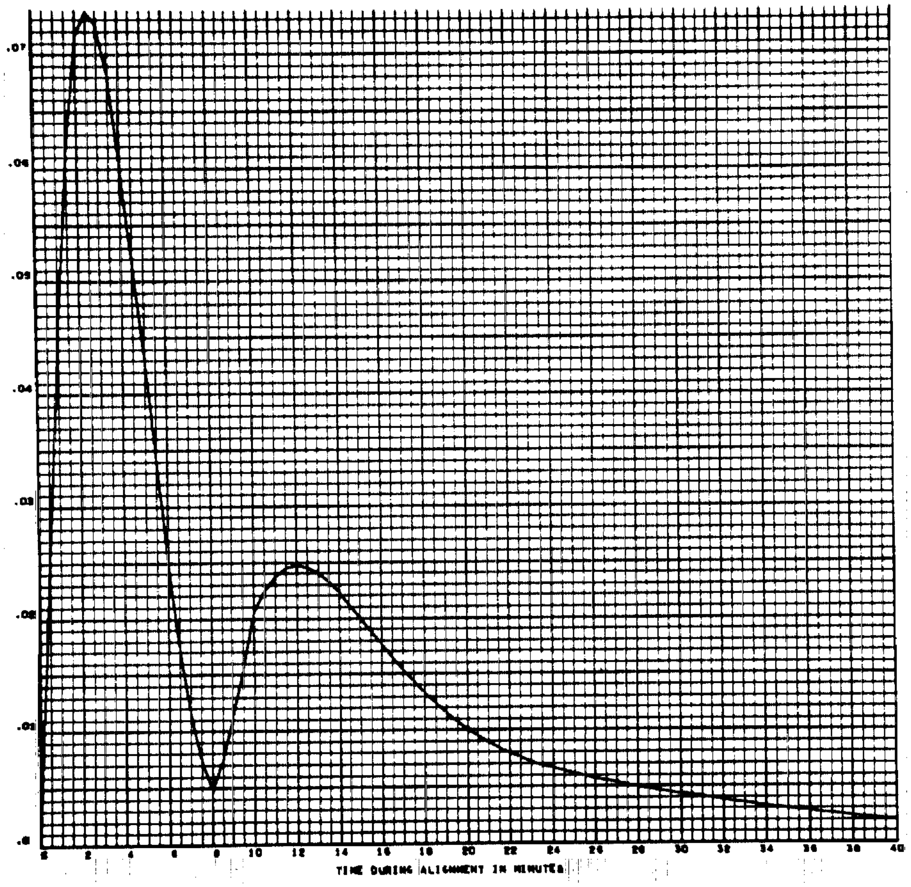

B28

LEVEL TILT IN ARCSECONDS - ORBITAL GYROCOMPASSING, CASE 10, RUN 2
X TILT DUE TO X GYRO MISALIGNMENT - 1 ARCSECOND

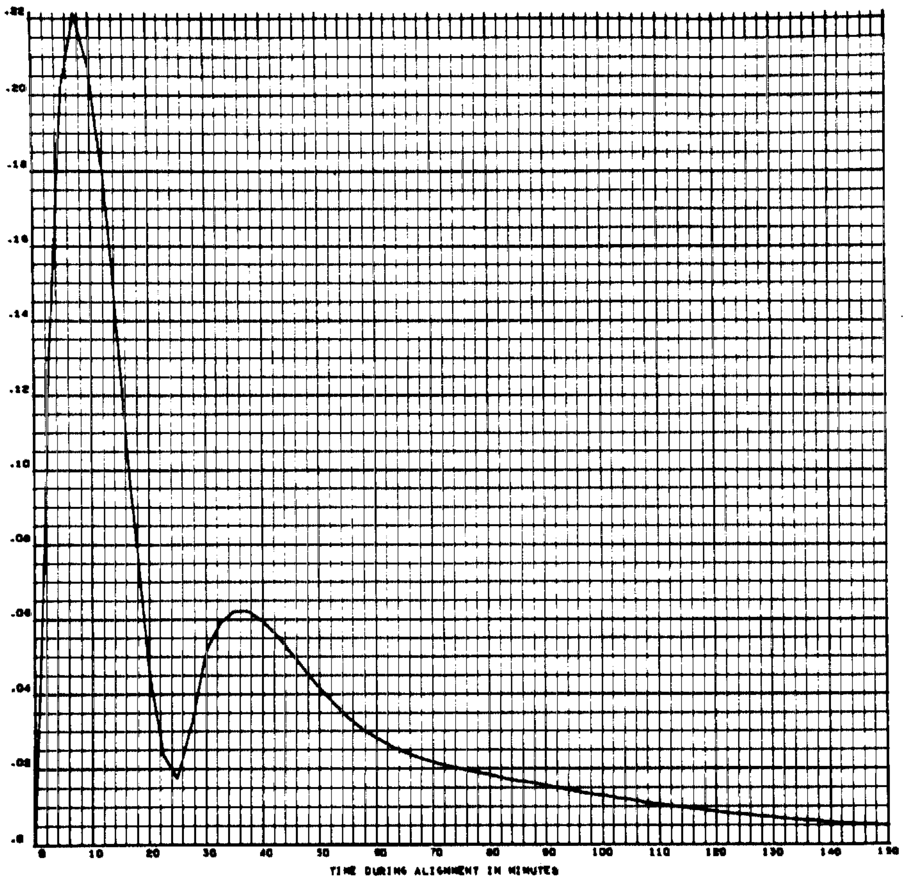

B29

LEVEL TILT IN ARCSECONDS - ORBITAL GYROCOMPASSING, CASE 14, RUN 1
X TILT DUE TO X GYRO MISALIGNMENT - 1 ARCSECOND

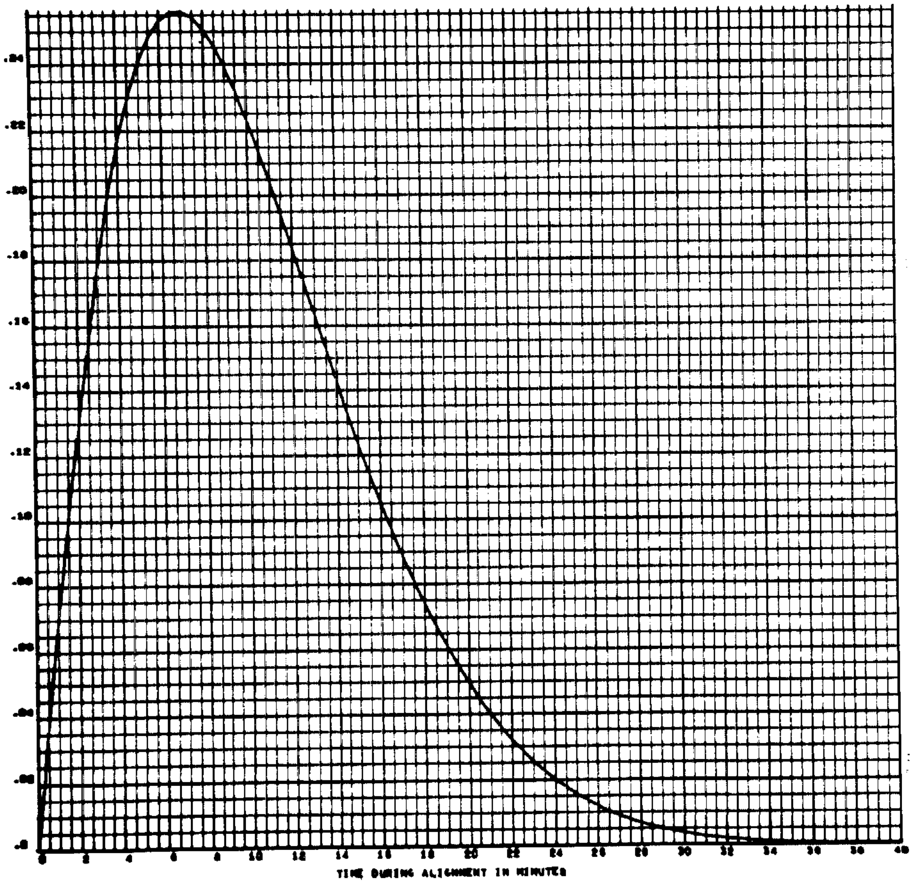

B30

LEVEL TILT IN ARCSECONDS - ORBITAL GYROCOMPASSING, CASE 14, RUN 2
X TILT DUE TO X GYRO MISALIGNMENT - 1 ARCSECOND

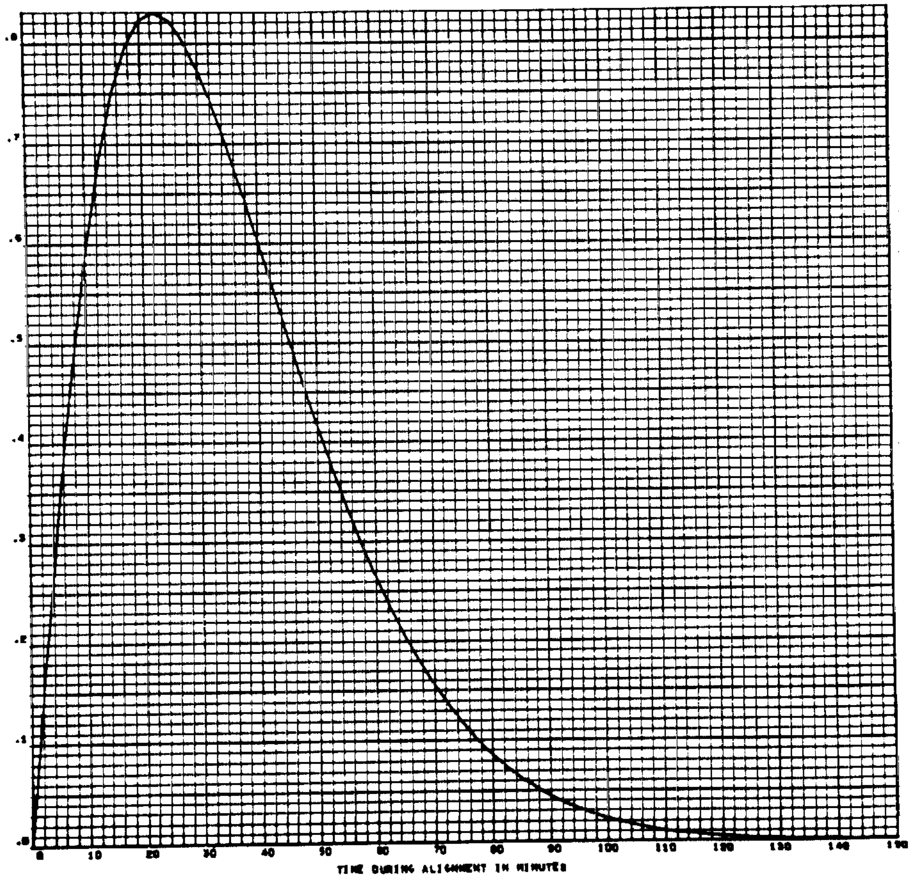

B31

LEVEL TILT IN ARCSECONDS - ORBITAL GYROCOMPASSING, CASE 4, RUN 1
X TILT DUE TO Z GYRO MISALIGNMENT - 1 ARCSECOND

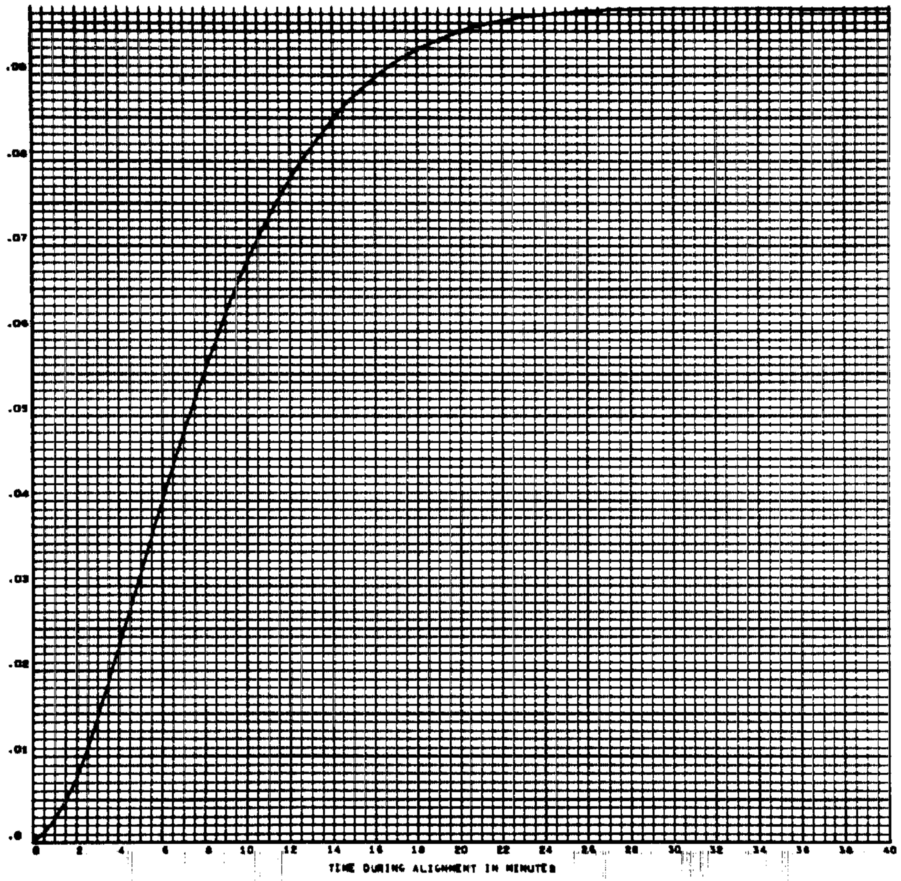

B32

LEVEL TILT IN ARCSECONDS - ORBITAL GYROCOMPASSING, CASE 4, RUN 2
X TILT DUE TO Z GYRO MISALIGNMENT - 1 ARCSECOND

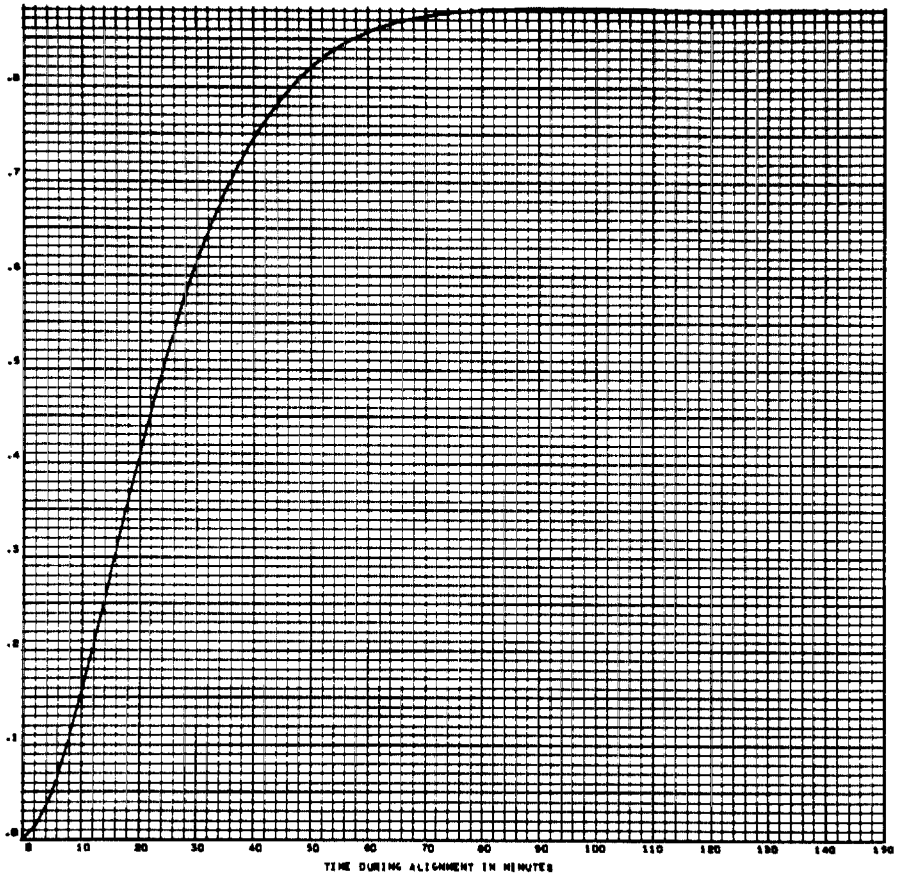

B33

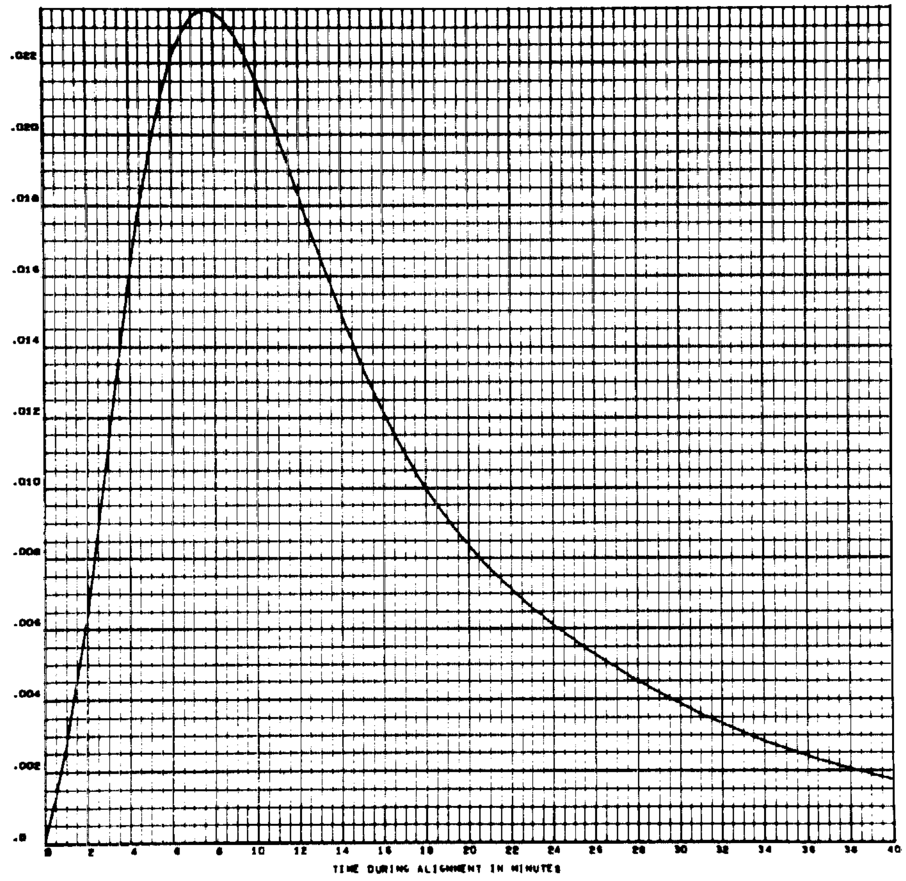
LEVEL TILT IN ARCSECONDS - ORBITAL GYROCOMPASSING, CASE 10, RUN 1
X TILT DUE TO Z GYRO MISALIGNMENT - 1 ARCSECOND

B34

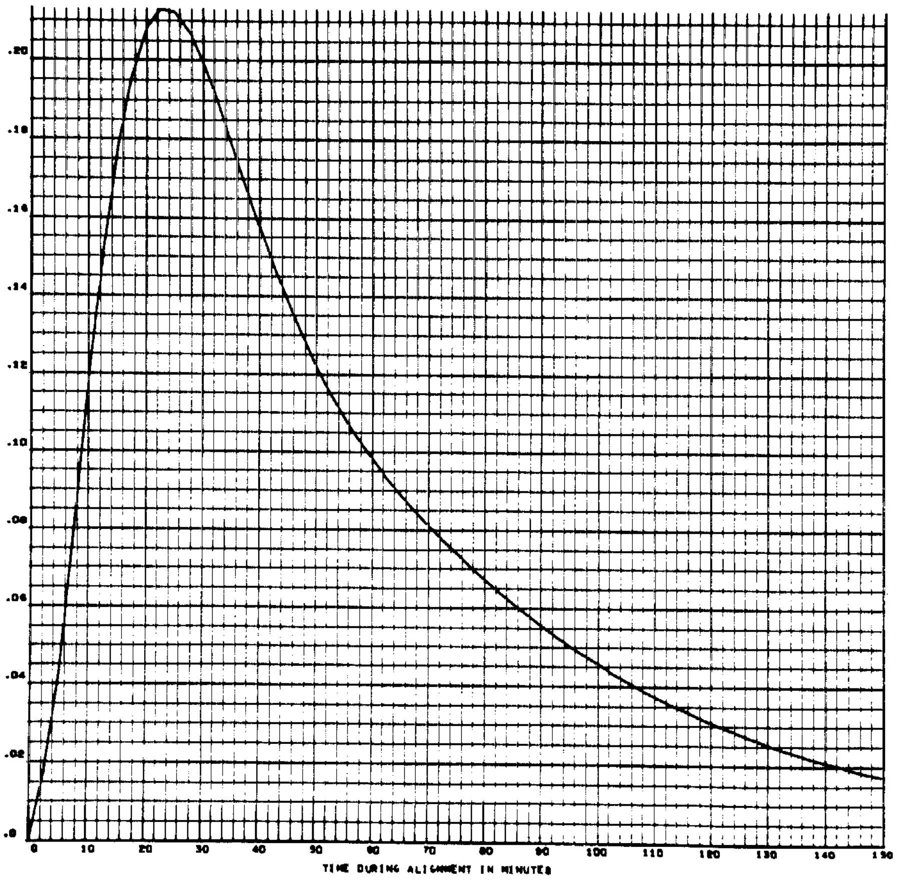
LEVEL TILT IN ARCSECONDS - ORBITAL GYROCOMPASSING, CASE 10, RUN 2
X TILT DUE TO Z GYRO MISALIGNMENT - 1 ARCSECOND

B35

LEVEL TILT IN ARCSECONDS - ORBITAL GYROCOMPASSING, CASE 14, RUN 1
X TILT DUE TO Z GYRO MISALIGNMENT - 1 ARCSECOND

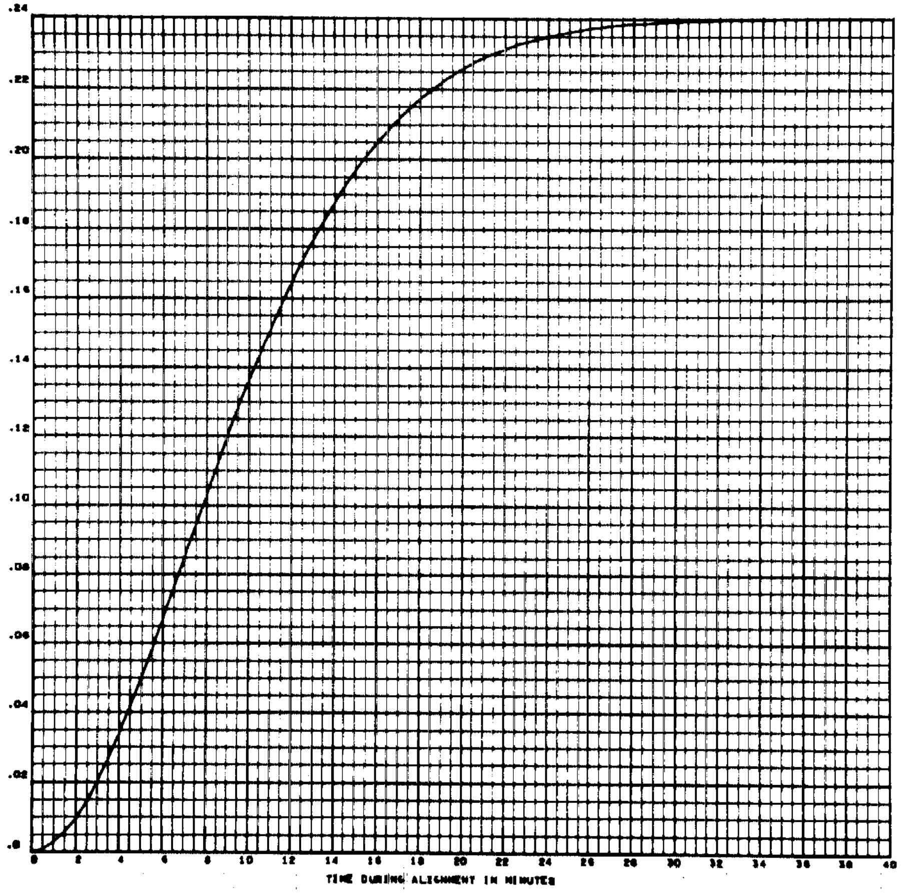

B36

LEVEL TILT IN ARCSECONDS - ORBITAL GYROCOMPASSING, CASE 14, RUN 2
X TILT DUE TO Z GYRO MISALIGNMENT - 1 ARCSECOND

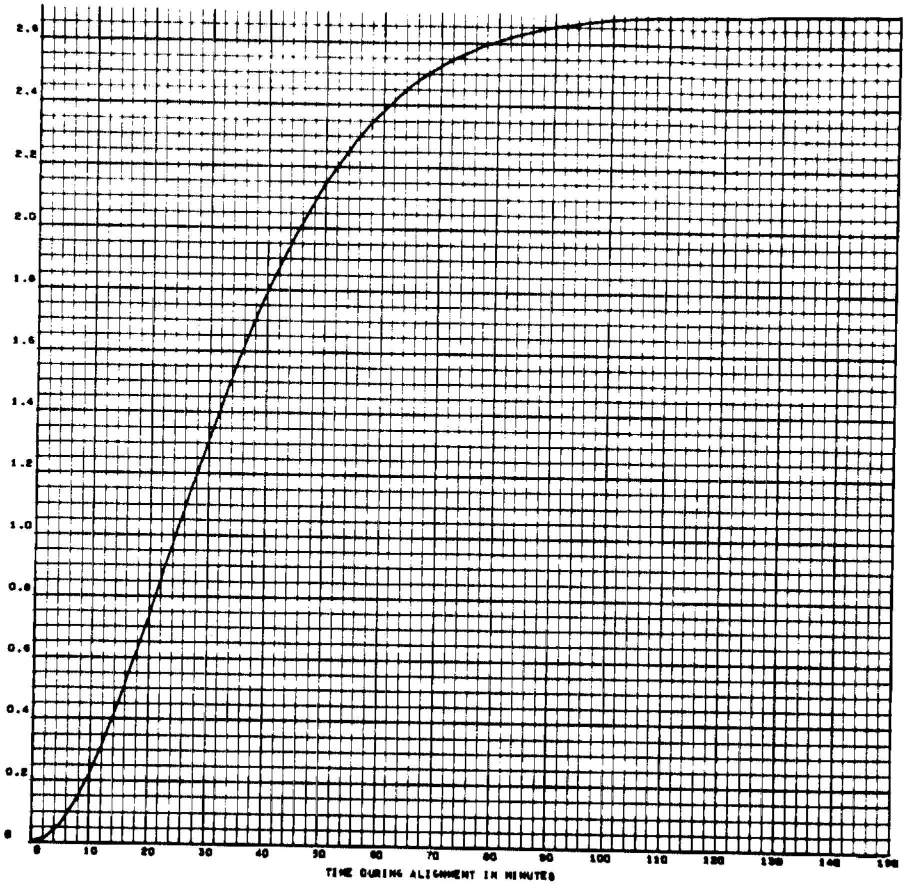

B37

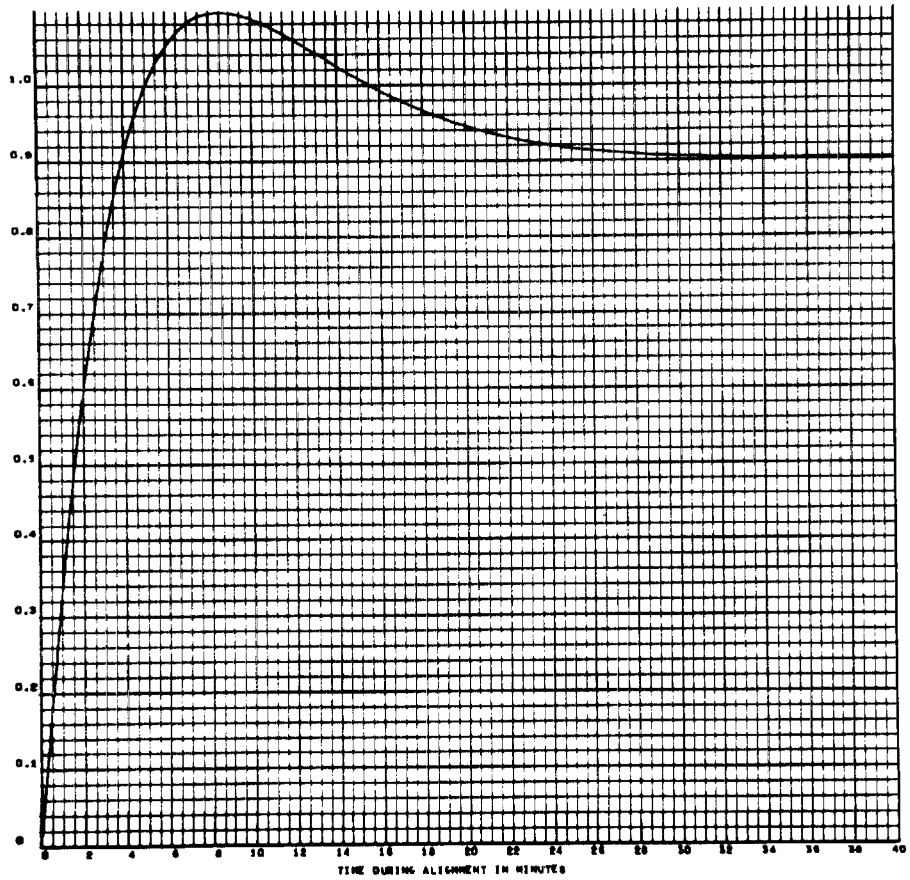
LEVEL TILT IN ARCSECONDS - ORBITAL GYROCOMPASSING, CASE 4, RUN 1
X TILT DUE TO HORIZON SENSOR MISALIGNMENT - 1 ARCSECOND

B38

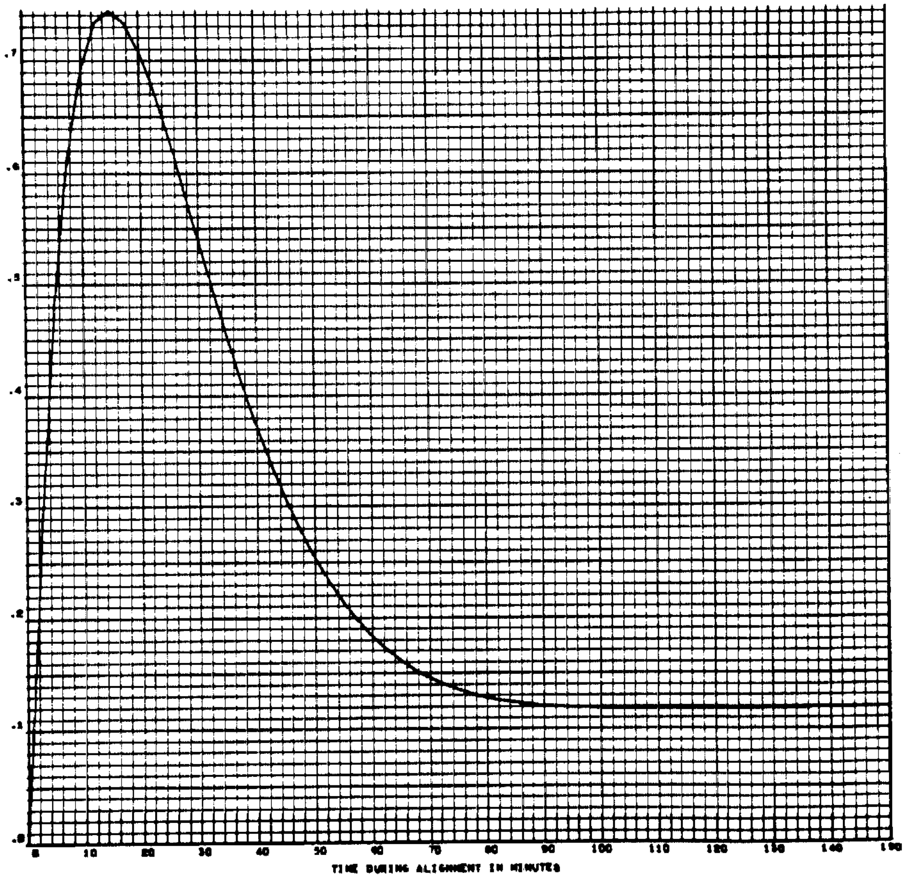
LEVEL TILT IN ARCSECONDS - ORBITAL GYROCOMPASSING, CASE 4, RUN 2
X TILT DUE TO HORIZON SENSOR MISALIGNMENT - 1 ARCSECOND

B39

LEVEL TILT IN ARCSECONDS - ORBITAL GYROCOMPASSING, CASE 10, RUN 1
X TILT DUE TO HORIZON SENSOR MISALIGNMENT - 1 ARCSECOND

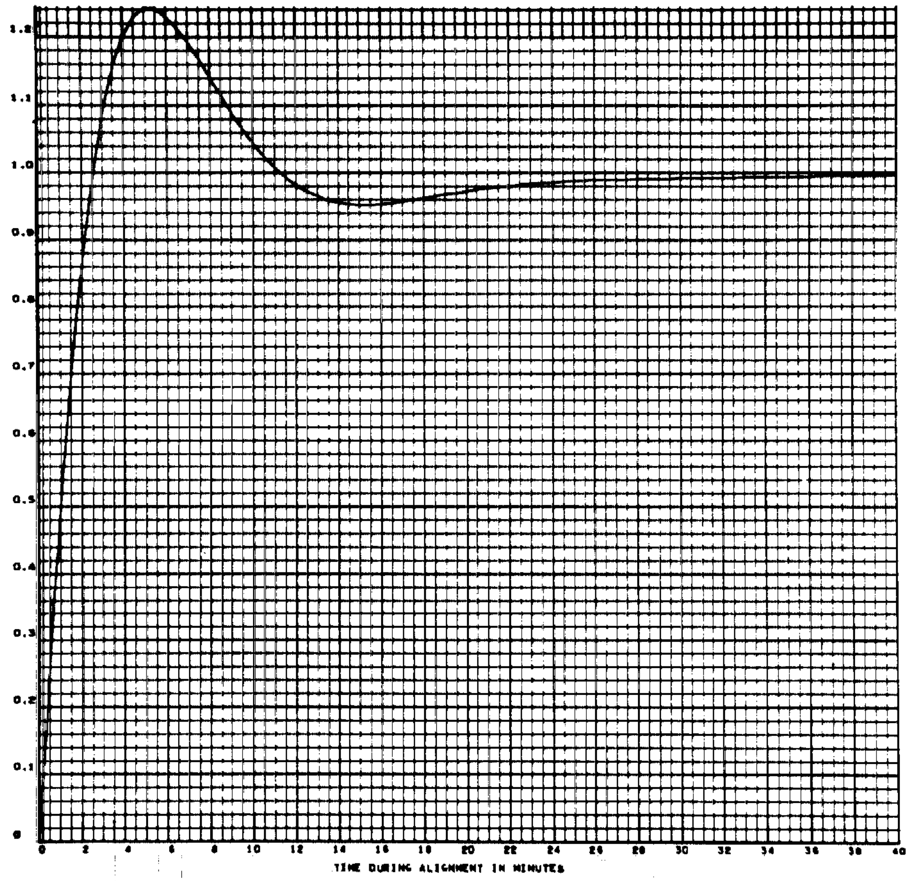

B40

LEVEL TILT IN ARCSECONDS - ORBITAL GYROCOMPASSING, CASE 10, RUN 2
X TILT DUE TO HORIZON SENSOR MISALIGNMENT - 1 ARCSECOND

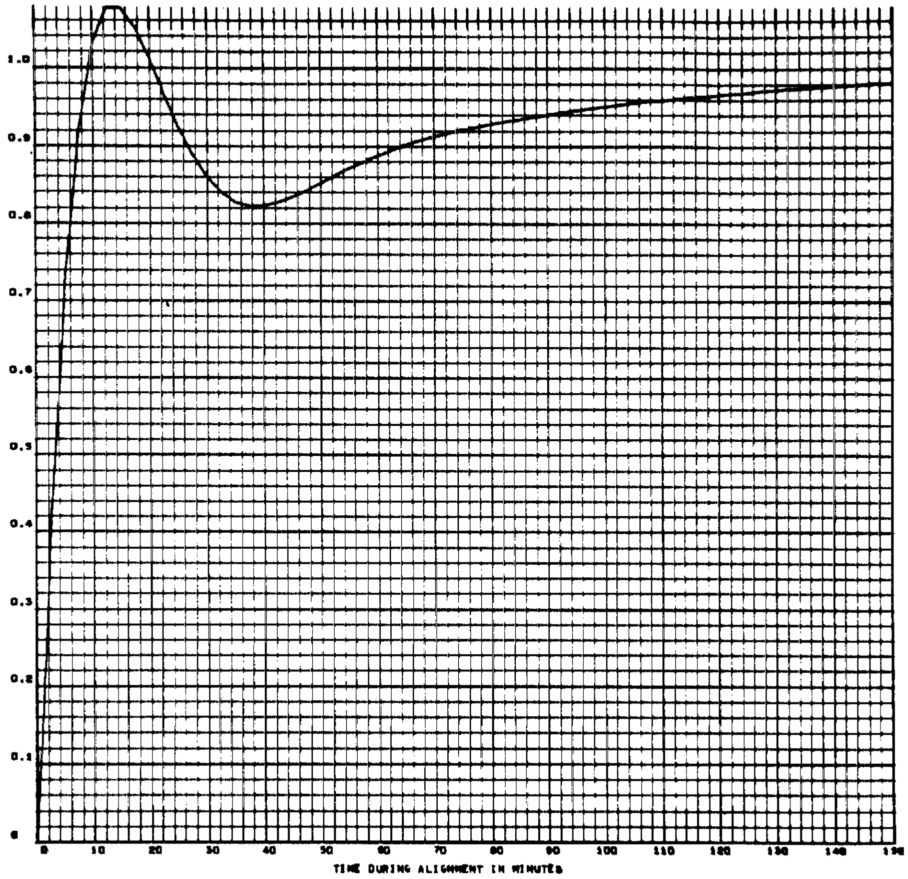

B41

LEVEL TILT IN ARCSECONDS - ORBITAL GYROCOMPASSING, CASE 14, RUN 1
X TILT DUE TO HORIZON SENSOR MISALIGNMENT - 1 ARCSECOND

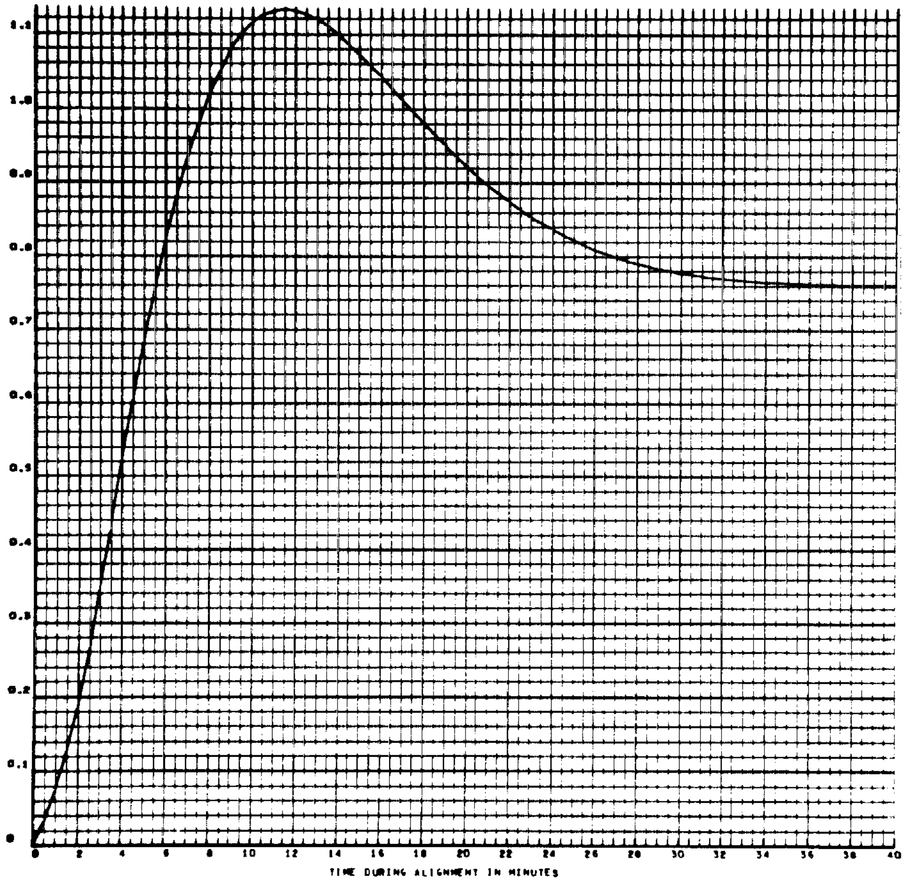

B42

LEVEL TILT IN ARCSECONDS - ORBITAL GYROCOMPASSING, CASE 14, RUN 2
X TILT DUE TO HORIZON SENSOR MISALIGNMENT - 1 ARCSECOND

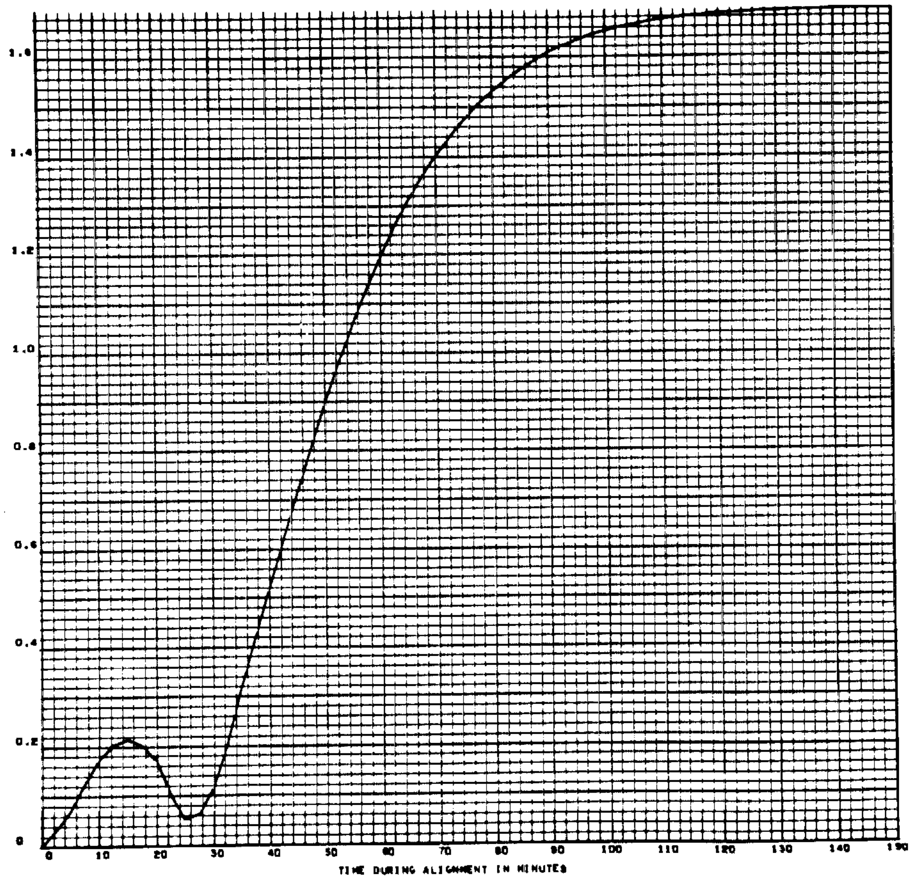

B43

LEVEL TILT IN ARCSECONDS - ORBITAL GYROCOMPASSING, CASE 4, RUN 1
X TILT DUE TO HORIZON SENSOR NOISE - 1 ARCSECOND, C.T. = 1 MINUTE

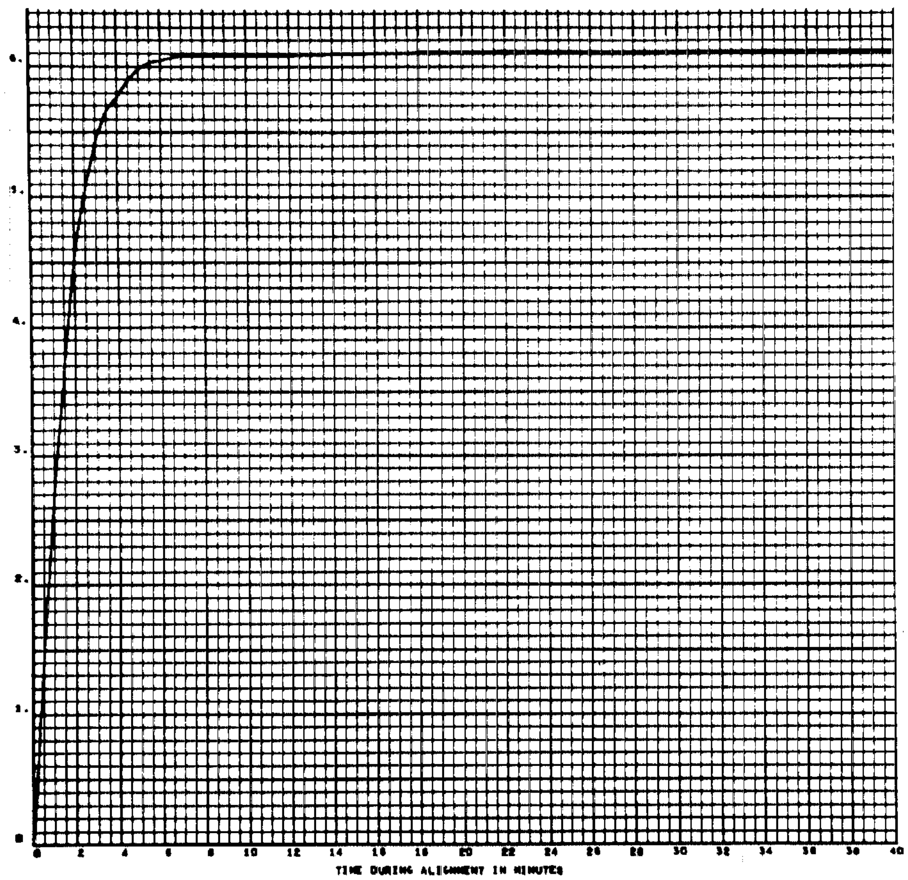

B44

LEVEL TILT IN ARCSECONDS - ORBITAL GYROCOMPASSING, CASE 4, RUN 2
X TILT DUE TO HORIZON SENSOR NOISE - 1 ARCSECOND, C.T. = 1 MINUTE

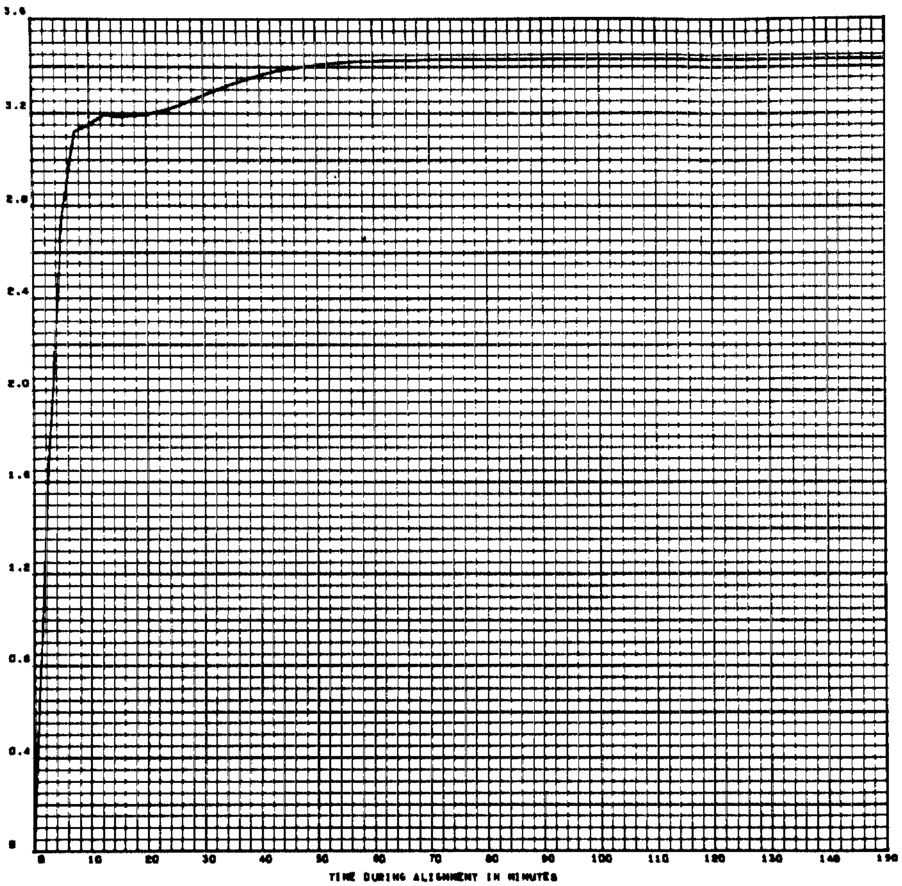

B45

LEVEL TILT IN ARCSECONDS - ORBITAL GYROCOMPASSING, CASE 1O, RUN 1
X TILT DUE TO HORIZON SENSOR NOISE - 1 ARCSECOND, C.T. = 1 MINUTE

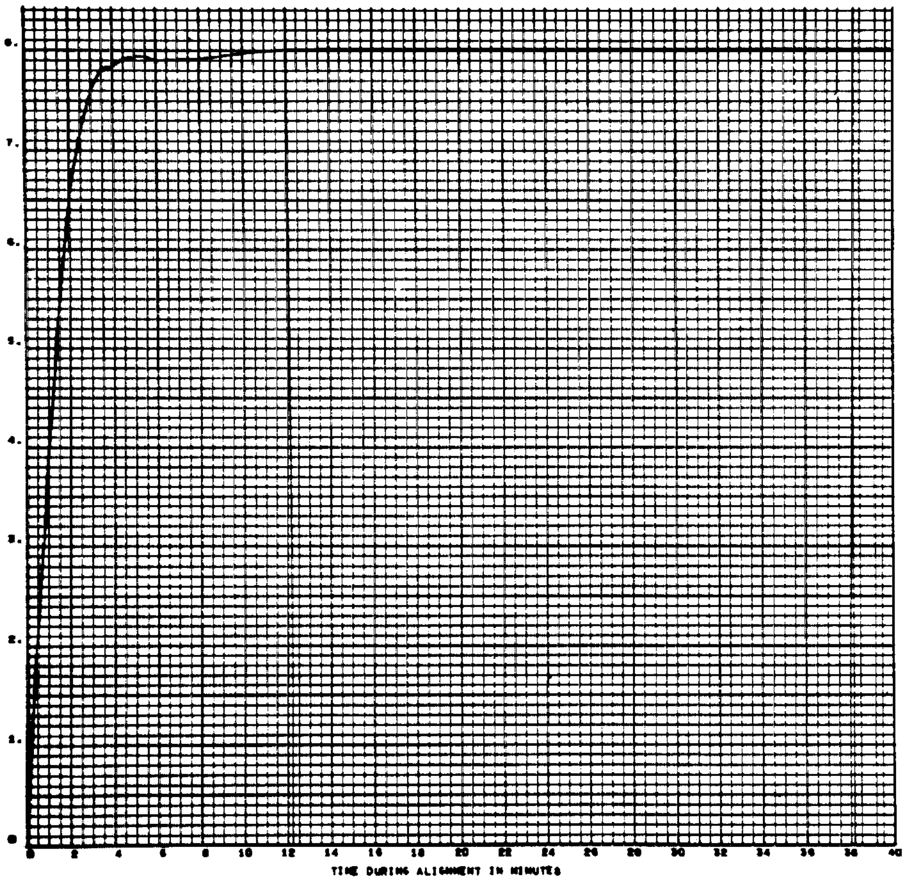

B46

LEVEL TILT IN ARCSECONDS - ORBITAL GYROCOMPASSING, CASE 1O, RUN 2
X TILT DUE TO HORIZON SENSOR NOISE - 1 ARCSECOND, C.T. = 1 MINUTE

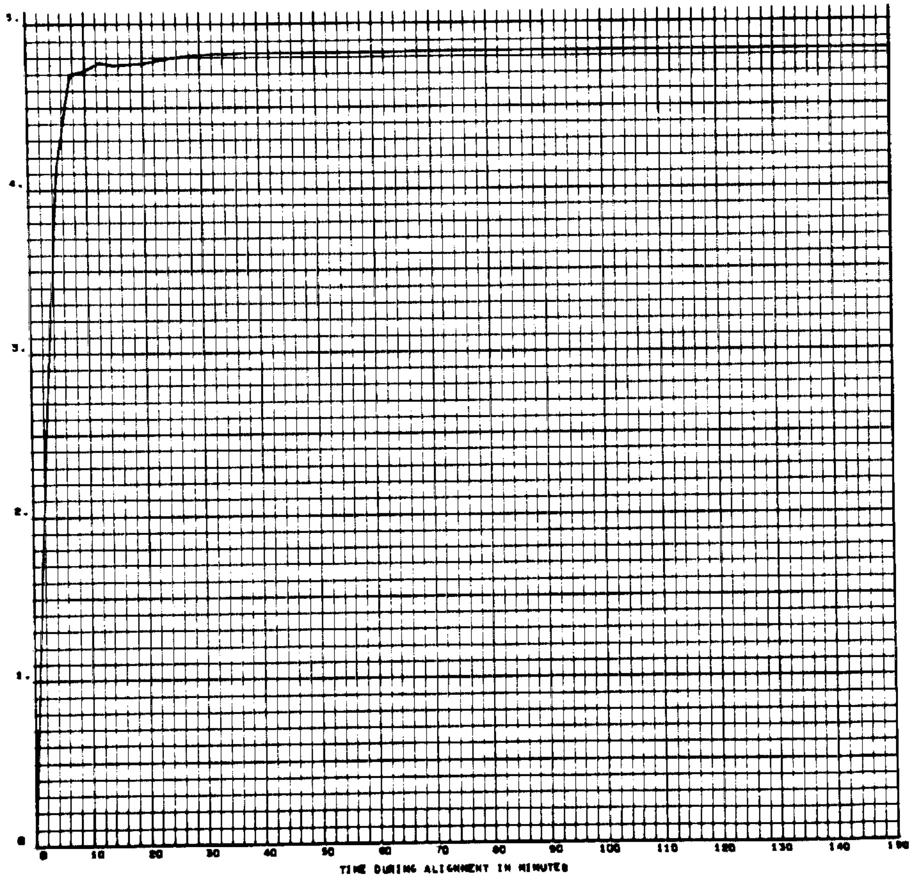

B47

LEVEL TILT IN ARCSECONDS - ORBITAL GYROCOMPASSING, CASE 14, RUN 1
X TILT DUE TO HORIZON SENSOR NOISE - 1 ARCSECOND, C.T. = 1 MINUTE

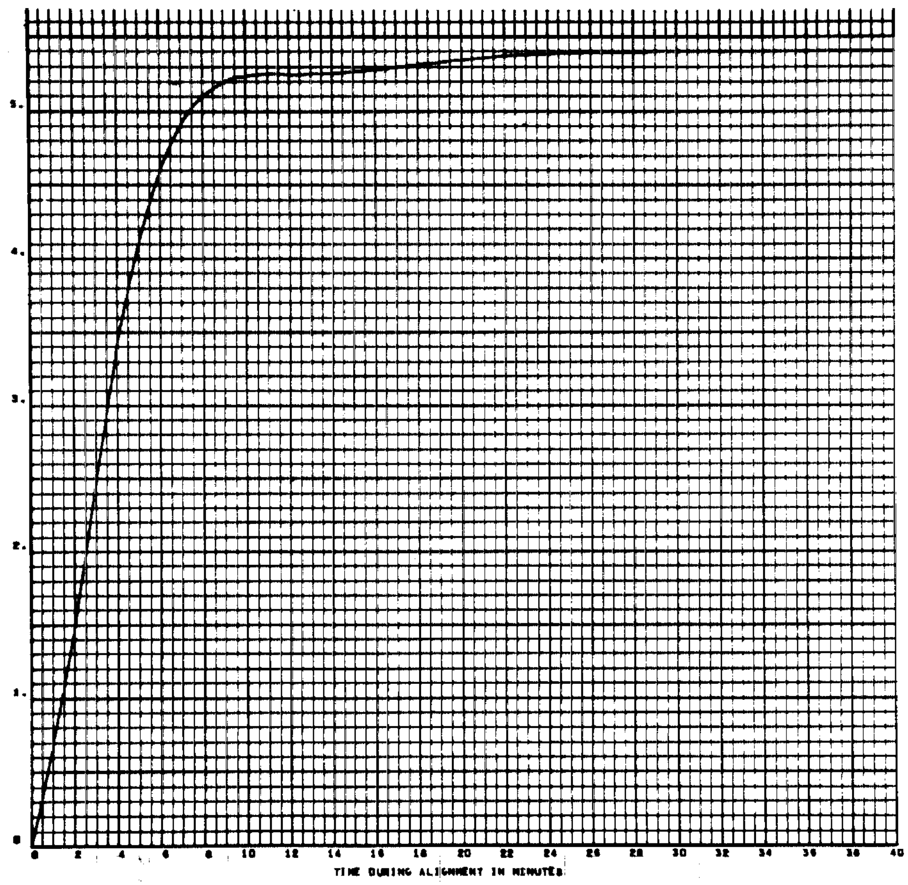

B48

LEVEL TILT IN ARCSECONDS - ORBITAL GYROCOMPASSING, CASE 14, RUN 2
X TILT DUE TO HORIZON SENSOR NOISE - 1 ARCSECOND, C.T. = 1 MINUTE

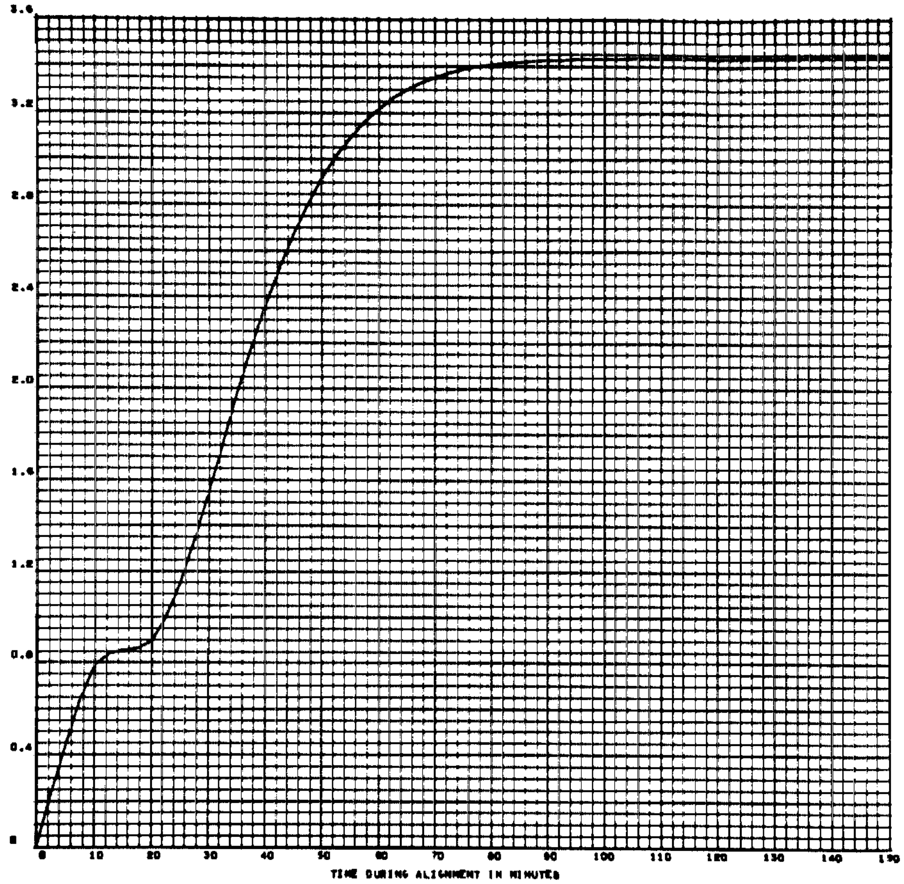

B49

LEVEL TILT IN ARCSECONDS - ORBITAL GYROCOMPASSING, CASE 4, RUN 1
X TILT DUE TO INITIAL X TILT - 10 DEGREES

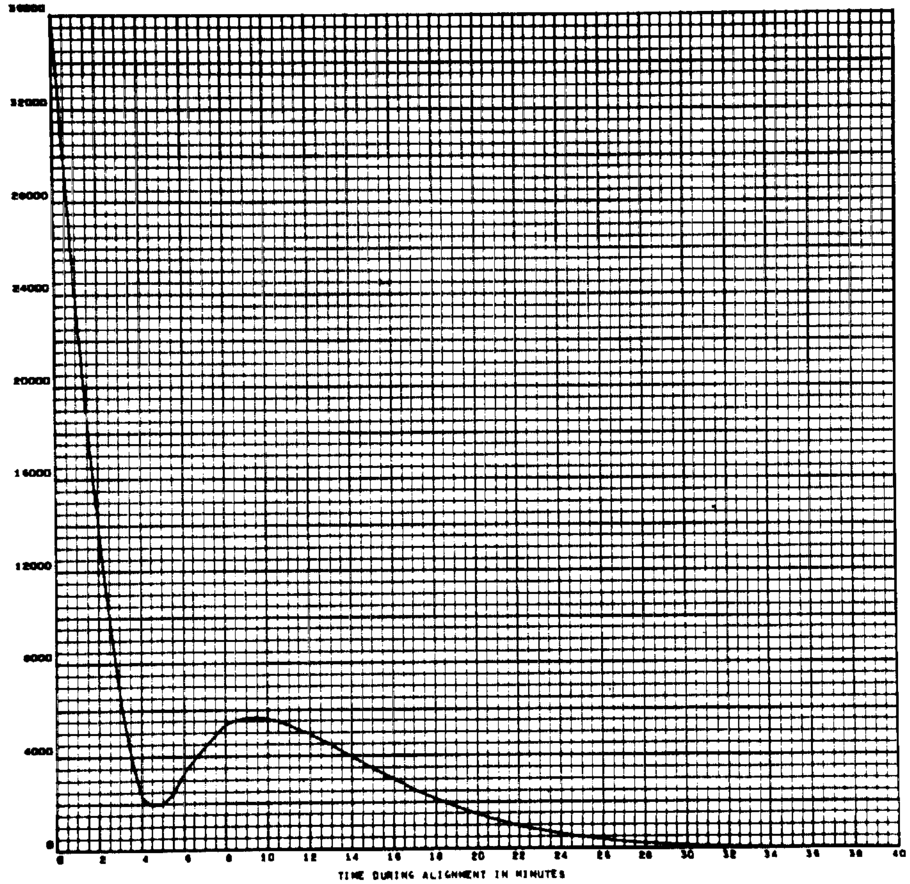

B50

LEVEL TILT IN ARCSECONDS - ORBITAL GYROCOMPASSING, CASE 4, RUN 2
X TILT DUE TO INITIAL X TILT - 10 DEGREES

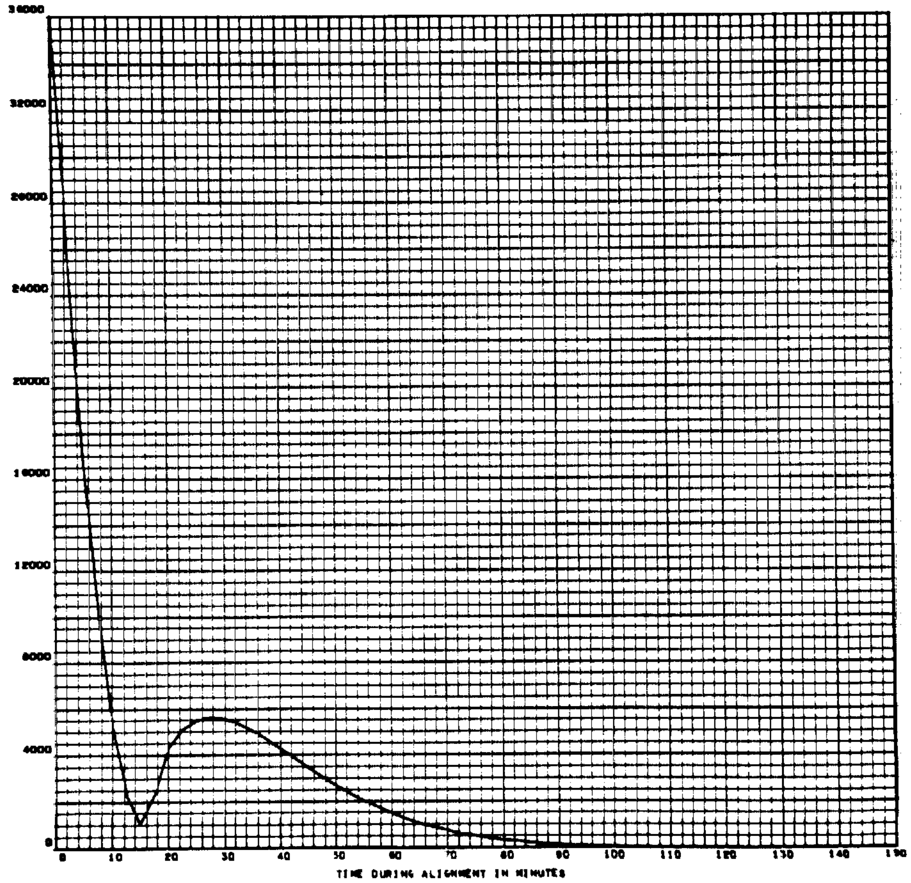

B51

LEVEL TILT IN ARCSECONDS - ORBITAL GYROCOMPASSING, CASE 10, RUN 1
X TILT DUE TO INITIAL X TILT - 10 DEGREES

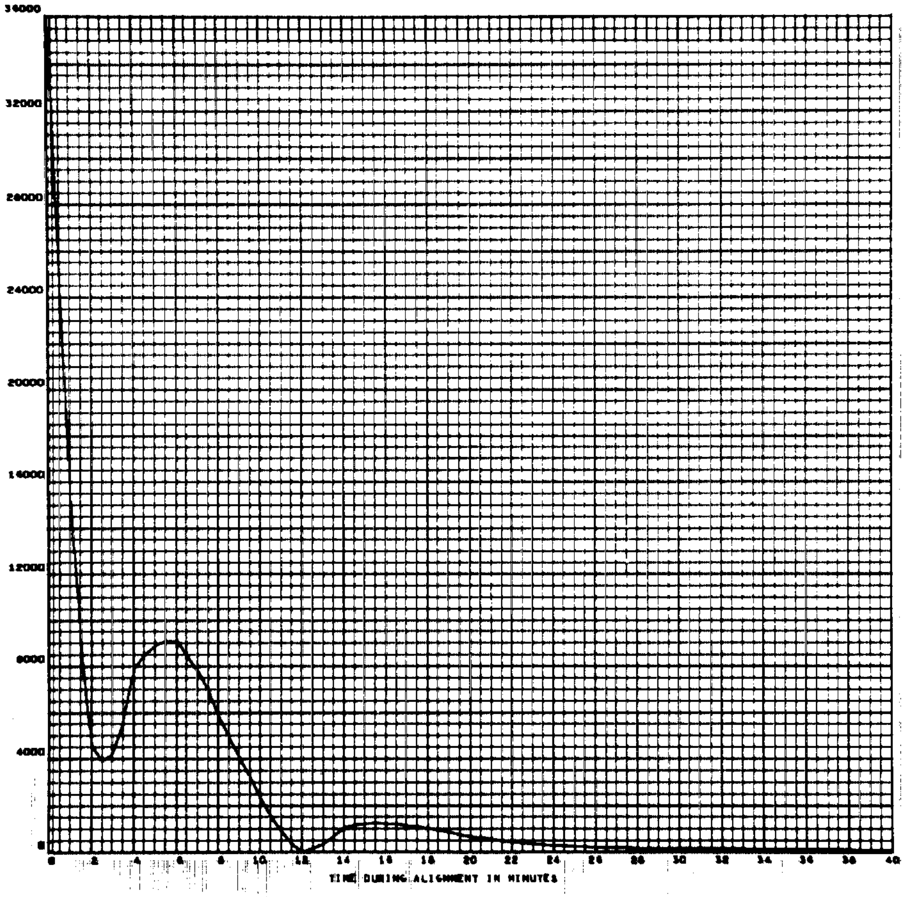

B52

LEVEL TILT IN ARCSECONDS - ORBITAL GYROCOMPASSING, CASE 10, RUN 2
X TILT DUE TO INITIAL X TILT - 10 DEGREES

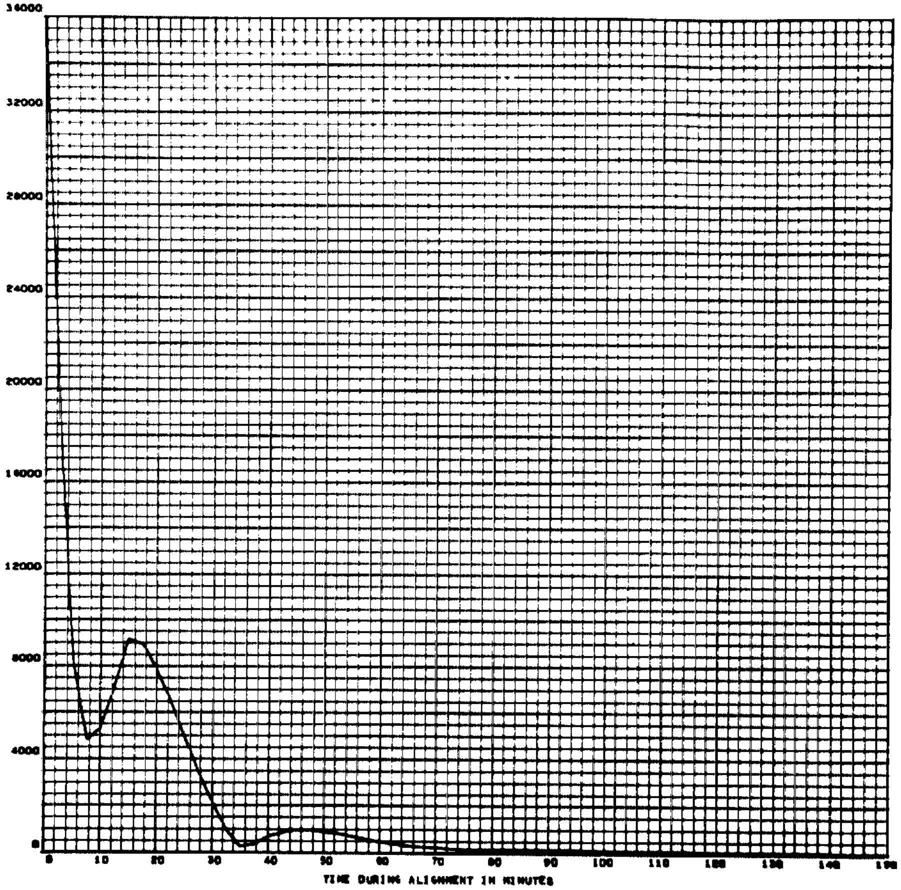

B53

LEVEL TILT IN ARCSECONDS - ORBITAL GYROCOMPASSING, CASE 14, RUN 1
X TILT DUE TO INITIAL X TILT - 10 DEGREES

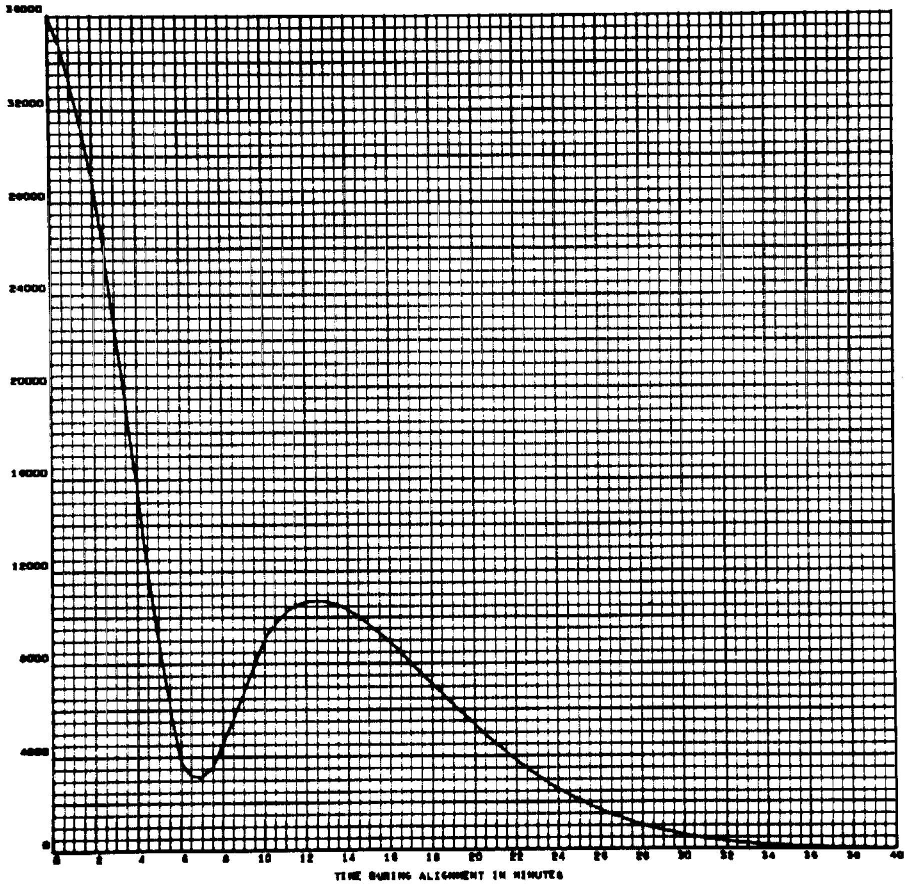

B54

LEVEL TILT IN ARCSECONDS - ORBITAL GYROCOMPASSING, CASE 14, RUN 2
X TILT DUE TO INITIAL X TILT - 10 DEGREES

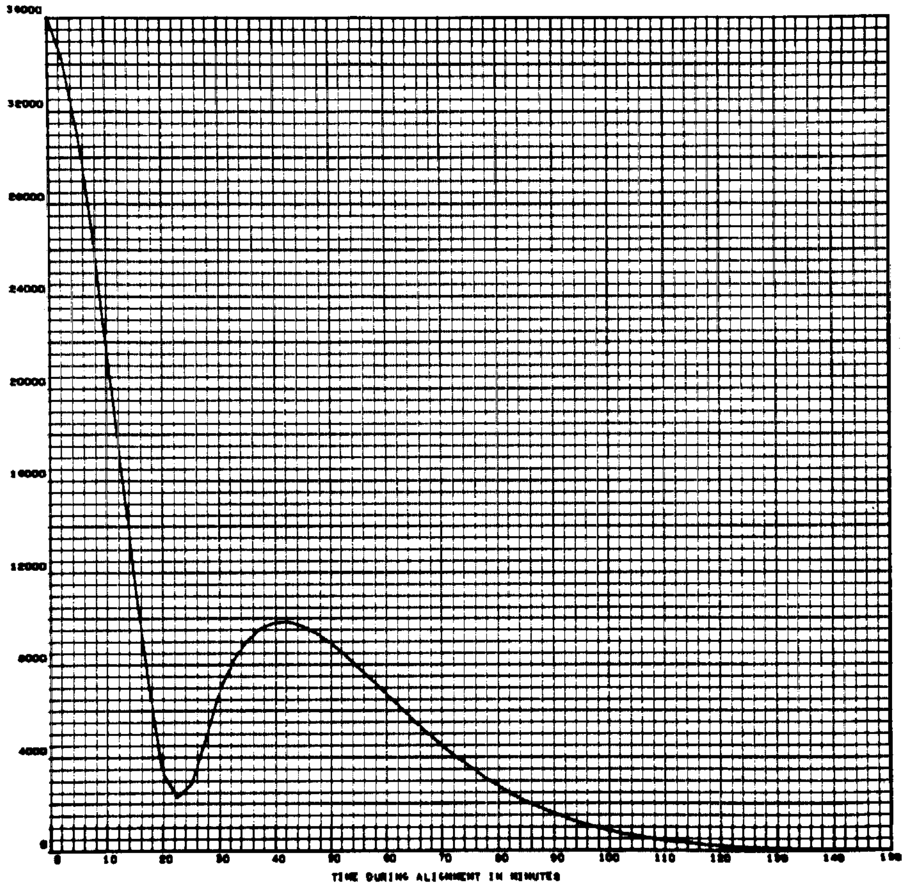

B55

LEVEL TILT IN ARCSECONDS - ORBITAL GYROCOMPASSING, CASE 4, RUN 1
X TILT DUE TO INITIAL AZIMUTH MISALIGNMENT - 10 DEGREES

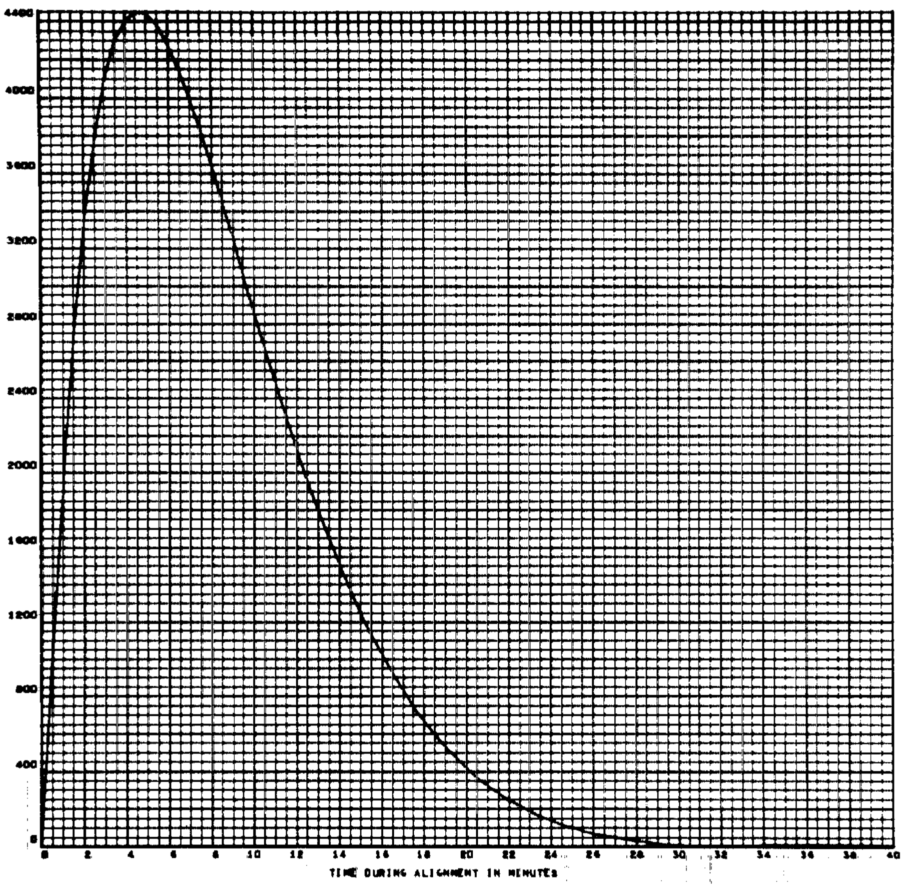

B56

LEVEL TILT IN ARCSECONDS - ORBITAL GYROCOMPASSING, CASE 4, RUN 2
X TILT DUE TO INITIAL AZIMUTH MISALIGNMENT - 10 DEGREES

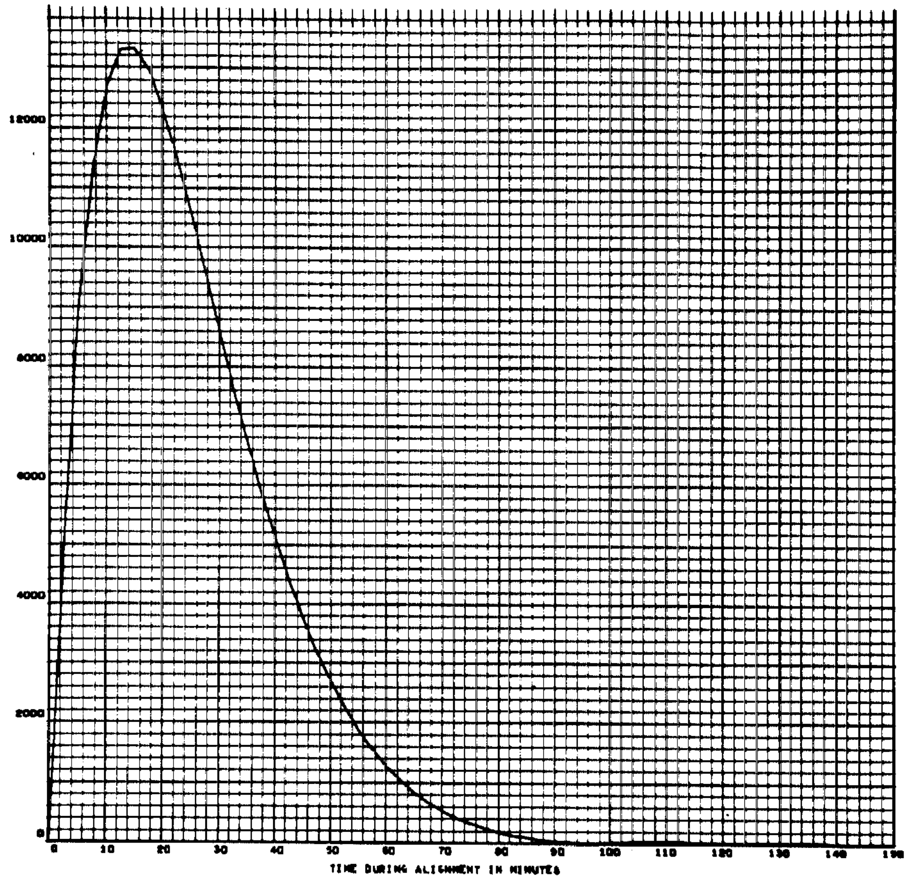

B57

LEVEL TILT IN ARCSECONDS - ORBITAL GYROCOMPASSING, CASE 10, RUN 1
X TILT DUE TO INITIAL AZIMUTH MISALIGNMENT - 10 DEGREES

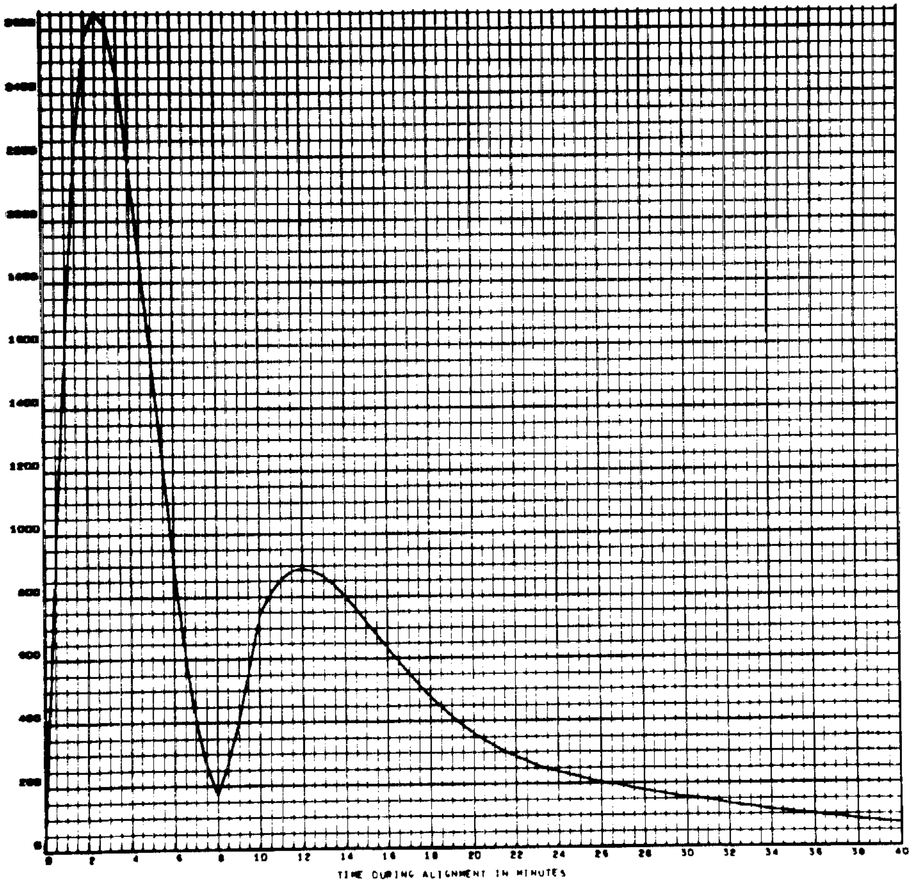

B58

LEVEL TILT IN ARCSECONDS - ORBITAL GYROCOMPASSING, CASE 10, RUN 2
X TILT DUE TO INITIAL AZIMUTH MISALIGNMENT - 10 DEGREES

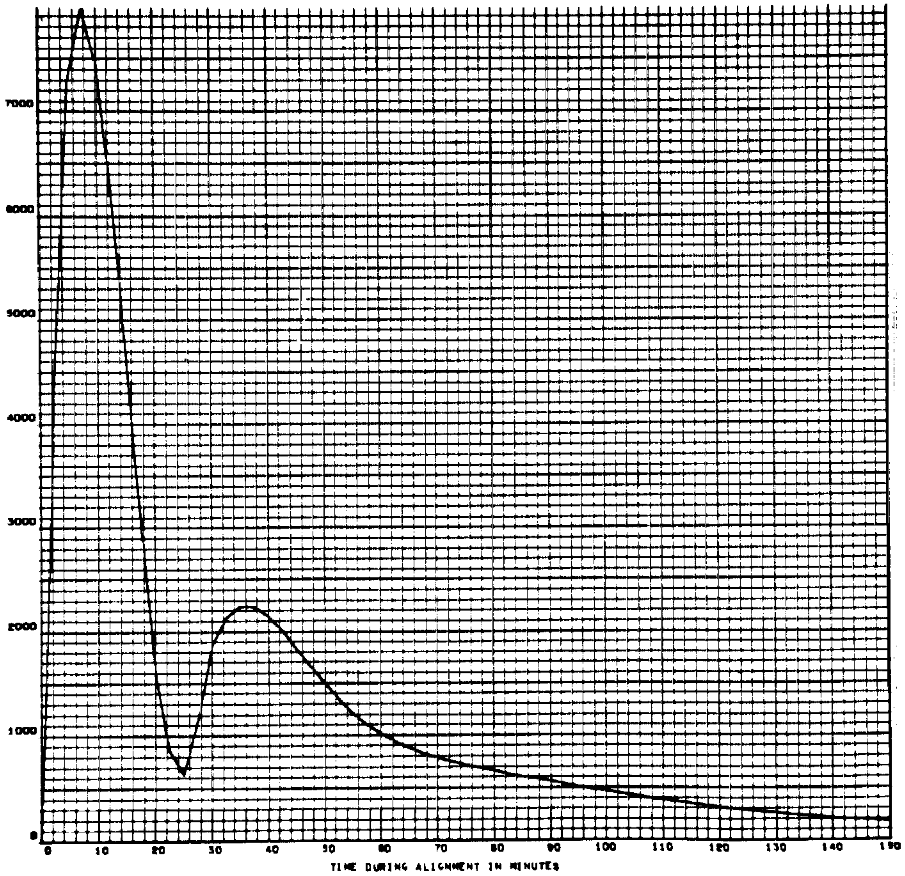

359

LEVEL TILT IN ARCSECONDS - ORBITAL GYROCOMPASSING, CASE 14, RUN 1
X TILT DUE TO INITIAL AZIMUTH MISALIGNMENT - 10 DEGREES

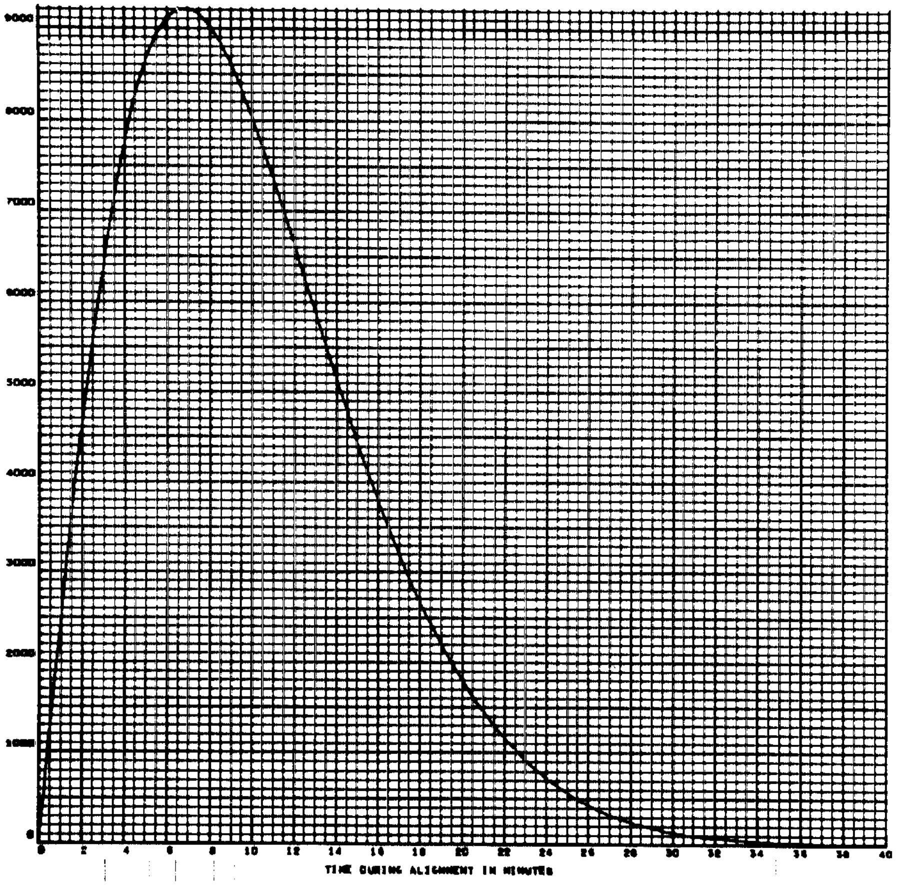

360

LEVEL TILT IN ARCSECONDS - ORBITAL GYROCOMPASSING, CASE 14, RUN 2
X TILT DUE TO INITIAL AZIMUTH MISALIGNMENT - 10 DEGREES

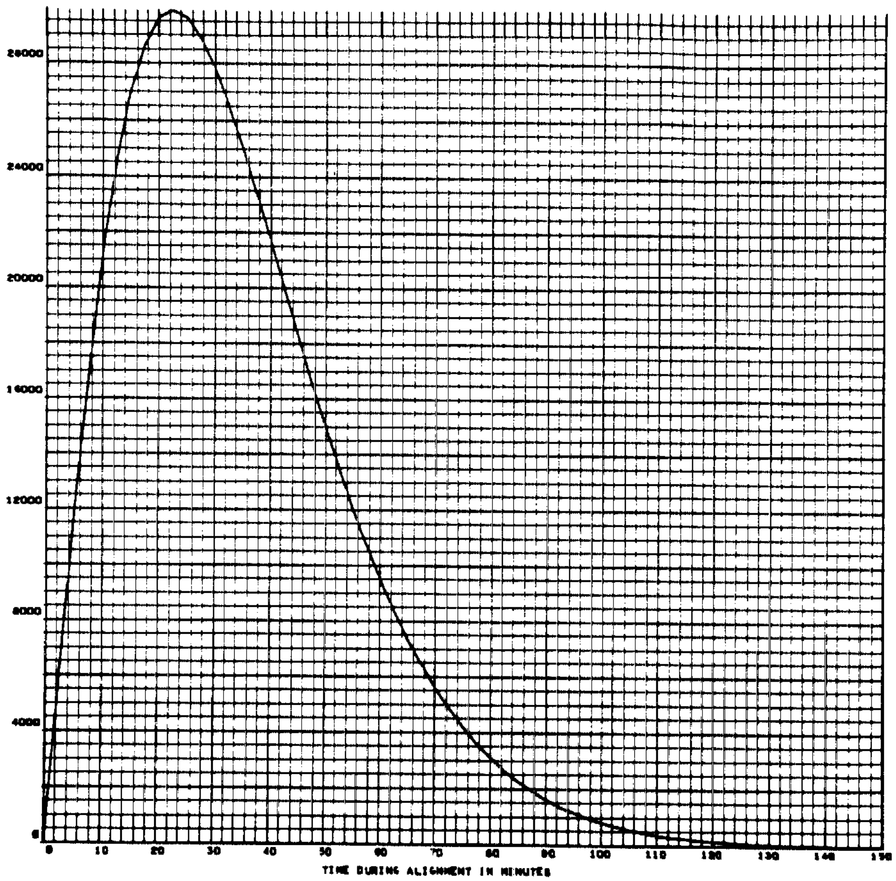

B61

AZIMUTH MISALIGNMENT IN ARCSECONDS - ORBITAL GYROCOMPASS, CASE 4, RUN 1
ERROR DUE TO X GYRO DRIFT - .01 DEGREES/HOUR

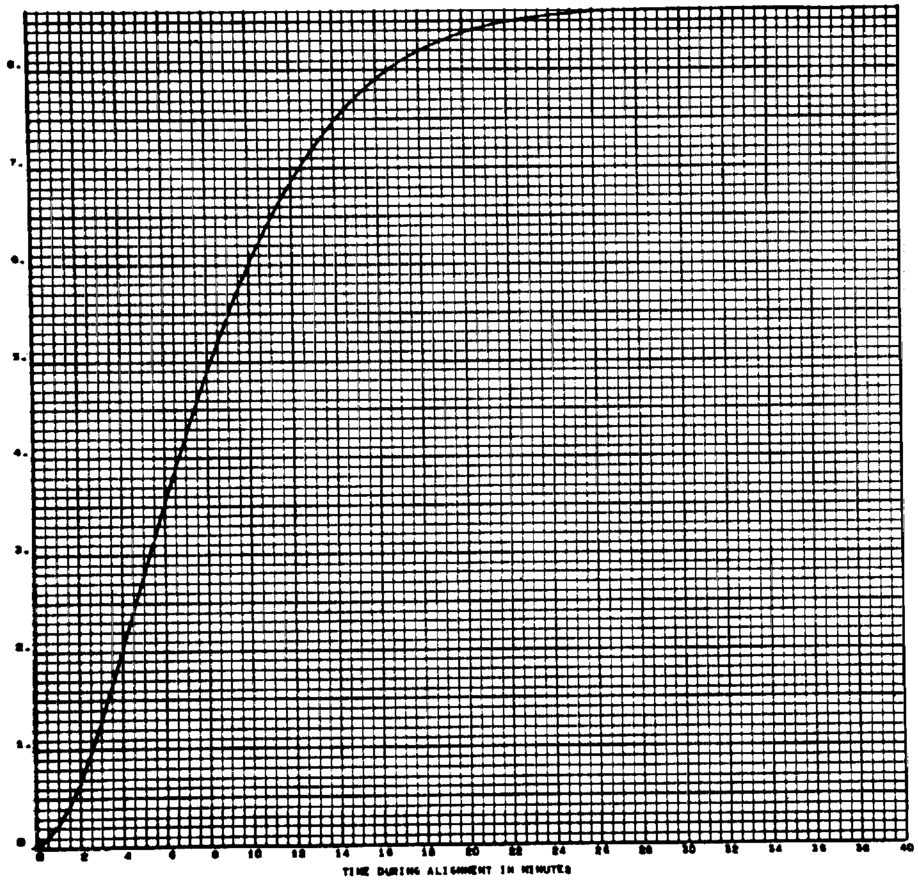

B62

AZIMUTH MISALIGNMENT IN ARCSECONDS - ORBITAL GYROCOMPASS, CASE 4, RUN 2
ERROR DUE TO X GYRO DRIFT - .01 DEGREES/HOUR

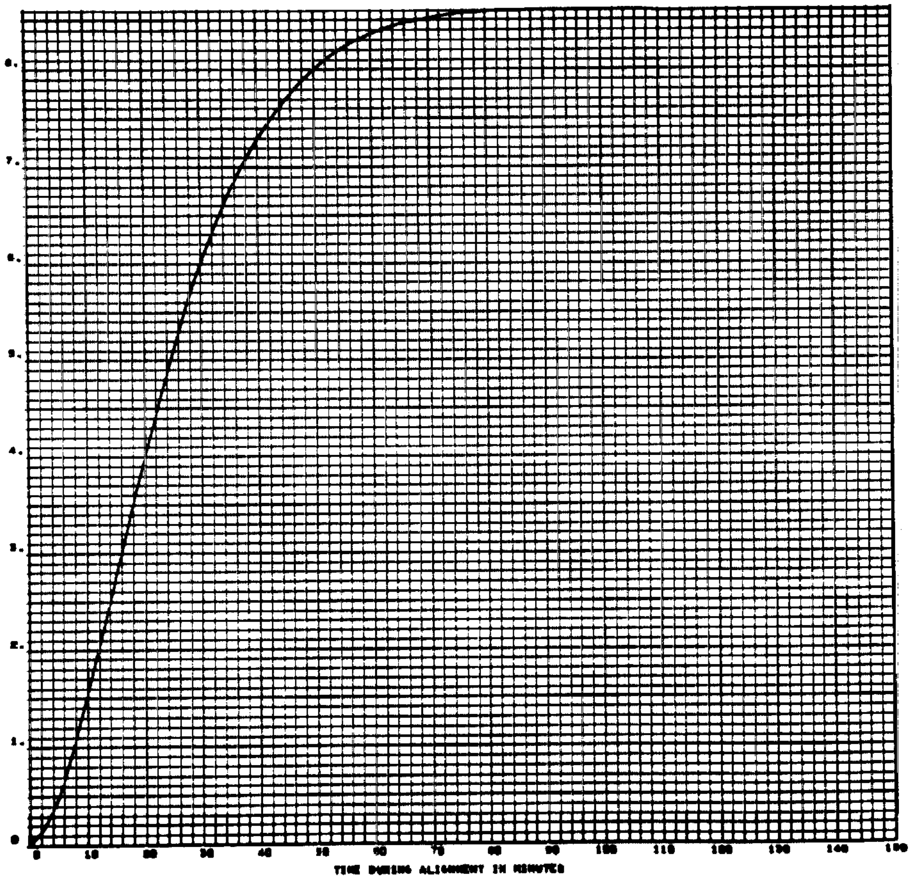

B63

AZIMUTH MISALIGNMENT IN ARCSECONDS - ORBITAL GYROCOMPASS, CASE 10, RUN 1
ERROR DUE TO X GYRO DRIFT - .01 DEGREES/HOUR

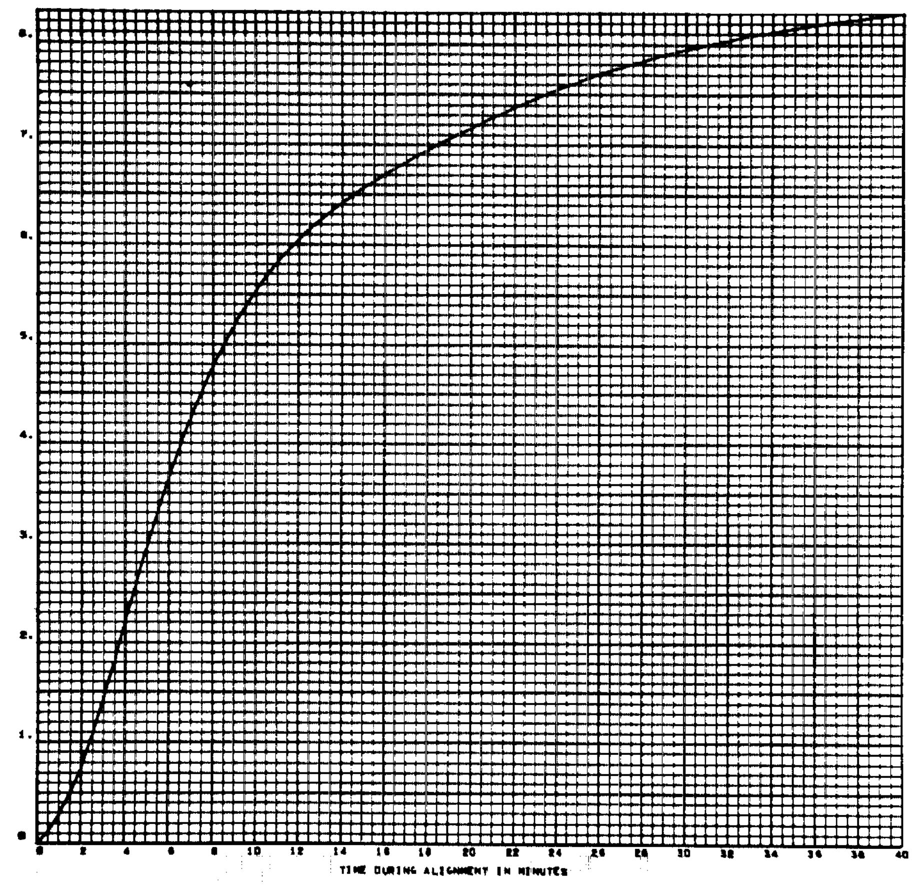

B64

AZIMUTH MISALIGNMENT IN ARCSECONDS - ORBITAL GYROCOMPASS, CASE 10, RUN 2
ERROR DUE TO X GYRO DRIFT - .01 DEGREES/HOUR

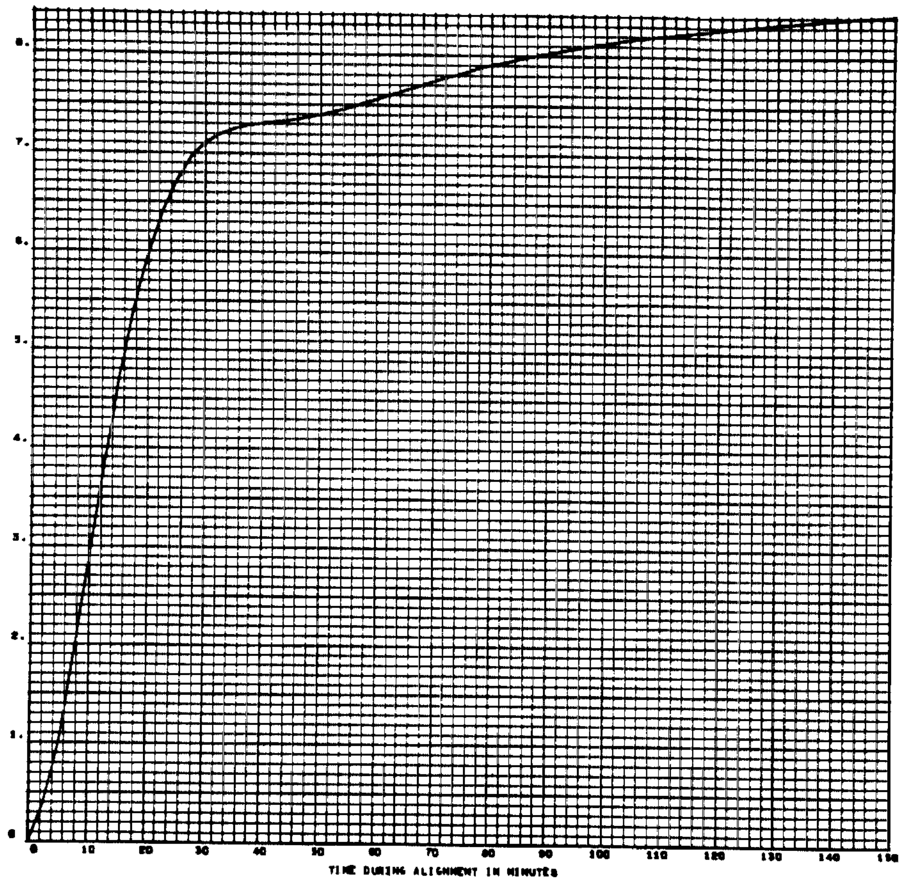

B65

AZIMUTH MISALIGNMENT IN ARCSECONDS - ORBITAL GYROCOMPASS, CASE 14, RUN 1
ERROR DUE TO X GYRO DRIFT - .01 DEGREES/HOUR

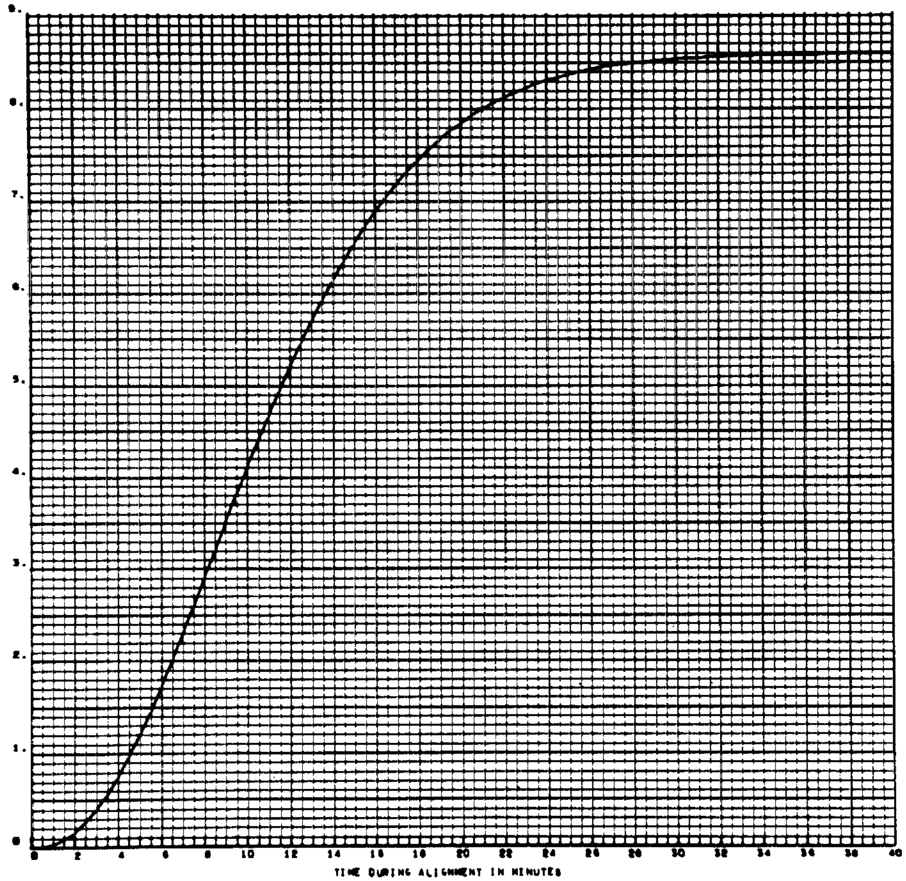

B66

AZIMUTH MISALIGNMENT IN ARCSECONDS - ORBITAL GYROCOMPASS, CASE 14, RUN 2
ERROR DUE TO X GYRO DRIFT - .01 DEGREES/HOUR

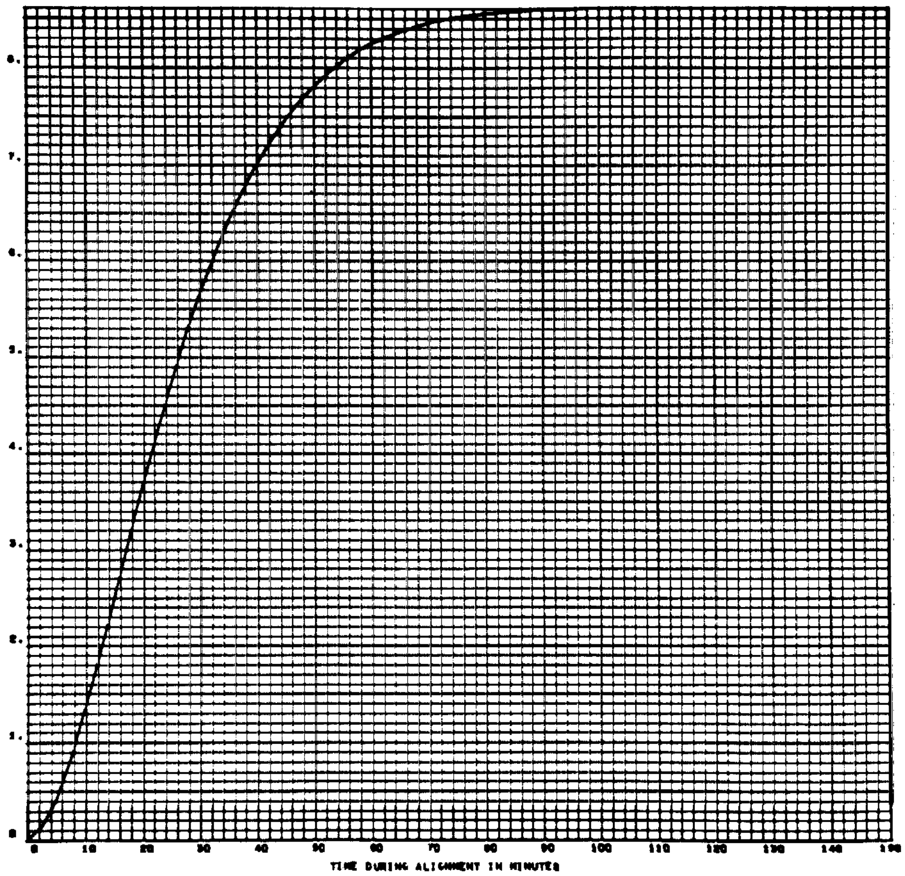

B67

AZIMUTH MISALIGNMENT IN ARCSECONDS - ORBITAL GYROCOMPASS, CASE 4, RUN 1
ERROR DUE TO Z GYRO NOISE - .01 DEGREES/HOUR, C.T. = 1 HOUR

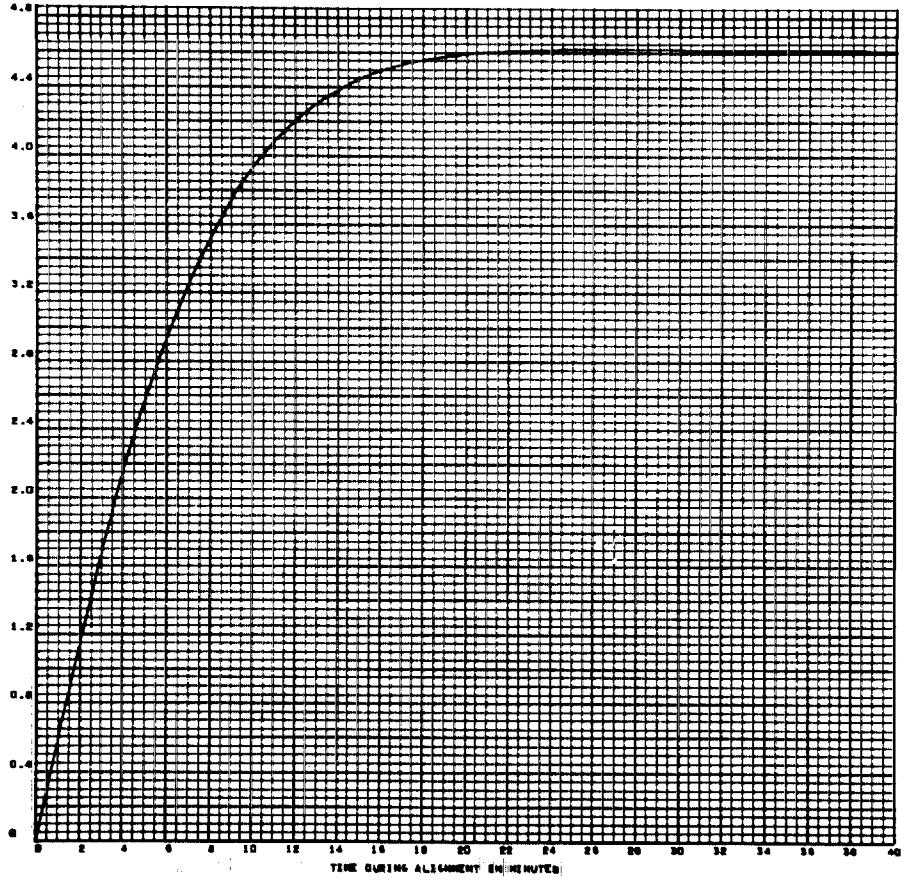

B68

AZIMUTH MISALIGNMENT IN ARCSECONDS - ORBITAL GYROCOMPASS, CASE 4, RUN 2
ERROR DUE TO Z GYRO NOISE - .01 DEGREES/HOUR, C.T. = 1 HOUR

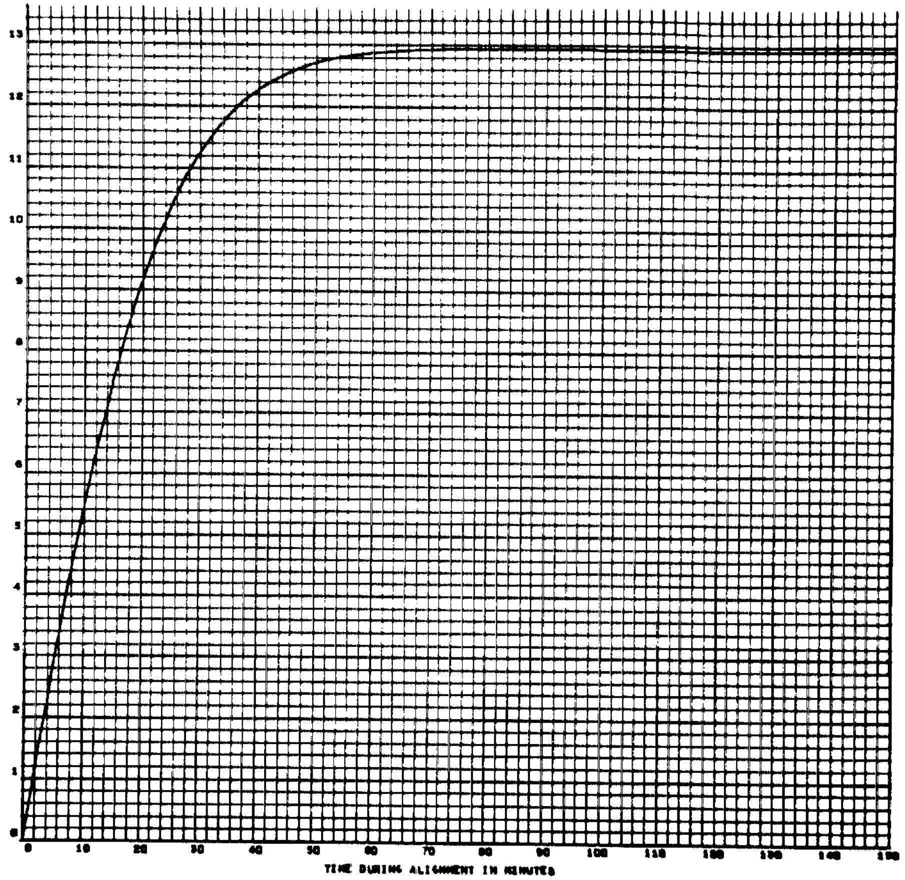

B69

AZIMUTH MISALIGNMENT IN ARCSECONDS - ORBITAL GYROCOMPASS, CASE 10, RUN 1
ERROR DUE TO Z GYRO NOISE - .01 DEGREES/HOUR, C.T. = 1 HOUR

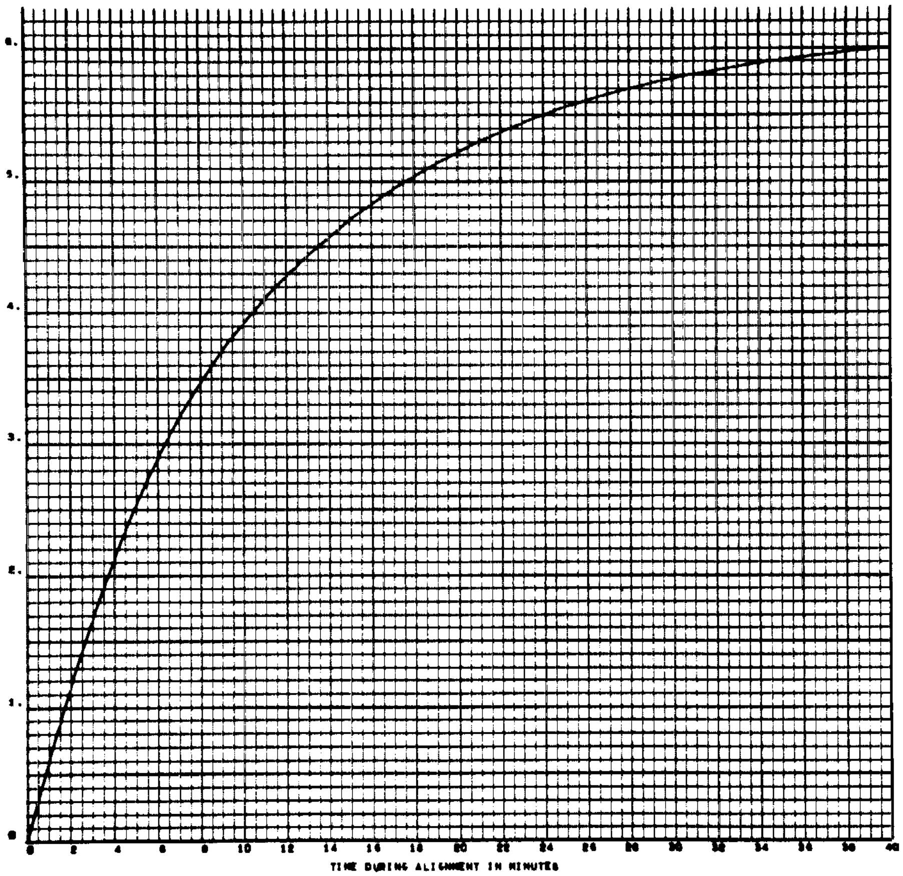

B70

AZIMUTH MISALIGNMENT IN ARCSECONDS - ORBITAL GYROCOMPASS, CASE 10, RUN 2
ERROR DUE TO Z GYRO NOISE - .01 DEGREES/HOUR, C.T. = 1 HOUR

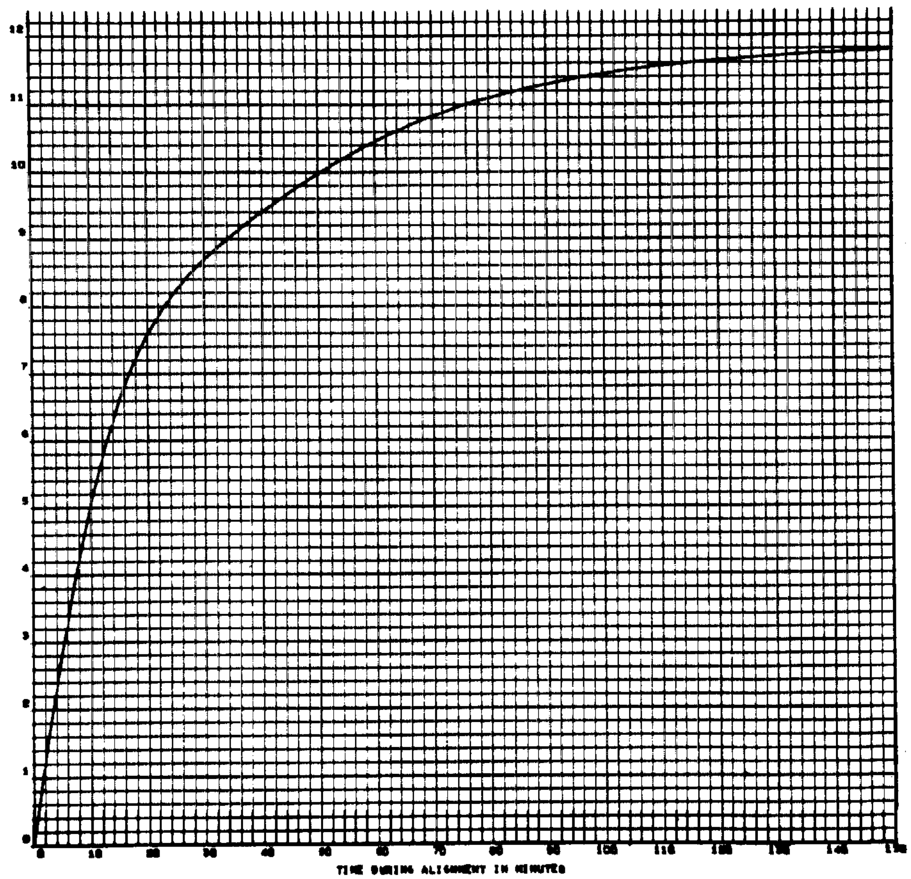

B71

AZIMUTH MISALIGNMENT IN ARCSECONDS - ORBITAL GYROCOMPASS, CASE 14, RUN 1
ERROR DUE TO Z GYRO NOISE - .01 DEGREES/HOUR, C.T. = 1 HOUR

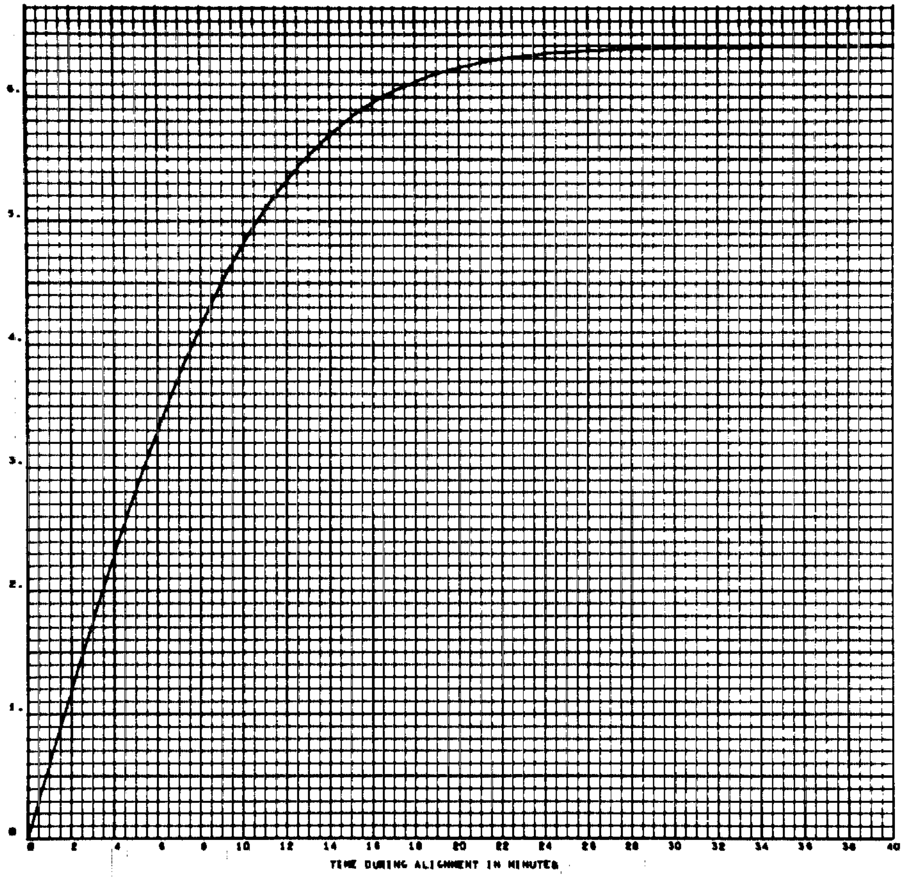

B72

AZIMUTH MISALIGNMENT IN ARCSECONDS - ORBITAL GYROCOMPASS, CASE 14, RUN 2
ERROR DUE TO Z GYRO NOISE - .01 DEGREES/HOUR, C.T. = 1 HOUR

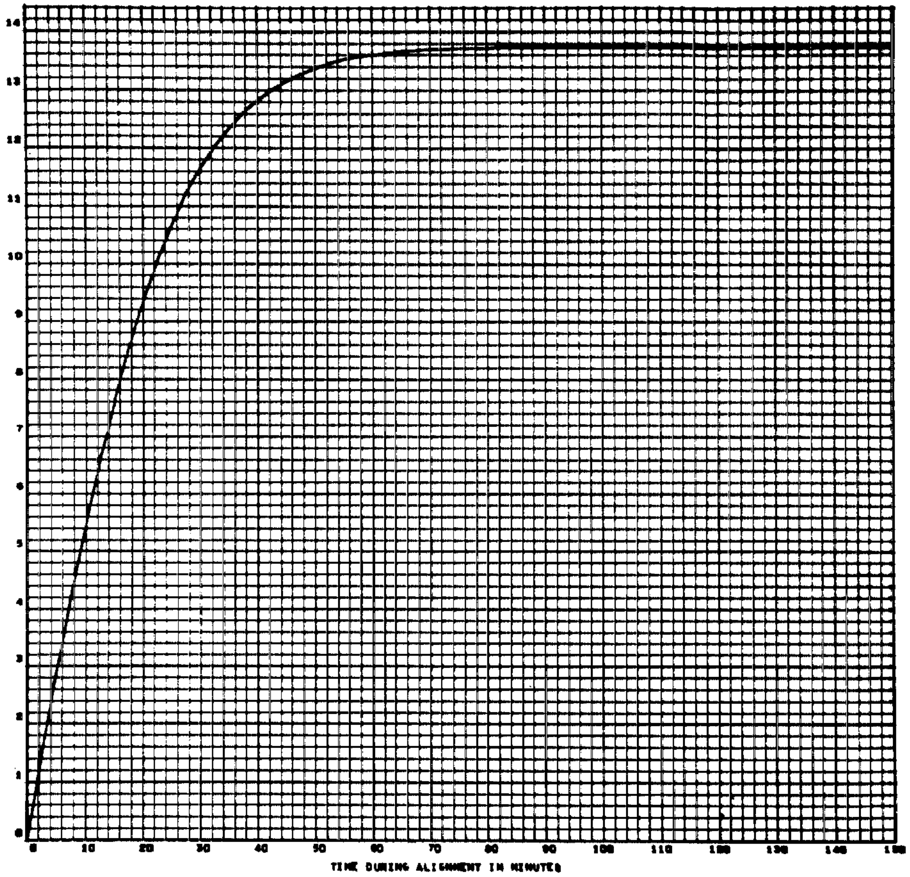

B73

AZIMUTH MISALIGNMENT IN ARCSECONDS - ORBITAL GYROCOMPASS, CASE 4, RUN 1
ERROR DUE TO X GYRO NOISE - .01 DEGREES/HOUR, C.T. = 1 HOUR

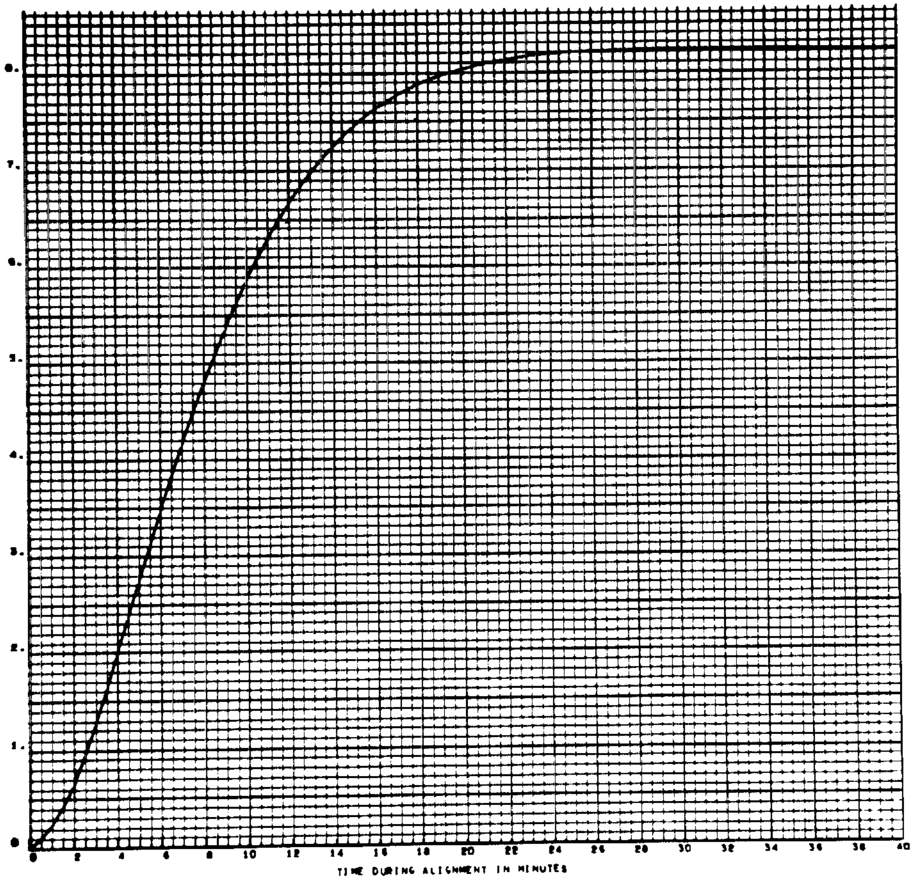

B74

AZIMUTH MISALIGNMENT IN ARCSECONDS - ORBITAL GYROCOMPASS, CASE 4, RUN 2
ERROR DUE TO X GYRO NOISE - .01 DEGREES/HOUR, C.T. = 1 HOUR

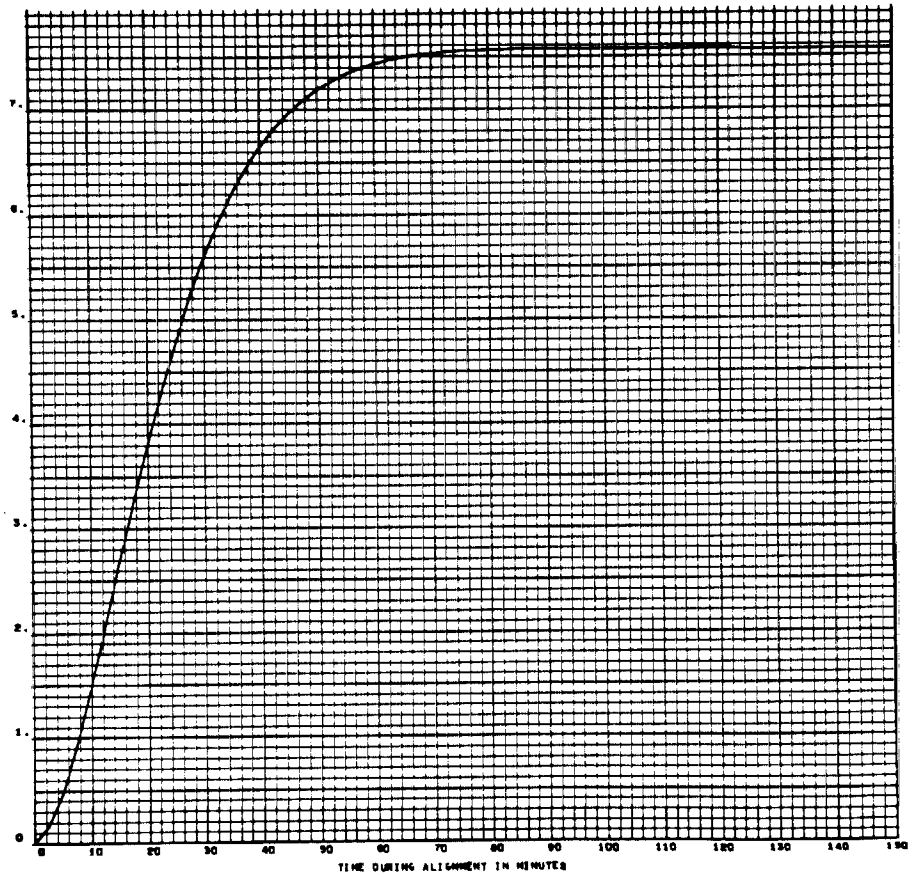

B75

AZIMUTH MISALIGNMENT IN ARCSECONDS - ORBITAL GYROCOMPASS, CASE 10, RUN 1
ERROR DUE TO X GYRO NOISE - .01 DEGREES/HOUR, C.T. = 1 HOUR

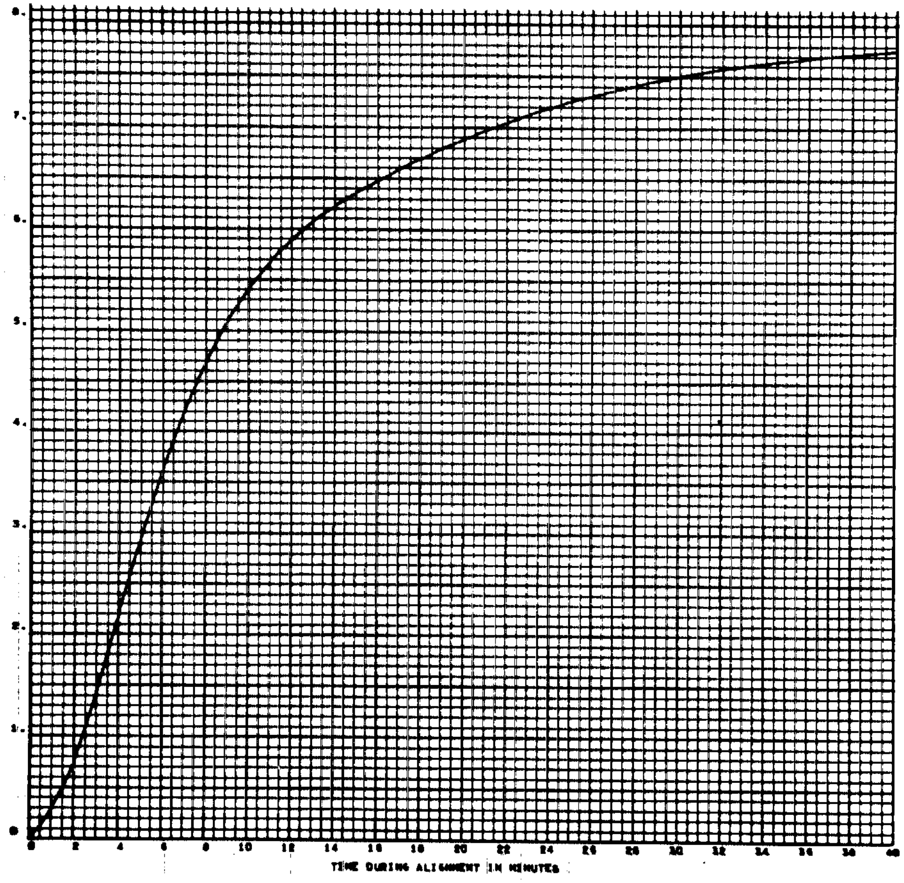

B76

AZIMUTH MISALIGNMENT IN ARCSECONDS - ORBITAL GYROCOMPASS, CASE 10, RUN 2
ERROR DUE TO X GYRO NOISE - .01 DEGREES/HOUR, C.T. = 1 HOUR

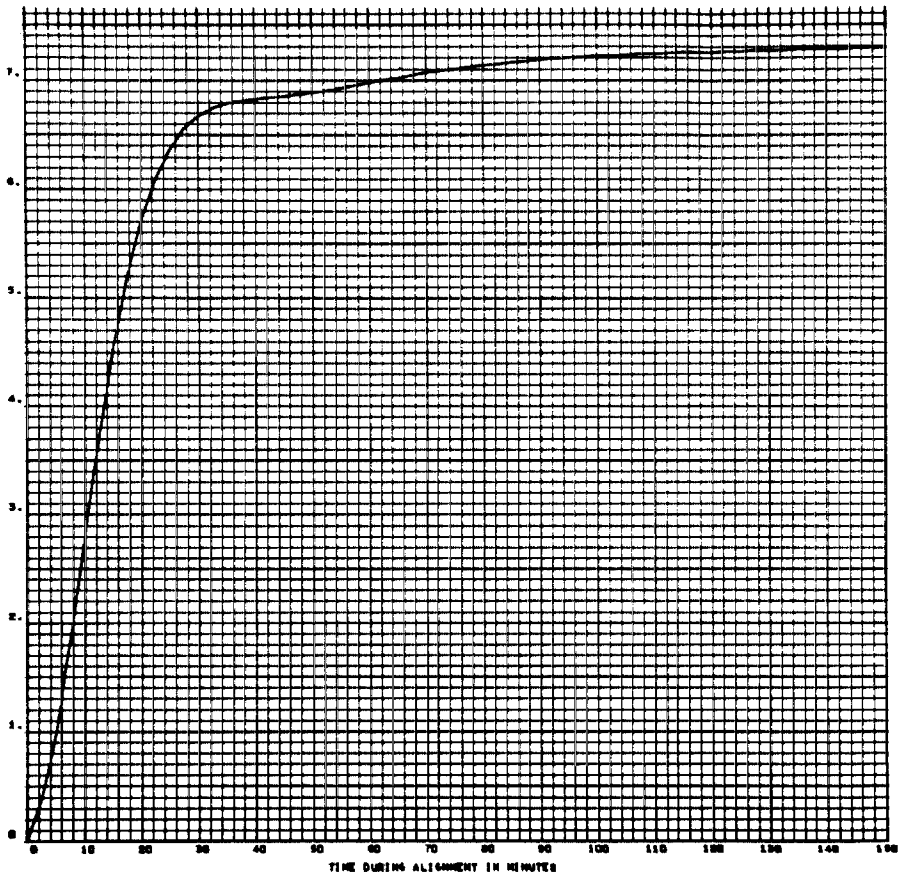

B77

AZIMUTH MISALIGNMENT IN ARCSECONDS - ORBITAL GYROCOMPASS, CASE 14, RUN 1
ERROR DUE TO X GYRO NOISE - .01 DEGREES/HOUR, C.T. = 1 HOUR

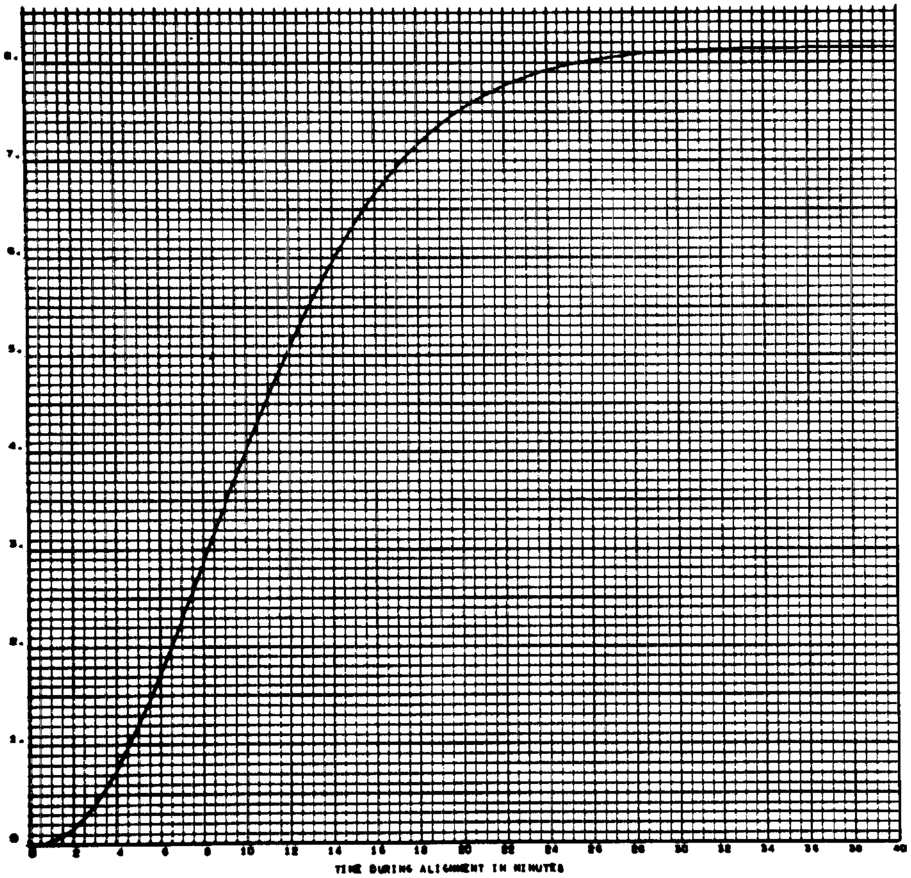

B78

AZIMUTH MISALIGNMENT IN ARCSECONDS - ORBITAL GYROCOMPASS, CASE 14, RUN 2
ERROR DUE TO X GYRO NOISE - .01 DEGREES/HOUR, C.T. = 1 HOUR

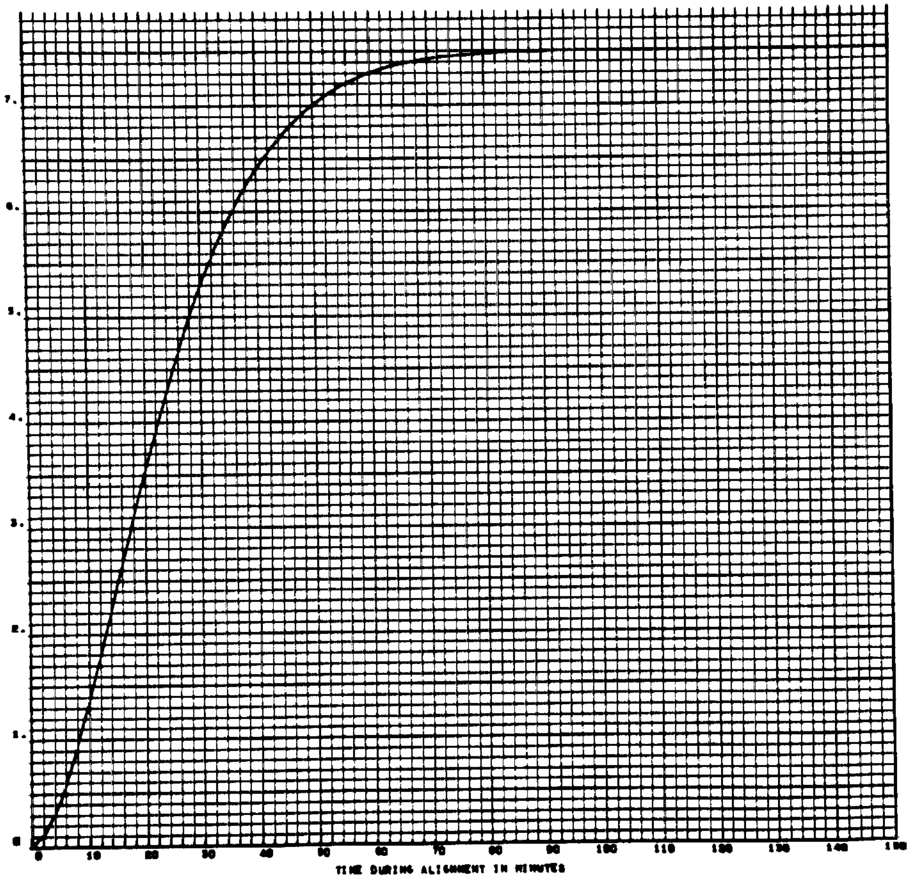

B79

AZIMUTH MISALIGNMENT IN ARCSECONDS - ORBITAL GYROCOMPASS, CASE 4, RUN 1
ERROR DUE TO X GYRO MISALIGNMENT - 1 ARCSECOND

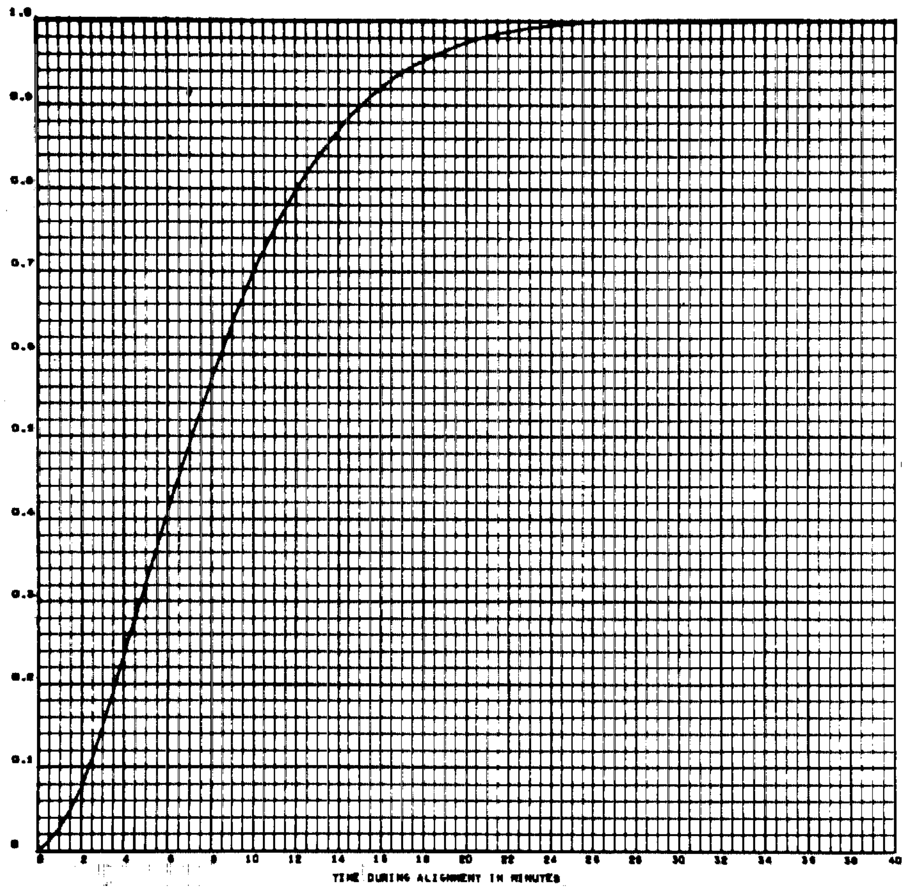

B80

AZIMUTH MISALIGNMENT IN ARCSECONDS - ORBITAL GYROCOMPASS, CASE 4, RUN 2
ERROR DUE TO X GYRO MISALIGNMENT - 1 ARCSECOND

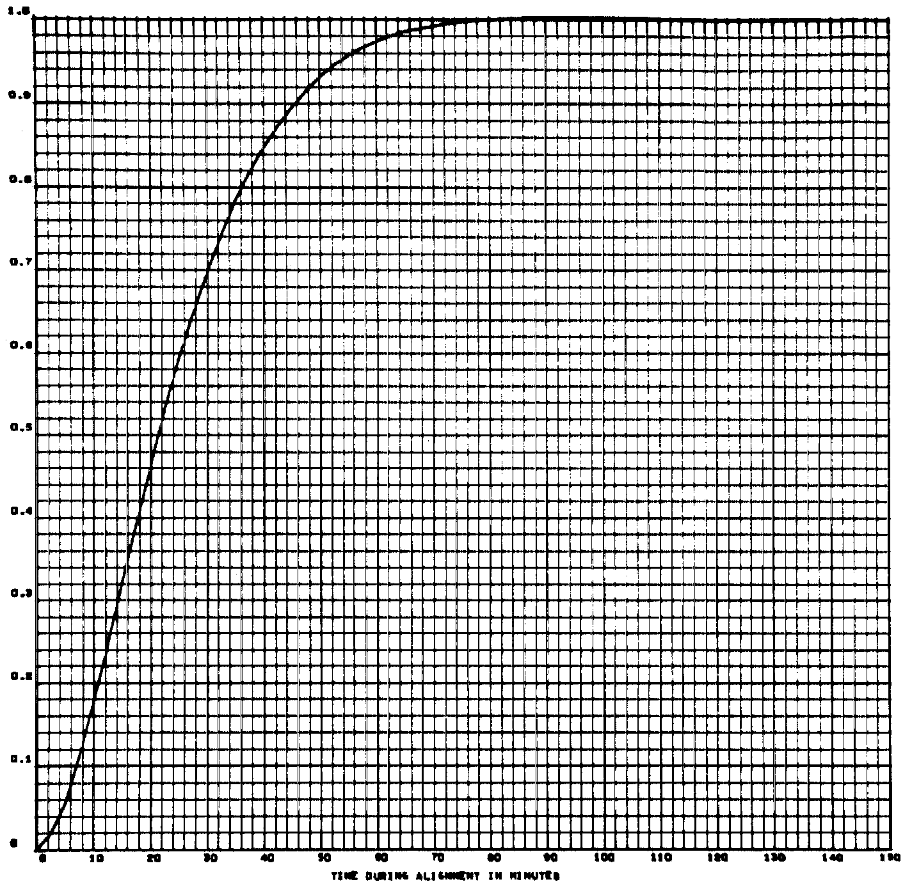

B81

AZIMUTH MISALIGNMENT IN ARCSECONDS - ORBITAL GYROCOMPASS, CASE 10, RUN 1
ERROR DUE TO X GYRO MISALIGNMENT - 1 ARCSECOND

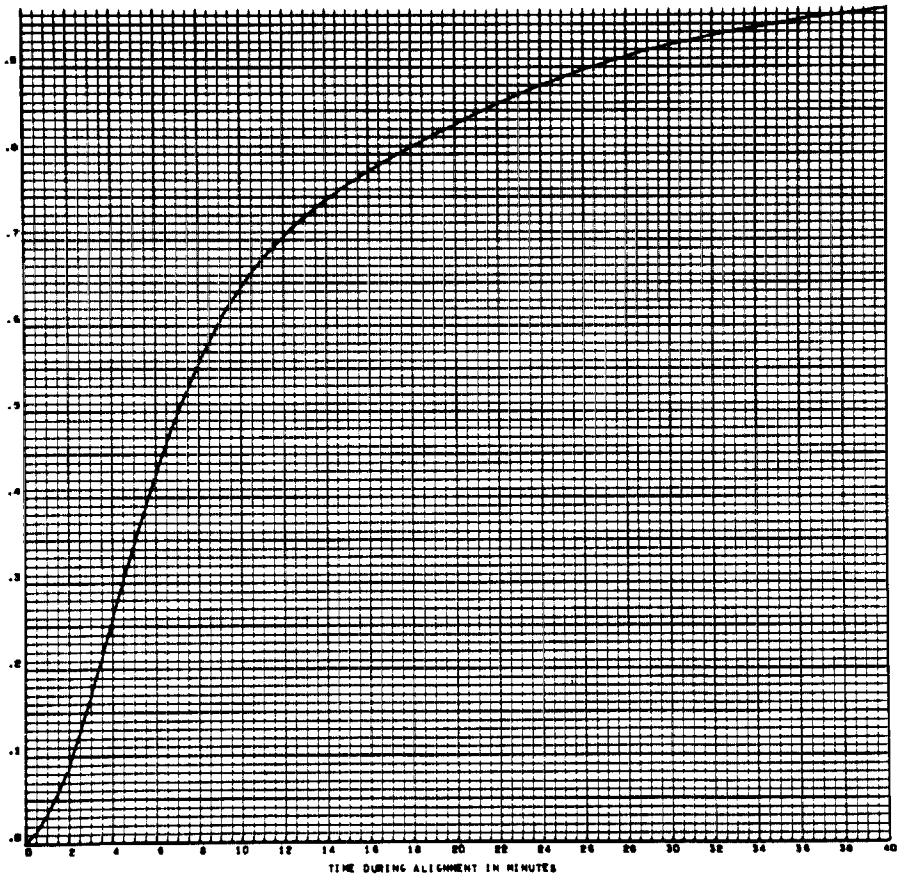

B82

AZIMUTH MISALIGNMENT IN ARCSECONDS - ORBITAL GYROCOMPASS, CASE 10, RUN 2
ERROR DUE TO X GYRO MISALIGNMENT - 1 ARCSECOND

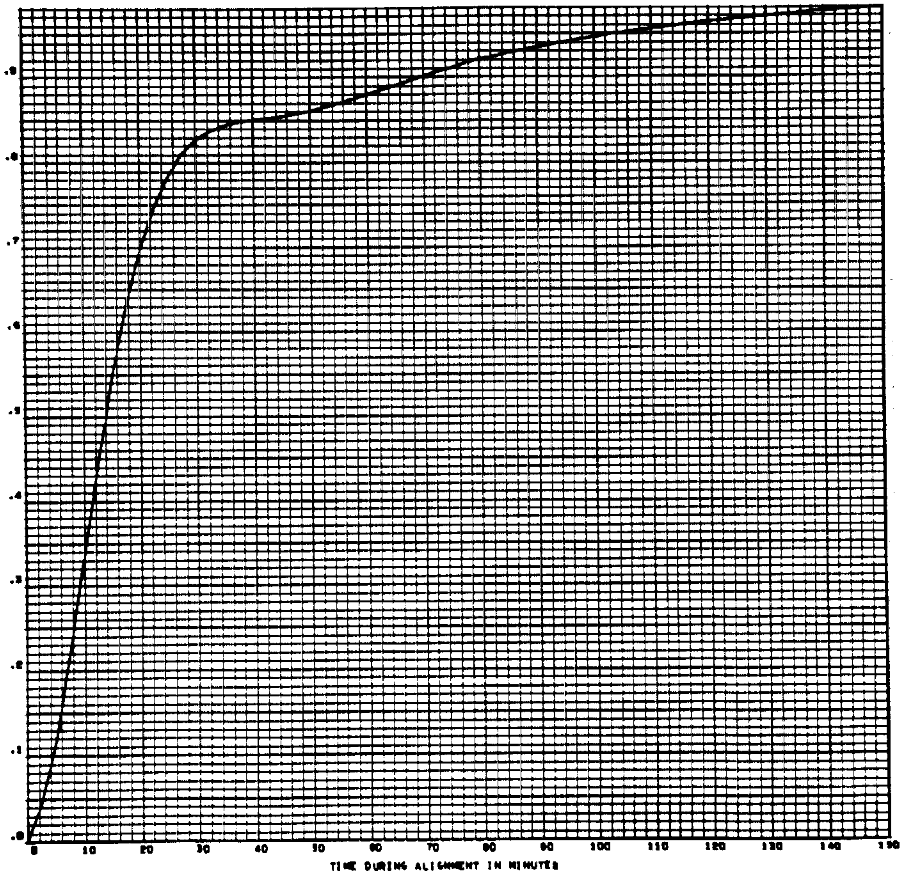

B83

AZIMUTH MISALIGNMENT IN ARCSECONDS - ORBITAL GYROCOMPASS, CASE 14, RUN 1
ERROR DUE TO X GYRO MISALIGNMENT - 1 ARCSECOND

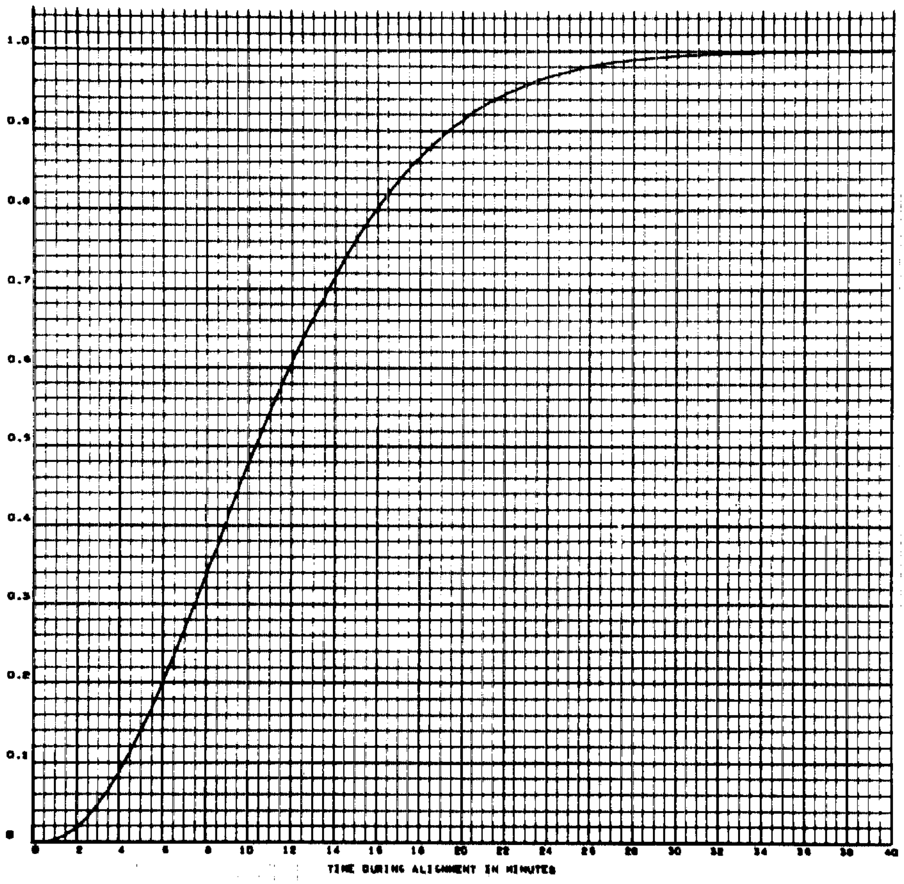

B84

AZIMUTH MISALIGNMENT IN ARCSECONDS - ORBITAL GYROCOMPASS, CASE 14, RUN 2
ERROR DUE TO X GYRO MISALIGNMENT - 1 ARCSECOND

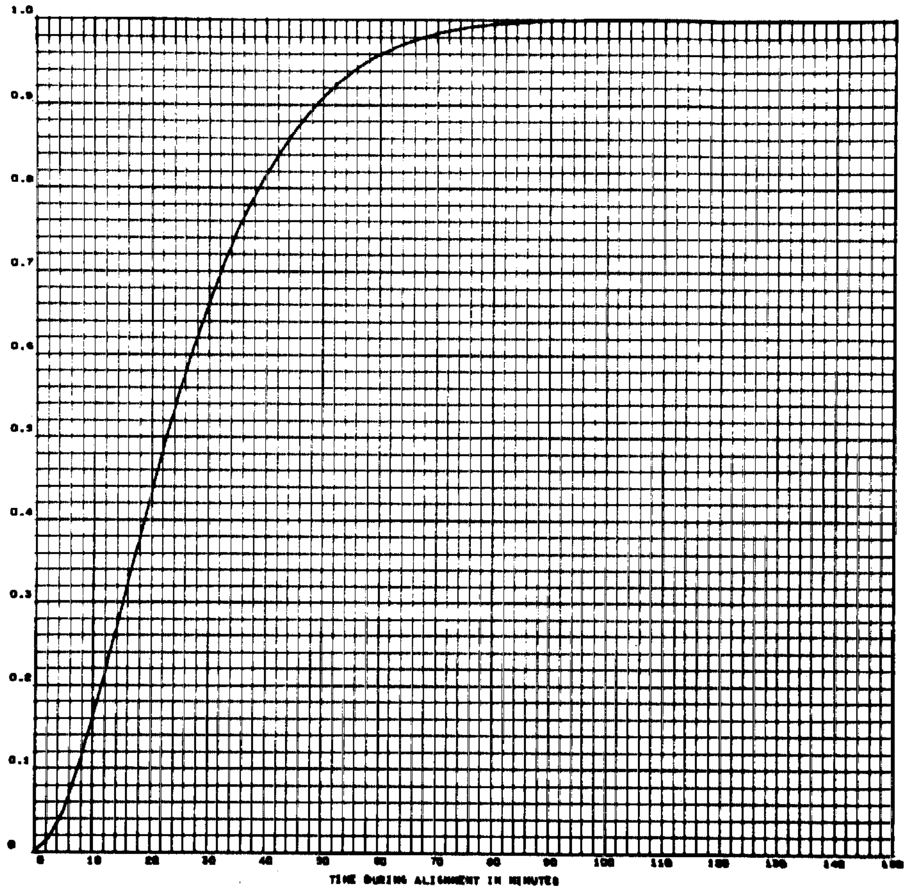

B85

AZIMUTH MISALIGNMENT IN ARCSECONDS - ORBITAL GYROCOMPASS, CASE 4, RUN 1
ERROR DUE TO Z GYRO MISALIGNMENT - 1 ARCSECOND

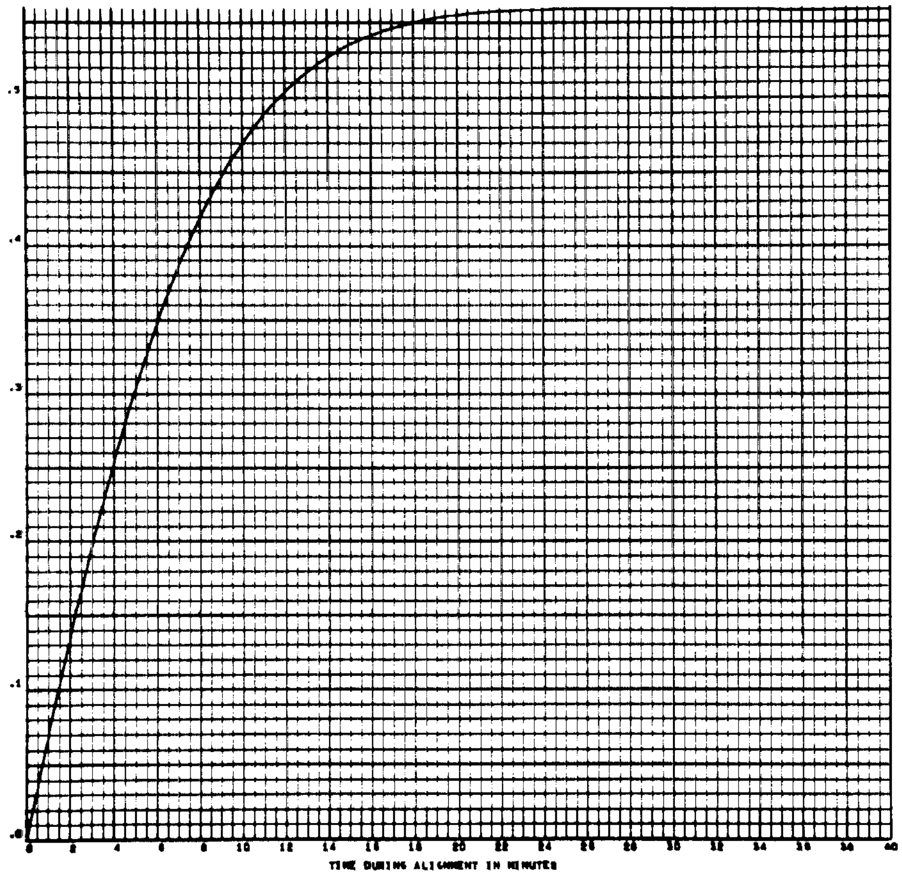

B86

AZIMUTH MISALIGNMENT IN ARCSECONDS - ORBITAL GYROCOMPASS, CASE 4, RUN 2
ERROR DUE TO Z GYRO MISALIGNMENT - 1 ARCSECOND

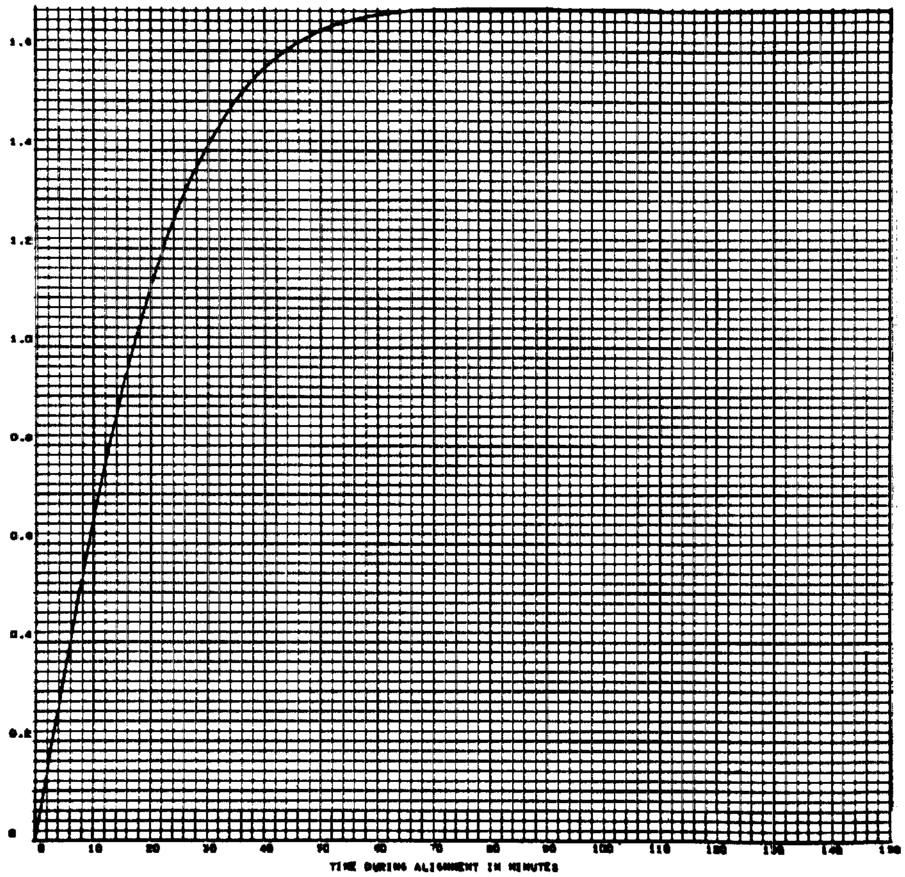

B87

AZIMUTH MISALIGNMENT IN ARCSECONDS - ORBITAL GYROCOMPASS, CASE 10, RUN 1
ERROR DUE TO Z GYRO MISALIGNMENT - 1 ARCSECOND

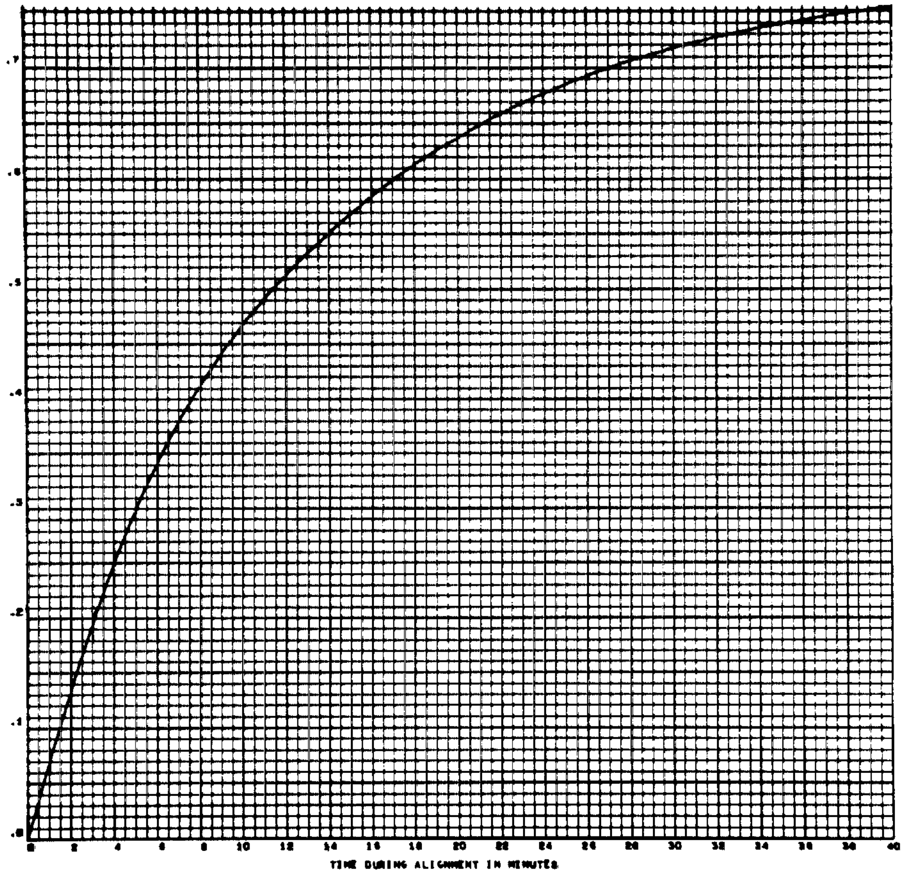

B88

AZIMUTH MISALIGNMENT IN ARCSECONDS - ORBITAL GYROCOMPASS, CASE 10, RUN 2
ERROR DUE TO Z GYRO MISALIGNMENT - 1 ARCSECOND

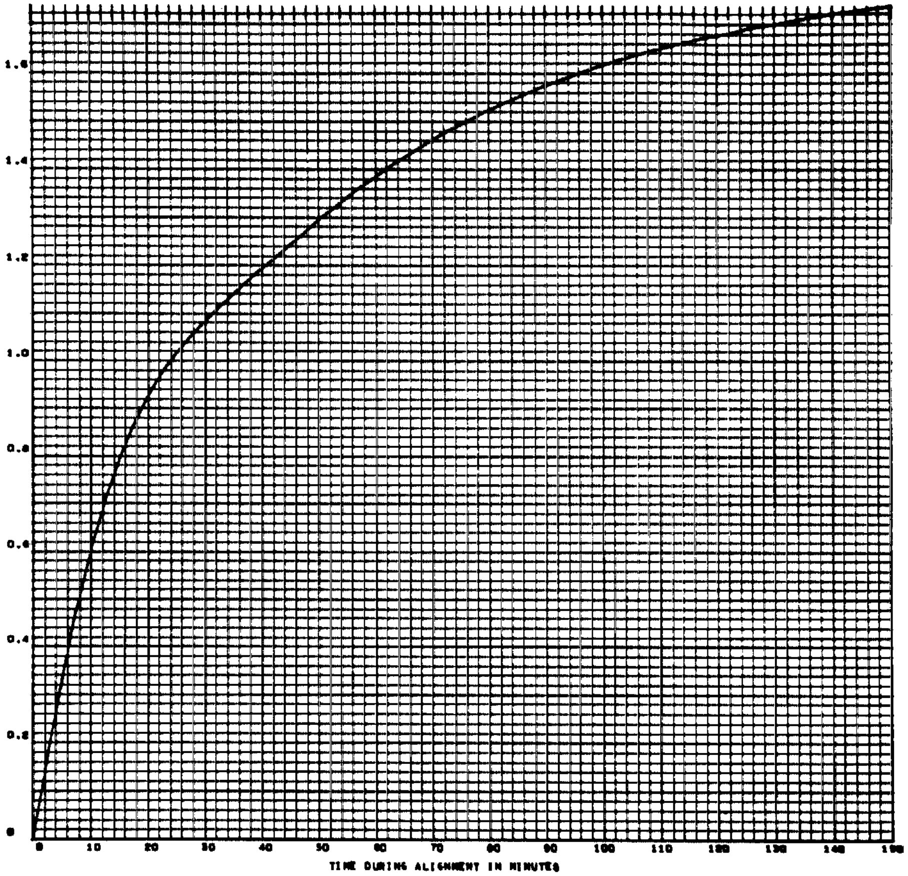

B89

AZIMUTH MISALIGNMENT IN ARCSECONDS - ORBITAL GYROCOMPASS, CASE 14, RUN 1
ERROR DUE TO Z GYRO MISALIGNMENT - 1 ARCSECOND

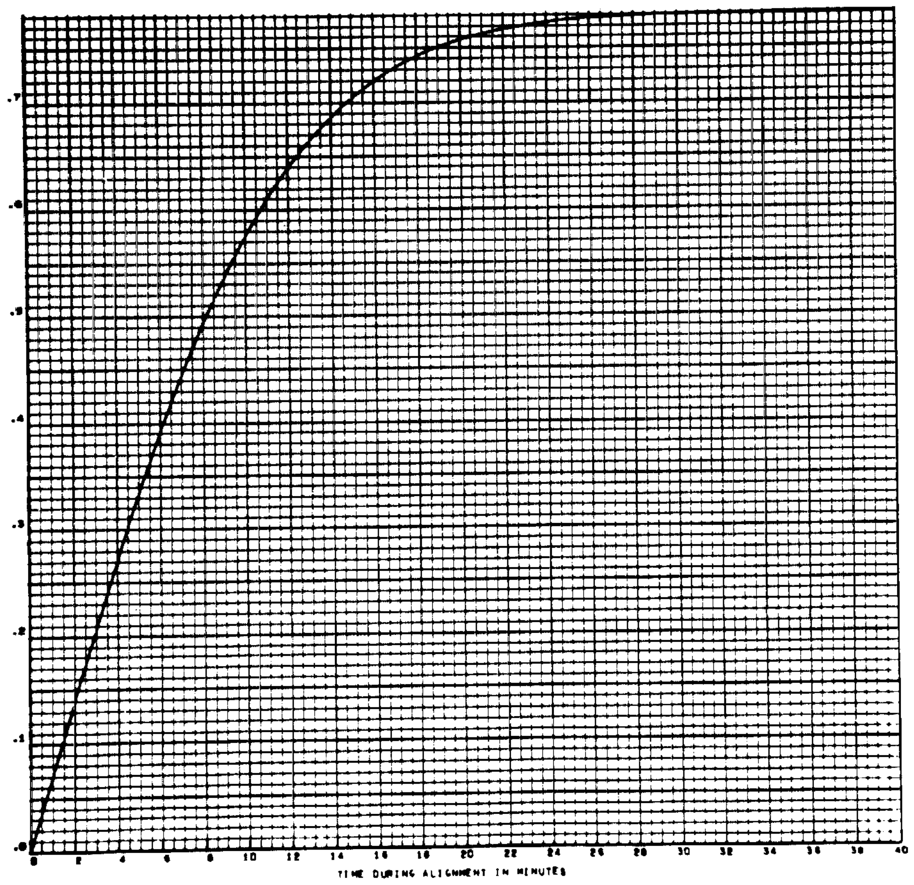

B90

AZIMUTH MISALIGNMENT IN ARCSECONDS - ORBITAL GYROCOMPASS, CASE 14, RUN 2
ERROR DUE TO Z GYRO MISALIGNMENT - 1 ARCSECOND

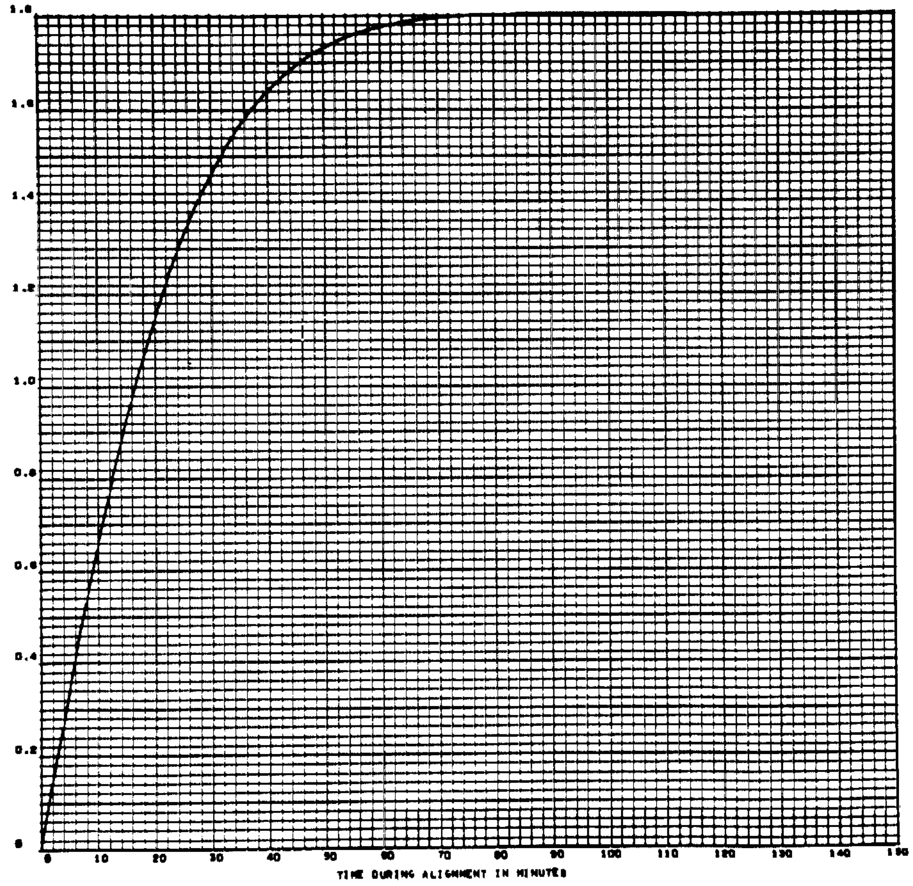

B91

AZIMUTH MISALIGNMENT IN ARCSECONDS - ORBITAL GYROCOMPASS, CASE 4, RUN 1
ERROR DUE TO HORIZON SENSOR MISALIGNMENT - 1 ARCSECOND

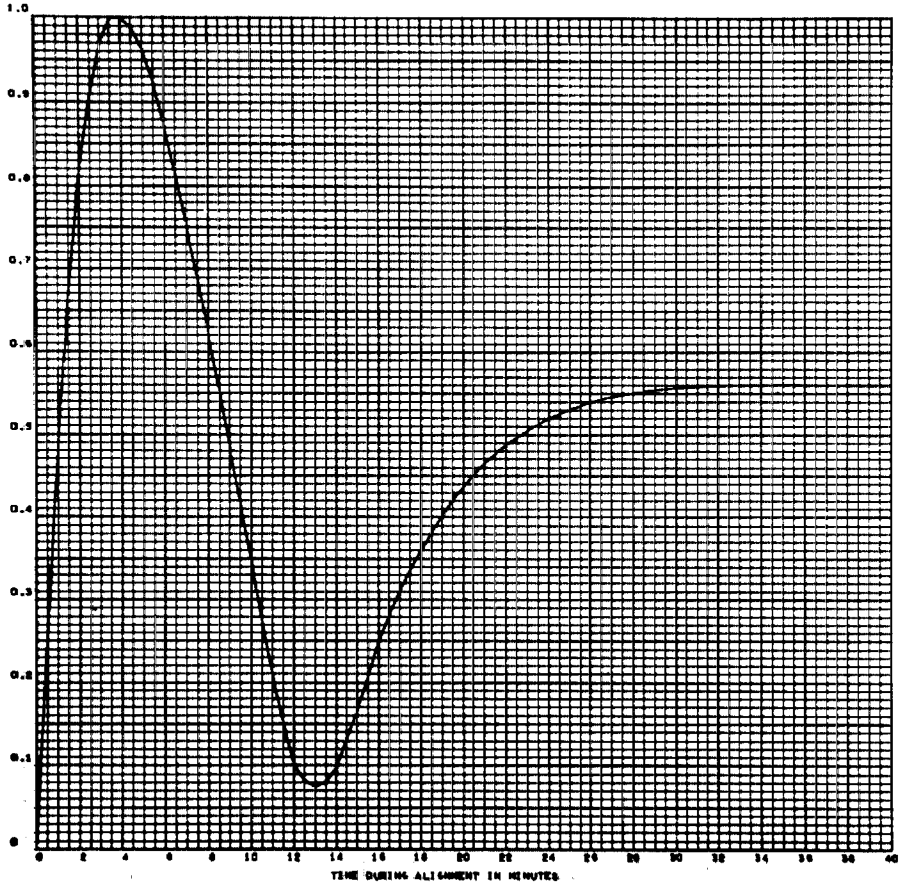

B92

AZIMUTH MISALIGNMENT IN ARCSECONDS - ORBITAL GYROCOMPASS, CASE 4, RUN 2
ERROR DUE TO HORIZON SENSOR MISALIGNMENT - 1 ARCSECOND

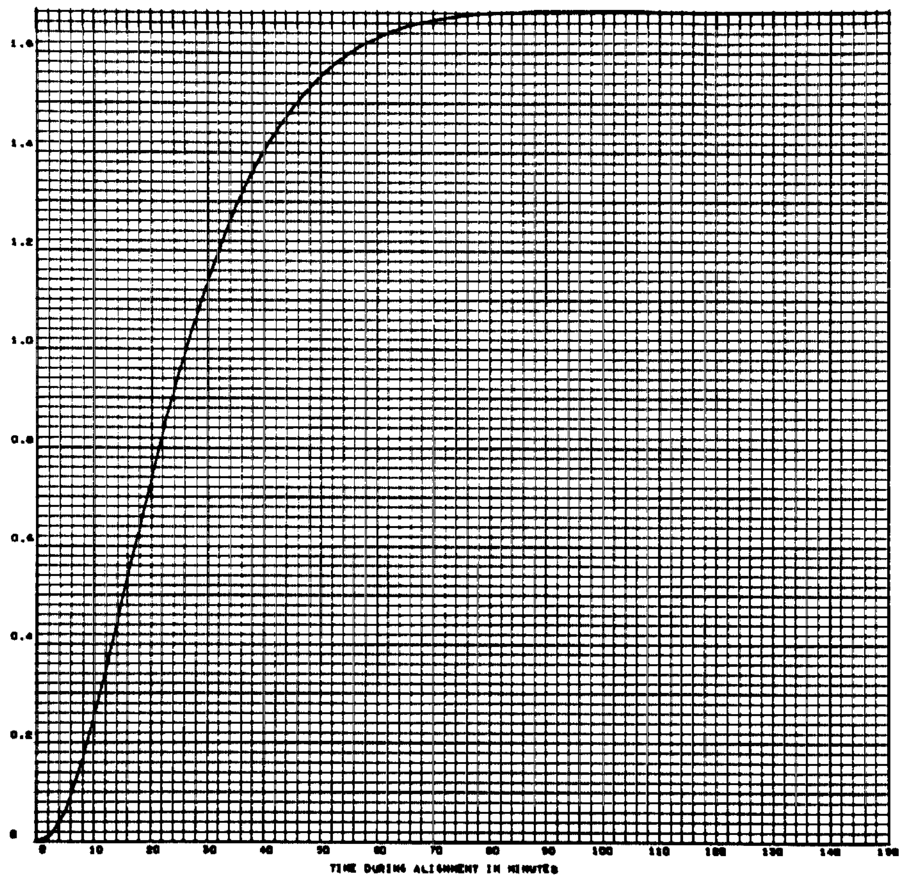

B93

AZIMUTH MISALIGNMENT IN ARCSECONDS - ORBITAL GYROCOMPASS, CASE 10, RUN 1
ERROR DUE TO HORIZON SENSOR MISALIGNMENT - 1 ARCSECOND

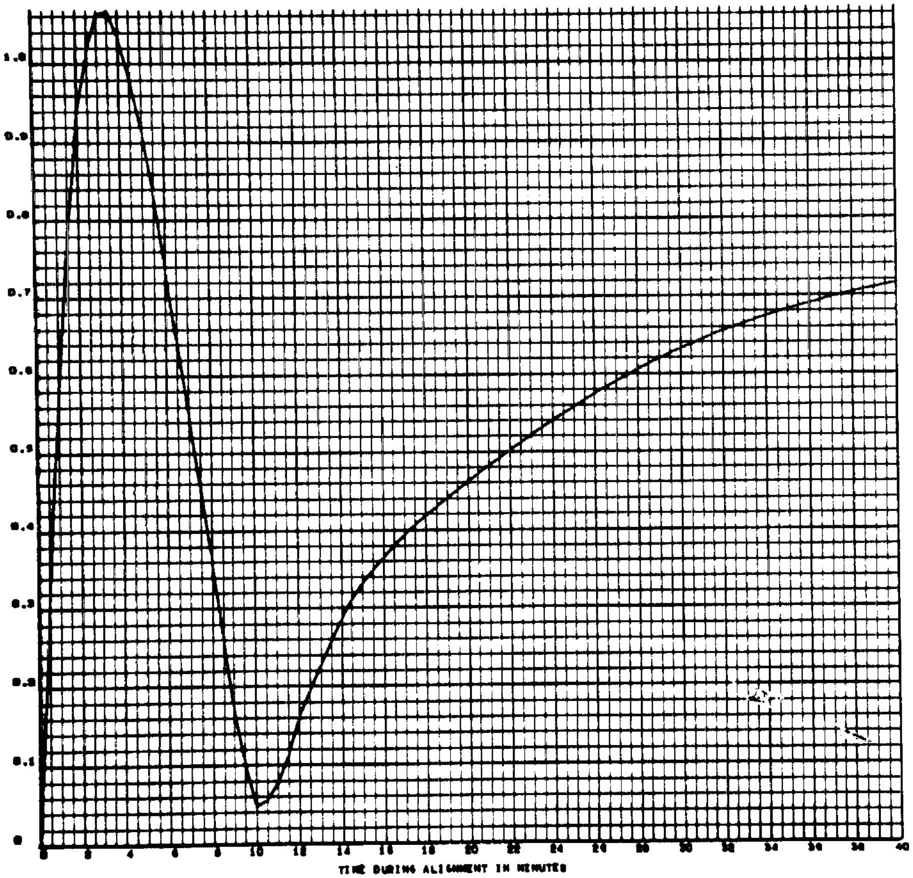

B94

AZIMUTH MISALIGNMENT IN ARCSECONDS - ORBITAL GYROCOMPASS, CASE 10, RUN 2
ERROR DUE TO HORIZON SENSOR MISALIGNMENT - 1 ARCSECOND

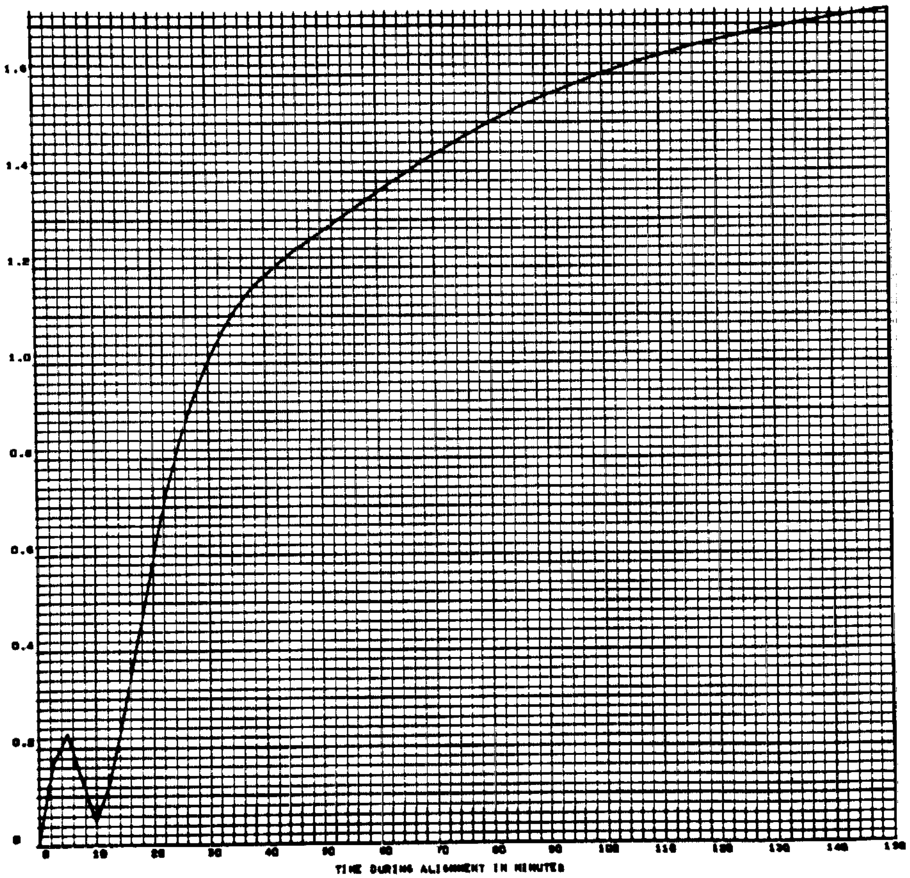

B95

AZIMUTH MISALIGNMENT IN ARCSECONDS - ORBITAL GYROCOMPASS, CASE 14, RUN 1
ERROR DUE TO HORIZON SENSOR MISALIGNMENT - 1 ARCSECOND

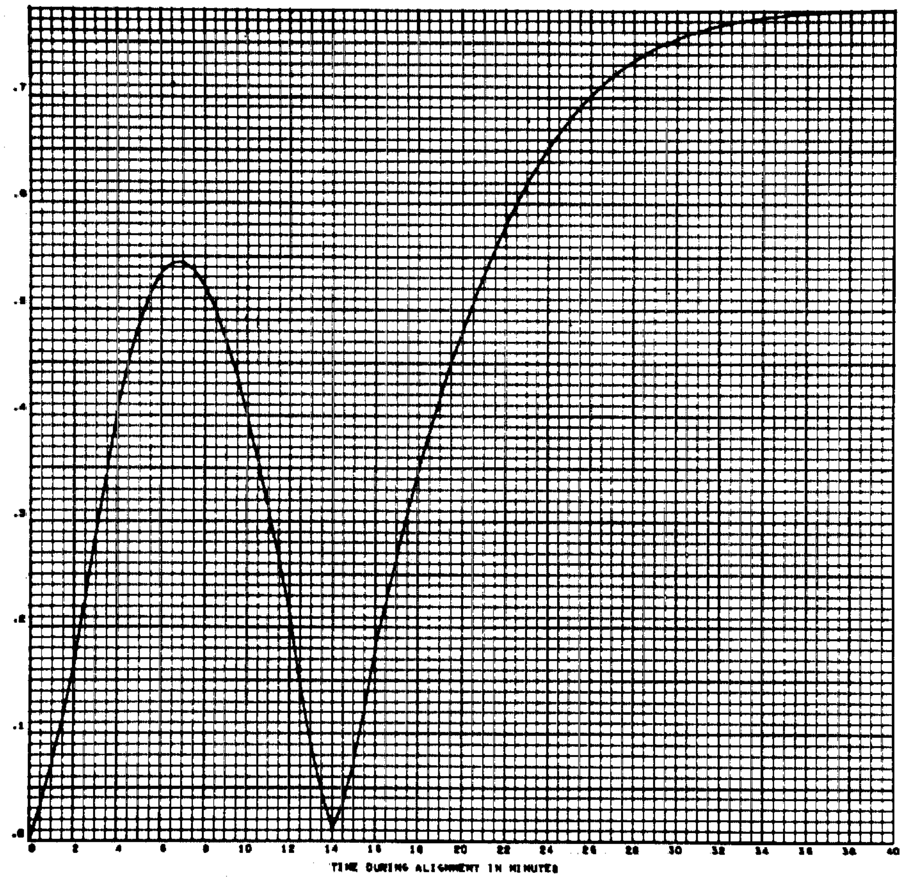

B96

AZIMUTH MISALIGNMENT IN ARCSECONDS - ORBITAL GYROCOMPASS, CASE 14, RUN 2
ERROR DUE TO HORIZON SENSOR MISALIGNMENT - 1 ARCSECOND

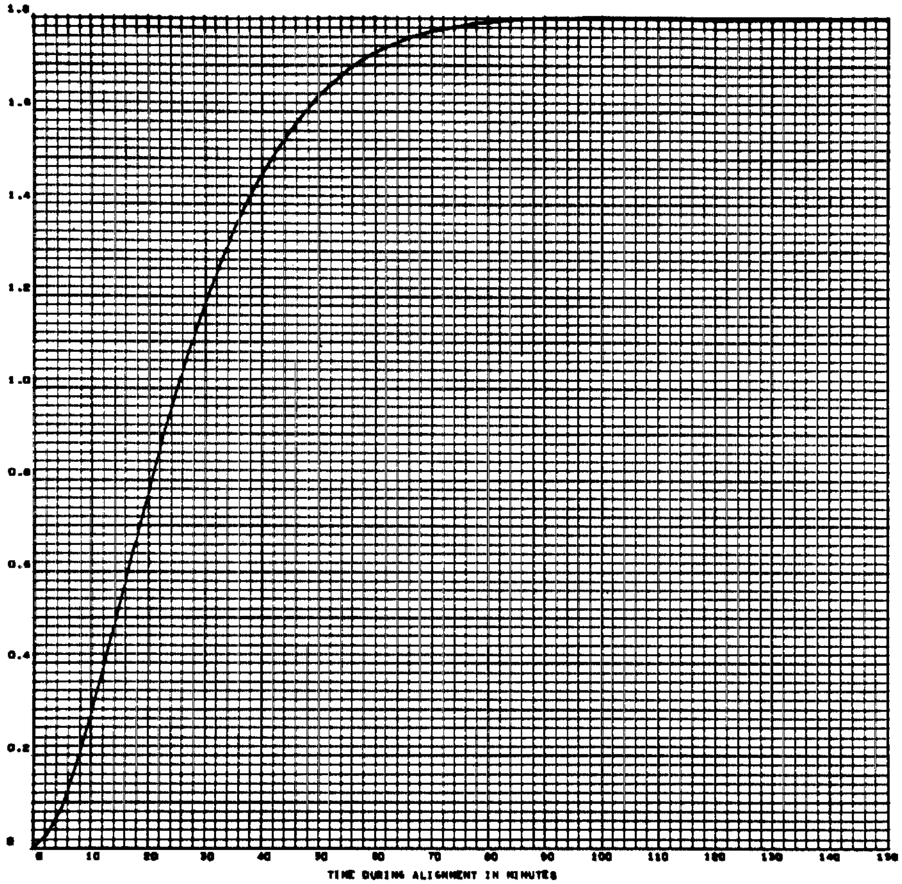

B97

AZIMUTH MISALIGNMENT IN ARCSECONDS - ORBITAL GYROCOMPASS, CASE 4, RUN 1
ERROR DUE TO HORIZON SENSOR NOISE - 1 ARCSECOND, C.T. = 1 MINUTE

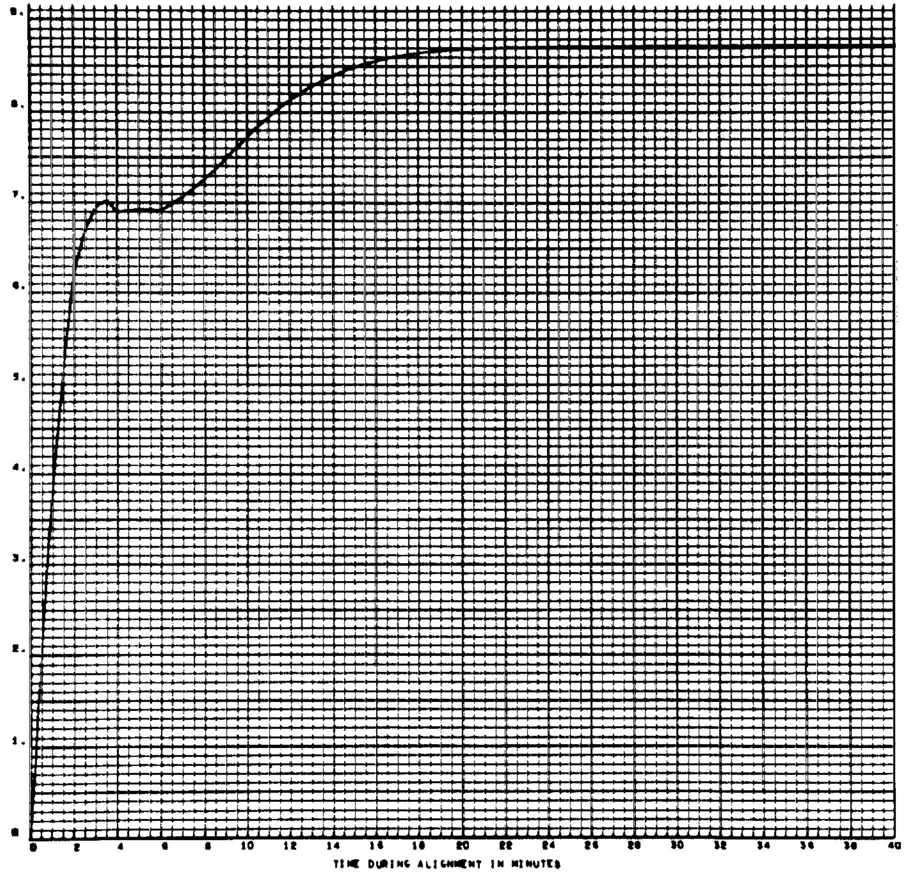

B98

AZIMUTH MISALIGNMENT IN ARCSECONDS - ORBITAL GYROCOMPASS, CASE 4, RUN 2
ERROR DUE TO HORIZON SENSOR NOISE - 1 ARCSECOND, C.T. = 1 MINUTE

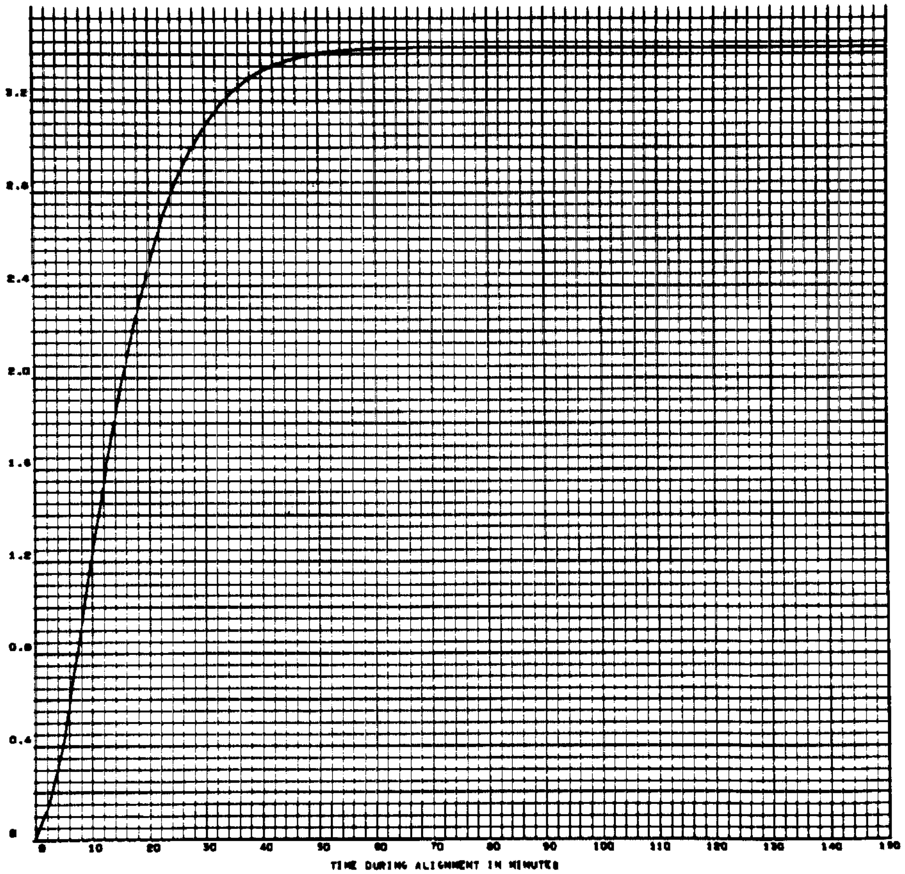

B99

AZIMUTH MISALIGNMENT IN ARCSECONDS - ORBITAL GYROCOMPASS, CASE 10, RUN 1
ERROR DUE TO HORIZON SENSOR NOISE - 1 ARCSECOND, C.T. = 1 MINUTE

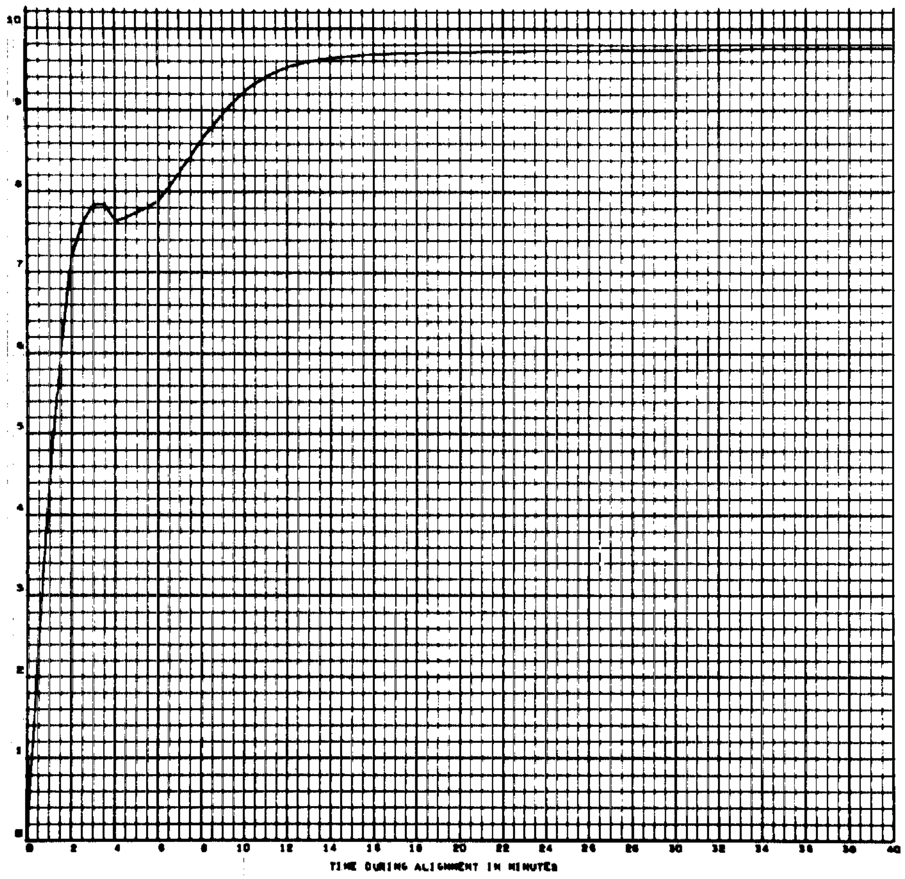

B100

AZIMUTH MISALIGNMENT IN ARCSECONDS - ORBITAL GYROCOMPASS, CASE 10, RUN 2
ERROR DUE TO HORIZON SENSOR NOISE - 1 ARCSECOND, C.T. = 1 MINUTE

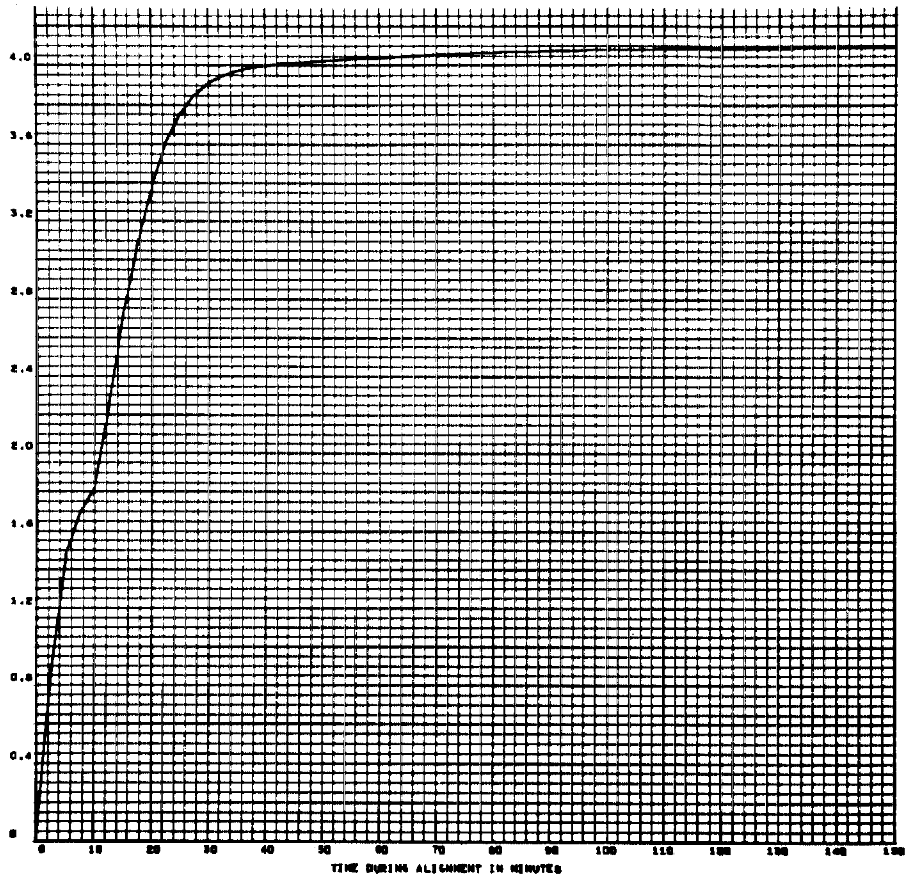

B101

AZIMUTH MISALIGNMENT IN ARCSECONDS - ORBITAL GYROCOMPASS, CASE 14, RUN 1
ERROR DUE TO HORIZON SENSOR NOISE - 1 ARCSECOND, C.T. = 1 MINUTE

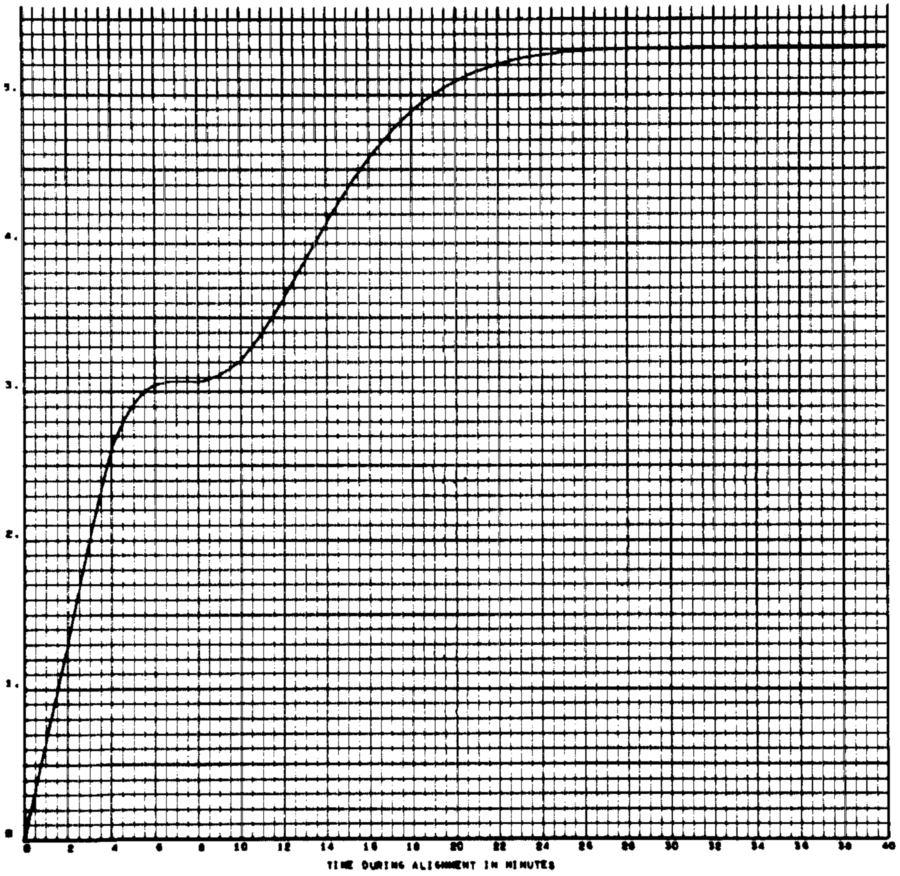

B102

AZIMUTH MISALIGNMENT IN ARCSECONDS - ORBITAL GYROCOMPASS, CASE 14, RUN 2
ERROR DUE TO HORIZON SENSOR NOISE - 1 ARCSECOND, C.T. = 1 MINUTE

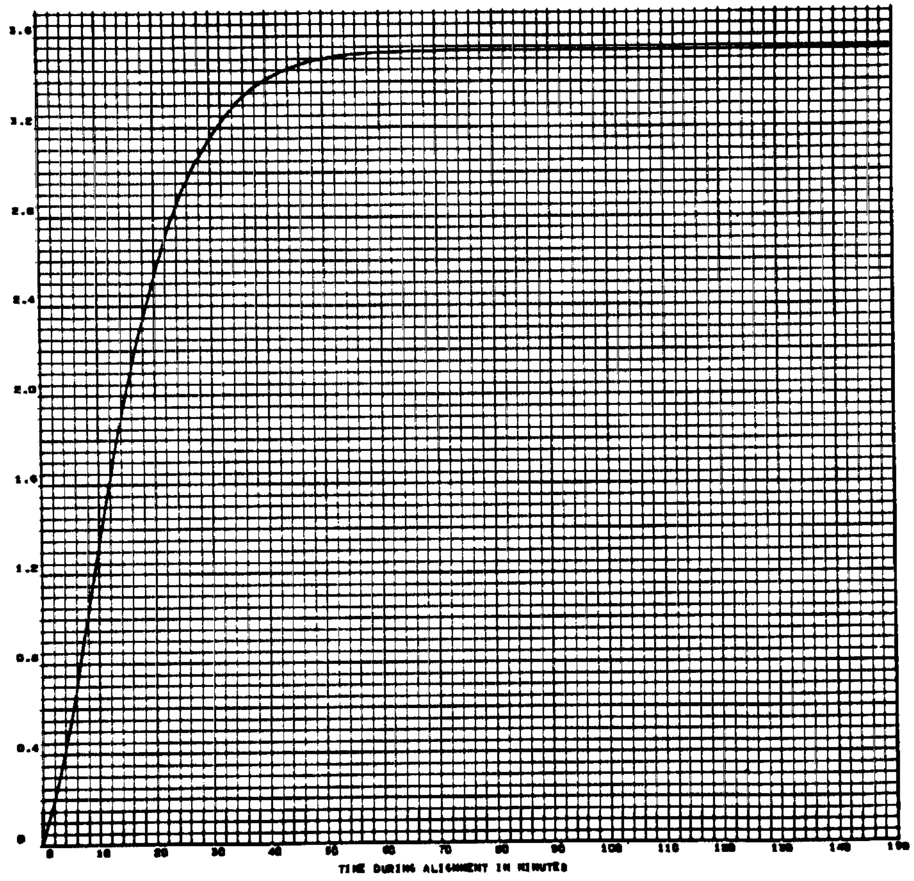

B103

AZIMUTH MISALIGNMENT IN ARCSECONDS - ORBITAL GYROCOMPASS, CASE 4, RUN 1
ERROR DUE TO INITIAL X TILT - 10 DEGREES

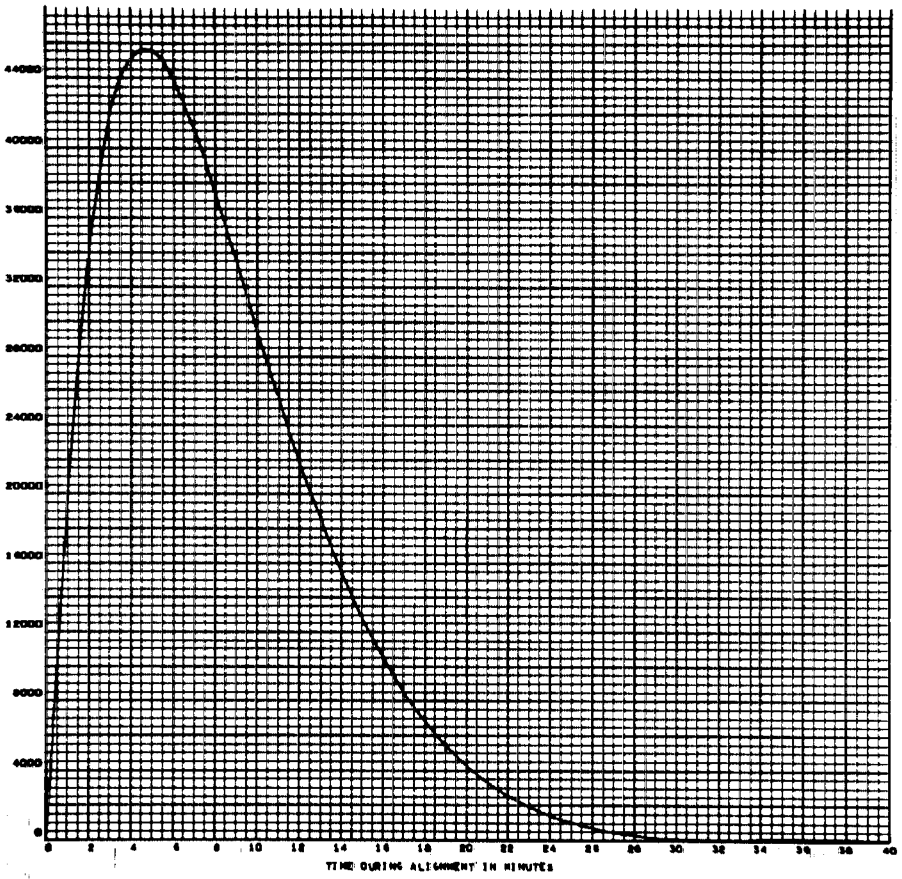

B104

AZIMUTH MISALIGNMENT IN ARCSECONDS - ORBITAL GYROCOMPASS, CASE 4, RUN 2
ERROR DUE TO INITIAL X TILT - 10 DEGREES

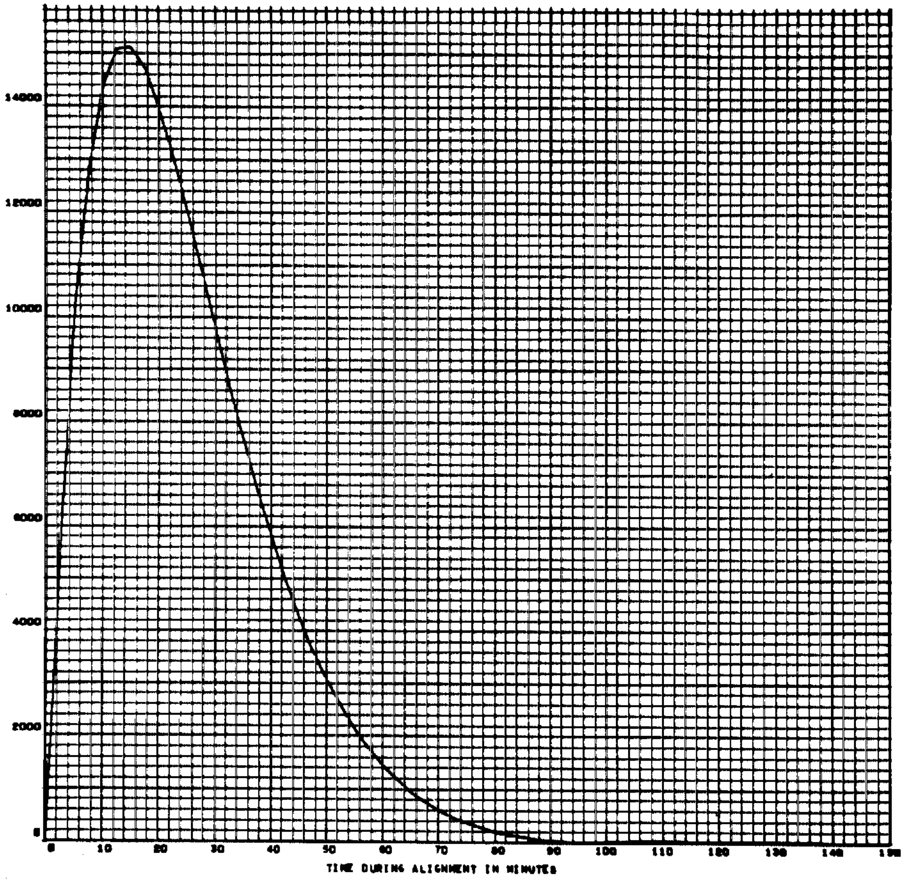

B105

AZIMUTH MISALIGNMENT IN ARCSECONDS - ORBITAL GYROCOMPASS, CASE 10, RUN 1
ERROR DUE TO INITIAL X TILT - 10 DEGREES

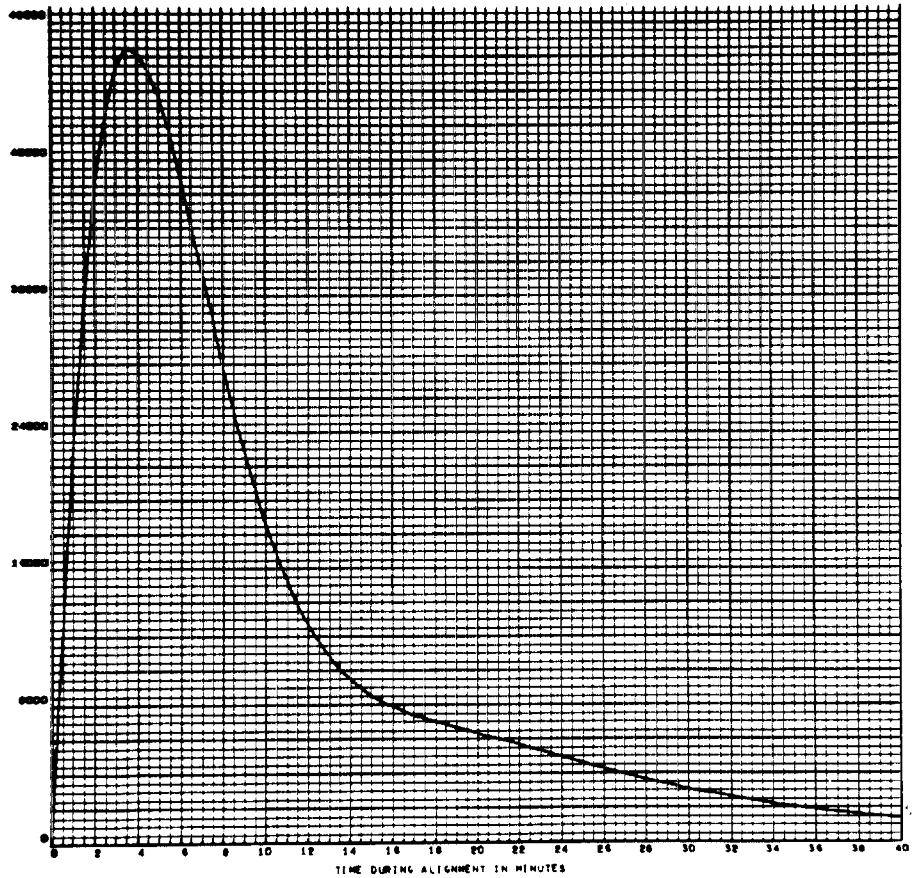

B106

AZIMUTH MISALIGNMENT IN ARCSECONDS - ORBITAL GYROCOMPASS, CASE 10, RUN 2
ERROR DUE TO INITIAL X TILT - 10 DEGREES

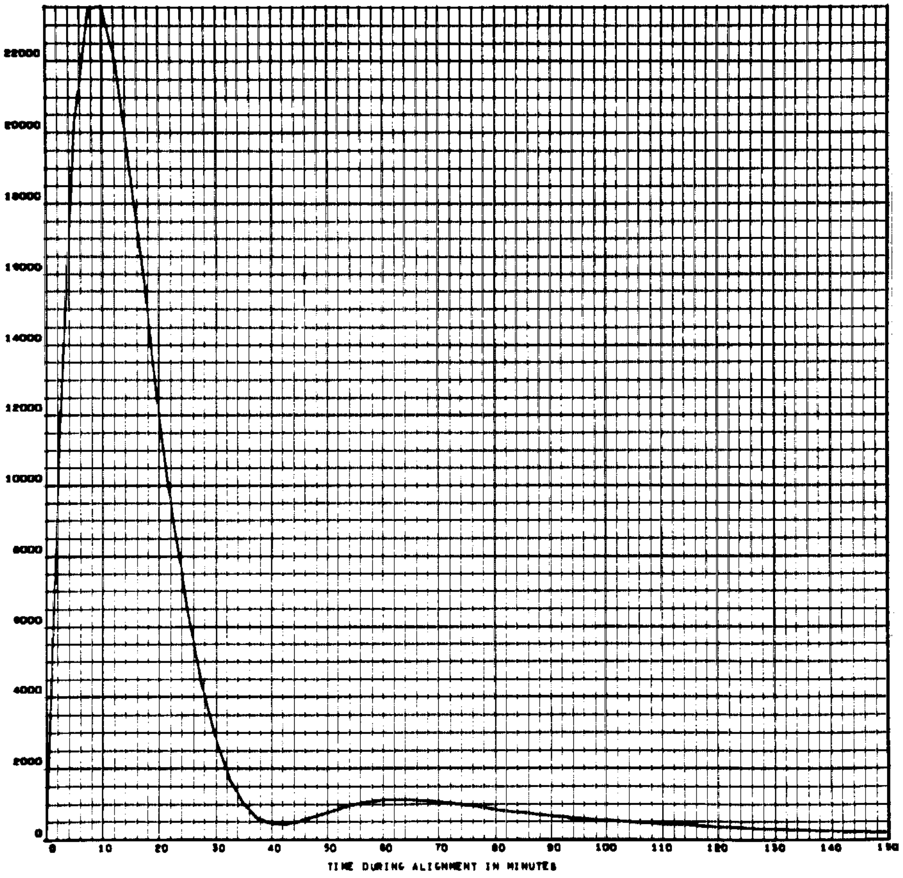

B107

AZIMUTH MISALIGNMENT IN ARCSECONDS - ORBITAL GYROCOMPASS, CASE 14, RUN 1
ERROR DUE TO INITIAL X TILT - 10 DEGREES

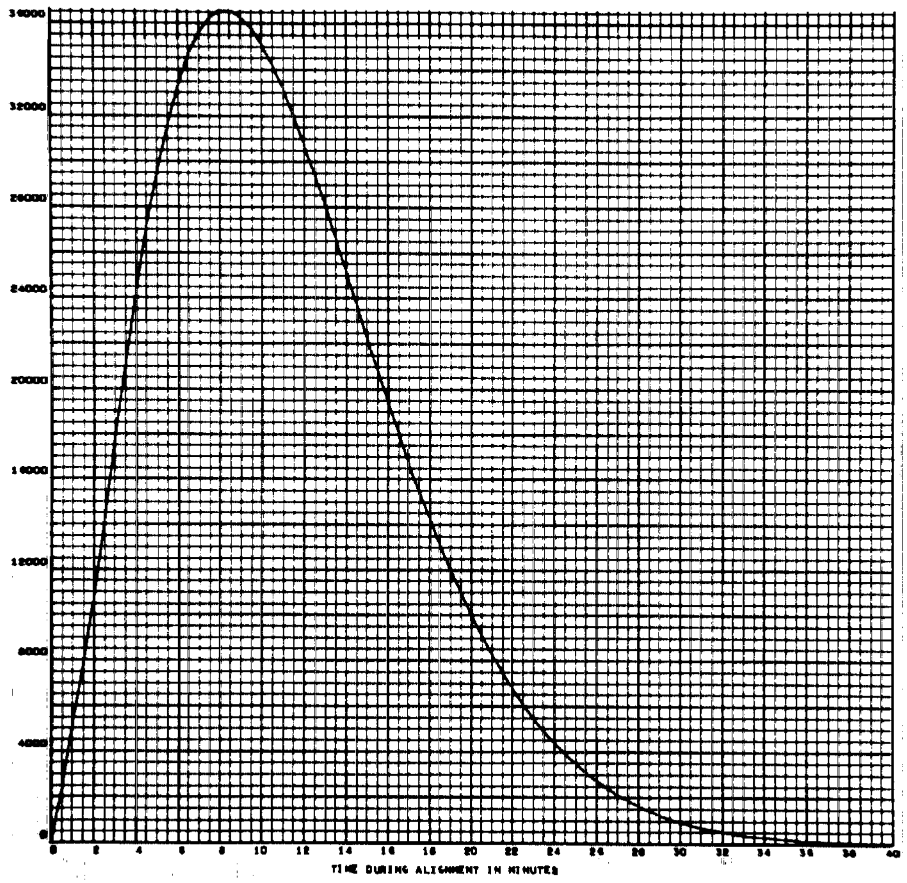

B108

AZIMUTH MISALIGNMENT IN ARCSECONDS - ORBITAL GYROCOMPASS, CASE 14, RUN 2
ERROR DUE TO INITIAL X TILT - 10 DEGREES

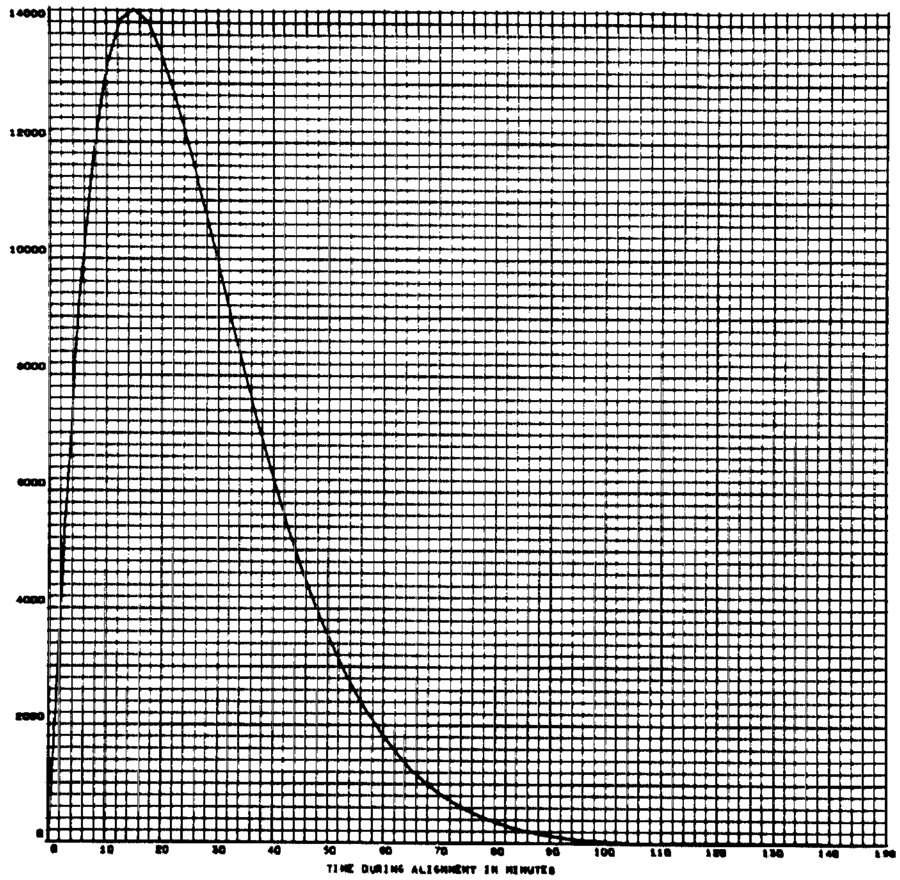

B109

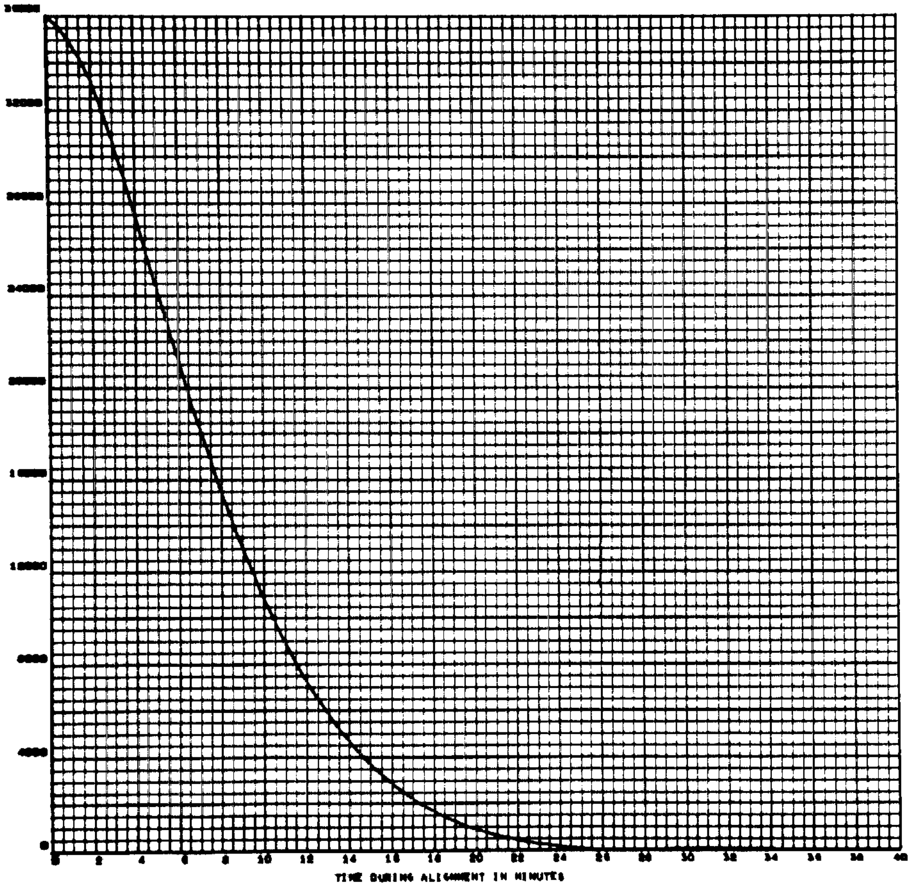

AZIMUTH MISALIGNMENT IN ARCSECONDS - ORBITAL GYROCOMPASS, CASE 4, RUN 1
ERROR DUE TO INITIAL AZIMUTH MISALIGNMENT - 10 DEGREES

B110

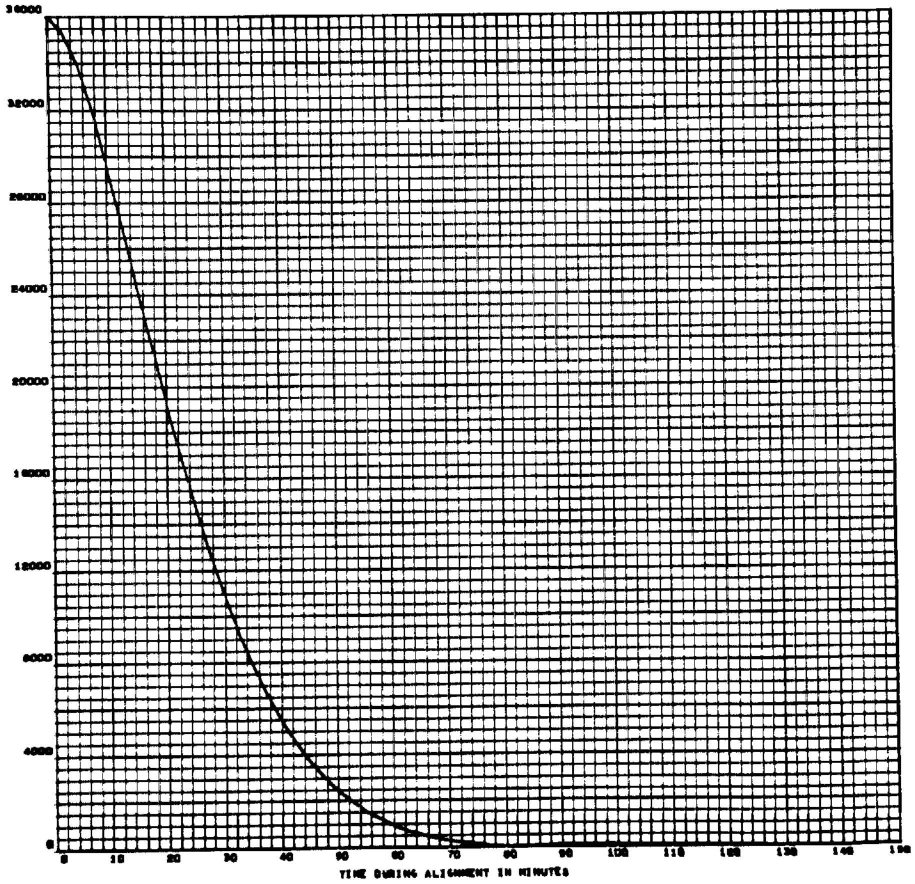

AZIMUTH MISALIGNMENT IN ARCSECONDS - ORBITAL GYROCOMPASS, CASE 4, RUN 2
ERROR DUE TO INITIAL AZIMUTH MISALIGNMENT - 10 DEGREES

B111

AZIMUTH MISALIGNMENT IN ARCSECONDS - ORBITAL GYROCOMPASS, CASE 10, RUN 1
ERROR DUE TO INITIAL AZIMUTH MISALIGNMENT - 10 DEGREES

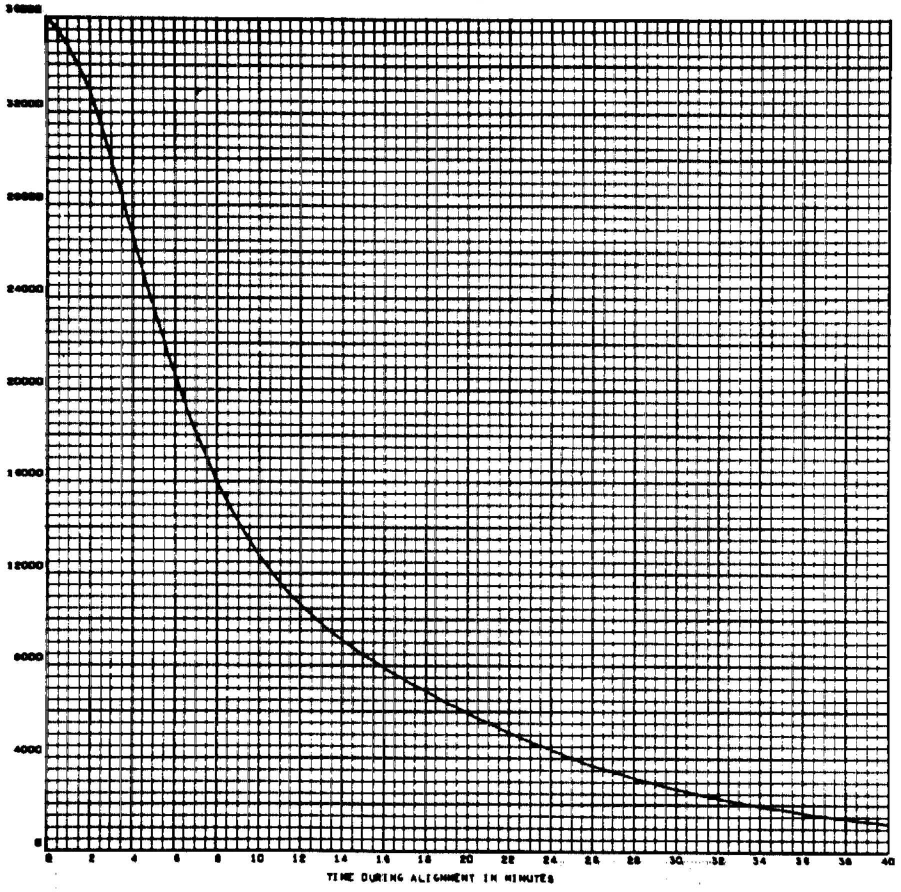

B112

AZIMUTH MISALIGNMENT IN ARCSECONDS - ORBITAL GYROCOMPASS, CASE 10, RUN 2
ERROR DUE TO INITIAL AZIMUTH MISALIGNMENT - 10 DEGREES

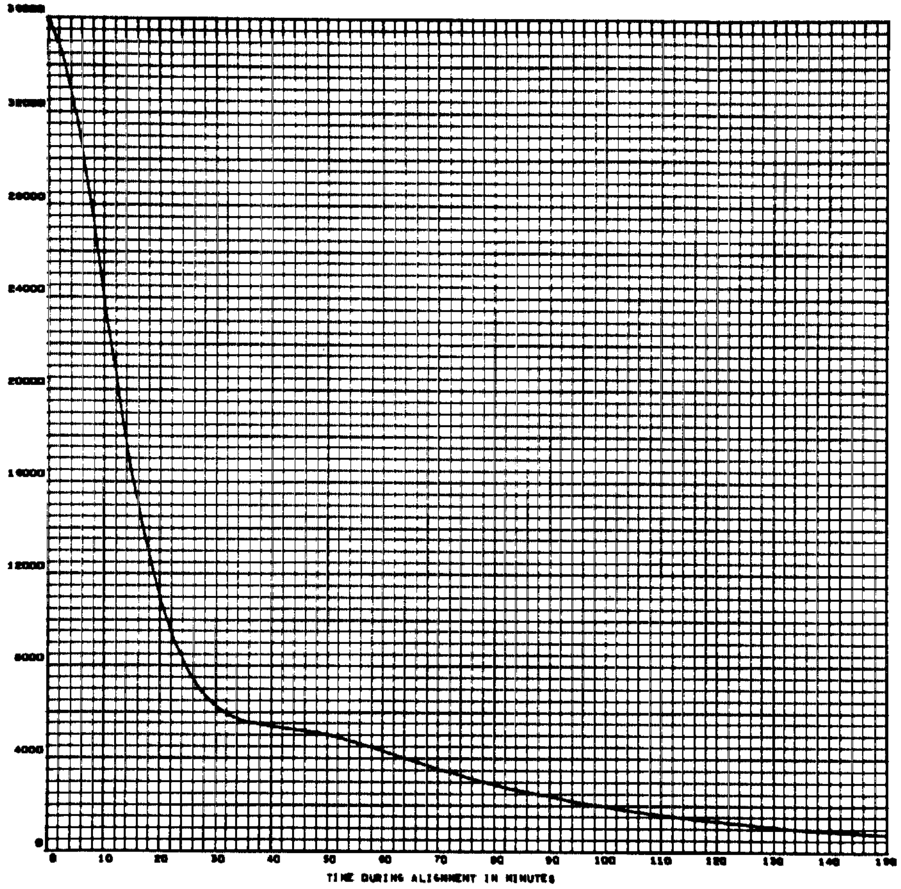

B13

AZIMUTH MISALIGNMENT IN ARCSECONDS - ORBITAL GYROCOMPASS, CASE 14, RUN 1
ERROR DUE TO INITIAL AZIMUTH MISALIGNMENT - 10 DEGREES

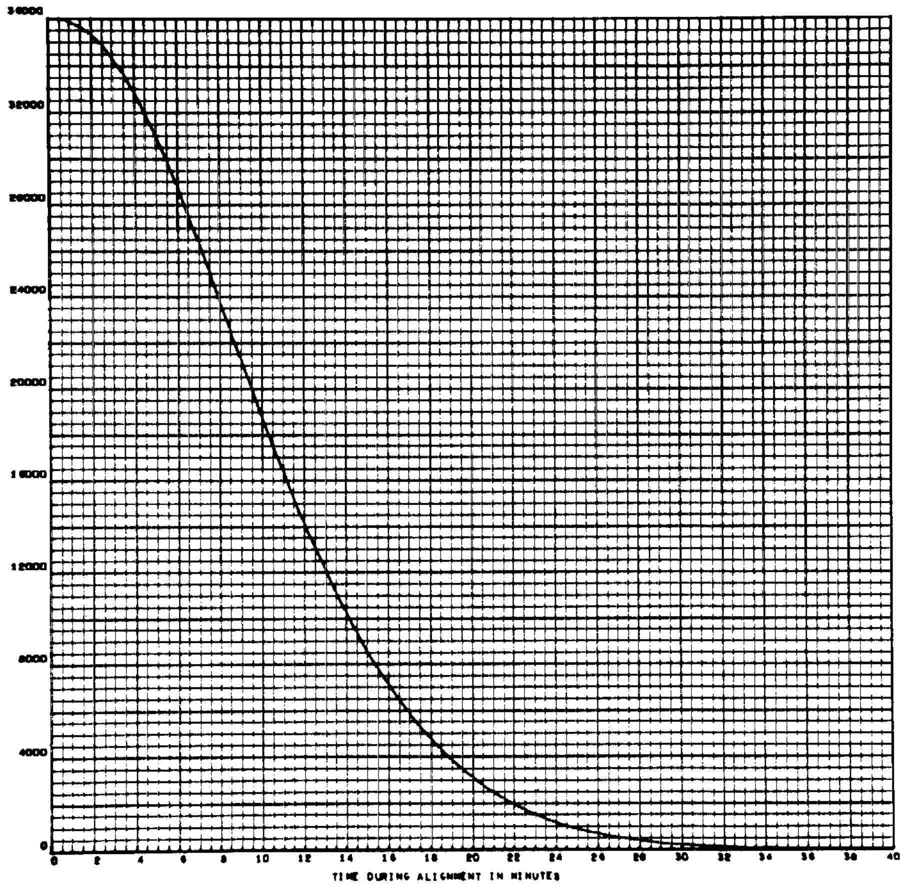

B14

AZIMUTH MISALIGNMENT IN ARCSECONDS - ORBITAL GYROCOMPASS, CASE 14, RUN 2
ERROR DUE TO INITIAL AZIMUTH MISALIGNMENT - 10 DEGREES

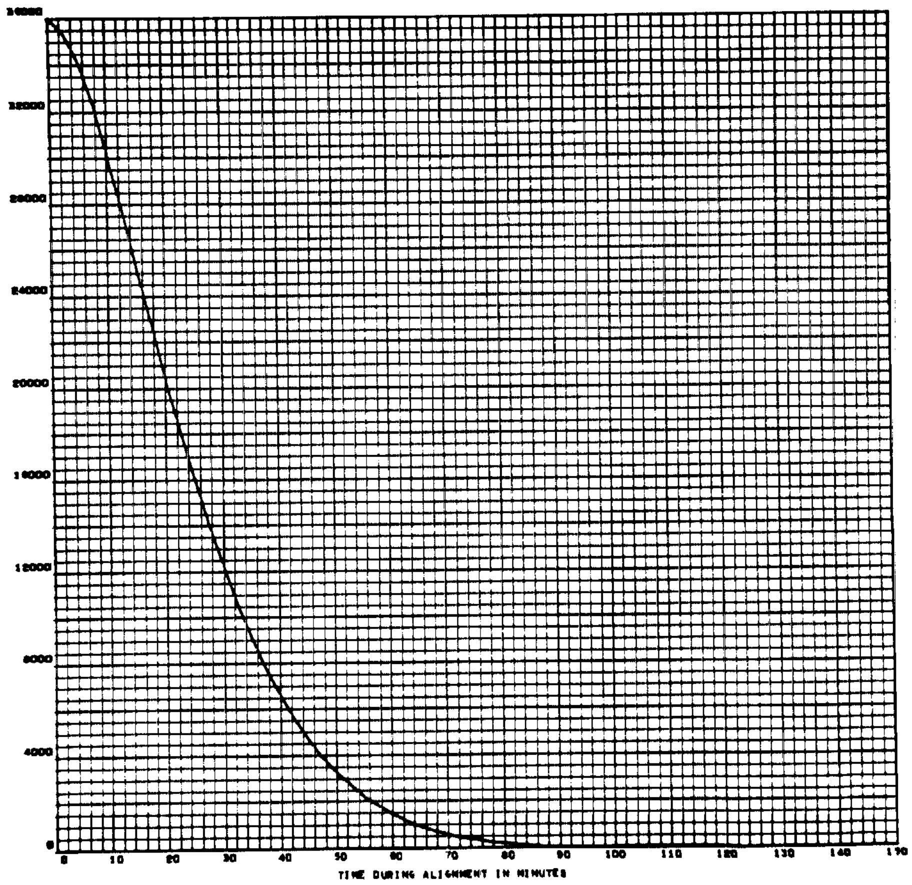

B115

AZIMUTH MISALIGNMENT IN ARCSECONDS - ORBITAL GYROCOMPASS, CASE 4, RUN 1
ERROR DUE TO Z GYRO DRIFT - .01 DEGREES/HOUR

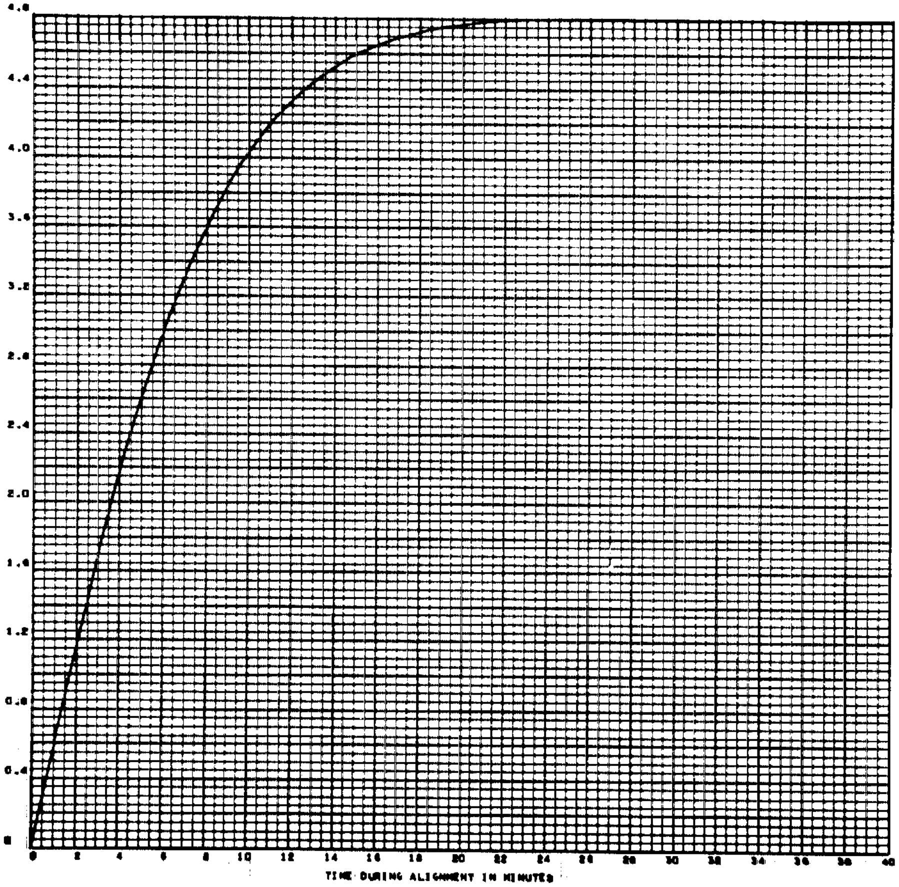

B116

AZIMUTH MISALIGNMENT IN ARCSECONDS - ORBITAL GYROCOMPASS, CASE 4, RUN 2
ERROR DUE TO Z GYRO DRIFT - .01 DEGREES/HOUR

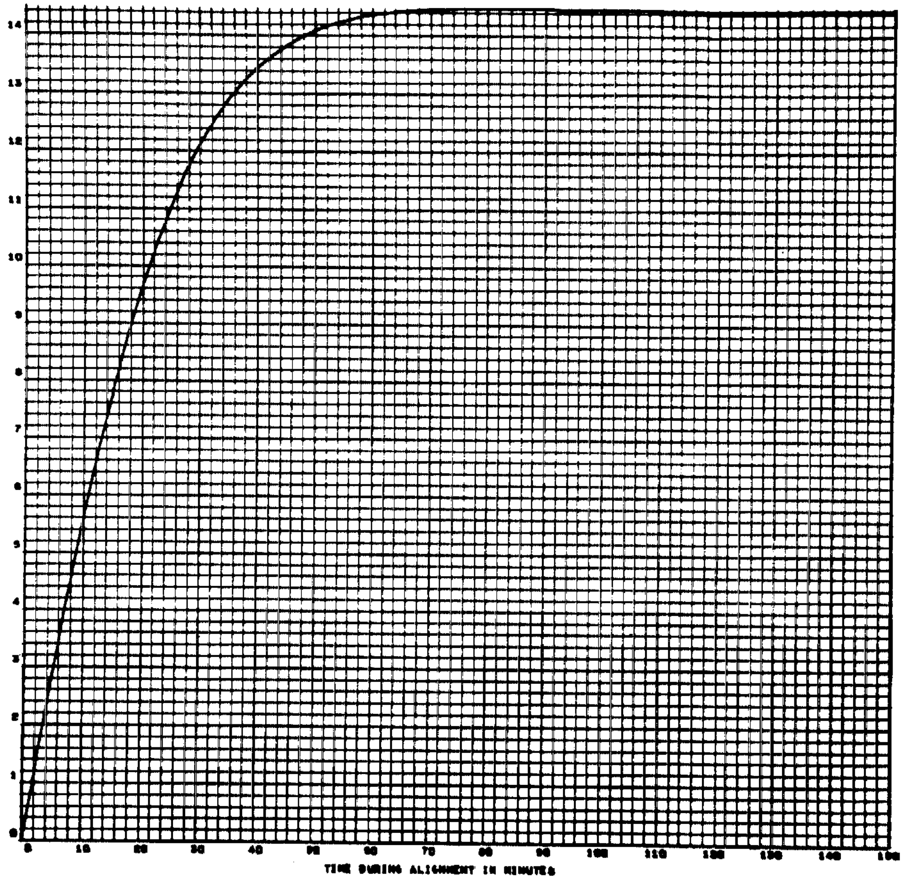

AZIMUTH MISALIGNMENT IN ARCSECONDS - ORBITAL GYROCOMPASS, CASE 10, RUN 1
ERROR DUE TO Z GYRO DRIFT - .01 DEGREES/HOUR

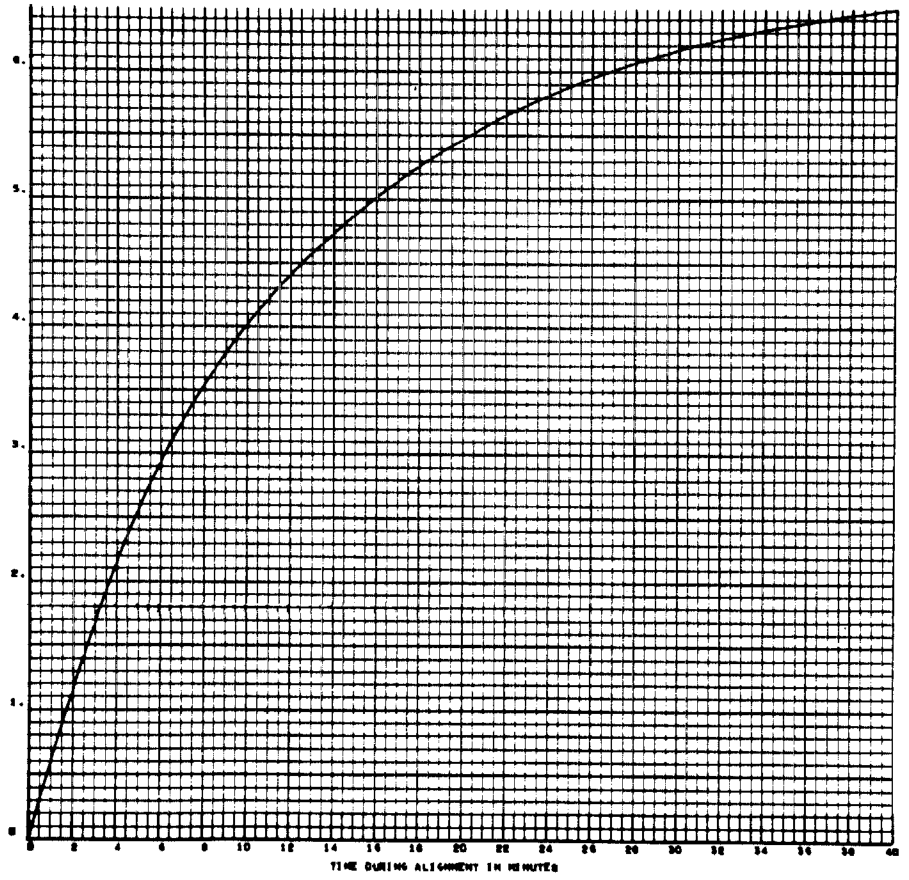

AZIMUTH MISALIGNMENT IN ARCSECONDS - ORBITAL GYROCOMPASS, CASE 10, RUN 2
ERROR DUE TO Z GYRO DRIFT - .01 DEGREES/HOUR

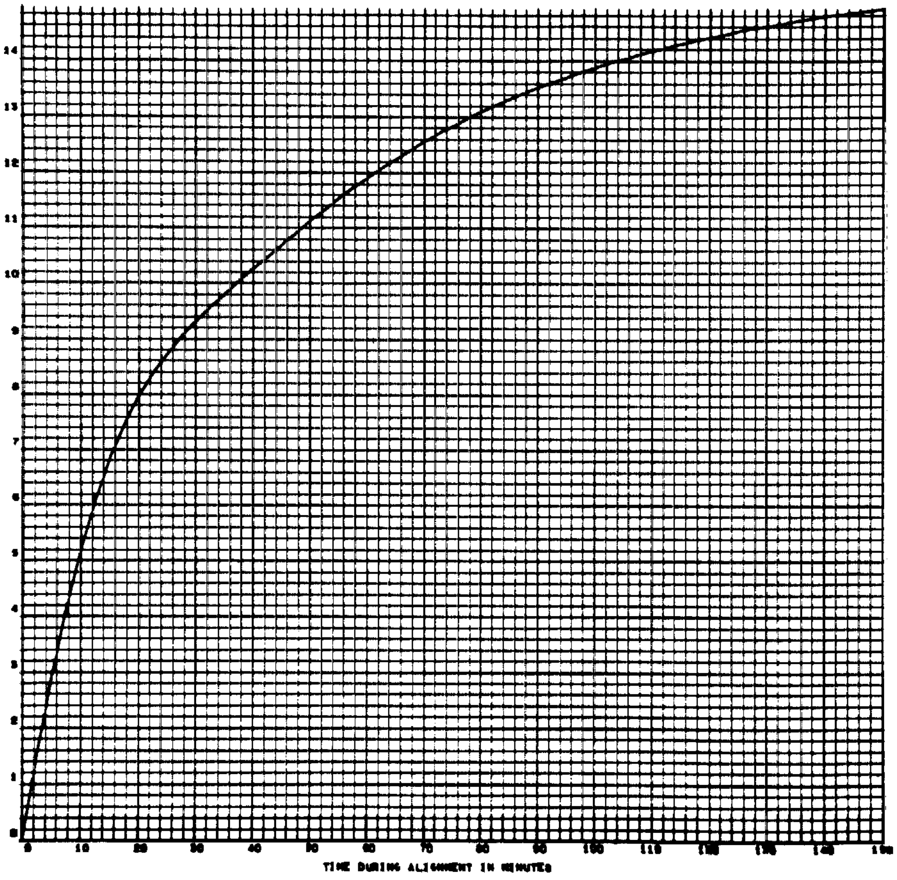

B119

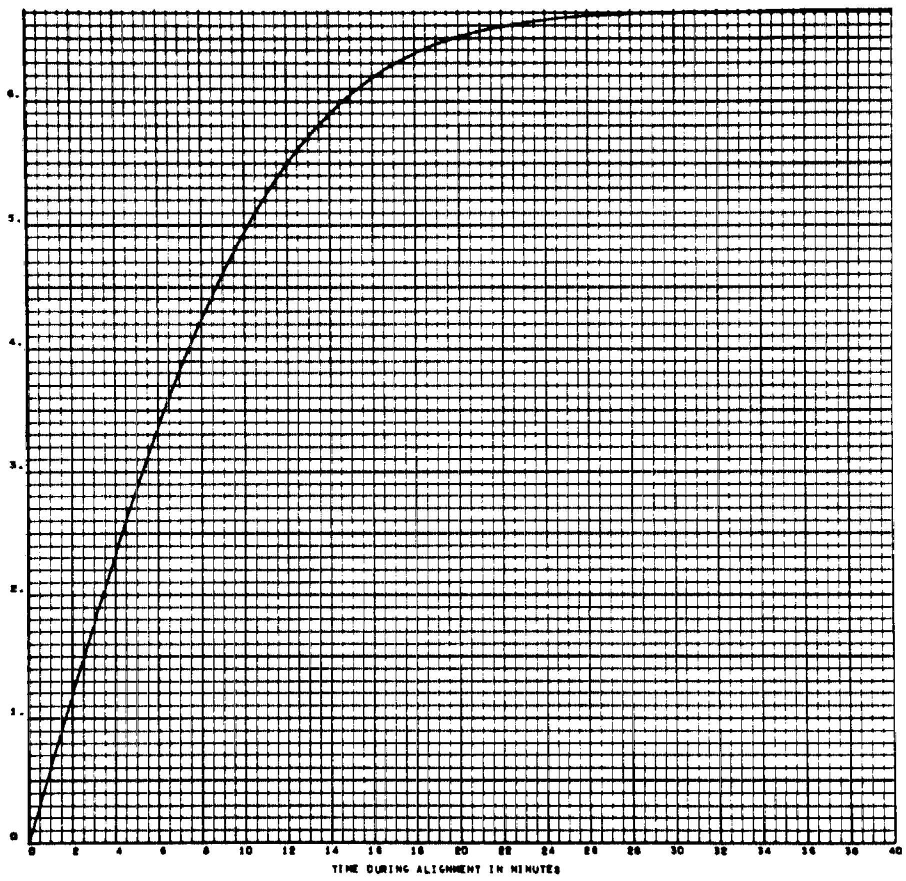

AZIMUTH MISALIGNMENT IN ARCSECONDS - ORBITAL GYROCOMPASS, CASE 14, RUN 1
ERROR DUE TO Z GYRO DRIFT - .01 DEGREES/HOUR

B120

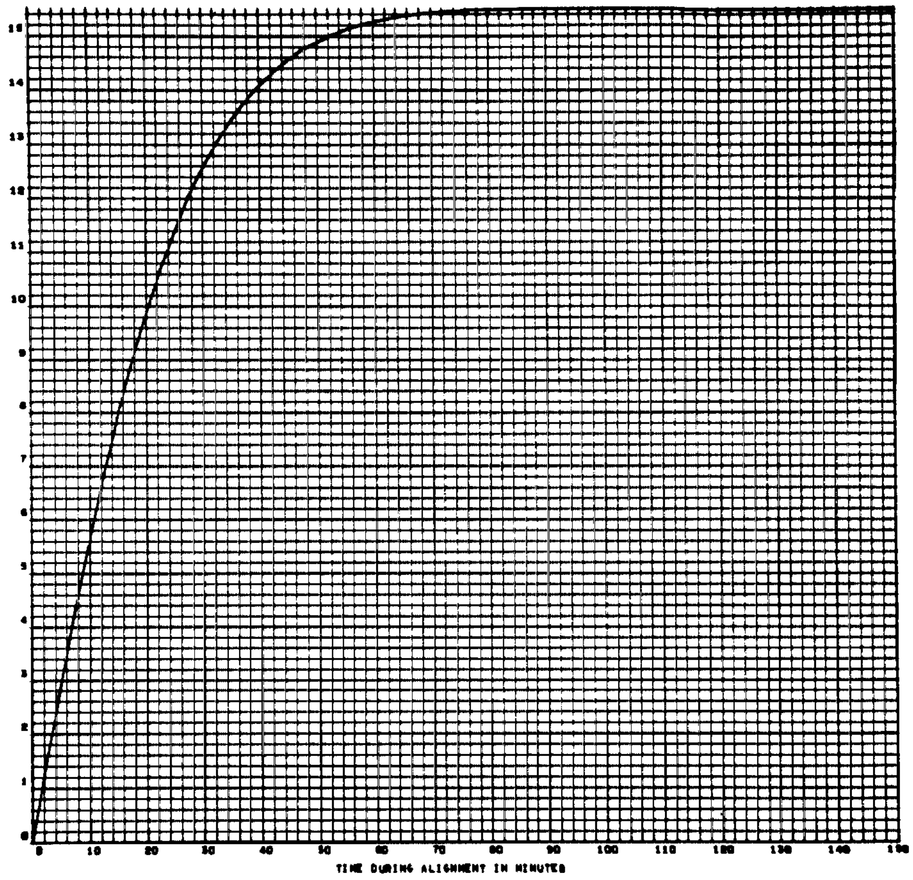

AZIMUTH MISALIGNMENT IN ARCSECONDS - ORBITAL GYROCOMPASS, CASE 14, RUN 2
ERROR DUE TO Z GYRO DRIFT - .01 DEGREES/HOUR

B121

LEVEL TILT IN ARCSECONDS - ORBITAL GYROCOMPASSING, CASE 4, RUN 1
Y TILT DUE TO INITIAL Y TILT - 10 DEGREES

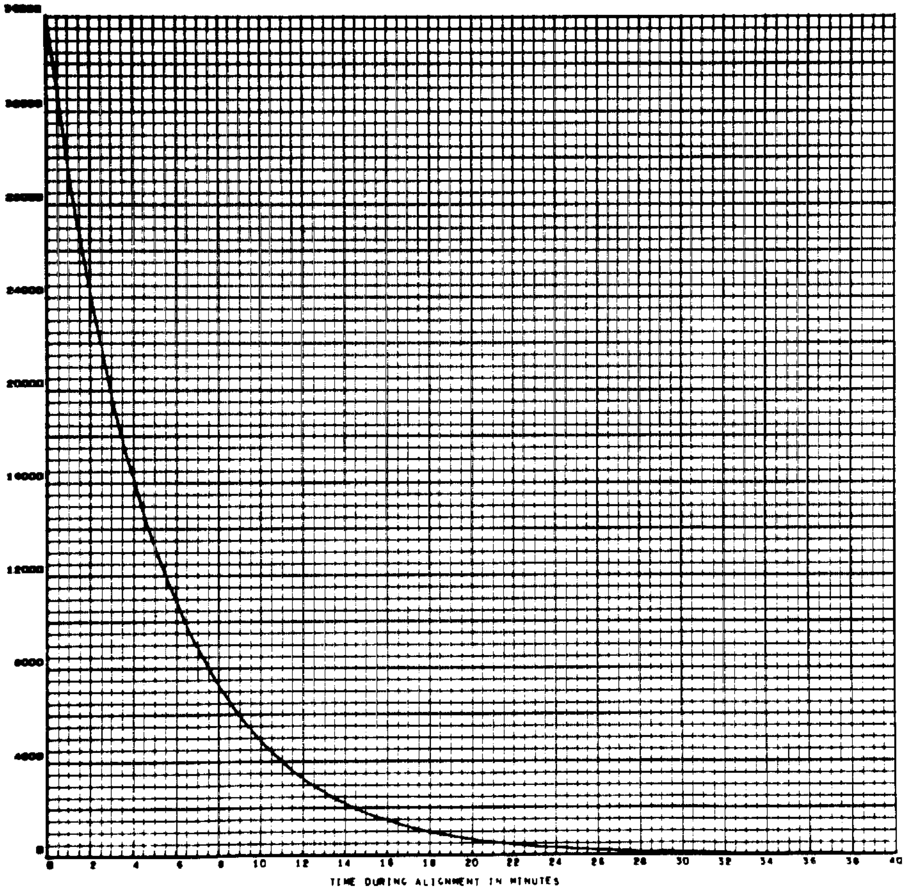

B122

LEVEL TILT IN ARCSECONDS - ORBITAL GYROCOMPASSING, CASE 4, RUN 2
Y TILT DUE TO INITIAL Y TILT - 10 DEGREES

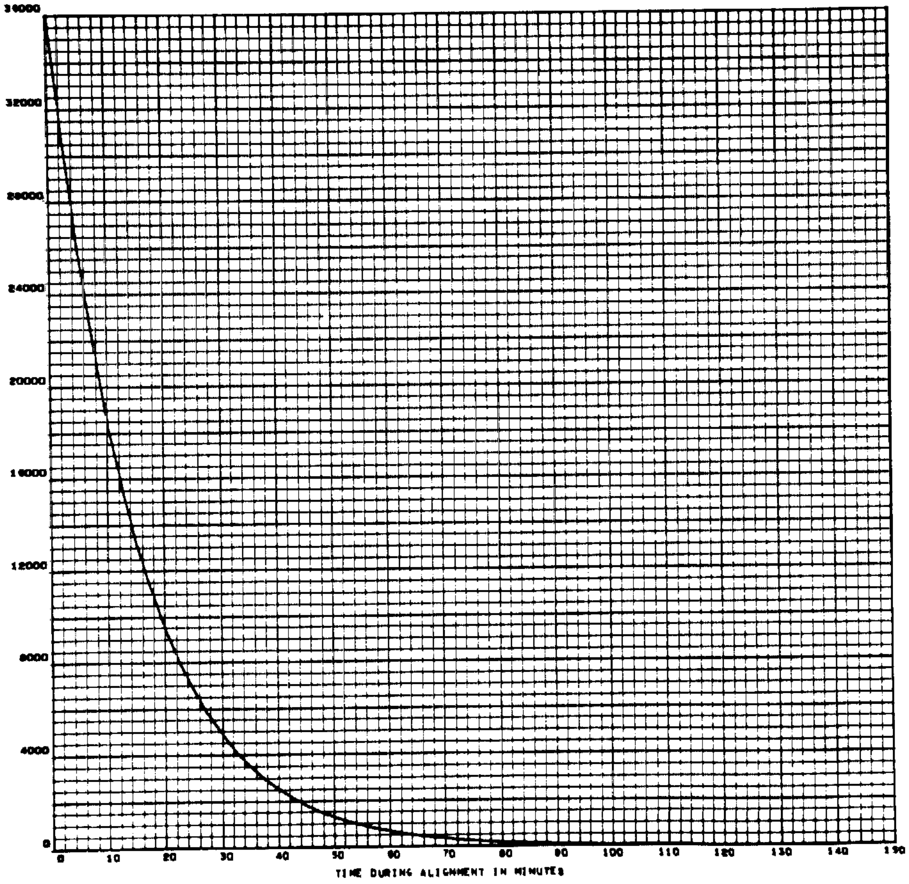

B/23

LEVEL TILT IN ARCSECONDS - ORBITAL GYROCOMPASSING, CASE 10, RUN 1
Y TILT DUE TO INITIAL Y TILT - 10 DEGREES

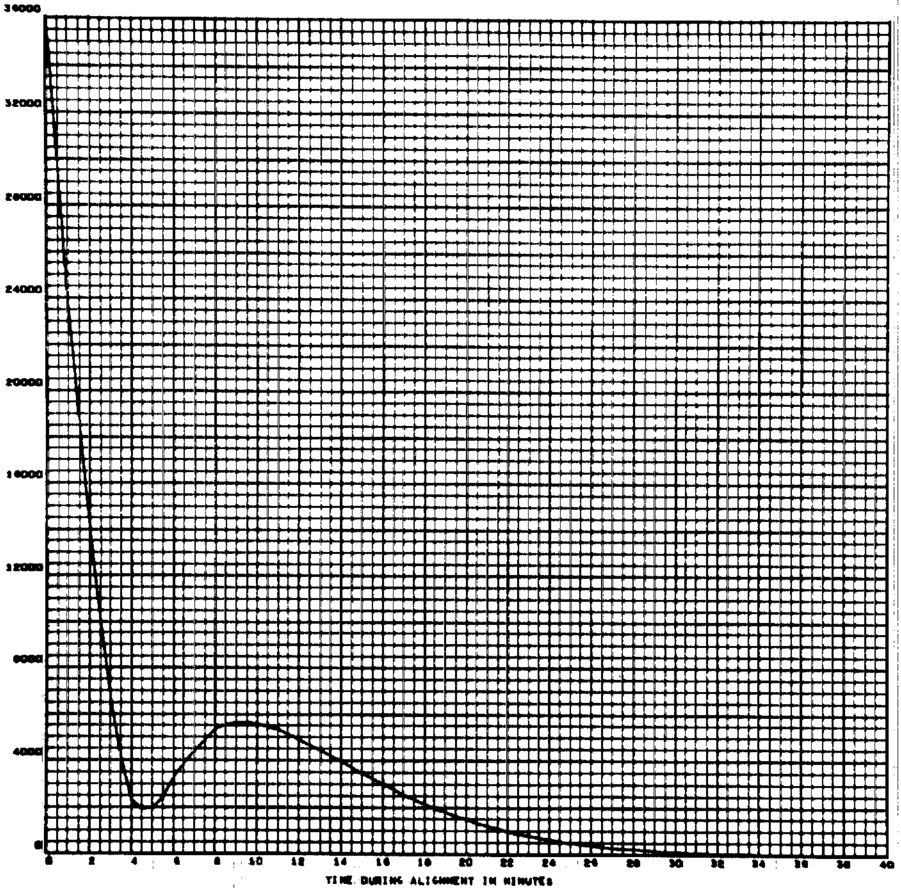

B/24

LEVEL TILT IN ARCSECONDS - ORBITAL GYROCOMPASSING, CASE 10, RUN 2
Y TILT DUE TO INITIAL Y TILT - 10 DEGREES

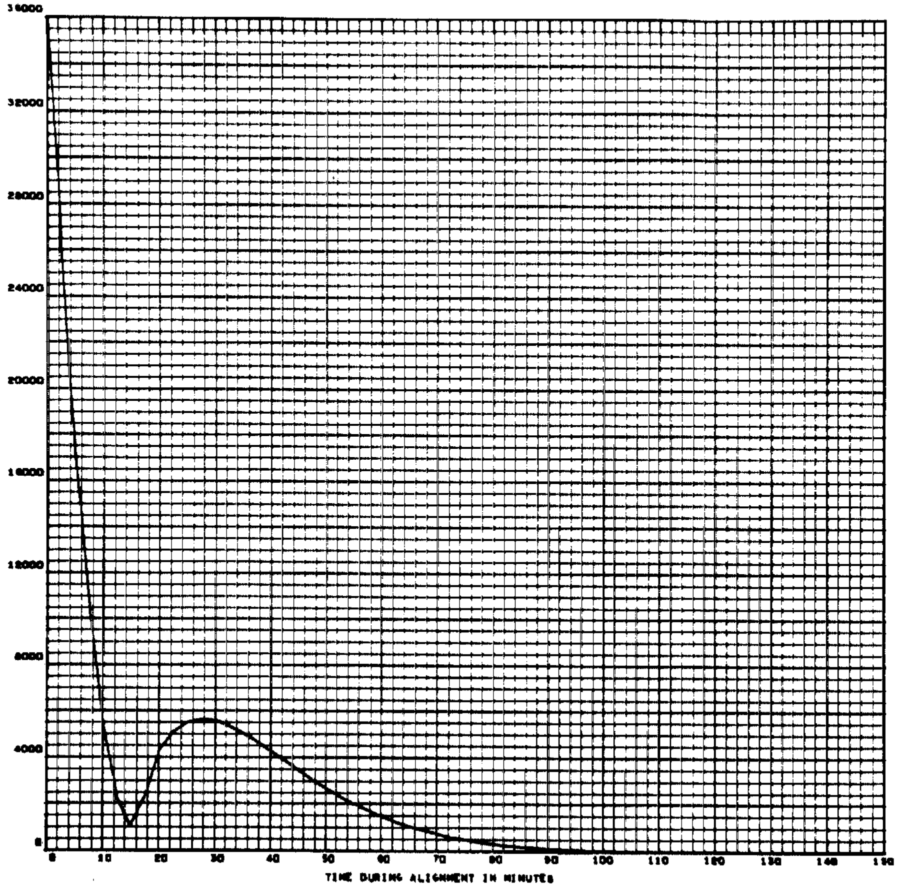

B/25

LEVEL TILT IN ARCSECONDS - ORBITAL GYROCOMPASSING, CASE 14, RUN 1
Y TILT DUE TO INITIAL Y TILT - 10 DEGREES

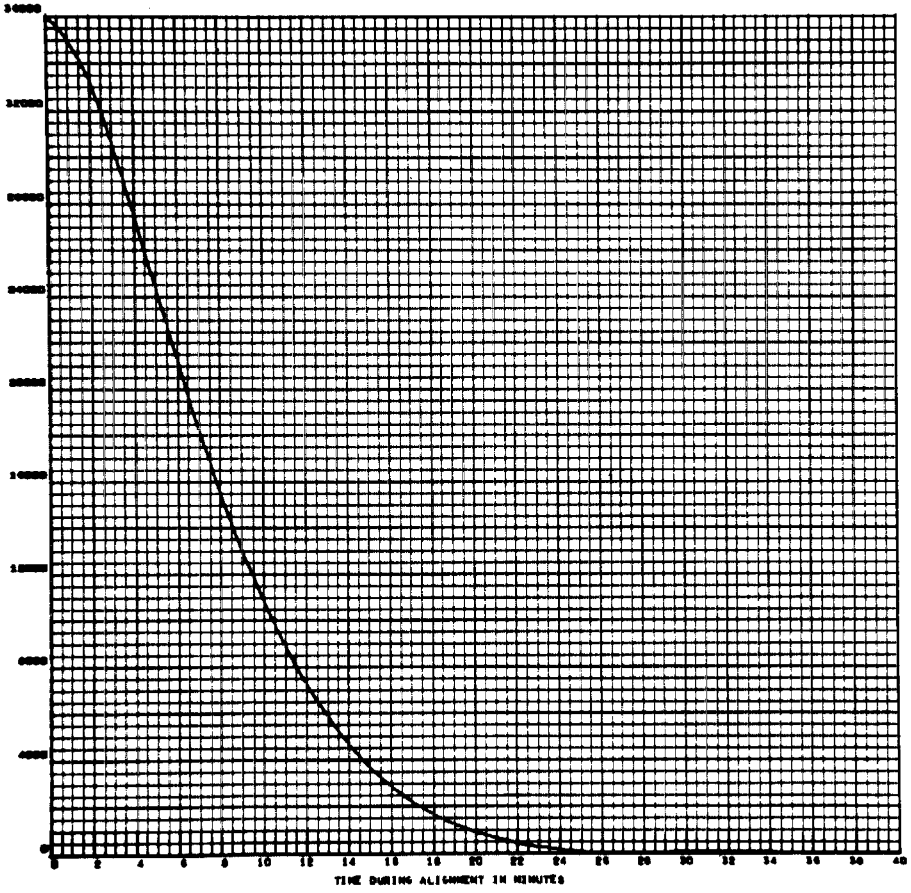

B/26

LEVEL TILT IN ARCSECONDS - ORBITAL GYROCOMPASSING, CASE 14, RUN 2
Y TILT DUE TO INITIAL Y TILT - 10 DEGREES

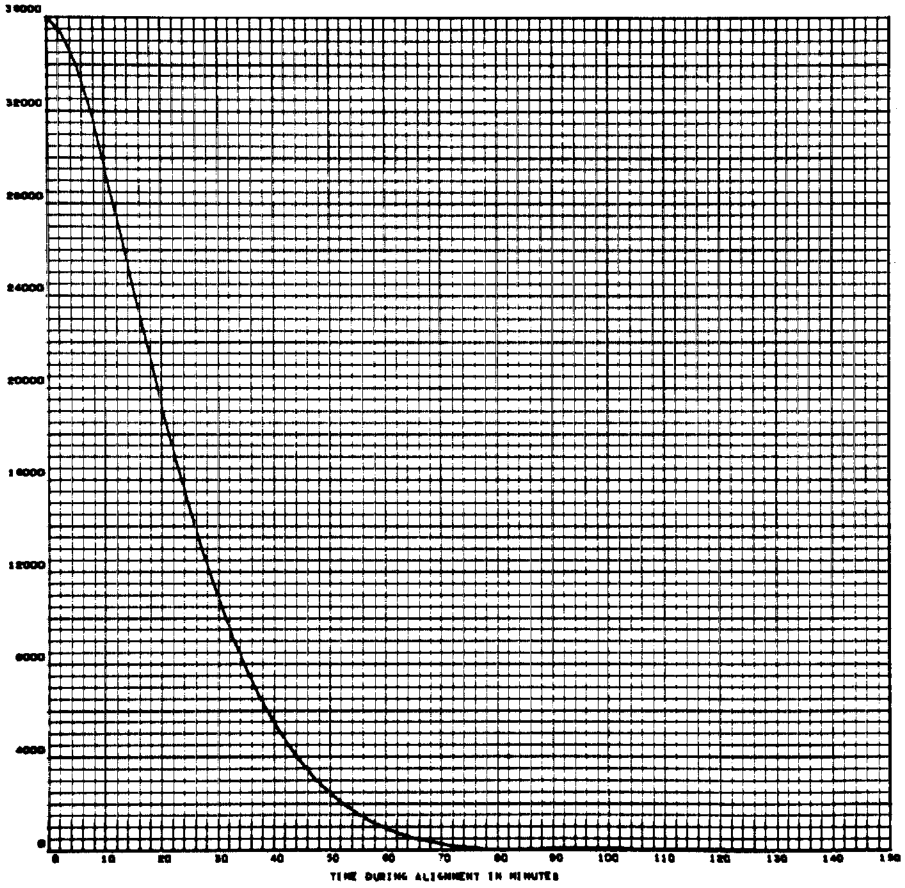

B/27

LEVEL TILT IN ARCSECONDS - ORBITAL GYROCOMPASSING, CASE 4, RUN 1
Y TILT DUE TO Y GYRO DRIFT - .01 DEGREES/HOUR

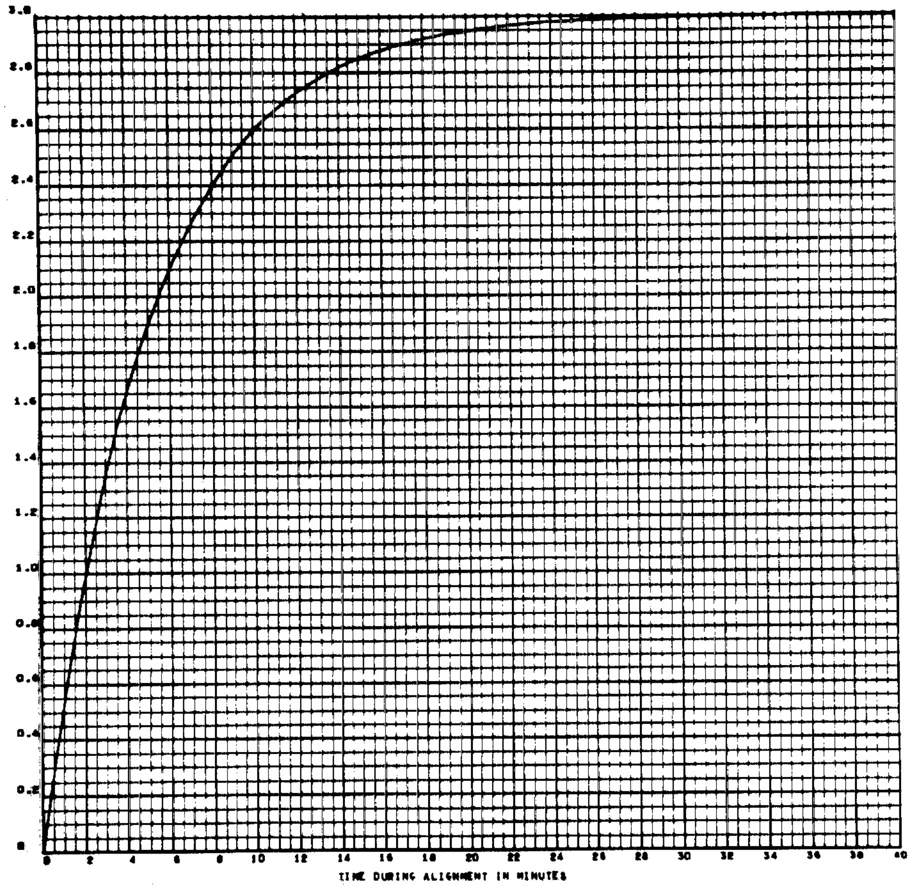

B/28

LEVEL TILT IN ARCSECONDS - ORBITAL GYROCOMPASSING, CASE 4, RUN 2
Y TILT DUE TO Y GYRO DRIFT - .01 DEGREES/HOUR

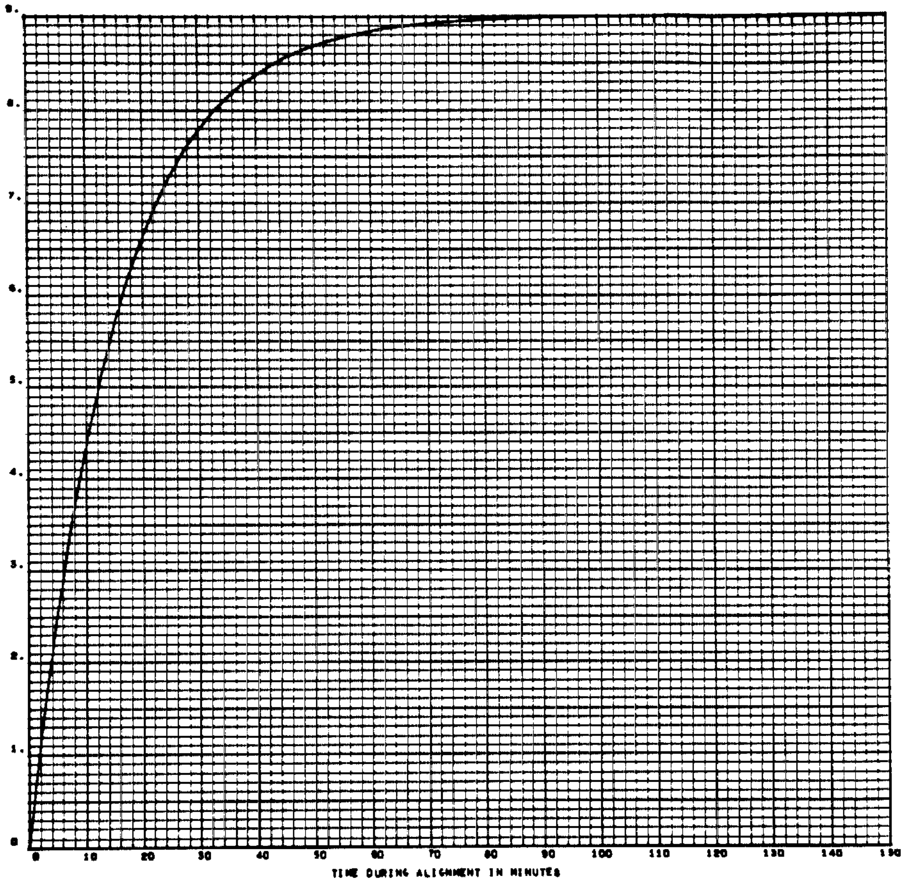

B/29

LEVEL TILT IN ARCSECONDS - ORBITAL GYROCOMPASSING, CASE 10, RUN 1
Y TILT DUE TO Y GYRO DRIFT - .01 DEGREES/HOUR

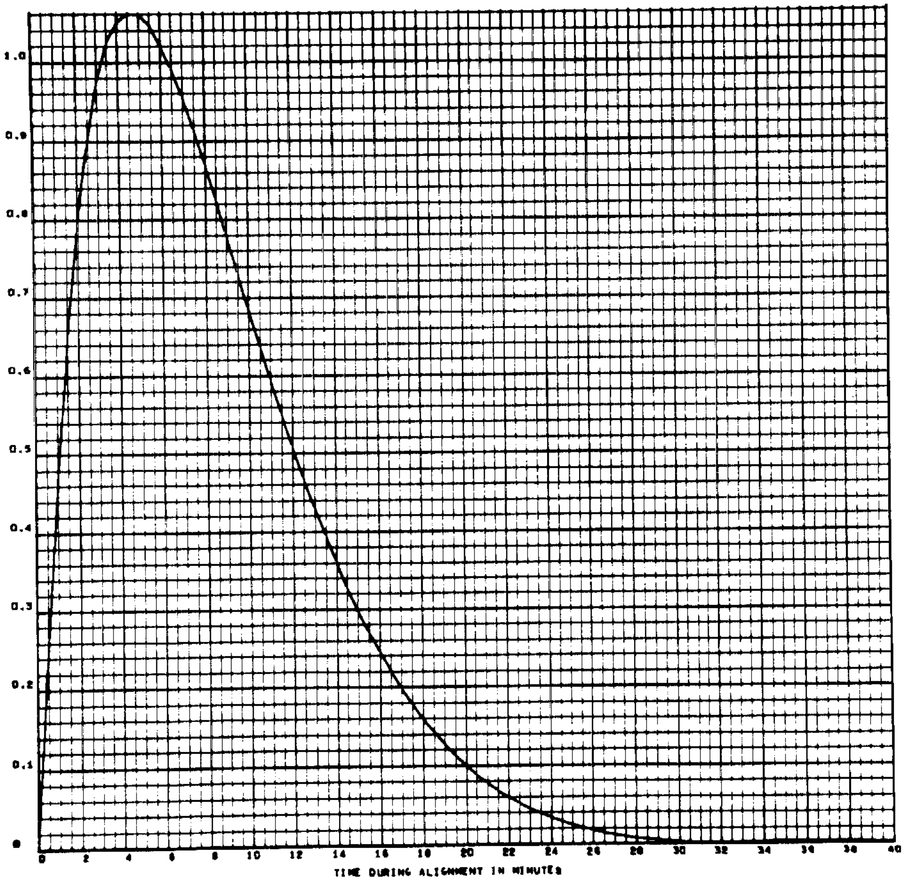

B/30

LEVEL TILT IN ARCSECONDS - ORBITAL GYROCOMPASSING, CASE 10, RUN 2
Y TILT DUE TO Y GYRO DRIFT - .01 DEGREES/HOUR

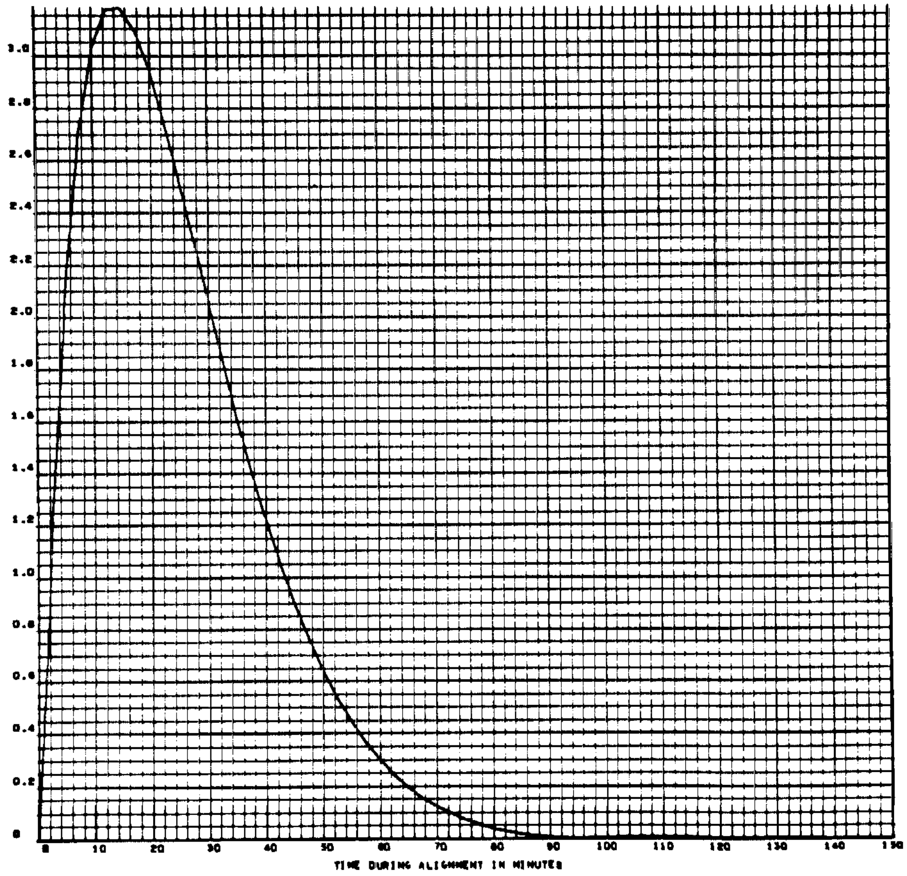

B131

LEVEL TILT IN ARCSECONDS - ORBITAL GYROCOMPASSING, CASE 14, RUN 1
Y TILT DUE TO Y GYRO DRIFT - .01 DEGREES/HOUR

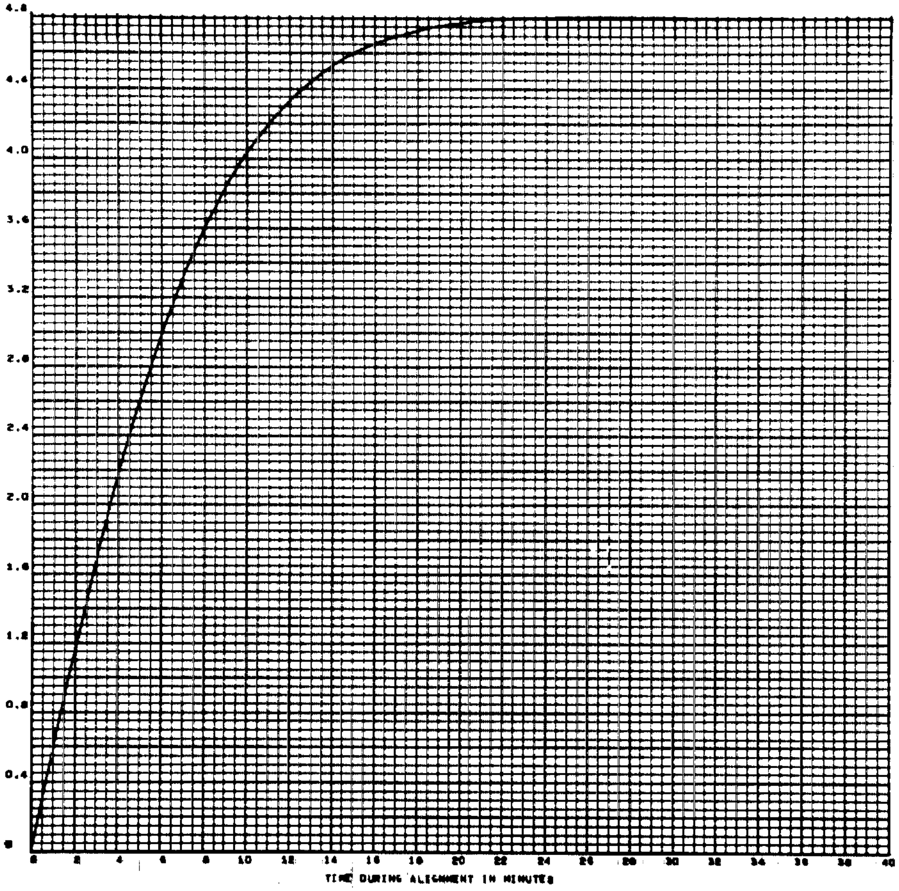

B132

LEVEL TILT IN ARCSECONDS - ORBITAL GYROCOMPASSING, CASE 14, RUN 2
Y TILT DUE TO Y GYRO DRIFT - .01 DEGREES/HOUR

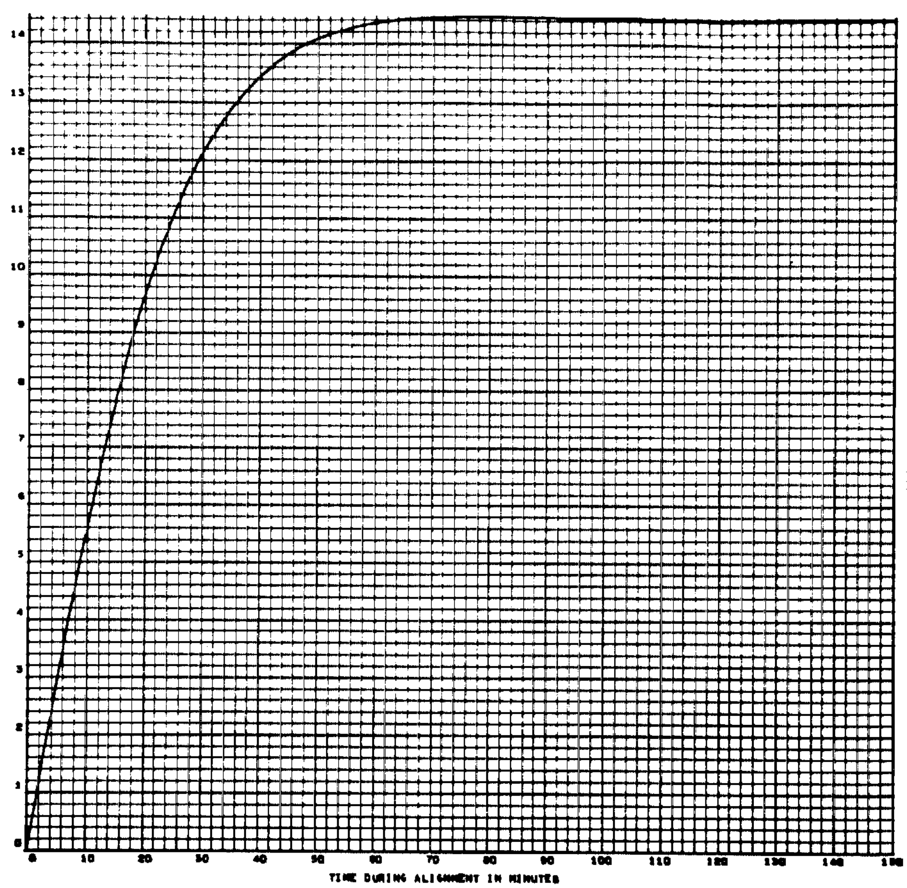

B133

LEVEL TILT IN ARCSECONDS - ORBITAL GYROCOMPASSING, CASE 4, RUN 1
Y TILT DUE TO Y GYRO NOISE - .01 DEGREES/HOUR, C.T. = 1 HOUR

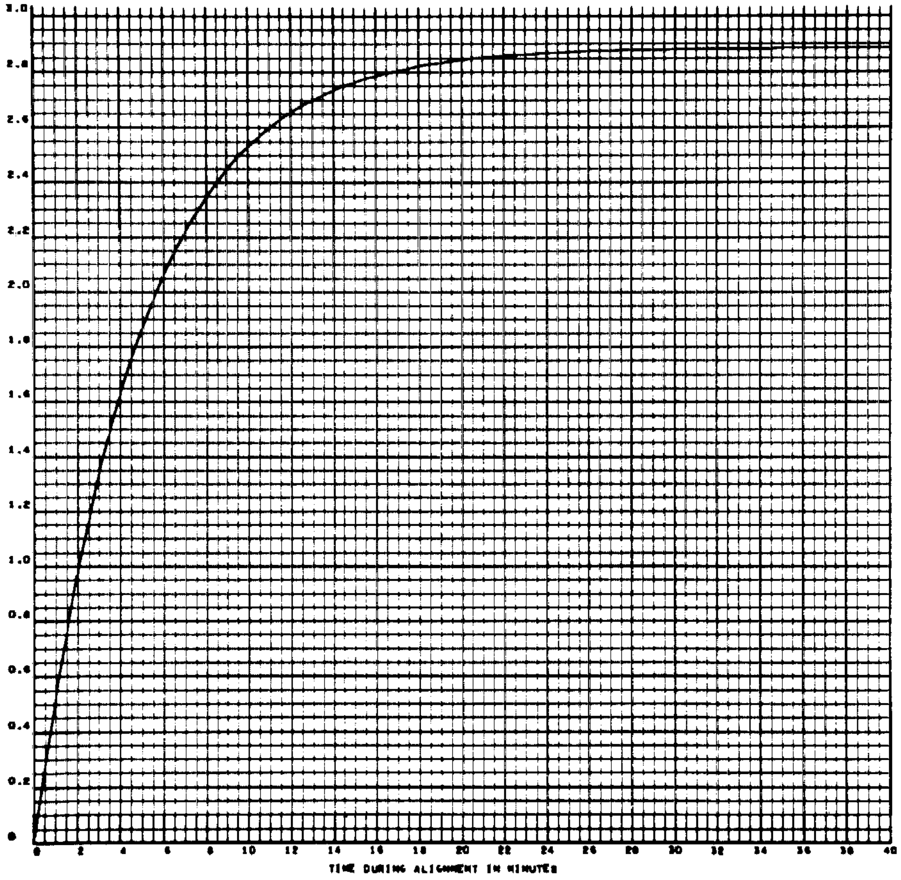

B134

LEVEL TILT IN ARCSECONDS - ORBITAL GYROCOMPASSING, CASE 4, RUN 2
Y TILT DUE TO Y GYRO NOISE - .01 DEGREES/HOUR, C.T. = 1 HOUR

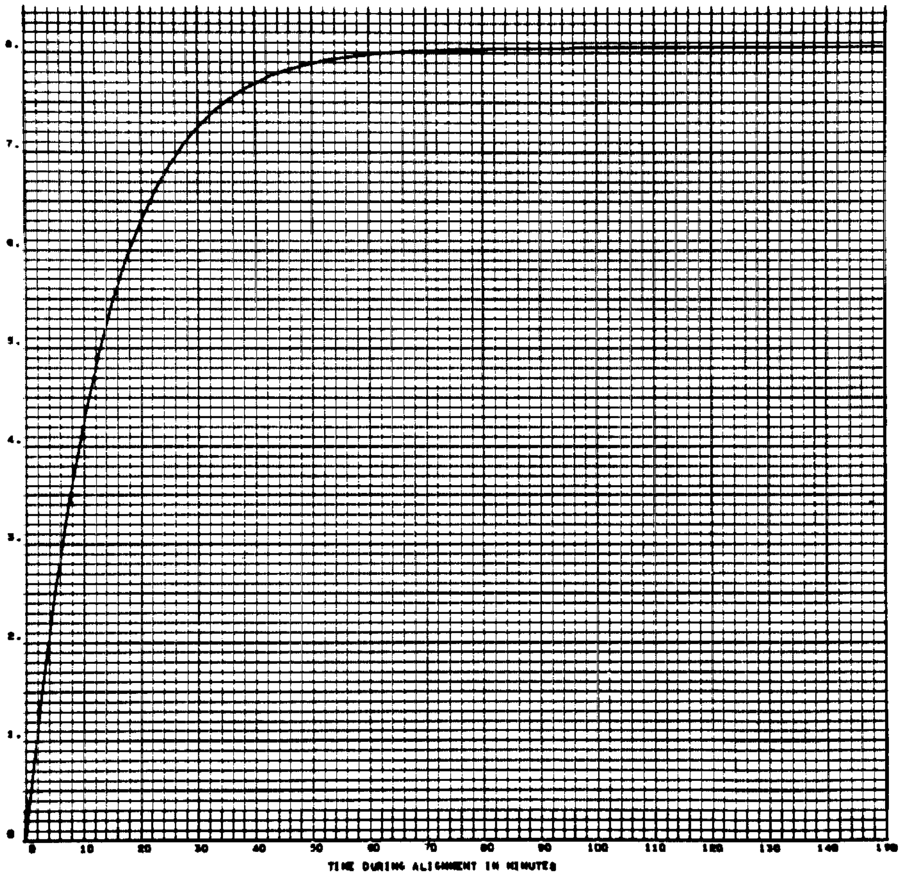

B135

LEVEL TILT IN ARCSECONDS - ORBITAL GYROCOMPASSING, CASE 10, RUN 1
Y TILT DUE TO Y GYRO NOISE - .01 DEGREES/HOUR, C.T. = 1 HOUR

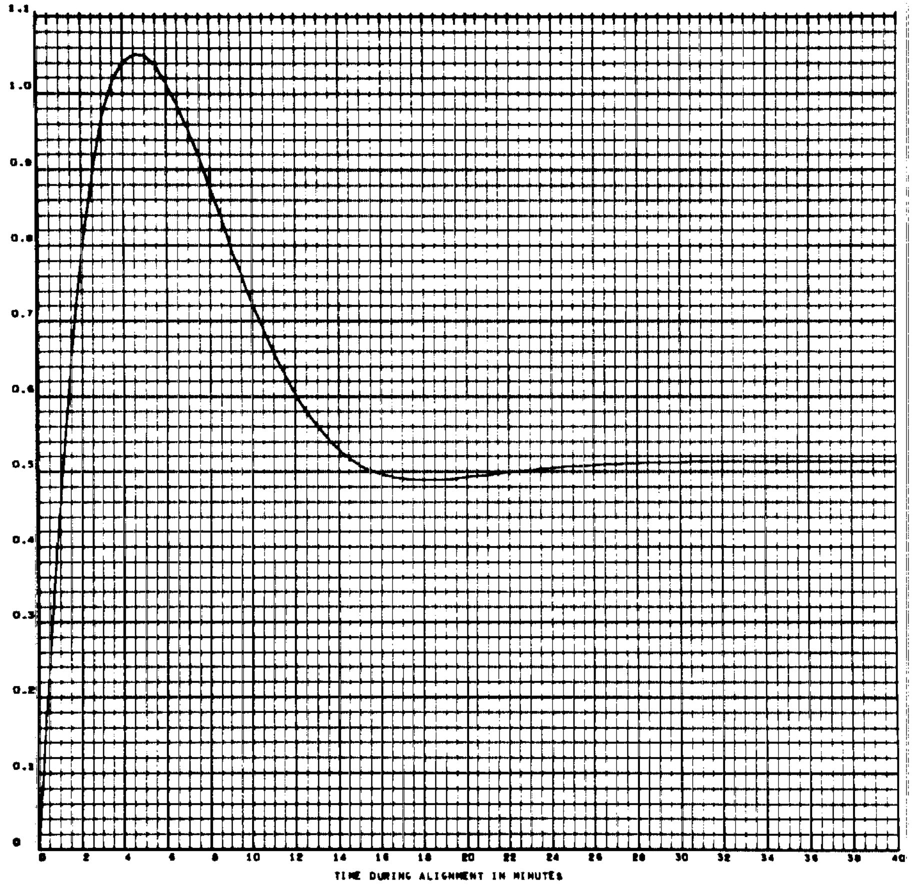

B136

LEVEL TILT IN ARCSECONDS - ORBITAL GYROCOMPASSING, CASE 10, RUN 2
Y TILT DUE TO Y GYRO NOISE - .01 DEGREES/HOUR, C.T. = 1 HOUR

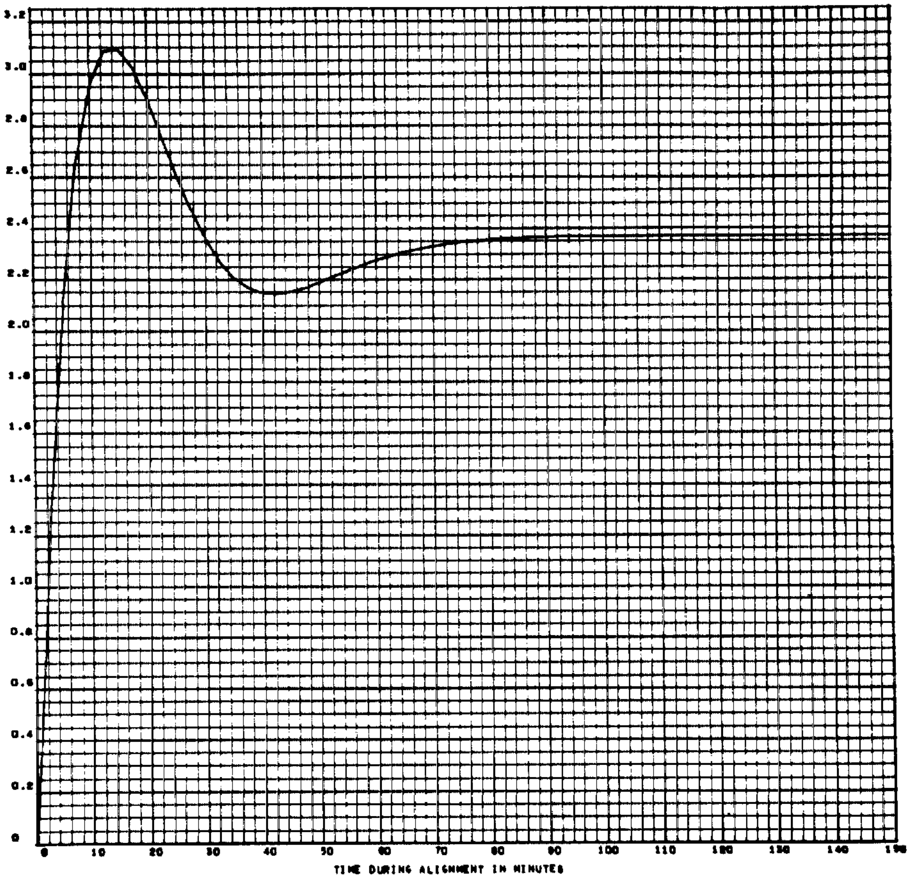

B137

LEVEL TILT IN ARCSECONDS - ORBITAL GYROCOMPASSING, CASE 14, RUN 1
Y TILT DUE TO Y GYRO NOISE - .01 DEGREES/HOUR, C.T. = 1 HOUR

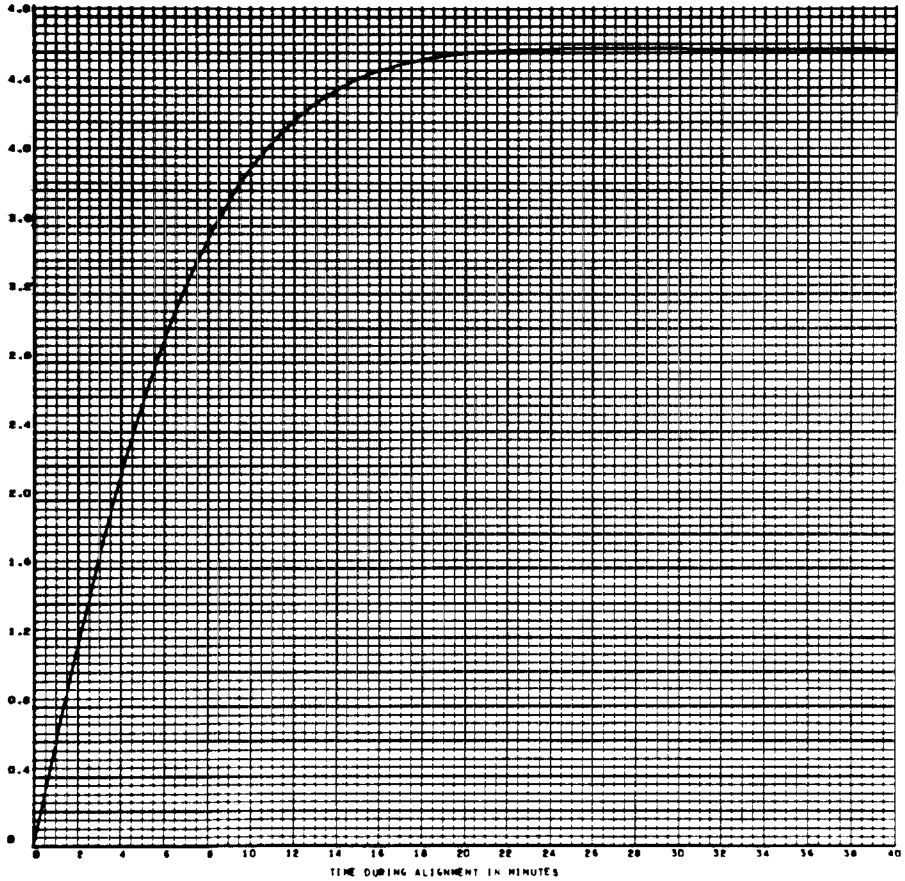

B138

LEVEL TILT IN ARCSECONDS - ORBITAL GYROCOMPASSING, CASE 14, RUN 2
Y TILT DUE TO Y GYRO NOISE - .01 DEGREES/HOUR, C.T. = 1 HOUR

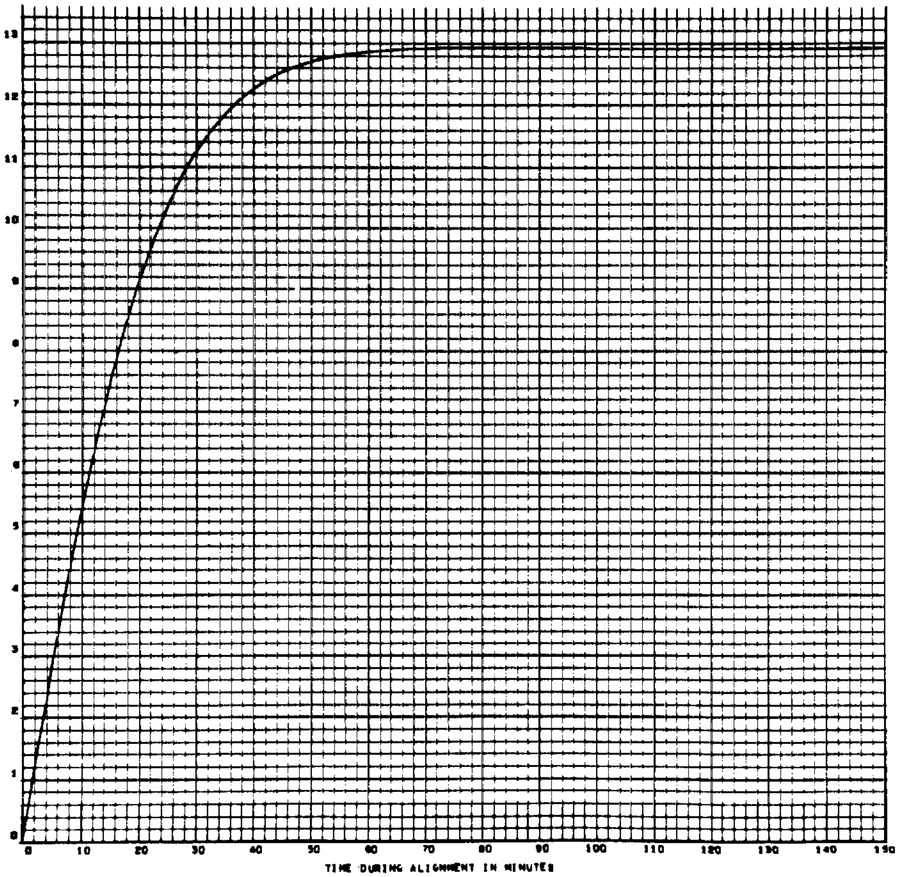

B139

LEVEL TILT IN ARCSECONDS - ORBITAL GYROCOMPASSING, CASE 4, RUN 1
Y TILT DUE TO HORIZON SENSOR MISALIGNMENT - 1 ARCSECOND

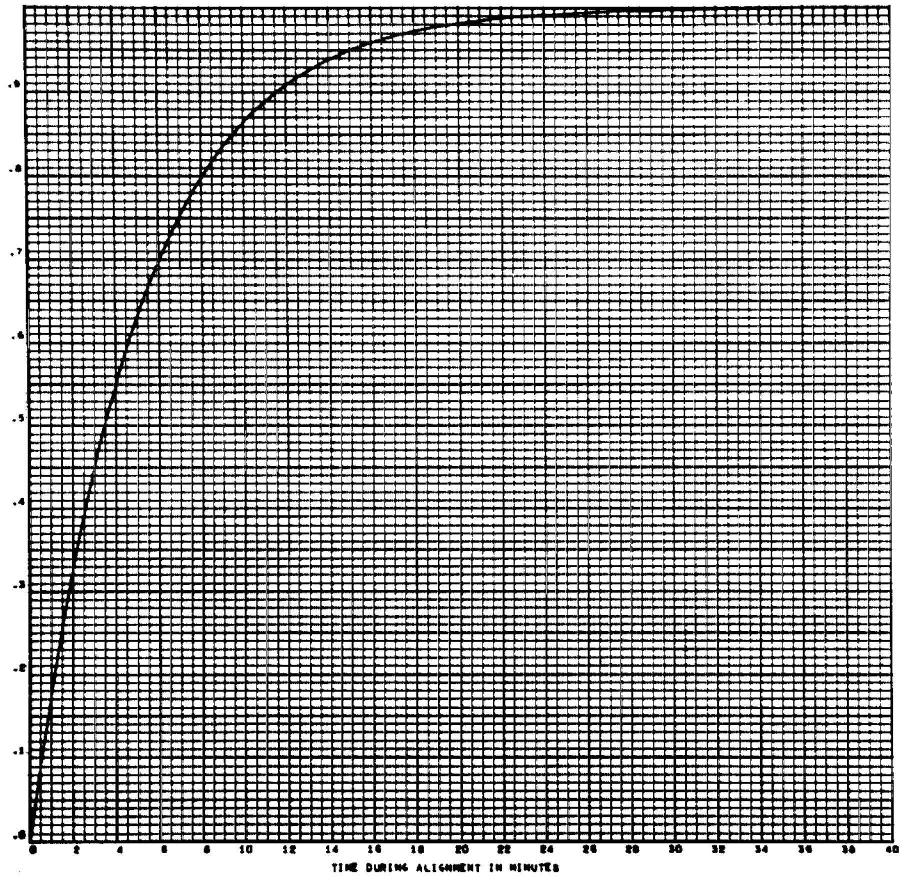

B140

LEVEL TILT IN ARCSECONDS - ORBITAL GYROCOMPASSING, CASE 4, RUN 2
Y TILT DUE TO HORIZON SENSOR MISALIGNMENT - 1 ARCSECOND

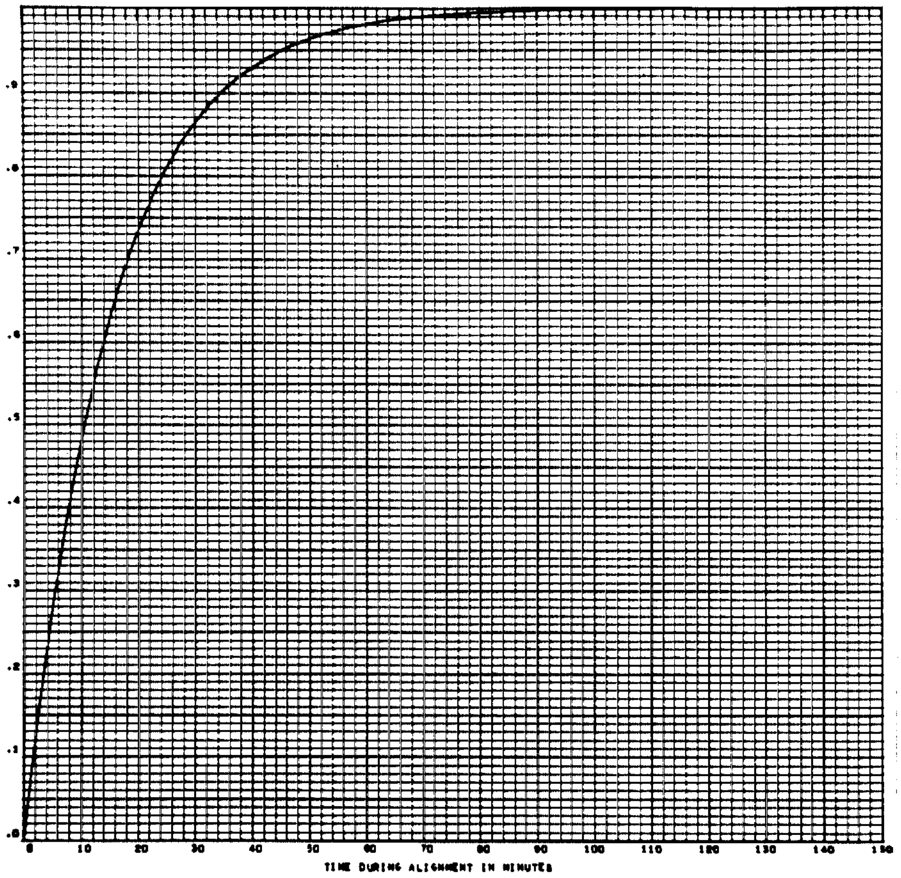

B/41

LEVEL TILT IN ARCSECONDS - ORBITAL GYROCOMPASSING, CASE 10, RUN 1
Y TILT DUE TO HORIZON SENSOR MISALIGNMENT - 1 ARCSECOND

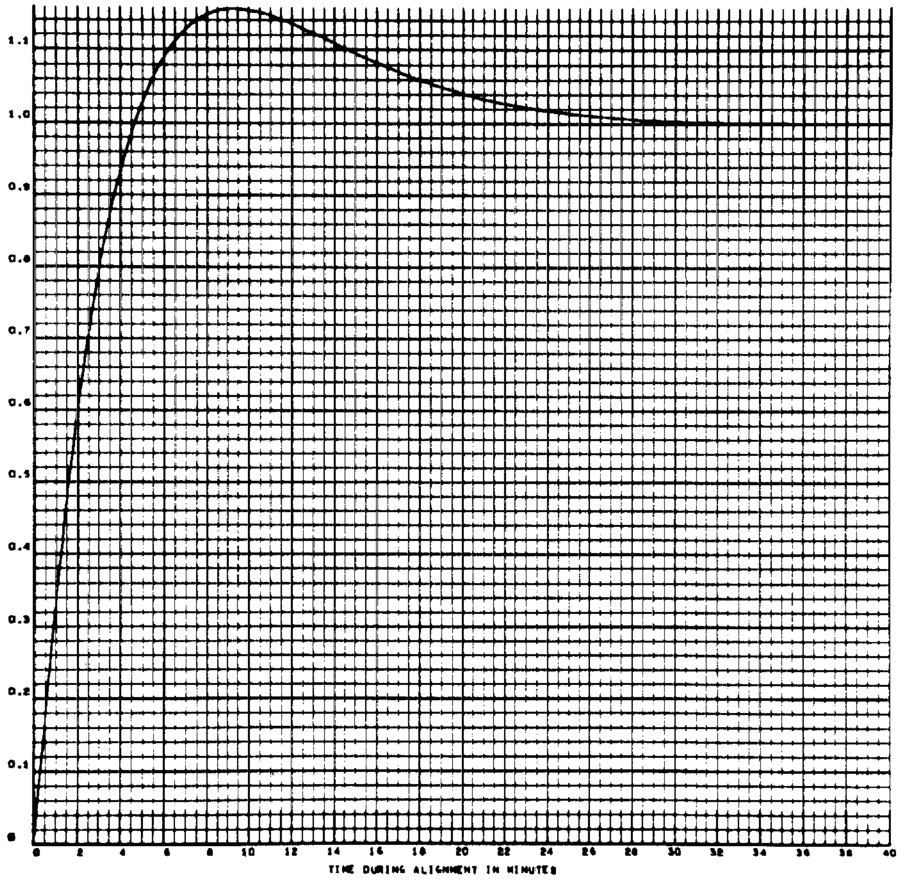

B/42

LEVEL TILT IN ARCSECONDS - ORBITAL GYROCOMPASSING, CASE 10, RUN 2
Y TILT DUE TO HORIZON SENSOR MISALIGNMENT - 1 ARCSECOND

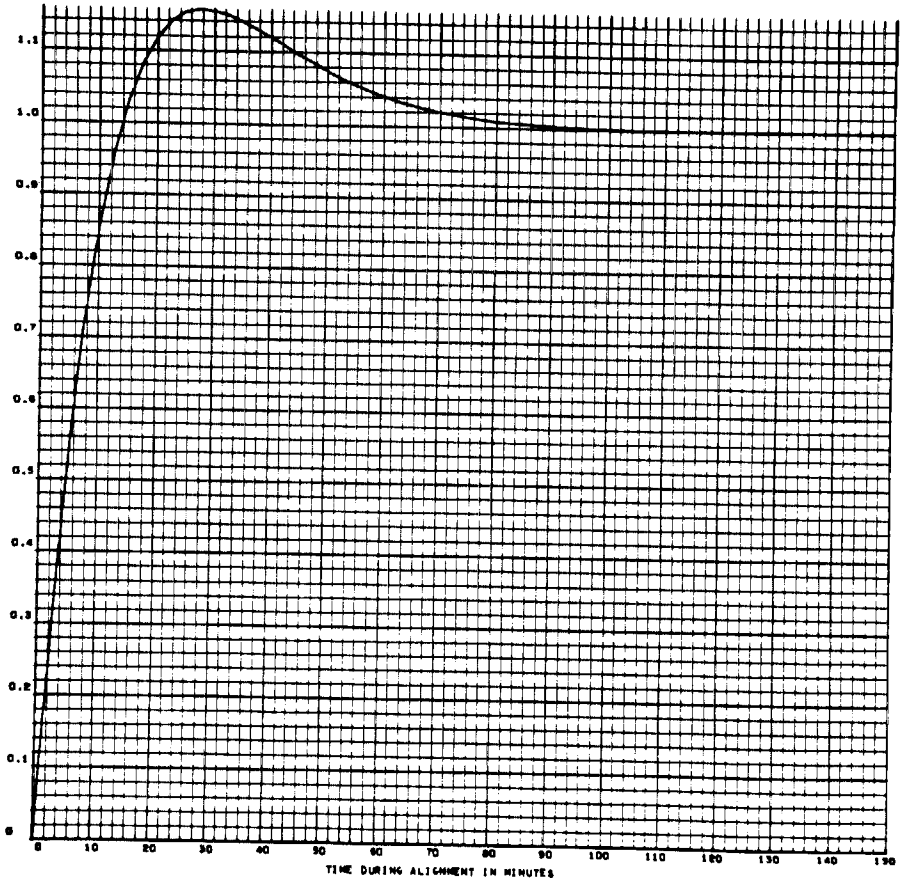

B/43

LEVEL TILT IN ARCSECONDS - ORBITAL GYROCOMPASSING, CASE 14, RUN 1
Y TILT DUE TO HORIZON SENSOR MISALIGNMENT - 1 ARCSECOND

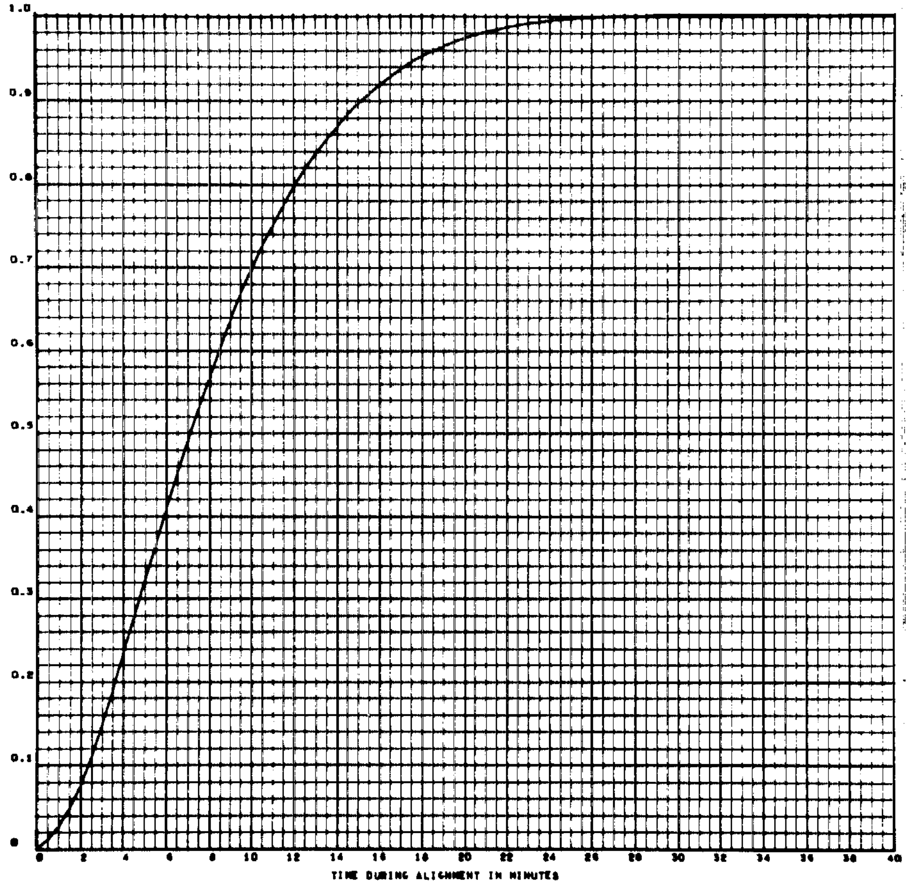

B/44

LEVEL TILT IN ARCSECONDS - ORBITAL GYROCOMPASSING, CASE 14, RUN 2
Y TILT DUE TO HORIZON SENSOR MISALIGNMENT - 1 ARCSECOND

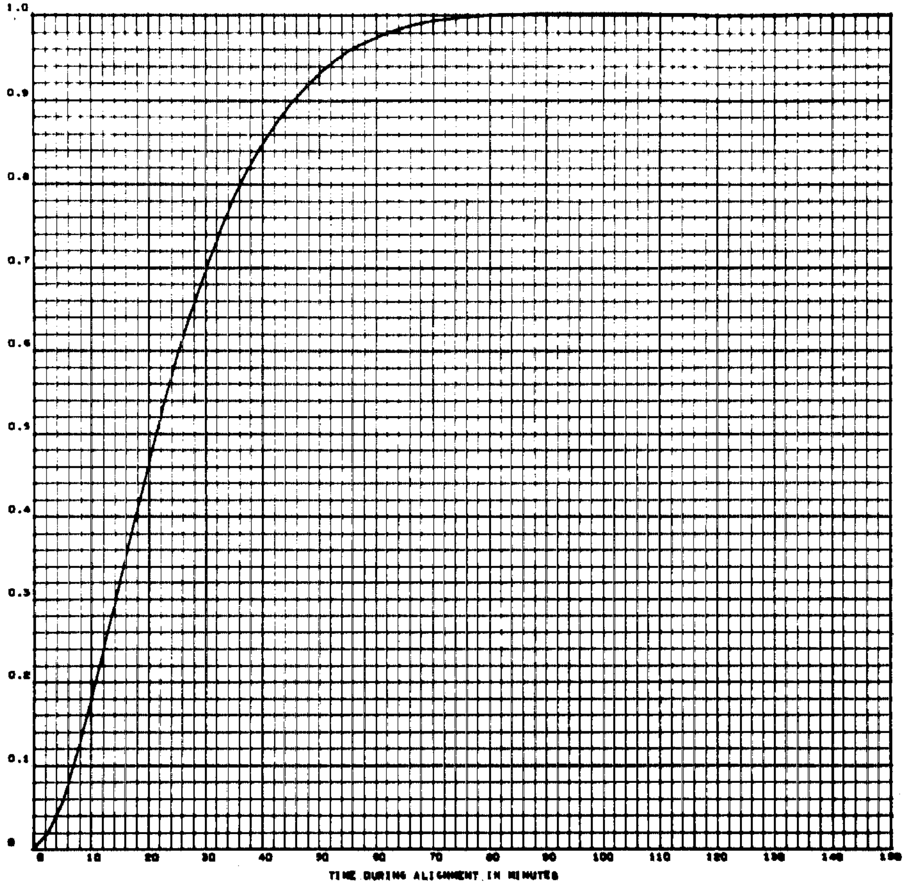

B145

LEVEL TILT IN ARCSECONDS - ORBITAL GYROCOMPASSING, CASE 4, RUN 1
y TILT DUE TO HORIZON SENSOR NOISE - 1 ARCSECOND, C.T. = 1 MINUTE

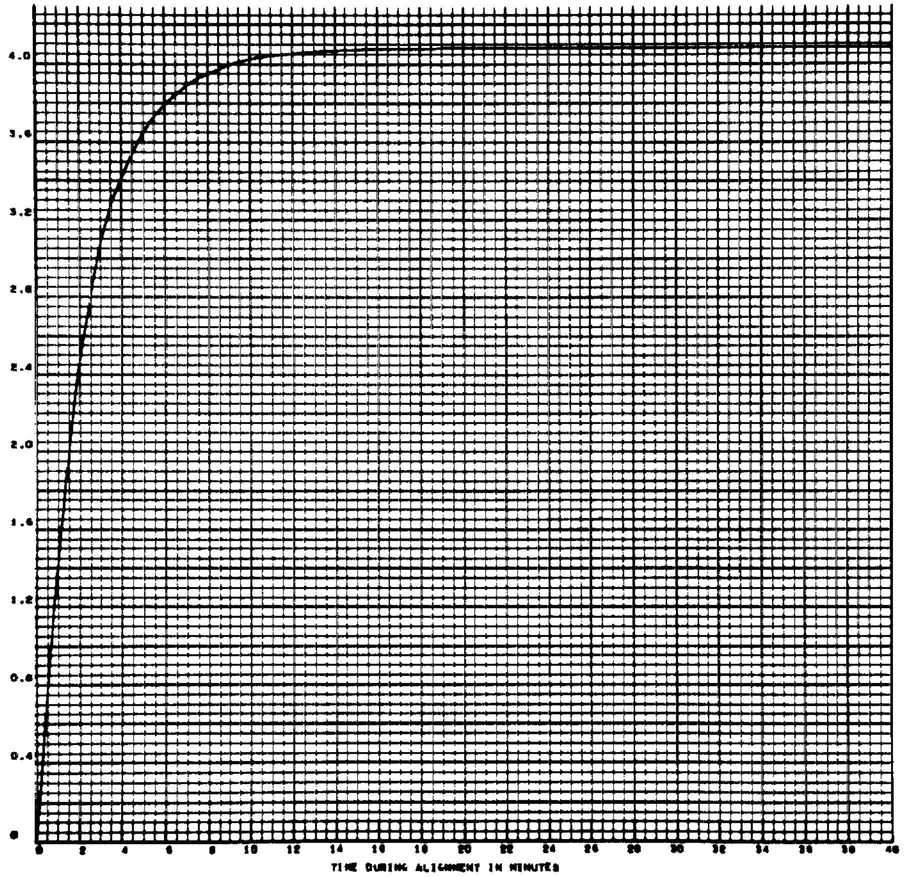

B146

LEVEL TILT IN ARCSECONDS - ORBITAL GYROCOMPASSING, CASE 4, RUN 2
y TILT DUE TO HORIZON SENSOR NOISE - 1 ARCSECOND, C.T. = 1 MINUTE

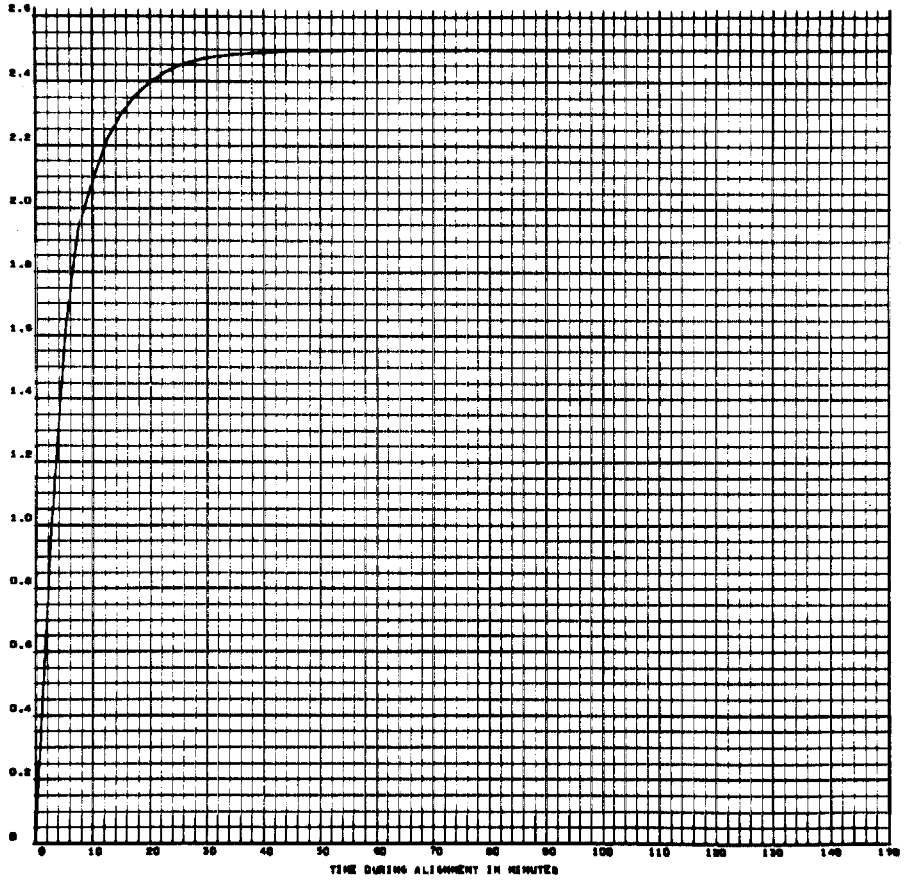

B147

LEVEL TILT IN ARCSECONDS - ORBITAL GYROCOMPASSING, CASE 10, RUN 1
Y TILT DUE TO HORIZON SENSOR NOISE - 1 ARCSECOND, C.T. = 1 MINUTE

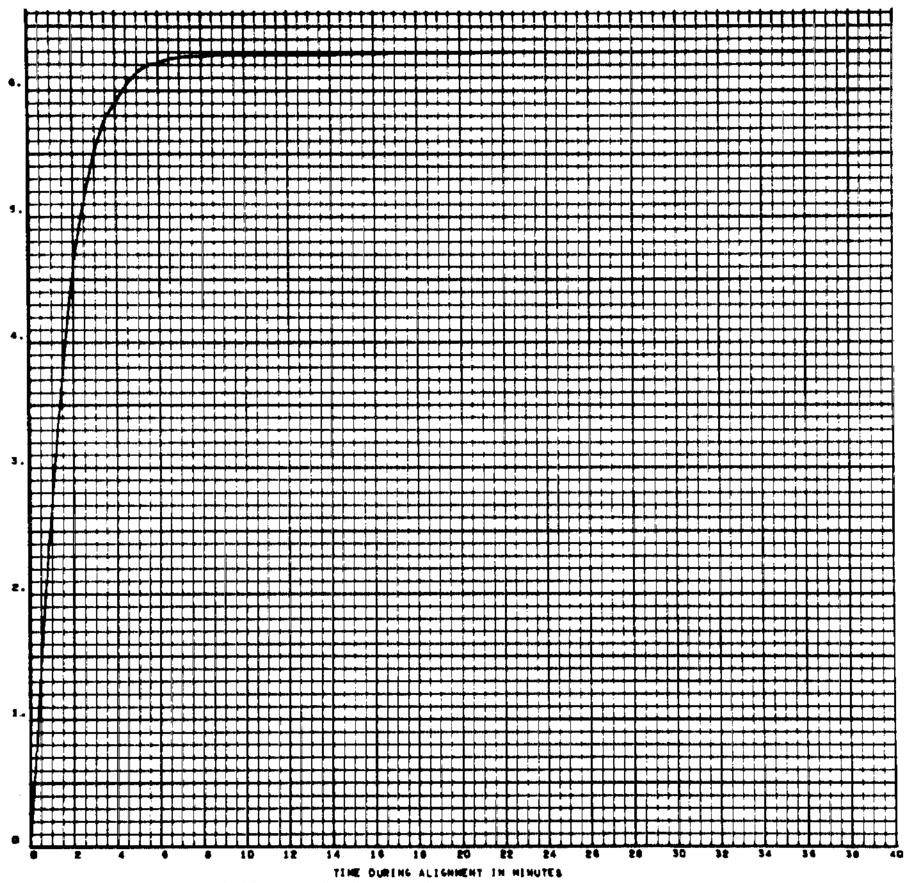

B148

LEVEL TILT IN ARCSECONDS - ORBITAL GYROCOMPASSING, CASE 10, RUN 2
Y TILT DUE TO HORIZON SENSOR NOISE - 1 ARCSECOND, C.T. = 1 MINUTE

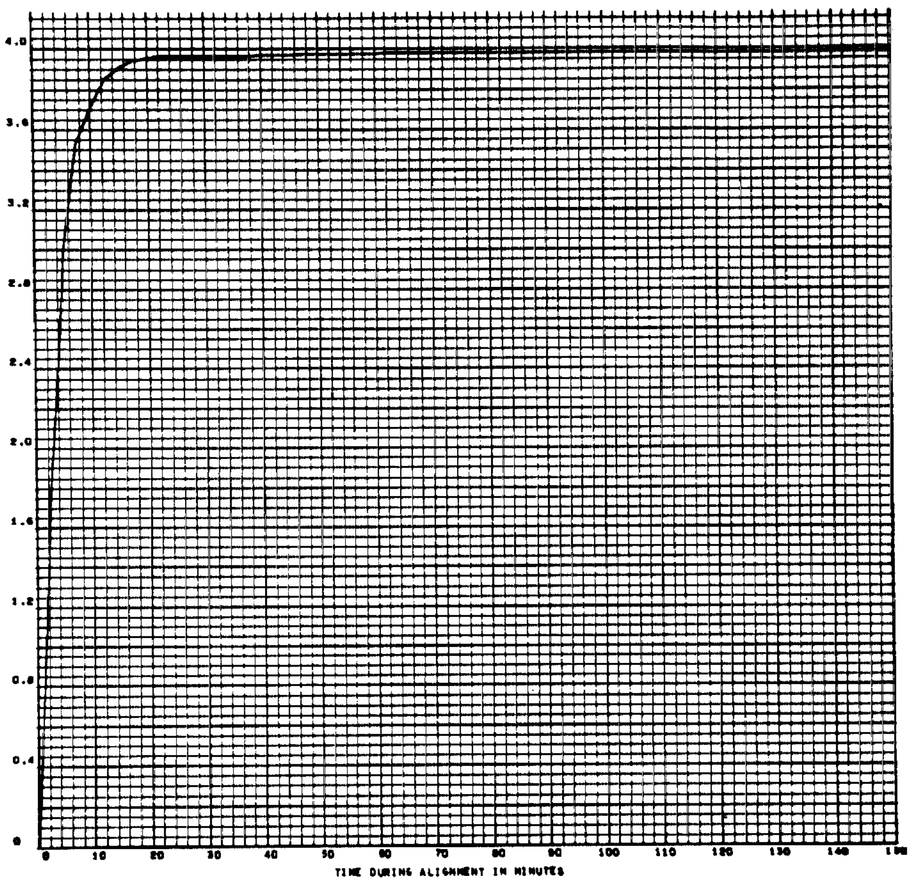

B149

LEVEL TILT IN ARCSECONDS - ORBITAL GYROCOMPASSING, CASE 14, RUN 1
Y TILT DUE TO HORIZON SENSOR NOISE - 1 ARCSECOND, C.T. = 1 MINUTE

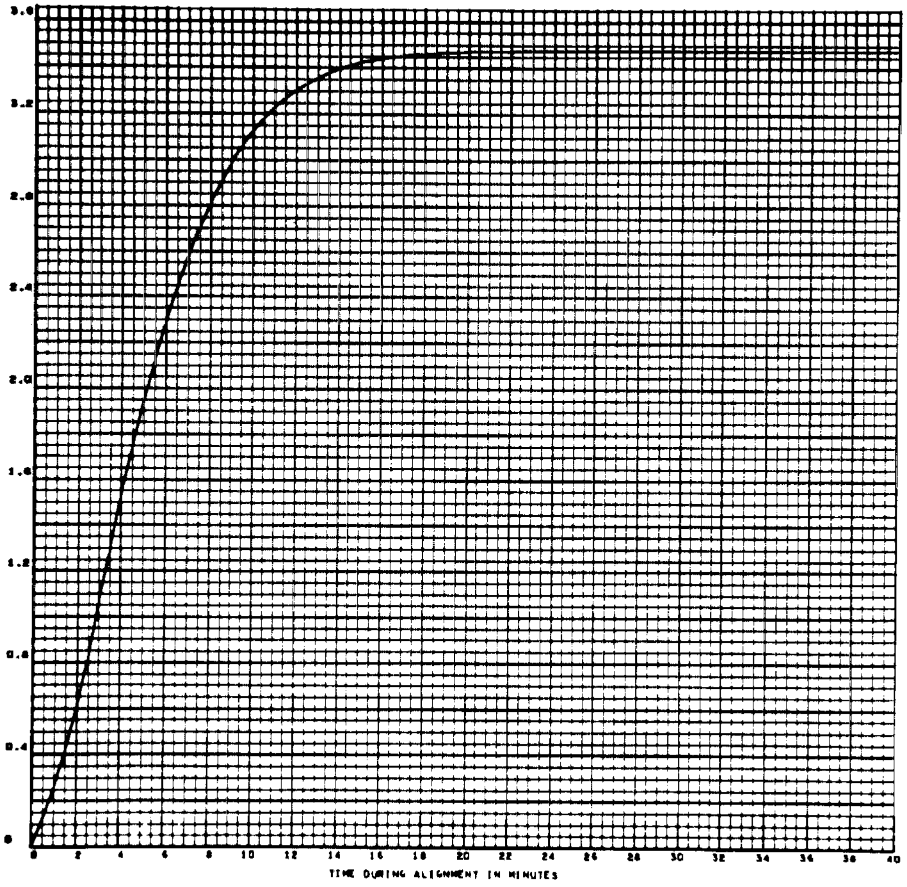

B150

LEVEL TILT IN ARCSECONDS - ORBITAL GYROCOMPASSING, CASE 14, RUN 2
Y TILT DUE TO HORIZON SENSOR NOISE - 1 ARCSECOND, C.T. = 1 MINUTE

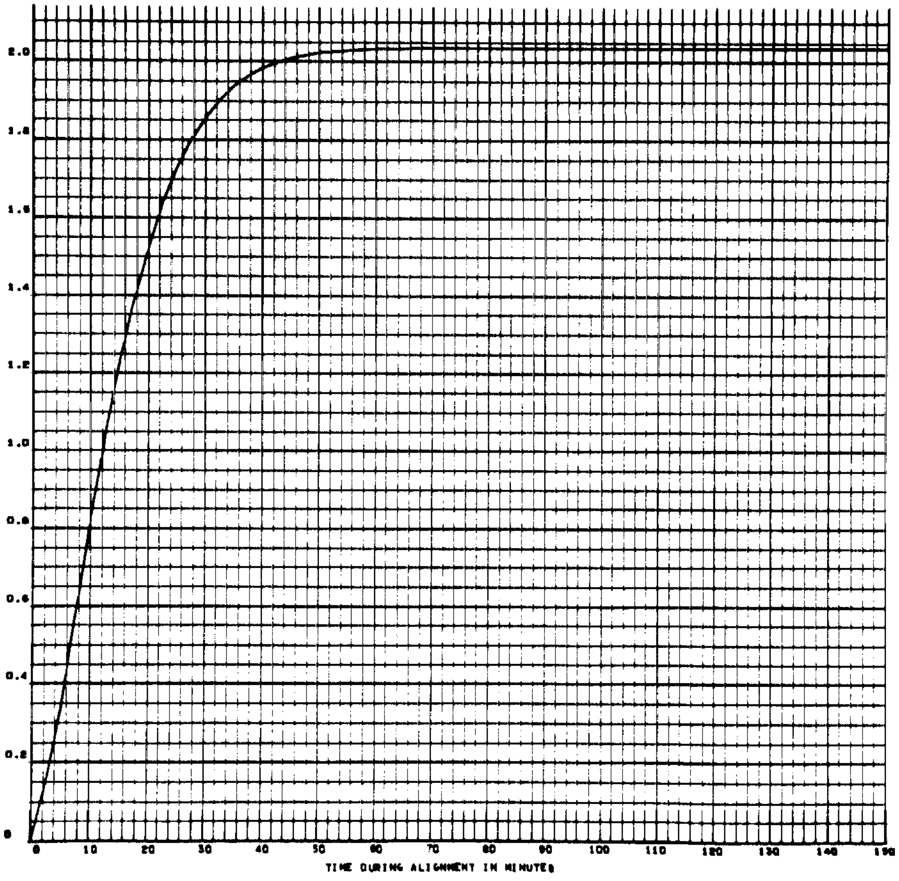

APPENDIX C

MECHANIZATION OF STRAPDOWN ESG ATTITUDE AND ANGULAR RATE DETERMINATION

To gyrocompass aline an ESG system it is necessary to measure angular rates. Since the pickoff data basically yields whole value direction cosines, the angular rate must be obtained by computation. The current literature on ESG attitude mechanization does not consider the problem of determining angular rate from direction cosines. In the following a derivation is given on one approach to computing vehicle rates from a series of direction cosine measurements.

First, it is necessary to give a discussion on how direction cosines are computed from the optical pickoff data. Figure A-1 shows a rotor with a scribed great circle which is canted relative to the rotor spin axis.

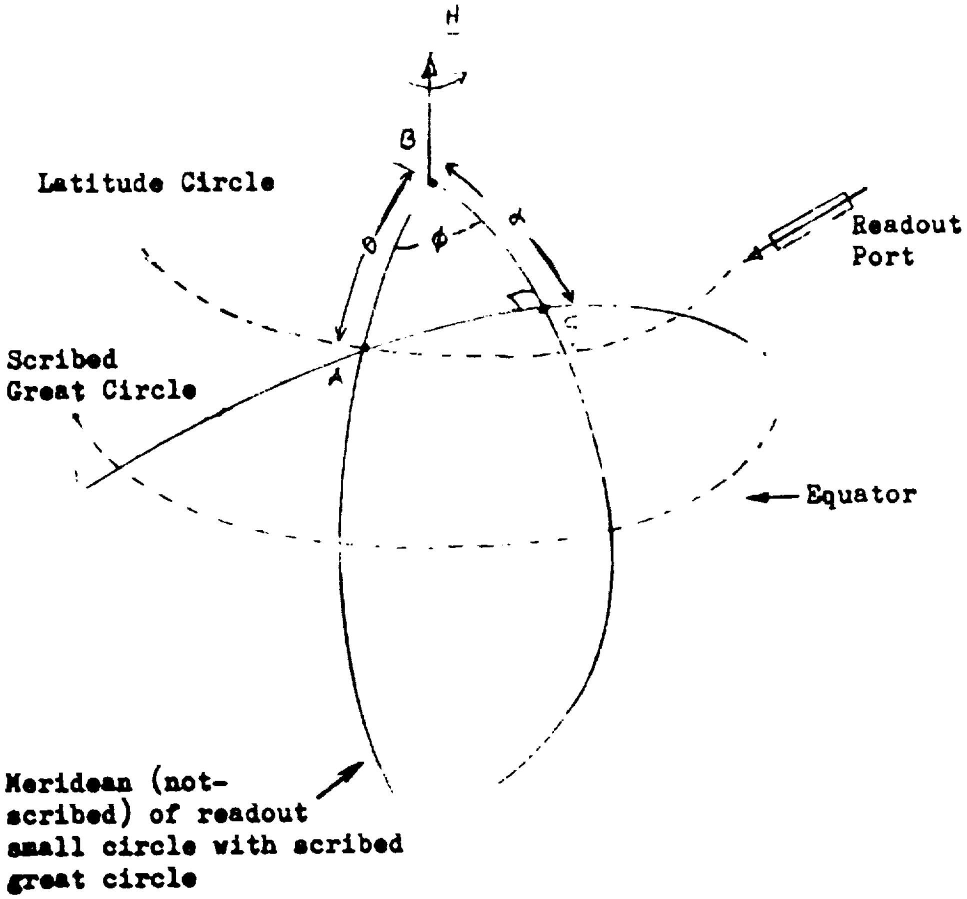
H
B
Latitude Circle
θ
φ
α
Readout Port
C
A
Scribed Great Circle
Equator
Meridean (not-scribed) of readout small circle with scribed great circle

Fig. A-1

ESG Gyro Readout Latitude Circle Geometry

The angle α is the colatitude of the point of closest approach of the scribed great circle and is a constant when there is no rotor drift. The angle θ is the desired colatitude of the readout port which defines the direction cosine of the port relative to the spin axis. This angle θ is a function of the difference in the times of crossing of the scribed great circle in the field of view of the port.

An optical pickoff senses a pulse whenever the great circle scribe line passes in its field of view. There are three pickoffs for each gyro, differently oriented; two of which yield independent data, and the third is used for redundancy. For each rotor revolution two pulses are registered. For a number of revolutions a series of pulses will be registered at each read port yielding three time series, one of which is typically shown in Fig. A-2.

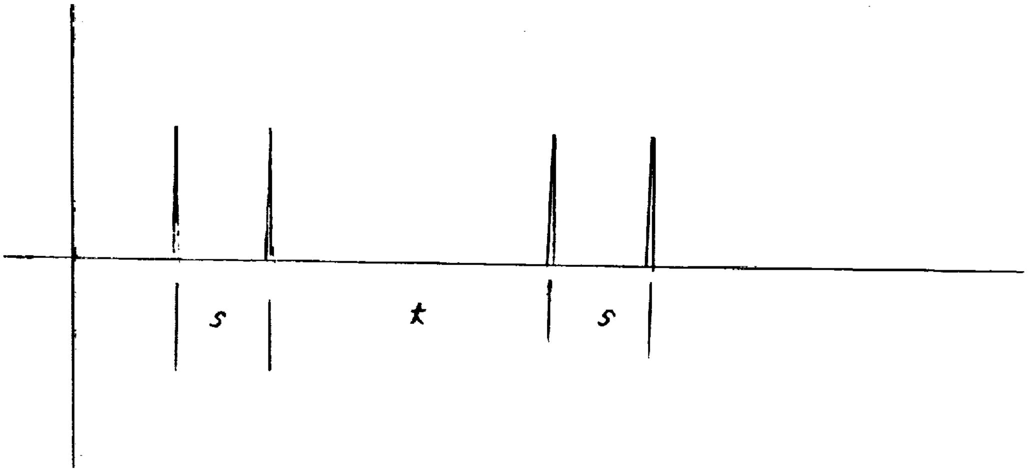

Fig. A-2

Time Series of Pulses Read From Pickoff Ports

The basic measurables which are recorded are the time spacing between two successive pulses. The measure of the latitude of the readout port to the spin axis is given by the ratio of the crossing times s and t. If s = t then this indicates the read port is located at the equator of the spinning rotor.

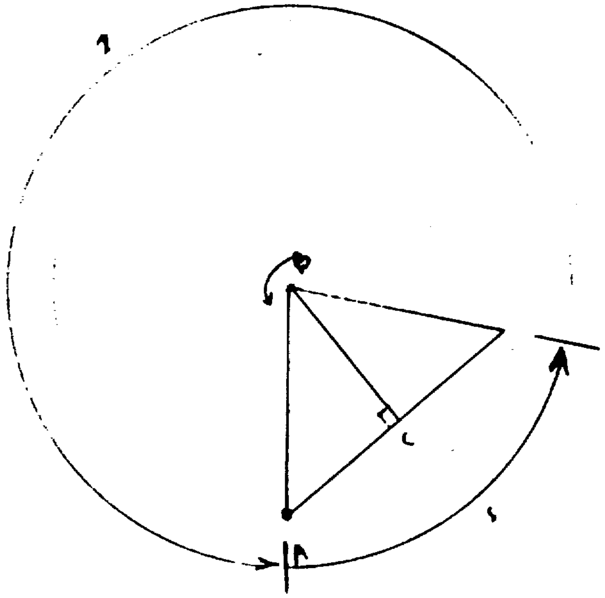

Fig. A-3

Top View of Readout Latitude Circle

A top view of the readout latitude circle corresponding to the time series Fig. A-2 is shown in Fig. A-3. From this figure it is seen that

$$\phi = \angle ABC = \pi \frac{s}{t+s} \qquad \text{(A-1)}$$

$$= \frac{\pi}{2}\rho + \frac{\pi}{2}$$

where

$$\rho = \frac{s-t}{s+t} \qquad \text{(A-2)}$$

and $s+t$ is the period of rotor revolution ($\approx$ constant). For mechanization purposes ρ is a better observable than the parameter s.

From Fig. A-3

$$c\theta = c\alpha \; c\angle AC \qquad (A\text{-}3)$$

$$s\theta = \frac{\sin\alpha}{s\angle BAC} = \frac{s\angle AC}{s\phi} \qquad (A\text{-}4)$$

$$c\phi = s\angle BAC \; c\angle AC \qquad (A\text{-}5)$$

$$= \frac{s\alpha}{s\theta} \; c\angle AC = \frac{s\alpha}{s\theta}\,\frac{c\theta}{c\alpha} = \tan\alpha \,\mathrm{ctn}\,\theta$$

$$= c\left(\frac{\pi}{2}\rho + \frac{\pi}{2}\right)$$

Therefore,

$$c\phi = -\,s\,\frac{\pi}{2}\rho = \tan\alpha\;\mathrm{ctn}\,\theta \qquad (A\text{-}6)$$

from which

$$\mathrm{ctn}\,\theta = -\,s\,\frac{\pi}{2}\rho\;\mathrm{ctn}\,\alpha \qquad (A\text{-}7)$$

Thus, for α = constant, meaning ρ yields a measure of θ. An alternate form yielding $c\theta$ directly can be obtained from the above equation

$$c\theta = \frac{\sin\frac{\pi}{2}\rho}{\left[\tan^2\alpha + \sin^2\frac{\pi}{2}\rho\right]^{\frac{1}{2}}} \qquad (A\text{-}8)$$

The sign ambiguity is resolvable by the redundant third readout.

Assuming, for simplicity, the readout ports corresponding to the orthogonal body frame axes, the three readouts yield the spin direction of the rotor

$$\underline{H} = c\theta_x \, \underline{1}_{px} + c\theta_x \, \underline{1}_{py} + c\theta_z \, \underline{1}_{pz} \tag{A-9}$$

A similar result is obtained for the second gyro.

The spin direction, as given by Eq. (A-9) is well defined if the gyrocase (vehicle frame) is not undergoing angular rotations. In the presence of angular motion, the cosine of each port must be initialized to the same time, because the computations occur at different times. Actually the ρ's are computed on the basis of smoothed values of s and t; therefore, high frequency rates greater than the sampling time (of the order of rotor revolution) are smoothed out. The smoothing algorithm must include the effect of rates and possibly accelerations. This, in essence, is equivalent to providing for an interpolation type algorithm to tie the cosine computations to the same epoch.

The vehicle angular rate in inertial space can be obtained in the following way. From the equation

$$S^{pI} = [\underline{H}_1^p \; \underline{H}_2^p \quad \underline{H}_1^p x \underline{H}_2^p] \, [\underline{H}_1 \; \underline{H}_2 \quad \underline{H}_1 x \underline{H}_2]^{-1} .$$

The angular rate is

$$\tilde{\omega}^{pI} = -\dot{S}^{pI} S^{Ip} = -[\dot{\underline{H}}_1^p \; \underline{H}_2^p \quad \dot{\underline{H}}_1^p x \underline{H}_2^p + \underline{H}_1^p x \dot{\underline{H}}_2^p] \, [\underline{H}_1^p \; \underline{H}_2^p \quad \underline{H}_1^p x \underline{H}_2^p]^{-1}$$

The time derivative $\dot{\underline{H}}_1^p$ typically is

$$\dot{\underline{H}}_1^p = \begin{bmatrix} -s\theta_x & \dot{\theta}_x \\ -s\theta_y & \dot{\theta}_y \\ -s\theta_z & \dot{\theta}_z \end{bmatrix}$$

To express $\dot{\theta}$ in terms of s and t, from Eq. (A-7)

$$-\csc^2\theta \quad \dot{\theta} = -c\,\frac{\pi}{2}\,\rho\ \mathrm{ctn}\,\alpha\ \frac{\pi}{2}\ \dot{\rho}$$

From

$$\rho = \frac{s-t}{s+t}$$

one can express

$$\rho = \rho_o + \dot{\rho}_o \tau + \ddot{\rho}_o\ \frac{T^2}{2}\ \cdots$$

Since ρ is measured by smoothing

$$\rho_i = \rho_o + \dot{\rho}_o(i\tau) + \ddot{\rho}_o\ \frac{(i\tau)^2}{2}\cdots$$

From which using pseudo inverse methods one can compute by inversion

$$\rho_o,\ \dot{\rho}_o,\ \ddot{\rho}_o$$

and finally to interpolate

$$\dot{\rho} = \dot{\rho}_o\tau + \ddot{\rho}_o\ \tau\quad\cdots$$

with this expression $\dot{\theta}$ is computed and the components of $\tilde{\omega}^{pI}$ are defined.

BIBLIOGRAPHY

Differential Accelerometer Determination of the Vertical

"A New Approach to Gravitational Gradient Determination of the Vertical", John W. Diesel, AIAA Journal, Volume 2, No. 7, July 1962 (pp 1189-1196)

"Sensing and Actuation Methods", Methods for the Control of Satellites and Space Vehicles, Volume I, WADD-TR60-643, July 31, 1960

"Mass Detection by Means of Measuring Gravity Gradients", by C. C. Bell, R. L. Forward, J. R. Morris, AIAA Paper No. 65-403

"Gravity Gradient Determination of the Vertical", by R. E. Roberson, American Rocket Society Paper 1496-60

Horizon Sensors

"Infrared Horizon Sensor Accuracy in the Atmospheric Absorption Bands", M. D. Earle, Electrical and Optical Department, Sensing and Information Systems Subdivision, Electronics Division, Aerospace Corporation Report TOR-268(4540-80), AD 460971

"An Orbital Gyrocompass Heading Reference for Satellite Vehicles", Robert Gordon, Sperry Gyroscope Co. AIAA Paper No. 64-238

"Standardized Space Guidance Study Program Definition Study-Phase 1a" Volume 7, Annex C-4, Prepared by Sperry Gyroscope Co., May, 1964, AD 353106

"Semiannual Report on Study of Attitude Sensors for Space Missions", E. I. Reeves, Space Technology Laboratories, Inc., 30 June, 1960, AD 242423

"Radiometric Observations of the Earth's Horizon from Altitudes Between 300 and 600 Kilometers", Thomas McKee, Ruth Whitman, and Charles Engle, Langley Research Center, Langley Station, Hampton, Va., NASA TN D-2528

"Infrared Horizon Sensor Techniques for Lunar and Planetary Approaches", Gerald Falbel, Technical Planning Staff, Barnes Engineering Co., Paper No. 63-358

"Physical Significance of the Tiros II Radiation Experiment", R. A. Hanel, Goddard Space Flight Center, and D. Q. Wark, U.S. Weather Bureau, NASA TN D-701, December 1961

"Study of a Proposed Infrared Horizon Scanner for Use in Space-Oriented Control System", Norman Hatcher and Ernst F. Germann, Jr., Langley Research Center, Langley Air Force Base, Va., NASA TN D-1005, January 1962

"Horizon Trackers for Lunar Guidance and Control Systems", Kenneth H. Kuhn and Edward W. Stark, Air Armament Div., Sperry Gyroscope Division of Sperry Rand Corp., Paper presented at the American Astronautical Society Lunar Flight Symposium, New York, N.Y., December 27, 1960

"Horizon Sensing for Attitude Determination", Barbara Kegerreis Lunde, NASA, Goddard Space Flight Center, Goddard Memorial Symposium, Paper No. 64-47

"IR Horizon Sensor Guides Planetary Orbiting", Bernard Kovit, Repring from Space and Aeronautics, February 1961

"Angular Distance of Outgoing Thermal Radiation in Different Regions of the Spectrum", Y. Ya, Kondrat'ev and K. E. Yakushevskaya, Acad. Sci. USSR (Artificial Earth Satellites) pp. 13-29

"The Infrared Horizon of the Planet Earth", R. A. Hanel, W. R. Bandeen, and B. J. Conrath, Journal of Atmospheric Science, No. 20, 1963

"Horizon-Based Satellite Navigation Systems", R. L. Lillestrand and J. E. Carroll, IEEE Trans on Aerospace and Navigational Electronics, 1963

"An Analytical Infrared Radiation Model of the Earth", R. A. McGee, Volume 1, No. 5, Applied Optics, September 1962

"Final Report on the TIROS I Meteorological Satellite System", Goddard Space Flight Center and U.S. Weather Bureau, NASA TR R-131, 1962

"A Meteorological Study of Cold Clouds as Related to Satellite Infrared Horizon Sensors", John E. Alder, Stanford Research Institute, AFCRL-63-413, N63-17752

"Estimation of Local Vertical and Orbital Parameters for an Earth Satellite on the Basis of Horizon Sensor Measurements", A. L. Knoll, M. M. Edelstein, Honeywell Aeronautical Division, Boston, Mass., January 20, 1964

"Proceedings of the First Symposium on Infrared Sensors for Spacecraft Guidance and Control", Barnes Engineering Co., Stamford, Conn., May 12,13 and 26,27, 1965.

"Horizon Sensors and Horizon Profile Measurements", M. D. Earle, Electrical and Optical Department, Sensing and Information Systems Subdivision, Electronics Division, Aerospace Corporation Report No. TOR-469(5107-38)-1, February 1965

"Infrared Horizon Sensors", John Duncan, Wm. Wolfe, G. Oppel, and James Burn, IRIA State of Art Report 2389-80-T, AD 466289, University of Michigan, April 1965

"Infrared Horizon Sensors, Description of Classified Instruments", John Duncan, IRIA State of the Art Report 2389-80-T, University of Michigan, April 1965

"Optical Attitude Sensors for Space Vehicle Application:Descriptive Survey of Recent Literature and Error Studies", a thesis submitted in partial satisfaction of the requirements for the degree Master of Science in Engineering, by James H. Spotts, University of California, Los Angeles

"Control, Guidance and Navigation of Spacecraft", NASA SP-17, December 1962